Seasonal organization of planktonic microbial communities with emphasis on the diversity and ecology of blooming taxa

Dimitra-Ioli Skouroliakou

Thèse de Doctorat

Mention Sciences agronomiques et écologiques
Spécialité Sciences de la Mer – Biologie et écologie

présentée à ***l'Ecole Doctorale en Sciences Technologie et Santé (ED 585)***

de l'Université du Littoral et de la Côte d'Opale

par

Dimitra-Ioli Skouroliakou

pour obtenir le grade de Docteur de l'Université du Littoral et de la Côte d'Opale

Organisation saisonnière des communautés microbiennes planctoniques en relation avec la diversité et l'écologie d'espèces responsables d'efflorescences

Soutenue le 18 Octobre 2023, après avis des rapporteurs, devant le jury d'examen :

Dr. François Schmitt
DR CNRS, Laboratoire d'Océanologie et des Géosciences (LOG) / Président
Dr. France Van-Wambeke
DR CNRS, Institut Méditerranéen d'Océanologie (MIO) / Rapportrice
Dr. Raffaele Siano
CR Institut Français de Recherche pour l'Exploitation de la MER (IFREMER) / Rapporteur
Dr. Loïs Maignien
MCF, Université de la Bretagne Occidentale (UBO) / Examinateur
Dr. Hera Karayanni
Assistant Professor, University of Ioannina (UOI) / Membre Invité
Pr. Urania Christaki
PR, Université du littoral Côte d'Opale (ULCO) / Directrice de thèse
Dr. Luis Felipe Artigas
MCF, Université du littoral Côte d'Opale (ULCO) / Co-encadrant

Preface

This thesis was funded via a PhD grant by the ‘Region des Hauts de France’ 50 % and the ‘Pôle métropolitain de la Côte d’Opale (PMCO)’ 50 % from October 2019 to September 2022. The ‘Université du Littoral Cote d’Opale’ provided complete funding for doctoral contract extension from October 2022 to March 2023, due to the Covid-19 lockdown.

Additionally, this thesis supported by the national monitoring network SOMLIT (https://www.somlit.fr/), the CPER MARCO (https://marco.univ-littoral.fr/), and the French Research program of INSU-CNRS via the LEFE-EC2CO 'PLANKTON PARTY'.

Acknowledgments

First of all, I would like to express my thanks to the ‘Region des Hauts de France’, the ‘Pôle métropolitain de la Côte d’Opale (PMCO)’, the Université du Littoral Côte d’Opale, the CPER-MARCO, and the research program of INSU-CNRS via the LEFE-EC2CO ‘PLANKTON PARTY’ for their funding, as well as the national monitoring network SOMLIT and the local monitoring transect DYPHYRAD for supporting this thesis. I extend also my thanks to Pr. Hubert Loisel for allowing me to work in the Laboratory of Oceanology and Geosciences.

I am grateful to France Van-Wambeke, Raffaele Siano, Loïs Maignien, François Schmitt and Hera Karayanni, for agreeing to evaluate this work. Furthermore, I am thankful to the committee members for their willingness to follow my PhD work and for their valuable comments over the years (Loïs Maignien, François Schmitt, Ludwig Jardillier, and Kostas Kormas). Merci Loïs pour m'avoir donné l'opportunité de participer à EBAME workshop. Merci à Ludwig (et également à Paola Bertolino) de m'avoir accueillie au l’laboratoire ESE, pour m'avoir formée aux extractions d'ADN et aux PCR, ainsi que pour tes conseils. Κώστα ευχαριστώ για τις πολύτιμες συμβουλές σου.

I want to convey my deepest gratitude to my supervisor Urania Christaki, for her continuous guidance, support and insights that have enriched my academic journey since my master’s internship.

I would like thank my co-supervisor, Felipe Luis Artigas, for giving me the opportunity to collect samples at the monitoring transect DYPHYRAD and for allowing me to gain my first teaching experience.

My sincere acknowledgments go to the crew of the marine vessel Sepia II, and the technicians Vincent Conille and Eric Lecuyer. I also thank Muriel Crouvoisier for conducting nutrient analysis.

I extend my warmest thanks to my colleagues at LOG, especially Elsa Breton who trained me in phytoplankton identification, collaborated with me over the years, and for sharing her enthusiasm for community ecology. I am also grateful to Solène Irion for her support and help during the first years of my thesis.

I share my thanks to all the students who helped me with sampling, cytometry analyses and DNA extractions (Léa Fourchault, Lola Miro Solé, Laura Cocquebert, Patrick Kagerer, et Aurelie Libeau).

Many thanks to Peter Magee and Clémantine Gallot for English proofreading.

Merci Jordan pour ton soutien et tes corrections des parties en français dans cette thèse.

My lasts thanks go to my family in Greece. Thank you for believing in me and for your support. Ευχαριστώ μαμά για όλα, εύχομαι να με βλέπεις και να είσαι περήφανη.

I dedicate this thesis to the memory of my mother

Ioli SKOUROLIAKOU – CV
Ph.D. student

Work Experiences

2019-in progress

Doctoral contract, Université du Littoral Côte d'Opale, UMR LOG 8187, Laboratory of Oceanography and Geosciences, Wimereux-France - supervised by Christaki U. and Artigas L. F.

2018-2019

Project Engineer, Université du Littoral Côte d'Opale, UMR LOG 8187, Laboratory of Oceanography and Geosciences, Wimereux-France - supervised by Christaki U.

2018

Master Internship, Université du Littoral Côte d'Opale, UMR LOG 8187, Laboratory of Oceanography and Geosciences, Wimereux-France - supervised by Christaki U.

Title: 'Temporal succession and small-scale variability of planktonic microbial communities in a meso-eutrophic coastal ecosystem'

2017

Master Internship at the HCMR: Hellenic Centre for Marine Research, Anavissos Greece - supervised by Giannakourou A.
Title: 'Study of the microbial food web in the Cretan Sea and Levant Basin'

Education

2019 – in progress

PhD student in Marine Sciences – Biology and Ecology, Université du Littoral Côte d'Opale - supervised by Christaki U and Artigas L. F.

Title: 'Seasonal organisation of planktonic microbial communities with emphasis on the diversity and ecology of blooming taxa'

2013-2018

Integrated Master (300 ECTS) in Biological Applications and Technology, University of Ioannina (Greece, Rank: 2nd /41, mark: 8.01/10)

List of publications

(In blue boxes: Papers and communications from this Ph.D. thesis)

Published papers

2023

1. Christaki U*, **Skouroliakou D-I***, Jardillier, (2023), Interannual dynamics of putative parasites (Syndiniales Group II) in a coastal ecosystem, *Environmental Microbiology*, DOI: https://doi.org/10.1111/1462-2920.16358, **the first two authors contributed equally,* (**3rd paper, Results section**)
2. Houliez E, Schmitt F, Breton E, **Skouroliakou D-I**, Christaki U. (2023). On the conditions promoting Pseudo-nitzschia spp. blooms in the Eastern English Channel and southern North Sea; *Harmful Algae*, DOI: https://doi.org/10.1016/j.hal.2023.102424

2022

3. **Skouroliakou D-I**, Breton E, Irion S, Artigas L F, Christaki U. (2022), Deterministic and stochastic processes regulate phytoplankton assemblages in a temperate coastal ecosystem; *Microbiology Spectrum*, DOI: https://doi.org/10.1128/spectrum.02427-22, (**1st paper, Results section**)

4. Breton E, Goberville E, Sautour B, OuadiA, **Skouroliakou D-I**, Seuront L, Beaugrand G, Kleparski L, Crouvoisier M, Pecqueur D, Salmeron C, Cauvin A, Pocquet A, Garcia N, Gohin F, Christaki U., (2022), Multiple phytoplankton community responses to environmental change in a temperate coastal system: a trait-based approach, *Frontiers in Marine Science*, DOI: https://doi.org/10.3389/fmars.2022.914

2021

5. Breton E, Christaki U, Sautour B, Demonio O**, Skouroliakou D-I**, Beaugrand G, Seuront L, Kléparski L, Poquet A, Nowaczyk A, Crouvoisier M, Ferreira S, Pecqueur D, Salmeron C, Brylinski J-M, Lheureux A, Goberville E; (2021) Seasonal Variations in the Biodiversity, Ecological Strategy, and Specialization of Diatoms and Copepods in a Coastal System With Phaeocystis Blooms: The Key Role of Trait Trade-Offs ; *Frontiers in Marine Science* .Vol8, DOI: https://www.frontiersin.org/article/10.3389/fmars.2021.656300
6. Christaki U, **Skouroliakou D-I**, Delegrange A, Irion S, Courcot L, Jardillier L, Sassenhagen I. (2021). Microzooplankton diversity and potential role in carbon cycling of contrasting Southern Ocean productivity regimes; *Journal of Marine Systems*, DOI: https://doi.org/10.1016/j.jmarsys.2021.103531

In preparation

7. **Skouroliakou** et al., Bacterial dynamics and interactions during distinct phytoplankton blooms in temperate coastal waters.
(2nd To be submitted in Environmental Microbiology, Results section)

Ouvrage colloque MARCO-2021 : Contribution dans trois chapitres de la session 'Biodiversité, réseaux trophiques et adaptation des organismes à l'environnement'

1. Breton E, Masson Neaud N, Courcot L, **Skouroliakou D-I**, Christaki U, (2022). Inventaire taxonomique illustré des diatomées (Phylum : Ochrophyta, Classe : Bacillariophyceae) récoltées au point Côte (Manche orientale) des Services Nationaux d'Observation SOMLIT/PHYTOBS sur la période 1996-2019.
2. Breton E, Goberville E, Sautour B, **Skouroliakou D-I**, Crouvoisier M, Seuront L, Beaugrand G, Pecqueur D, Salmeron C, Cauvin A, Garcia N, Christaki U, (2022). Dynamique et facteurs de contrôle des efflorescences de la micro-algue mucilagineuse du genre *Phaeocystis* : synthèse de 24 ans d'observation à la station « Wimereux Côte » des Services Nationaux d'Observation SOMLIT/PHYTOBS.
3. Breton E, Christaki U, Sautour B, **Skouroliakou D-I**, Crouvoisier M, Cauvin A, Goberville E, (2022). De l'intérêt des approches basées sur les traits de vie pour la compréhension des processus régulateurs de la biodiversité et leur rôle sur le fonctionnement des écosystèmes : exemples avec le plancton des eaux côtières de la Côte d'Opale.

List of communications

International conferences

1. Christaki U, **Skouroliakou D-I**, Irion S., Sequencing data and empirical evidence of interannual patterns of putative parasites (Group II Syndiniales) in a coastal ecosystem, Jacques-Monod Conference, 5 – 9 September 2022, (https://cjm3-2020.sciencesconf.org/), France. (*Poster presentation*)
2. **Skouroliakou D-I**, Breton E, Irion S, Artigas F, Christaki U., Stochastic and deterministic processes regulate phytoplankton assemblages in a coastal temperate ecosystem, ISME18 Conference 14 – 19 August 2022, (https://isme18.isme-microbes.org/), Switzerland. (*Poster presentation*)
3. **Skouroliakou D-I,** Irion S, Christaki U., Ecological processes driving phytoplankton assemblages with null model approach based on phylogenetic information, Ocean sciences meeting 27 February – 4 March 2022, online conference, (https://www.aslo.org/osm2022/), USA. (*Oral presentation)*

4. **Skouroliakou D-I,** Irion S, Christaki U., Ecological processes driving phytoplankton blooming taxa in a coastal meso-eutrophic ecosystem: a phylogenetic approach, 10th Hellenic conference of ecology 14 – 17 October 2021, online conference (https://helecos10.gr/en/), Greece. (*Oral presentation*)
5. Sassenhagen I, Breton E, **Skouroliakou D-I,** Cornille V, Jardillier L, Christaki U., Species specific interactions among microalgae and parasitic marine alveolates, ISME17 12-17 August 2018, Germany. (*Poster presentation*)
6. Sassenhagen I, Breton E, **Skouroliakou D-I**, Cornille V, Jardillier L, Christaki U., Species specific interactions among microalgae and parasitic marine alveolates. The 18th ICHA meeting 21 -16 October 2018, France. (*Poster Presentation*)

Local conferences

7. **Skouroliakou D-I,** Irion S, Christaki U., Ecological processes driving phytoplankton blooming taxa in a coastal meso-eutrophic ecosystem: a phylogenetic approach, MARCO meeting, 13 – 15 October 2021 (https://marco.univ-littoral.fr), France. *(Poster presentation)*
8. Houliez E, Breton E, **Skouroliakou D-I**, Schmitt F G, Christaki U., Conditions favorisant les efflorescences des diatomées du genre *Pseudo-nitzschia spp*. en Manche orientale et sud de la Mer du Nord, MARCO meeting, 13 – 15 October 2021 (https://marco.univ-littoral.fr), France (*Oral presentation*).
9. Houliez E, Breton E, **Skouroliakou D-I**, Schmitt F G, Christaki U., Conditions favorisant les efflorescences des *Pseudo-nitzschia spp.* en Manche orientale et sud de la Mer du Nord : apports des réseaux d'observation et des analyses de niches, Colloque EVOLECO 2021, La Rochelle, 3-5 novembre 2021. (*Oral presentation*)
10. **Skouroliakou D-I,** Christaki U., Diversity and biomass of the microzooplankton during MOBYDICK,comparison with KEOPS data. Workshop MOBYDICK, Museum Histoire Naturelle, Paris 14-15 Mai 2019. (*Oral presentation*)

Student co-supervising

1. M2- Yanis Maire – Aix-Marseille Université, 'Effects of turbulence on diatoms of the genus Pseudo-nitzschia spp. and associated bacteria', January 2023 – June 2023.
2. Bcs – Léa Fourchault – University of St Andrews, UK, 'Marine Microbial Ecology in the Eastern English Channel: An Introduction to Conventional and Molecular Approaches', June - July 2020.
3. M1– Lola Miro Solé - Université du Littoral Côte d'Opale, 'Succession of microbial communities in the Eastern English Channel', June-July 2020.
4. L2 - Laura Cocquebert- Université du Littoral Côte d'Opale, 'Temporal dynamics and micro-scale variability of viruses in the Eastern English Channel', January 2020.
5. L2 - Patrick Kagerer - Université de Franche-Comté, 'Initialisation in planktonic ecology: Sampling and observation', June-July 2019.
6. L3 – Aurèlie Libeau – Université de la Rochelle, 'Cytometry and phytoplankton identification in English Channel', April-May 2019.

Teaching

Developmental biology, 48 hrs (2nd year of BSc in Life Sciences) Calais 2020-2022, France

Field experiences

ECOPEL Leg1 Plankton sampling in English Channel, 2 weeks on board of R/V 'Antea', April 2018, PI: Artigas L.F.

Sampling at the local monitoring stations DYPHYRAD (DYnamique PHYtoplanctonique le long de la RADiale) in the Eastern English Channel on bord of R/V 'Sepia II', 2019-2021, PI: Artigas L.F.

Science communication

'Fête de la Mer', 8- 11 July 2021, and 11- 14 July 2019: 'Demonstration of plankton sampling and observation techniques'

Workshops-Trainings

1. *EBAME*6 Workshop on Computational Microbial Ecogenomics, 25 October – 5 November, 2021 Brest – France, organized by Maignien L.
2. *Research ethics,* 27 May 2021, organised by the Sciences, Technology, Health Doctoral School.
3. *Efficient composition of a thesis with LaTex,* 10 – 18 March 2021, organised by the Sciences, Technology and Health Doctoral School.
4. *Conducting your thesis as a project,* 06 -30 April 2020, organised by the Sciences, Technology, Health Doctoral School.
5. *From researcher today to entrepreneur tomorrow?* 03-04 December 2019, organised by the Sciences, Technology, Health Doctoral School.
6. *Metabarcoding training* at UMR 8079 Diversité, Ecologie et Evolution Microbiennes, Laboratoire Ecologie, Systématique et Evolution Orsay, 12-14 November 2019, organized by Jardillier L.
7. *PHYTOBS* Workshop on microphytoplankton identification, 27 – 29 May 2019, Roscoff – France, organized by: M. Lemoine, Claquin P., Chomérat N. and Rigaut-Jalabert F.
8. *Cytometry training,* initiation in the use of the 'CYTOFLEX' flow cytometer, 24 – 25 October 2017, organized by Beckman coulter France S.A.

Contribution in projects beyond thesis

1. *INSU-CNRS, LEFE-CYBER*, 'Turbu-diatox' project: 'Effets de la turbulence sur la prolifération et la toxicité des diatomées', 2021 -2022, PIs: Urania Christaki and François Schmitt.
   During the last year of my thesis, I participated in the Turbu-diatox project. My contributions involved conducting laboratory analyses, such as cytometry, DNA and RNA extractions. I also provided early training to a Master's student in bioinformatic analyses. Additionally, I handled tasks related to quotation and communication with sequencing companies.
2. *OFB, INDIGENE project* : 'Données génétiques et indicateurs de biodiversité microbienne pélagique', 2020 – 2022, PI : Simon (Roscoff), colaborators : U. Christaki (Wimereux), L Maignen (Brest)
   I provided a portion of my thesis metabarcoding data (16S and 18S datasets) to the INDIGENE project.
3. *ANR, MOBYDICK* Marine Ecosystem Biodiversity and Dynamics of Carbon around Kerguelen: an integrated view, https://www.mio.univ-amu.fr/mobydick/, 2018 – 2022, PI: Bernard Quéguiner
   During my Project Engineer contract (2018-2019), I analyzed 89 microzooplankton samples (dinoflagellates and ciliates) using inverted microscopy and I participated in data analysis.

Funding

2019 – 2023

Grant for doctoral salary from Région Hauts-de-France, Pôle Métropolitain de la Côte d'Opale and Université du Littoral Côte d'Opale

2018 – 2019

Erasmus grant grant for 9-month internship in France from the state scholarships foundation 'IKY', https://www.iky.gr/en/, Erasmus + 'IKY', 4500 €

2017 Grant for 2-month internship from the Greek state scholarships foundation 'IKY', https://www.iky.gr/en/, 912 €

Table of Contents

Abbreviations

ASV: amplicon sequence variant

EEC: Eastern English Channel

db-RDA: distance-based redundancy analysis

DNA : deoxyribonucleic acid

DYPHYRAD : dynamique phytoplanctonique le long de la radiale

eLSA: extended local similarity analysis

FISH: fluorescence in situ hybridization

HNF: heterotrophic nanoflagellate

HTS: high-throughput sequencing

FSC: forward scatter

NGS: next generation sequencing

OTU: operational taxonomic unit

PNF: phototrophic nanoflagellate

RNA: ribonucleic acid

Chl-a: chlorophyl-a

S : salinity

SOMLIT : service d'observation du milieu littoral

SSC: side scatter

T: temperature

PAR: photosynthetic active radiation

PicoNano: picophytoplankton and nanophytoplankton

PCA : principal component analysis

PCR : Polymerase chain reaction

$Si(OH)_4$: silicates

NO_2+NO_3: nitrite and nitrate

PO_4: phosphate

NRI: nearest related index

βNRI: beta nearest related index

List of figures

List of supplementary figures

List of Tables

List of supplementary tables

List of annexes

Chapter 1: General Introduction

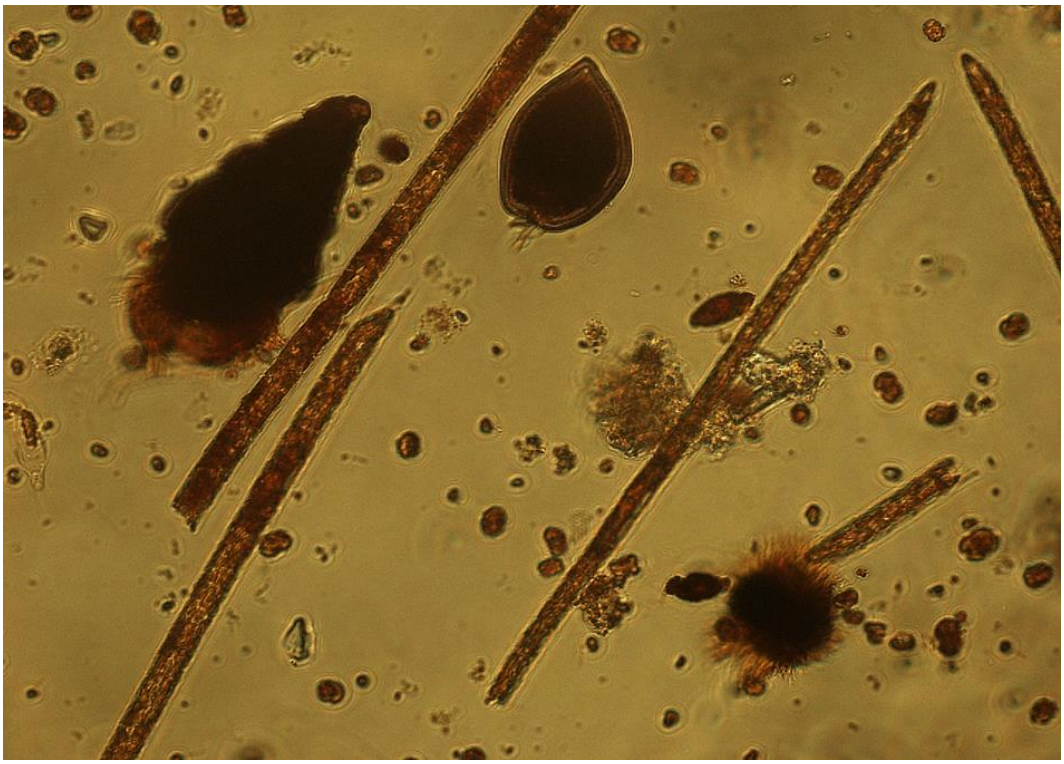

1. Introduction

1.1. General overview of plankton

The term plankton (Hensen, 1987; in ancient greek πλαγκτός / plagkos: drifter) encompasses all organisms that live in the water column and cannot actively move against currents (Fig. 1.1). Their movement is therefore determined by passive transport through currents that disperse them. However, some organisms are capable of active movement (e.g., vertical migrations) and may have morphological structures related to movement such as flagella and cilia. Some of drifting organisms that called 'tychoplankton' are benthic, but under certain conditions (e.g., physical mixing), they suspended in water column (Kuhn *et al.,* 1981). The definition of plankton does not have a phylogenetic basis (i.e., there is no common ancestor), but rather a functional one. Plankton is an extremely diverse group in terms of morphology, phylogeny (Woese *et al.*, 1990; Worden *et al.*, 2015), taxonomic and functional level (Barton *et al.*, 2013), spanning across several orders of magnitude in size (microns to meters). It has representatives from all domains of life, including prokaryotes (i.e., bacteria, archaea), protists (unicellular eukaryotes), small to large metazoans, as well as viruses, sharing common ecological futures (e.g., high growth rate, wide and diverse populations). However, there are strong differences in physiology, metabolic capacities, or trophic behaviour (e.g., Massana and Logares, 2013). It includes autotrophs (i.e., they produce their own food from inorganic compounds), heterotrophs (i.e., they feed on existing organic matter), mixotrophs that combine both autotrophic and heterotrophic trophic modes (Stoecker *et al.*, 2017), and parasites which infect other organisms in the ocean, having a significant impact on marine trophic networks (Hudson *et al.*, 2006).

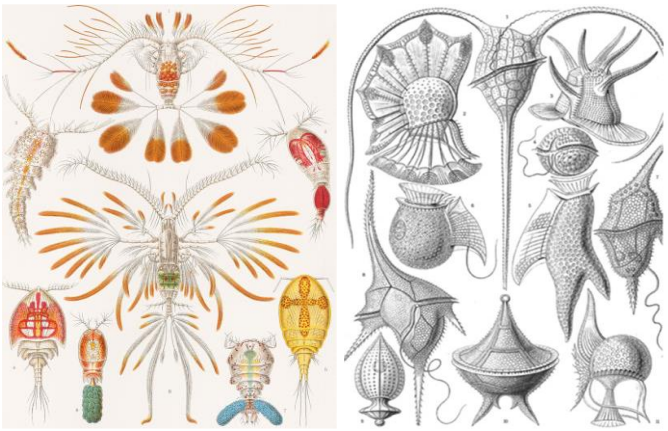

Figure 1.1. *Schematic illustration of morphological plankton diversity (i.e., copepods on the left), armoured dinoflagellates on the right plate drawn by Ernst Haeckel for 'Art Forms of Nature' in 1904.*

In the late 1970's, Sieburth categorised plankton and nekton[1] in several size spectra (Fig. 1.2). Autotrophic organisms are arbitrarily distributed over three size classes: picophytoplankton (0.2 – 2.0 µm), nanophytoplankton (2.0 – 20 µm), and microphytoplankton (> 20 µm). The first class is mainly made of cyanobacteria of the genera *Synechococcus* and *Prochlorochococcus*, although eukaryotic species have been described (e.g., *Ostreococcus tauri*, Courties *et al.*, 1994). The other two classes are more diverse, as they include coccolithophores, cryptophytes, haptophytes, autotrophic dinoflagellates, and diatoms. The latter ones are emblematic components within microphytoplankton. Diatoms account for 40% of the total primary production in the ocean by dominating export production (Sarthou *et al.*, 2005), and exert a major influence upon the biogeochemical cycles of macro-nutrients, nitrogen (N), phosphorus (P), and silicon (Si) (e.g., Tréguer *et al.*, 2018).

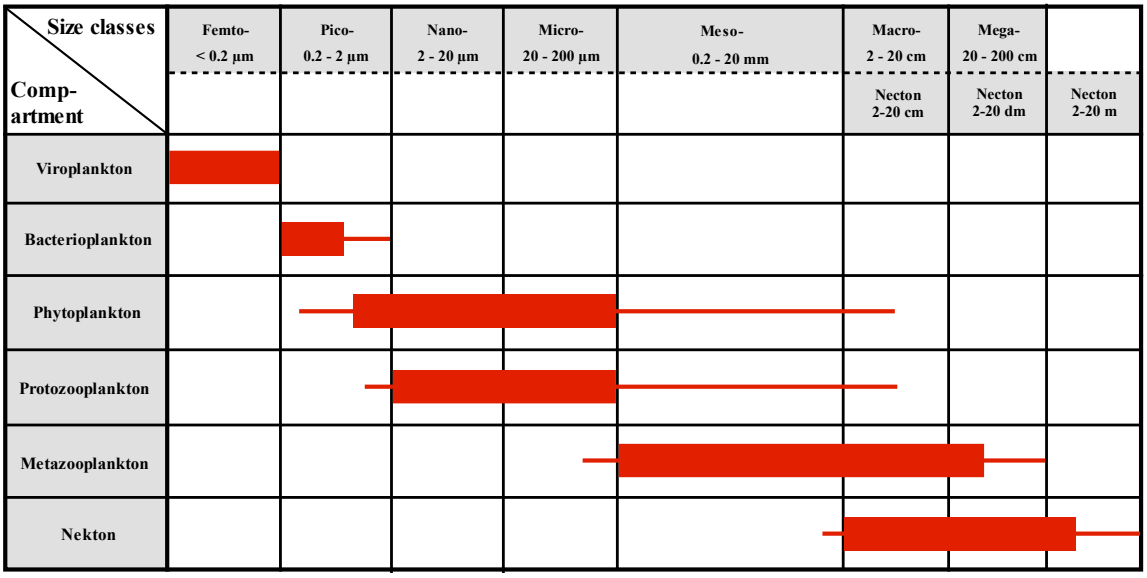

Figure 1.2. *Distribution of size spectra of different taxonomic/trophic groups of plankton and nekton, in rows, according to different size classes, in columns (modified from Sieburth et al. 1978).*

The other five compartments are heterotrophic and / or mixotrophic and are associated with relatively well-constrained size classes: viruses lie in the femtoplankton (0.02-0.2 µm), free bacteria and archaea in the picoplankton, and fungi (mycoplankton) in the nanoplankton (Fig. 1.2). The protozooplankton is the group whose size spectrum overlaps the most with that of the phytoplankton. Protozooplankton includes unicellular eukaryotes, such as ciliates, that feed on bacteria or graze on smaller-sized phytoplankton, heterotrophic nanoflagellates, and dinoflagellates. They play a pivotal role in oceanic ecosystems as they consume phytoplankton, they are grazed by mesozooplankton and thus contribute to nutrient remineralization (e.g.,

[1] ***Nekton****: organisms that can move against currents.*

Sherr and Sherr, 2002). This thesis, will focus on planktonic microbial communities spanning from bacteria to protists living in the surface waters of a coastal ecosystem.

1.2. Plankton: Tiny but powerful ocean organisms

Knowledge of distribution patterns, composition, and ecology of planktonic communities is of great interest for many reasons (e.g., Lombard *et al.*, 2019). Life is thought to have begun in the ocean, and planktonic organisms, therefore, provide important evolutionary insights on diversity, complex life forms, and adaptations to highly variable environments. Plankton forms the foundation of most marine food webs. In marine ecosystems, plankton account for more than 60 % of marine biomass (Bar-On and Milo, 2019; Fig. 1.3). This biomass is shared between producers ~1 Gt C (i.e., bacteria, protists, plants) and consumers ~ 5 Gt C (i.e., animals, protists, and bacteria). Phytoplankton account for less than 1% of Earth's photosynthetic biomass, but are responsible for almost half of the global annual net primary production (Falkowski *et al.*, 1998; Field *et al.*, 1998). In contrast to terrestrial ecosystems, a small mass of producers sustains a significantly larger mass of consumers. This is because of the high turnover occurring over small time scales (hours to days) and their small size, while consumers such as fish have much longer turnover, spanning from months to years (Sheldon *et al.*, 1972). Furthermore, planktonic organisms play significant roles in global cycles of the majority of oceanic chemical elements, and they are key mediators of the Biological Carbon Pump (BCP)[2]. The organic material produced by phytoplankton is consumed by herbivorous zooplankton that provide a crucial source of food for higher trophic levels. In particular, larval stages of many commercially important fish species are zooplankton, and larval recruitment directly depends on the abundance of phytoplankton (e.g., Platt *et al.*, 2003). Because of their restricted environmental preferences and relatively short life spans, plankton abundance and composition

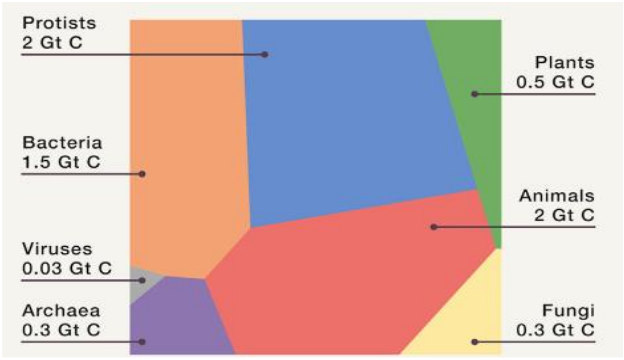

Figure 1.3*. The composition of marine biomass represented using a Voronoi treemap (Source: Bar-On and Milo, 2019).*

[2] ***BCP****: vertical transfer processes including passive sinking of organic particles, physical mixing of particulate and dissolved organic carbon (POC and DOC, respectively), and active transport by zooplankton migration. The mineralization of the organic matter increases with depth the concentration of dissolved inorganic carbon. The net effect of this phytoplankton-fuelled biological pump, is the transport of CO_2 from the atmosphere to the deep ocean, where it may be sequestered over the timescales of deep-ocean circulation (100 to 1000 years).*

react tightly to both local and global environmental changes (e.g., Edwards *et al.*, 2013; Beaugrand and Kirby, 2010; Beaugrand *et al.*, 2015). Some planktonic organisms can be directly toxic to humans, or cause disease and parasitism in animals, including commercial ones. For example, the diatom *Pseudonitzschia* spp. produces domoic acid, a neurotoxin that contaminates mussels, fishes, birds, and humans (Husson *et al.*, 2016). Given these important functions, the biomass and diversity of both phytoplankton and zooplankton were identified as Essential Ocean Variables (EOVs) by the Global Ocean Observing System (e.g., Miloslavich *et al.*, 2018).

1.3. Planktonic microbes in a changing world

With the advent of the industrial era and the intensification of agriculture, there has been a continuous increase in greenhouse gas emissions for a little over a century, primarily due to the growing use of fossil fuels, modifying environments and threatening ecosystems (IPCC 2023). Atmospheric concentrations of greenhouse gases such as CO_2, CH_4, N_2O contribute to an increase in positive radiative forcing on the climate, resulting in atmospheric warming (Luthi *et al.*, 2008). Among these gases, the atmospheric concentration of CO_2 has risen from 280 parts per million (ppm) during the pre-industrial era to over 415 ppm today (IPCC 2023). Models even predict atmospheric concentrations reaching up to 430 ppm by 2060, with an associated warming of 1.3°C (Davis *et al.*, 2010; Fig. 1.4). Warming induces changes in water stratification, as well as a decrease in pH, and dissolved oxygen (Bopp *et al.*, 2013; Kwiatkowski *et al.*, 2020).

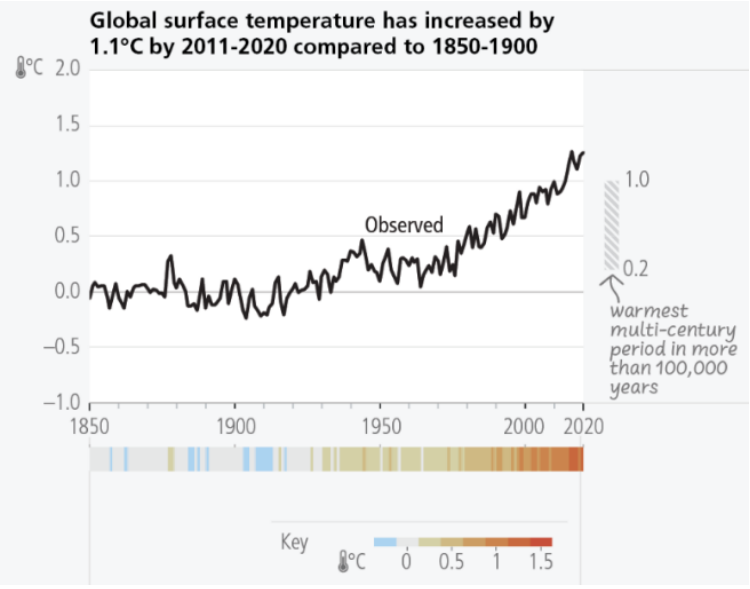

Figure 1.4. *Global average surface air temperature since 1850 (Source: IPCC report 2023).*

In this context, plankton are experiencing changes in their abundance and distribution. Studies have shown that globally, both phytoplankton and zooplankton are appearing earlier in the year, but the situation becomes more complex when considering specific groups and regions (e.g., Friedland *et al.*, 2018). For instance, in the North-East Atlantic, dinoflagellates are blooming[3] about thirty days earlier, while diatoms are not showing significant changes in their timing, although there is variation among different species within these groups (Chivers *et al.*, 2020; CPR data 1958-2016). There is also evidence of a global decline in the overall biomass of phytoplankton (Boyce *et al.*, 2010). Plankton distribution is also shifting poleward in order to track their optimal thermal habitats (e.g., Poloczanska *et al.*, 2013; Burrows *et al.*, 2014; Benedetti *et al.*, 2021). However, the extent of these shifts varies for different species within the diatom and dinoflagellate groups (Chivers *et al.*, 2017). Additionally, the average size of calanoid copepods (a type of zooplankton) is decreasing, primarily due to a northward movement of smaller warm-water species and a decline in larger cold-water species (Beaugrand *et al.*, 2010). These changes in the timing, abundance, and distribution of plankton have significant implications for marine ecosystems. The composition of plankton communities and their interactions are being altered, leading to a decline in fisheries (e.g., Karl *et al.*, 2001). Besides the shifts associated with temperature increase, sediment archives evidenced that human contaminations irreversibly affect protist communities (Siano *et al.*, 2021).

A fundamental objective in marine microbial ecology is to elucidate the diversity and dynamics of planktonic microbes and determine the factors that influence their diversity patterns. This knowledge is crucial for predicting how these patterns may be altered by human activities and climate change.

[3] ***Blooms*** *have been described as periods of rapid (or even 'explosive') growth in planktonic biomass (Platt et al., 1991) that can last from days to weeks. Regarding phytoplankton, blooms are considered as a condition of elevated phytoplankton concentration, although there is no established quantitative threshold defining "elevated." The concentration of the photosynthetic pigment chlorophyll (Chl) is commonly used as an index of phytoplankton abundance, and has the benefit of being detectable from space (Behrenfeld and Boss, 2014).*

1.4. Ecological theories and processes controlling diversity patterns

Different conceptual frameworks allow studying of the processes that define diversity patterns. In this section, main theories and ecological processes[4] explaining community diversity will be presented (Fig. 1.5). Several theories of biodiversity have been formulated that could explain community assemblages and their spatio-temporal distribution. Community assembly describes how processes interact to determine species composition and local biodiversity of a community (e.g., Chase and Myers, 2011). These theories, based on different principles, are not mutually exclusive. They involve environmental mechanisms, interactions, and stochastic ones (see Table 1.1 for terminology included in this section).

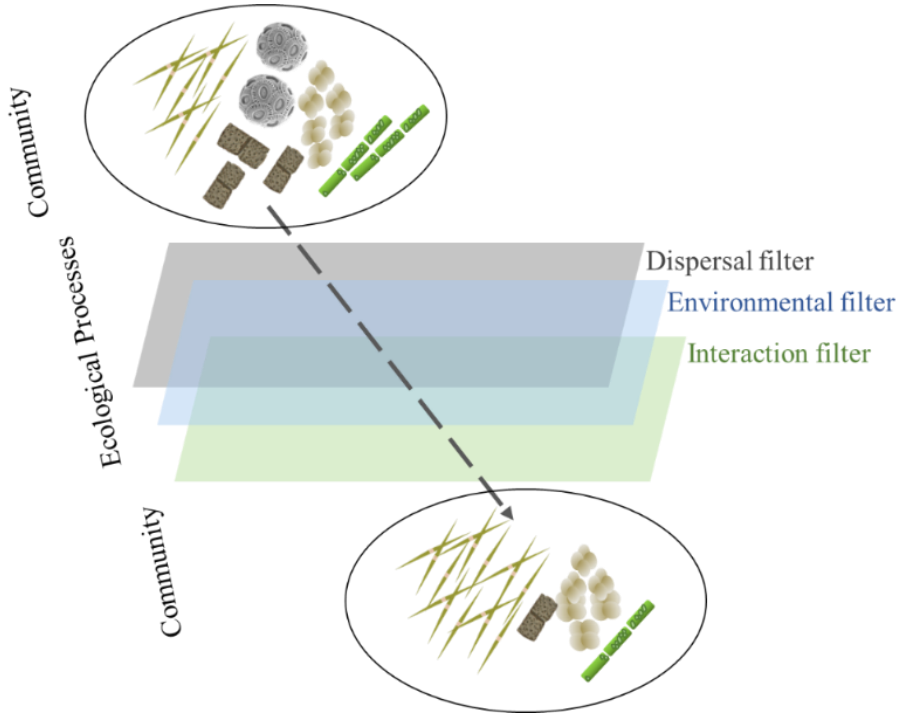

Figure 1.5. *Example of ecological filters (i.e., processes), including dispersal limitation, abiotic and biotic constraints that determine the community composition (modified from Cadotte and Tucker 2017).*

[4] ***Ecological processes****: Community ecologists infer ecological processes of community assembly by considering that any local community is a subset of a regional species pool shaped by biogeographical and historical effects (Weiher et al., 1998; Grime, 2006): species thriving local community have successfully passed a hierarchy of ecological filters, including dispersal limitation, abiotic and biotic constraints (Cadotte and Tucker, 2017; Figure 1.5).*

Table 1.1. *Key terminology in community assembly (Source: Zhou et al., 2017 and references therein; Cadotte and Tucker 2017).*

	Definition
Community assembly	The occurrence and abundance of species in a community. It describes how assemblages interact to determine species composition and local biodiversity of a community.
Species pool	A set of species occurring in a particular region that can potentially inhabit a site because of suitable local conditions.
Historical effects	The effects of the order and timing of past biotic or abiotic events on community assembly
Deterministic processes	Deterministic factors such as species traits, species interactions and environmental conditions that govern community structure
Stochastic processes	Random changes in community structure with respect to species identities and/or functional traits due to stochastic processes of birth, death, colonization, extinction and speciation.
Environmental filtering	The effect of environmental conditions selecting those species capable of survival and reproduction in a given environment.
Drift	Random changes, with respect to species identity, in the relative abundances of different species within a community over time due to inherent stochastic processes of birth, death, and reproduction.
Selection	Niche-based process that shapes community structure due to fitness differences (e.g., survival, growth, and reproduction) among different organisms, including effects of abiotic conditions and biotic interactions.
Dispersal	Movement and successful establishment of a community from one location to another via both active and passive mechanisms.

1.4.1. Environment

Two main complementary views exist regarding the influence of the environment on community assemblages. The first view considers the neutral model of biodiversity developed by Hubbell (2001), which was inspired by MacArthur and Wilson's (1967) theory of island biogeography. In Hubbell's model, all individuals are assumed to have the same prospects for reproduction and death (neutrality). The variability in relative abundances across species is solely due to demographic stochasticity or 'ecological drift'. The neutral theory[5] of biodiversity has been heavily debated, particularly due to its assumption of ecological equivalence. This means that individuals have similar birth, death, speciation and immigration rates, and there are no significant differences in fitness or competitive abilities among species. Therefore, the presence or absence of specie is determined primarily by chance rather that by its specific characteristics or competitive advantages. Although the neutral theory assumes the ecological equivalence of all individuals, it has been able to successfully predict several key ecological patterns in many communities, such as species abundance distributions and species-area

[5] ***Comment on neutrality by science journalist Jhon Whitfield (2002) in Nature News****: 'Vive la différence ? Forget it. La différence est morte. That is the message from the proponents of neutrality, a view of ecology that is anathema to many in the field. Rather than focusing on how differences between species allow them to coexist, neutrality assumes that trees in the rainforest, or corals on a tropical reef, are basically all the same.'*

relationships, even outperforming the niche theory in some cases (Adler *et al.*, 2007; Rosindell *et al.*, 2012).

The second view considers the concept of ecological niche, coined by Hutchinson (1957). Hutchinson's multidimensional niche is an n-dimensional hypervolume, with each dimension corresponding to an environmental variable. This volume represents the range of values of abiotic characteristics within which an organism can survive, grow, and reproduce. For each environmental variable, the range of values within which an organism can survive may vary in size. It defines a tolerance around an optimum. Hutchinson's definition of the niche is based on species coexistence. According to it, the separation of niches between species is governed by the principle of Gause (1934). Gause executed a series of co-culture experiments. He observed that for a number of species pairs, each species grew well in the absence of the other. However, when these species were co-cultured, one species (e.g., *Paramecium aurelia*) dominated and suppressed the other species (e.g., *Paramecium caudatum*). Based on these observations, he formulated the law of competitive exclusion, which states that two species with identical or closely similar ecological requirements cannot coexist indefinitely in the same environment. Consequently, each species cannot occupy the entirety of its fundamental niche (Pulliam, 2000).The realized niche of a species is therefore narrower than its fundamental niche, due to abiotic factors or biotic interactions, which represents the actual niche of a species (Hutchinson, 1957).

Once the concept of the ecological niche was established, it was widely accepted that all organisms across different kingdoms of life are subject to the niche concept (review Colwell and Rangel, 2009). However, Hutchinson observed that in the case of phytoplankton, multiple species were capable of coexisting in the same environment (Hutchinson, 1961). This observation contradicted the principle of competitive exclusion and became known as the "paradox of the plankton". *'The problem that is presented by the phytoplankton is essentially how it is possible for a number of species to coexist in a relatively isotropic or unstructured environment all competing for the same sorts of materials... According to the principle of competitive exclusion, we should expect that one species alone would outcompete all the others so that in a final equilibrium situation the assemblage would reduce to a population of a single species*. Hutchinson proposed the hypothesis that equilibrium in the environment is never reached because the environment (including abiotic and biotic factors) undergoes changes before equilibrium can be achieved. As a result, competitive exclusion never reaches its peak, allowing species to coexist. Several hypotheses have been proposed over the past sixty years

to resolve the paradox of plankton, including trophic exclusion, stochastic processes, genome-size evolution, and implications of asexual reproduction on speciation (Behrenfeld *et al.*, 2021).

Through the lens of community ecology, according to Chesson's theory, coexistence is possible when species have distinct ecological niches and exhibit niche differences (Chesson, 2000). The theory suggests that coexistence is facilitated by two main mechanisms: niche partitioning and species interactions. Niche partitioning refers to the differentiation of species in their resource use or habitat preference, allowing them to coexist by reducing competition for limited resources. Species interactions, such as predation, competition, facilitation, or mutualism, can also contribute to coexistence. These interactions may lead to the stabilization of species abundances, creating conditions for multiple species to persist in the community. Chesson's coexistence theory provides a theoretical framework to understand community assembly and diversity patterns, emphasizing the importance of niche differentiation and species interactions in promoting species coexistence.

1.4.2. Interactions

Interactions are ubiquitous in the living world. There is no species that does not depend on another for its survival. These interactions vary greatly in their effects and can be obligatory, facultative, or opportunistic, occurring either briefly or over longer periods, thus rendering individuals more or less interdependent. Long-lasting interactions are referred to as symbiotic and can have diverse impacts on the partners involved. The following types of interactions are commonly observed: mutualism, predation, parasitism, commensalism, competition, amensalism, and neutralism (Fig. 1.6; Faust and Raes, 2012). In this section I will present the interactions that have been studied or discussed during this thesis.

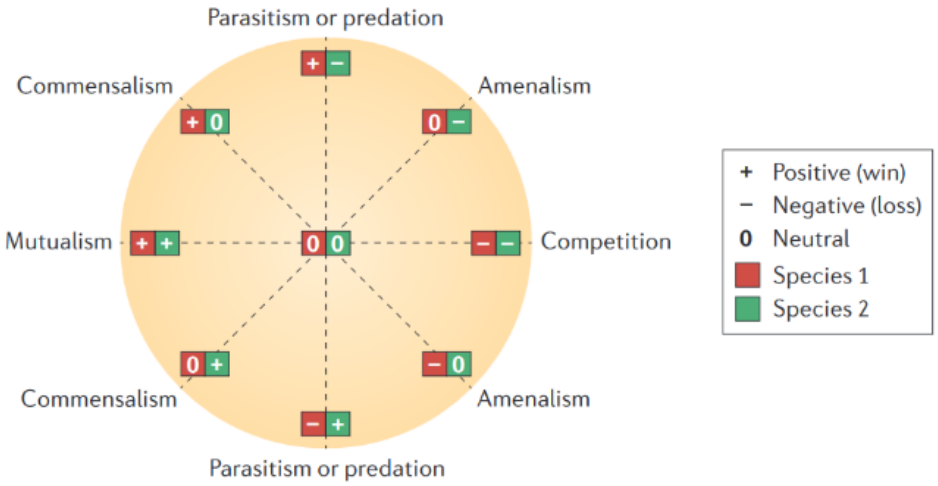

Figure 1.6. *Summary of ecological interactions between members of different species. For each interaction partner there are three possible outcomes: positive (+), negative (-), and neutral (0) (Source: Faust and Raes, 2012).*

Biological interactions are increasingly recognized as a major force modulating microbial community structure and function, in some cases more than abiotic factors (e.g., Genitsaris *et al.*, 2015; Lima-Mendez *et al.*, 2015). Interactions between microorganisms have significant effects on the circulation of energy, nutrient cycling, and transfer efficiency to higher trophic levels (review Worden *et al.*, 2015; Fig. 1.7). Among microbial interactions, predator-prey interactions involve the transfer of carbon from phytoplankton and bacterial biomass to higher trophic levels (Fenchel, 1988; Calbet and Landry, 2004). Heterotrophic and mixotrophic protists are key players in this process. Grazers, through the excretion of organic matter, contribute to the organic matter pool and promote the growth of microorganisms such as bacteria and phytoplankton. This process, known as cross-feeding, facilitates the availability of nutrients and enhances microbial productivity (Morris *et al.*, 2013).

One of the most important interactions in microbial communities concern those of phytoplankton and heterotrophic bacteria, and can span from cooperative to competitive (Seymour *et al.*, 2017). Heterotrophic bacteria primarily consume organic material released by phytoplankton, such as dissolved organic carbon (DOC), which is abundant and easily degradable (Ducklow *et al.*, 2001). They also consume more complex products like polysaccharides, and senescent or dead phytoplankton biomass (Teeling *et al.*, 2012). From the perspective of phytoplankton, bacteria can serve as providers of essential macronutrients through the process of remineralization, where bacteria release previously bound nutrients back into the environment (Azam *et al.*, 1983; Buchan *et al.*, 2014). When external nutrient supply is limited, phytoplankton growth is expected to benefit from bacterial recycling of nitrogen and phosphorus. Moreover, specific interactions between phytoplankton and bacteria can develop

based on bacterial production of vitamins, such as vitamin B12, and enhancement of bioavailability of micronutrients like iron (Amin *et al.*, 2012; Durham *et al.*, 2015). On the other side of the spectrum bacteria can also compete with phytoplankton for inorganic nutrients (Joint *et al.*, 2002), or have a negative effect on phytoplankton growth (Mitchell, 1971; Meyer *et al.*, 2017). For example, algicidal bacteria produce lytic enzymes causing lysis, growth inhibition, and death of phytoplankton (Mayali and Azam, 2004; Meyer *et al.*, 2017). They frequently follow algal blooms of diatoms, coccolithophores and *Phaeocystis spp.*, as well as toxic species belonging to the group of dinoflagellates (Demuez *et al.*, 2015). These findings emphasize the intricate ecological connections between these two groups of microorganisms in aquatic ecosystems.

Another essential but still poorly understood interaction concerns parasitism. Parasitism is a biological relationship between two organisms, in which the parasite benefits from its host (Combes, 1996). Parasitism is an essential mechanism in trophic networks, altering or even controlling the dynamics of host populations. However, such interactions are not stable over time, as the host constantly seeks to escape from the parasite, while the parasite strives to enhance its infection potential and counter the host's defence mechanisms (Thompson, 1988). Parasites have the potential to strongly influence community composition and nutrient cycling in an ecosystem by terminating for instance phytoplankton blooms, or even favouring the growth of species through the infection of its grazers or competitors (Skovgaard and Saiz, 2006; Chambouvet *et al.*, 2008; Velo-Suárez *et al.*, 2013). One of the most abundant sequences in marine protistan diversity surveys belong to Syndiniales, known to be parasitic and to control blooms of dinoflagellates, to infect ciliates and other protists (e.g., Chambouvet *et al.*, 2008; Guillou *et al.*, 2008 and references therein). Yet, current knowledge regarding spatiotemporal structures and host range of Syndiniales is scarce, due to difficulties with microscopic counts and culturing of these organisms (e.g., Sassenhagen *et al.*, 2020).

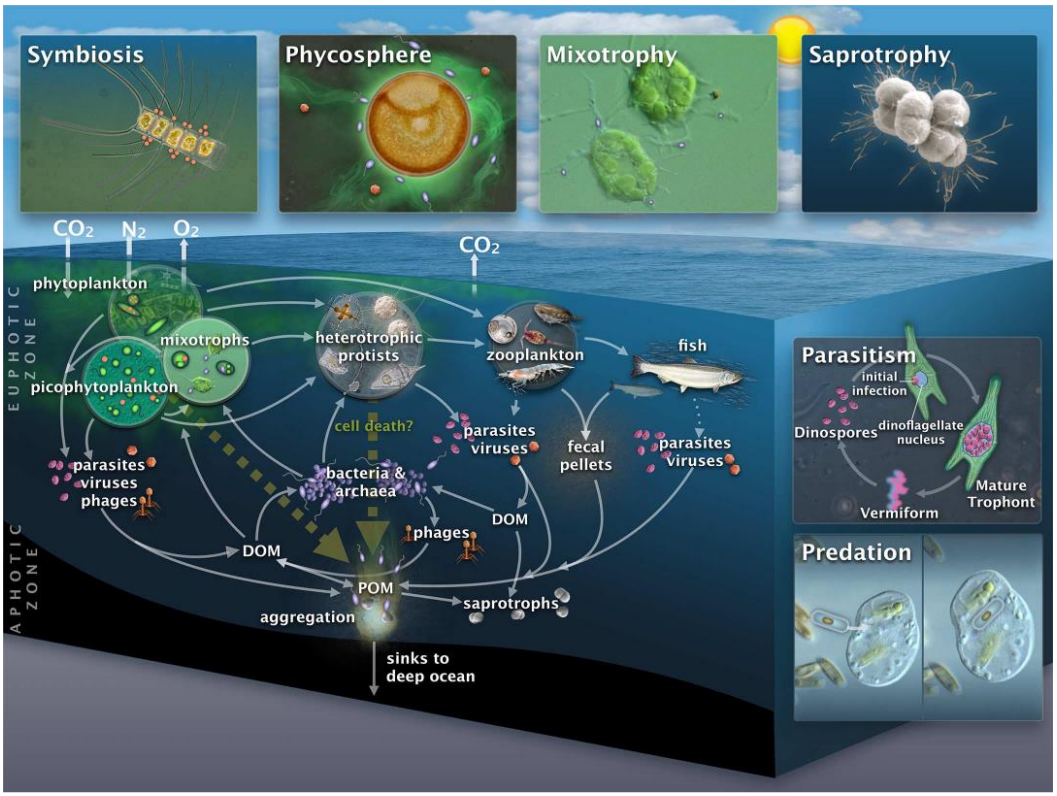

Figure 1.7. *Microbes and their interactions structuring oceanic ecosystems (Source: Worden et al., 2015).*

1.4.3. Dispersal

Dispersal is a major process in ecology and evolution. In community ecology dispersal is referred to the movement and successful establishment of organisms across space (e.g., Vellend, 2010). Several factors influence their successful establishment, including for instance biotic interactions and environmental filtering. Environmental filtering is the effect of environmental conditions selecting those species capable of survival and reproduction in a given environment (Emerson and Gillespie, 2008). Dispersal can be viewed as a deterministic process (i.e., biotic and abiotic conditions under which a species can persist), a stochastic one (i.e., random changes), or both (Lowe and McPeek, 2014; Vellend *et al.*, 2014). For example, if dispersal rates are dependent on the population size, then dispersal is stochastic because it is more probable for more abundant species to disperse than less abundant species. However, dispersal rates could be different among different species, depending on their traits (e.g., spores, dormancy). From this point of view, dispersal is a deterministic process (Zhou and Ning, 2017).

The investigation of microbial dispersal processes has been relatively limited compared to other organisms due to the small size, high abundance, wide distribution, and short generation time of microorganisms (Nemergut *et al.*, 2013). Consequently, our understanding of microbial

dispersal remains incomplete (e.g., Fenchel and Finlay, 2004). A central question in microbial ecology revolves around whether microorganisms are limited in their ability to disperse, which has generated debate within the scientific community. Historically, microorganisms were considered to be everywhere and hence not limited by dispersal capacities (Bass-Becking 1934[6]). However, it is now accepted that microorganisms show strong biogeographic patterns, which is evidence for dispersal limitation (e.g., Hanson *et al.*, 2012; Zhou and Ning, 2017). More importantly, although some microorganisms can propel themselves to a certain degree within a short distance, microbial dispersal is typically considered passive (Nemergut *et al.*, 2013). Since passive dispersal is usually stochastic with respect to species identity, microbial dispersal can be largely viewed as stochastic (Vellend *et al.*, 2014). However, passive dispersal may not always be stochastic. In marine systems the carrying capacity of the physical dispersal vector (e.g., currents, upwelling, eddies) depend on the physical properties of microorganism such as their size and their shape.

Conceptual Synthesis in Community ecology: Vellend's framework

'Community ecology is a mess. The rules are contingent in so many ways…as to make the search for patterns unworkable'

(Lawton 1999:181)

Disentangling the mechanisms that shape communities is a challenge in ecology. There are numerous ecological theories that aim to explain the composition and abundance of species within communities. However, reconciling and unifying these different ecological theories is complicated from both mathematical and conceptual perspectives (Chase, 2005). Vellend (2010) proposed that patterns can be explained by four major processes: speciation, selection, drift, and dispersal. Speciation refers to the generation of new species, selection involves deterministic changes based on the selective value of species, drift encompasses stochastic changes, and dispersal represents the movements of species. By assigning varying levels of importance to these processes, all previously formulated ecological theories can be conceptualized (Vellend, 2010). This classification into four ecological processes has the potential to combine different ecological approaches and contribute to the development of a general framework.

[6] *'**Everything is everywhere, but the environment selects' (Bass-Becking 1934)**: this hypothesis does not strictly rule out patterns caused by geographical effects on ecology and historical founder effects, it does propose that the remarkable dispersal potential of microbes leads to distributions generally shaped by environmental factors rather than geographical distance.*

To study the patterns of living organisms and understand the underlying mechanisms, it is necessary to quantify biodiversity, their properties and to identify their variation. This helps establishing connections with potential driving forces.

1.5. Methods to study planktonic microbes

Methods for studding marine microbes and their environment have progressed greatly, from early approaches based on microscopy that have been used since the first oceanographic expedition '*Challenger'* in 1872, to the present use of advanced methods. These methods aim to a complete understanding of the complex and multiscale processes of the ocean. For example: i) flow cytometry characterises cells according to fluorescence and scattering properties, ii) automated cell imaging techniques allows characterisation of natural state and traits of organisms (e.g., CytoSence[7], FlowCam[8], UVP[9]), iii) remote sensing defines taxonomic composition of phytoplankton in relation to satellite derived chlorophyl-a (Alvain *et al.*, 2005), and iv) exploitation of molecular methods and gene sequencing approaches to characterise diversity. In particular, ocean observation through satellites and autonomous mobile platforms such as floats and gliders have resulted in a considerable increase in the amount of data acquired on the oceanic environment since the early 2000s (e.g., Chai *et al.*, 2020). The use of these new technologies has led to an increase in the spatial, vertical, and temporal coverage of the ocean (3D observations), enabling a finer characterization of biotic and abiotic variability at multiple spatiotemporal scales. The purpose of this section is not to present all the existing methods, but rather to focus on the advantages and limitations of those used in the present thesis (Fig. 1.8). In this thesis classical tools were combined (microscopy and cytometry) that provide data on abundance and biomass, and molecular techniques that provide genetic diversity data.

[7] ***CytoSense*** *(scatter/fluorescence scan) show one-dimensional morphology and optical features of big cells, colonies, chains and filaments. The optional camera makes bright field images of individual particles, hydrodynamically focused along their long axis by low shear acceleration in a sheath.*

[8] ***FlowCam*** *uses a similar imaging principle as the CytoSense (but lacks the hydrodynamic focusing provided by the sheath flow). Images are acquired either continuously or after the detection of a fluorescent (Chl-a) particle.*

[9] ***UVP*** *consists of a camera connected to a red-emitting light unit, which purpose is to illuminate a volume of water sampled by the camera in order to capture particles and organisms.*

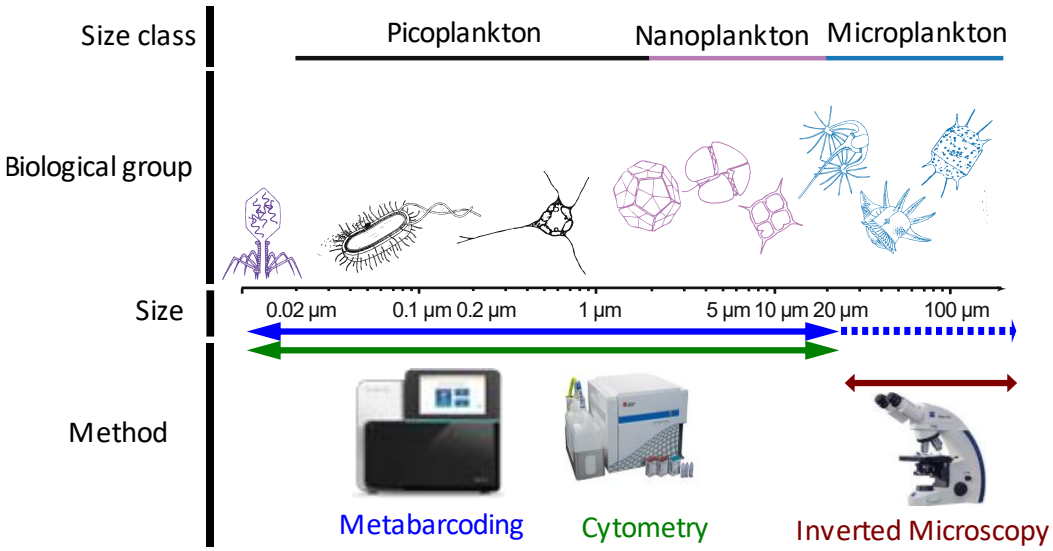

Figure 1.8*. Methods applied to quantify abundance, biomass and diversity of planktonic microbes in this thesis (Modified from* Sunagawa *et al.*, 2020*).*

1.5.1. Inverted Microscopy – Utermöhl method

In 1931 Utermöhl invented a sedimentation method that relies on observation under an inverted optical microscope for identifying and enumerating microplankton. Utermöhl method has barely evolved in almost a century (Fig. 1.9). First, natural samples are fixed (e.g., acid lugol's solution) to maintain the features and organelles of the observed organisms. The samples can be stored in 4 ^{o}C for long periods of time, even for several years. Then, samples are settled in a cylinder with a capacity ranging from 10 to 200 ml depending on cell concentration. After 16 to 48 hours, the sedimented cells are observed using objectives positioned under the inverted microscope stage. Microplankton such as diatoms, dinoflagellates and ciliates are then identified down to the species level when possible, using available documentation for the study areas and counted by scanning all or part of the chamber. Then the abundance (i.e., cells/L) is determined by measuring the counted volume. Through inverted microscopy, it is also possible to calculate microplankton biomass (i.e., µgC/L). For this, the sizes of different species are measured, corresponding to simple geometric forms (e.g., ellipse, cylinder) allowing the calculation of their biovolume (Hillebrand *et al.*, 1999). The biovolume is then converted into carbon content using conversion factors specific to the microplankton group of interest (e.g., Menden-Deuer and Lessard, 2000).

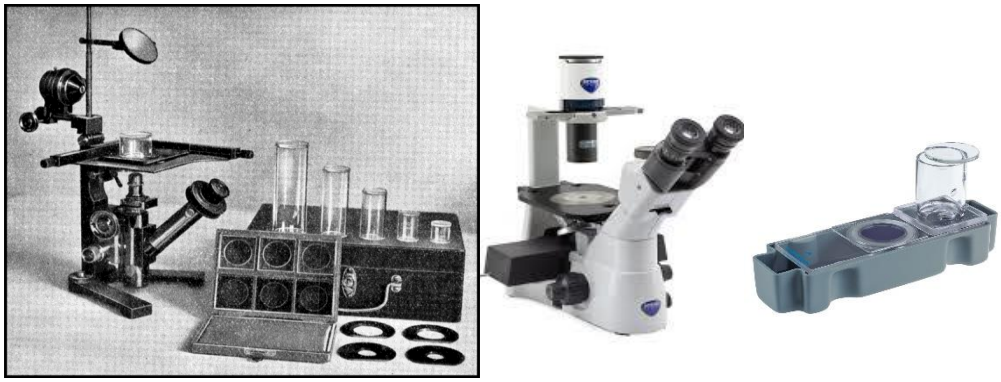

Figure 1.9. *Left: Illustration of Utermöhl method from the original paper in 1931, right: inverted microscope and sedimentation chamber used today.*

Despite the importance of microscopy, this method does have general limitations. Most notably, it is time consuming and depends heavily on the expertise of the observer to discriminate taxa, also including an observer-dependent bias. Taxonomic identification is based on morphological characteristics, and thus can be difficult even for experts to identify cells. For example, nanoplankton is difficult to identify because of their small size and lack of distinctive morphological features. A further complication is that fixation of samples may not work equally for all taxa and thus enumeration may be biased. For example, alkaline or neutral lugol's solution is most appropriate for coccolithophorids rather than acid lugol's solution. Also, improvements are still needed to refine the relationships between biovolumes and biomasses, which differ depending on plankton group, size range and life stage. For example, there is no unified formula for all diatoms to convert their resting spores into carbon biomass based on biovolume (Kuwata *et al.*, 1993; Leblanc *et al.*, 2021).

1.5.2. Flow cytometry

In contrast to microscopy, flow cytometry is a rapid, easy and accurate method for quantification of the abundance of small autotrophic and heterotrophic cells based on their optical properties. Four decades ago, this method adapted from medical tools designed for counting blood cells, to count instead autoflorescent particles (i.e., phytoplankton) present in water, and has proven to be invaluable for the study of picoplankton and nanoplankton in the ocean (e.g., Trask *et al.*, 1982; Chisholm *et al.*, 1988; Amann *et al.*, 1990; Lomas *et al.*, 2011; Sunagawa *et al.*, 2020). A flow cytometer measures and counts cells by hydrodynamically aligning them in sheath fluid, which is a solution that runs through a narrow stream (10 to 20 mm wide). When a cell passes in front of the laser beam, the light of the laser scatters depending on the cell's size and shape. The direction of the scattering, (i.e., Forward Scatter (FSC), Side

Scatter (SSC)) indicates the cell size. In contrast to FSC, SSC is also influenced by the cell surface and internal cellular structure (granularity).

Biomedical uses of flow cytometry usually involve treatment of cells with fluorescent dyes or probes before analysis, but the most common oceanographic applications entail measurement of untreated phytoplankton cells that naturally exhibit fluorescence associated with their photosynthetic pigments. Presence of chlorophyll-a and Phycoerythrin fluorescence allows to discriminate phytoplankton from other particles, and flow cytometric analysis permits enumeration of abundance, quantification of cell properties such as size and pigmentation, and some level of taxonomic, optical and/or sized-based discrimination (e.g., *Prochlorococcus*, *Synechococcus*, picoeukaryotes) (e.g., Olson *et al.*, 1989). Cells without pigments such as virus, bacteria and heterotrophic nanoflagellates (HNF) need to be stained with a fluorochrome for detection by a cytometer. The most common fluorochromes for marine samples are the nucleid acid stains DAPI (4,6-diamidino-2-phenylindole; Porter and Feig, 1980) and SYBR-Green I; (Marie *et al.*, 1999, 2000). Furthermore, staining with fluorochromes, coupled with cytometric analysis, has made possible to study: 1) the life cycle of organisms and the determination of organism growth rates (e.g., Dunker *et al.*, 2018) 2) enzymatic activity by evaluating fluorescence levels after staining (e.g., González-Gil *et al.*, 1998). 3) The use of probes (FISH: Fluorescence in situ hybridization) coupled with flow cytometry allows the study of harmful algae (e.g., *Gyrodinium aureolum*; Vrieling *et al.*, 1996), or they provide in a certain way taxonomic discrimination (e.g., Biegala *et al.*, 2003).

There are some important limitations of conventional flow cytometry. First, flow cytometry does not provide taxonomic discrimination (with exception of cyanobacteria). Even if flow cytometry is combined with molecular probes, this approach remains technically challenging and difficult to apply systematically for characterization of many plankton species (Biegala *et al.*, 2003). Flow cytometry provides much faster analysis of cells than microscopy, but the sample volumes are still small (from tens of μl to a few ml) and relatively few discrete samples can be processed compared with the space and time scales of change in the natural environment. Moreover, flow cytometers are typically optimized so that analysis of small (pico- and nano-sized) plankton is effective, but relatively rare and larger microplankton are missed or poorly characterised.

1.5.3. Metabarcoding

The first sequencing techniques were described in 1977: the Maxam-Gilbert chemical method (Maxam and Gilbert, 1977) and the Sanger enzymatic method (Sanger *et al.*, 1977). The Sanger method, still used today, was quickly preferred over the Maxam-Gilbert method. It has supported considerable progress and allowed the sequencing of the first human genome as part of the Human Genome Project (1998 – 2003; Collins *et al.*, 1998) . However, Sanger sequencing is limited for large genomes and it is costly. New sequencing methods have been developed in the last 20 years, leading to increasingly massive sequencing of living organisms. In 2005, high-throughput sequencing (HTS or NGS: Next Generation Sequencing) was developed. This technology is based on a principle of massive parallel sequencing that allows to determine DNA/RNA sequences for whole genome or specific regions of interest at a much lower cost than traditional Sanger sequencing (review Goodwin *et al.*, 2016).

Among the NGS techniques, the environmental metabarcoding has revolutionized the way scientists assess microbial diversity in natural environments. To study planktonic microbes, DNA is extracted from samples collected in a particular environment. PCR amplification is performed using general primers to target a small fragment of a DNA marker gene, resulting in thousands of sequences per sample. Bioinformatic processing of the sequences obtained from the pool of amplicons makes allows to describe the molecular diversity present in an environmental sample (Fig. 1.10).

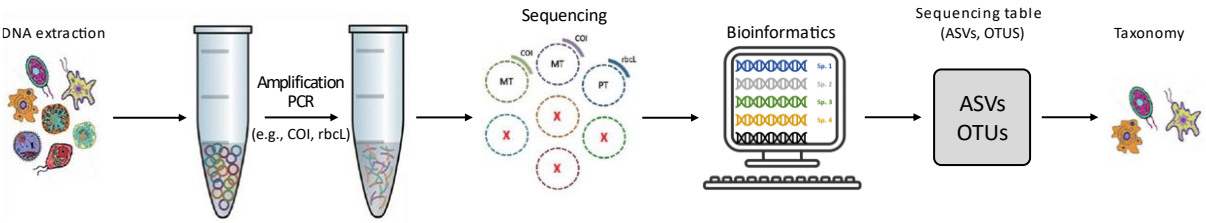

***Figure 1.10**. Overview of the different steps involved in metabarcoding of planktonic communities (Source:* Jo *et al.*, 2019).

Metabarcoding allows the determination of the taxonomy of organisms and the study of their phylogenetic relationships. This method is particularly interesting as it provides diversity data on organisms that cannot be observed by microscopy, that are hard to cultivate, fragile, or rare. Metabarcoding has revealed a previously hidden taxonomic richness, including rare species and parasites (López-García *et al.*, 2001) . As a result, metabarcoding studies have yielded much higher biodiversity estimates compared to traditional microscopy-based methods (Bachy

et al., 2013). Metabarcoding data have evidenced that a quite large proportion of eukaryotic diversity remains unknown (Leray and Knowlton, 2016).

Despite the importance of metabarcoding in microbial ecology, each step of this method is associated with potential biases. These biases can lead to the under- or overestimation of certain taxa. For example, PCR biases lead to problems of i) quantification as some taxa are over amplified (Gong and Marchetti, 2019; Sinclair *et al.*, 2015), and ii) the creation of chimeric sequences. These artificial sequences are made with the fusion of two (or more) sequences, but are by definition lower in abundance than the "parent" sequences and can be identified by software. Taxonomic groups such as dinoflagellates have a high number of gene copies (Wisecaver and Hackett, 2011), resulting in their overrepresentation in molecular data (Potvin and Lovejoy, 2009; Georges *et al.*, 2014; Genitsaris *et al.*, 2016; Christaki *et al.*, 2021; Santi *et al.*, 2021; Caracciolo *et al.*, 2022). Additionally, the number of copies depends on cell size, and larger ones exhibit variations in the number of copies that can differ by several orders of magnitude among taxa (see Figure 1 in Biard *et al.*, 2017), leading to a higher representation of larger organisms in sequencing datasets. As a consequence, metabarcoding data are semi-quantitative, they do not present an accurate image of abundance and biomass (Lamb *et al.*, 2019). Another challenge is the clustering of sequences to ecologically relevant units. Amplicons are clustered into Operational Taxonomic Units (OTUs) to account for intra-species variability. Traditionally, a minimum similarity of 97% was required to consider two rRNA sequences to belong to the same microbial species (Stackebrandt and Goebel, 1994). But the use of an a priori genetic distance threshold to delineate fundamental units of diversity is not always applicable or relevant (Brown *et al.*, 2015) and limits the resolution of diversity analysis by masking important patterns occurring between closely related organisms (Eren *et al.*, 2013). The recent development of new high-resolution methods: i) sequencing error analysis (DADA2[10]; Callahan *et al.*, 2016), ii) information entropy analysis (oligotyping; Eren *et al.*, 2013), iii) error distribution profiles (SWARM; Mahé *et al.*, 2015) constitutes an important advance in microbial diversity analysis. These methods are supposed to provide a more accurate image of the diversity by avoiding artificial similarity thresholds.

Metabarcoding has revolutionized the study of marine microbial diversity on a global scale, (e.g., Massana and Pedrós-Alió, 2008; Massana *et al.*, 2015; De Luca *et al.*, 2021). Despite this

[10] ***DADA2****: It implements a novel algorithm that models the errors introduced during amplicon sequencing, and uses that error model to infer the true sample composition. DADA2 replaces the traditional "OTU-picking" step in amplicon sequencing workflows, producing instead higher-resolution tables of amplicon sequence variants (ASVs).*

progress, a major challenge in microbial ecology remains the identification of microorganisms responsible for specific functions in the environment and understanding the factors that regulate these functions (Madsen, 2005; Gutierrez-Zamora and Manefield, 2010). To assess this challenge, metagenomics and metatranscriptomics have emerged as powerful tools for estimating the function potential (DNA-based) and functional activities (RNA-based) of microbial communities. Unlike metabarcoding, which focuses on a specific genomic region, shotgun metagenomic sequencing enables the sequencing of all genomic DNA present in a sample. This approach provides extended genomic information, allowing both taxonomic identification and functional characterization of the environment (Su *et al.*, 2014). Although these methods are currently used in several microbial studies (e.g., Gilbert and Dupont, 2011; Mineta and Gojobori, 2016; Delmont *et al.*, 2018), their integration into monitoring programs is not yet fully realized because they are more expensive and computationally more complex than metabarcoding.

1.5.4. Fluorescence in situ hybridization (FISH)

Given the above-mentioned biases associated with marker-gene sequencing, it is important to complement it with true quantitative methods. One such technique is fluorescence in situ hybridization (FISH) of ribosomal RNA (rRNA) (Gall and Pardue, 1969). The rRNA of fluorescently labelled groups can be visualized under an epifluorescence microscope, enabling the detection, identification, and enumeration of active microorganisms without the need for culture (Amann *et al.*, 1990; Fig. 1.11). These microorganisms are free in the environment and/or in association with other organisms (e.g., attached or within their hosts for parasites). This technique is based on the use of an oligonucleotide probe coupled with a fluorochrome that will specifically hybridize to a target sequence (conventional FISH). The TSA-FISH (Tyramide Signal Amplification-FISH, also called CARD-FISH; Catalyzed Reported Deposition-FISH), on the other hand, involves a probe coupled to the HRP

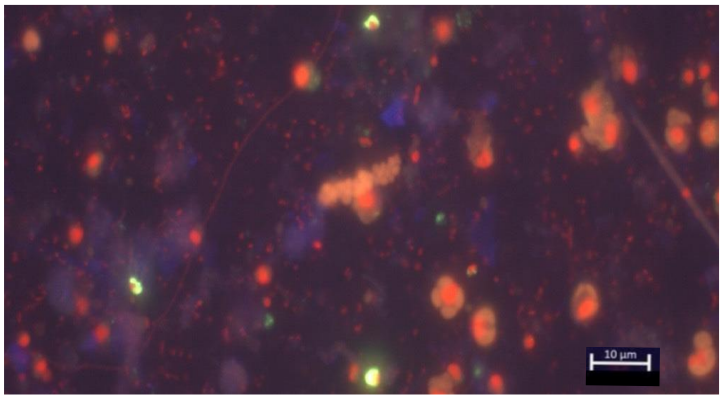

Figure 1.11. *Epifluorescence microscopy of planktonic microbes in the Eastern English Channel. Hybridization with ALV01 probe targeting Syndiniales Group II (planktonic parasites) that cannot be detected by conventional microscopy. Cytoplasm of Syndiniales Group II in green; nucleus in red. Scale bar = 10 µm (Christaki et al., 2023).*

(Horseradish Peroxidase) enzyme and the substrate of this enzyme (tyramide) associated with a fluorochrome (Schönhuber *et al.*, 1997). TSA-FISH allows up to 10 to 20 times more intense signal amplification than with the conventional FISH method. This improved method is therefore essential for environmental samples for which the conventional method does not provide intense enough fluorescent signals. This is the case for pico-sized cells with low rRNA copy numbers. Most probes designed for prokaryotes and eukaryotes target broad taxonomic groups, however some species-specific probes also exist (e.g., Eilers *et al.*, 2000; Simon *et al.*, 2000; Not *et al.*, 2004; Schattenhofer *et al.*, 2009). The TSA-FISH approach also has its inherent limitations: it is time-consuming, few probes are available as of now, and fine taxonomic resolution is very challenging or even impossible to be provided. As the genetic similarity among taxa increases, it becomes difficult to identify unique sequences that can be targeted by probes. This can lead to a higher probability of cross-reactivity, where a probe may bind to unintended targets, resulting in false-positive signals (Kubota, 2013).

To comprehensively understand the composition of planktonic microbes, it is essential to employ a diverse range of complementary techniques that effectively capture their inherent advantages while considering their respective limitations. By adopting a multi-faceted approach, encompassing various methodologies (Table 1.2), we can obtain a holistic representation of the planktonic microbial structure, thereby enabling long-term deployment and sustainable monitoring.

Table 1.2. *Overview of advantages and limitations of traditional and molecular methods, applied in this thesis, to study planktonic microbes.*

Method	Principle	Data Type	Advantages	Limitations
Inverted Microscopy	Morphological identification	Quantitative data	-Functional groups (identification of traits: e.g., colony formation, spores, cysts) -Possible biomass estimation - Reproductible -Low cost	-Time consuming -No characterization of pico- and nanoplankton, parasites -Need expertise in identification - Subject to human observer biases
Flow Cytometry	Laser-based detection of hydrodynamically aligned fluorescent cells	Quantitative data	-Fast -Reproductible -Enumeration of pico- and nanoplankton -Functional groups to a certain extent	- No precise taxonomic identification -No precise biomass data -No microphytoplankton counting -Costly instrument
Metabarcoding	Amplification of a specific region of DNA to identify organisms to species or genus level using databases	Semi-quantitative data: relative abundance of reads (e.g., % ASVs) within a sample	-Fast -Low cost (approx. 25€/sample) -Detailed diversity containing small sized, cryptic organisms, and parasites	-No absolute abundance and biomass -PCR biases -Different amplification rates among species -Different quantitative estimates between sequencers and runs -Different bioinformatic analyses can yield different community composition
FISH (Fluorescence In Situ Hybridization)	Identification of groups of interest using a fluorescent probe matching rRNA	Quantitative data	Ideal for quantification pico- and nanoplankton, parasites	-Difficult to create probes that target specific taxa -Time consuming - Relatively Expensive

1.6. Eastern English Channel

1.6.1. Importance and challenges of coastal ecosystems

Coastal regions comprise various interconnected ecosystems, ranging from estuaries to continental shelves. These areas act as a boundary between the land and the ocean and are affected by both terrestrial inputs and interactions with the open sea. Coastal zones offer a wide range of ecosystem services, which represent the economic benefits that humans gain from natural habitats. These services may account for up to one third of the earth's economic value (Costanza et al., 1997). Coastal ecosystems are some of the most fertilized systems in the world, promoting primary and secondary productivity (Nixon and Buckley, 2002). Even though they only cover 8% of the ocean's surface, they account up to 10 to 30 % in primary production, supporting fisheries (Nixon and Buckley, 2002; Bauer et al., 2013; Cloern et al., 2014). Their position at the interface between the continent and the ocean makes them particularly active areas from a biogeochemical perspective. They play a major role in all biogeochemical cycles including carbon, nitrogen, phosphorus, silicon (Siefert and Plattner, 2004). Their diversity and productivity are also influenced by local hydrodynamism, such as currents (also influenced by wind), and freshwater inflow, which are significant regulators of the onset of spring blooms (Behrenfeld and Boss, 2014). Coastal hydrodynamism also contributes to the development of mesoscale (10 – 200 km) and sub-mesoscale (1-10 km) physical structures, such as frontal zones and eddies. These features have a significant impact on the ecosystem's biology, starting with the microbial compartment (e.g., Casotti et al., 2000).

The major drivers of seasonal succession of plankton in shallow coastal systems are light, temperature, day length and inorganic nutrients (Sverdrup, 1953; Margalef, 1958, 1963)). In coastal temperate zones, seasonality results in major phytoplankton bloom in spring-summer and/or a second one in autumn. The spring phytoplankton bloom is usually dominated by phytoplankton of large size, such as diatoms (Fenchel, 1988). Blooms are an important, widespread natural phenomenon in coastal ecosystems, supporting food webs with key roles in ecosystem functioning (Behrenfeld and Boss, 2014 and references therein). These periodic bursts in biomass are ecological hotspots, and the life cycles of many grazers are evolutionarily tuned to the timing and location of these major events notably in coastal areas (Longhurst, 2007). Large diatoms typically dominate phytoplankton spring blooms due to their high ability to use winter nutrient stocks and increasing irradiance (e.g., Chan, 1980). In these ecosystems, heterotrophic protists are dominated by ciliates and dinoflagellates and they may consume up

to 57% of primary production (e.g., Calbet and Landry, 2004). The end of the diatom bloom in late spring coincides with decreasing nutrient levels and is followed by a drastic shift in phytoplankton composition towards pico- and nanophytoplankton and motile microphytoplankton cells (i.e., flagellates and dinoflagellates) which prevail during summer. This generally fuels the microbial loop[11] and short-circuits the classical herbivorous food chain (e.g., Azam *et al.*, 1983; Sherr and Sherr, 1994), thus profoundly affecting the food-web structure.

Despite their importance, coastal environments have become fragile due to growing anthropogenic pressures in recent decades (Cloern *et al.*, 2014; Newton *et al.*, 2020). Various pollutants, including nutrients, hydrocarbons, metals, and plastics are impacting coastal areas (Cloern *et al.*, 2014; Newton *et al.*, 2020). One of the most significant threats to coastal systems is eutrophication, caused by excessive nutrient loading from rivers. The intensification of agricultural practices, urbanization, and industrialization in coastal zones has led to a significant increase in nutrient inputs over the years (e.g., Grizzetti *et al.*, 2012). In fact, since the 1980s, there has been a global rise in the relative nitrogen to phosphorus content of major riverine inputs to coastal zones, linked to an increased use of nitrogen fertilizers and improved phosphorus removal from wastewater during re-oligotrophication efforts (Turner *et al.*, 2003; Grizzetti *et al.*, 2012; Glibert *et al.*, 2014). This has resulted in a strong nitrogen to phosphorus imbalance in the inputs of most rivers, which affects coastal waters (Grizzetti *et al.*, 2012; Burson *et al.*, 2016). These disturbances affect the functioning of coastal systems, leading to increased phytoplankton production, changes in species composition, shifts in bloom intensities and duration, and sometimes the proliferation of toxic algae, leading to mortality events of several species (Cadée and Hegeman, 2002; Philippart *et al.*, 2000; Lancelot *et al.*, 1987; Anderson *et al.*, 2002).

Phytoplankton blooms are particularly frequent and intense in coastal ecosystems across the globe. A recent study using daily satellite data evidenced a relationship between blooms and ocean circulation, and identified the stimulatory effects of increasing temperature (Dai et

[11] ***The microbial loop*** *describes a trophic pathway in the marine microbial food web where dissolved organic carbon (DOC) is returned to higher trophic levels via its incorporation into bacterial biomass, and then coupled with the classic food chain formed by phytoplankton-zooplankton-nekton. The term microbial loop was coined by Azam et al., 1983 to include the role played by bacteria in the carbon and nutrient cycles of the marine environment*

al., 2023). Due to the importance of coastal ecosystems and the influence of human activities, microbial surveys have been established worldwide.

The oldest and the most geographically extensive monitoring program in the world is the Continuous Plankton Recorder (CPR). It started in 1931 and is operated until today by the Marine Biological Association, based in Plymouth, UK. Commercial ships or other ships-of-opportunity tow the CPR along their regular routes in near-surface waters (e.g., Batten *et al.*, 2003). The CPR filters plankton from seawater using a mesh with nominal size of 270 μm, and thus targets only zooplankton and some phytoplankton (although because of the silk wave it may captures phytoplankton down to 10 μm; Richardson *et al.*, 2006). In France, national microbial surveys have been investigating coastal regions for the past four decades. Their primary goal is to examine the relationships between anthropogenic activities and the functioning of the ecosystem. To achieve this, laboratories associated with IFREMER, CNRS, and Universities are conducting diverse microbial surveys, including (Table 1.3):

1) REMI, (Réseau de contrôle microbiologique des zones de production conchylicoles ; microbial survey of shellfish production areas),

2) REPHY (Réseau d'Observation et de surveillance du Phytoplancton et de l'HYdrologie dans les eaux littorales ; phytoplankton and phycotoxin survey),

3) SOMLIT (Service d'Observation du Milieu LITtoral),

4) PHYTOBS (Réseau d'observation du phytoplancton), and

5) ROME (Réseau d'Observatoires pour la recherche en Microbiologie Environnementale intégrée)

Several parameters acquired in these surveys contribute to the evaluation of ecological status of the marine environment across Europe according to the frameworks Marine Strategy Framework Directive (MSFD 2008/56/EC) and Water Framework Directive (2000/60/EC).

Table 1.3. *French national microbial surveys across coastal ecosystems.*

Surveys	Creation	Institute	Objectives	Stations	Frequency	Depth	Methods
REMI	1989	IFREMER	Enumeration of *E. coli* in live shellfish	363	Monthly or bimonthly	Surface	Most probable number (MPN)
REPHY	1984	IFREMER	-Monitoring biomass, abundance and composition of phytoplankton in coastal and lagoon waters, as well as the associated hydrological parameters	300	Monthly or bimonthly	Surface	-Hydrological parameters - Microscopy
SOMLIT	1995	CNRS	- Characterise the evolution of coastal and littoral ecosystems - Determine the climatic and anthropogenic forces	20	Biweekly	From surface to bottom	- Hydrological parameters - Microscopy - Cytometry
PHYTOBS	1987	CNRS, IFREMER, Universities	-Study the responses of microphytoplankton diversity in response to climate change - Asses the quality of the coastal environment through indicators -Define ecological niches, -Detect variations in bloom phenology	25	Biweekly	Surface	-Hydrological parameters - Microscopy
ROME	2020	IFREMER	Study the spatio-temporal dynamics of virus, bacteria, and microalgae communities, as well as potentially emerging toxic and pathogenic species along coasts	4	-Biweekly seawater sampling -Monthly microbial shellfish sampling	ND	Environmental DNA (eDNA)

1.6.2. Hydrological characteristics of the EEC

The English Channel (EC) is a shallow epicontinental sea, with a maximum depth of 175 m, situated on the continental shelf of the Northeast Atlantic and between the south coast of England and the northern coast of France (Tappin and Reid, 2000). The EC is divided into two distinct basins in terms of oceanographic characteristics, the western English Channel (WEC) and the Eastern English Channel (EEC) (Dauvin, 2012; Fig. 1.12).

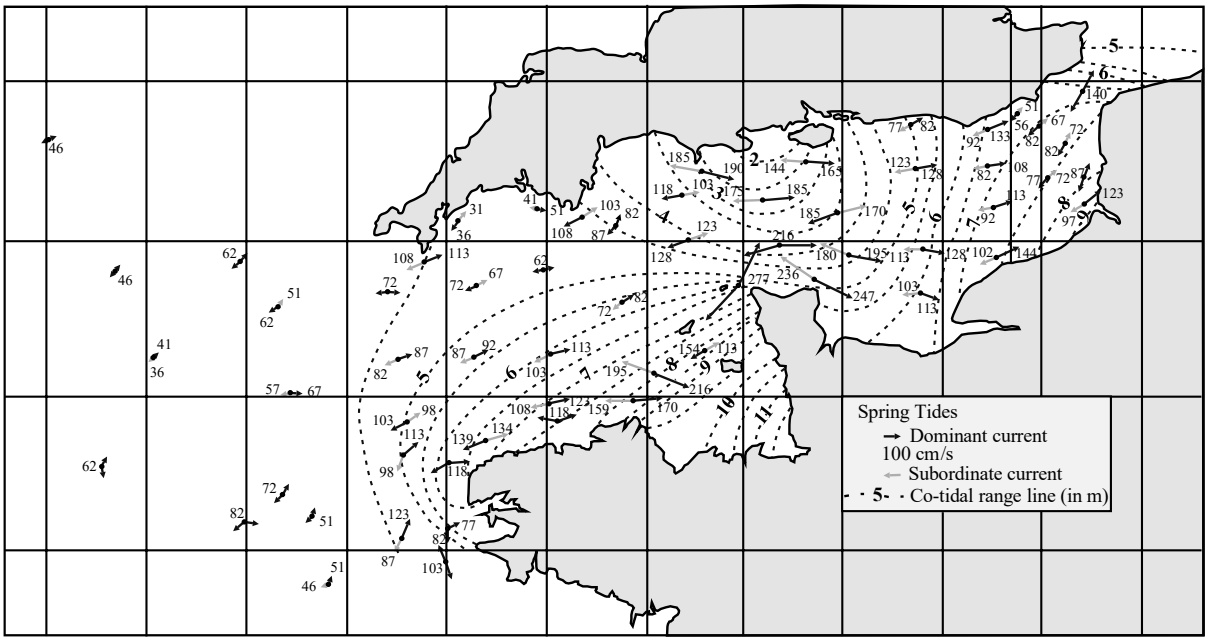

Figure 1.12. *Surface currents in the English Channel (Source: Reynaud et al., 2003).*

The EEC stretches from the Strait of Dover to the Cap de la Hague. It is characterised by a mega-tidal regime with semidiurnal tides (i.e., two high and low tides per day). The tidal range in the EEC varies between 3 and 9 meters, during neap-tides and spring-tides, respectively. The tide currents flow parallel to the coast, with northward flood streams during high tides and southward ebb streams during low tides. The residual circulation parallel to the coast generates a permanent water mass, which is continuously maintained by the riverine inputs, originating from the local rivers, such as Somme, Authie, and Canche, as well as the Bay of Seine. As a result, near-shore waters are less salty and more turbid compared to the open sea, and they are separated the offshore waters by a frontal area called the coastal flow or 'fleuve côtier' (Brylinski *et al.*, 1991; Lagadeuc *et al.*, 1997; Sentchev *et al.*, 2006). The coastal flow spans from 3 to 5 miles and is characterised by phytoplankton richness and significant pollution. It drifts northward due to residual circulation, dominant south-west winds, and the narrowing of the Channel in the Dover Strait (Brylinski et al., 1991; Fig. 1.13). This coastal flow acts as a

transition zone for material fluxes from the WEC to the North Sea, transferring dissolved and particulate material towards the North Sea ; Velegrakis *et al.*, 1999).

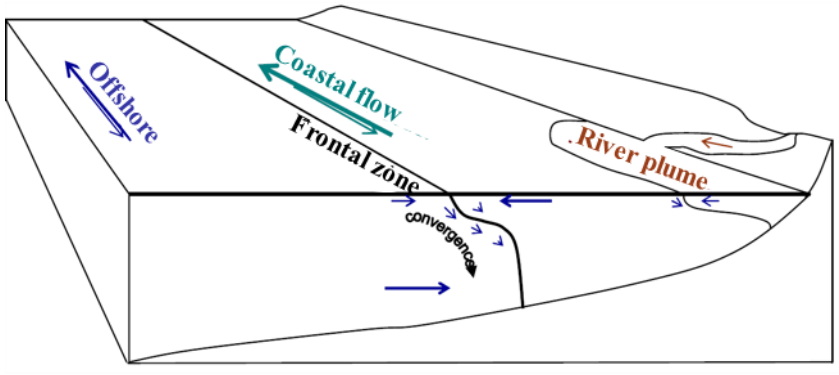

Figure 1.13. *Illustration of the coastal flow 'fleuve côtier' and the frontal zone in the Eastern English Channel (Source: Brylinski et al., 1991).*

The meteorological conditions of the EEC and especially temperature, irradiance, winds, and precipitation, exhibit cyclic changes throughout the year and cause spatiotemporal variability of the physicochemical properties of water masses. Warmer water masses are observed in summer than in winter due to increased irradiance that warms the first few meters of the water column. The shallow depth and strong tidal current (1.0 to 2.5 m s^{-1}) generate constant mixing of the water column preventing the formation of a seasonal thermocline (Gentilhomme and Lizon, 1997).

1.6.3. Planktonic microbes in the EEC

The EEC is characterised by strong repeating patterns in phytoplankton succession, including the annual spring nontoxic blooms of the haptophyte *Phaeocystis globosa* that can represent up to 90% of the phytoplankton biomass (e.g., Schapira *et al.*, 2008; Grattepanche *et al*., 2011a; b, Breton et al., 2017).

Phaeocystis is widely distributed in a variety of marine habitats around the world. It presents a polymorphic life cycle exhibiting phase alteration between colonies and two types of cells: flagellates and non-flagellates (colonial) (Rousseau *et al.*, 2007). Three out of the six *Phaeocystis* species are associated with bloom events in nitrogen-rich areas. (Reviewed in Schoemann *et al.*, 2005). For example, *Phaeocystis globosa* forms big gelatinous colonies reaching several millimeters, consisting of thousands of cells embedded in a polysaccharidic matrix, in coastal and offshore waters (Schoemann *et al*., 2005). *Phaeocystis* is exceptional because of its unique physiology, which impacts food-web structures, global biogeochemical cycles and climate regulation (e.g., Lancelot *et al*., 1995). Furthermore, it is of particular

interest due to its production of dimethylsulfoniopropionate (DMSP) (Liss *et al*. 1994) and also its massive release of organic matter during the decline of the bloom (van Boekel *et al.*, 1992). This latter phenomenon often results in foam accumulation on the coast (Lancelot 1995, Hubas et al. 2007). The foam formation occurs under specific windy conditions and the amount of foam is dependent on wind speed and direction (Lancelot, 1995). While *Phaeocystis globosa* blooms are not toxic, foam accumulation may result in anoxic conditions impacting marine ecosystems significantly (Spilmont *et al.*, 2009).

For the past two decades extensive research has been demonstrating the major drivers defining *Phaeocystis globosa* blooms in the EEC (Breton *et al.*, 1999, 2006; Seuront *et al.*, 2006; Spilmont *et al.*, 2009; Grattepanche *et al.*, 2011, 2011; Lefebvre *et al.*, 2011; Monchy *et al.*, 2012; Christaki *et al.*, 2014; Genitsaris *et al.*, 2015, 2015, 2016; Breton *et al.*, 2017; Rachik *et al.*, 2018; Breton *et al.*, 2021, 2022). The depletion of silicates, a nutrient used only by diatoms triggers colony formation and bloom of *Phaeocystis* in the laboratory, but abundant nitrogen and silicate depletion are not the only reasons for *Phaeocystis* proliferation. The need for sufficient irradiance has been considered to be higher than those of diatoms for maximum growth, and thus could result in *Phaeocystis globosa* blooms (Peperzak *et al.*, 1998). *Phaeocystis globosa* has also a strong protection against grazing by forming colonies and may further benefit from the increased grazing of mesozooplankton on the microzooplankton, potential predators of *Phaeocystis* (Nejstgaard *et al.*, 2007; Grattepanche *et al.*, 2011a,b; Fig. 1.14). Furthermore, the re-oligotrophication and reduction in river inputs observed along the coast over the past decade have promoted the blooms of *Phaeocystis globosa* by exacerbating the imbalance between nitrates and phosphates (Breton *et al.*, 2022).

Figure 1.14. *Schematic illustration of microbial food web during Phaeocystis globosa bloom. In the Eastern English Channel, heterotrophic protists, particularly large heterotrophic dinoflagellates, are the main predators of diatoms and the only consumers of small Phaeocystis globosa colonies (Modified from Grattepanche 2011 thesis).*

Microscopic observations and metabarcoding have shown that besides the intense bloom of *Phaeocystis globosa*, other plankton microorganisms including diatoms, dinoflagellates, bacteria and eukaryotic parasites prevail, and some of them present blooms or increases in the EEC (e.g., Breton et al., 2000; Schapira *et al*., 2008; Lamy *et al.*, 2009; Grattepanche et al., 2011a, b; Hernández-Fariñas *et al*., 2014; Genitsaris *et al*., 2015; 2016; Christaki *et al.*, 2017). The structure and seasonal succession of microbial communities have been studied using sequencing approaches (e.g., Christaki *et al.*, 2014; Genitsaris *et al.*, 2015, 2016). Genitsaris *et al*. (2015) stated that biotic interactions appeared to be the main factor governing the structure and temporal succession of protist communities. Another sequencing study revealed a highly diverse community of eukaryotic endosymbionts, parasites, and organic matter degraders (Christaki *et al.*, 2017). The dominant members of this community are the Syndianiales Group II a phylogenetically related group to dinoflagellates (Lopez-García *et al*., 2001). However, massive sequencing techniques such as High Throughput Sequencing (HTS) only provide a semi-quantitative estimation of a taxon, not its absolute abundance. In the case of endosymbionts, HTS cannot determine their hosts and therefore their role. On the other hand, microscopic observations focusing on phytoplankton using trait-based approaches have shown that phytoplankton are regulated through competition-defence trade-offs (Breton *et al*., 2021).

However, little is known regarding the mechanisms regulating 'blooming taxa', as the previously referred studies were particularly focused on *P. globosa* blooms. In this thesis the term 'blooming taxa' includes the planktonic microorganisms that bloom or present relatively important increases.

1.7. Thesis Objectives

The aim of this thesis was to investigate the seasonal organization mechanisms of microbial communities in the Eastern English Channel. In particular this thesis looked into ecological processes through a community ecology approach, and interactions (i.e., between heterotrophic bacteria and phytoplankton, and dinoflagellates and Syndiniales Group II)

This work was supported by the State-Region Contract Plan (CPER) 'Hauts-de-France' MARCO (Recherche Marine et Littorale en Côte d'Opale – 2014-2020; https://marco.univ-littoral.fr/) under the work package 2.3: 'Taxonomic and functional diversity of procaryotes, protists and planktonic metazoans'. The objective of the work package 2.3, was to enhance our knowledge of the biological processes carried out by small planktonic organisms (viruses, prokaryotes, photosynthetic and heterotrophic protists and zooplankton) that constitute the basis of marine food webs, using both conventional and molecular methods. The preliminary results of the work package 2.3, which inspired this thesis, showed that several planktonic taxa marked the ecological succession with momentary proliferations or peaks, especially after the wane of *P. globosa bloom*. These organisms belonged to different phylogenetic groups such as bacteria, protists, potentially toxic phytoplankton and eukaryotic parasites, all of which have in common their small size and rapid growth rate. While microbial surveys usually collect samples every 2 weeks (Table 1.3). Two different frequencies were conducted to better capture the temporal changes of planktonic communities (bi-weekly during 2016–2020 and at a higher frequency during 2018–2020).

For this, 322 samples were gathered at 5 neighbouring coastal stations across 15 km. The coastal and offshore stations south of Boulogne-sur-Mer on the frame of the National Observation Service (SNO) 'SOMLIT', as well as three stations of the local monitoring transect called 'DYPHYRAD' (DYnamique PHYtoplanctonique le long de la RADiale), from 2016 to 2020.

- **Chapter 2 aimed to investigate the ecological processes regulating phytoplankton assemblages in the coastal waters of the Eastern English Channel.**

i) Which phytoplankton taxa bloom or show increases in the EEC?

ii) Do stochastic and/or deterministic processes regulate the seasonal succession of phytoplankton?

Skouroliakou, D-I., Irion S., Breton E., Artigas F-L., Christaki U., (2022), Stochastic and deterministic processes regulate phytoplankton assemblages in a temperate coastal ecosystem, *Microbiology Spectrum*, https://doi.org/10.1128/spectrum.02427-22

- **Chapter 3 aimed to describe heterotrophic bacterial dynamics and identify putative interactions during *Phaeocystis globosa* and transient diatoms blooms.**

i) Do heterotrophic bacteria present seasonal patterns?

ii) Does heterotrophic bacteria composition vary between different blooming events?

iii) Are there any taxon-specific relationships between phytoplankton and heterotrophic bacteria?

To be submitted in Environmental Microbiology.

- **Chapter 4 aimed to investigate interannual dynamics, diversity and identify potential hosts of Syndiniales Group II.**

i) Do Syndiniales Group II have seasonal patterns and do they relate to dinoflagellate dynamics?

ii) Do stochastic and/or deterministic ecological assembly processes prevail in the Syndiniales Group II community assembly?

iii) Is sequencing an accurate method to infer dinospore abundances?

Christaki U*, **Skouroliakou D-I***, Jardillier, (2023), Interannual dynamics of putative parasites (Syndiniales Group II) in a coastal ecosystem, *Environmental Microbiology*, DOI: https://doi.org/10.1111/1462-2920.16358, **the first two authors contributed equally*

The last chapter (**Chapter 5**) consists of a general discussion of the results obtained, the conclusions, as well as the perspectives that will be developed.

Chapter 2: Phytoplankton community assembly processes in a temperate coastal ecosystem

Preamble

While ecological deterministic processes are conducive to modeling, stochastic ones are far less predictable. Understanding the overall assembly processes of phytoplankton is critical in tracking and predicting future changes. The novelty of this study is that it addresses for the first time, and on a pluri-annual scale, a long-posed question: Is seasonal phytoplankton succession influenced by deterministic processes (e.g., abiotic environment) or by stochastic ones (e.g., dispersal, or ecological drift). Our results provided strong support for a seasonal and repeating pattern with stochastic processes (drift) prevailing during most of the year, and in particular, during the periods that presented monospecific phytoplankton peaks.

Stochastic and deterministic processes regulate phytoplankton assemblages in a temperate coastal ecosystem

Dimitra-Ioli Skouroliakou[1] *, Elsa Breton[1], Solène Irion[1], Luis Felipe Artigas[1], and Urania Christaki[1]

[1] Univ. Littoral Côte d'Opale, CNRS, Univ. Lille, UMR 8187 LOG, Wimereux, France

Keywords: community assembly, phytoplankton, seasonality, ecological processes

This chapter has been published in the Microbiology Spectrum Journal

DOI : https://doi.org/10.1128/spectrum.02427-22

Résumé en Français

Dans cette étude, nous avons émis l'hypothèse que les processus écologiques déterministes et stochastiques régulant le phytoplancton présentent des schémas saisonniers et répétitifs. Cette hypothèse a été explorée lors d'une étude de 5 ans (287 échantillons) menée à petite échelle spatiale (~15km). Les données de microscopie, cytométrie et de séquençage (metabarcoding) ont permis une évaluation approfondie de la diversité et l'exploration des processus écologiques régulant le phytoplancton, à l'aide d'une analyse de '*null modelling*' (modèle nul). Le renouvellement temporel de la communauté (diversité bêta) a mis en évidence un schéma inter-annuel cohérent qui a déterminé la structure saisonnière du phytoplancton. En hiver et au début du printemps le déterminisme (sélection homogène) était le processus majeur dans l'assemblage de la communauté phytoplanctonique (moyenne globale de 38 %). Des processus stochastiques (*ecological drift*, dérive écologique) ont prévalu pendant le reste de l'année (moyenne globale de 55 %) avec des valeurs maximales enregistrées à la fin du printemps et en été, qui présentaient souvent des pics phytoplanctoniques monospécifiques transitoires. Nous avons ainsi montré que globalement, la prévalence des processus stochastiques rend à priori moins prévisible la dynamique saisonnière des communautés phytoplanctoniques face aux changements environnementaux futurs**.**

Abstract

Assessing the relative contributions of the interacting deterministic and stochastic ecological processes for phytoplankton community assembly is crucial in understanding and predicting community organization and succession at different temporal and spatial scales. In this study, we hypothesized that deterministic and stochastic ecological processes regulating phytoplankton, present seasonal and repeating patterns. This hypothesis was explored during a

five-year survey (287 samples) conducted at a small spatial scale (~15km) in a temperate coastal ecosystem (eastern English Channel). Microscopy and flow-cytometry quantified phytoplankton abundance and biomass, while metabarcoding data allowed an extended evaluation of diversity and the exploration of the ecological processes regulating phytoplankton, using null model analysis. Alpha diversity of phytoplankton was governed by the effect of environmental conditions (environmental filtering). Temporal community turnover (beta diversity) evidenced a consistent inter-annual pattern that determined the phytoplankton seasonal structure. In winter and early spring (from January to March), determinism (homogeneous selection) was the major process in the phytoplankton community assembly (overall mean of the year was 38%). Stochastic processes (ecological drift) prevailed during the rest of the year (from April to December, overall mean for the year was 55%) with maximum values recorded in late spring and summer, which often presented recurrent and transient monospecific phytoplankton peaks. Overall, the prevalence of stochastic processes renders, *a priori* less predictable the seasonal dynamics of phytoplankton communities to future environmental change.

2.1. Introduction

Understanding the mechanisms that shape species' community structure is a central topic in ecology (e.g., Connor and Simberloff, 1979; Chesson, 2000; Hubbell, 2001). 'Niche theory' hypothesises that species coexist due to their intraspecific and interspecific interactions, and changing environmental conditions (Hutchinson, 1957). On the contrary, 'neutral theory' assumes that all species are ecologically functionally equivalent, and species coexist due to random changes in the community structure because of stochastic processes of birth, death, colonisation, extinction, and speciation (Chase and Myers, 2011). Given these two theories, Chesson recognised that both niche and neutral processes act concomitantly in structuring communities. In line with these perspectives, Vellend's conceptual framework grouped four major ecological processes that drive species composition and diversity: selection, dispersal, speciation, and ecological drift. Selection refers to deterministic fitness differences between individuals of the same or different species, including environmental filtering and interactions among species (competition, predation, and facilitation); dispersal is the movement of species across space; speciation is the generation of new genetic variation; and ecological drift represents random changes in species' relative abundance over time due to the inherent stochastic processes.

Assessing the relative importance of these processes has recently attracted the attention of microbial ecologists mostly in soil and freshwater environments by using concepts developed in terrestrial ecology (e.g., Stegen *et al.*, 2012; Wang *et al.*, 2013; Liu *et al.*, 2017; Wu *et al.*, 2018; Aguilar and Sommaruga, 2020). These studies revealed the concomitant action of deterministic and stochastic processes in shaping communities. Deterministic processes are related to environmental conditions such as nutrient availability (Liu *et al.*, 2017), species traits or interactions (Zhou and Ning, 2017; and references therein), while stochastic processes that include inherent randomness are less predictable and they are related to dispersal mechanisms, drift, and speciation (Vellend, 2010). The majority of literature developing ecological theories (such as, Hubbel's, 2001) and the respective methodology derive from terrestrial ecology.

Historically, phytoplankton assemblages have been studied from a deterministic perspective based on their traits (e.g., Tilman *et al.*, 1982; Violle *et al.*, 2007), and their environment (Longobardi *et al.*, 2022). However, deterministic processes in structuring phytoplankton communities (Litchman and Klausmeier, 2008) are insufficient to explain overall community structure and diversity patterns (Behrenfeld *et al.*, 2021). Marine phytoplankton studies have been partly focused on stochastic (e.g., Chust *et al.*, 2013) or dispersal processes (e.g., Spatharis *et al.*, 2019). Yet, there is a need to understand how deterministic and stochastic processes potentially change in one ecosystem at different time scales (Jia *et al.*, 2018; Aguilar and Sommaruga, 2020). Two existing phytoplankton studies have quantified the relative contribution of both deterministic and stochastic processes focused on large spatial scale (Xu *et al.*, 2022) or short time periods (less than a year; Ramond *et al.*, 2021). However, the present study is the first one to quantify both deterministic and stochastic phytoplankton assembly processes at a seasonal scale over a pluri-annual sampling period.

Given the annual emergence of *P. globosa* blooms and the high seasonal turnover in environmental conditions and phytoplankton, the eastern English Channel is a very suitable natural ecosystem to explore these ecological processes. It is a constantly mixed meso-eutrophic epicontinental sea, which has been undergoing anthropogenic disturbances since the last century (McLean *et al.*, 2019). The nitrate enrichment with parallel silicate depletion in late winter promotes annual spring blooms of the Haptophyte *Phaeocystis globosa* (Egge and Aksnes, 1992; Breton *et al.*, 2006). Yet, after the wane of the *P. globosa* bloom, the seasonal succession is also marked by the increase in abundance and biomass of other planktonic taxa, such as heterotrophic bacteria, reaching high abundances (Lamy *et al.*, 2009), peaks of parasitic

Syndiniales (Christaki *et al.*, 2017), diatoms (Breton *et al.*, 2017), and dinoflagellates (Gómez and Souissi, 2007, 2008).

Previous studies investigating drivers structuring planktonic communities in the eastern English Channel focused only on deterministic processes such as inter-taxa relations (Genitsaris *et al.*, 2016), environmental filtering (Breton *et al.*, 2021), and predation (Grattepanche, Breton, *et al.*, 2011). The present study aimed to explore the stochastic and deterministic ecological processes driving the seasonal organisation of phytoplankton assemblages, and how these processes varied across seasons. We hypothesized that deterministic and stochastic ecological processes regulating phytoplankton, present seasonal and repeating patterns. For this, first, the seasonal diversity patterns combining morphological (i.e., counts by microscopy and flow cytometry) and metabarcoding (18S rDNA amplicon sequencing) data of phytoplankton obtained at five neighboring coastal stations in the eastern English Channel from 2016 to 2020 were investigated. Second, the phylogenetic structure (alpha diversity) and the phylogenetic turnover (beta diversity) in metabarcoding data using null models according to (Stegen *et al.*, 2012, 2013) were explored. Then finally, considering the theoretical framework of Vellend, the relative importance of stochastic and deterministic ecological processes across seasons was quantified.

2.2. Material and Methods

2.2.1. Sampling strategy

Subsurface seawater (2 m depth) of five coastal stations along a ca. 15 km transect was sampled from March 2016 to October 2020 in the eastern English Channel (Figure S2.1). During, the first two years, the S1 inshore station and the S2 offshore station of the SOMLIT monitoring network (https://www.somlit.fr/) were sampled on a bi-weekly basis. From 2018 to 2020 three stations were added: the coastal stations R1, R2 and the offshore station R4 from the local monitory transect DYPHYRAD. The sampling was carried out weekly and more intensively for some periods between 2018 and 2020. A total of 322 samples were gathered during 169 sampling campaigns at these five stations.

2.2.2. Environmental variables

Sea surface temperature (T, °C) and salinity (S, PSU) were measured in situ with a CTD Seabird profiler. The average subsurface daily PAR experienced by phytoplankton in the water column for six days before sampling was obtained from global solar radiation (GSR, Wh m^{-2}) as described in Breton *et al.*, (2021). Wind stress (Pa) was calculated as described in Smith (1988). In addition, seawater macronutrients concentration were analysed according to Aminot

and Kérouel (2004). Chlorophyll-a (Chl-a) concentration was measured by fluorometry as described in (Lorenzen, 1966). Additional details on environmental data acquisition and sample analysis can be found at https://www.somlit.fr/en/ and in supplementary information.

2.2.3. Phytoplankton microscopic and cytometric counts (morphological data)

For diatoms and *P. globosa* counting, 110 mL water samples were collected and fixed with Lugol's-glutaraldehyde solution (1% v/v). For dinoflagellates, another 110 mL were fixed with acid Lugol's solution (1% v/v) (data for dinoflagellates are available from 16/02/2018. Phytoplankton was examined, when possible, to the species or genus level using an inverted microscope (Nikon Eclipse TE2000-S) at 400x magnification after sedimentation in a 10, 50, or 100 mL Hydrobios chamber, as described previously in Breton *et al*., (2021).

The abundance of pico- and nanophytoplankton (PicoNano, 0.2-20 µm) and cryptophytes was enumerated by flow cytometry with a CytoFlex cytometer (Beckman Coulter). For all samples, 4.5 ml were fixed with paraformaldehyde (PFA) at a final concentration of 1% and stored at -80 °C until analysis (Marie *et al.*, 1999). Phytoplankton cells were detected according to the autofluorescence of their pigments (Chl-a, Phycoerythrin). *P. globosa* was discriminated from the PicoNano group based on orange fluorescence (Phycoerythrin, 496 nm).

Biovolumes for diatoms and cryptophytes, dinoflagellates, and *P. globosa* were estimated using an image analyser system and standard geometric forms according to (Hillebrand *et al.*, 1999). Then, the carbon-biovolume relationships were estimated following Menden-Deuer and Lessard, (2000), Verity (1992), and Schoemann (2005; see Table S2.1 for details).

2.2.4. DNA barcoding

For DNA extraction 4 to 7 L of seawater was filtered on 0.2µm polyethersulfone (PES) membrane filters (142 mm, Millipore, U.S.A.) after a pre-filtration step through 150 µm nylon mesh (Millipore, U.S.A.) to remove metazoans. All filters were stored at −80 °C for 18S rDNA amplicon Illumina MiSeq sequencing. A quarter of PES filter was used for DNA extraction following the DNAeasy PowerSoil Pro Kit (QIAGEN, Germany) manufacturer's protocol. The 18S rRNA gene V4 region was amplified using EK-565F (50-GCAGTTAAAAAGCTCGTAGT) and UNonMet (50-TTTAA GTTTCAGCCTTGCG) primers (Bower *et al.*, 2004). Pooled purified amplicons were then paired-end sequenced on an Illumina MiSeq 2 × 300 platform. Quality filtering of reads, identification of amplicon sequencing variants (ASV), and taxonomic affiliation based on the PR2 database were done in

the R-package (Guillou *et al.*, 2008; Callahan *et al.*, 2016). Raw sequencing data have been submitted to the Short Read Archive under BioProject number PRJNA851611.

A total number of 41,179 ASVs were identified from 6,366,087 reads in 287 samples, containing Metazoa, Streptophyta, Excavata, Alveolata, Amoebozoa, Apusozoa, Archaeoplastida, Hacrobia, Opisthokonta, Rhizaria, and Stramenopiles. For the purpose of this study only ASVs affiliated to Hacrobia, Stramenopiles, and Archaeoplastida were kept. In addition, mixotrophic dinoflagellates ASVs related to *Gymnodinium* and *Prorocentrum* were considered for their ecological importance. *Gymnodinium* is known to dominate dinoflagellate abundance and biomass in the eastern English Channel (Grattepanche, Breton, *et al.*, 2011), while *Prorocentrum* showed a momentary increase in this study. Unaffiliated eukaryotic ASVs, singletons and doubletons were removed, obtaining a final phyloseq object containing 6,471 ASVs corresponding to 2,448,955 reads, in 287 samples. The dataset was rarefied to the lowest number of reads (1,020), resulting in 274,380 reads corresponding to 4,141 ASVs from 269 samples.

2.2.5. Diversity, statistical and community assembly analyses

To describe the phytoplankton communities, the alpha diversity and Faith's phylogenetic diversity indices were calculated. Kruskal-Wallis and the post-hoc Nemenyi test were used to test if phytoplankton groups significantly differ among stations. To explore and summarize seasonal variations in the abiotic environment the multivariate Principal Component Analysis (PCA) was performed. Distance-based RDA analysis was applied considering morphological and metabarcoding data. All analysis was performed in R (R Core Team, 2021).

To infer ecological assembly processes governing alpha and beta diversity, null models based on metabarcoding data were applied according to Stegen's framework (Stegen *et al.*, 2012, 2013) reviewed by Zhou and Ning (2017). All tests presented here, were applied according to this framework. Briefly, the community assembly analysis, is based on the comparison of observed community turnovers (shifts in composition across samples), phylogenetic turnovers (shifts in composition weighted by the phylogenetic similarity between taxa) and turnovers expected by chance (in null-models), to estimate whether the differences between pairs of communities are explained by dispersal, selection, or ecological drift. According to phylogenetic community composition (alpha diversity) within each sample, phylogenetic structure is divided into environmental filtering and overdispersion, which are deterministic processes (Table 1). Based on phylogenetic turnover in community composition (beta

diversity), deterministic processes are divided into homogeneous selection (i.e., consistent environmental factors cause low compositional turnover) and heterogeneous selection (i.e., high compositional turnover caused by shifts in environmental factors). However, stochastic processes are divided into homogeneous dispersal (i.e., low compositional turnover caused by high dispersal rates), dispersal limitation (i.e., high compositional turnover caused by a low rate of dispersal), and ecological drift that can result from fluctuations in population sizes due to chance events (Stegen *et al.*, 2012, 2013; Segura *et al.*, 2013; Table 1). The implicit hypothesis is that phylogenetic conservatism exists, which means that ecological similarity between taxa is related to their phylogenetic similarity (i.e., phylogenetic signal; Losos, 2008). Mantel correlograms were applied to detect phylogenetic signals, which correlate the phylogenetic distances to the niche distances at different distance classes (e.g., Liu *et al.*, 2017; Doherty *et al.*, 2020; further information in supplementary). Significant positive correlations indicate that ecological similarity among ASVs is higher than expected by chance within the distance class. Alternatively, significant negative correlations indicate that ASVs are more ecologically dissimilar than expected by chance. Here the *cal_mantel_corr* function in the microeco package was used (Liu *et al.*, 2021).

To characterise if alpha diversity (i.e., phylogenetic structure) of phytoplankton is governed by environmental filtering or overdispersion we used the NRI index (Nearest Related Index, see also Table 2.1). For this, first, the phylogenetic metric MPD (Mean Pairwise Distance) was calculated as it considers the mean phylogenetic distance among all pairs of species within a community (Webb *et al.*, 2002). Phylogenetic structure (alpha diversity) was then assessed by the NRI for each community with null models based on 999 randomizations with the random shuffling of the phylogenetic tree labels with MicrobiotaProcess package v.1.5.4.990 (i.e., the *get_NRI_NTI* function). The NRI index is obtained by multiplying the standardized effect size of mean pairwise phylogenetic distance by -1.

The phylogenetic temporal turnover between pairwise communities among sampling dates (beta diversity) was quantified to investigate the action of deterministic and stochastic ecological processes with microeco R package v.0.6.0 (Liu *et al.*, 2021), using the *trans_nullmodel* function. The phylogenetic distance between pairwise communities (beta mean pairwise distance: βMPD) was computed with null models based on 999 randomizations with the random shuffling of the phylogenetic tree labels as in Stegen *et al*., (2013). The βNRI was calculated via the z score, as the difference between the observed βMPD and the mean of the βMPD null models divided by the standard deviation of the null models. βNRI scores less

than -2 indicate that the observed phylogenetic turnover is significantly lower than ~95% of the null values and thus that homogeneous selection between the compared communities causes higher than expected phylogenetic similarity. Similarly, βNRI scores greater than +2 indicate the dominance of heterogeneous selection. The Raup-Crick distances based on the Bray-Curtis similarity (RC_{bray}) were also calculated to further differentiate the stochastic processes structuring the community assembly, when βNRI scores varied between -2 and +2 . Values, of RC_{bray} less than -0.95 and greater than 0.95 indicate less and more compositional turnover, respectively, than the null expectation and that is attributed to homogeneous dispersal in the former case and to dispersal limitation in the latter. All definitions of the different assembly processes corresponding to the values of NRI and βNRI are shown in Table 1. Non-weighted metrics were used as metabarcoding data are semi-quantitative and the rarefied dataset was considered to prevent any bias due to potential under-sampling (Ramond *et al.*, 2021). The analysis in August has not been considered for further discussion in the present study because of insufficient sampling (i.e., only three samples).

To evaluate whether phylogenetic structure (i.e., NRI) and turnover (i.e., βNRI) is attributed to different environmental variables a Permutational Multivariate Analysis of Variance (PERMANOVA) was performed based on the Bray-Curtis distance.

2.3. Results

2.3.1. Seasonality of the environmental variables and phytoplankton communities

Prior to the quantification of ecological processes regulating the phytoplankton communities across seasons, the seasonal variations of the environment and the phytoplankton communities were investigated. The environmental variables and phytoplankton community composition measured in the eastern English Channel at the SOMLIT and DYPHYRAD stations evidenced clear seasonal patterns from December 2016 to October 2020, typical of temperate marine waters. Wind stress, nutrients, and chlorophyll showed great variability across seasons (Table S2.2). Nutrient inputs originated mainly from local rivers and reached relatively high values during fall and winter (Fig. S2.2A). For example, silicate concentrations recorded in winter were high (e.g., on average 5.9 ± 1.9 µM in January), whereas values in spring and summer were low on average (e.g., 0.9 ± 0.9 µM in June, Table S2.2, Fig. S2.2A). The N/P molar ratio varied greatly across seasons (from 0.4 to 316), and most of the time strongly deviated from the Redfield ratio (1958), (N/P=16, Table S2.2). A comparison of the mean ranks (Kruskal Wallis and Nemenyi *post hoc* test) of environmental variables between the different stations revealed significant differences in salinity, phosphate, silicate, and Chl-a between the stations

(Fig. S2.2B). However, the environmental variables were of the same range and showed the same seasonal variation at all stations (Fig. S2.2B). Principal Component Analysis (PCA) performed on the environmental dataset showed that the first two principal components contributed to 58 % of the total variance (Fig. 2.1A). The first principal component (PC1: 39.2 %) was mainly formed, by decreasing order, by phosphate, PAR, nitrite and nitrate, silicate, temperature, and wind stress, opposing winter and summer conditions (Fig. 2.1A, Fig. S2.2A). The second principal component (PC2: 18.8 %) was mainly formed by decreasing order by Chl-a, salinity and temperature associated with spring and autumn. Overall, summer and autumn samples formed tighter groups on the PCA biplot than spring and winter samples which were more dispersed (Fig. 2A).

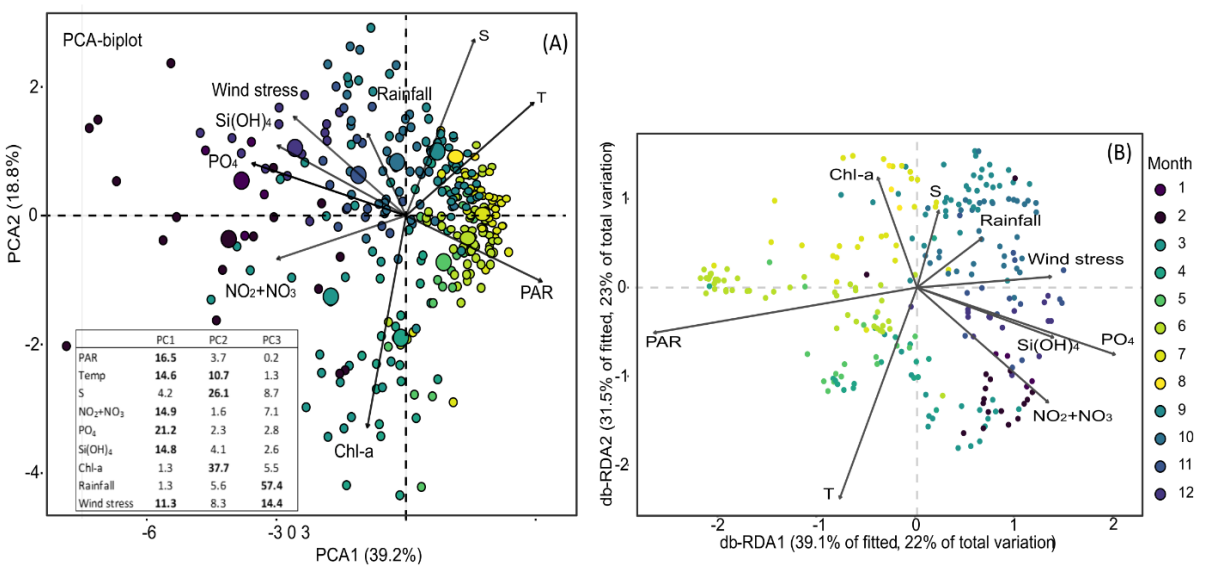

Figure 2.1. *(A) Principal component analysis (PCA) illustrating the variations of the environmental variables (arrows) at all sampling dates (coloured points with the size corresponding to the cos2 values of the PCA): Photosynthetic Active Radiation (PAR, E m^{-2} d^{-1}), temperature (T, °C), salinity (S, PSU), nitrite and nitrate (NO_2+NO_3 µM), silicate ($Si(OH)_4$, µM), phosphate (PO_4, µM), chlorophyll-a (Chl-a, µg L^{-1}), rainfall (Kg m^{-2}), wind stress (Pa). The table on the bottom left represents the % of the contribution of the different environmental variables in the building of the PCA axis (the most important contributors are in bold). (B) Distance-based redundancy (db-RDA) ordination illustrating the variations of the phytoplankton communities, based on metabarcoding data, (samples, coloured dots) in relation to the environmental variables (black arrows) in the eastern English Channel at the DYPHYRAD and SOMLIT stations from March 2016 to October 2020.*

The distance-based redundancy analysis (db-RDA) applied to metabarcoding data of phytoplankton communities and the environmental variables showed that the first two axes explained 45 % of the total variation in phytoplankton composition data (23 % and 22 % of the total variability for db-RDA1 and db-RDA2, respectively; Fig. 2.1B) with db-RDA1 and db-RDA2 highlighting a seasonal succession similar the PCA. The permutation test showed that PAR and temperature mainly contributed to the overall variability by 21 % (p=0.001) and 18 % (p=0.001), respectively, followed by nutrients (nearly 10 %, p=0.01, Table S2.3). Our study

is one of the rare ones considering both morphological and metabarcoding data using a relatively large data set (287 samples). Accordingly, since metabarcoding data are subjected to PCR biases and are always expressed in relative abundances, while morphological data are absolute abundances, it was important to confront the two data sets and see if they show similar trends. For this, the db-RDA was also applied to the microscopy data, which revealed similar seasonal trends (Fig. S2.3). The first two axes showed that the selected environmental variables explained nearly 37 % of the total variation (db-RDA1: 24 % and db-RDA2: 13 %) in phytoplankton data. The permutation test showed that PAR (24 %, p=0.001), temperature (10 %, p=0.001), and nutrients (10 %, p<0.05) mainly contributed to the overall variability (Table S2.4).

2.3.2. Phytoplankton community inferred with metabarcoding and morphological data

Phytoplankton communities showed high variability in alpha diversity (Fig. 2.2 A-D). The overall trend observed was decreasing Richness, Phylogenetic Faith's diversity (PD) and Shannon index from winter to spring, with the lowest observed values during the *P. globosa* spring bloom (April, May) and highest observed values in summer and autumn. Accordingly, the Simpson diversity index (1-D), showed the lowest values during the *P. globosa* spring bloom and relatively high values during the rest of the year (Fig. 2.2A-D).

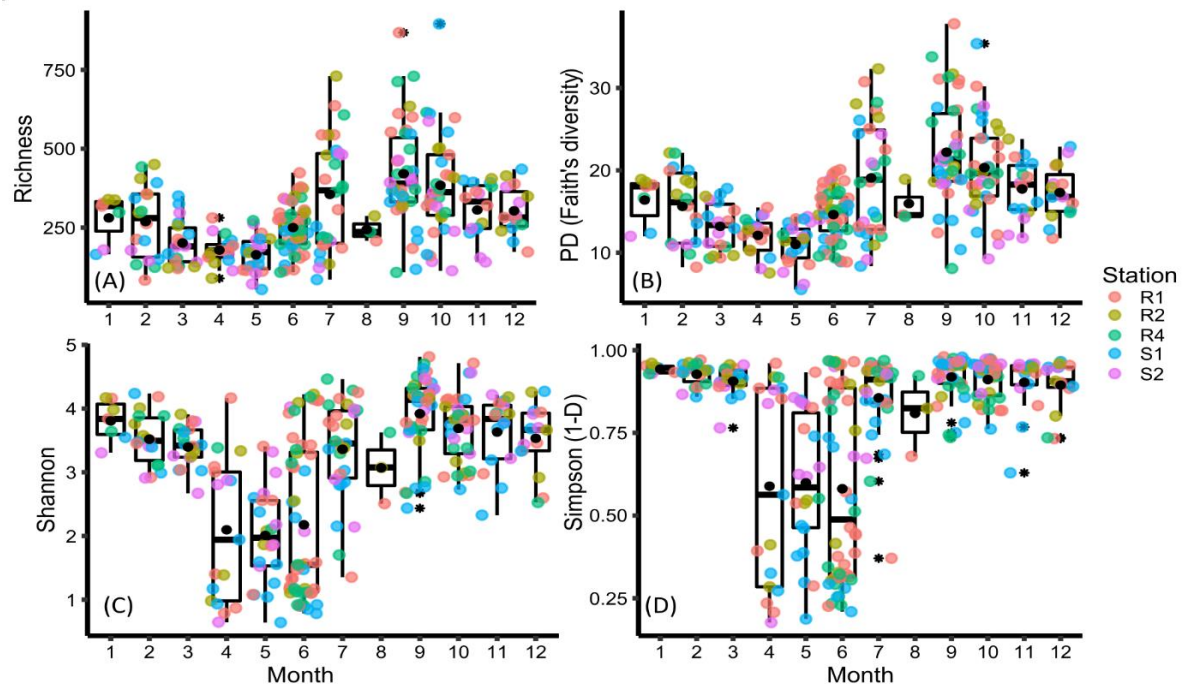

***Figure 2.2**. Alpha diversity of the phytoplankton communities based on metabarcoding data collected in the eastern English Channel at the DYPHYRAD and SOMLIT stations from March 2016 to October 2020. (A) Richness, (B) PD, Faith's phylogenetic diversity, and the (C) Shannon and (D) Simpson (1-D) indices. Solid black lines represent the median, black dots the mean, colored dots the samples according to stations, and the black stars the outliers.*

Based on morphological data (i.e., microscopy and cytometry counts), diatoms dominated the phytoplankton biomass (mean 55 %) across all seasons except in April-May, when the haptophyte *P. globosa* increased in biomass (42 % and 28 %, respectively, Fig. 2.3A). Pico-nanophytoplankton contributed 32 % of the total biomass, while cryptophytes and dinoflagellates accounted for only 4 % and 3 % of the total phytoplankton biomass, respectively (Fig. 2.3A). Metabarcoding data also reflected the dominance of diatoms as relative read abundance (mean 60 %) in the community and the *Phaeocystis* bloom in April and May (43 % and 41 %, respectively). Pico-nanophytoplankton, cryptophytes, and dinoflagellates contributed 20 %, 0.5%, and 6, % of the mean relative read abundance, respectively (Fig. 2.3B). Furthermore, no significant differences were found among the stations for the number of reads, cell counts, and biomass of the different phytoplankton groups recorded in this study (Fig. S2.4).

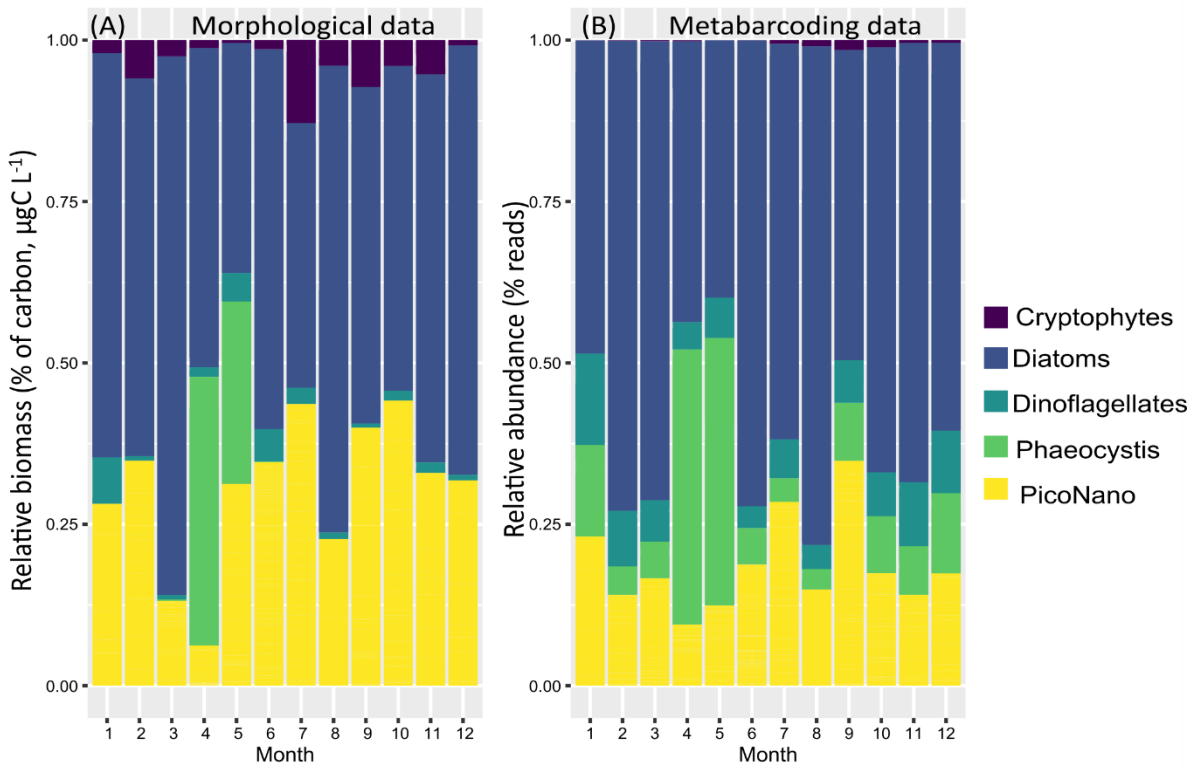

***Figure 2.3**. Phytoplankton community structure in the eastern English Channel at the DYPHYRAD and SOMLIT stations from March 2016 to October 2020. (A) From microscopy and cytometry (relative biomass as a percentage of carbon, see Table S2.1 in Supplemental information for biomass calculation). (B) From rarefied metabarcoding data (relative abundance as the percentage of reads of the ASVs).*

Besides the *P. globosa* bloom in April and May (Fig. 2.4A), several important peaks belonging to different groups were observed in spring, summer, and autumn, in both datasets. In July 2016, the planktonic diatom *Chaetoceros socialis* reached a maximum value of 3.1 10^6 cells L^-

[1] (Fig. 2.4B, Fig. S2.5), which coincided with a relatively high number of *Chaetoceros* reads (32 %, Fig. S2.5). In July 2017, *Guinardia* showed a relatively high number of reads (69 %, Fig. S2.6) in contrast to low abundance (18 10^3 cells L^{-1}) in microscopy data. In June 2018, a peak of the pennate diatom *Pseudo-nitzschia pungens*, reached 4.8 10^6 cells L^{-1} (Fig. 2.4B). The transient *P. pungens* peak was also clearly observed in metabarcoding data, reaching 73% of relative read abundance (Fig. S2.7). In addition, the centric diatom *Leptocylindrus danicus* marked diatom community structure also in June with a maximum concentration of 1.5 10^6 cells L^{-1} in 2018 (Fig. 2.4B, Fig. S2.7) and was also abundant in June of 2019 and 2020 (Fig. 2.4A, Figs. S2.8-S2.9). Dinoflagellates showed a peak in June 2018 (13.5 10^3 cells L^{-1}, Fig. 2.4C) attributed to *Prorocentrum minimum,* which contributed up to 9 % of the total relative abundance of reads (Fig. S2.7). Pico- and nanophytoplankton showed peaks of abundance generally in spring and summer, while the maximum abundance was recorded in September 2020 (35.4 10^6 cells L^{-1}, Fig. 2.4D). According to metabarcoding, pico- nanophytoplankton was dominated by the coccolithophorid *Emiliania* and the nanoplanktonic diatom *Minidiscus*. Several peaks were observed in cryptophyte's abundance in July 2016, 2018, and 2020; in 2016 peaks were also observed in April and September (Fig. 2.4E). Based on metabarcoding, the dominant cryptophyte was assigned to *Plagioselmis.*

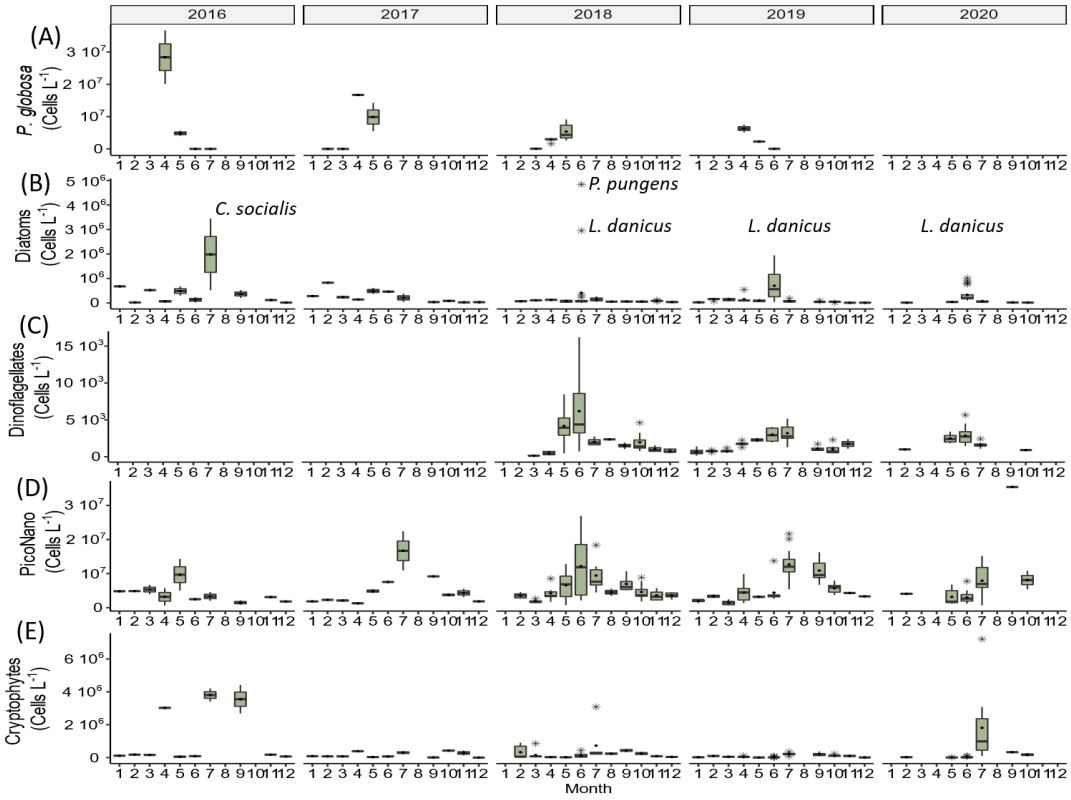

Figure 2.4*. Abundance (cells L^{-1}) of the phytoplankton groups identified in the eastern English Channel at the SOMLIT and DYPHYRAD stations from March 2016 to October 2020 based on microscopy and flow cytometry data. (A) P. globosa, (B) diatoms, (C) dinoflagellates (Gymnodinium and Prorocentrum), (D) PicoNano, and (D) cryptophytes. No data were available from 2016 to 2017 for dinoflagellates and all phytoplankton from February 14, 2020 to May 20, 2020 because of the sanitary crisis). Solid black lines represent the median, black dots the mean, and the black stars the outliers.*

2.3.3. Phylogenetic structure, temporal turnover, and ecological processes driving the phylogenetic phytoplankton community structure

Mantel correlograms correlating the phylogenetic distances to the niche distances at different distance classes detected significant positive correlations across short phylogenetic distances (< 0.4 phylogenetic distance, Fig. S2.10). Except for salinity, all the evaluated environmental variables showed significant negative correlations over intermediate phylogenetic distances. These results supported that phylogenetic metrics can be applied to infer ecological assembly processes. Significant positive correlations across long phylogenetic distances were observed for PAR (nearly 0.8 phylogenetic distance, Fig. S2.10).

Ecological processes governed the alpha diversity of phytoplankton (i.e., phylogenetic structure) were investigated using the NRI index. It showed that, phylogenetic clustering prevailed during all seasons suggesting environmental filtering (NRI > 0, Table 2.1). The strongest values of phylogenetic clustering were detected from January to March (NRI > 3,

Fig. 2.5). From April to July, NRI values showed a decreasing trend, indicating a tendency towards a weaker phylogenetic clustering at this time of the year. From September to December, NRI values showed again an increasing trend (Fig. 2.5).

***Table 2.1**. Definitions of the different assembly processes, and respective model conditions referenced from Webb et al. 2002, Stegen et al. (2012, 2013), and Zhou and Ning (2017).*

Process	**Deterministic**		**Stochastic**		
Diversity	**Alpha diversity**				
Clustering	Phylogenetic clustering	Phylogenetic overdispersion			
Definition	Environmental conditions, selecting those species capable of survival and persistence in a local environment (environmental filtering)	Competitive exclusion, resulting in limiting similarity (overdispersion)			
Phylogenetic structure index	NRI>0	NRI<0			
Diversity			**Beta Diversity**		
Process	Homogeneous selection	Heterogeneous selection	Dispersal limitation	Homogeneous dispersal	Drift
Definition	Consistent environmental factors cause a low compositional turnover	Shifts in environmental factors cause a high compositional turnover	Movement of an individual is restricted	High rate of movement of an individual from one location to another	Population size fluctuates due to chance events
Phylogenetic turnover index	βNRI < -2	βNRI >2	-2 < βNRI <2		
Taxonomic turnover index	-	-	$RC_{bray} > 0.95$	$RC_{bray} < - 0.95$	$-0.95<RC_{bray}<0.95$

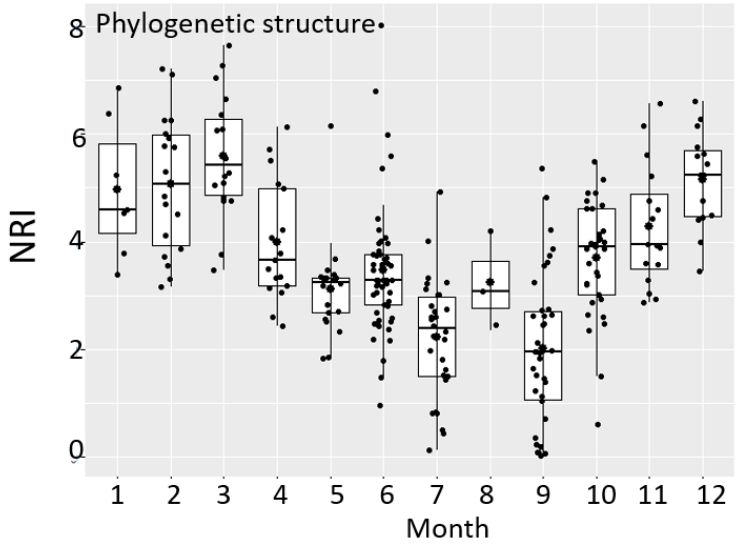

***Figure 2.5**. Phylogenetic structure (alpha diversity) of the phytoplankton community in the eastern English Channel at the DYPHYRAD and SOMLIT stations from March 2016 to October 2020 based on metabarcoding data. Phylogenetic structure based on the net relatedness index (NRI) with NRI > 0and NRI < 0 suggested phylogenetic clustering and overdispersion, respectively (see Table 2.1). Solid black lines represent the median and black dots the mean.*

To test if phylogenetic structure (i.e., NRI) and turnover (i.e., βNRI) were attributed to different environmental variables a PERMANOVA was applied. PAR and temperature -although they explained a very small amount of the variance of the data set- were the only variables significantly linked with phytoplankton phylogenetic structure and phylogenetic turnover (Tables S2.5, S2.6, $p < 0.001$). Most of the variance remained unexplained with residuals presenting 67 % and 87% for the phylogenetic structure and phylogenetic turnover (Tables S2.5, S2.6).

The different ecological processes, selection, dispersal and drift were quantified using the null model analysis. The analysis applied to the entire data set showed that drift and homogeneous selection were the dominant ecological processes driving the seasonal succession of the phytoplankton community, contributing to 55 % and 38 %, respectively, over the entire period of study (Fig. 2.6A). Heterogeneous selection contributed weakly to the seasonal succession of the phytoplankton community (6 %) and dispersal did not have any significant influence. The null model analysis applied additionally at the monthly scales showed three distinct patterns. First, phytoplankton succession in winter-early spring was dominated by the homogeneous selection, contributing to 83 %, 52 %, and 54 % of the assembly processes in January, February, and March, respectively. Second, spring and summer periods were mostly dominated by drift mechanisms (contributing from 69 % to 87 %, depending on the month). Third, autumn was

dominated primarily by drift, contributing from 52 % to 65 % to the assembly processes with homogeneous selection accounting from 25 % to 38 % (Fig. 2.6B, Table S2.5).

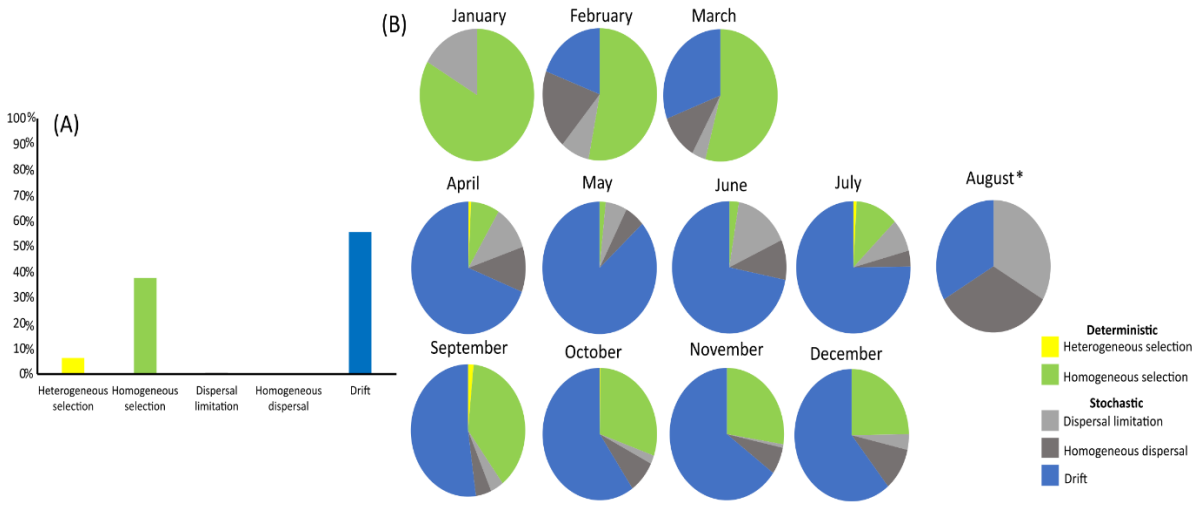

Figure 2.6*. The relative importance of the ecological processes (beta diversity) driving phytoplankton communities in the eastern English Channel at the DYPHYRAD and SOMLIT stations from March 2016 to October 2020. A: considering the whole data set, B: data discriminated per month. *, only three samples were available for August, so the data was not interpretable.*

2.4. Discussion

In the present study, microscopy and flow cytometry allowed phytoplankton biomass to be quantified, while metabarcoding data provided an extended evaluation of its diversity. Alpha diversity of phytoplankton communities was regulated by environmental filtering. Drift, followed by homogeneous selection, were the major mechanisms regulating the temporal turnover in community composition (beta diversity) and prevailed across seasons. Three periods were evidenced: (i) Winter-early spring, with homogeneous selection as the major process regulating the phytoplankton communities, composed mainly of diatoms communities (e.g., *Thalassiosira*); (ii) Spring-summer, with drift as the major process in community assembly during the bloom of *P. globosa* and during the transient peaks of various taxa (diatoms, dinoflagellates, and pico-nanophytoplankton); and (iii) Autumn, with a combination of drift and homogeneous selection as a major ecological process in phytoplankton community assembly dominated by diatoms (Table 2.2). Overall, we evidenced that deterministic and stochastic ecological processes varied across seasons in alpha and beta diversity.

Table 2.2. *Summary of the seasonal characteristics of the phytoplankton community in coastal waters of the eastern English Channel. The median values are given in parentheses. The relative terms "High," "Moderate," and "Low" refer to the median of the entire data set.*

	Median in entire dataset	**January-March**	**April-July**	**September-December**
Dominant phytoplankton (morphological and metabarcoding)		*Thalassiosira sp.*	*Phaeocystis globosa, Chaetoceros socialis, Leptocylindrus danicus, Pseudonitzschia pungens, Prorocentrum minimum, piconanophytoplankton*	*Thalassiosira sp., Ditylum sp., piconanophytoplankton*
PAR (E m^{-2} d^{-1})	60.8	Low (35.5)	High (84.9)	Low (41.7)
T(ºC)	15	Low (7.7)	Moderate (15.2)	Moderate (16.5)
NO_2+NO_3	1.0	High (4.3)	Low (0.5)	Moderate (1.3)
$Si(OH)_4$	1.3	High (2.9)	Low (0.8)	Moderate (1.8)
PO_4	0.2	High (0.4)	Low (0.1)	Moderate (0.2)
Windstress (Pa)	0.04	High (0.1)	Moderate (0.04)	High (0.1)
Rainfall (kg m^2)	1.3	Moderate (1.1)	Low (0.8)	High (2.0)
Richness	272	Low (213)	Low (218)	High (361)
Taxonomic alpha diversity (Shannon)	3.4	High (3.5)	Low (2.5)	High (3.8)
Ecological processes (Alpha diversity)	1.4	Environmetnal filtering (3.1)	Environmental filtering (0.8)	Environmental filtering (1.5)
Ecological processes (Beta diversity)		Homogeneous selection	Drift	Drift + Homogeneous selection

2.4.1. Seasonal diversity patterns

Overall, the relative abundance of the major phytoplankton groups inferred by metabarcoding was in good accordance with the relative carbon biomass inferred by morphological approaches in particular for pico- nanophytoplankton and cryptophytes and to a lesser degree for diatoms (Durkin *et al.*, 2022, Fig. 2.3). Moreover, the distance-based RDA analysis showed similar seasonal patterns in both datasets (Figs. 2.1B, S2.3).

The most abundant diatom taxa were common in both data sets. Three diatom taxa showed transient blooms in summer (June-July): (i) the chain-forming centric diatom *L. danicus* has been previously reported in high abundances in the sampling area during summer (Genitsaris *et al.*, 2015; Breton *et al.*, 2017) . A good correspondence between a high number of reads and cell counts of *Leptocylindrus* has been reported also in the Gulf of Naples (Piredda *et al.*, 2018); (ii) The chain-forming diatom *Pseudo-nitzschia* is known to form dense blooms along the French coast of the eastern English Channel and is often a co-occurring species of the *P. globosa* (Bottin *et al.*, 2016 and references therein); and (iii) The colony-forming diatom *C. socialis* observed in July has been reported in the English Channel in spring and summer (Napoléon *et al.*, 2014; Breton *et al.*, 2017).

Dinoflagellates are known to be over-represented in sequencing data, and their use in numerical analysis can lead to important biases (e.g., Medinger *et al.*, 2010; Christaki *et al.*, 2021). In this study, two small mixotrophic dinoflagellates (*Gymnodinium* and *Prorocentrum*) were included in the analysis for the reason that they were the only dinoflagellates to exhibit relatively high abundances in microscopy data, while they did not represent an exaggerated number of reads in metabarcoding data (Fig. 2.3, S2.4). *Gymnodinium* and *Prorocentrum* were prominent members of the protist community in previous studies in the western and eastern English Channel (Widdicombe *et al.*, 2010; Grattepanche, Breton, *et al.*, 2011). The genus *Gymnodinium* showed relatively stable cell numbers across seasons, while the species *P. minimum* showed a peak in 2018. Intense but brief blooms of *P. minimum* have been previously reported during the summer months in the Western English Channel (Widdicombe *et al.*, 2010). The *P. globosa* bloom in April and May was clear in both datasets, however, metabarcoding data evidenced the presence of low relative abundances of *P. globosa* all year long (Fig. 2.3B), which were not recorded by microscopy and cytometry because of its very low abundance. Pico- nanophytoplankton showed maximum concentrations also in summer reaching 2 10^7 cells L^{-1}, and one in fall 3.5 10^7 cells L^{-1} (Chase *et al.*, 2009; Fig. 2.4D)

2.4.2. Ecological processes shaping phytoplankton seasonal organization

The NRI index calculated for the whole phytoplankton community evidenced that alpha diversity of phytoplankton communities governed by environmental filtering (Webb *et al.*, 2002; Tables 2.1, 2.4, and Fig. 2.5). Environmental filtering is the effect of environmental conditions selecting those species capable of survival and persistence in a local environment (Emerson and Gillespie, 2008; Kraft *et al.*, 2015) and it is known to play a major role in structuring marine phytoplankton communities (Segura *et al.*, 2013; Bottin *et al.*, 2016; Klais *et al.*, 2017; Burson *et al.*, 2019). Phytoplankton communities, based on the phylogenetic temporal turnover (beta diversity), assembled across seasons through a concomitant action of deterministic and stochastic processes. However, stochastic processes (i.e., drift) contributed by far more than ecological selection to community assembly, except for winter and early spring (from January to March), when homogeneous selection regulated phytoplankton communities (Figs. 2.5, 2.6).

The dominance of homogeneous selection in winter and early spring is coherent with the strong environmental filtering conditions, such as, the high nutrient concentration values, and low light availability recorded during this period (NRI > 4 Fig. 2.5A, see also Table 2.1, and 2.2). Hence, homogenous selection has been seen as the selection of species with common and

appropriate genomic architecture and metabolic strategies for surviving and persisting in a local environment (Grzymski and Dussaq, 2012; Louca *et al.*, 2016) implying an increase in community similarity (Stegen *et al.*, 2015). This process dominates in community assembly when environmental conditions are spatially homogenous (Fig. S2.2B; Segura *et al.*, 2013; Jia *et al.*, 2018). In the geographic scale of our study (ca 15 km), the coastal waters of the eastern English Channel represented an homogeneous pool of phytoplankton taxa undergoing similar selection processes (Figs. 2.6, S2.4). The dominance of diatoms at this time of the year, mainly of the genus *Thalassiosira*, was coherent with the worldwide observations of diatoms thriving in light-limited, nutrient-enriched, and colder waters submitted to relatively high wind-driven turbulence (Schapira *et al.*, 2008; Armbrust, 2009). Silica frustule and large centric vacuole are considered as key traits for diatom success in winter and early spring for protecting against mechanical and salinity shocks (Logares *et al.*, 2009; Hoef-Emden, 2014) and optimizing light affinity (Hansen and Visser, 2019).

The prevalence of stochastic processes in phytoplankton community assembly in beta diversity was observed during the rest of the year (from April to December, Fig. 2.6, Table 2.2). Maximum drift values were recorded in late spring and summer - periods that presented monospecific phytoplankton peaks. This was coherent with the large quantity of unexplained variance between environmental variables and the phytoplankton community in terms of abundance, and phylogenetic structure and turnover (db-RDA and PERMANOVA, respectively). The dominance of drift is in accordance with a previous study quantifying the ecological processes in natural ecosystems using the same analytical approaches of the present study (Logares *et al.*, 2018) . These authors found that microeukaryotic communities were governed by drift (72%), while the relative contribution of selection and dispersal were low.

However, identifying the underlying mechanisms and factors favouring stochasticity is challenging. Hence, studies are still scarce and detecting stochastic processes may suggest the non-consideration of unmeasured environmental variables (Zhou and Ning, 2017), as well as from a mixture of antagonistic processes (Powell *et al.*, 2015). Moreover, multiple factors may influence the relative importance of stochastic versus deterministic processes in community assembly, including predation (Chase *et al.*, 2009), productivity (Chase, 2010), community size (Orrock and Watling, 2010), resource availability (Kardol *et al.*, 2013), as well as disturbance (Dini-Andreote *et al.*, 2015). For example, predators can increase the importance of stochastic processes by reducing the number of individuals that can live in a given environment, and thus the community size, by increasing the probability of species going extinct locally (Chase *et al.*,

2009). Nonetheless, the minor role played by dispersal in shaping phytoplankton communities in this study area (Fig. 2.6) is coherent with the small spatial scale investigated (~15 km) (e.g., (Heino *et al.*, 2015; Logares *et al.*, 2020).

In this study, the continuous decrease in species richness observed from February to May (Fig. 2.2A) potentially suggests intense stress for the diatom community which -despite increasing light- faces silicate limitation during this period (Breton *et al.*, 2006; Fig. S2.2A). This presumption of stress is reinforced by the low degree of silicification and the decrease of the functional evenness observed by Breton (2021) in May. Note that functional evenness describes the evenness of abundance distribution in a functional trait space (Mason *et al.*, 2005). In fact, a decrease in functional evenness, which reflects under-used parts of the niche (Mason *et al.*, 2005), is considered a fingerprint of disturbance (Mouillot *et al.*, 2013). *P. globosa*, although it is a poor competitor for nitrate and has a lower maximum growth rate than diatoms (Breton *et al.*, 2017) does not require silicate and thus it blooms under limiting silicate and excess of nitrate in spring (Lancelot *et al.*, 1998). *Phaeocystis* has also a strong protection against grazing by forming colonies and may further benefit from the increased grazing of mesozooplankton on the microzooplankton, potential predators of *Phaeocystis* (Grattepanche, *et al.*, 2011).

Despite the relatively low nutrient levels after the *P. globosa* bloom, phytoplankton richness and PD values increased (Table 2) and several transient peaks belonging to different phylogenetic groups (diatoms, dinoflagellates, and pico- nanophytoplankton) appeared in summer (Fig. 2.4; Christaki *et al.*, 2017). This suggests that other mechanisms lowered the competitive exclusion in shaping phytoplankton communities at this time of the year. One plausible explanation is that the new niche opportunities that might have resulted from intense bacteria activity remineralising the organic resource derived from *P. globosa*. This resource is recurrently released in May in the seawater (Lamy *et al.*, 2009), and/or from the under-used and the vacant niches left open after the species loss at the end of the *Phaeocystis* bloom. Such a large input of dissolved organic material may be compared to large inputs of nutrients, which is typically considered a perturbation that favours ecological drift (Chase and Myers, 2011) through the enhanced growth of a variety of species and by reducing competition. Jurburg et al., (2017) stated that ecological drift in soil microbial communities was due to the niche enlargement after a perturbation. Mixotrophy typically reflects such a possibility (Xu *et al.*, 2022). The dinoflagellate *P. minimum* which showed a peak in abundance in June is mixotrophic (Fig. 2.4B; Fan *et al.*, 2003). This species grows photosynthetically on inorganic nutrients, but compensates for low concentrations of inorganic nitrogen by mixotrophic

utilization of organic nitrogen and other compounds released at the end of *P. globosa* bloom. Other alternative strategies also exist, such as, adaptation to high light levels. Indeed, the diatoms *L. danicus* and *P. pungens* are considered adapted to high light conditions (Widdicombe *et al.*, 2010; Polimene *et al.*, 2014), whereas pico- nanophytoplankton and cryptophytes, can acquire nutrients in low concentration; outcompeting larger cells for nutrient uptake (Reynolds, 1984) due to the high surface/volume ratio reducing the "package effect" (Finkel, 2001), and increasing nutrient diffusion (Raven, 1984), compared to larger cells. Overall, these specific adaptations provide a better efficiency for growth that is necessary for maintenance and ecological success during seasons with low nutrient and high light levels.

Autumn phytoplankton communities were subjected to the combined action of drift and selection processes. The local environment progressively increased the action of environmental filtering and, consequently, the contribution of homogeneous selection to community assembly increased (Fig. 2.5, 2.6, and Table 2.2). Nutrients became progressively available again, light and temperature diminished, while high turbulence values (wind stress as a proxy) enhanced physical mixing (Fig S2.2). This could explain the high richness, diversity, and a community characterized by large diatoms such as *Thalassiosira sp.* and *Ditylium sp.* (e.g., Fig. S2.7). Drift remained a major mechanism in autumn, potentially related to high grazing pressure in late summer-autumn (Grattepanche, Breton, *et al.*, 2011). External forces such as wind stress and salinity showed high variability and extreme values particularly in September (Fig. S2.2), which seemed to be a transitional period between summer and autumn conditions (Figs. 2.1A, S2.2, S2.3).

It is acknowledged that there are several limitations to discuss. Inferring ecological processes based on phylogenetic metrics is challenging. The phylogenetic signal is required, which was indeed detected in our study (Fig. S2.10). The phylogenetic signal has been confirmed in natural phytoplankton communities and based on evolutionary models (Bruggeman, 2011), but the opposite has been demonstrated in an experimental study focused on eight species of freshwater green algae (Narwani *et al.*, 2013). However, our results present the overall action of ecological processes at the whole community level, and not on a particular taxonomic group. Different taxonomic classes may be structured by different processes (Xu *et al.*, 2022). The sampling effort is also important. For example, in this study, only three samples were available for August, and thus the results could not be interpreted (Fig. 2.6). Finally, the biases derived from PCR and sequencing may add bias in calculating the importance of the ecological processes in community assembly. Nonetheless, in this study, there was -as discussed above-

a relatively good correspondence between morphological and metabarcoding data. Molecular and morphological data are complementary but unfortunately are rarely considered together in actual marine planktonic studies, and this is one of the strong points of our work.

Concluding this study, null modeling based on phytoplankton metabarcoding data revealed that stochastic and deterministic processes presented seasonal and repeating patterns. Our results provided strong support that, except for winter and early spring, the ecological drift prevailed during the rest of the year and in particular during the periods that presented by recurrent and transient monospecific phytoplankton peaks. The prevalence of stochastic processes renders *a priori* the seasonal dynamics of phytoplankton communities less predictable. In this context, the exploration of ecological processes driving phytoplankton communities in the long term is critical in our understanding of pelagic ecosystems' response relative to environmental variability.

Acknowledgments

We would like to thank the Captain and the crew of the RV ‘Sepia II’; M. Crouvoisier for nutrient analysis; V. Cornille and E. Lecuyer for help with the fieldwork; E. Goberville for meteorological data; and P. Magee for English proofing. We thank the SCoSI/ULCO (Service COmmun du Système d’Information de l’Université du Littoral Côte d’Opale) providing us with the computational resources to run all the bioinformatic analyses via the CALCULCO computing platform (https://www-calculco.univ-littoral.fr/). This work was logistically supported by the national monitoring network SOMLIT (https://www.somlit.fr/) and funded by the CPER MARCO (https://marco.univ-littoral.fr/) and the French Research program of INSU-CNRS via the LEFE-EC2CO 'PLANKTON PARTY' and the OFB through the INDIGENE project. DIS was funded via a PhD grant by the 'Region des Hauts de France’ and the ‘Pôle métropolitain de la Côte d’Opale (PMCO)’. We also thank the reviewers for their comments and suggestions that helped to improve our manuscript.

Contributions

Samples were collected from the national monitoring network SOMLIT and the local transect DYPHYRAD (PI: Dr. Artigas Luis-Felipe) by the crew of ‘Sepia II’, and the assistance of technicians Vincent Cornille and Eric Lecuyer. I participated in some of these samplings from 2018 to 2020. Since 2018, I have been responsible for fixing microscopy and cytometry data and conducting filtrations for metabarcoding. I enumerated and identified separately phytoplankton (diatoms and *Phaeocystis*), and dinoflagellates using inverted microscopy.

Additionally, I conducted extractions, prepared libraries, and performed purifications for 18S metabarcoding for all samples. Phytoplankton data from 2016 to 2017 were enumerated by Dr. Breton Elsa, and nutrient and chlorophyll-a measurements were carried out by Crouvoisier Muriel. All samples were sequenced by Genewiz platform. I conducted bioinformatic and statistical analysis with the help of Dr. Irion Solène. I applied null-model analysis and I did all the visualisations. Pr. Chrisraki Urania conceptualised, leaded, and acquired funding for this study.

2.5. Supplementary

Supplementary Materials and Methods

DNA barcoding

Different molecular barcodes of 10 bp were added to both forward and reverse primers to tag amplicons and allow to differentiate them after sequencing. Polymerase chain reaction (PCR) mixtures comprised 1 µL of DNA, 12.5 µL of DreamTaq Green PCR Master Mix (Thermo Fisher Scientific, U.S.A.), 1 µL of each primer (10 µmol L^{-1}), and 9.5 µL nuclease-free water in a total volume of 25 µL. PCR settings included an initial step of denaturation at 94 ^{o}C for 2 min, 25 cycles of denaturation at 94 ^{o}C for 15 s, annealing at 55 ^{o}C for 30 s, an extension at 72 ^{o}C for 1 min and 30 sec, and a final step of extension at 72 ^{o}C for 5 min. About 4 µL PCR product was used to check amplification on 1% agarose gel. The remaining amplicon products from five different PCR reactions of each sample were pooled and purified together using the QIAquick PCR purification kit (Qiagen, Germany), according to the manufacturer's instructions. DNA concentrations after purification were measured with a Qubit 2.0 fluorometer (Thermo Fischer Scientific Inc) with the dsDNA High Sensitivity Assay Kit (Life Technologies Corp., U.S.A.) and adjusted at equal concentrations depending on the sequencing run (20 to 47 ng/µL).

Diversity and statistical analysis

The alpha diversity indices Richness, Shannon and Simpson were calculated with the "vegan" package (Oksanen *et al.,* 2020) and Faith's phylogenetic diversity index was calculated with the "Picante" package (Kembel *et al.,* 2010). Heatmaps were generated to illustrate the overall phytoplankton community composition and diversity of the 30 most common genera in all samples (i.e, 0.5 % of reads in the entire dataset), using the "Ampvis2" R-package (Andersen *et al.,* 2018) after pooling ASVs belonging to the same genus. Monthly boxplots were built

using the "ggplot2" package (Wickham, 2016) to illustrate seasonal variations of the environmental variables, the alpha diversity indexes, the phylogenetic indexes and the different phytoplankton groups. To test how the environmental variables and the different phytoplankton groups' abundance, biomass and number of reads differed among stations the non-parametric test Kruskal-Wallis was performed, followed by a post hoc Nemenyi test (package "PMCMRplus"; Pohlert, 2015). To explore the seasonal environmental gradient a Principal Component Analysis (PCA) was performed on environmental variables using the "ade4", "FactoMineR" and "factoextra" packages (Dray *et al.*, 2007; Lê *et al.*, 2008; Kassambara and Mundt, 2020). The significance of each environmental variable in driving the phytoplankton community structure was assessed by distance-based redundancy analysis (db-RDA) (Legendre and Anderson, 1999) based on Bray-Curtis dissimilarity distance matrix using the "microeco" R package v.0.6.0 (Liu *et al.*, 2021). The significance of db-RDA models was tested with a permutation test using the *permutest* function with 999 permutations.

Community assembly

Mantel correlograms were applied to detect phylogenetic signals (closely related taxa have similar habitat associations). The phylogenetic signal was evaluated for PAR, temperature, salinity, nitrite and nitrate, phosphate, and silicate. It allowed characterizing the continuous correlations by comparing each matrix of between-ASV environmental optima (or "niche value") differences and the second matrix of between-ASV phylogenetic distances. For example, for PAR we took all the records of a given ASV (this was done for all ASVs) and recorded the PAR of each record, the ASV's abundance in each record, and then found the abundance -weighted mean of PAR. This is the ASV's 'niche value' for PAR. The analogous procedure was used to estimate ASV niche values for all the other environmental parameters. To summarize major trends in this relationship, between-ASVs niche differences were placed in phylogenetic distance bins and median niche difference was found in each bin (which are represented by the squares in the graph). X axis shows the phylogenetic distances (0: lowest, 1.0 maximum). Y axis shows the correlation between environmental optima and phylogenetic distances. All mantel correlograms showed positive correlation between niche optima and phylogenetic distances at short phylogenetic distances, which justifies the utilisation of the phylogenetic metrics to infer community assembly (Stegen *et al.*, 2012).

The βNRI was calculated as the difference between the observed βMPD and the mean of the βMPD null models divided by the standard deviation of the null models. Beta net relatedness values (βNRI) lower than expected (i.e., βNRI < -2) indicate a dominance of homogeneous

selection. In contrast, βNRI values which are greater than expected (i.e., βNRI > 2) indicate that communities are experiencing heterogeneous selection. When the deviation was low (i.e., -2 < βNRI ≤ 2), an additional step was conducted to define whether the beta diversity of the communities could be structured by dispersal or drift (Table 1). In this step, the Raup–Crick metric (RCbray) (Chase *et al.*, 2011) was calculated using the Jaccard's distance. For this, RCbray compares the measured b-diversity against the b-diversity that would be obtained if drift was driving community turnover (i.e., under random community assembly). The randomization was run 999 times based on the presence-absence of all ASVs across each pairwise community comparison that is randomized. RCbray values less than - 0.95 indicate that community turnover is driven by dispersal limitation, RCbray values greater than 0.95 indicate homogeneous dispersal respectively, and values between -0.95 and +0.95 point to a community assembly governed by drift or other undominated mechanisms.

Supplementary Tables

Table S2.1. *Cell to carbon biomass conversion factors used in this study for the estimation of biomass of the different phytoplankton groups identified in the eastern English Channel at the SOMLIT and DYPHYRAD stations from March 2016 to October 2020.*

	Conversion factor	References
Diatoms	pgC $cell^{-1}$=0.288 x $(biovolume)^{0.811}$	Based on linear dimensions the biovolume was calculated according to the cell shape (Hillebrand et al 1999). Conversion from biovolume to biomass according to Menden Deuer & Lessard 2000 and according to microscopic observations over the period 2007-2015 (Breton et al., 2017)
Dinoflagelates	pgC $cell^{-1}$=0.76 x $(biovolume)^{0.819}$	Based on linear dimensions the biovolume was calculated according to the cell shape (Hillebrand et al 1999). Conversion from biovolume to biomass according to Menden Deuer & Lessard 2000 and according to microscopic observations over the period 2018-2020 (this study)
Phaeocystis free flagellate cell *Phaeocystis* colonial cells	8 pgC $cell^{-1}$ 14.2 pgC $cell^{-1}$	Schoemann et al., 2005
Nanophytoplankton	4.98 pgC $cell^{-1}$	Cell carbon was estimated using the empirical relationship between biovolume and cell carbon of Verity et al. (1992). 0.433x $(biovolume)^{0.86}$.Mean ESD=3.03 µm (ecquivalent sphere diameter) according to microscopic observations
Picophytoplankton	1.19 pgC $cell^{-1}$	As above, based on mean ESD=1.74
Cryptophytes	11 pgC $cell^{-1}$	Conversion from biovolume to biomass according to Menden Deuer & Lessard 2000 and according to microscopic observations over the period 2007-2015 (Breton et al., 2017)

1

Table S2.2. *Monthly range, mean (±SD) and median values of the mean Photosynthetic Active Radiation (PAR_{10m}, E m^{-2} d^{-1}), sea surface temperature (T, °C), salinity (S, PSU), nutrients (nitrite and nitrate: NO_2 + NO_3, phosphate: PO_4, all in µM, the N/P molar ratio, silicate $Si(OH)_4$, µM), chlorophyll-a (Chl-a, µg L^{-1}), rainfall (Kg m^2), and wind stress (Pa) in the eastern English Channel at the SOMLIT (S1, S2) and DYPHYRAD (R1, R2, R4) stations from March 2016 to October 2020. Note that only three samples were available for August (with grey color).*

	January	February	March	April	May	June	July	August	September	October	November	December
PAR_{10m} (E m^{-2} d^{-1})												
Range	17.4-21.3	23.2-35.5	36.2-52.8	56.5-69.3	73.03-83.86	84.3-86.7	79.7-86.7	66.5-66.5	46.6-64.0	29.4-46.4	20.2-28.3	14.8-17.5
Mean±SD	19.2±1.6	29.1±3.8	46.7±4.7	62.3±3.1	79.67±3.57	86.1±0.7	84.2±2.1	66.5±0.0	55.6±5.7	39.7±5.5	22.7±2.8	16.0±1.0
Median	19	28.6	48.2	63.7	81.27	86.4	84.9	66.5	55.2	38.3	22.2	15.9
CV(%)	8.4	13.1	10.0	5.1	4.48	0.9	2.5	0.0	10.2	14.2	12.5	6
T (°C)												
Range	5.4-7.9	6.0-8.3	5.8-9.5	8.6-11.4	11.03-14.7	13.7-18.2	16.5-20.1	19.1-19.5	12.4-19.8	14.4-18.1	10.6-14.9	8.1-11.4
Mean±SD	7.1±0.8	7.4±0.7	8.0±1.3	9.6±0.7	12.91±1.06	15.4±1.0	17.8±0.8	19.3±0.2	18.1±1.3	16.2±0.9	12.6±1.3	10.2±0.8
Median	7	7.5	8.2	9.7	12.86	15.4	17.8	19.5	18.6	16.4	12.8	10.4
CV(%)	11.8	10.2	16.6	7.5	8.19	6.4	4.2	1.2	7.4	5.4	10.4	7.9
S (µM)												
Range	33.8-34.9	32.9-34.8	33.3-34.9	32.6-35.2	33.5-35.0	31.2-35.1	33.4-34.9	0.03-0.1	33.8-34.9	33.6-35.1	34.1-35.0	33.9-35.0
Mean±SD	34.2±0.4	34.0±0.6	34.2±0.5	34.1±0.6	34.2±0.4	34.3±0.5	34.6±0.3	34.6±0.2	34.5±0.2	34.5±0.3	34.6±0.3	34.4±0.3
Median	34.1	34.1	34.2	34.2	34.09	34.4	34.6	34.6	34.6	34.5	34.6	34.3
CV(%)	1.0	1.7	1.5	1.7	1.27	1.4	0.9	0.5	0.5	0.8	0.8	0.8
NO_2+NO_3 (µM)												
Range	3.4-10.6	0.3-23.9	1.1-20.7	0.3-9.3	0.14-1.6	0.01-4.4	0.2-1.1	0.2-0.5	0.3-2.8	0.2-3.5	0.4-5.2	1.1-8.6
Mean±SD	8.0±4.0	7.6±6.6	5.2±4.4	2.2±2.3	0.53±0.4	0.9±1.0	0.5±0.2	0.4±0.2	1.0±0.6	1.5±0.8	2.2±1.4	3.5±2.4
Median	10.0	4.2	4.2	1.5	0.41	0.5	0.5	0.5	0.7	1.5	1.8	2.9
CV(%)	49.8	86.5	85.2	104.1	74.01	113.5	42.0	44.2	67.8	52.4	66.3	68.6
PO_4 (µM)												
Range	0.4-0.6	0.2-1.0	0.01-0.6	0.03-0.3	0.01-0.29	0.01-0.4	0.01-0.2	0.1-0.2	0.01-0.5	0.03-0.4	0.01-0.5	0.1-0.8
Mean±SD	0.5±0.1	0.5±0.2	0.3±0.1	0.1±0.1	0.1±0.07	0.1±0.1	0.1±0.05	0.1±0.1	0.17±0.1	0.2±0.1	0.3±0.2	0.4±0.2
Median	0.5	0.5	0.2	0.2	0.11	0.1	0.1	0.1	0.14	0.2	0.2	0.4
CV(%)	14.0	39.3	51.3	47	71.24	91.7	57.0	52.2	64.0	46.5	56.4	47.3
N/P												
Range	7.0-24.2	0.4-35.2	4.8-52.7	1.5-43.7	0.82-262.5	2.1-316.1	1.1-15.3	3.0-3.9	2.3-78.0	2.7-16.3	0.4-5.2	3.8-21.1
Mean±SD	16.6±8.7	14.7±10.5	18.5±13.2	13.0±12.0	25.71±61.0	17.4±42.4	7.3±3.3	3.4±0.4	8.4±12.2	7.7±2.7	2.2±1.4	9.1±4.6
Median	18.5	9.4	14.6	9.3	4.22	7.5	6.5	3.3	5.3	7.1	1.8	9.0
CV(%)	52.8	71.8	71.7	92.0	237.3	243.6	44.8	12.2	145.0	35.0	66.3	50.2
$Si(OH)_4$ (µM)												
Range	4.6-8.8	1.8-14.1	0.1-5.2	0.1-3.6	0.05-2.68	0.01-3.0	0.01-3.4	1.1-2.9	0.01-4.8	0.1-6.1	0.3-5.5	1.0-9.3
Mean±SD	5.9±1.9	5.2±3.6	1.9±1.5	0.9±0.8	1.04±0.70	0.9±0.9	1.3±1.1	2.1±0.9	1.2±1.1	1.8±1.7	2.7±1.5	4.6±2.7
Median	5.1	3.3	1.8	0.6	0.9	0.6	1.2	2.3	0.7	1.5	3.1	4.3
CV(%)	33	68.3	79.2	88.9	67.52	96.5	84.2	41.9	92.8	92.7	53.5	58.6
Chl-a (µg L^{-1})												
Range	1.01-2.77	0.6-7.9	1.6-9.3	0.6-15.2	0.6-10.9	0.6-9.6	0.6-8.5	0.8-1.5	0.5-7.9	1.0-6.9	0.7-4.6	0.5-3.5
Mean±SD	1.7±0.6	3.9±2.2	5.1±2.3	5.7±3.1	2.9±3.0	2.3±1.7	2.1-1.5	1.1±0.3	1.6±1.2	2.4±1.3	2.5±1.4	1.5±0.9
Median	1.6	3.5	5.1	5.4	1.7	1.8	1.7	0.9	1.3	2.0	2.6	1.3
CV(%)	33.7	56.7	44.3	54.9	102.2	74.1	70.8	32.6	73.5	53.0	56.9	61.2
Rainfall (Kg m^2)												
Range	1.0-2.6	0.0002-5.5	0.1-4.3	0.01-3.2	0.02-4.6	0.02-4.6	0.01-3.8	2.3-2.4	0.05-6.5	0.1-8.0	0.2-4.6	0.05-0.1
Mean±SD	1.8±0.6	1.8±2.1	1.6±1.4	1.6±1.2	1.3±1.4	1.3±1.4	1.0±1.1	2.4±0.0	2.7±2.4	2.7±2.1	2.0-1.7	0.1±0.03
Median	1.7	1.0	1.1	2.5	0.7	0.7	0.6	2.4	2.4	2.4	1.4	0.1
CV(%)	36	117.9	88.2	75.5	103.2	103.2	109.5	0.5	87	77.8	83.3	32.1
Wind stress (Pa)												
Range	0.03-0.1	0.05-0.2	0.02-0.2	0.02-0.1	0.01-0.07	0.01-0.1	0.01-0.1	0.1-0.1	0.02-0.2	0.03-0.1	0.02-0.1	0.05-0.1
Mean±SD	0.1±0.03	0.1±0.1	0.1±0.1	0.04±0.02	0.04±0.02	0.04±0.02	0.04±0.02	0.1±0.0	0.06±0.04	0.1±0.04	0.1±0.03	0.1±0.03
Median	0.05	0.1	0.1	0.04	0.04	0.04	0.03	0.1	0.04	0.1	0.1	0.1
CV(%)	52.6	60.3	69.6	41.6	43.45	42.7	61.1	2.5	70.3	49.2	42.9	32.1

Table S2.3. *Permutation test for distance-based redundancy analysis (db-RDA) under the reduced model of phytoplankton communities based on metabarcoding data in relation to environmental variables in the eastern English Channel at the SOMLIT and DYPHYRAD stations from March 2016 to October 2020. P-value significant codes: 0 '***', 0.001 '**', 0.01 '*', 0.05 '.', 0.1, ' ' 1.*

Parameter	Unit	df	Sum of squares	Pseudo-F	Pseudo-r^2	p-value
PAR_{10m}	E m^{-2} d^{-1}	1	6.49	21.53	0.001	***
SST	^{o}C	1	5.43	18.05	0.001	***
SSU	nu	1	0.75	2.49	0.002	**
NO2+NO3	µM	1	1.39	4.62	0.001	***
PO4	µM	1	0.91	3.03	0.001	***
SiO4	µM	1	0.75	2.49	0.001	***
Chla	mg L^{-1}	1	0.81	2.68	0.001	***
Rainfall	Kg m^2	1	0.52	1.73	0.02	*
Wind Stress	Pa	1	0.49	1.62	0.029	*
Residual	235	70.65				

Table S2.4. *Permutation test for distance-based redundancy analysis (db-RDA) under the reduced model of phytoplankton communities based on morphological data in relation to environmental variables in the eastern English Channel at the SOMLIT and DYPHYRAD stations from March 2016 to October 2020. P-value significant codes: 0 '***', 0.001 '**', 0.01 '*', 0.05 '.', 0.1 ' ', 1.*

Parameter	Unit	df	Sum of squares	Pseudo-F	Pseudo-r^2	p-value
PAR_{10m}	E m^{-2} d^{-1}	1	7.47	23.50	0.001	***
T	^{o}C	1	3.14	9.88	0.001	***
S	nu	1	0.40	1.25	0.210	n.s.
NO_2+NO_3	µM	1	0.94	2.95	0.001	***
PO_4	µM	1	1.40	4.41	0.001	***
$Si(OH)_4$	µM	1	0.76	2.10	0.013	*
Chl-a	µg L^{-1}	1	1.63	5.12	0.001	***
Rainfall	Kg m^2	1	0.86	2.71	0.003	**
Wind Stress	Pa	1	0.57	1.79	0.035	*
Residual		212	67.38			

Table S2.5. *The relative contribution of each ecological process in community assembly is presented by the percentage per month (see also Fig. 2.6).*

Month	Heterogeneous selection	**Homogeneous selection**	Dispersal limitation	Homogeneous dispersal	**Drift**
January	0	**83**	17	0	0
Fabruary	0	**52**	8	19	19
March	0	**54**	4	11	31
April	1	8	11	11	**69**
May	0	2	6	6	**87**
June	0	3	16	10	**72**
July	1	12	8	4	**75**
August	0	0	33	33	33
September	2	**38**	4	4	**52**
October	0	**30**	2	8	**60**
November	0	**28**	1	7	**65**
December	0	**25**	4	10	**61**

Table S2.6. *Permutational multivariate analysis of variance (PERMANOVA) between the phylogenetic community structure of eukaryotic phytoplankton (NRI) and the environmental variables measured in the eastern English Channel at the SOMLIT and DYPHYRAD stations from March 2016 to October 2020. P-value significant codes: 0 '***', 0.001 '**', 0.01 '*', 0.05 '.',0.1, ' ' 1.*

Phylogenetic structure (NRI)						
Parameter	Unit	df	Sum of squares	R^2	F	p-value
PAR_{10m}	E m^{-2} d^{-1}	1	0.69	0.02	7.76	***
T	^{o}C	1	2.48	0.07	27.95	***
S	nu	1	0.17	0.006	1.96	
NO_2+NO_3	µM	1	0.12	0.004	1.36	
PO_4	µM	1	0.15	0.005	1.67	
$Si(OH)_4$	µM	1	0.05	0.001	0.51	
Rainfall	Kg m^2	1	0.14	0.004	1.53	
Wind Stress	Pa	1	0.005	0.005	1.77	
Residual		236	21.98	0.670		
Total		244	31.13	1.00		

Table S2.7. *Permutational multivariate analysis of variance (PERMANOVA) between the phylogenetic community turnover of eukaryotic phytoplankton (betaNRI) and environmental variables measured in the eastern English Channel at the SOMLIT and DYPHYRAD stations from March 2016 to October 2020. P-value significant codes: 0 '***', 0.001 '**', 0.01 '*', 0.05 '.',0.1, ' ' 1.*

Phylogenetic turnover (betaNRI)						
Parameter	Unit	df	Sum of squares	R^2	F	p-value
PAR_{10m}	E m^{-2} d^{-1}	1	1.60	0.05	13.05	***
T	^{o}C	1	2.27	0.07	18.55	***
S	nu	1	0.07	0.002	0.63	
NO_2+NO_3	µM	1	0.02	0.001	0.14	
PO_4	µM	1	0.06	0.002	0.52	
$Si(OH)_4$	µM	1	0.05	0.001	0.37	
Rainfall	Kg m^2	1	0.19	0.006	1.59	
Wind Stress	Pa	1	0.10	0.003	0.79	
Residual		236	28.85	0.87		
Total		244	33.58	1.00		

Supplementary Figures

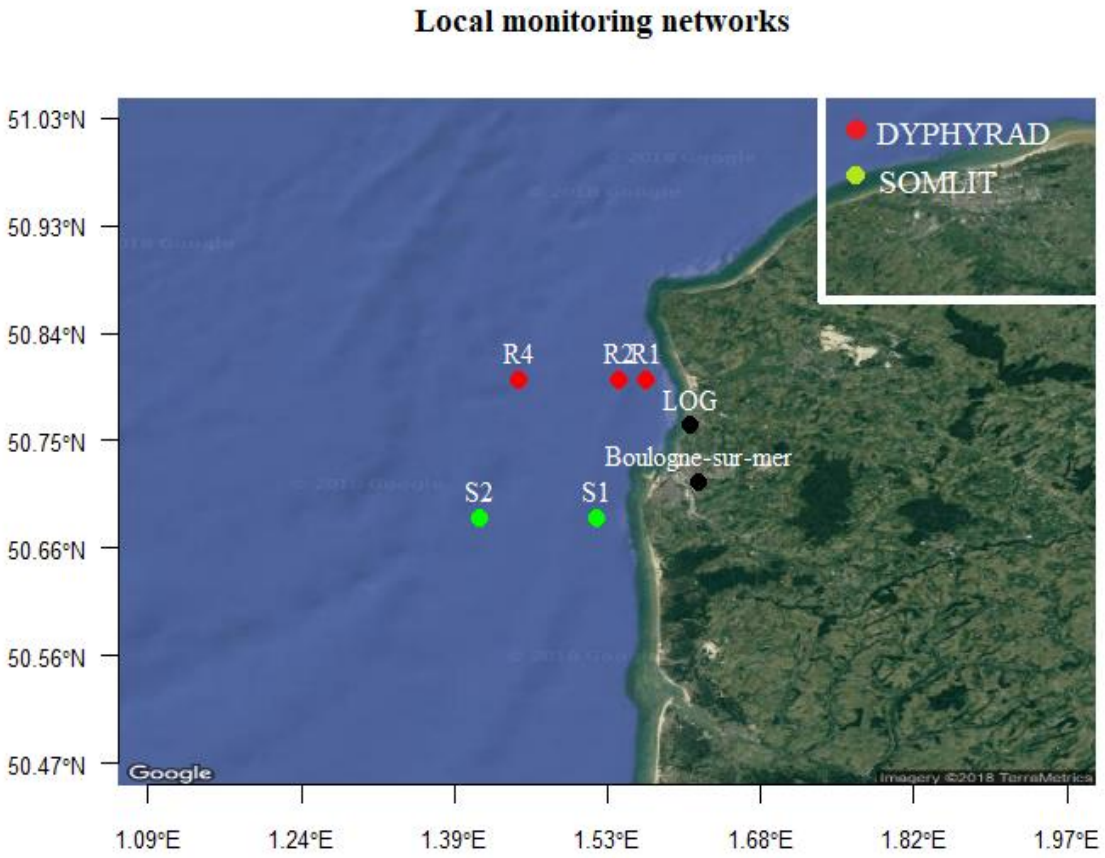

Figure S2.1. *Location of the SOMLIT (S1, S2) and DYPHYRAD (R1, R2, R4) stations in the eastern English Channel (map creation with R software using the package Googlemap).*

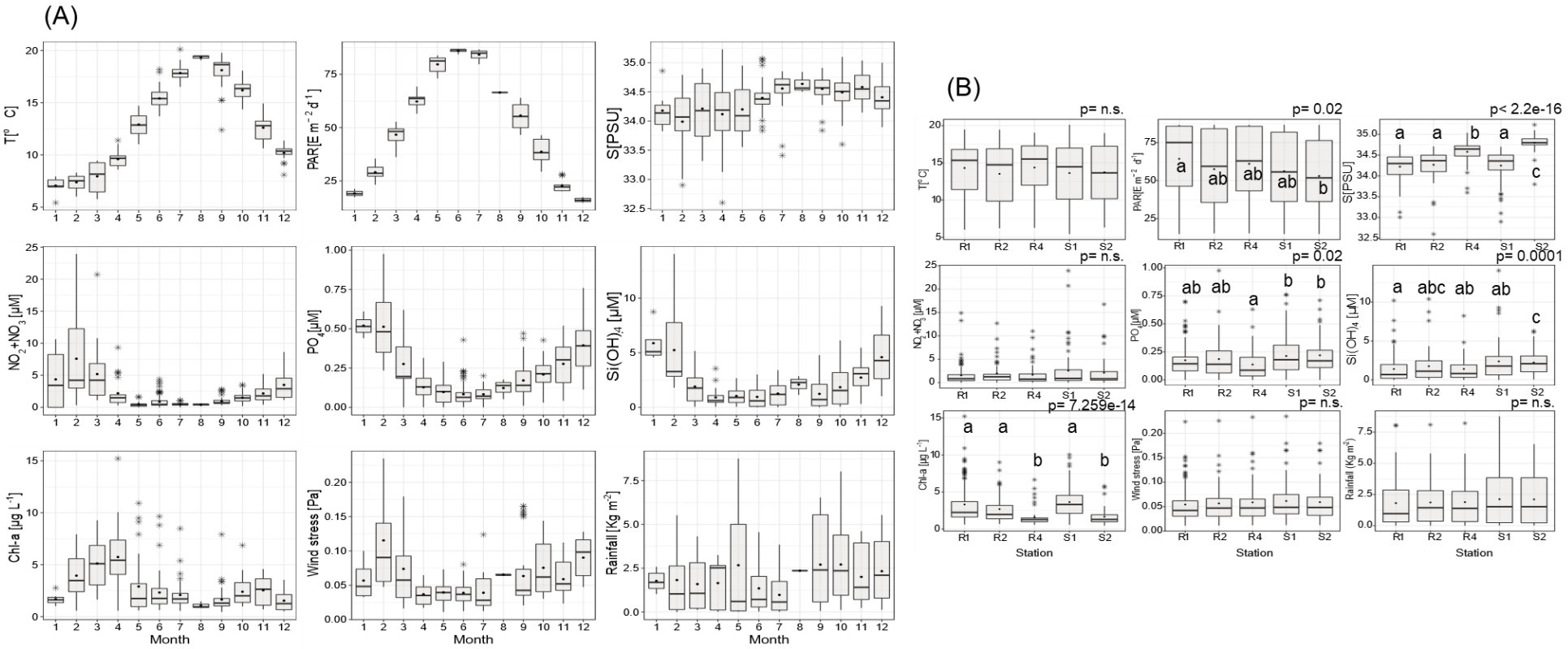

Figure S2.2. *(A) Monthly variations of the environmental variables: Temperature (T, °C), Photosynthetic Active Radiation (PAR, E m^{-2} d^{-1}), Salinity (S, PSU), nitrite and nitrate (NO_2+NO_3 µM), phosphate (PO_4, µM), silicate ($Si(OH)_4$, µM), chlorophyll-a (Chl-a, µg L^{-1}), wind stress (Pa), rainfall (Kg m^{-2}) (B) Spatial variations of the environmental variables measured in the eastern English Channel at the DYPHYRAD and SOMLIT stations from March 2016 to October 2020. The letters indicate significant differences ($p < 0.05$) between stations based on Kruskal-Wallis and Nemenyi post-hoc test on the top of the graphs. Solid black lines represent the median, black dots the mean and the black stars the outliers.*

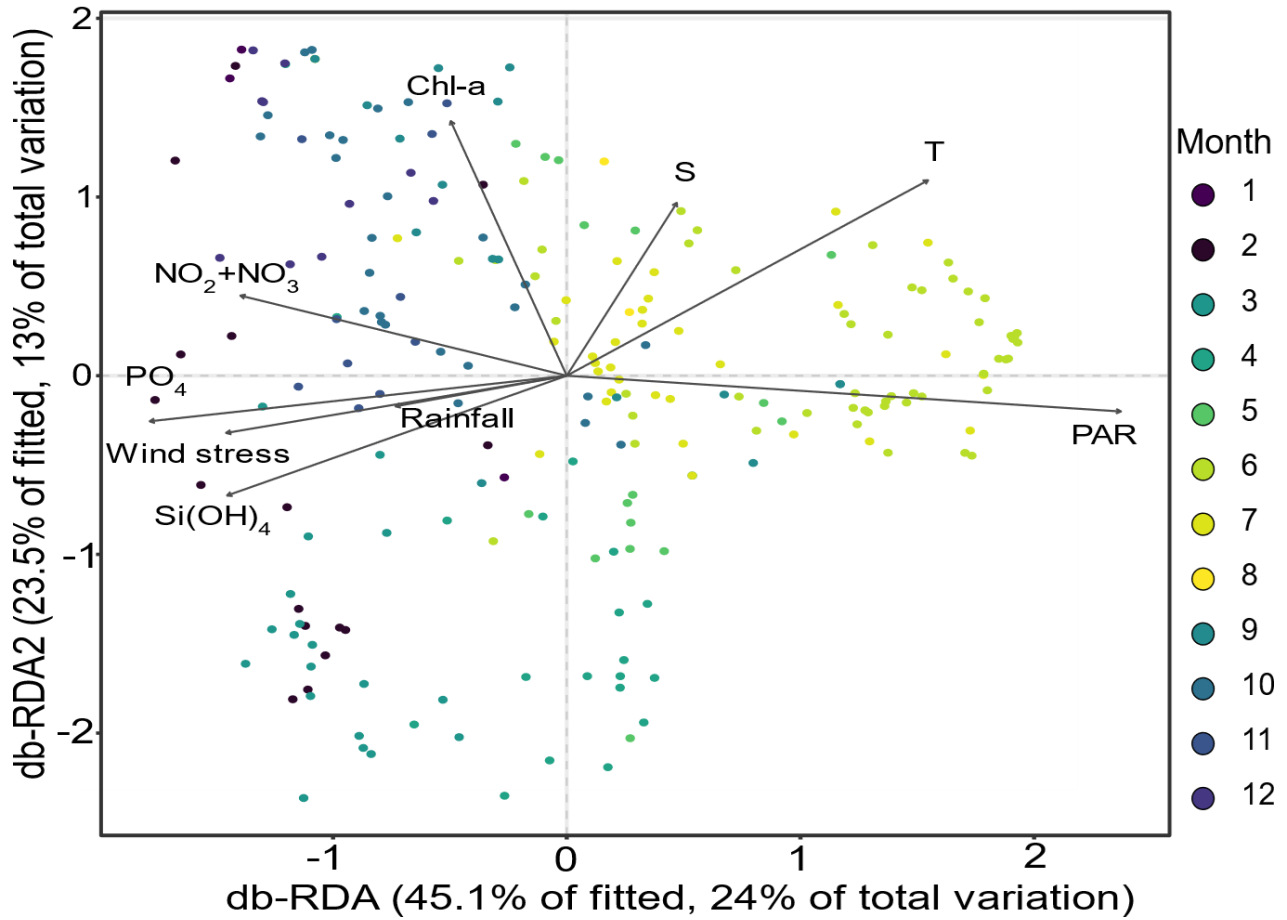

Figure S2.3. *Distance-based redundancy (db-RDA) ordination plot of the phytoplankton communities based on morphological data (coloured dots with colour varying according to the months) to explore the link between the structure of the phytoplankton communities and the environmental variables (black arrows; temperature (T, °C), Photosynthetic Active Radiation (PAR, E m^{-2} d^{-1}), salinity (S, PSU), nitrite and nitrate (NO_2+NO_3 µM), phosphate (PO_4, µM), silicate ($Si(OH)_4$, µM), chlorophyll-a (Chl-a, µg L^{-1}), wind stress (Pa), rainfall (Kg m^{-2}) measured in the eastern English Channel at the DYPHYRAD and SOMLIT stations from March 2016 to October 2020.*

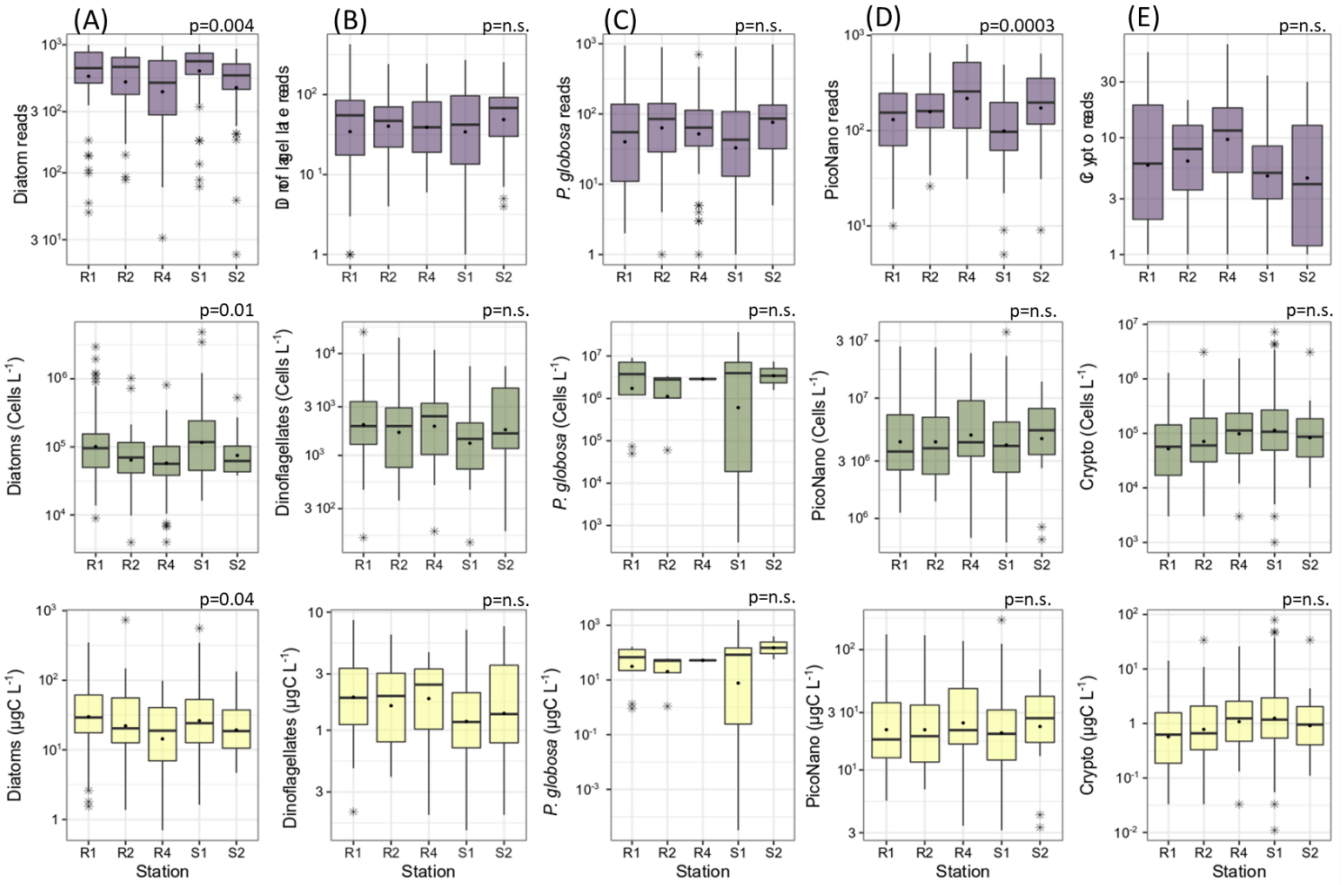

Figure S2.4. *Spatial variations of the number of reads (purple), abundance (number of cell cell L^{-1}, in green) and biomass (µgC L^{-1}, in yellow) of the different phytoplankton groups (A: diatoms, B: dinoflagellates, C: P. globosa, D: pico- nanophytoplankton (PicoNano), and E: cryptophytes) identified in the eastern English Channel from March 2016 to October 2020. The letters indicate significant differences ($p < 0.05$) between stations based on Kruskal-Wallis and Nemenyi post-hoc test. Solid black lines represent the median, black dots the mean and the black stars the outliers.*

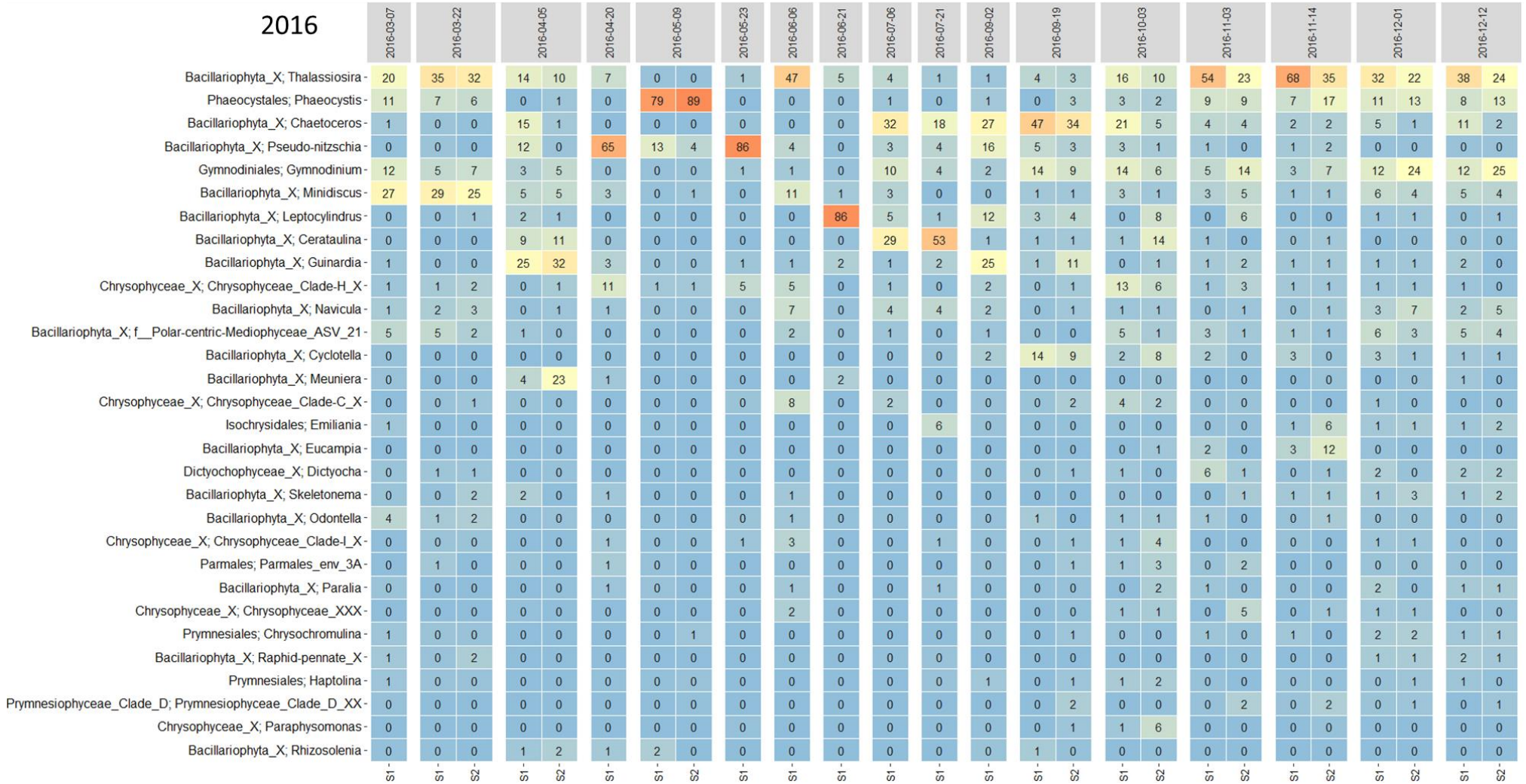

Figure S2.5. *Heatmap illustrating the relative abundance of reads of the 30 most abundant phytoplankton genera (i.e., contributing to at least 0.5 % of reads in the whole data set), occurring in the eastern English Channel at the SOMLIT (S1, S2) stations in 2016.*

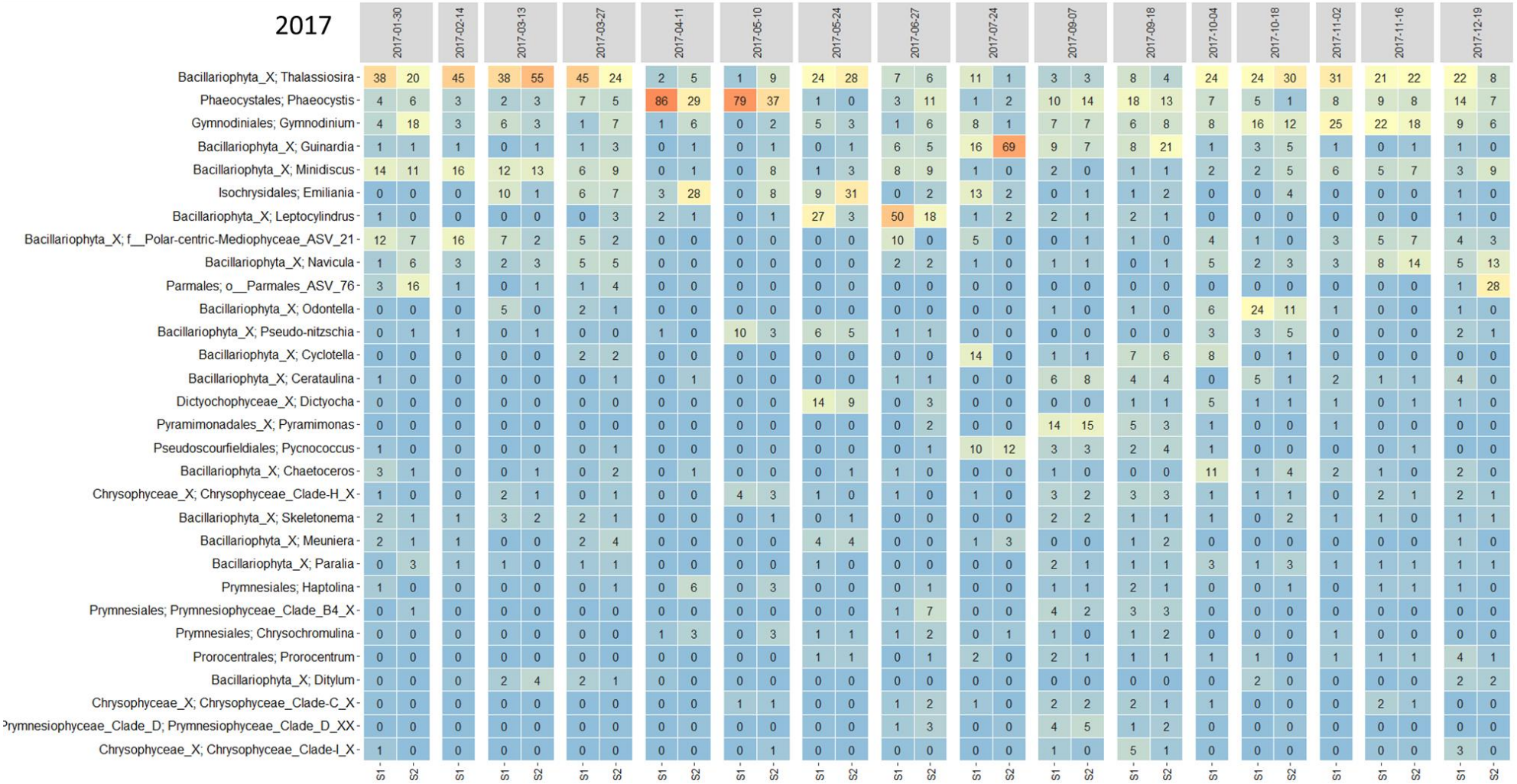

Figure S2.6. *Heatmap illustrating the relative abundance of reads of the 30 most abundant phytoplankton genera (i.e., contributing to at least 0.5 % of reads in the whole data set), occurring in the eastern English Channel at the SOMLIT (S1, S2) stations in 2017.*

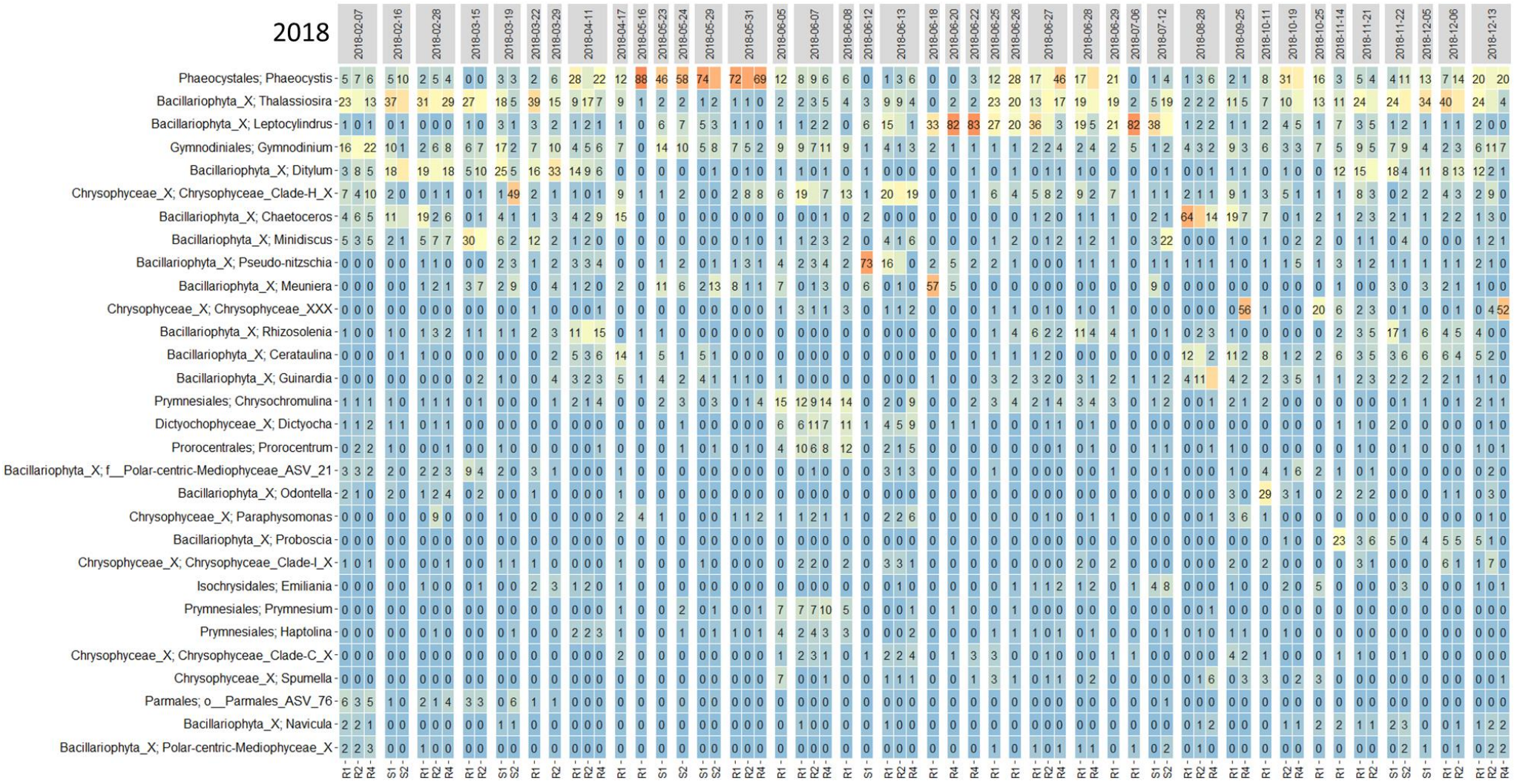

Figure S2.7. *Heatmap illustrating the relative abundance of reads of the 30 most abundant phytoplankton genera (i.e., contributing to at least 0.5 % of reads in the whole data set), occurring in the eastern English Channel at the SOMLIT (S1, S2) and DYPHYRAD (R1, R2, R4) stations in 2018.*

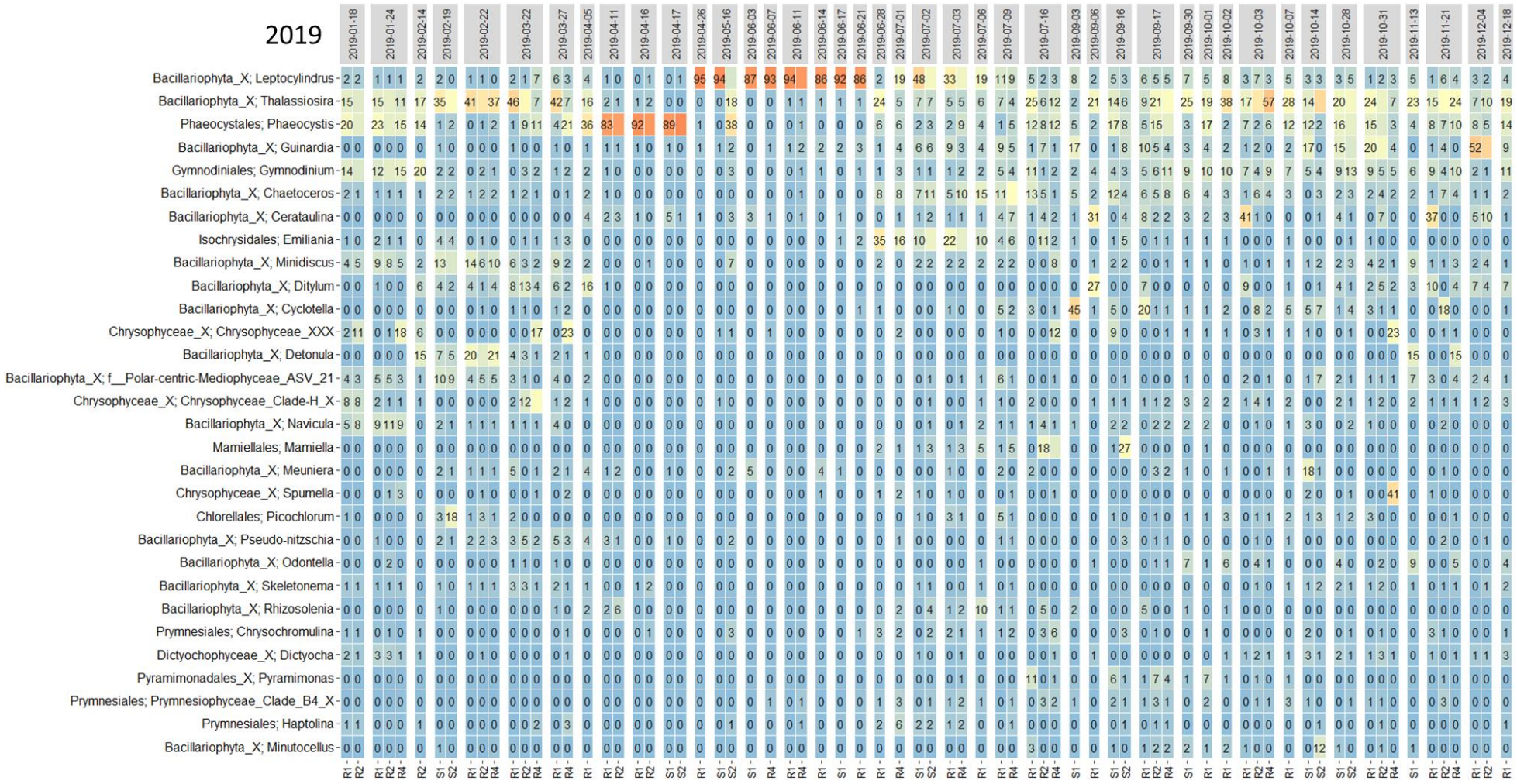

Figure S2.8. *Heatmap illustrating the relative abundance of reads of the 30 most abundant phytoplankton genera (i.e., contributing to at least 0.5 % of reads in the whole data set), occurring in the eastern English Channel at the SOMLIT (S1, S2) and DYPHYRAD (R1, R2, R4) stations in 2019.*

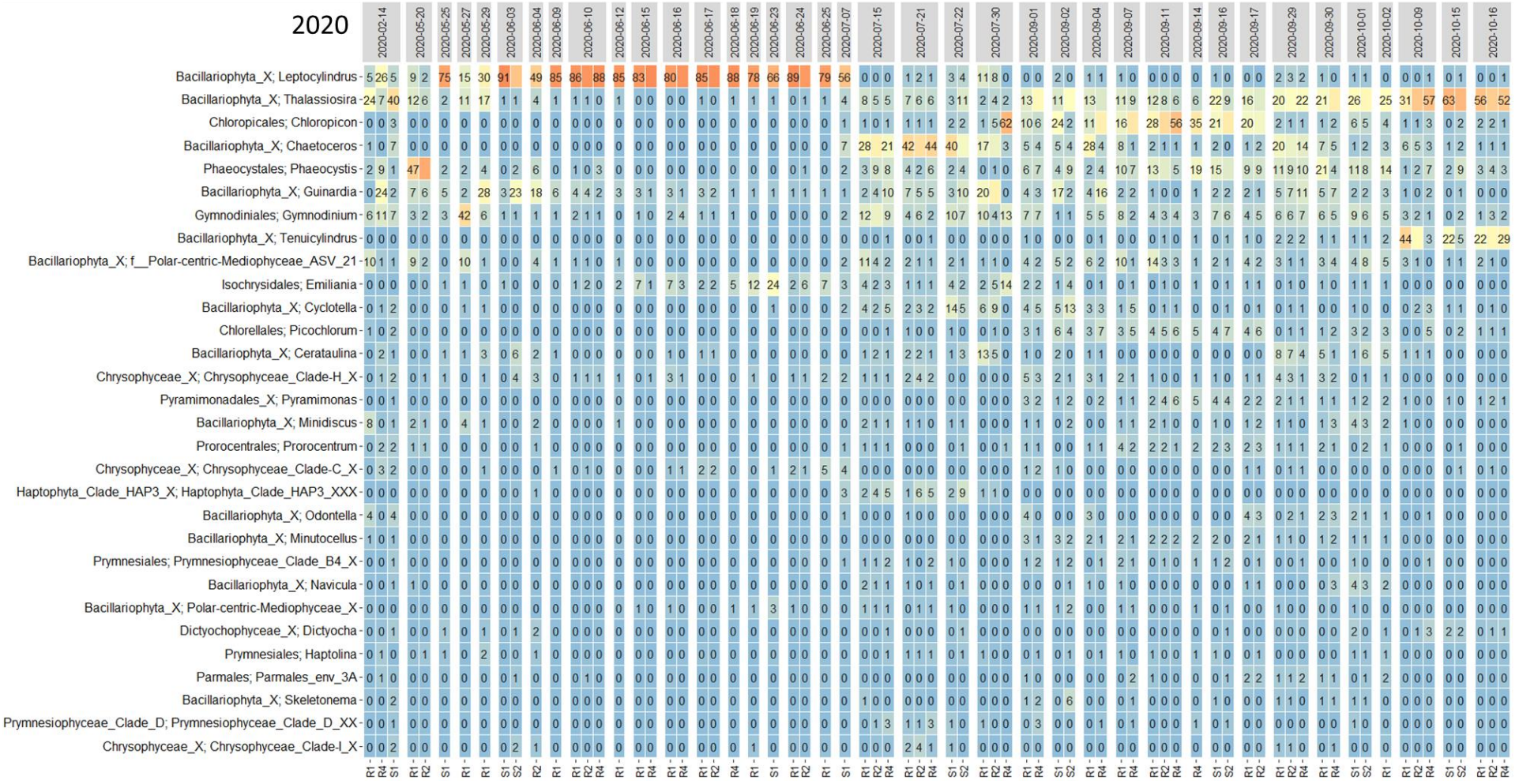

Figure S2.9. *Heatmap illustrating the relative abundance of reads of the 30 most abundant phytoplankton genera (i.e., contributing to at least 0.5 % of reads in the whole data set), occurring in the eastern English Channel at the SOMLIT (S1, S2) and DYPHYRAD (R1, R2, R4) stations in 2020.*

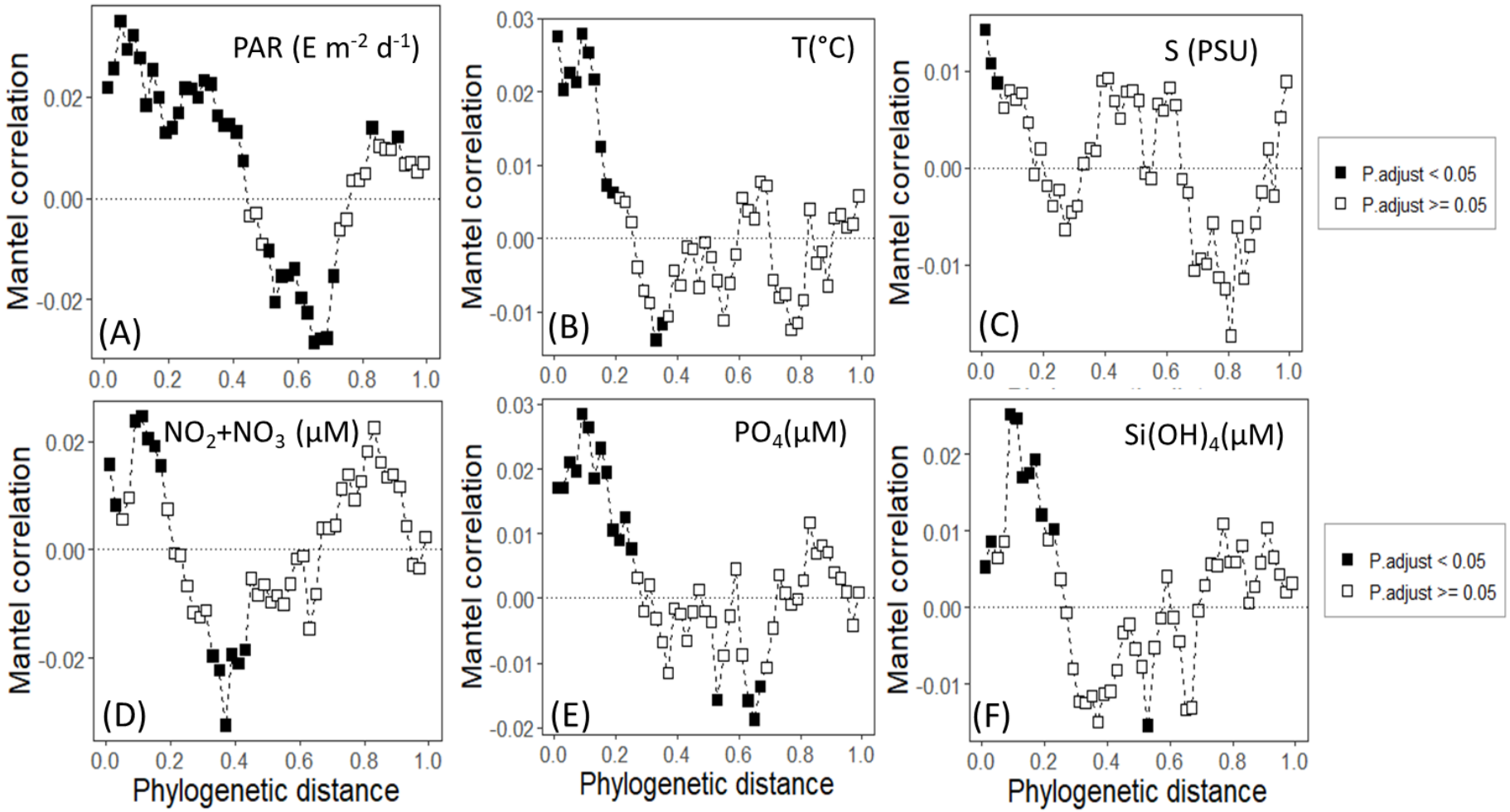

Figure S2.10. *Exploration of the phylogenetic signal of the phytoplankton communities in the eastern English Channel at the SOMLIT and DYPHYRAD stations from March 2016 to October 2020 through Mantel correlograms between the Euclidean distance matrix of ASVs environmental optima for (A) Photosynthetic Active Radiation (PAR, E m^{-2} d^{-1}), (B) temperature (T, °C), (C) salinity (S, PSU), (D) nitrite and nitrate (NO_2+NO_3 µM), (E) phosphate (PO_4, µM), (F) silicate ($Si(OH)_4$, µM), and the phylogenetic distance matrix. Black and white squares indicate significant ($p<0.05$) and non-significant correlation values, respectively.*

Chapter 3: Bacterial dynamics and interactions with phytoplankton

Preamble

One of the most important interaction in microbial communities concerns phytoplankton and heterotrophic bacteria, and can span from cooperative to competitive (Seymour *et al.*, 2017). The rapid responses of bacteria are directly linked to changes in their physicochemical and biological environment, even if their community structure can be relatively predictable (e.g., review Fuhrman *et al.*, 2015). Bacteria therefore represent the biological intermediate link between physicochemical changes in the environment and phytoplanktonic community responses. However, in the EEC the study of bacteria communities in relation to phytoplankton has been overlooked with the last study dating 14 years ago. In this chapter, microscopy data were used to describe diatom communities and *P. globosa*, and metabarcoding data to describe heterotrophic bacterial communities over five years. Extended local similarity (eLSA) network analysis was applied to identify potential relationships with *P. globosa* and diatom blooms.

Bacterial dynamics and interactions during distinct phytoplankton blooms in temperate coastal waters

Keywords: Bacteria, diatoms, *Phaeocystis globosa*, interactions, network analysis

This chapter is a draft paper

Résumé en français

Cette étude a visé à contribuer à notre compréhension des interactions complexes entre le phytoplancton et les bactéries hétérotrophes dans les écosystèmes côtiers. Pour cela, la dynamique du phytoplancton et des bactéries hétérotrophes a été étudié en combinant le séquençage 16S rDNA, la microscopie et la cytométrie en flux dans un écosystème côtier mésotrophe sur une période de cinq ans (soit 282 échantillons). Cette étude s'est concentrée sur deux groupes de phytoplancton concurrents et phylogénétiquement éloignés (les Haptophytes, i.e., *P. globosa*, et les Bacillariophyta, i.e., les diatomées). L'analyse eLSA a été utilisée pour construire des réseaux pendant les périodes sans efflorescences et les périodes d'efflorescences. Dans l'ensemble, les résultats de cette étude ont mis en évidence l'importance des interactions saisonnières et spécifiques. L'hiver a été caractérisé par des communautés riches et diversifiées de diatomées, le printemps par des efflorescences de *P. globosa*, tandis que l'été était marqué par de courtes efflorescences monospécifiques de diatomées. L'hiver a montré des communautés bactériennes interconnectées, indiquant une dégradation synergique de divers substrats dérivés du phytoplancton. Au printemps, malgré des variations dans l'intensité des efflorescences de *P. globosa*, la composition des communautés bactériennes est restée constante d'une année à l'autre, suggérant l'établissement d'un environnement stable pour les communautés bactériennes pendant ces efflorescences. En été, des associations spécifiques entre les efflorescences transitoires monospécifiques de diatomées et les bactéries hétérotrophes ont été observées.

Abstract

Marine phytoplankton and bacteria form the foundation of marine food webs. The specific interactions taking place between phytoplankton and bacteria have been mainly focused in diatom blooms. This study aimed to contribute to our understanding of the intricate interactions between phytoplankton and bacteria in coastal ecosystems. For this we studied the dynamics of phytoplankton and heterotrophic bacteria combining 16S rDNA amplicon sequencing,

microscopy and flow cytometry in a meso-eutrophic coastal ecosystem over a period of five years (i.e., 282 samples). We focused on two competing and phylogenetically distant phytoplankton groups (Haptophytes (i.e., *Phaeocystis globosa*) and Bacillariophyta (diatoms)). We applied extended local similarity analysis (eLSA) to construct networks during non-blooming and blooming periods. Overall, our results highlighted the importance of seasonal and species-specific interactions between phytoplankton and evidenced the bacterial community dynamics in the EEC. Winter was characterised by a rich and diverse diatom communities, spring by *P. globosa* blooms, while summer by short monospecific diatom blooms. Winter showed interconnected bacterial communities, indicating a synergistic degradation of diverse phytoplankton-derived substrates. In spring, despite variations in the intensity of *P. globosa* blooms, the composition of bacterial communities remained consistent across years, suggesting the establishment of stable-state environment for bacterial communities during these blooms. In summer, specific associations between transient monospecific diatom blooms and heterotrophic bacteria were observed.

3.1. Introduction

Despite making up only 0.2% of the total biomass of primary producers on earth, marine phytoplankton contributes up to 50% of global primary production (Falkowski *et al*., 1998; Field *et al*., 1998). Heterotrophic bacteria in the marine environment are responsible for remineralizing at least half of this production (Azam *et al.*, 1983). The abundance, diversity, and functions of these microorganisms are influenced by various factors, including temperature, light, nutrient availability, and biotic interactions (review Fuhrman 2015). The latter are increasingly recognised as the determinant force modulating microbial community structure and function (e.g., Genitsaris *et al.*, 2015; Lima-Mendez *et al.*, 2015).

Thus, the interactions between heterotrophic bacteria and phytoplankton represent a fundamental ecological relationship in marine ecosystems (review Seymour *et al.*, 2017). Interactions span the spectrum of ecological relationships from cooperative to competitive (Amin *et al.*, 2012). For example, a typically cooperative (i.e., mutualistic) relationship concerns the release of dissolved organic carbon by phytoplankton, which provides carbon and energy to bacteria. In return, bacteria can facilitate access to nutrients, including vitamins, to support phytoplankton growth (e.g., Durham *et al.*, 2015). The interactions of these two biological compartments strongly influence nutrient cycling and biomass production and affect carbon and oxygen fluxes (Cole, 1982; Azam and Malfatti, 2007). While on the other side of

the spectrum, algicidal bacteria induce negative effects on phytoplankton targets (Mayali and Azam, 2004; Meyer *et al.*, 2017).

The associations between phytoplankton and bacteria have been explored through experimental and *in situ* studies (e.g., Lelong *et al.*, 2012; Delmont *et al.*, 2014; Amin *et al.*, 2015; Cooper and Smith, 2015; Durham *et al.*, 2015). Experimental studies have evidenced important roles through species-specific associations. For example, using the exudates of diatom species as a growth substrate allowed to establish specific links between the substrate preferences of several bacteria (Landa *et al.*, 2016). *In situ* studies have investigated heterotrophic bacterial dynamics, and have shown predictable recurrent seasonal patterns at taxonomic and functional levels, in oligotrophic and eutrophic ecosystems (Teeling *et al.*, 2012, 2016; Chafee *et al.*, 2018; Auladell *et al.*, 2023). These patterns were influenced by abiotic factors including temperature, stratification, mixed layer depth, nutrients and winds, as well as, biotic factors including phytoplankton blooms (e.g., Buchan *et al.*, 2014; Teeling *et al.*, 2016; Bunse and Pinhassi, 2017).

Processing phytoplankton-derived organic matter requires diverse heterotrophic bacteria with different adaptive strategies (Buchan *et al.*, 2014). Heterotrophic bacteria are generally distinguished as either oligotrophs or copiotrophs. (Koch, 2001; Lauro *et al.*, 2009). Oligotrophs grow in low labile organic matter environments such as winter and deep offshore waters, while copiotrophs develop during high productivity periods such as phytoplankton blooms (e.g., Giovannoni *et al.*, 2014; Lemonnier *et al.*, 2020). They also present different degrees of ecological specialization, with generalist bacteria being able to assimilate broad range of substrates, while specialists can only assimilate a narrow range of substrates (e.g., Mou *et al.*, 2008).

Actually, the majority of our knowledge regarding the influence of phytoplankton blooms on bacteria dynamics is related to diatom-dominated blooms. (e.g., Teeling *et al.*, 2012, 2016; Chafee *et al.*, 2018; Arandia-Gorostidi *et al.*, 2022). This is due to the ecological significance of diatoms on a global scale (e.g., Tréguer *et al.*, 2018). It remains unclear whether similar patterns are extended to other phytoplankton, particularly those that may compete with diatoms. *Phaeocystis globosa* typically competes with diatoms and often dominates spring blooms in coastal waters (e.g., Peperzak *et al.*, 1998). *P. globosa* can form colonies of cells embedded in a mucopolysaccharide matrix reaching up to a centimetre in diameter (review, Schoemann *et al.*, 2005). Specific polysaccharides define which bacteria are attracted to

colonize the organic matter excreted by phytoplankton (e.g, review, Mühlenbruch *et al.*, 2018). The availability of distinct polysaccharides in the *Phaeocystis* colony matrix, along with other chemical properties, such as the presence of amino-sugars and abundant dimethylsulfoniopropionate (DMSP), suggest that a unique bacterial consortium thrive in the *Phaeocystis* microenvironment (Solomon *et al.*, 2003; Shen *et al.*, 2011; Mars Brisbin *et al.*, 2022). The few existing studies focused on *P. globosa* and associated bacteria showed drastic shifts in bacteria composition and activity at different phases of the bloom, however these studies conducted in short period of time (less than a year; Alderkamp *et al.*, 2006; Lamy *et al.*, 2009; Gibson *et al.*, 2022).

The present study aimed to improve our understanding relative to phytoplankton and heterotrophic bacterial communities in particular during blooming periods. For this, phytoplankton and heterotrophic bacteria dynamics were investigated in the coastal waters of the meso-eutrophic Eastern English Channel (EEC) characterized by blooms of two phylogenetically distant and competing groups, Haptophytes (i.e., *Phaeocystis globosa*) and Bacillariophyta (diatoms). The phytoplankton succession in this area is characterized by a rich diatom winter community, recurrent *P. globosa* bloom in spring (e.g., Breton *et al.*, 2006), showing variable blooming intensities across years (Houliez *et al.*, 2023), and transient diatom blooms in summer (Skouroliakou *et al.*, 2022). It remains to determine whether variable blooming intensities of *P. globosa* exhibit similar bacteria structures on multiple years, and whether they are comparable to those of diatom blooms. It is noteworthy that there are only few studies on bacterial dynamics in the EEC, with the last one dating 14 years ago extended on small temporal scale during the growth, bloom, and senescence phases of *P. globosa* bloom (four months; Lamy *et al.*, 2009). Our objective here was to describe bacteria interannual patterns and taxon-specific relationships between bacteria and phytoplankton on a pluriannual scale. We hypothesized that bacterial seasonal community structure was associated with different seasonal phytoplankton communities, but also affected by *P. globosa* and transient summer diatom blooms. The temporal patterns of phytoplankton and bacterial communities were investigated using microscopy, flow cytometry, and 16S rRNA gene amplicon sequencing at the surface coastal waters of the EEC from 2016 to 2020 (i.e., 282 samples). The extended local Similarity Analysis (eLSA) was used to investigate potential relations between phytoplankton and bacteria.

3.2. Material and methods

3.2.1. Sampling

Subsurface seawater samples were collected (2 m depth) at five neighboring stations in the EEC (Fig. S3.1). From 2016 to 2020, the SOMLIT (French Network of Coastal Observatories; https://www.somlit.fr/) coastal S1 and offshore S2 stations were sampled on a bi-weekly basis. From 2018 to 2020 the sampling effort was intensified with weekly samplings at three additional stations (R1, R2, and R4) from the local monitoring transect 'DYPHYRAD' situated approximately 15 km north of the SOMLIT stations (Fig. S3.1, Table S3.1). Higher frequency samplings (2-3 times per week) were also carried out after the end of the spring bloom in June-July and in autumn September-October at stations R1-R4. The higher frequency was applied to catch rapidly changing heterotrophic bacteria and phytoplankton dynamics. The post-spring bloom period (June-July) was chosen because high bacterial abundance and activity were observed after a *P. globosa* bloom (e.g., Lamy *et al.*, 2009), as well as high diatom abundance and biomass (e.g., Breton *et al.*, 2017). High frequency sampling was carried out in September and October because it is a transitional period from summer to winter conditions (e.g., Breton, 2000). Only three samples were collected in August due to the unavailability of the boat during this month. For this reason, the August data are presented but not further discussed.

3.2.2. Environmental variables

Sea surface temperature (T, °C) and salinity (S, PSU) were measured in situ with a CTD Seabird profiler (SBE 25). The average subsurface daily PAR experienced by phytoplankton in the water column for six days before sampling was obtained using global solar radiation (GSR, Wh m^{-2}) recorded by the Copernicus Atmosphere Monitoring Service (CAMS) radiation service (http://www.soda-pro.com/web-services/radiation/cams-radiation-service). GSR was converted into PAR by assuming PAR to be 50% of GSR and by considering 1 W m^{-2} = 0.36 E m^{-2} d^{-1} (Morel and Smith 1974). Seawater macronutrient concentrations, nitrate, (NO_3^-), nitrite (NO_2^-), phosphate (PO_4^{3-}), and silicate ($Si(OH)_4$) were analyzed according to Aminot and Kérouel (2004). Chlorophyll-a (Chl-a) concentration was measured by fluorometry as described in (Lorenzen 1966). Additional details on environmental data acquisition and analysis can be found at https://www.somlit.fr/en/.

3.2.3. Phytoplankton

For diatoms and *P. globosa* (colonies, free flagellate, and colonial cells) counting, 110 mL water samples were collected and fixed with Lugol's-glutaraldehyde solution (1% v/v, which does not disrupt *P. globosa*'s colonies (Breton *et al.*, 2006). Phytoplankton species

were identified to the genus or species level when possible, using an inverted microscope (Nikon Eclipse TE2000-S) at 100-400x magnification, after sedimentation for 24 h in a 10 mL Hydrobios chamber (e.g., Breton *et al*., 2021). Biovolumes were estimated based on standard geometric forms according to (Hillebrand *et al.*, 1999). Then, the carbon-biovolume relationships were assessed according to (Menden-Deuer and Lessard, 2000; Schoemann *et al.*, 2005; see Table S3.2).

The bloom periods were defined based on abundance data according to the IFREMER REPHY/REPHYTOX thresholds based on 30-year data at the French coasts including those of the EEC (REPHY/REPHYTOX station is situated 2 km west of the R1 station; https://www.phytobs.fr/Stations/Boulogne). These thresholds were $\geq 10^5$, or $\geq 10^6$ for diatoms (depending on the species), and $\geq 10^6$ for *Phaeocystis globosa* (Belin *et al.*, 2021).

3.2.4. Heterotrophic bacteria

Samples for heterotrophic bacteria (1.5 mL) were fixed with paraformaldehyde (PFA) at a final concentration of 1%, then stored at 4°C for 40 min, flash frozen in liquid nitrogen, and then kept at -80°C until analysis. Heterotrophic bacteria were stained with SYBR Green I (Marie *et al.*, 1999) and enumerated by flow cytometry with a CytoFlex cytometer (Beckman Coulter).

For diversity, four to seven litres of seawater were first screened through 150 µm nylon mesh (Millipore, U.S.A.) to remove metazoans, and then filtered on 0.2 µm polyethersulfone (PES) membrane filters (142 mm, Millipore, U.S.A.). Filters were stored at -80°C for 16S rRNA genes amplicon Illumina MiSeq 2x300 bp sequencing. A quarter of the PES filter was used for DNA extraction following the DNAeasy PowerSoil Pro kit (Qiagen, Germany) manufacturer's protocol. Then the 16S rRNA gene V3-V4 region was amplified with the primers 341F (CCTACGGGNGGCWGCAG) and 785R (GACTACHVGGGTATCTAATCC) (Klindworth *et al.*, 2013). The library preparation was performed in a laminar flow hood, and all materials were exposed to UV light for 30 minutes before use to eliminate contamination. Additionally, the PCR decontamination kit (OZYME, France) was used to remove contaminating DNA from the PCR master mix. All PCRs were performed on four replicates before being pooled together. PCR products were purified using the QIAquick kit and then the DNA quantity was measured using the Qubit dsDNA HS assay kit. Pooled purified amplicons were then paired-end sequenced on an Illumina MiSeq 2 X 300 platform (Genewiz South Plainfield, NJ, USA, approximate sequencing depth: 50K reads/sample).

After sequencing, quality filtering of reads, identification of amplicon sequencing variants (ASV), and taxonomic affiliation based on the SILVA database (release 138.1; Quast *et al.*,

2013) were processed with the R-package DADA2 (v.1.20.0; (Callahan *et al.*, 2017). A total number of 34,508 ASVs were identified from 11,294,899 reads in 282 samples. For this study only ASVs affiliated to heterotrophic bacteria were kept. Several filtering steps of the dataset were done with the package phyloseq (McMurdie and Holmes, 2013). The ASVs that were taxonomically unclassified at Phylum rank or were not assigned to bacterial lineages were excluded from further analysis. Furthermore, ASVs assigned to mitochondria, chloroplast, and autotrophic bacteria (i.e., Cyanobacteria and Chloroflexi) were removed from the dataset. Singletons were additionally excluded and the dataset was rarefied at the lowest number of reads (8,000). Out of a total of 282 samples 26 were excluded from the analysis with less than 8000 reads, resulting in 2,071,296 reads corresponding to 9,745 ASVs, in 256 samples. Raw sequencing data have been submitted to the Short Read Archive under BioProject number: PRJNA917476.

3.2.5. Statistical analyses

All statistical analyses and data visualizations were performed in R version 4.1.0. (R Core Team, 2021). To illustrate seasonal variations of environmental variables, heterotrophic bacteria, diatom and *P. globosa* counts, boxplots were constructed with the ggplot2 package (Wickham, 2016). Seasonal patterns were further explored with the distance-based RDA analysis using the microeco package (Liu *et al.*, 2021). To illustrate the composition of bacteria in family and genus level and phytoplankton taxa bar plots, bubble plots, and heatmaps were built with ggplot2 and amvis2 packages (Wickham, 2016; Andersen *et al.*, 2018). Bacterial community structures were described at the family and genus levels. Alpha diversity indices (Richness, Shannon, Simpson (1-D)) were calculated after rarefying the read depths based on the sample with the lowest reads count (i.e., 8,000 reads) with the package microeco (Liu *et al.*, 2021).

3.2.6. Network analysis

Sixty-nine samples from stations S1 and R1, which were most frequently sampled (Table S3.1), were chosen for the network analysis. Thirty-eight samples corresponded to dates when blooms occurred in spring and summer (from March to July), and thirty-one winter samples (from December to February) corresponded to a reference non-blooming period. The extended local similarity analysis (eLSA) was used to assess significant positive and negative correlations among: i) dominant bacteria at genus taxonomic level (i.e., ≥ 1% number of reads in the 69 selected samples), ii) environmental variables including nutrients (NO_2, NO_3, PO_4, $Si(OH)_4$),

PAR and temperature, and iii) dominant phytoplankton taxa at genus or species level presenting > 10 % of biomass in the selected samples.

eLSA was chosen because it is optimized to detect non-linear, time-sensitive relationships that cannot otherwise be identified by other network analyses (Ruan *et al.*, 2006; Xia *et al.*, 2011). The eLSA analysis looks through time series networks for associations that are strong enough, that they are likely to be realistic associations. eLSA calculates the highest local similarity score (LS) between any pair of factors considering the length of the time series (Ruan *et al.*, 2006). This score represents the strength of the correlation between two nodes, and its range depend on the dataset (Xia *et al.*, 2011; Arandia-Gorostidi *et al.*, 2022). In our dataset we compared the strength of the associations relatively to mean LS value of the entire dataset (i.e., $LS_{median} = 31.5$; $LS_{observed} \geq LS_{median}$ defined as 'strong', $LS_{observed} < LS_{median}$, defined as 'weak'). Weiss *et al.*, (2016) compared eLSA with seven other existing network analyses methods (e.g., SparCC, MIC, CoNet) and found that eLSA was the most suitable for time-series data. They also highlighted that eLSA is capable of correctly inferring three-member relationships. Here, the analysis was conducted following the tutorial (https://bitbucket. org/charade/elsa/wiki/Home), using a delay of one-time point to identify time-lag correlations, and without any delay (Ruan *et al.*, 2006; Xia *et al.*, 2011; Steele *et al.*, 2015). Only correlations with $p < 0.05$ and false-discovery rate corrected q-value < 0.05 (Storey and Tibshirani, 2003) were taken into consideration.

Network visualization and statistics were performed with Cytoscape v3.9. (Shannon *et al.*, 2003). The network was characterized by the numbers of positive and negative edges as well as nodes and connected nodes. The network *mean degree* corresponds to the average number of edges established by each node. The *Characteristic Path Length* represents the average shortest number of steps (number of nodes) between all node pairs. Network complexity was estimated using the *Clustering Coefficient*, which is the probability of two nodes having similar neighbour are connected to each other (Delmas *et al.*, 2019). The clustering coefficient varies between 0 and 1, low values indicate globally poorly connected neighbourhood.

3.3. Results

3.3.1. Environmental context

In the EEC, environmental parameters displayed seasonal patterns typical of temperate marine waters (Fig. 3.1 A-F, Table S3.3). Temperature increased from January to August and decreased from August to December with mean monthly values ranging from 7.1 to 19.3 ^{o}C

(Fig. 3.1A, Table S3.3). Mean monthly salinity ranged between 34.1 and 34.6 PSU, and showed relatively high variability from winter to spring and several extreme values across seasons (Fig. 3.1B, Table S3.3). Macronutrients decreased from January to March and increased from September to December (Fig. 3.1 C-D). The N/P ratio ranged from 0.4 to 316 (Table S3.3). Chl-a values ranged from 0.5 to 15.2 µg L^{-1} with mean monthly values from 1.5 to 5.7 µg L^{-1}. A comparison of the mean ranks (Kruskal Wallis and Nemenyi post-hoc test) of environmental variables revealed significant differences in salinity, phosphate, silicate, and Chl-*a* between stations (Fig. S3.2, Table S3.3). However, the environmental variables were of the same range and showed the same seasonal variation at all stations (Fig. 3.1, Fig. S3.2).

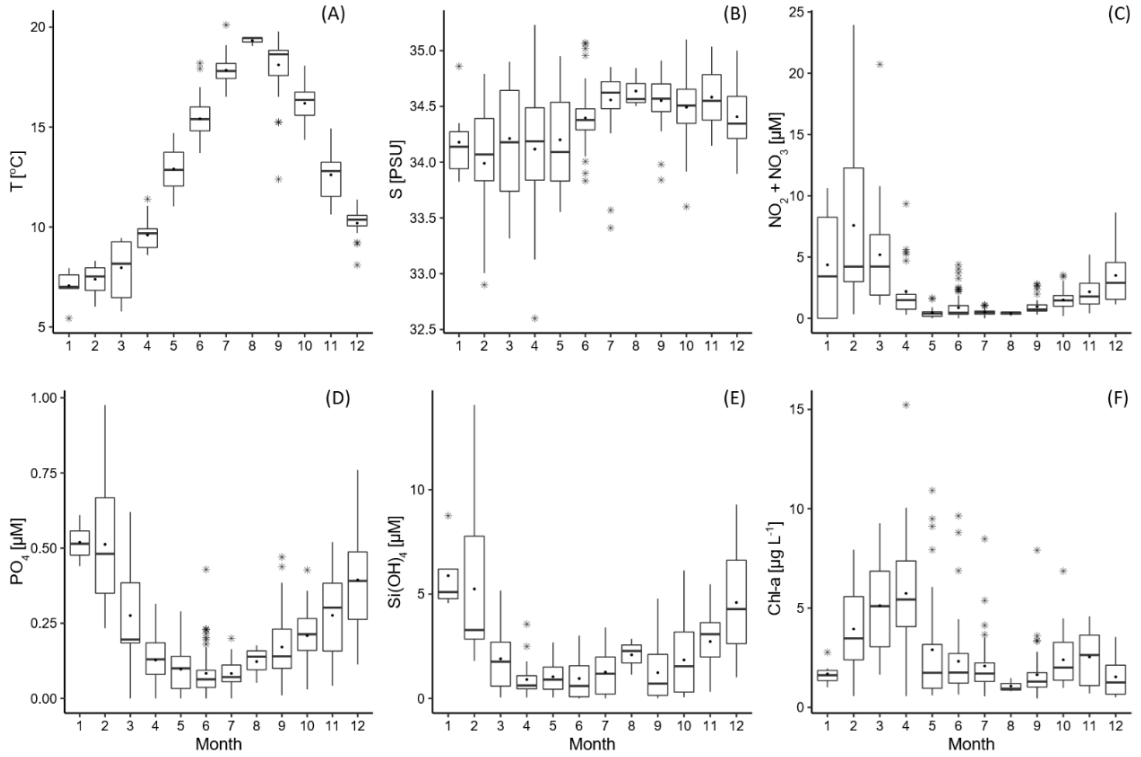

Figure 3.1. *Seasonal variation of environmental variables: (A) Temperature [T, °C], (B) S: Salinity [S, PSU], (C) Nitrites and Nitrates [NO_2+NO_3 µM], (D) Phosphates [PO_4, µM], (E) Silicates: S [$Si(OH)_4$, µM], (F) Chlorophyll-a [Chl-a, µg L^{-1}] in the EEC at the DYPHYRAD and SOMLIT stations (Fig. S3.1, Table S3.1) from March 2016 to October 2020.*

3.3.2. Phytoplankton community structure and succession

In this study, 90 diatoms were identified mostly to species level and their abundance ranged from 4.0 10^3 to 4.8 10^6 cells L^{-1} (Fig. S3.3). In winter, phytoplankton was dominated by diatoms with a mean abundance of 102 10^3 cells L^{-1}. *Thalassiosira* spp., dominated winter phytoplankton in terms of abundance (24.7 ± 12.3 10^3 cells L^{-1}, 24 %, Fig. 3.2A) and biomass (3.2 ± 5.1 µg C L^{-1}), accounting for 21% of diatom biomass. Besides *Thalassiosira* spp., several

other diatom species contributed to the winter biomass (i.e., *Guinardia striata*; 21%, *Coscinodiscus* spp.; 16%, *Ditylum brightwelli*; 10%). Spring phytoplankton communities were dominated by *P. globosa* which bloomed in April and May, featuring though differences in its abundance and biomass across years (i.e., annual maximum abundance ranged from 7.5 to 36.7 10^6 cells L^{-1}, and annual maximum biomass from 132 to 1555 µg C L^{-1}, Fig. 3.2B; S3.3B). The summer phytoplankton community showed several transient diatom blooms. *Chaetoceros socialis* showed a peak in July 2016, reaching 3.1 10^6 cells L^{-1} (Fig. 3.2A, S3.3A). The centric diatom *Leptocylindrus danicus* peaked in the summer from 2018 to 2020, with a maximum concentration of 5.9 10^6 cells L^{-1}, and the pennate diatom *Pseudo-nitzschia pungens*, reached 4.8 10^6 cells L^{-1} in June 2018 (Fig. 3.2A, S3.3A). In autumn phytoplankton was also dominated by diatoms, however their abundance was 2 orders of magnitude lower than in summer (i.e., mean abundance 3.9 10^4 cells L^{-1}).

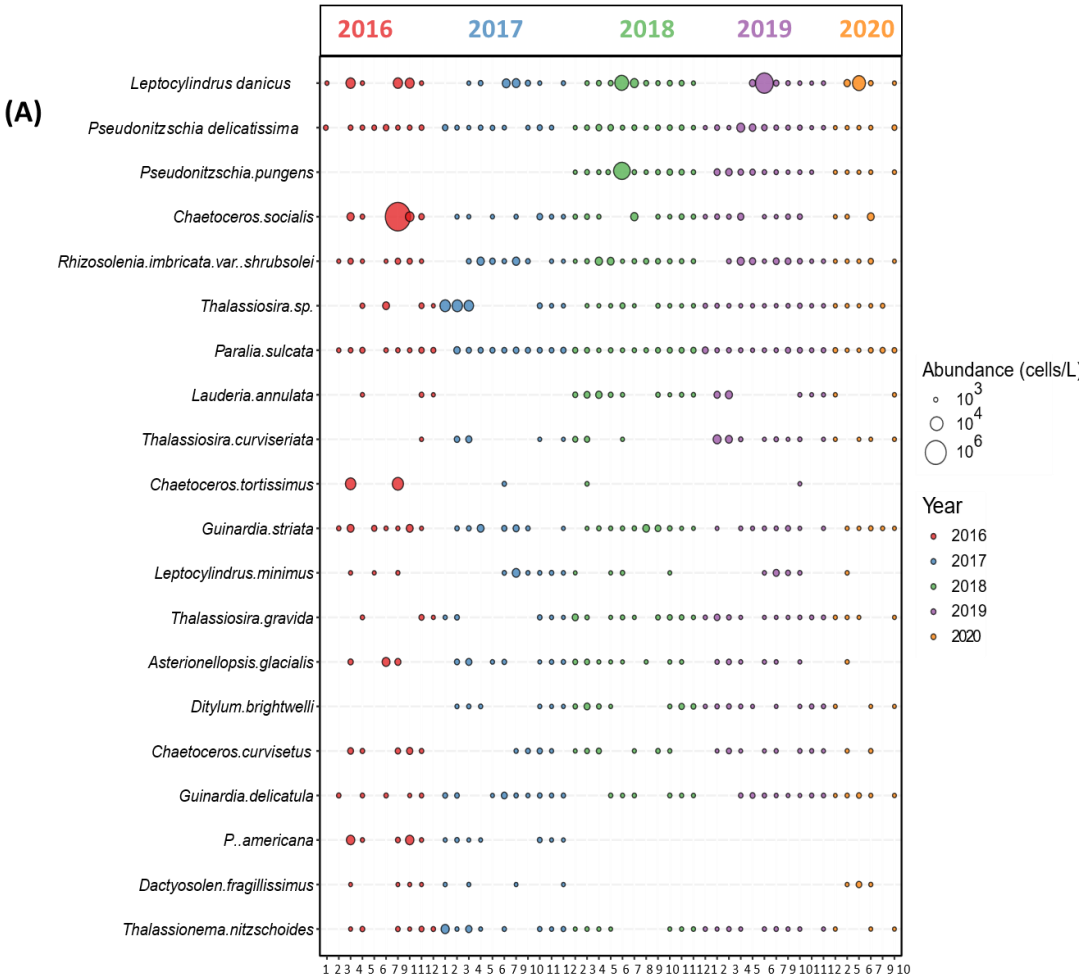

(Figure continued to the next page)

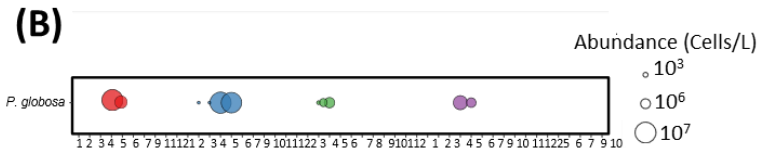

***Figure 3.2**. Bubble plot illustrating the mean monthly abundance (cells L^{-1}) of (A) 20 most abundant diatoms in total abundance, and (B) Phaeocystis globosa identified by microscopy, occurring in the EEC at the DYPHYRAD and SOMLIT stations from March 2016 to October 2020. No data were available for P. globosa in April-May 2020 due to Covid-19 restrictions. The size of the circles in the plot corresponds to the abundance classes (10^3, 10^4, and 10^6). The colours correspond to the different years.*

3.3.3. Heterotrophic bacteria community structure and succession

According to metabarcoding data, the most abundant groups at the family taxonomic level were assigned to Actinomarinaceae (15.5 %), followed by Flavobactericeae, contributing to 13.7 % of the total number of reads (Fig. S3.4). Actinomarinaceae exclusively consisted of the genus *Candidatus Actinomarina* (15.5%), the most abundant genus across the dataset. Flavobactericeae were more diversified, with the most dominant genera affiliated to NS5 marine group (2.8 %), *Tenacibaculum* (2.5 %), and *NS4 marine group* contributing to and 2.1 % in relative abundance. (Fig. S3.4). In terms of alpha diversity, bacterial communities showed low seasonal variability (Fig. S3.5). Richness mean highest values were recorded in September (585 ASVs) and lowest in May (402 ASVs). Shannon and Simpson's mean monthly values ranged from 3.8 to 4.3, and from 0.89 to 0.95 respectively (Fig. S3.5).

The distance-based redundancy analysis (db-RDA) between environmental variables and bacterioplankton communities explained 45 % of the total variation in bacterial composition with db-RDA1 and db-RDA2 contributing to 33 % and 12% of the total variation (Fig. 3.3). Autumn (from September to November) communities formed tighter groups on the db-RDA plot, while summer -which presented diatom transient blooms- were more dispersed. Winter communities were associated to macronutrients (NO_2+NO_3, PO_4, $Si(OH)_4$), spring communities to chlorophyll-a, and summer communities to temperature. The permutation test showed that temperature, phosphates, and nitrates mostly contributed to the overall variability by 18 % ($p < 0.001$), 16.5 % ($p < 0.001$), and 11.3 % ($p < 0.001$), respectively.

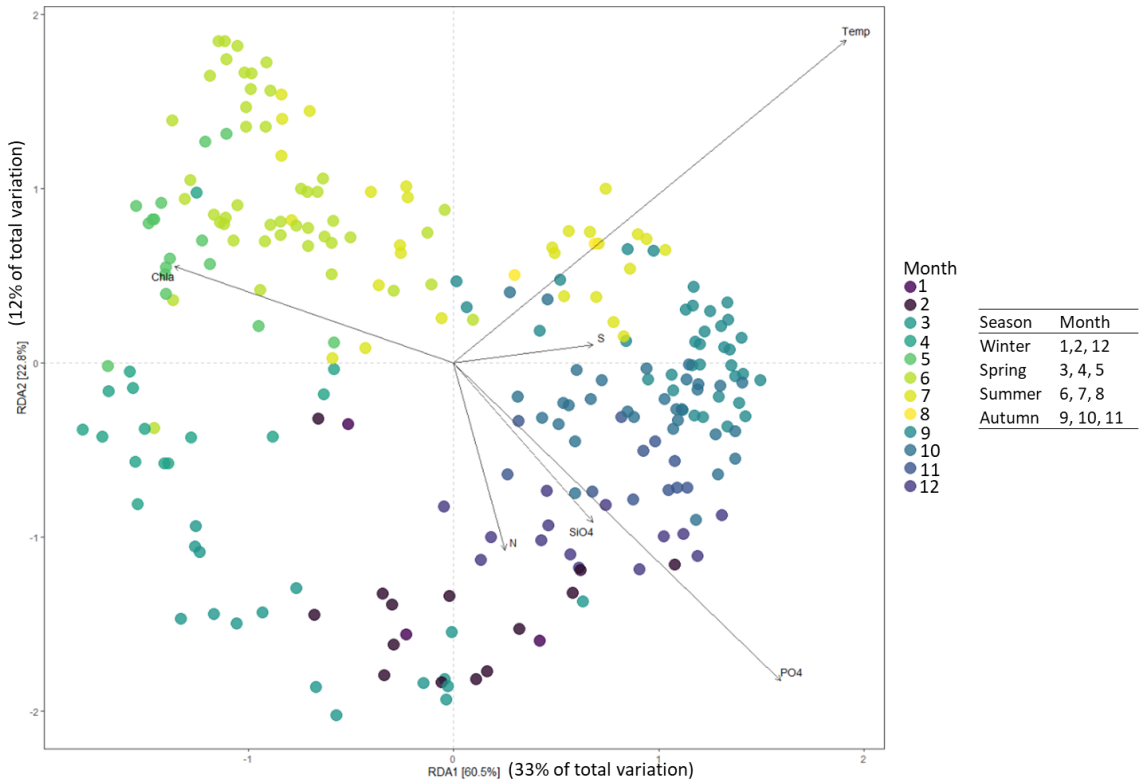

***Figure 3.3**. Distance-based redundancy (db-RDA) ordination illustrating the variations of the heterotrophic bacterial communities, based on metabarcoding data, (samples, colored dots) in relation to the environmental variables (black arrows) in the EEC at the DYPHYRAD and SOMLIT stations from March 2016 to October 2020.*

Heterotrophic bacteria abundance ranged from 0.3 to 4.9 10^6 cells mL^{-1}; it increased from winter to summer and a decreased from summer to autumn. Higher abundance was always evidenced after the wane of *P. globosa* bloom in June and July (Fig. 3.4A). Among the 10 dominant bacterial families accounting for 69.8 % of total read abundance, three families (Actinomarinaceae, Flavobacteriaceae, and Rhodobacteraceae) contributed to 41.2 % in relative read abundance of the entire dataset (Fig. 3.4B). Actinomarinaceae dominated heterotrophic bacteria community in winter (December – February) and autumn (September – November) reaching a maximum of 39 % relative abundance of reads in winter (Fig. 3.4B). However, during the spring (March-April) and summer (June-July) blooms, Flavobacteriaceae and Rhodobacteraceae relative abundance increased dominating over Actinomarinaceae. Flavobacteriaceae ranged from 4 % in winter to 40 % in summer respectively (Fig. 3.4B).

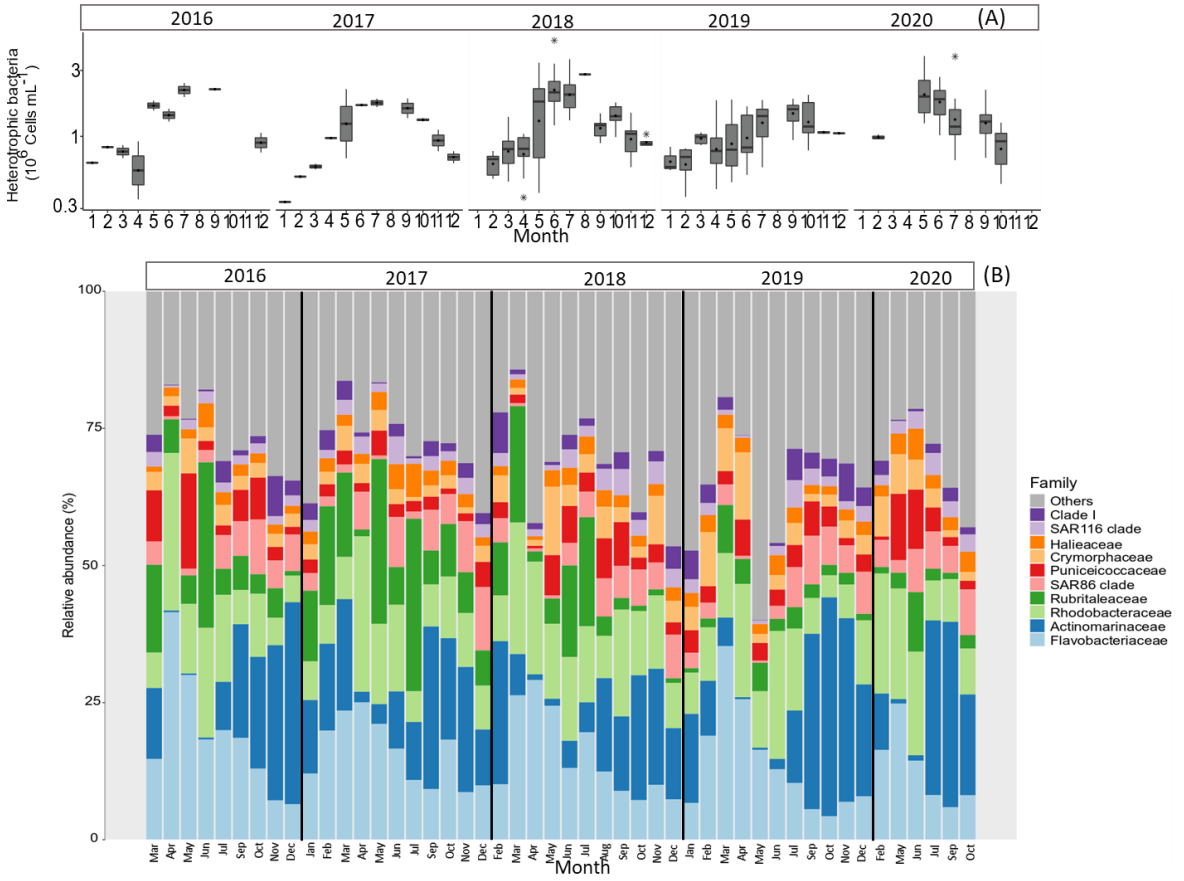

Figure 3.4*. (A) Seasonal variation of mean monthly abundance (cells L^{-1}) of heterotrophic bacteria enumerated by cytometry in the EEC at the SOMLIT and DYPHYRAD stations from March 2016 to October 2020, the Y axis is log10 transformed. (B) Seasonal variation of the ten most abundant families based on rRNA gene metabarcoding data.*

Twenty-one genera of the most abundant heterotrophic bacteria (i.e., ≥ 1 % relative read abundance in the entire dataset; 282 samples) were visually classified to temporal patterns (Fig. 3.5). About half of them (12 out of 21 genera) were seasonal corresponding to winter-autumn or spring. Five out of twenty-one bacteria showed peaks mainly during the monospecific diatom blooms in summer, thus their presence was irregular across years and were defined as 'episodic'. Four out of twenty-one genera showed low variability across seasons and were defined as 'ubiquitous'. In winter and autumn (from September to February) *Candidatus Actinomarina*, *Clade Ia*, *OM43 clade*, *SUP05 cluster*, and *MB11C04 marine group* dominated bacteria community with the first one contributing the most in relative read abundance (e.g., 63 % in October 2019). In spring, despite the variation in intensity of *P. globosa* blooms across years bacterial communities were always dominated by six genera (*Amylibacter*, *NS5 marine group*, *Planktomarina*, *Lentimonas*, *SAR92 clade*, *Polaribacter*, and *Tenacibaculum*). These bacteria contributed to more than 10 % in relative read abundance during the *P. globosa*

blooms. The first three were relatively abundant also out of the blooming period (> 5 %), while the last three contributed to less than 3 % in total relative read abundance. *Ilumatobacter*, *Persicirhabdus*, *Luteolibacter*, *Formosa*, and *Roseibacillus*, dominated bacterial communities mainly during the summer monospecific diatom blooms, and they exhibited 'episodic' patterns, however *Luteolibacter* peaked once during a *P. globosa* bloom. *Ilumatobacter* showed maximum relative abundance in June (i.e., 32 %) during the *L. danicus* bloom in 2019. *Persicirhabdus* peaked in June 2017 (i.e., 36 %). *Luteolibacter* showed peaks in June 2016 (i.e., 33.5 %), in 2018 (i.e., 25%), and 2020 (i.e., 54 %). *Formosa*'s and *Roseibacillus*' relative read abundance fluctuated across the years with a maximum in September 2016 and November 2017 (i.e., 11.7 and 11.6%). *NS4 marine group, OM60.NOR5 clade* and *Blastopirellula* contributed to 7.8, 8.5, 4.7, and 6.5 % relative read abundance in the entire dataset, they were consistently present across years (i.e., ubiquitous).

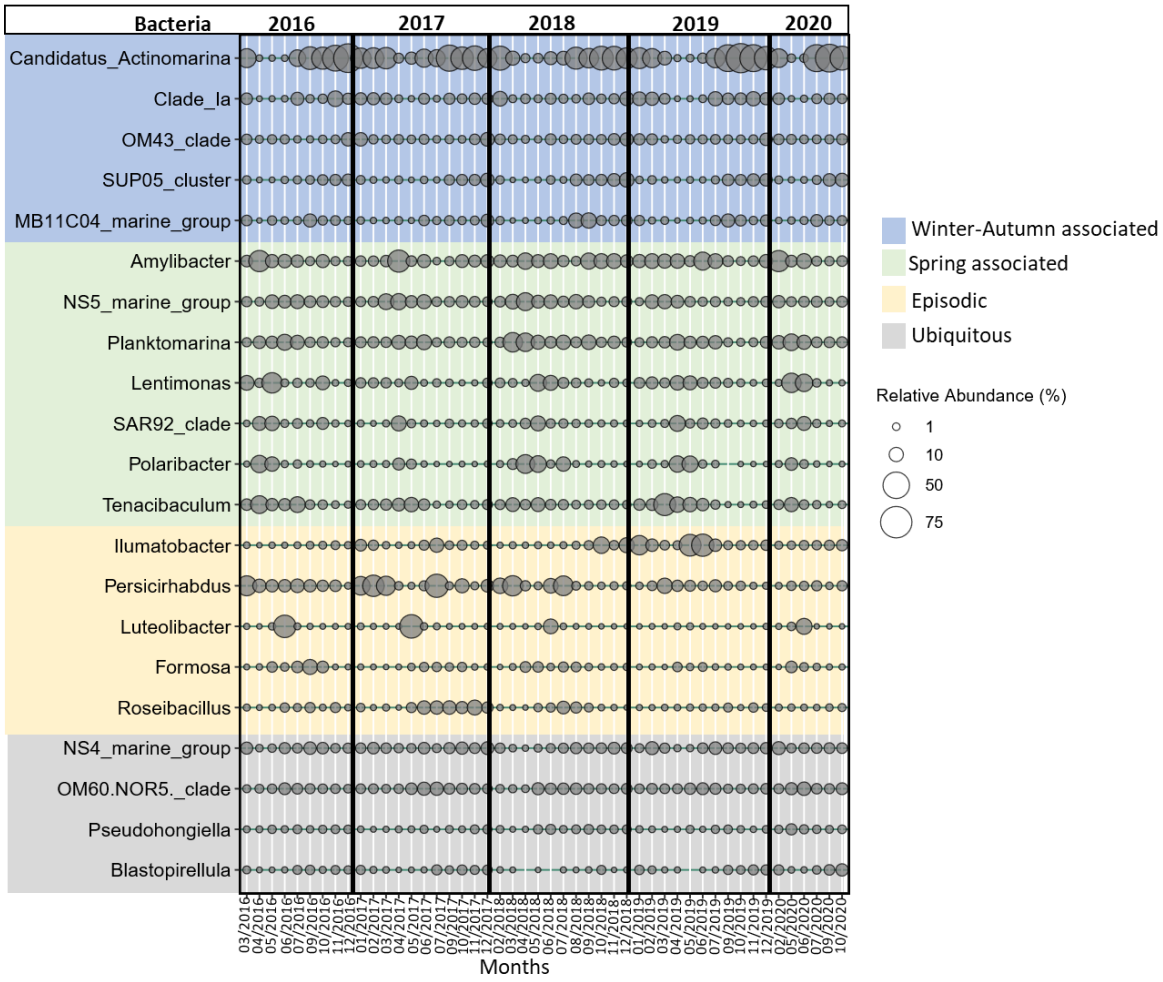

Figure 3.5. *Bubble plot illustrating the mean relative abundance of 21 dominant bacteria in genus taxonomic level (i.e., ≥ 1 % reads relative abundance in the entire dataset; 282 samples). The size of the circles in the plot corresponds to the relative abundance classes (1 %, 10%, 50%, and 75%). The colours correspond to the different patterns that were visually assigned to: i) winter-autumn associated (blue), ii) spring associated (green), iii) episodic (yellow), iv) ubiquitous.*

3.3.4. Bacteria putative associations with phytoplankton

For network analysis sixty-nine samples were selected. Thirty-eight samples corresponded to dates when blooms occurred in spring and summer (from March to July), and thirty-one winter samples (from December to February) corresponded to a 'reference' non-blooming period. The winter season in opposition to spring and summer, presented diverse diatom communities, relatively low mean temperature (i.e., 8.2 ^{o}C; Fig. 3.1 A), and relatively low bacterial abundance (i.e., 0.7 10^{6} cells mL^{-1}; Fig., 3.4A). Both lag-delayed and no-lag networks showed only significant positive correlations for six phytoplankton species (i.e., *D. brightwellii, G. striata, P. globosa, C. socialis, L. danicus, P.pungens*) and two genera (i.e., *Thalassiosira* spp., *Coscinodiscus* spp.*).* These phytoplankton taxa, accounted for more than 10 % of biomass in the sixty-nine samples. Additionally, twenty-three bacterial genera, representing more than 1% in relative abundance in the selected samples, along with five environmental variables, were included in the analysis (Figs. 3.6, S3.6 respectively). The lag-delayed and no-lag networks had similar topological characteristics (Table S3.4), and showed three sub-networks: i) the winter non-blooming period characterised by a mixed diatom community ii) the *Phaeocystis globosa* recurrent spring bloom, and iii) the summer transient monospecific diatom blooms. The no-lag sub-networks were clearer (Fig. 3.6), and therefore they will be the one described and discussed here.

Bacterial associations with phytoplankton and environmental variables comprised in total 36 nodes and 95 edges. The strength of connection between nodes was expressed by the local similarity score (LS). The lowest LS score was detected between *Coscinodiscus* spp. and phosphates (i.e., 0.02) and the highest between *L. danicus* and temperature (i.e., 225). The highest number of connections (i.e., 11 edges) was found for *Candidatus Actinomarina* and *NS4 marine group* (Fig. 3.6).

The winter ‘mixed diatom community’ sub-network had the highest clustering coefficient (mean ± SD, 0.66 ± 0.24) compared to the other two sub-networks (0.43 ± 0.25, 0.53 ± 0.30; Table S3.5). In the ‘mixed diatom community’ sub-network bacteria were highly interconnected and they shared connections with phytoplankton and nutrients (Fig. 3.6) The sub-network was consisted by four diatoms (i.e., *Coscinodiscus* spp., *D. brightwellii, G. striata, Thalassiosira* spp.*),* nine bacteria (i.e., *Candidatus Actinomarina, SUP05 cluster, Persicirhabdus, OM43 clade, Clade Ia, MB11C04 marine group, Brevundimonas, NS2b marine group, NS4 marine group*) and environmental variables (nitrites and nitrates, phosphates and silicates). The most connected bacteria *Candidatus Actinomarina* (i.e., 11

edges) and *NS4 marine group* (i.e., 11 edges) shared more connections with bacteria than with phytoplankton (i.e., 2 edges). The less connected bacterium *Bervudimonas* was connected to two bacteria (*NS2b marine group,* and *Persicirhabdus*). The most connected phytoplankton was *Thalassiosira* spp., (i.e., 7 edges; six connections with bacteria and one with nutrients), followed by *Coscinodiscus* spp. (i.e., 5 edges; three connections with bacteria and two with nutrients), and *D. brightwellii* (i.e., 5 edges; connections with bacteria), while *G. striata* was the less connected one (i.e., 2 edges; connections with bacteria). Out of nine bacteria that consisted this sub-network, only three (i.e., *MB11C04 marine group, Brevundimonas, NS2 marine group*) showed unique connections with phytoplankton, while the rest of them were connected with more than one phytoplankton. For example, *Candidatus Actinomarina* was connected with *Coscinodiscus* spp. and *Thalassiosira* spp., and OM43 clade was connected with *D. bridhtwelli* and *G. striata*. (Table S3.5).

The '*P. globosa bloom*' sub-network consisted by nine bacteria, *P. globosa,* and chlorophyl-a. Six out of the nine bacteria belonging in this sub-network were directly connected to *P. globosa* (i.e., *Polaribacter, Tenacibaculum, Ulvibacter, Planktomatina, SAR92 clade and Amylibacter*). They were also connected between them and with the other three bacteria (i.e., *Lentimonas, Pseudoalteromonas, NS5 marine group*). Chlorophyll-a was connected with *Amylibacter and Lentimonas*. The 'Transient diatom blooms' sub-network consisted by five bacteria, three diatoms that showed transient peaks in summer, and temperature. This sub-network evidenced unique connections between phytoplankton and bacteria. *L. danicus* was strongly connected to *Ilumatobacter,* and to a lesser degree to *Tetayamaria*, and *OM60(NOR5) clade*. *C. socialis* was connected to *Formosa,* and *P. pungens* was connected to *Luteolibacter*. Not surprisingly temperature was the environmental variable that appeared in this network and was directly connected to four out of five bacteria, and to two phytoplankton genera (Fig. 3.6).

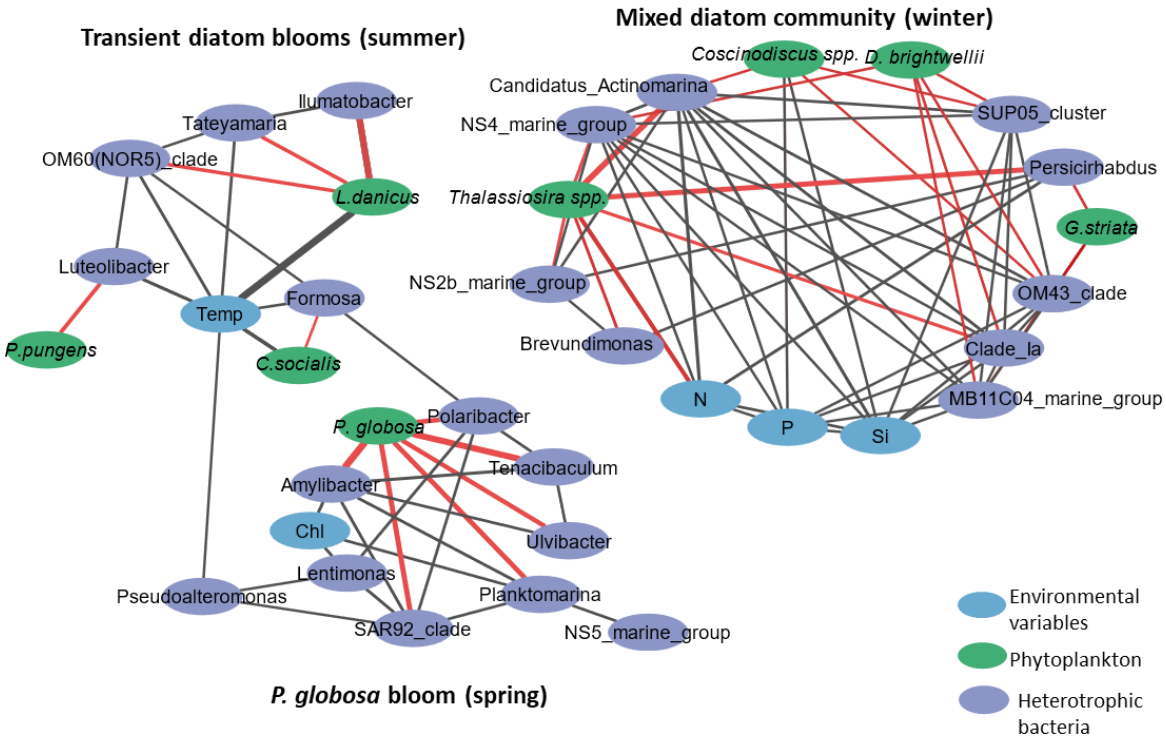

Figure 3.6. *Network diagram of significant correlations ($p<0.05$) between the 23 dominant bacteria in genus level (i.e., ≥1% number of reads in 69 samples selected for network analysis), 8 phytoplankton species/genus representing 10% of biomass in 69 samples and 5 environmental variables (Si $(OH)_4$, NO_2+NO_3, PO_4, temperature and Chl-a) as determined by eLSA analysis without delay. To facilitate reading, purple circles represent the bacteria, blue ones the environmental variables, and green ones the phytoplankton taxa. The width of the lines (edges) is proportional to the strength of the association and corresponds to LS score. The red colour of the lines represents bacteria-phytoplankton connections.*

3.4. Discussion

Previous studies investigated bacteria dynamics in temperate coastal regions were mostly focussed to spring / summer diatoms blooms (e.g., Teeling *et al.*, 2016; Bunse and Pinhassi, 2017; Chafee *et al.*, 2018; Arandia-Gorostidi *et al.*, 2022). In this study bacteria and phytoplankton succession and putative interactions were investigated in a coastal ecosystem characterised by mixed diatom communities in winter, recurrent blooms of *Phaeocystis globosa* in spring, and transient diatom blooms in summer. The major findings of this work were that bacteria presented seasonal, (Fig. 3.3), and 'episodic' patterns (Fig. 3.5) due to transient diatom blooms (Figs. 3.2). We evidenced that diatoms and *P. globosa* defined distinct bacteria communities that were seasonal and / or substrate driven. This was further reflected on the network analysis. The network analysis showed: i) consistent bacteria in winter, that showed several connections between them and with diatoms, and ii) well-defined blooming sub-networks with 'strong' connections between bacteria and *P. globosa*, and unique associations between transient diatom blooms and bacteria (Fig. 3.6).

3.4.1. Seasonal dynamics of bacteria and phytoplankton communities

Seasonality in bacterioplankton community structure has been already reported in previous studies and is considered to remain recurrent year after year (Fuhrman *et al*., 2015; Gilbert *et al*., 2012). Three families, (i.e., Actinomarinaceae, Flavobacteriaceae, and Rhodobacteriaceae) accounting for a total 41.2% number of reads, exhibited seasonal variations (Fig. 3.4B). This seasonality was further supported by examining the dynamics at the genus level. For example, *Candidatus Actinomarina* (Actinomatinaceae), which thrives in cold and nutrient rich waters, displayed a preference for winter-autumn seasons (Chafee *et al.*, 2018; López-Pérez *et al.*, 2020; Hu *et al.*, 2022; Table 3.1). In winter phytoplankton communities were dominated by diverse diatoms, favoured by high nutrient concentrations, low light availability and wind-driven turbulence (e.g., Schapira *et al.*, 2008). By the end of March, depletion of silicates and abundant nitrates triggered the growth of *P. globosa* (e.g., Breton *et al.*, 2006). Flavobacteriaceae showed peaks during *P. globosa* blooms, while Rhodobacteraceae or other families dominated summer diatom blooms. Flavobacteriaceae and Rhodobacteraceae families possess a wide range of hydrolytic enzymes and membrane transporters to degrade and assimilate organic matter, mostly saccharides, released by phytoplankton (Riemann *et al.*, 2000; Pinhassi *et al.*, 2004; Teeling *et al.*, 2012). These findings align with a recent experimental study that showed strong seasonal differences of bacterial communities characterised by distinct polysaccharide utilization (laminarin, xylan, and chondroitin) in the North Sea (Giljan *et al*., 2022). Seasonality was also evident in bacterial abundance (Fig. 3.4A). However, alpha diversity remained stable across seasons (Figs. 3.4; 3.5; S3.5). This stability could be attributed to the large species pool (e.g., 9,745 ASVs, 394 genera in the entire dataset), and the consistent availability of substrates provided by phytoplankton communities across the seasons.

The distance-based RDA analysis indicated that environmental variables contributed to 45 % in total variation, with nutrients and temperature explaining 27 % and 18 % of the variation in community composition, respectively (Fig. 3.3). Temperature is known to be key environmental factor as it impacts the metabolic kinetics of al organisms *(Brown et al., 2004)*. Nutrients contribute directly in bacterioplankton composition and indirectly via the promotion of specific phytoplankton species which in turn promote specific bacterial groups. While distance-based RDA evidenced generally well clustered bacterial communities across seasons, this was less clear in summer, suggesting a ‘break of seasonality’ due to the setup of transient

diatom blooms. This was further confirmed by the visually assigned temporal patterns that showed the dominance of 'episodic' genera particularly in summer (Fig. 3.5).

3.4.2. Exploring taxon-specific phytoplankton-bacteria relationships

A major finding in the present study was that network analysis showed three distinct well defined sub-networks for the non-blooming winter period, the *P. globosa* and the transient summer diatom blooms. However, co-occurrence networks should not be over-interpreted as they rely on pairwise comparisons, and may not necessarily reveal true interactions (e.g., Blanchet *et al.*, 2020). Additionally, metabarcoding can overestimate or underestimate the proportions of eukaryotic taxa for which DNA is more easily extracted and amplified (e.g., Santi *et al*., 2021). A strength of the present work was that phytoplankton was enumerated by microscopy, which is rarely considered in network studies (e.g., Arandia-Gorostidi *et al.*, 2022). Regarding bacteria metabarcoding biases are considered less pronounced than in eukaryotes because bacteria have less complex genomes (Cooper, 2000). Also, comparisons of relative abundance of bacterial families using 16S metabarcoding and staining with specific probes (FISH method) have generally showed accordance (e.g., Telling *et al*., 2016).

The winter sub-network consisted of well-connected bacteria between them and with phytoplankton, having various strategies including, copiotrophs and oligotrophs (Table 3.1). The oligotrophic *Candidatus Actinomarina* dominated in winter and showed various connections with bacteria and diatoms. Little is known about the ecology of the smallest free living bacteria *Candidatus Actinomarina* (Ghai *et al.*, 2013). It is considered photoheterotroph and they have been found during winter season in the North Sea (Chafee *et al.*, 2018), and in deep water levels below the DCM (López-Pérez *et al.*, 2020). Low-abundant bacteria (containing < 5 % reads in the dataset) also showed several connections. Among these bacteria, *OM43 clade* comprises methylotrophs known to feed on algae's C1 compound (i.e., compounds containing one carbon; e.g., methanol; Halsey *et al.*, 2012). They have been associated to phytoplankton spring blooms in the North Sea (Teeling *et al.*, 2016), and they have been found during winter months in northwestern Atlantic Ocean, suggesting a broad biogeographic distribution at different biotic and abiotic conditions (Georges *et al.*, 2014). Another interesting observation involves the *MB11C04 marine group*, which was connected to the diatom *D. brightwelli* (Fig. 3.6). This copiotroph bacterium is specialised in consuming complex sulphated methyl pentoses (polysaccharides) produced by diatoms (Orellana *et al.*, 2022). Both *OM43 clade* and *MB11C04 marine group* exhibited seasonal patterns (Fig. 3.5). However, *Persicirhabdus*, connected to *Thalassiosira* spp., showed variations across years

(Fig. 3.5). It is suggested that local conditions are necessary for their development, such as phytoplankton structure, that determines the type of organic matter present in the environment (Zhang *et al.*, 2015). The intensity of the response of *Persicirhabdus* seems to be proportional to the substrate quantity could be important in their development (Hellweger, 2018; Lemonnier, 2019). This is consistent with our observation of *Thalassiosira* spp. showing variable abundance during the non-blooming period (0.08 – 711.4 10^3 cell L^{-1}; Fig. 3.2A). It can be hypothesized that during the non-blooming period, there was a greater variety of substrates derived from a diversified diatom community. Therefore, several bacteria may collaborate to assimilate these substrates. This is in line with previous studies stressing out that in winter carbon in more recalcitrant and thus there is a need of various transporters and carbohydrate genes to process it, while in summer carbon is more labile (Ward *et al.*, 2017). Taking together, diverse diatom-derived substrates require a consortium of interconnected bacteria with specific strategies including the degradation of simple and complex saccharides. An unexpected observation in this sub-network concerns the *SUP05 cluster*, which showed a recurrent seasonal pattern (Fig. 3.5). It has been reported to be more abundant at the bottom of the water column, but can rise to the surface when the water column is mixed in winter and early spring (Chun *et al.*, 2021). This could be explained by strong hydrodynamism, and wind particularly in winter in the EEC (Breton *et al*., 2021).

Table 3.1. *Bacteria detected in network analysis corresponding to: i) non-blooming period, ii) P. globosa bloom, and iii) transient diatom blooms and strategies reported in previous studies.*

	Genus	Family	Strategies	References
Non-blooming period				
	Candidatus Actinomarina	Actinomarinaceae	oligotroph, preference in cold waters	e.g., Chafee et al., 2018
	NS4 marine group	Flavobacteriaceae	copiotroph	e.g., Lemonnier et al., 2020
	NS2b marine group	Flavobacteriaceae	copiotroph	e.g., Arandia-Gorostidi et al., 2022
	Brevundimonas	Caulobacteraceae	algicidal	e.g., Coyne et al., 2022
	MB11C04 marine group	Puniceicoccaceae	copiotroph, specialised consumers of	e.g., Orellana et al., 2022
			sulfated methyl pentoses	
	Clade Ia	SAR11 Clade	oligotroph	e.g., Giebel et al., 2010
	OM43 clade	Methylophilaceae	methylotroph known to feed on algae C1	e.g., Hasley et al., 2012
			compound	
	Persicirhabdus	Rubritaleaceae	copiotroph, specialised consumer of complex	e.g., Buchan et al., 2014
			molecules of organic matter	
	SUP05 cluster	Thioglobaceae	Sulfur-oxidizing bacteria. They can be found in	e.g., Chun et al., 2021
			anoxic and oxygenated waters that appear to	
			lack reduced sources of sulfur for cell growth	
***P. globosa* bloom**				
	Polaribacter	Flavobacteriaceae	copiotroph, exploit large variaty of resources	e.g., Teeling et al., 2016
	Tenacibaculum	Flavobacteriaceae	copiotroph	e.g., Teeling et al., 2016
	Ulvibacter	Flavobacteriaceae	copiotroph	e.g., Teeling et al., 2016
	Planktomarina	Rhodobacteraceae	copiotroph, exploit large variaty of resources	e.g., Teeling et al., 2016
	NS5 marine group	Flavobacteriaceae	copiotroph	e.g., Teeling et al., 2016
	SAR92 clade	Porticoccaceae	copiotroph	e.g., Teeling et al., 2016
	Lentimonas	Puniceicoccaceae	copiotroph	e.g., Teeling et al., 2016
	Pseudoalteromonas	Pseudoalteromonadaceae	algicidal, it produces extracellular	e.g., Mayali and Azam 2004
			bioactive molecules to kill phytoplankton cells	
	Amylibacter	Rhodobacteraceae	copiotroph	e.g., Lemonnier et al., 2020
Transient diatom blooms				
	Formosa	Flavobacteriaceae	copiotroph	e.g., Teeling et al., 2016
	Luteolibacter	Rubritaleaceae		
	OM60(NOR5) clade	Halieaceae	copiotroph	e.g., Teeling et al., 2016
	Tateyamaria	Rhodobacteraceae		
	Ilumatobacter	Ilumatobacteraceae		

The '*P. globosa*' sub-network showed 'strong' connections (LS varied from 108 to 240 which exceed LS_{median}) between *P. globosa* and six copiotroph bacteria (Fig. 3.6; Table 3.1). Despite the variations in the intensity of *P. globosa* blooms over the years (Fig. 3.2B), these six bacteria exhibited recurrent patterns (Fig. 3.5). These findings provide valuable insights into the bacteria dynamics complementing a recent experimental study focused on the microbiome of *P. globosa* strains isolated from various geographic regions (Mars Brisbin *et al.*, 2022). These authors showed that different strains of *P. globosa* harbour similar bacterial communities. They were affiliated to the orders Alteromonadales, Burkholderiales, and Rhizobiales, and they promoted growth of *Phaeocystis* through opportunistic and symbiotic strategies. However, in our study analysing the whole bacterial community (free-living and attached), dominant orders were affiliated to: Flavobacteriales, Rhodobacteriales, Cellvibrionales and Opitutales. The bulk of bacteria during phytoplankton blooms are free-living and not particle attached to phytoplankton or particles (e.g., Teeling *et al.*, 2016). Therefore, bacteria associated to *P. globosa* in our study were likely dominated by the free-living compartment. The genera found in our study (Figs, 3.5; 3.6) have been previously detected in diatom blooms responding to high substrate loading (e.g., Tada *et al.*, 2012; Teeling *et al.*, 2016). The 'strong' connections of the

six bacteria with *P. globosa* (Fig. 3.6) and the recurrence of bacterial composition (at Family and genus level; Figs. 3.2 B, 3.5) during the blooms suggested that *P. globosa* blooms were stable-state systems for bacteria communities. An interesting observation concerns the copiotroph *Pseudoalteromonas* which can be algicidal (Fig. 3.6). It produces extracellular bioactive molecules to kill phytoplankton such as cyanobacteria, dinoflagellates and diatoms (Mayali and Azam, 2004; Seymour *et al.*, 2009). Experimental studies have shown that bacteria of genus *Bacillus* and *Streptomycetes* had strong algicidal activity against *Phaeocystis* (Zhang *et al.*, 2014; Guan *et al.*, 2015). An existing study underlined the importance of viruses in the termination of *P. globosa* blooms (Brussaard *et al.*, 2007), the algicidal bacteria implication in *P. globosa* blooms is an area of research that deserves further investigation. Furthermore, *P. globosa* blooms and the associated bacteria probably conditioned the abiotic environment for summer bacteria-phytoplankton communities. This is in line with a recent study which showed that *P. pungens* belonging to the '*P. seriata complex'* bloomed only after low intensity of *P. globosa* bloom (Houliez *et al.*, 2023). Finally, the blooming diatoms present in the summer sub-network showed unique connections with several bacteria (Fig. 3.6). This can be attributed to the different substrates produced by different diatoms (Grossart *et al.*, 2005).

Concluding, this study expands previous reports describing the seasonal dynamics of bacterial communities focusing in coastal ecosystems subjected to phytoplankton blooms. Bacterial communities were seasonal and substrate driven. However, during winter in presence of a diverse diatom community, bacteria were associated with all phytoplankton species and between them, while during monospecific *P. globosa* and diatom blooms specific bacterial genus were strongly associated with the blooming species. In a context of global change, recurrent spring and transient summer blooms are influenced in terms of length and intensity. Further studies are needed to explore the functional potential of associated bacterial communities and the importance of algicidal bacteria in the termination of *P. globosa* and diatom blooms.

Contributions

Samples were collected from the national monitoring network SOMLIT and the local transect DYPHYRAD (PI: Dr. Artigas Luis-Felipe) by the crew of 'Sepia II', and the assistance of technicians Cornille Vincent and Lecuyer Eric. I participated in some of these samplings from 2018 to 2020. Since 2018, I have been responsible for fixation of microscopy data and conducting filtrations for metabarcoding. I enumerated and identified phytoplankton (diatoms

and *Phaeocystis*) using inverted microscopy and heterotrophic bacteria with cytometry. Additionally, I conducted extractions, prepared libraries, and performed purifications for 16S metabarcoding for all samples. Phytoplankton data from 2016 to 2017 were enumerated by Dr. Breton Elsa, and all nutrient and chlorophyll-a measurements were carried out by Muriel Crouvoisier. All samples were sequenced by Genewiz platform. I conducted bioinformatic, statistical, network analysis and data visualisations. Pr. Chrisraki Urania conceptualised, leaded and acquired funding and for this study.

3.5. Supplementary

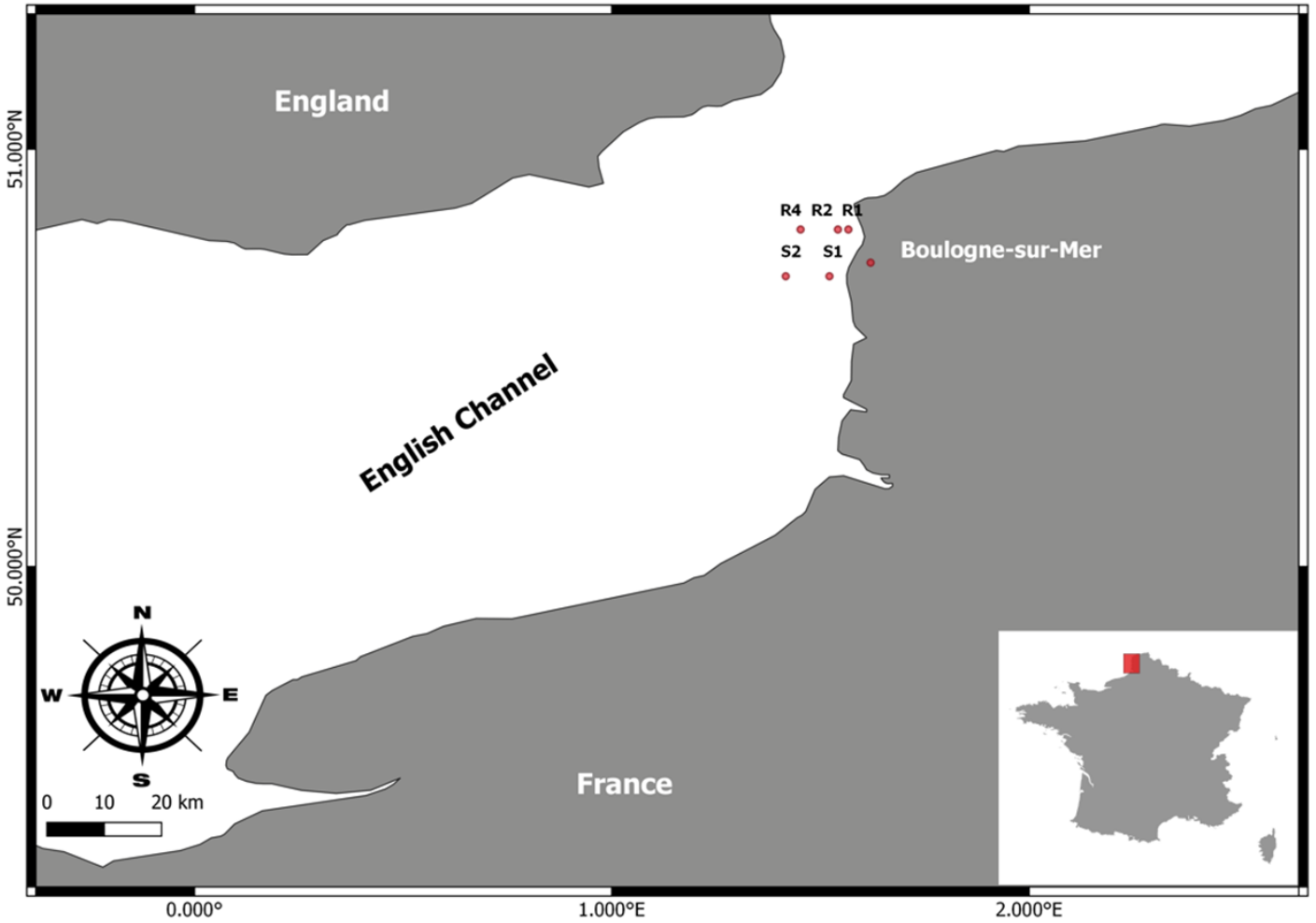

Figure S3.1. *Location of the SOMLIT (S1, S2) and DYPHYRAD (R1, R2, R4) stations in the EEC (map creation with QGIS software V.3.10.1).*

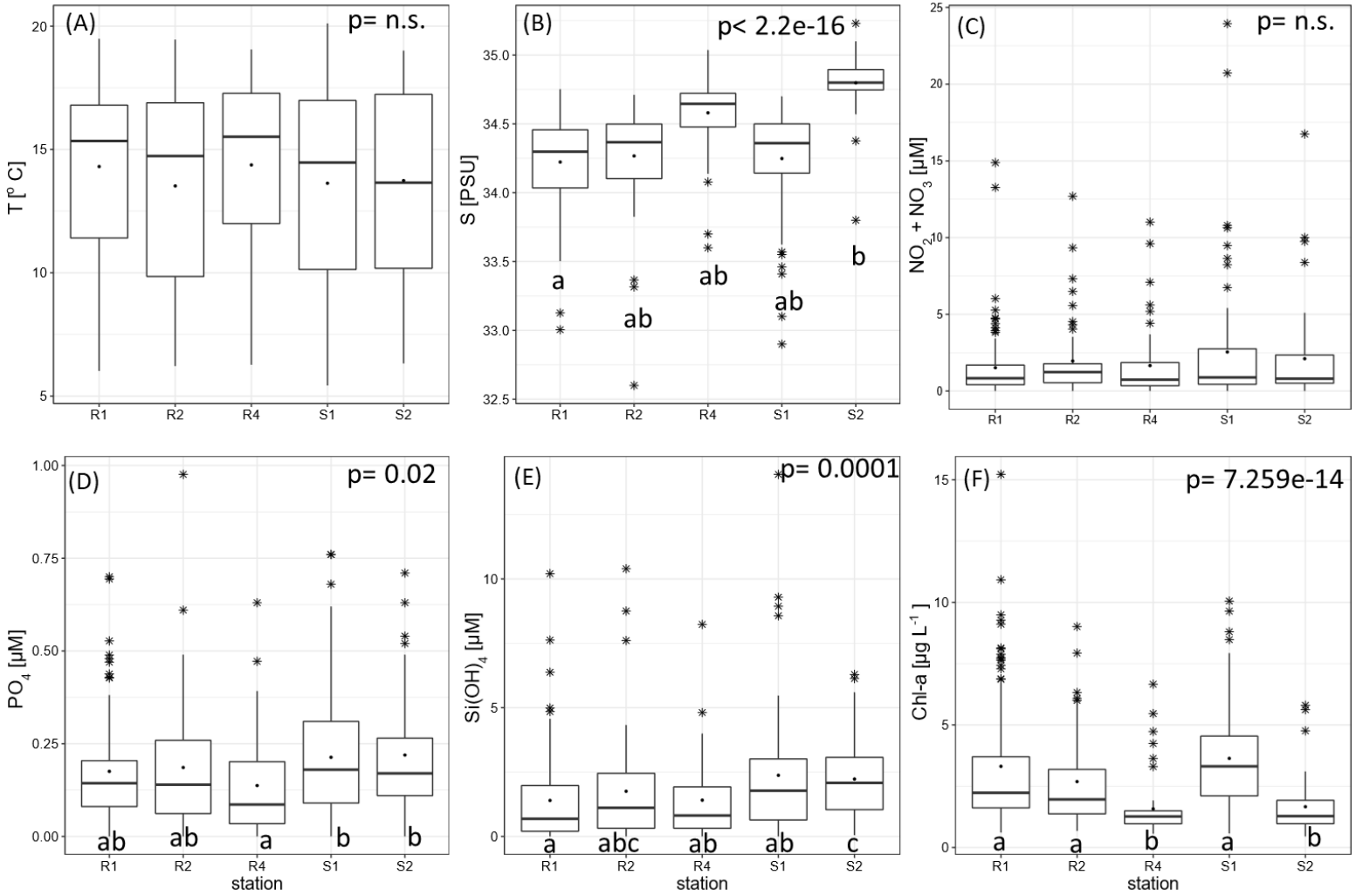

Figure S3.2. *Spatial variation of environmental variables measured in the EEC at the DYPHYRAD and SOMLIT stations from March 2016 to October 2020: (A) Temperature [T, °C], (B) S: Salinity [S, SSU], (C) Nitrites and Nitrates [NO_2+NO_3 µM], (D) Phosphates [PO_4, µM], (E) Silicates: [Si $(OH)_4$, µM], (F) Chlorophyll-a [Chl-a, µg L^{-1}]. The letters indicate significant differences ($p < 0.05$) between stations based on Kruskal-Wallis and Nemenyi post-hoc test on top and bottom of the boxplots respectively. Solid black lines represent the median, black dots the mean and the black stars the outliers.*

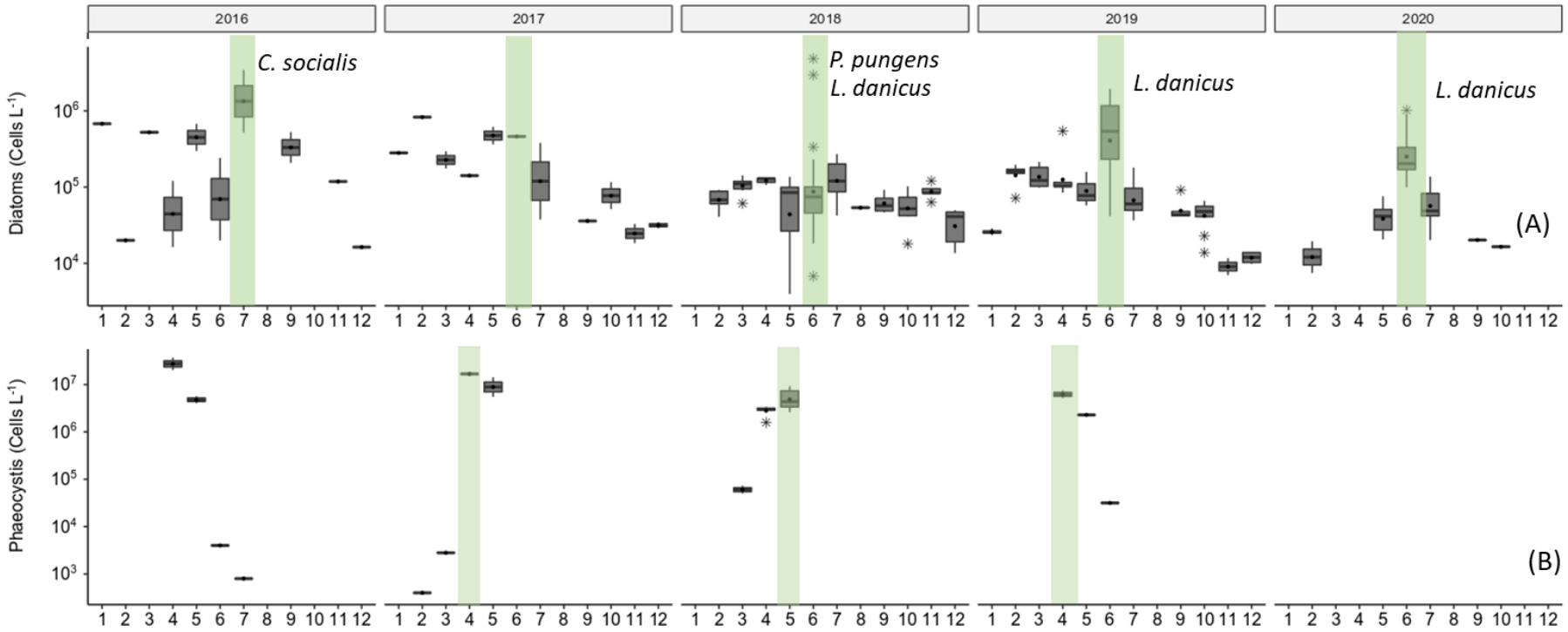

***Figure S3.3**. Abundance (cells L^{-1}) of phytoplankton (diatoms and Phaeocystis globosa) identified by microscopy in the EEC at the SOMLIT and DYPHYRAD stations from March 2016 to October 2020 based on microscopy and flow cytometry data., (A) diatoms, (B) Phaeocystis globosa. Y axis is log10 transformed. No data were available from February 14, 2020 to May 20, 2020 because of the sanitary crisis and on August due to annual leave of the personnel). Solid black lines represent the median, black dots the mean, and the black stars the outliers. The green stripe indicates the period presenting peaks.*

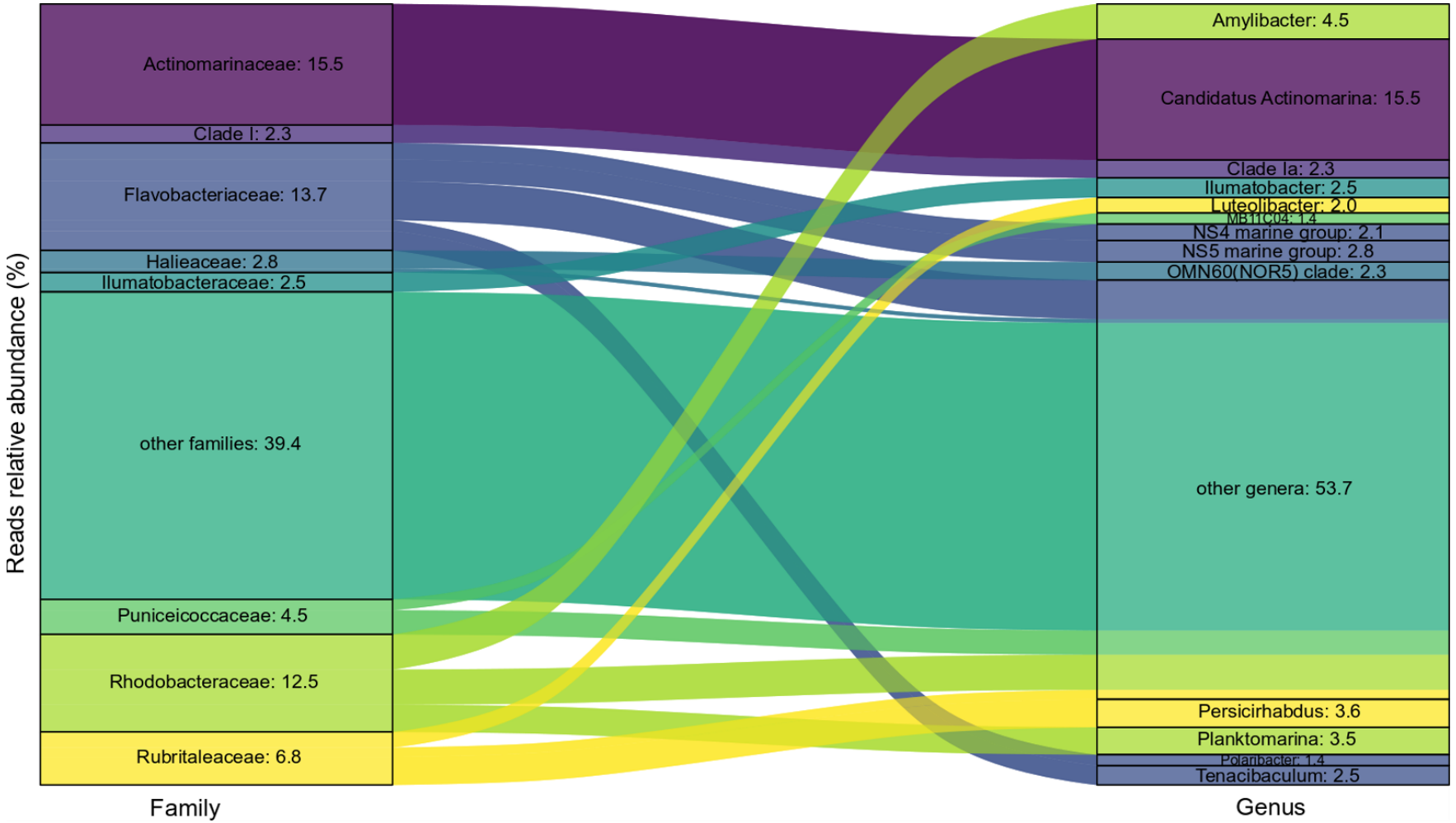

Figure S3.4. *Alluvial plot representing the relative abundance (%) of heterotrophic bacteria (X- axis) across family and genus taxonomic ranks (Y-axis), from March 2016 to October 2020 in the EEC at the DYPHYRAD and SOMLIT stations. The area of the alluvial being proportional to the taxa relative abundance. The 60.6 % of the families and their corresponding genera are presented in the alluvial plot, while the rest 39.4 % of the families is grouped as «other families» to facilitate the reading of the plot. Colors correspond to different families (the direction of the alluvial carries no meaning). Samples were rarefied at 8,000 reads.*

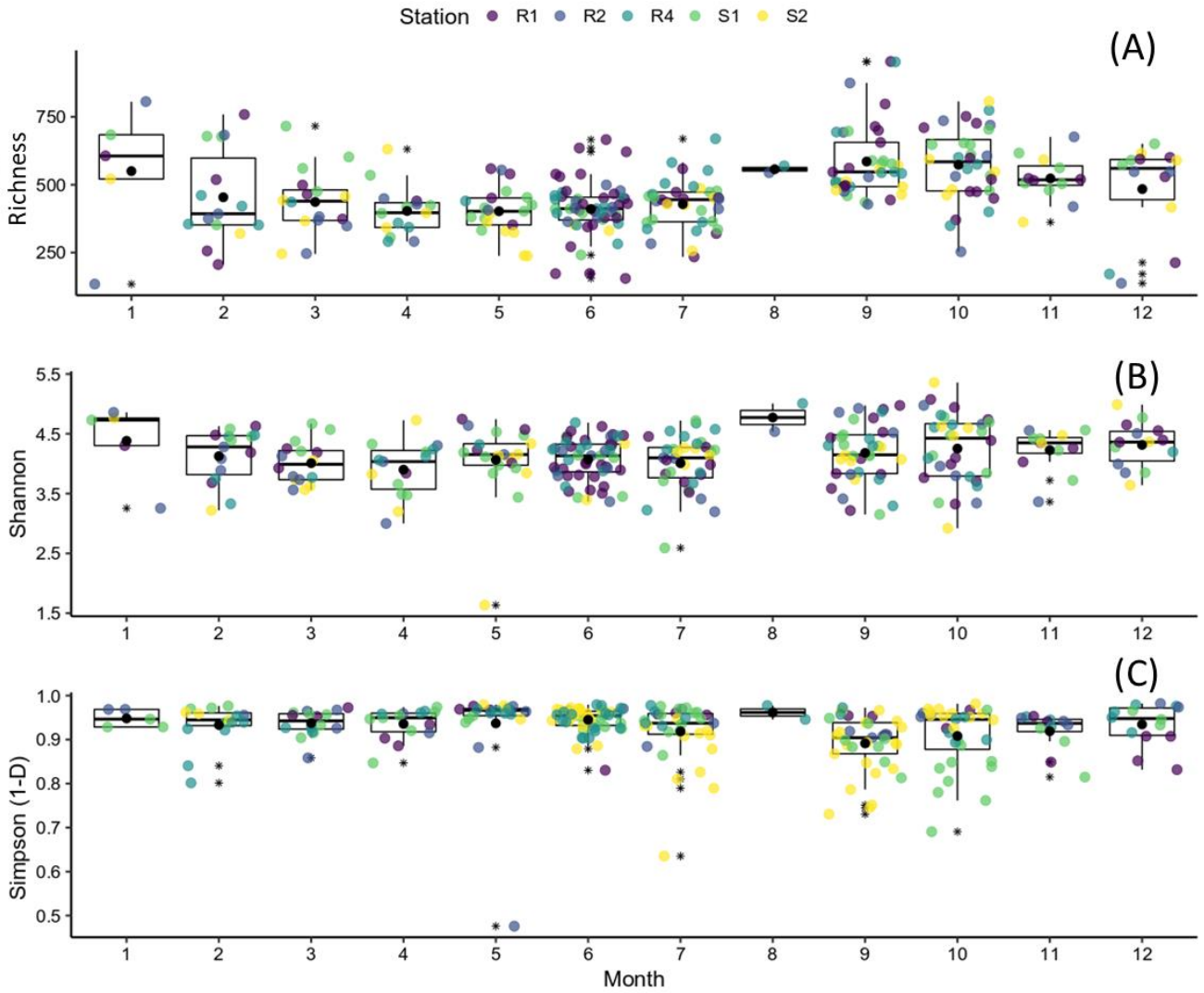

Figure S3.5. *Alpha diversity variations of the heterotrophic bacterial communities in the EEC at the DYPHYRAD and SOMLIT stations from March 2016 to October 2020. (A) Richness, (B) Shannon and (C) Simpson (1-D) indices. All samples were rarefied at 8,000 reads. Solid black lines represent the median, black dots the mean, coloured dots the samples according to stations and years, and the black stars the outliers.*

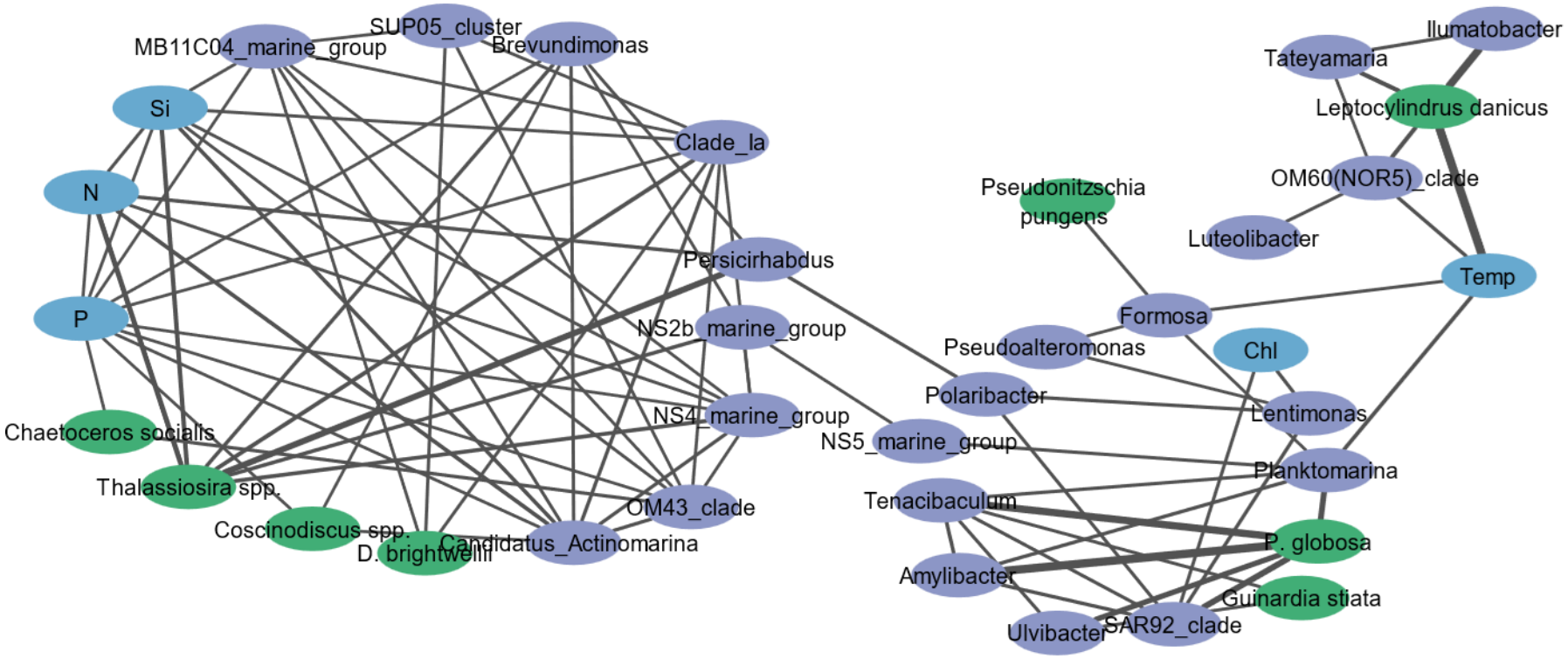

Figure S.3.6*. Network diagram of positively significant correlations (p<0.05) between the 22 dominant bacteria, 8 phytoplankton taxa (see Material and Methods), 5 environmental variables ($Si(OH)_4$, NO_2+NO_3, PO_4, temperature and Chl-a) as determined by eLSA analysis using a delay of one time point. To facilitate purple circles, represent the bacteria, blue ones the environmental variables, and green ones the phytoplankton taxa. The width of the lines (edges) corresponds to the LS score.*

Table S3.1. *Station and sample description. Max. depth corresponds at highest tide. To note that S1 and R1 being closer to the coast were easier to sample under difficult weather conditions (see also Fig. S3.1). Environmental parameters and 16S rDNA amplicon sequencing were realized for all samples (i.e.,282) from 2016 to 2020. Microscopic counts for phytoplankton and flow cytometry acquired from 2018 to2020 at all stations.*

Station	Date	Long (°E)	Lat (°N)	Max. depth	Distance from the coast (km)	Sampling Frequency	No of samples
S1	2016-2020	1.521389	50.6875	27	2	Bi-weekly	65
S2	2016-2020	1.416667	50.6875	56	9.8	Bi-weekly	41
R1	2018-2020	1.566667	50.79944	19	2.6	Once/twice a week	85
R2	2018-2020	1.541667	50.79944	23	4.3	Once a week	43
R4	2018-2020	1.452222	50.79944	52	10.9	Once/twice a week	48

Table S3.2. *Cell to carbon biomass conversion factors used in this study for the estimation of biomass of Phaeocystis globose and diatoms identified in the EEC at the SOMLIT and DYPHYRAD stations from March 2016 to October 2020.*

	Conversion factor	References
Diatoms	pgC $cell^{-1}$=0.288 x $(biovolume)^{0.811}$	Based on linear dimensions, the biovolume was calculated according to the cell shape (Hillebrand *et al*., 1999). Conversion from biovolume to biomass according to Menden Deuer & Lessard 2000 and according to microscopic observations over the period 2007 - 2015 (Breton *et al*., 2017)
Phaeocystis free flagellate cells	8 pgC $cell^{-1}$	Schoeman *et al*., 2005
Phaeocystis colonial cells	14.2 pgC $cell^{-1}$	

***Table S3.3**. Monthly range, mean (±SD) and median values of the mean sea surface temperature (T, °C), salinity (S, PSU), nutrients (nitrite and nitrate: NO_2 + NO_3, phosphate: PO_4, all in µM, the N/P molar ratio, silicate $Si(OH)_4$, µM, chlorophyll-a (Chl-a, µg L^{-1}) in the EEC at the DYPHYRAD and SOMLIT stations from March 2016 to October 2020. Note that only three samples were available for August.*

	January	February	March	April	May	June	July	August	September	October	November	December
PAR_{10m} (E m^{-2} d^{-1})												
Range	17.4-21.3	23.2-35.5	36.2-52.8	56.5-69.3	73.03-83.86	84.3-86.7	79.7-86.7	66.5-66.5	46.6-64.0	29.4-46.4	20.2-28.3	14.8-17.5
Mean±SD	19.2±1.6	29.1±3.8	46.7±4.7	62.3±3.1	79.67±3.57	86.1±0.7	84.2±2.1	66.5±0.0	55.6±5.7	39.7±5.5	22.7±2.8	16.0±1.0
Median	19	28.6	48.2	63.7	81.27	86.4	84.9	66.5	55.2	38.3	22.2	15.9
CV(%)	8.4	13.1	10.0	5.1	4.48	0.9	2.5	0.0	10.2	14.2	12.5	6
T (°C)												
Range	5.4-7.9	6.0-8.3	5.8-9.5	8.6-11.4	11.03-14.7	13.7-18.2	16.5-20.1	19.1-19.5	12.4-19.8	14.4-18.1	10.6-14.9	8.1-11.4
Mean±SD	7.1±0.8	7.4±0.7	8.0±1.3	9.6±0.7	12.91±1.06	15.4±1.0	17.8±0.8	19.3±0.2	18.1±1.3	16.2±0.9	12.6±1.3	10.2±0.8
Median	7	7.5	8.2	9.7	12.86	15.4	17.8	19.5	18.6	16.4	12.8	10.4
CV(%)	11.8	10.2	16.6	7.5	8.19	6.4	4.2	1.2	7.4	5.4	10.4	7.9
S (µM)												
Range	33.8-34.9	32.9-34.8	33.3-34.9	32.6-35.2	33.5-35.0	31.2-35.1	33.4-34.9	0.03-0.1	33.8-34.9	33.6-35.1	34.1-35.0	33.9-35.0
Mean±SD	34.2±0.4	34.0±0.6	34.2±0.5	34.1±0.6	34.2±0.4	34.3±0.5	34.6±0.3	34.6±0.2	34.5±0.2	34.5±0.3	34.6±0.3	34.4±0.3
Median	34.1	34.1	34.2	34.2	34.09	34.4	34.6	34.6	34.6	34.5	34.6	34.3
CV(%)	1.0	1.7	1.5	1.7	1.27	1.4	0.9	0.5	0.5	0.8	0.8	0.8
NO_2+NO_3 (µM)												
Range	3.4-10.6	0.3-23.9	1.1-20.7	0.3-9.3	0.14-1.6	0.01-4.4	0.2-1.1	0.2-0.5	0.3-2.8	0.2-3.5	0.4-5.2	1.1-8.6
Mean±SD	8.0±4.0	7.6±6.6	5.2±4.4	2.2±2.3	0.53±0.4	0.9±1.0	0.5±0.2	0.4±0.2	1.0±0.6	1.5±0.8	2.2±1.4	3.5±2.4
Median	10.0	4.2	4.2	1.5	0.41	0.5	0.5	0.5	0.7	1.5	1.8	2.9
CV(%)	49.8	86.5	85.2	104.1	74.01	113.5	42.0	44.2	67.8	52.4	66.3	68.6
PO_4 (µM)												
Range	0.4-0.6	0.2-1.0	0.01-0.6	0.03-0.3	0.01-0.29	0.01-0.4	0.01-0.2	0.1-0.2	0.01-0.5	0.03-0.4	0.01-0.5	0.1-0.8
Mean±SD	0.5±0.1	0.5±0.2	0.3±0.1	0.1±0.1	0.1±0.07	0.1±0.1	0.1±0.05	0.1±0.1	0.17±0.1	0.2±0.1	0.3±0.2	0.4±0.2
Median	0.5	0.5	0.2	0.2	0.11	0.1	0.1	0.1	0.14	0.2	0.2	0.4
CV(%)	14.0	39.3	51.3	47	71.24	91.7	57.0	52.2	64.0	46.5	56.4	47.3
N/P												
Range	7.0-24.2	0.4-35.2	4.8-52.7	1.5-43.7	0.82-262.5	2.1-316.1	1.1-15.3	3.0-3.9	2.3-78.0	2.7-16.3	0.4-5.2	3.8-21.1
Mean±SD	16.6±8.7	14.7±10.5	18.5±13.2	13.0±12.0	25.71±61.0	17.4±42.4	7.3±3.3	3.4±0.4	8.4±12.2	7.7±2.7	2.2±1.4	9.1±4.6
Median	18.5	9.4	14.6	9.3	4.22	7.5	6.5	3.3	5.3	7.1	1.8	9.0
CV(%)	52.8	71.8	71.7	92.0	237.3	243.6	44.8	12.2	145.0	35.0	66.3	50.2
$Si(OH)_4$ (µM)												
Range	4.6-8.8	1.8-14.1	0.1-5.2	0.1-3.6	0.05-2.68	0.01-3.0	0.01-3.4	1.1-2.9	0.01-4.8	0.1-6.1	0.3-5.5	1.0-9.3
Mean±SD	5.9±1.9	5.2±3.6	1.9±1.5	0.9±0.8	1.04±0.70	0.9±0.9	1.3±1.1	2.1±0.9	1.2±1.1	1.8±1.7	2.7±1.5	4.6±2.7
Median	5.1	3.3	1.8	0.6	0.9	0.6	1.2	2.3	0.7	1.5	3.1	4.3
CV(%)	33	68.3	79.2	88.9	67.52	96.5	84.2	41.9	92.8	92.7	53.5	58.6
Chl-a (µg L^{-1})												
Range	1.01-2.77	0.6-7.9	1.6-9.3	0.6-15.2	0.6-10.9	0.6-9.6	0.6-8.5	0.8-1.5	0.5-7.9	1.0-6.9	0.7-4.6	0.5-3.5
Mean±SD	1.7±0.6	3.9±2.2	5.1±2.3	5.7±3.1	2.9±3.0	2.3±1.7	2.1-1.5	1.1±0.3	1.6±1.2	2.4±1.3	2.5±1.4	1.5±0.9
Median	1.6	3.5	5.1	5.4	1.7	1.8	1.7	0.9	1.3	2.0	2.6	1.3
CV(%)	33.7	56.7	44.3	54.9	102.2	74.1	70.8	32.6	73.5	53.0	56.9	61.2

***Table S3.4**. Network statistics of the eLSA analysis without lag and with lag delay of 1 time point. The connections with $p < 0.05$ are shown. All topological parameters were calculated with Cytoscape v.3.9.1 (Shannon et al., 2003).*

	no lag	lag 1
Nodes	36	36
Edges (pairs)	95	84
Avg. number of neighbours	3,900	4,667
Network diameter	6	8
Network radius	3	4
Characteristic path length	2,737	3,757
Clustering coefficient	0.478	0.529
Network density	0.205	0.133
Network heterogeneity	0.421	0.539
Network centralization	0.181	0.161
Connected components	2	1

***Table S3.5**. Topological statistics (Characteristic Path Length, Clustering Coefficient, Edges) of the network without lag corresponding to bacteria, phytoplankton and environmental variables shown in the network (Fig. 3.6).*

Sub-networks	**Characteristic Path Length**	**Clustering Coefficient**	**Edges**
Non-blooming period			
Phytoplankton			
Thalassiosira spp.	1.53	0.52	7.00
Coscinodiscus spp.	1.87	0.90	5.00
D. brightwellii	1.80	1.00	5.00
Guinardia stiata	1.93	0.00	2.00
Bacteria			
Candidatus_Actinomarina	1.27	0.58	11.00
NS4_marine_group	1.27	0.58	11.00
NS2b_marine_group	1.67	0.60	5.00
SUP05_cluster	1.60	0.79	8.00
MB11C04_marine_group	1.47	0.67	9.00
Persicirhabdus	1.93	0.40	5.00
Clade_Ia	1.40	0.72	9.00
OM43_clade	1.53	0.78	9.00
Brevundimonas	2.27	1.00	3.00
Environmental variables			

NO_2	1.60	0.60	6.00
PO_3	1.53	0.75	8.00
$Si(OH)_4$	1.47	0.75	9.00
Mean±SD	**1.63±0.27**	**0.66±0.24**	**7.00±2.68**
***P. globosa* bloom**			
Phytoplankton			
P. globosa	2.47	0.53	6.00
Bacteria			
Polaribacter	2.16	0.30	5.00
Tenacibaculum	2.68	0.67	4.00
Ulvibacter	3.26	1.00	3.00
Lentimonas	2.37	0.33	4.00
SAR92_clade	2.16	0.40	6.00
Planktomarina	2.68	0.40	5.00
NS5_marine_group	3.63	0.00	1.00
Amylibacter	2.63	0.47	6.00
Pseudoalteromonas	2.11	0.33	3.00
Environmental variables			
Chl-a	2.79	0.33	3.00
Mean±SD	**2.63±0.47**	**0.43±0.25**	**4.18±1.60**
Diatom blooms			
Chaetoceros socialis	2.79	1.00	2.00
Leptocylindrus danicus	2.84	0.67	4.00
Pseudonitzschia pungens	3.84	0.00	1.00
Bacteria			
Luteolibacter	2.89	0.33	3.00
Formosa	2.21	0.33	4.00
Ilumatobacter	3.74	1.00	2.00
Tateyamaria	2.84	0.67	4.00
OM60(NOR5) clade	2.53	0.50	5.00
Environmental variables			
Temp	2.11	0.29	7.00
Mean±SD	**2.87±0.6**	**0.53±0.3**	**3.56±1.8**

Chapter 4: Interannual dynamics of putative parasites (Syndiniales Group II)

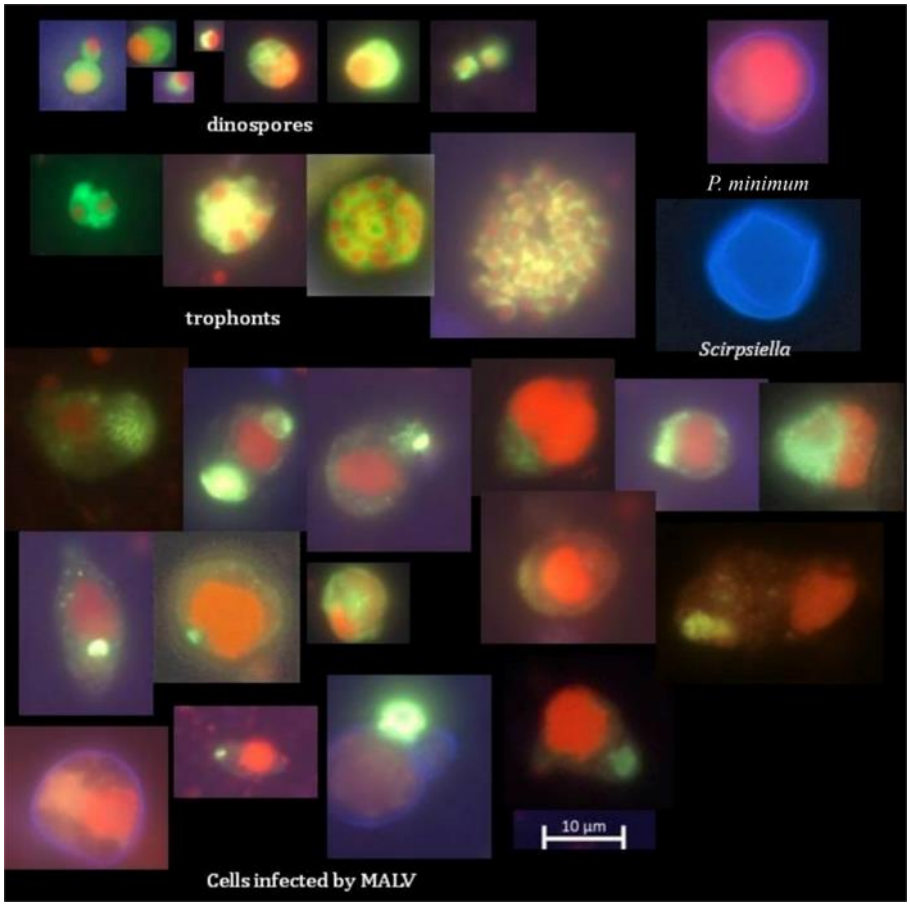

Preamble:

Parasitism is a biological relationship between two organisms, in which the parasite benefits from its host (Combes, 1996). One of the most abundant sequences in marine protistan diversity surveys belong to Syndiniales, known to be parasitic and to control blooms of dinoflagellates (e.g., Chambouvet *et al.*, 2008). Yet, current knowledge regarding spatiotemporal structures and host range of Syndiniales is scarce, due to difficulties with microscopic counts and culturing of these organisms (e.g., Sassenhagen *et al.*, 2020). A previous study in the EEC evidenced that Syndiniales Group II sequences showed peaks in April – May during the *Phaeocystis globosa* bloom (Christaki *et al*., 2017). However, co-occurrence network analysis, found no association between them. Metabarcoding only provides a relative abundance estimation of a taxon and not its absolute abundance. In the case of endosymbionts, metabarcoding does not allow for the identification of their hosts and thus their role. Direct observations are crucial for this purpose. In this chapter morphological data were used to describe protists communities (i.e., inverted microscopy), and to enumerate for the first time Group II Syndiniales spores (ie., FISH method) in the EEC. Furthermore, null models based on a phylogenetic metric according to the framework of Vellend were used to infer the ecological processes, governing the Syndiniales Group II assembly.

Interannual dynamics of putative parasites (Syndiniales Group II) in a coastal ecosystem

Urania Christaki[1*], Dimitra-Ioli Skouroliakou[1*], Ludwig Jardillier[2]

[1] Univ. Littoral Côte d'Opale ULCO, Univ. Lille, UMR CNRS 8187 LOG, 62930 Wimereux, France

[2] Université Paris-Saclay, CNRS, AgroParisTech, Ecologie Systématique Evolution, 91190 Gif-sur-Yvette, France

*the first two authors have equal contribution

This chapter has been published in the Environmental Microbiology Journal

*DOI: https://doi.org/10.1111/1462-2920.*16358

Résumé en Français

La dynamique temporelle du groupe II des Syndiniales a été étudiée en combinant le séquençage des amplicons 18S rDNA et le dénombrement direct par microscopie (hybridation in situ en fluorescence - amplification du signal à la tyramide (FISH-TSA) sur une période de 5 ans. L'étude a été menée dans un écosystème dominé par les diatomées, l'haptophyte *P. globosa* et présentant une abondance relativement faible de dinoflagellés. Une dynamique temporelle cohérente du groupe II des Syndiniales a été observé sur plusieurs années consécutives, mettant en évidence l'existence de populations locales. Selon les données de séquençage, le groupe II des Syndiniales a montré une abondance et une richesse croissantes en été et en automne. Les dinospores dénombrées par microscopie étaient présentes à de faibles abondances et étaient ponctuées par des pics transitoires. En été, l'abondance maximale de dinospores et leur prévalence ont coïncidé avec le pic d'abondance du dinoflagellé *Prorocentrum minimum*, tandis qu'en automne, le groupe II des Syndiniales avait probablement des hôtes plus diversifiés. Bien que plusieurs pics d'abondance de dinospores et de lectures (reads) coïncidassent, aucune relation cohérente n'a pu être démontrée entre eux. Les processus d'assemblage écologique à l'échelle saisonnière ont révélé que les processus stochastiques étaient les principaux moteurs (80 %) de l'assemblage de la communauté du groupe II, bien que des processus déterministes soient perceptibles (20 %) en juin et en juillet. Cette dernière observation pourrait refléter les interactions spécifiques entre les Syndiniales et les dinoflagellés en été.

Abstract

Temporal dynamics of Syndiniales Group II were investigated combining 18S rDNA amplicon sequencing and direct microscopy counts (Fluorescence in Situ Hybridization, FISH-TSA) during five years. The study was undertaken in meso-eutrophic coastal ecosystem, dominated by diatoms, the haptophyte *Phaeocystis globosa* and exhibiting relatively low dinoflagellate abundance (max. 18.6 × 10^3 cells L^{-1}). Consistent temporal patterns of Syndiniales Group II were observed over consecutive years highlighting the existence of local populations. According to sequencing data, Syndiniales Group II showed increasing abundance and richness in summer and fall. Dinospores counted by microscopy, were present at low abundances and were punctuated by transient peaks. In summer dinospore highest abundance (559 × 10^3 L^{-1}) and prevalence (38.5 %) coincided with the peak abundance of the dinoflagellate *Prorocentrum minimum* (13 × 10^3 L^{-1}) while in autumn Syndiniales Group II likely had more diversified hosts. Although, several peaks of dinospore and read abundances coincided, there was no consistent relation between them. Ecological assembly processes at a seasonal scale revealed that stochastic processes were the main drivers (80%) of the Syndiniales community assembly though deterministic processes were noticeable (20%) in June and July. This latter observation may reflect the specific Syndiniales - dinoflagellate interactions in summer.

4.1 Introduction

Parasitism greatly influences ecosystem functioning by altering food web structure carbon flow (Hudson *et al.,* 2006; Worden *et al.*, 2015). For example, by damaging their phytoplanktonic hosts, parasites decrease the primary production that sustains the trophic web (e.g., *Kagami et al.,* 2007; Rasconi *et al.*, 2011). Consequently, they produce labile dissolved organic matter that can be used by heterotrophic prokaryotes and zoospores that are consumed by zooplankton (Gleason *et al.,* 2008). In particular, Syndiniales which are known to infect a wide range of organisms have attracted additional attention in recent decades due to their repeated occurrence in sequence datasets (López-García *et al.,* 2001; Guillou *et al.,* 2008). High-throughput sequencing of marine planktonic communities have shown that the putative parasites Syndiniales are likely to be the most abundant and diversified members of the planktonic parasite community (e.g., Guillou *et al.,* 2008; Christaki *et al.,* 2017). Current knowledge concerning spatio-temporal structuring and the host range of Syndiniales is scarce, due to the difficulties of identifying the parasite-host consortia and their ecology (e.g., Sassenhagen *et al.*, 2020 and references therein). Within the order of Syndiniales, the dominance of Group I is well established in coastal and open-ocean waters (e.g., Guillou *et al*., 2008; Christaki *et*

al., 2017; Sassenhagen *et al.,* 2020; Sehein *et al.*, 2022). Direct observation on ciliates evidenced association of Group I with ciliates (reviewed by Skovgaard *et al.,* 2014) and single cell amplification has suggested that Group I could be associated to diatoms (Sassenhagen *et al*., 2020). Syndiniales Group II association with dinoflagellates has been directly evidenced through microscopic observations of hybridized cells (e.g., Chambouvet *et al*., 2008; Salomon *et al*., 2009; Siano *et al.*, 2011) thanks to specific FISH probes (Chambouvet *et al*., 2008) and has been also indirectly inferred via statistical approaches using metabarcoding data (e.g network analysis, Christaki *et al.*, 2017; Anderson and Harvey, 2020). The life-cycle of these parasites is well understood since 1964 (Cachon, 1964). It is characterized by an alternation between a biflagellated free-living infective stage (the dinospore) and an intracellular stage (the trophont) which grows and expands to fill up the host cell volume. The maturation of the trophont, takes a few days, it eventually kills the host and releases a motile worm-shaped multinucleated and multiflagellated structure (the vermiforme), which within a few hours, releases hundreds of dinospores, each potentially capable of infecting a novel host (Cachon 1964, Coats and Park, 2002).

Owing to the potential of Syndiniales Group II to terminate toxic dinoflagellate blooms most of the previous studies focusing on these algae's have been restricted to environments and periods in relation to dinoflagellate blooms (Chambouvet *et al*., 2008; Alves-de-Souza *et al.*, 2012; Velo-Suárez *et al.*, 2013). High prevalence of Syndiniales is usually associated with marked densities of host organisms, stratification, and may be influenced by the availability in nutrients (Alves-de-Souza *et al.*, 2015; Sehein *et al.*, 2022) though it has also been reported that dinospores (free-living, small flagellated Syndiniales forms, typically <10 μm) were able to infect dinoflagellates at relatively low dinoflagellate abundances (Salomon *et al.*, 2009) and in oligotrophic waters (Siano *et al.*, 2011).

The main objective of this study was to investigate the temporal dynamics of Syndiniales Group II in a productive constantly mixed coastal system - the Eastern English Channel (EEC). The EEC is characterized by diatom communities punctuated by spring blooms of the haptophyte *Phaeocystis globosa* and exhibiting relatively low dinoflagellate abundances (e.g., Grattepanche *et al.,* 2011; Breton *et al.*, 2017 and references therein). A previous temporal survey in the same area revealed the occurrence of Syndiniales in the EEC and provided insights into their temporal dynamics inferring their potential hosts through network analysis (Christaki *et al.*, 2017). However, co-occurrence networks allow inferring putative associations but do not

necessarily reveal real interactions. Direct observations are needed to identify microbial interactions such as parasitism.

Parasitic taxa usually present short transient peaks, that is, their abundance is usually low or below detection limit and they occasionally increase to a noticeable abundance at the community level) they could present annual and inter-annual distributions identified as of 'Conditionally Rare Taxa' (CRT, Shade *et al.,* 2014). Thus, the frequency of a conditionally rare taxon's abundance over time exhibits a bimodal distribution (Shade *et al*., 2014). Furthermore, as the overall community assembly processes is critical in tracking and predicting future changes in planktonic communities (e.g., Ramond *et al*., 2021; Xu *et al*., 2022, Skouroliakou *et al*., 2022 and references therein); an exploratory analysis was undertaken for Syndiniales Group II at a seasonal scale applying the null model analysis framework (Stegen *et al*., 2012, 2013). The *rationale* was that while ecological deterministic processes are conducive to modeling, stochastic ones are far less predictable. The results of a recent study analyzing processes regulating phytoplankton assemblages at the same area, provided strong support for a seasonal and repeating pattern with stochastic processes prevailing during most of the year, and in particular, during the periods that presented transient monospecific phytoplankton peaks (Skouroliakou *et al*., 2022). The main question in this study is whether the stochastic and deterministic ecological processes varied across seasons for Syndiniales Group II. Our hypothesis was that similarly to phytoplankton stochastic ecological processes prevail in Syndiniales Group II community assembly.

Overall, this study focused on the following specific questions: (i) On a technical aspect, is sequencing an accurate method to infer dinospore abundances? (ii) Do Syndiniales Group II, have seasonal patterns and do they relate to dinoflagellate dynamics? (iii) Do stochastic or deterministic ecological processes prevail in the Syndiniales Group II community assembly?
To answer these questions, a multiple year temporal survey at two different frequencies was conducted to better capture the temporal changes of planktonic communities (bi-weekly during 2016-2020 and at a higher frequency during 2018-2020 an effort to catch rapidly changing dinoflagellate Syndiniales Group II abundance dynamics). 18S rDNA amplicon Illumina Mi-Seq sequencing and dinospore enumeration were combined with the FISH-TSA method, microscopical examination of microplankton, and flow cytometry for nano- and picoplankton, along with measurements environmental parameters.

4.2 Material and Methods

4.2.1. Study site, sample collection

Samples were collected at 2 m depth at five neighboring stations between March 2016 and October 2020 (Fig. S4.1) using 12 L Niksin bottles. From 2016 to 2020, the SOMLIT coastal S1 and the offshore S2 stations (French Network of Coastal Observatories; https://www.somlit.fr/) were sampled bi-weekly (Table 4.1). Stations (R1, R2, and R4) belonging to the 'DYPHYRAD' transect situated about 15km north of the SOMLIT stations (Fig. S4.1, Table 4.1) were sampled weekly. Higher frequency samplings (2-3 times a week) were also carried out after the end of the spring bloom in June-July and in autumn in September-October at stations R1 and R4. *Phaeocystis globosa* spring bloom occurs every year in April-May (e.g Grattepanche, *et al*. 2011; Christaki *et al*., 2014, 2017; Breton *et al*., 2017, 2021). The higher frequency was applied in an effort to catch rapidly changing dinoflagellate Syndiniales Group II abundance dynamics. The post spring bloom and autumn periods were chosen as there are the ones where higher Syndiniales Group II and /or dinoflagellate abundances were observed in previous studies (eg. Grattepanche, *et al.*, 2011; Genitsaris *et al*., 2016; Christaki *et al*., 2014, 2017. To note that only three samples were collected in August due to the unavailability of the boat crew during their annual leave. For this reason, the August data are presented but not further discussed.

Table 4.1. *Station and sample description. Max. depth corresponds at highest tide. To note that S1 and R1 being closer to the coast were easier to sample under difficult weather conditions (see also Fig. S4.1). Environmental parameters and 18S rDNA amplicon sequencing were realized for all 2016-2020 samples. Microscopy counts of microplankton, flow cytometry and FISH-TSA for 2018-2020 samples at all stations (total 269 samples).*

Station	Date	Long (°E)	Lat (°N)	Max. depth	Distance from the coast (km)	Sampling Frequency	No of samples
S1	2016-2020	1.521389	50.6875	27	2	Bi-weekly	63
S2	2016-2020	1.416667	50.6875	56	9.8	Bi-weekly	39
R1	2018-2020	1.566667	50.79944	19	2.6	Once/twice a week	79
R2	2018-2020	1.541667	50.79944	23	4.3	Once a week	42
R4	2018-2020	1.452222	50.79944	52	10.9	Once/twice a week	46

4.2.2. Environmental variables

Seawater temperature (◦C) and salinity were measured *in situ* using a conductivity-temperature-depth profiling system (CTD Seabird SBE 25). The average subsurface daily PAR experienced by phytoplankton in the water column for a six-day period before sampling was obtained using a global solar radiation (GSR, Wh m^{-2}) recorded by the Copernicus Atmosphere Monitoring Service (CAMS) radiation service (http://www.soda-pro.com/web-services/radiation/cams-radiation-service). GSR was converted into PAR by assuming PAR to be 50% of GSR and by considering 1 W m^{-2} = 0.36 E m^{-2} d^{-1} (Morel and Smith, 1974). Inorganic nutrient concentrations (nitrate, NO_3^-), nitrite (NO_2^-), phosphate (PO_4^{3-}), and silicate ($Si(OH)_4$) were analysed according to Aminot and Kérouel (2004). Chlorophyll *a* (Chl-*a*) concentrations were measured by fluorometry (Lorenzen, 1966). Wind speed (m s^{-1}), wind direction (deg), and rainfall (kg m^{-2}) were obtained from the National Aeronautics and Space Administration (NASA) and Goddard Space Flight Center (http://gmao.gsfc.nasa.gov/reanalysis/MERRA-2, resolution 0.625°×0.5° , longitude x latitude). Wind stress (Pa) was calculated from wind speed as described in Smith, (1988). Additional details on environmental data acquisition and sample analysis can be found at https://www.somlit.fr/.

4.2.3. DNA barcoding, bioinformatic analysis

Four to seven liters of seawater depending on the quantity of the particulate material in the water i.e until signs of clogging of the filter) were filtered onto 0.2µm polyesthersulfone (PES) membranes (142mm, Millipore, U.S.A.) after a pre-screening step through 150 µm nylon mesh (Millipore, U.S.A.) to remove metazoans. Filters were stored at -80°C for 18S rDNA amplicon Illumina MiSeq sequencing. DNA extraction was performed according to the DNAeasy PowerSoil kit protocol (QIAGEN, Germany). To describe protist diversity, the V4 hypervariable region of the 18S rDNA gene (527 bp) was amplified using the primers EK-565F (5'-GCAGTTAAAAAGCTCGTAGT) and UNonMet (5'-TTTAAGTTTCAGCCTTGCG) biased against Metazoa (Bower *et al.*, 2004). Pooled and purified amplicons were then paired-end sequenced on an Illumina MiSeq 2 × 300 platform by Genewiz (South Plainfield, NJ, USA).

Quality filtering of reads, identification of amplicon sequencing variants (ASV), and taxonomic affiliation based on the PR2 database (Guillou *et al*., 2013) were done in the R-

package DADA2 (Callahan *et al*., 2016). A total number of 41,179 ASVs were identified from 6,366,087 reads in 287 samples containing Metazoa, Streptophyta, Excavata, Alveolata, Amoebozoa, Apusozoa, Archaeoplastida, Hacrobia, Opisthokonta, Rhizaria, and Stramenopiles. ASVs affiliated to Excavata, Metazoa, Streptophyta, unaffiliated ASVs and singletons were removed, obtaining a phyloseq object containing 20,651 taxa by eight taxonomic ranks. After eliminating samples with less than 5,000 reads, the number of reads per sample was rarefied to the lowest number of reads (5,234) which produced 15,250 ASVs distributed in 269 samples. Then, only taxa affiliated to the order Syndiniales Group II were kept, resulting in a new phyloseq object composed of 663 taxa detected in 269 samples (for more details on DNA barcoding and bioinformatic analysis, see Suppl. Information). Raw sequencing data have been submitted to the Short Read Archive under BioProject number PRJNA851611.

4.2.4. Fluorescent in situ Hybridisation (FISH-TSA)

Fluorescent in situ hybridization (FISH) coupled with tyramide signal amplification (TSA) was used to enumerate Syndiniales Group II dinospores and observe infected hosts. Dinospores and infected hosts were enumerated on the same hybridized filters. Samples (300 mL) were fixed with paraformaldehyde (1% final concentration) for 1 hour at 4°C and then filtered onto 0.6 µm polycarbonate membranes. The filters were dehydrated by several successive ethanol baths (50%, 70%, and 100%) and stored at -80°C until analysis. The oligonucleotide probe ALV01 (5'-GCC TGC CGT GAA CAC TCT-3') was used to target Syndiniales Group II dinospores (Chambouvet *et al*., 2008). A total of 199 filters over the period 2018-2020 were proceeded with FISH-TSA following the protocol described in (Piwosz *et al*., 2021 and references therein). Following the TSA reaction, the filters were counter stained 15 min with calcofluor (100 ng ml^{-1}) to visualise armored dinoflagellates. All counts were performed with an epifluorescence microscope at 100x (Zeiss Imager M2) with different fluorescence filters (for calcofluor, excitation: 345 nm; emission: 475 nm), promidium iodide (excitation: 536 nm; emission: 617 nm) and FITC (excitation: 495 nm; emission: 520 nm), 150 optical fields at x100 corresponding to 873±149 µl of initial sample (390-1333 µl) were observed for each filter (for more details see Suppl. Information).

4.2.5. Microscopic and cytometric counts (morphological data)

For diatoms and *P. globosa* colonies and free cells counting, 110 mL water samples were collected and fixed with Lugol's-glutaraldehyde solution (1% v/v, which does not disrupt *P. globosa's* colonies, Breton *et al*., 2006). For dinoflagellates, another 110 mL were fixed

with acid Lugol's solution (1% v/v) (data for dinoflagellates are available for 2018-2020, Table 4.1). Phytoplankton was identified to the species or genus level when possible using an inverted microscope (Nikon Eclipse TE2000-S) at 400x magnification after sedimentation in a 10, 50, or 100 mL Hydrobios chamber, as described previously in (Breton *et al*., 2021). The abundance of pico- and nanophytoplankton (PicoNano, 0.2-20 µm) and *P. globosa* free cells were enumerated by flow cytometry with a CytoFlex cytometer (Beckman Coulter). For all samples, 4.5 ml were fixed with paraformaldehyde (PFA) at a final concentration of 1% and stored at -80 °C until analysis (Marie *et al*., 1999). Phytoplankton cells were detected according to the autofluorescence of their pigments (Chl-a, 488 nm). *P. globosa* was discriminated from the PicoNano group based on orange fluorescence (Phycoerythrin, 496 nm) and size (FSC). Heterotrophic nanoflagellates (HNF) were enumerated after staining with SYBRGreen I following (Christaki *et al*., 2011).

4.2.6. Abundance distribution and community assembly of Syndiniales Group II

Shade *et al*., (2014) suggested a simple method for detecting conditionally rare taxa (CRT) based on the coefficient of bimodality (b) defined by Ellison (1987),

$$b=(1+skewness^2)/(kurtosis+3) \quad (1)$$

According to Shade *et al*., (2014) when b > 0.9, taxa are conditionally rare (CRT). The "b" coefficient was calculated for abundant ASVs representing a relative abundance ≥ 0.01 in the Syndiniales Group II (this corresponded ≥ 500 reads, and 72 % of the total Syndiniales Group II reads). For comparison, the bimodality coefficient was also calculated for the 55 ASV with ≥ 100 reads (84% of the total reads).

To explore the ecological assembly processes regulating Syndiniales Group II at a seasonal scale null models based on metabarcoding data were applied according to Stegen's framework (Stegen *et al*., 2012, 2013) reviewed by Zhou and Ning (2017). Briefly, the community assembly analysis is based on the comparison of observed community turnovers (shifts in composition across samples), phylogenetic turnovers (shifts in composition weighted by the phylogenetic similarity between taxa), and turnovers expected by chance (in null-models). This information is used to estimate whether the differences between pairs of communities are explained by dispersal, selection, or ecological drift. According to this framework, deterministic processes are divided into homogeneous selection (i.e., consistent abiotic or biotic conditions filter which parasites can persist) and heterogeneous selection (i.e., high compositional turnover caused by shifts in environmental factors or hosts). Stochastic processes are divided into homogeneous dispersal (i.e., low compositional turnover caused by high dispersal rates),

dispersal limitation (i.e., high compositional turnover caused by a low rate of dispersal), and ecological drift that can result from fluctuations in population sizes due to chance events (Table 4.2).

***Table 4.2**. Definitions of the different assembly processes, and respective model conditions referenced from Webb 2002, Stegen et al. (2012, 2013) and Zhou and Ning 2017.*

	Deterministic processes		**Stochastic processes**		
	Homogeneous selection	Heterogeneous selection	Dispersal limitation	Homogeneous dispersal	Drift
Definition	Consistent biotic (i.e., hosts) or abiotic factors cause low compositional turnover	Shifts in biotic (i.e., hosts) or abiotic factors cause high compositional turnover	Movement of individual is restricted	High rate of movement of an individual from one location to another	Population size fluctuates due to chance events
Phylogenetic turnover index	βNRI < -2	βNRI > 2		-2 < βNRI < 2	
Taxonomic turnover index	-	-	RC_{bray} > 0.95	RC_{bray} < -0.95	-0.95 < RC_{bray} < 0.95

The implicit hypothesis is that phylogenetic conservatism exists, which means that ecological similarity between taxa is related to their phylogenetic similarity (i.e., phylogenetic signal) (Losos, 2008). The Mantel correlogram was applied to detect phylogenetic signal (e.g., Liu *et al*., 2017; Doherty *et al*., 2020, for details see Suppl. Information). The phylogenetic temporal turnover (betaNRI) between pairwise communities among sampling dates was quantified to investigate the action of deterministic and stochastic ecological processes with microeco R-package v.0.6.0 (Liu *et al*., 2021), using the trans_nullmodel function. The phylogenetic distance between pairwise communities (beta mean pairwise distance: βMPD) was computed with null models based on 999 randomizations with the random shuffling of the phylogenetic tree labels, as in Stegen et al., 2013. All definitions of the different assembly processes corresponding to the values of βNRI are shown in Table 4.2. Non-weighted metrics were used as metabarcoding data are semi-quantitative and the rarefied dataset was considered to prevent any bias due to potential under-sampling (Ramond *et al*., 2021). All analysis was run with R version 4.1. 0 (R core team 2021).

4.3. Results

4.3.1. Environmental variables

The environmental variables showed seasonal patterns typical of temperate marine waters. Nutrient inputs originated mainly from local rivers and reached relatively high values during autumn and winter with the highest values in February (Fig. S4.2A). The N/P ratio was highly variable ranging from 0.4 to 316, strongly deviating most of the time from the Redfield ratio (N/P=16, Redfield, 1958). Overall, the environmental variables were of the same range and showed the same seasonal variations at all stations. A comparison of the mean ranks (Kruskal Wallis and Nemenyi post hoc test) of environmental variables between the different stations revealed significant differences in salinity, phosphate, silicate, and Chl-*a* between the stations (Fig. S4.2B). Principal Component Analysis (PCA) performed on the environmental dataset showed a seasonal pattern opposing winter and summer conditions. Overall, summer and autumn samples formed tighter groups on the PCA biplot than spring and winter samples which were more dispersed (Fig. S4.3).

4.3.2. Planktonic eukaryotic diversity and abundance

Microscopic counts of diatoms and *Phaeocystis globosa*, and flow-cytometric counts of pico-nanophytoplankton showed that diatoms were always abundant with highest abundances from winter to early summer (range 4×10^3 - 5×10^6 cells L^{-1}, Fig. 4.1A). *P. globosa* bloomed in April and May, reaching a peak of 3.6×10^7 cells L^{-1} (Fig. 4.1B). Pico-nanophytoplankton showed clear seasonal variations, with the highest abundance in early summer after the phytoplankton spring bloom and then in autumn (Fig. 4.1C). Heterotrophic nanoflagellates highest values were recorded each year in May - June after the spring phytoplankton bloom (range 0.2×10^6 - 1.8×10^7 cells L^{-1}, Fig. 4.1D). Dinoflagellates -although they presented the highest number of reads- were three orders of magnitude less abundant than diatoms (ranging from 0.76 to 18.6×10^3 cells L^{-1}). Dinoflagellates reached their lowest abundances in winter and highest in summer after the end of *P. globosa* bloom (Fig. 4.1E). *Gymnodinium* spp. was the most abundant dinoflagellate genus in almost all samples while two other dinoflagellates (*Prorocentrum minimum* and *Scrippsiella* spp.) showed moderate increases in summer (Fig. S4.4). Ciliates presented relatively low abundances from <100 cells L^{-1} to 7.4×10^3 cells L^{-1} (Fig. 4.1F).

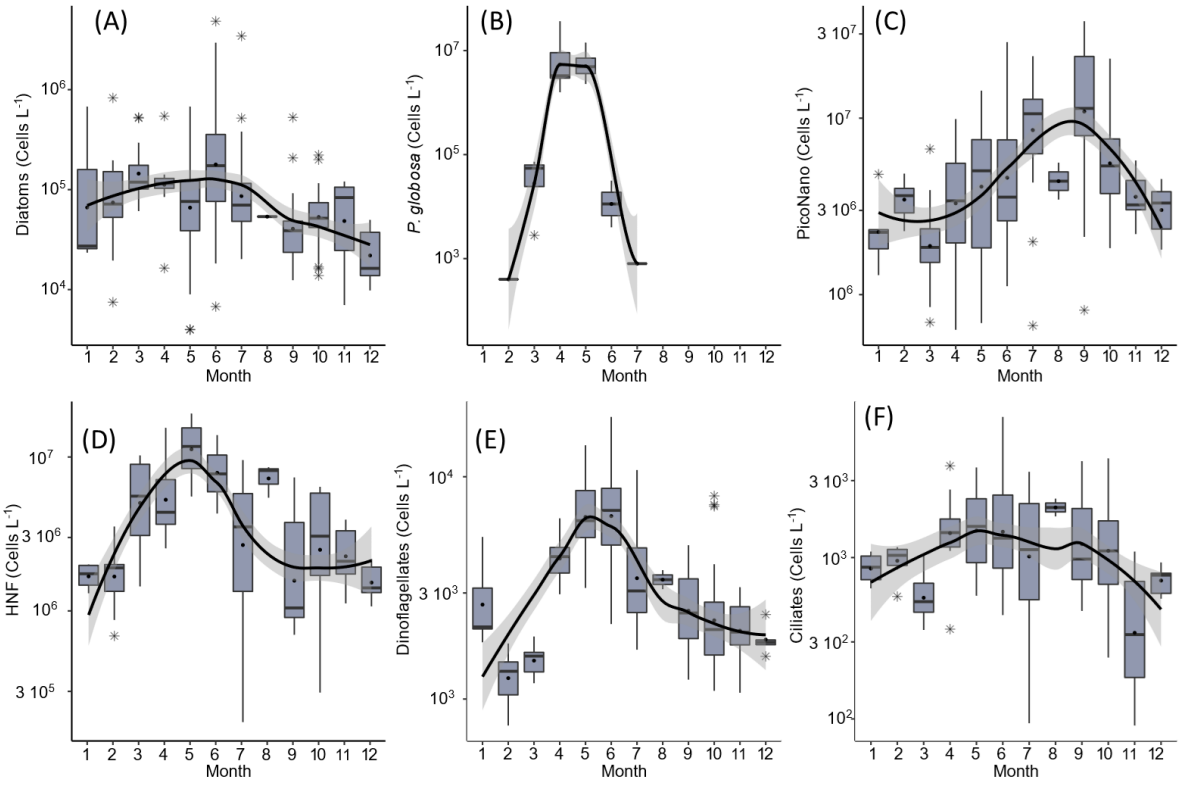

Figure 4.1. *Seasonal variation of protist abundance (cells L^{-1}): (A) Diatoms, (B) P. globosa, (C) PicoNano: pico-nanophytoplankton, (D) HNF: heterotrophic nanoflagellates, (E) dinoflagellates, and (F) ciliates, identified in the eastern English Channel at the SOMLIT and DYPHYRAD stations from March 2016 to October 2020. Y scale is log10 transformed. Solid black lines in the boxplot represent the median, black dots the mean, and the black stars the outliers. The solid line and ribbon represent LOESS smoothing and the 95% confidence interval. Data for ciliates and dinoflagellates were available for 2018-2020*

Sequence data showed that the most abundant group in terms of number of reads was Dinophyceae (30%), followed by Baccilariophyta (25%), and Syndiniales (10%) (Fig. 4.2A). Within Syndiniales, Group I was the most abundant (61 %, 6 Clades, 285 ASVs, Fig. 4.2B) while Group II was the most diversified (35 %, 27 Clades, 663 ASVs). Within Syndiniales Group II, Clades 10, 11, and 8 dominated (21, 25 and 9 % of the reads, respectively, Fig. 4.2C). Syndiniales Group II showed highest abundance and richness in June, July, and September and lowest in winter; the highest number of reads occurring in June 2018 (Fig. 4.3 A, B). Fifteen samples showed high Syndiniales Group II abundance (> 600 reads, Fig. 4.3A). Clade 8 was the most abundant clade in terms of reads, followed by Clades 10, 11, 14, 30, 5, and 13, respectively (Fig. S4.5). The most important peaks were observed at the beginning of summer and autumn (Fig. 4.3A-B). While the summer peaks were mostly dominated by Clade 8, a variety of clades and ASV dominated in the autumn peaks (Fig. S4.5). The highest values of Syndiniales Group II read abundance and richness were recorded at station R1 which was the

closest to the coast but also the most visited (Fig. S4.6 A-B, Table 4.1). The cumulative number over time of ASVs affiliated to Syndiniales Group II constantly increased. The cumulative plot based on new ASVs between two consecutive dates revealed that the slope of the cumulative curve became steeper with the influx of new ASVs in summer and autumn and with a particular high number of new ASV in autumn 2020 (Fig. S4.7).

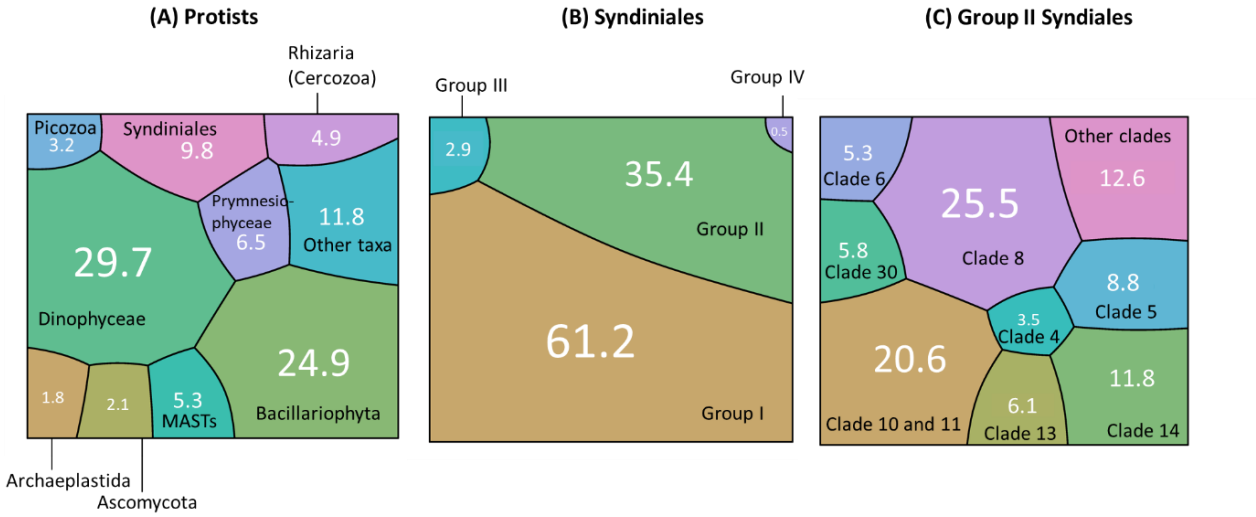

Figure 4.2. *Voronoi diagrams representing the relative abundance, given in percentage, of different protist taxonomies from 2016 to 2020 in the eastern English Channel at the SOMLIT (S1, S2) and DYPHYRAD (R1, R2, and R4) stations. The area of each cell being proportional to the taxa relative abundance (the specific shape of each polygon carries no meaning). This type of visualization is similar to pie charts but represents better small contributors (A) Relative abundance of the nine identified supergroups, (B) Relative abundance of Dino-Group Syndiniales within the taxonomic Class Syndiniales, (C) Relative abundance of Clades within Group II Syndiniales. Visualisation performed using the online tool http://www.bioinformatics.com.cn/srplot.*

Dinospores cells were counted by microsopy (on FIST-TSA hybridized filters) ranged from undetectable to 5.6×10^5 L^{-1} (Fig. 4.3C) and generally followed a seasonal pattern similar to the one of dinoflagellate microscopy abundances (Figs. 4.1E, 4.3C). The highest values of dinospore abundance were also recorded at station R1 (Fig. S4.6C, Table 4.1). Although dinospore abundances followed similar seasonal patterns with Syndiniales Group II reads (Fig. 4.3A-C, 4.2E) the number of reads cannot be used a predictor of number of dinospores and *vice versa* as there was no consistent numerical relationship between them (Fig. S4.8).

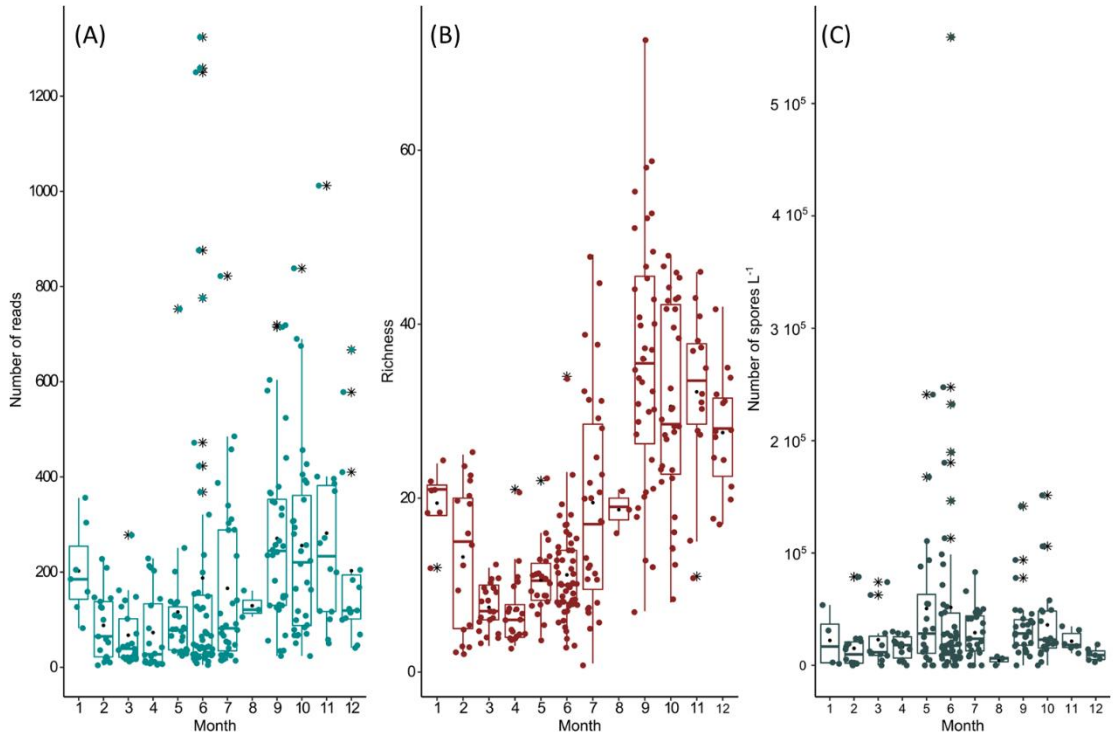

Figure 4.3. *Seasonal variation of Group II Syndiniales in the eastern English Channel at the SOMLIT and DYPHYRAD stations. (A) Number of reads, (B) Richness, (C) Dinospores. Solid lines in the boxplot represent the median, black dots the mean, and the black stars the outliers.*

4.3.3. Syndiniales Group II occurence and potential hosts

The maximum likelihood tree of the 20 most abundant Syndiniales Group II ASVs (i.e., ASVs representing at least 1% of the reads affiliated to Syndiniales within the rarefied dataset), showed that ASVs belonging to Clade 8 (ASV13 and ASV124) were the most phylogenetically distant from the rest of the Clades present. Clades 10, 11, and 14 were those phylogenetically closer to each other (Fig. 4.4). The majority of the most abundant ASVs were present every year at low or very low abundances and showed a few transient peaks. Indeed, 13 out of the 20 ASVs were found every year, while 7 were absent at least one year and up to three years (Fig. 4.4). Among these most abundant ASVs, several ASVs can be characterized as "highly persistent" such as ASV13 (Clade 8), ASV50 (Clade 4) and ASV101 (Clade 4), since they were present every year and in more than 50% of all samples (Fig. 4.4). At the opposite, ASV401 (Clade 6), ASV439 (Clade 47) were found only in 2019 and 2020 (5% of the samples) where they showed a unique peak.

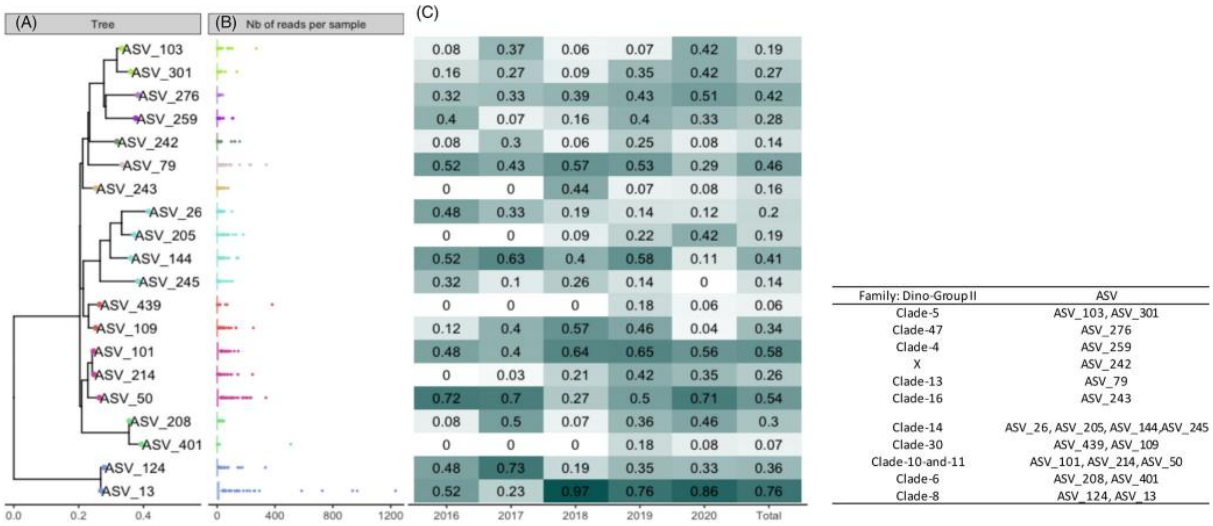

Figure 4.4. *Maximum likelihood tree of the 20 most abundant Group II Syndiniales ASVs (ASVs representing at least 1% of the Syndiniales affiliated reads on the rarefied dataset); (B) Boxplots of the number of reads per sample. Note that for all boxplots the median value is close to zero and high abundances are visible as outliers (C) ASVs relative abundance of samples where at least one read of each ASV was present for each year (2016-2020). To note that the number of samples differs between the years as follows 2016: 26 samples, 2017: 30 samples, 2018: 76 samples, 2019: 72 samples and 2020: 65 samples.*

Prevalence of infection was assessed when hosts were abundant enough to make accurate microscopy observations. Hosts were clearly identified during two infection events (Table 4.3). The first observed infection occurred during the *P. minimum* increase (up to 1.3×10^3 L^{-1}) coinciding with the dominance of Clade 8 (ASV 13) and the second was related to *P. micans* and *Scrippsiella spp.* and coinciding again to the dominance of Clade 8 in July 2019 (Table 4.3). Infected cells were rare and/or not possible to identify based on their morphology in the other samples although dinospores were detected. Host morphologies were diverse and represented athecate and thecate dinoflagellate cells and a few cells resembling ciliates. Trophont and veriform like Syndiniales were rarely observed in the samples (Fig. S4.9). It is worth noting, that microscopy observations of *P. globosa* and diatom cells, which reached very high abundances during the study, showed no sign of infection by Syndiniales Group II.

***Table 4.3**. Prevalence (%) of infected hosts identified in individual samples where it was possible to count at least 50 morphologically recognizable potential hosts were observed (for station position see Table 4.1 and Fig. S4.1). The clades present at each date are detailed in Fig. S4.5.*

Station, Date	R1 05/06/2018	R1 06/06/2018	R2 07/06/2018	R1 08/06/2018	S1 12/06/2018	R1 14/11/2018	R1 05/07/2019	R1 09/10/2019
Prevalence (%)	11.5	10.5	4.7	38.5	17.6	9.1	12.8	14.3
Infected protist	*P. minimum*	*P. minimum*	*P.minimum*	*P.minimum*	*P. minimum* *Amphidinium* sp. .	various	*Scripsiella* Sp. *P. minimum*	various

4.3.4. Abundance distributions and Syndiniales Group II Community Assembly

For the 20 most abundant ASVs (≥ 0.01 relative abundance), the coefficient of bimodality varied from 0.62 to 0.99 with only two ASVs identified as conditionally rare taxa (b > 0.9 ASV401 and ASV439). Applying the same calculation to the ASVs having ≥ 100 reads, the result was similar as the factor "b" varied between 0.62 and 0.99 and only three additional ASVs were detected as conditionally rare (b >0.9, see also Fig. S4.10).

In order to complement the abundance distribution analysis, the potential of stochasticity *vs* determinism regulating the Syndiniales Group II community was explored, and then, the associated ecological processes were quantified. The Mantel correlograms indicated phylogenetic signals at short phylogenetic distances (10-30 %, Fig. S4.11). The phylogenetic temporal turnover (βNRI) values ranged from -2 to 4.6 (Fig. 4.5A). The monthly variability of βNRI showed that the median value was between -2 and 2 (i.e., 1.4), defining stochastic assembly processes in Syndiniales Group II. However, βNRI values were somewhat greater than 2 defining '*determinism*' in June and July (Fig. 4.5A Table 4.2). The null model analysis suggested that 'ecological drift' was the major ecological process regulating the community assembly of Syndiniales Group II (80 %) with heterogenous selection accounting for 20% (Fig. 4.5B).

4.4. Discussion

In the present study, microscopy and flow cytometry were used to quantify pico- and nano-microplankton as well as dinospores, while metabarcoding data provided an extended evaluation of their diversity. The present study is original in its observation frequency -less than a week - and the duration of the survey - over a multiple of years -. In addition, contrary to most

previous studies, it was conducted in a meso-eutrophic coastal area with an expected low-host abundance of dinoflagellates and Syndiniales Group II.

4.4.1. Environmental context

During this study, environmental variables showed clear seasonal patterns typical of the Eastern English Channel (EEC; e.g., Grattepanche *et al*., 2011; Breton *et al*., 2017, Fig. S4.2A). This coastal area is highly dynamic, characterized by a mega-tidal hydrological regime and strong tidal currents parallel to the coast, with coastal water drifts towards the shoreline Thus, the less salty and more turbid near-shore waters remain separated from the open sea by this tidal front (Brylinski *et al*., 1991; Lagadeuc *et al*., 1997; Senchev *et al*., 2006). The stations nearer to the coast (R1, S1) -being more influenced by coastal run-off-, showed several extreme values of environmental variables (Genitsaris *et al*., 2016, Fig. S4.2B) and also the highest chlorophyll-a concentrations (Fig. S4.2B) and dinospore abundance (R1, Fig. 4.3C). Since dinoflagellates proliferate in relatively warm, stratified and nutrient enriched waters (Smayda, 2002), the highly dynamic hydrological conditions and the absence of stratification can explain the relatively low dinoflagellate abundances in this area. In the EEC, while dinoflagellates showed their highest abundances during the summer months (Gómez and Souissi, 2007; Grattepanche *et al*., 2011), these abundances remain relatively low compared to diatoms and nano- picoplankton (Fig. 4.2) and to other close or distant coastal areas (Table 4.4).

***Table 4.4**. Comparative table between the present and several previous studies Widdicombe et al. 2010 and Grattepanche et al., 2011 studies are reported for comparison with the dinoflagellate abundances of the present study.*

Dinoflagellates10^3 L^{-1}	Dinospores 10^3 L^{-1}	Prevalence (% of infected protists)	Site	Observations	References
Max ~400	Max ~800	Mean 21 Max 46	Penzé estuary (northern Brittany, France)	June, during dinoflagellate bloom	Chambouvet *et al.* 2008
Mean 70 Min < 1 Max>500 *Prorocentrum* up to 3360	ND	ND	Western English Channel (coastal)	Year round, Weekly, 15 years	Widdicombe *et al.*, 2010
Mean 5.3 Mino 0.3 Max 32.4	ND	ND	Eastern English Channel (station S1, Fig. s4.1)	Year round, Bi-weekly, 52 samples	Grattepanche *et al*., 2011
ND	Min 4.2 Max 1500	Min ~ 1 Max 25	Mediterranean	Summer, East-West transect	Siano *et al*., 2011
Min < 10 Max >100 Prorocentrum up to 103	Max 1680	Min undetectable Max~12	Reloncaví Fjord, southern Chile (coastal)	Summer, bi-weekly, during *Prorocentrum* bloom	Alves-de-Souza *et a*l., 2012
Range ~ 1-1000	Min < 0.1 Max 1000	Min undetectable Max ~70	Salt pond (Eastham, MA USA)	March-May, 1-3 days, 13 samples	Velo-Sarez *et al.*, 2013
ND	Min 0 Max 335	Min 0 Max 2.56	Salt pond (Falmouth, MA, USA)	March-October, twice a week	Sehein *et al*., 2022
Mean 4.5 Min 0.76 Max 18.6 *Prorocentrum* up to 15	Mean 35,3 Min 0 Max 559	Min undetectable Max 38.5	Eastern English Channel (coastal Fig. S4.1)	Year round, once/twice a week, 205 samples	This study

4.4.2. Sequence vs. abundance data, is sequencing an accurate method to infer dinospore abundances?

The comparison of the abundances of taxa obtained by sequencing (relative abundance of reads) and microscopy (cell abundance) is not straightforward. In silico analysis considering zero mismatches revealed that the ALV01 probe sequence matched with 80% of the ASVs affiliated to Syndiniales Group II found in this study. These results suggest that a relative increase in Syndiniales Group II reads was generally the consequence of an increase in dinospore

abundance measured by FISH-TSA counts. This was particularly the case in summer, in general, and autumn 2018 and 2019, in particular. Conversely, there was no relation between of the dinospores counted by microsopy and the read abundances (Fig. S4.8). This result implies that the dinospore abundance cannot be used as a predictor of relative read abundance and vice-versa. This discrepancy can be explained by: (i) Metabarcoding captures all cells while FISH-TSA targets only active cells. Massana *et al*., 2015 reported that Group I and Syndiniales Group II were found about 4-times more in RNA relative to DNA data; (ii) there is a lag time of about 2-3 days between the infection and the spore release (e.g., Coats and Park, 2002; Alves-de-Souza *et al*., 2015); (iii) it cannot be ruled out that several abundant Group II taxa were missed, although the estimated in silico coverage of the probe was high.

4.4.3. Syndiniales Group II communities and temporal patterns.

In this study, Group II was, as expected, the most diversified Syndiniales group (Guillou *et al*., 2008), accounting for 27 out of the 44 identified clades. Syndiniales Group II reads were always recorded and, in a few cases, very abundant. The sampling effort during this study was intensified during the last two years of the survey (2018-2020), with an increase in the frequency of 25-30 samples/year to 70-75 samples/year, producing a total of 269 samples. The cumulative plots of ASV affiliated to Syndiniales Group II did not reach a plateau and new ASV between two consecutive dates (defined as 'new arrivals' herein) were detected until the end of the study (Fig. S4.8 A, B). These intriguing observations may be explained by the introduction of new taxa via transportation of water masses travelling northwards in the English Channel. However, our data also showed consistent temporal patterns providing an indication of the existence of 'local populations'. The repeating patterns of the most abundant clades and ASVs have already been observed in two previous studies (Chambouvet *et al*., 2008; Christaki *et al*., 2017). Indeed, dominant taxa of Syndiniales Group II varied from one year to the other, though most of them were detected every year (Fig. 4.4). The bimodality coefficient (b) showed that only two among the 20 most abundant ASVs (≥ 0.01 relative abundance) were identified as 'Conditionally Rare Taxa' ($b > 0.9$) i.e., their abundance was usually low or below detection limit and they occasionally increased to an abundance 'appreciable' at the community level (sensu Shade *et al*., 2014, see also Material and Methods). The majority of ASVs exhibited a “b” coefficient lower than 0.9, suggesting that they had seasonal and/or irregular dynamics (Shade *et al*., 2014).

In a previous two and a half years survey in the same area, Syndiniales Group II was dominated by Clades 30, 8, and 10+11 (16, 13 and 7% of total Group II reads, Christaki *et al*., 2017), in the present study Clades 8, 10+11, and 14 dominated (Fig. 4.1C). Among these clades, only Clade

14 was known to reach high abundances related to dinoflagellate blooms in summer in the North-Western English Channel (Chambouvet *et al*., 2008). Clade 8 has not been reported previously as dominant in the North-Western English Channel (Chambouvet *et al*., 2008) or in other long term coastal studies (e.g., Käse *et al*., 2021, supplementary material). This clade was clearly dominating within the Group II community (25.5 % of the reads), prevailing in 8 out of the 15 samples that showed important peaks (>600 reads). Clade 8 also showed the highest occurrence during all years, being present in up to 97 % of the samples (in 2018, Fig. 4.4).

Dinospores were present throughout the sampling period at low abundances (ca. 10^3 cells L^{-1}) and were punctuated by a few transient peaks (ca. 10^5 cells L^{-1}). In a modeling study, the critical carrying capacity that ensures stable coexistence of dinoflagellate host and parasitoid varied from 10^3 to 10^5 L^{-1} (Salomon and Stolte, 2010). The dinospore abundances observed here imply that there is a 'seed populations' that could rapidly develop when the hosts reach a certain abundance. However, grazing by heterotrophic dinoflagellates and ciliates of the dinospores is most likely another important factor that keeps dinospore populations under control since their size fits within the range of their prey's size range (e.g Sherr and Sherr, 2002; Grattepanche *et al.*, 2011)

4.4.4. Dinospore and Dinoflagellates dynamics

In natural systems, the strength of infection by Syndiniales Group II has been related to the abundance of the dinoflagellate hosts because higher hosts density enhances encounter rates (Park *et al*., 2004). Consequently, dinoflagellate blooms are associated with the increase of the abundance and therefore prevalence of dinospores (e.g., Chambouvet *et al*., 2008; Alves-de-Souza *et al*., 2012, 2015; Velo-Suárez *et al*., 2013; Anderson and Harvey, 2020; Sehein *et al*., 2022). Not surprisingly, Syndiniales Group II showed seasonal patterns similar to dinoflagellates, characterized by increases in abundance and richness during summer and autumn, (Figs. 4.2, 4.3). The dinoflagellate abundances in this study were drastically lower than most of those previously reported in coastal ecosystems. However, the abundance of dinospores and the proportion of infected cells were comparable (Table 4.4). Given that each infection produces hundreds of dinospores (Coats and Park, 2002), even a small increase in the number of available hosts would result in a significant increase in the number of dinospores released throughout the parasite-host dynamics (Alves-de-Souza *et al*., 2015). The strongest infection witnessed during this study (June 2018), corresponded to the highest dinospore and dinoflagellate abundances (*P. minimum*) (Figs 4.2E and 4.3C), lasted more than a week and reached a prevalence of 38.5% (Table 4.3). Prevalence in natural populations of infected dinoflagellates is highly variable and can escalate up to 80% or even higher values during

epidemics (Coats *et al*., 1996) though most commonly reported infection prevalence is much lower (Coats and Bockstahler, 1994; Chambouvet *et al*., 2008; Salomon *et al.*, 2009; Siano *et al.*, 2011; Alves-de-Souza *et al*., 2012; Li *et al.*, 2014, Table 4.4). In this study, the *P. minimum*'s 'rise and fall' coincided with the temporal dynamics of Clade 8 and particularly to a specific ASV (ASV13). Two other dinoflagellates (*Scirpsiella sp.* and *Amphidinium spp*.) showed signs of infections. Although prevalence in natural dinoflagellate populations is usually observed at host densities of the order of 10^5-10^6 L^{-1}, an infection can occur at considerably lower host conditions (Salomon *et al*., 2009). One feature that can explain our observation is that dinospores are flagellated, allowing them to chase their host and thus increase infection rates. Also, the ability of parasites to have a diversity of hosts could be an adaptive/survival feature when certain hosts become scarce. Our study supports this hypothesis since Syndiniales Group II may have had diversified larger range of hosts in autumn. During the autumn peaks of dinospores, various cells presented signs of infection and metabarcoding data revealed that samples were dominated by a variety of Syndiniales Group II clades and ASVs. However, despite the large number of samples processed in this study -at the exception of the association between *P. minimum* and ASV13 in June 2018, -it was not possible to evaluate the extent of specific versus non-specific infections. Finally, given that the infective parasite cells have an ephemeral life (e.g., Cachon, 1964; Coats and Park, 2002) and should have to rapidly find a host, one may speculate how they manage to do this in such highly complex planktonic communities with low host abundances. Moreover, the production of allelopathic compounds by dinoflagellates as a defense mechanism killing dinospores and preventing infection (Long *et al*., 2021) could further complicate the chances of survival of these ephemeral swimmers. As such, these dinospores should have their own strategies to increase the chances of finding their hosts (by chemotaxis, for example); an area of research that deserves further investigation.

4.4.5. Community Assembly processes of Syndiniales Group II

Including parasitism in planktonic food web models is vital to better understand the dynamics of hosts and parasites and to better appreciate the role of parasitism in the functioning of planktonic ecosystems (e.g., Montagnes *et al*., 2008; Salomon and Stolte, 2010; Alves-de-Souza *et al*., 2015). In several studies Syndiniales dynamics have been related to environmental variables such as temperature, salinity, light intensity, and nutrient concentrations (Yih and Coats, 2000; Alves-de-Souza *et al*., 2012, 2015; Li *et al*., 2014; Käse *et al*., 2021 and references therein). In this study, a PCA (Fig. S4.2) revealed clear seasonal patterns of environmental

variables. However, multivariate analysis such as CCA and dbRDA between environmental parameters and Syndiniales Group II did not show any consistent pattern (data not shown). This is not surprising, since environmental variables such as the ones mentioned above are not expected to have direct influence on Syndiniales Group II, but affect them indirectly through the dynamics of their hosts. Here, as an alternative to multivariate analysis of environmental variables and ASVs abundance, ecological processes regulating the Syndiniales Group II community were explored. Community assembly describes how processes interact to determine species composition and local biodiversity of a community (e.g., Chase and Myers, 2011). This exploratory analysis showed the prevalence of stochastic (i.e., drift) processes in Syndiniales Group II community assembly (Fig. 4.5B). However, June and July were the only months when part of the processes could be infered as deterministic (Fig. 4.5A). It is hypothesised here, that deterministic processes were related to specific Syndiniales-dinoflagellate interactions observed during these months (see previous section & Table 4.2).

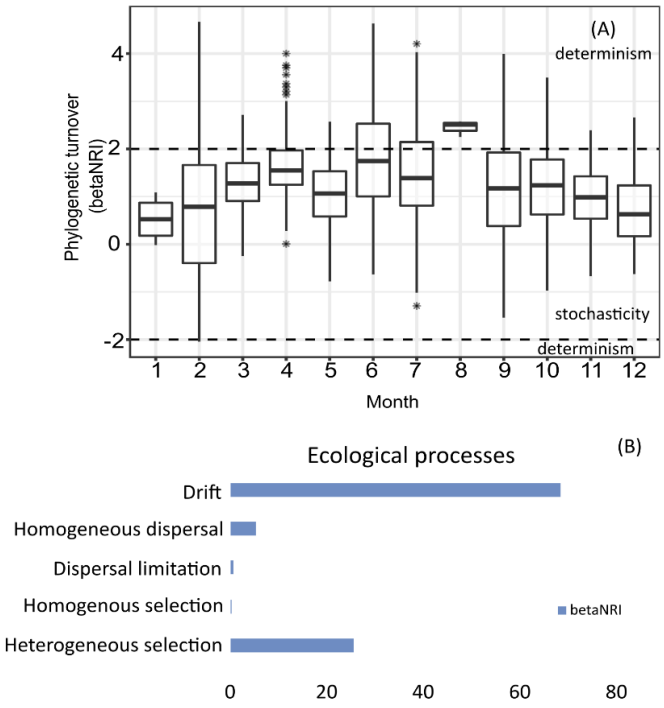

Figure 4.5. *(A) Phylogenetic turnover index (βNRI) Group II Syndiniales ASVs in the eastern English Channel at the SOMLIT and DYPHYRAD stations from March 2016 to October 2020. Solid black lines represent the median and black dots the mean. βNRI> 2, βNRI<- 2 indicating deterministic processes and -2<βNRI< 2indicattin stochastic processes (see also Table 4.2). (B) Relative importance of the ecological processes driving Group II Syndiniales communities in the eastern English Channel at the DYPHYRAD and SOMLIT stations from March 2016 to October 2020. Note that only three samples were available for August – data not interpretable.*

In conclusion we considered both morphological and metabarcoding data using a relatively large dataset (287 samples) which is an approach rarely undertaken. Since metabarcoding data are subjected to PCR biases and are always expressed in relative abundances, and morphological data are absolute abundances but do not provide a precise image of the diversity, it is important to combine these two complementary data sets. Most abundant clades and ASVs affiliated to Syndiniales Group II were observed in consecutive years, providing an indication of the existence of local populations, and featured consistent temporal patterns. Increasing abundance and richness were always observed during the second half of the year. In summer, they were related to dinoflagellate hosts; in autumn, Syndiniales Group II could have more diversified hosts than earlier in the year. The originality of this study makes it a study case for coastal ecosystems presenting abundant nutrients but no dinoflagellates blooms. While the dinoflagellate abundances in this study were much lower than most of those previously reported in coastal ecosystems, the number of dinospores and the prevalence were comparable. The low abundance of dinospores in the great majority of samples was consistent with the low host abundance, indicating a stable coexistence punctuated by rare transient peaks. Given all the above, the strategies of dinospores to increase their chances of survival in highly complex planktonic communities and in low host abundances deserves further attention. Overall, the prevalence of stochastic processes renders, *a priori* less predictable the seasonal dynamics of Syndiniales Group II communities to future environmental change.

Acknowledgments

We would like to thank the Captain and the crew of the RV ‘Sepia II’; L. Guillou for providing filters with cultures of infected dinoflagellates to test our FISH-TSA procedures, F. Artigas for setting-up the DYPHYRAD sampling, M. Crouvoisier for nutrient analysis; V. Cornille for help with the fieldwork, P. Magee for English proofing, the SCoSI/ULCO (Service COmmun du Système d’Information de l’Université du Littoral Côte d’Opale) providing us with the computational resources to run all the bioinformatic analyses via the CALCULCO computing platform (https://www-calculco.univ-littoral.fr/). This work was logistically supported by the national monitoring network SOMLIT (https://www.somlit.fr/) and funded by the CPER MARCO (https://marco.univ-littoral.fr/) and the French Research program of INSU-CNRS via the LEFE-EC2CO 'PLANKTON PARTY' project. D.I.S was funded via a PhD grant by the 'Region des Hauts de France’ and the ‘Pôle métropolitain de la Côte d’Opale (PMCO)’.

Contribution:

Samples were collected from the national monitoring network SOMLIT and the local transect DYPHYRAD (PI: Dr. Artigas Luis-Felipe) by the crew of 'Sepia II', and the assistance of technicians Vincent Cornille and Eric Lecuyer. I participated in some of these samplings from 2018 to 2020. Since 2018, I have been responsible for fixation of microscopy and cytometry data and conducting filtrations for metabarcoding and for FISH samples. I enumerated and identified separately phytoplankton (diatoms and *Phaeocystis*), and microzooplankton (dinoflagellates and ciliates) using inverted microscopy. I enumerated pico- naophytoplankton and heterotrophic nanoflagellates by cytometry. Additionally, I conducted extractions, prepared libraries, and performed purifications for 18S metabarcoding for all samples. Phytoplankton data from 2016 to 2017 were enumerated by Dr. Breton Elsa, and all nutrient and chlorophyll-a measurements were carried out by Crouvoisier Muriel. All samples were sequenced by Genewiz platform. I conducted bioinformatic and statistical analysis, I applied null-model analysis and I did all the visualisations. FISH experiment conducted by two master students under the supervision of Pr. Christaki Urania and Pr. Ludwig Jardillier. Syndiniales Group II spores and hosts were enumerated and identified by Pr. Christaki Urania. Pr. Chrisraki Urania conceptualised, leaded and acquired funding for this study.

4.5. Supplementary

Supplementary Materials and Methods

DNA barcoding

Different molecular barcodes of 10 bp were added to both forward and reverse primers to tag amplicons and allow to differentiate them after sequencing.Polymerase chain reaction (PCR) mixtures comprised 1 µL of DNA, 12.5 µL of DreamTaq Green PCR Master Mix (Thermo Fisher Scientific, U.S.A.), 1 µL of each primer (10 µmol L^{-1}), and 9.5 µL nuclease-free water in a total volume of 25 µL. PCR settings included an initial step of denaturation at 94 ^{o}C for 2 min, 25 cycles of denaturation at 94 ^{o}C for 15 s, annealing at 55 ^{o}C for 30 s, and extension at 72 ^{o}C for 1 min and 30 sec, and a final step of extension at 72 ^{o}C for 5 min. About 4 µL PCR product was used to check amplification on 1% agarose gel. The remaining amplicon products from five different PCR reactions of each sample were pooled and purified together using the QIAquick PCR purification kit (Qiagen, Germany), according to the manufacturer's instructions. DNA concentrations after purification were measured with a Qubit 2.0 fluorometer (Thermo Fischer Scientific Inc) with the dsDNA High Sensitivity Assay Kit (Life Technologies Corp., U.S.A.) and adjusted at equal concentrations

depending on sequencing run (20 to 47 ng/µL).

Bioinformatic analysis

Quality filtering of reads, identification of amplicon sequencing variants (ASV), and taxonomic affiliation based on the PR2 database (Guillou *et al.*, 2013) were done in the R- package DADA2 (Callahan et al. 2021). All paired-end sequences from the same sequencing run were imported and demultiplexed in Qiime (Caporaso *et al.*, 2010) based on each sample's 10 bp molecular identifier with the functions *extract_barcodes.py* (Qiime1) and *demux emp-paired* (Qiime 2-2018.8). Processing of sequences without primers and barcodes was further performed with the R-software (R Core Team 2021) using the DADA2 package v.1.10.1 (Callahan *et al.*, 2016) to define Amplicon Sequence Variants (ASVs). During filtering 6 maximum errors were allowed, while barcodes and primers were trimmed at 270 bp and 280 bp at the end of the forward and the reverse reads respectively. The minimum allowed read length was set to 245 bp. After dereplicating forward and reverse reads, the DADA2 pipeline identified amplicon sequence variants (ASV) in the dataset. The forward and reverse reads were merged and chimeras were identified and removed based on matches with combinations of 3'- and 5'-segments of different sequences. The taxonomy of the ASVs was assigned with the naïve Bayesian classifier method implemented in DADA2 based on the PR^2 database (Guillou *et al.*, 2013). A total number of 41,179 ASVs were identified from 6,366,087 reads in 287 samples, containing Metazoa, Streptophyta, Excavata, Alveolata, Amoebozoa, Apusozoa, Archaeoplastida, Hacrobia, Opisthokonta, Rhizaria, Stramenopiles.

All ASVs sequences were aligned in Geneious Prime 2021.1.1 with MAFFT V7.450 plugin using the FFT-NS-2 algorithm for analysis (Katoh and Standley, 2013) to deal with a large dataset. A phylogenetic tree was then built with FastTree V2.1.11 (Price *et al.*, 2009) using the default parameters. Then, the ASV table, and the phylogenetic tree were combined into one object with phyloseq R package v.1.37 (McMurdie and Holmes, 2013), to filter, subset, and pre-processing.ASVs affiliated to Excavata, Metazoa, Streptophyta, not assigned to Eukaryotes ASVs and singletons were removed, obtaining a phyloseq (phyloseq R package) object containing 20,651 taxa by 8 taxonomic ranks. A total number of 41,179 ASVs were identified from 6,366,087 reads in 287 samples containing Metazoa, Streptophyta, Excavata, Alveolata, Amoebozoa, Apusozoa, Archaeoplastida, Hacrobia, Opisthokonta, Rhizaria, Stramenopiles. ASVs affiliated to Excavata, Metazoa, Streptophyta, not assigned to Eukaryotes ASVs and singletons were removed, obtaining a phyloseq object containing 20,651 taxa by 8 taxonomic ranks. After eliminating samples with less than

5000 reads, the number of reads per sample was rarefied to the lowest number of reads (5234) which finally resulted to 15250 ASVs in 269 samples by 8 taxonomic ranks.

Fluorescent in situ Hybridisation (TSA-FISH)

Samples (1L) were fixed with paraformaldehyde (1% v/v) for 1 hour at 4°C. Samples were screened through 20 µm filters and 400-600 mL were then filtered on 0.6 µm Nuclepore filters (47 mm). The filters were dehydrated by several successive ethanol baths (50%, 70%, 100%) for three minutes each and stored at -80°C until analysis. The oligonucleotide probe ALV01 (5'-GCC TGC CGT GAA CAC TCT-3') was used to target Syndiniales Group II dinospores (Chambouvet *et al.*, 2008)TSA-FISH was prefromed following the protocol described in Piwosz et al. (2021 and references therein).

The filters were thawed and cut. Each filter piece was soaked in three successive baths of HCl (0.01M) to desactivate peroxidases, MilliQ sterile water and 96% ethanol (Piwosz *et al.*, 2021) and dried on Whatman paper. The filters, were then covered with hybridisation buffer (40% deionized formamide, 0.9M NaCl, 20mM Tris-HCl pH 7.5, 0.01% sodium dodecylsufate (SDS), 10% Blocking agent, Boehringer Mannheim) and the oligonucleotide probe (50 ng μl^{-1} final concentration), placed in hybridisation chambers, and incubated for three hours at 42°C. After the hybridisation step, the filters were washed twice at 46°C for 20 minutes with freshly prepared washing buffer (56mMNaCl, 5mM EDTA, 0.01% SDS, 20mM Tris-HCl pH 7.5) and then equilibrated in TNT buffer (100mMTris-HCl pH 7.5, 150mMNaCl, 0.05% Tween 20) for 15 min at room temperature in the dark. For TSA-reaction, each filter piece was then transferred to a slide onto which a drop of TSA reaction (Tyramide Flurorescein kit, Akoya Biosciences, Marlborough, MA, USA) and incubated for 30 min in the dark. Freshly made TSA mix consisted of 1:1 dextran sulfate and amplification diluent, 1:50 fluorescein tyramide and the mixture). The next "equilibration" step, consisted of two successive baths of TNT buffer pre-warmed to 55°C for 20 min each and then dried in an ethanol bath (96%) to improve the background. Finally, the filters were counter stained 15 min with calcofluor to visualize the dinoflagellate theca (100 ng ml^{-1}), rinsed with MilliQ sterile water and then mounted in an anti-fading Citifluor AF1 oil and propidium iodide (10 µg ml^{-1}) to visualize the nuclei. The filters were finally covered with cover glass and kept at 4°C until counting the next morning. All counts were performed with an epifluorescence microscope at 100x (Zeiss Imager M2) with different fluorescence filters (for calcofluor, excitation: 345 nm; emission: 475 nm), promidium iodide (excitation: 536 nm; emission: 617 nm) and FITC (excitation: 495 nm; emission: 520 nm), 150

optical fields at x100 corresponding to 873±149 µl of initial sample (390-1333 µl) were observed for each filter.

Community assembly processes

To detect phylogenetic signal a Mantel correlogram was applied (closely related taxa have similar habitat associations, Losos, 2008). The Mantel correlogram was applied to detect phylogenetic signal (e.g., Liu et al., 2017; Doherty et al., 2020). The Mantel correlogram correlates the phylogenetic distances to the niche distances. It is well established that dinoflagellates are over-represented in sequencing data (e.g., Georges et al., 2014, Christaki et al., 2021 and references therein). The niche value of an ASV was defined as the weighted mean of dinoflagellate abundance (Cells L^{-1}). Significant positive correlations indicate that ecological similarity among ASVs is higher than expected by chance. Alternatively, significant negative correlations indicate that ASVs are more ecologically dissimilar than expected by chance (Stegen et al., 2013). Here, the cal_mantel_corr function was used in the microeco R-package (Liu et al., 2021). To infer phylogenetic signal of Syndiniales Group II ASVs, we defined the niche value for each ASV using the dinoflagellate abundance that was chosen for their ecological role of being hosts. X axis shows the phylogenetic distances (0: lowest, 1.0 maximum). Y axis shows the correlation between the niche value and phylogenetic distances. The mantel correlogram showed a positive correlation between niche value and phylogenetic distances at short phylogenetic distances, which justifies the utilisation of the phylogenetic metrics to infer community assembly (Stegen *et al.*, 2012). This methodology to detect the phylogenetic signal have been previously described in several studies (e.g., Wang *et al.*, 2013; Doherty *et al.*, 2020; Fodelianakis *et al.*, 2021).

The βNRI was calculated as the difference between the observed βMPD and the mean of the βMPD null models divided by the standard deviation of the null models. Beta net relatedness values (βNRI) lower than expected (i.e., $\beta NRI < -2$) indicate a dominance of homogeneous selection. In contrast, βNRI values which are greater than expected (i.e., $\beta NRI > 2$) indicate that communities are experiencing heterogeneous selection. When the deviation was low (i.e., $-2 < \beta NRI \leq 2$), an additional step was conducted to define whether the beta diversity of the communities could be structured by dispersal or drift (Table 2). In this step, the Raup–Crick metric (RCbray) (Chase *et al.*, 2011) was calculated using the Jaccard's distance. For this, RCbray compares the measured b-diversity against the b-diversity that would be obtained if drift was driving community turnover (i.e., under random community assembly). The randomization

was run 999 times based on the presence-absence of all ASVs across each pairwise community comparison that is randomized. RCbray values less than - 0.95 indicate that community turnover is driven by dispersal limitation, RCbray values greater than 0.95 indicate homogeneous dispersal respectively, and values between -0.95 and +0.95 point to a community assembly governed by drift or other undominated mechanisms. Analysis wascarried out using R 4.1.0 (R Core Team, 2021).

Statistical analysis

Principal component analysis (PCA) illustrating variations of the abiotic parameters (arrows) at all sampling dates was realized using the packages ADE4 (Dray *et al*., 2006), FactomineR (Lê *et al*., 2008) and Fatoextra (Kassambara and Mundt, 2020).

Heatmaps were generated to illustrate the overall Syndiniales Group II community composition and diversity of the 30 most common genera in all samples (i.e, 1 % of reads in the entire dataset), using the "Ampvis2" R-package (Andersen *et al.*, 2018) after pooling ASVs belonging to the same genus. Monthly boxplots were built using the "ggplot2" package (Wickham, 2016) to illustrate seasonal variations of the environmental variables, the different protists' groups and the Syndiniales Group II. Boxplots were also computed combining with LOESS (Locally Weighted Scatterplot Smoothing), a nonparametric regression technique, to better reveal the seasonal trends in protists. To test how the environmental variables and the Syndiniales Group II differed among stations the non-parametric test Kruskal-Wallis was performed, followed by a post-hoc Nemenyi test (Legendre and Legendre, 1998; package "PMCMRplus", Pohlert, 2015). To explore the seasonal environmental gradient a Principal Component Analysis (PCA) was performed on environmental variables using the "ade4", "FactoMineR" and "factoextra" packages (Dray *et al*. 2007; Lê *et al*. 2008; Kassambara and Mundt 2020). Analysis was carried out using R 4.1.0 (R Core Team, 2021).

Supplementary Figures

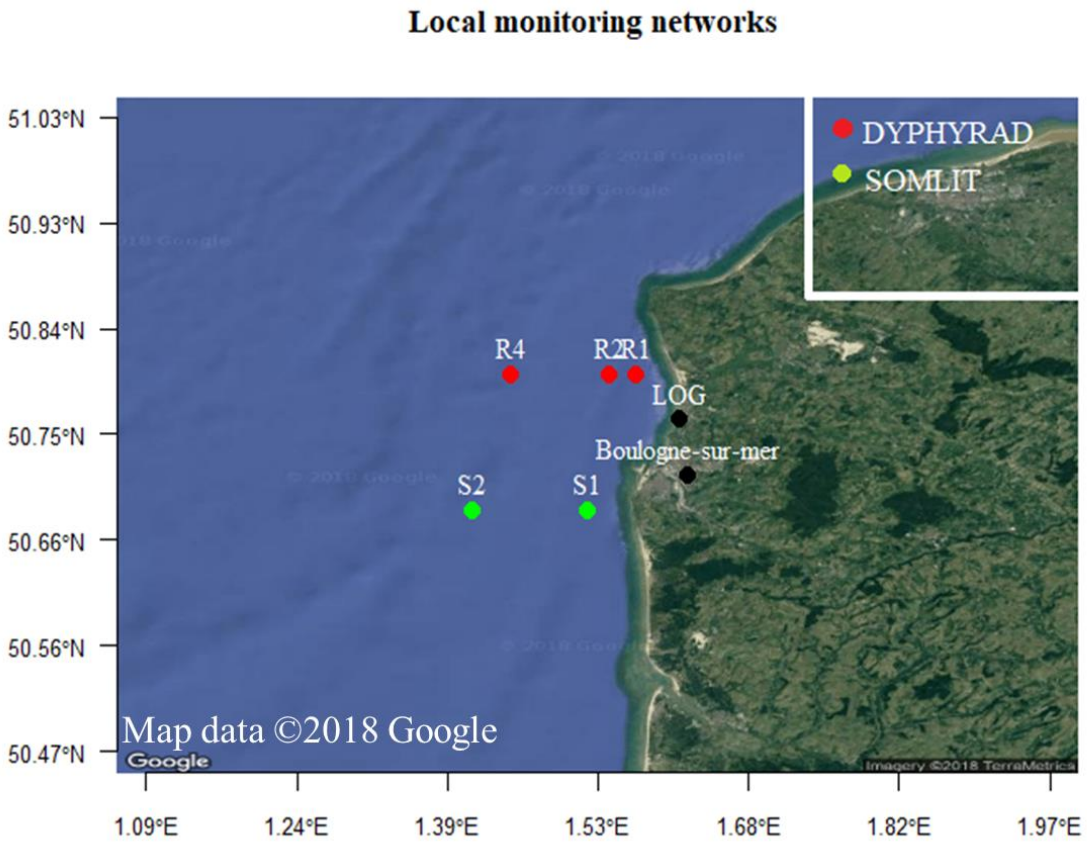

Figure S4.1. *Location of the SOMLIT (S1, S2) and DYPHYRAD (R1, R2, R4) stations in the eastern English Channel (map creation with R software using the package Googlemap, Map data © 2018 Google).*

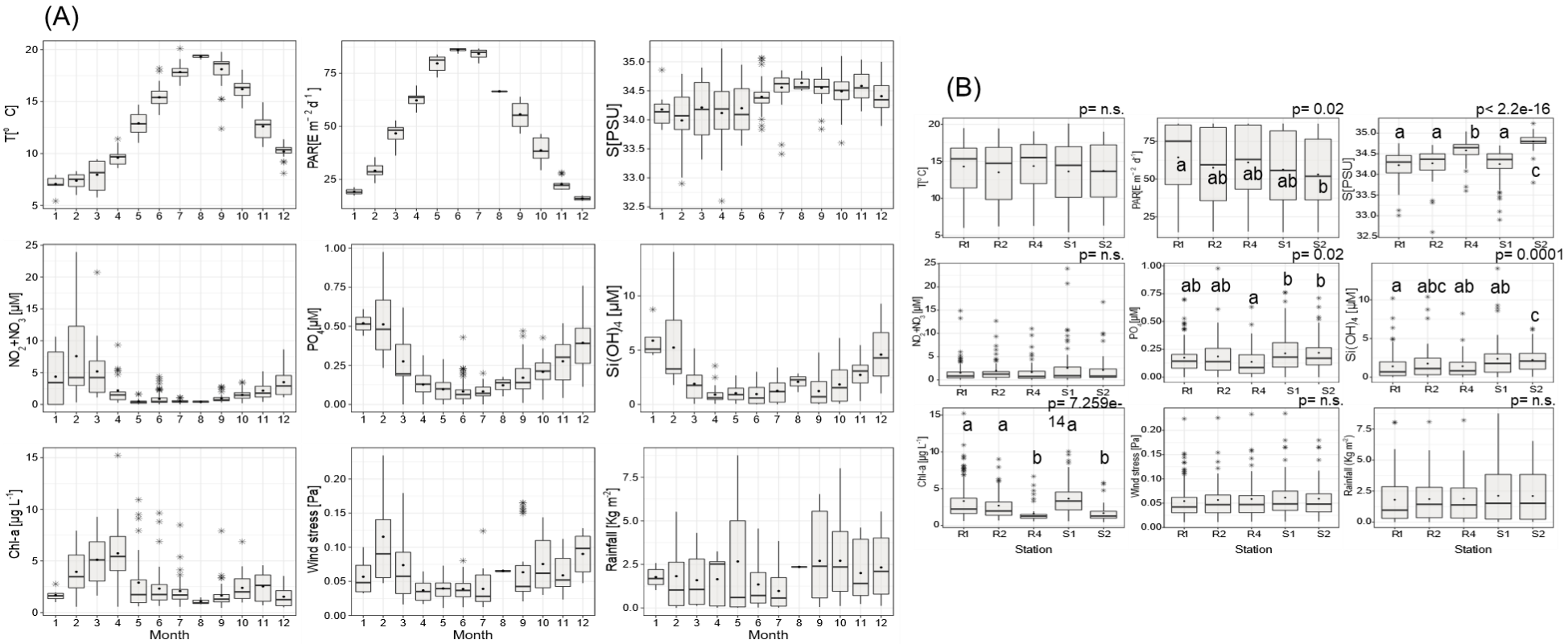

Figure S4.2. ***(A)*** *Seasonal variation of environmental variables: Temperature [T, ^oC], Photosynthetic Active Radiation [PAR, E m^{-2} d^{-1}], S: Salinity [S, PSU], Nitrites and Nitrates [NO_2+NO_3 µM], Phosphates [PO_4, µM], Silicates [$Si(OH)_4$, µM], Chlorophyll-a [Chl-a, µg L^{-1}], Wind stress [Pa], Rainfall [Kg m^{-2}].* ***(B)*** *The letters indicate significant differences ($p < 0.05$) between stations based on Kruskal-Wallis and Nemenyi post-hoc test in the top right of the graphs. Solid black lines represent the median, black dots the mean and the black stars the outliers.*

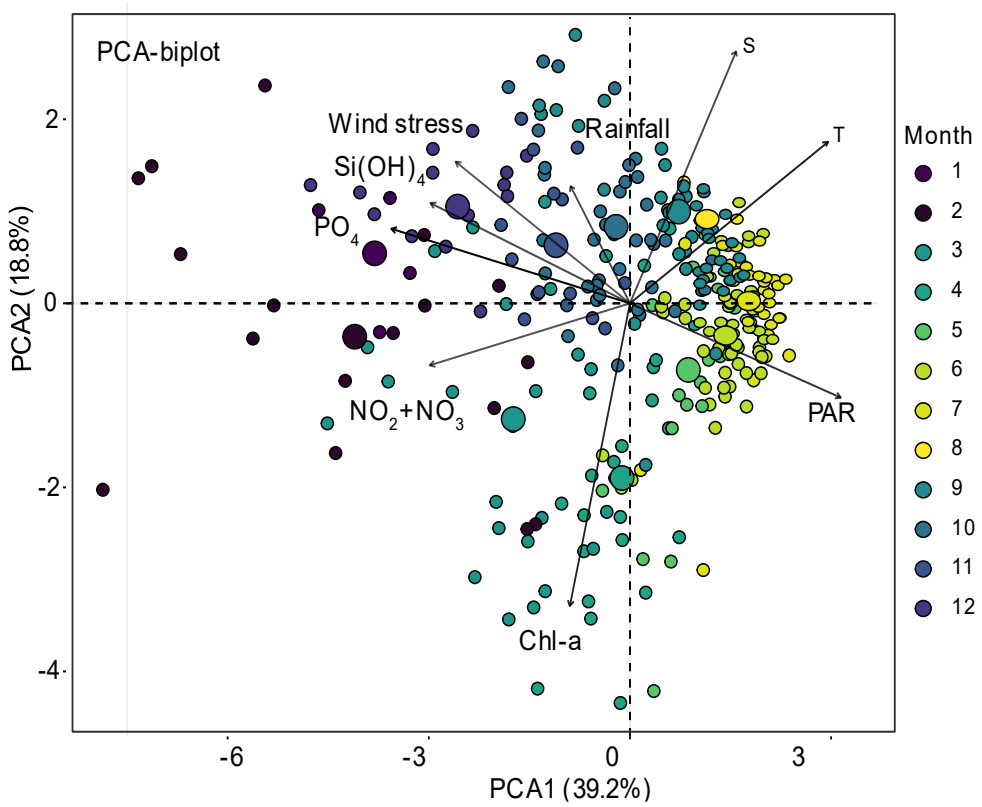

Figure S4.3. *Principal component analysis (PCA) illustrating variations of the abiotic parameters (arrows) at all sampling dates (colored points). Samples were grouped by seasons according to Silicates: $Si(OH)_4$ (µM), Phosphates: PO_4 (µM), Nitrite and Nitrates: NO_2+NO_3 (µM), Salinity, Temperature (^oC), Chl-a: Chlorophyll-a (μg^{-1}), PAR: Photosynthetic Active Radiation ($E\ m\text{-}2\ day^{-1}$), Wind stress (Pa), Rainfall ($Kg\ m^{-2}$) at the SOMLIT and DYPHYRAD stations from 2016 to 2020. The environmental variables are represented by arrows whose contribution to the construction of the axes varies according to the color gradient. The bigger color points represent the centroid for each month.*

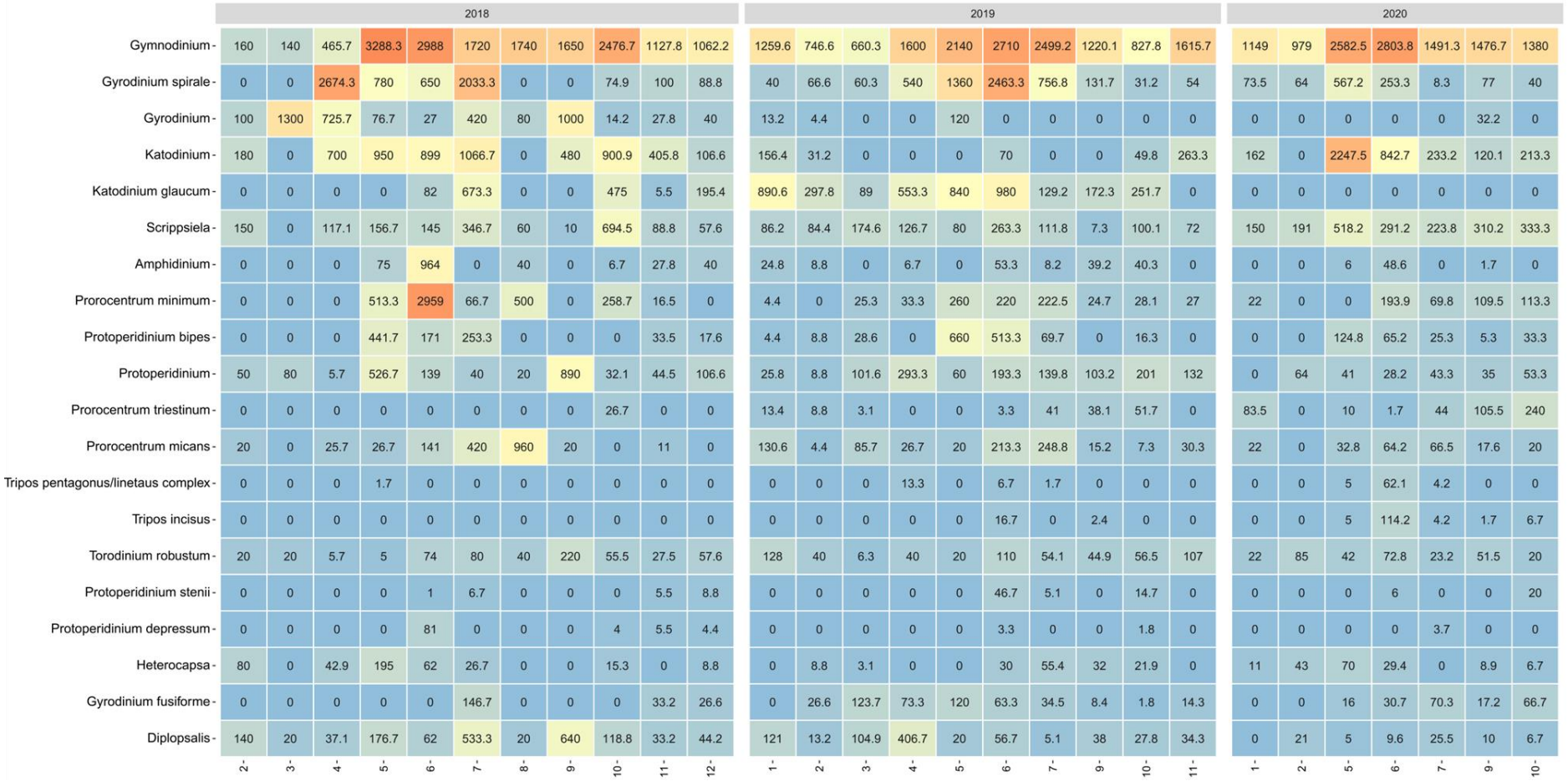

Fig. S4.4. *Heatmap illustrating the mean monthly cell abundance L^{-1} of dinoflagellates counted by microsopy in the eastern English Channel at the SOMLIT (S1, S2) stations from February 2018 to October 2020. Heatmaps were generated to illustrate the seasonal and interannual changes in the community composition of the 30 most common genera of Syndiniales Group II (i.e., 1 % of reads in the entire metabarcoding dataset) and 20 most common dinoflagellates detected by microscopy, using the "Ampvis2" R-package (Andersen et al., 2018).*

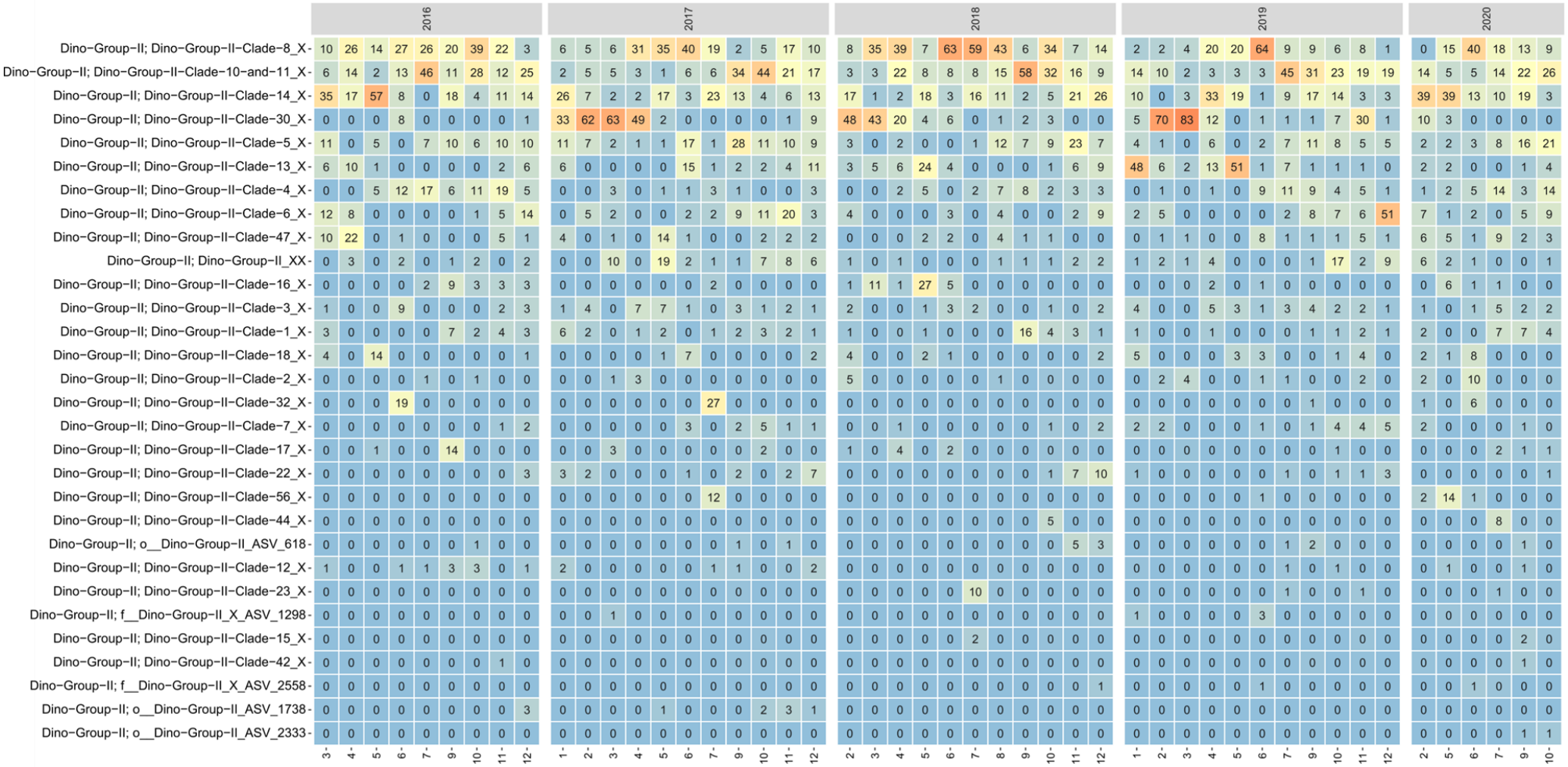

Figure S4.5. *Heatmap illustrating the relative abundance of reads of the 30 most abundant Syndiniales Group II genera (i.e., contributing to at least 1 % of reads in the whole data set), occurring in the eastern English Channel at the SOMLIT (S1, S2) stations from March 2016 to October 2020.*

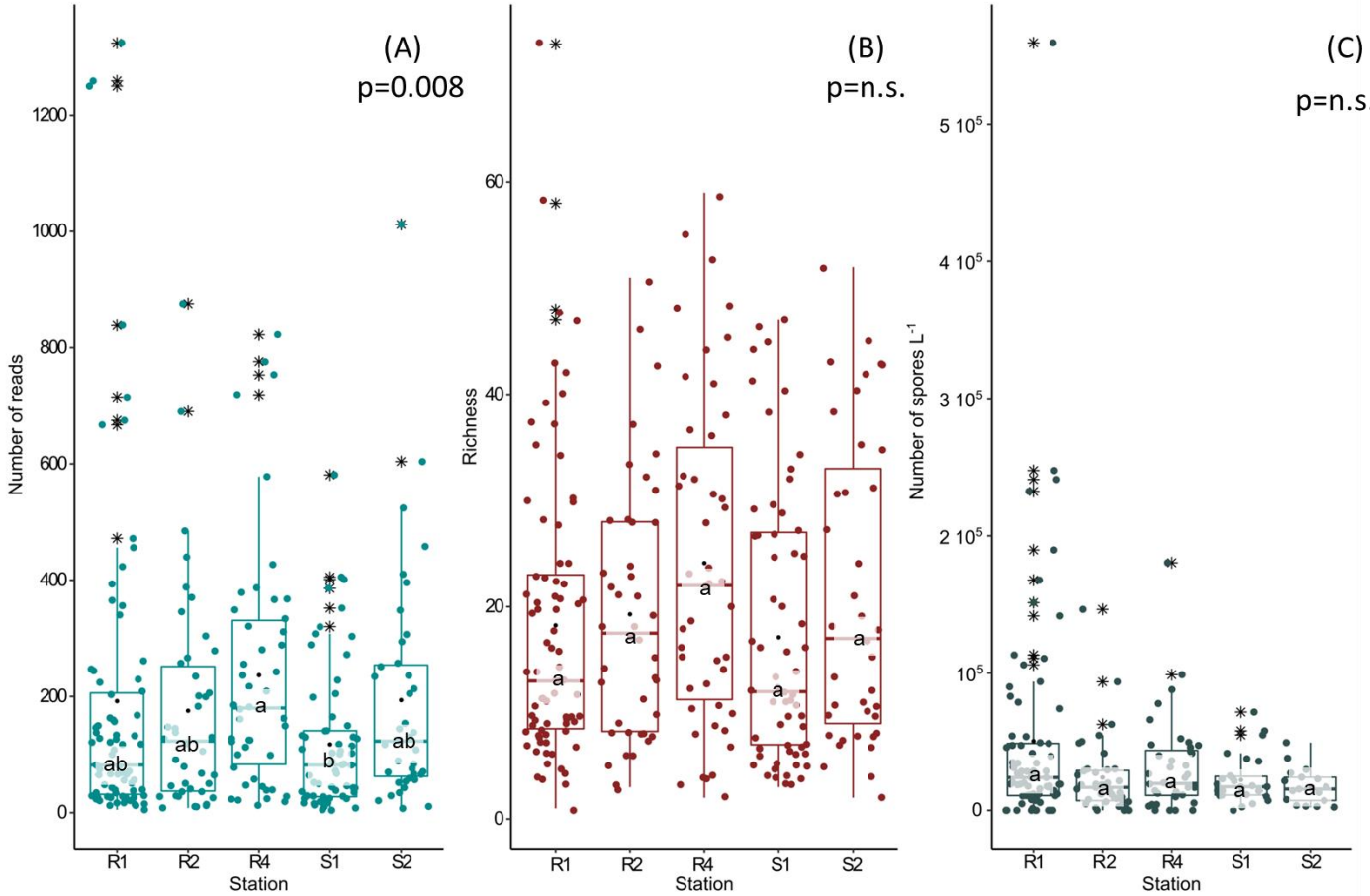

Figure S4.6. *Syndiniales Group II in the eastern English Channel at the SOMLIT (S1, S2) and DYPHYRAD stations (R1, R2, R4).* ***(A)*** *Number of reads,* ***(B)*** *Richness,* ***(C)*** *Dinospores. Solid lines in the boxplot represent the median, black dots the mean, and the black stars the outliers. The letters indicate significant differences (p < 0.05) between stations based on Kruskal-Wallis and Nemenyi post-hoc test in the top right of the graphs. Solid black lines represent the median, black dots the mean and the black stars the outliers.*

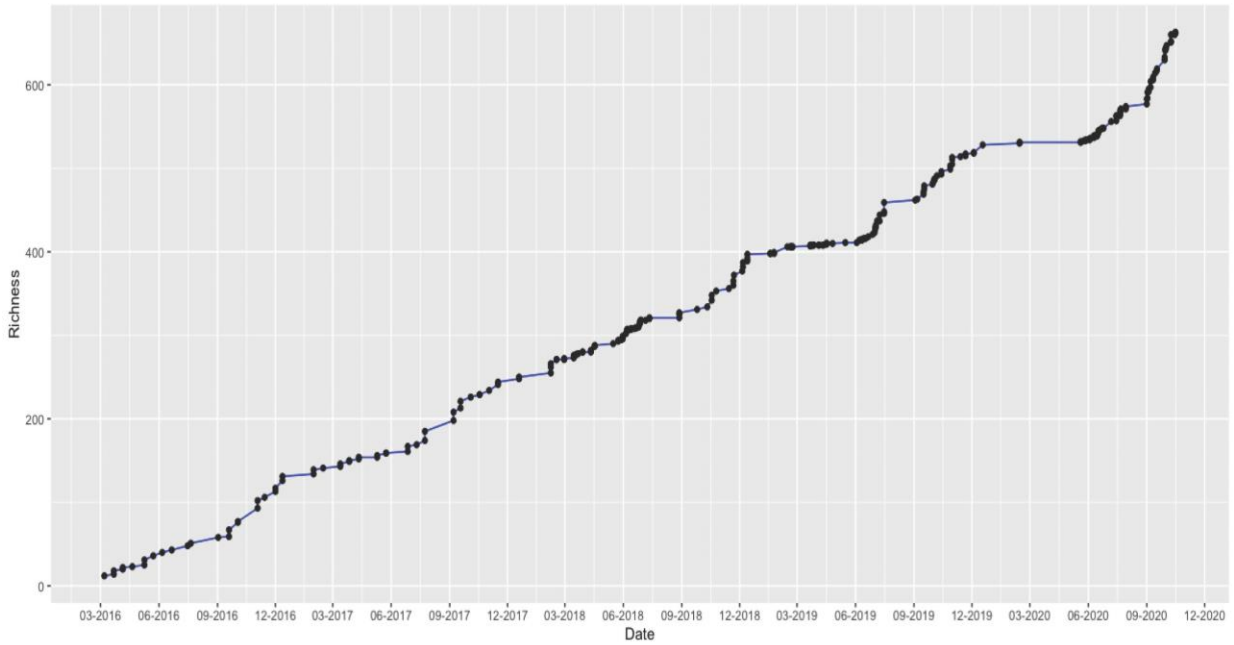

Figure S4.7. *Plot of the cumulative number of ASVs between two consecutive sampling dates. The influx of newly introduced ASVs is clearly noticeable in summer and autumn (when the slope becomes steeper) with a high number of "new arrivals" in autumn 2020.*

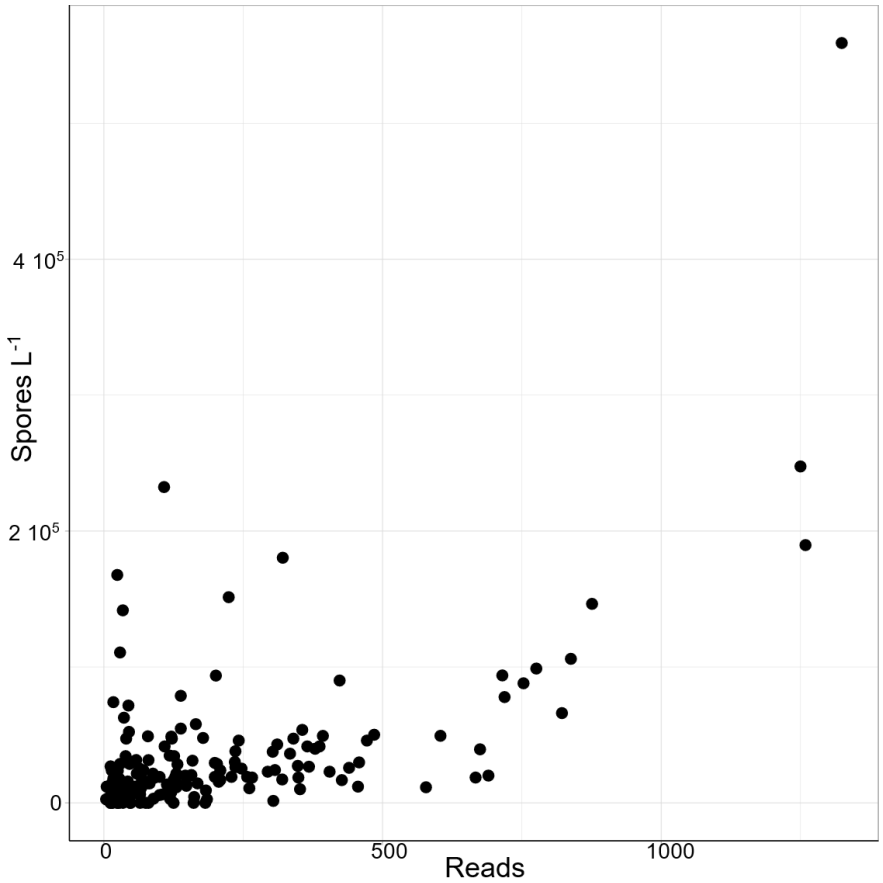

Figure S4.8. *Scatterplot of number of reads of Syndiniales Group II (from the rarefied data set) vs number of dinospores obtained from TSA- FISH counts in the eastern English Channel at the SOMLIT and DYPHYRAD stations from February 2018 to October 2020 (n= 199).*

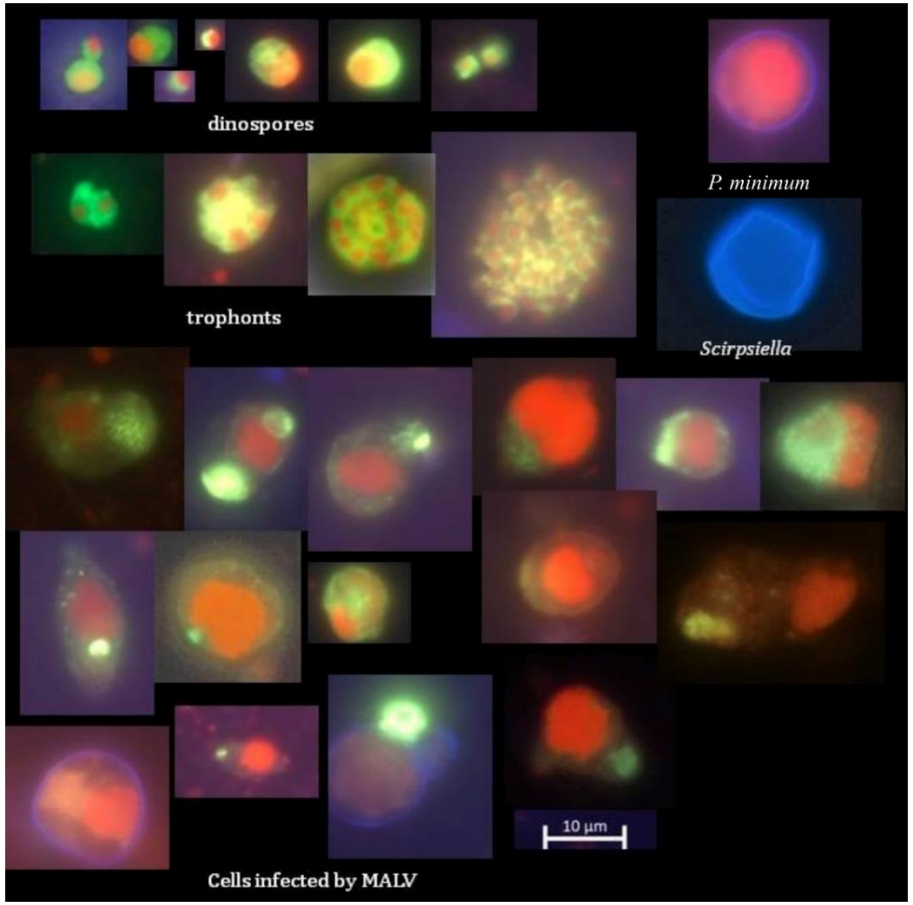

Figure S4.9. *A selection of pictures during the three larger infection events. Parasites are labelled with the CARD-FISH probe ALV01 and stained green when observed with a FITC filter set. Host theca are stained with Calcofluor when present and blue when visualized with a DAPI filter. Both host and parasite nuclei are stained with propidium iodide and are red when viewed with a Cy3 filter set. (a-g) cells with heterocapsid morphology, (h-m) cells with scrippsielloid morphology, (n-s) cells with shared athecate morphology, and (t-z) other interesting, but less common, infection morphotypes. All scale bars denote 5 µm. Finally, it is not excluded that several of the dinospores observed within ciliates or heterotrophic dinoflagellates were simply ingested.*

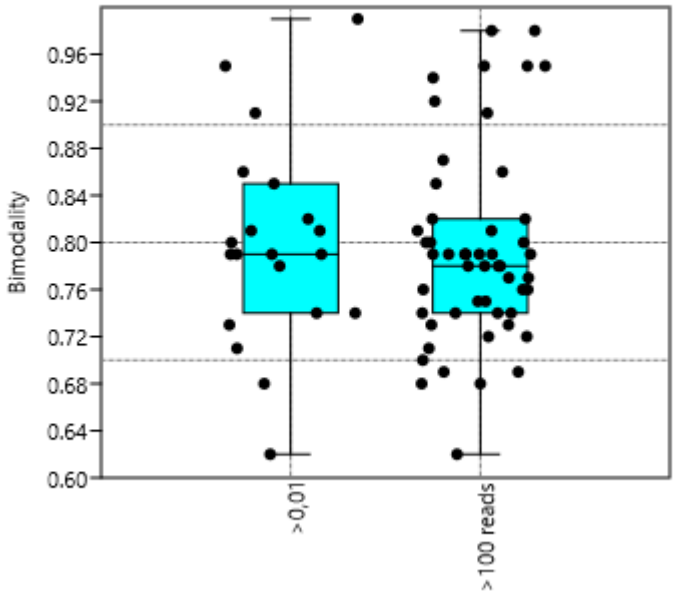

Figure S4.10. *Boxblot of the coefficient of bimodality of most abundant Syndiniales Group II taxa representing ≥ 0.01 relative abundance and the taxa with at least 100 reads in the whole data set. b varies between 0 and 1.*

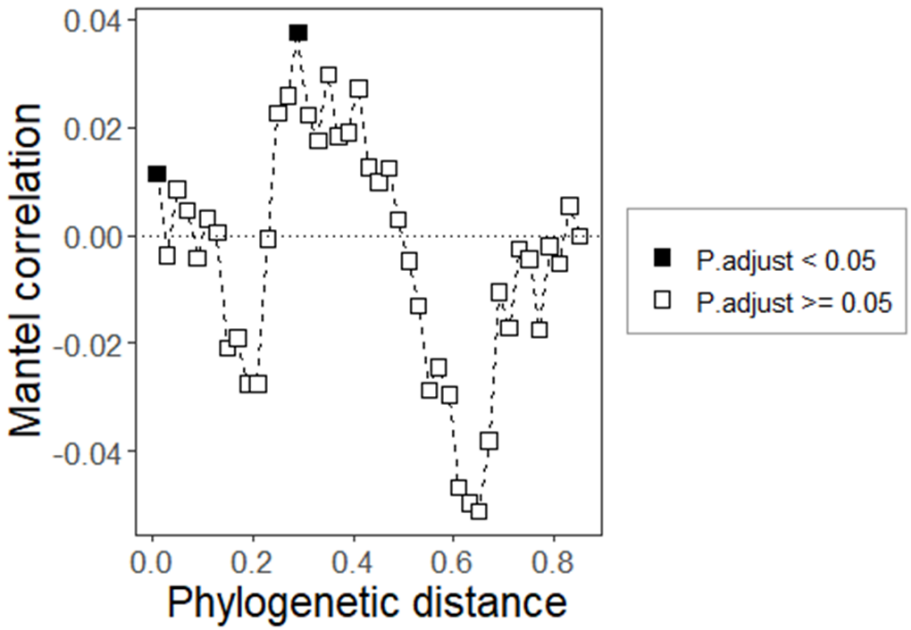

Figure S4.11. *Exploration of the phylogenetic signal of Syndiniales Group II in the eastern English Channel at the SOMLIT and DYPHYRAD stations from March 2016 to October 2020 through Mantel correlograms between the Euclidean distance matrix of ASVs niche distance and the phylogenetic distance matrix. Black and white squares indicate significant ($p<0.05$) and non-significant values respectively.*

Chapter 5: General Discussion

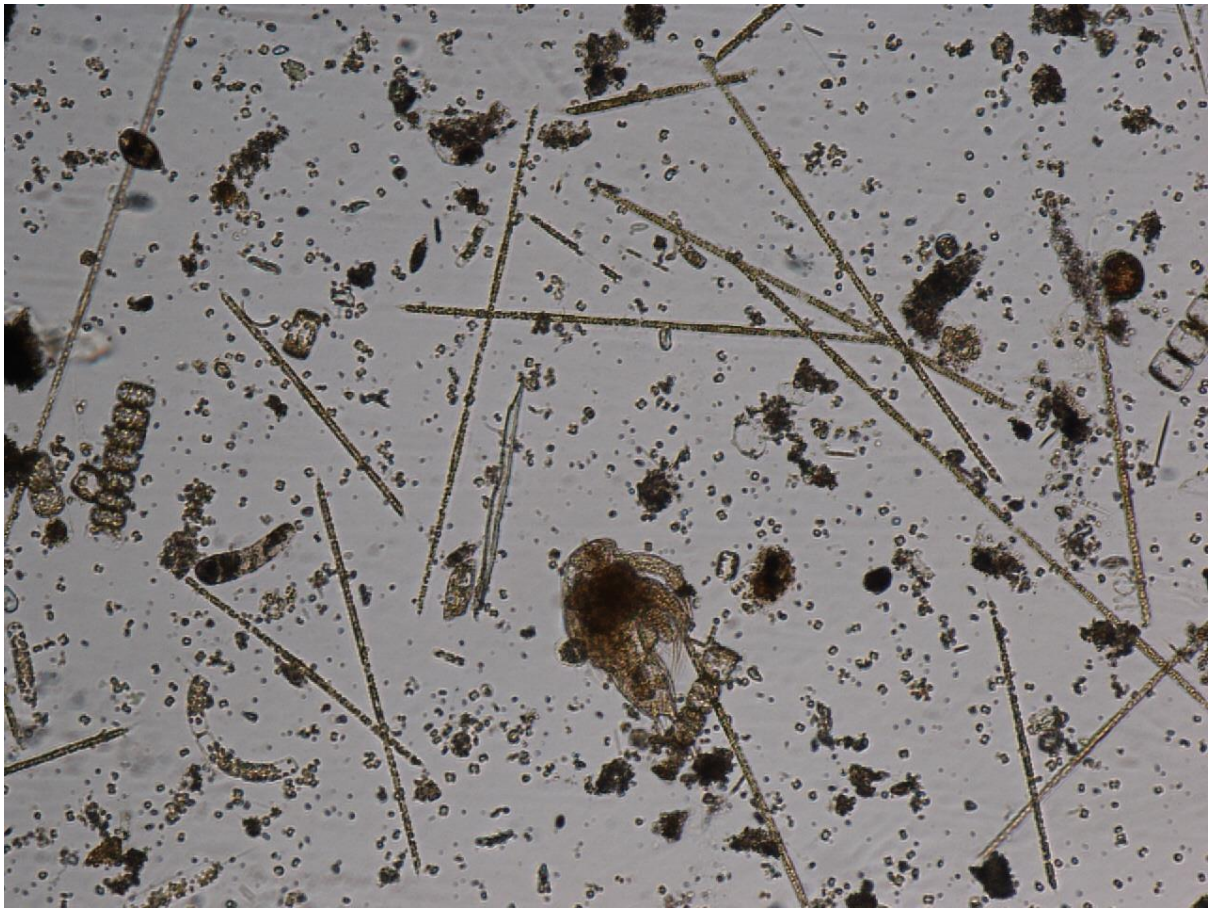

5. Discussion

The objective of this thesis was to investigate the seasonal organization mechanisms of plankton microbial communities in the Eastern English Channel (EEC). Conventional tools were used (i.e., microscopy and cytometry) to estimate abundance and biomass, and metabarcoding (i.e., 16S and 18S rRNA gene sequencing) to provide a more extended evaluation of the diversity. Besides the recurrent spring blooms of the haptophyte *Phaeocystis globosa*, it was evidenced that transient diatoms, small mixotrophic dinoflagellates (Chapter 2), and heterotrophic bacteria (Chapter 3) prevailed, and showed peaks, particularly in summer. Pico- and nanophytoplankton (Chapter 2) showed peaks in summer and autumn. Syndiniales Group II (reads and spores) showed peaks and infections in summer and autumn. The ecological processes that shape the seasonal organisation of phytoplankton and Syndiniales Group II were investigated. Moreover, this work focused on specific relationships concerning: i) putative hosts and parasites through direct observations (using the FISH method), ii) phytoplankton (i.e., diatoms, and *P. globosa*) and heterotrophic bacteria through indirect observations (i.e., inferring biological associations using network analysis).

In this chapter, the main conclusions of the three different studies will be summarized. A general scheme of the seasonal succession of microbial communities will be depicted (Fig. 5.1), and the scope of the discussion will be widened in the context of global changes. Finally, general perspectives of observatory surveys will be suggested.

5.1. Seasonal organisation of planktonic microbes in the coastal waters of the EEC

Using complementary approaches, this thesis provided new insights into the seasonal organisation of planktonic microbes in the EEC (Fig. 5.1 A). The dominance of deterministic ecological processes was in line with the high environmental filtering in winter (Chapter 2). These ecological filters (i.e., processes) resulted in a diverse diatom community during this period. Diatoms in winter are typically adapted to low light, high nutrient concentration, and turbulent conditions (Armbrust, 2009). Their silica frustule provides structural support and protection against mechanical stresses and salinity shocks (e.g., Logares *et al.*, 2009). Diatoms, especially those of the genus *Thalassiosira,* and other centric ones, identified with both microscopy and metabarcoding techniques, have developed adaptations to thrive under light-limited and turbulent waters (Schapira *et al.*, 2008). The presence of a large centric vacuole plays an important role in optimizing light affinity, and thus helping diatoms to persist (Hansen and Visser, 2019). The diverse diatom communities provided various substrates shaping a co-

occurring heterotrophic bacteria, that need to act synergistically to process a recalcitrant carbon fraction (Ward *et al.*, 2017; Chapter 3).

P. globosa exhibited blooms in April-May as expected. However, the metabarcoding dataset evidenced the presence of a low relative abundance of *P. globosa*, all year around (Fig. 2.3 B). The limiting volumes of water analysed by microscopy (from 10 to 100 ml) and cytometry (0.18 ml), could lead to misidentification or overlooking of *P. globosa* cells. However, metabarcoding allowed better detection of *P. globosa* at low abundance, as larger volumes of seawater were filtered (from 4 to 7 litres).

Regarding *P. globosa* bloom, network analysis revealed a strong association between *P. globosa* and copiotroph bacteria (Chapter 3). The composition of bacteria at family and genus levels remained consistent across years despite variations in blooming intensities. This suggested that *P. globosa* provides a 'stable-state' environment for heterotrophic bacteria communities (Mars Brisbin *et al.*, 2022). During this period, one noteworthy observation was the presence of the copiotrophic bacterium *Pseudolateromonas*. Previous research (e.g., Lemonnier *et al.*, 2020), has noted that this genus is typically found during productive periods, which aligns with the conditions of the *P. globosa* bloom. Moreover, *Pseudoalteromonas* has the potential to be algicidal, as it may produce bioactive molecules that can kill phytoplankton cells (Mayali and Azam, 2004). This algicidal activity could serve as a mechanism contributing to the bloom termination. At the end of the bloom in late spring, bacteria remineralized the large organic resources derived from *P. globosa.* In Chapter 2, it was hypothesized that the significant inputs of organic matter may act as perturbations that favour stochastic processes in phytoplankton community assembly (e.g., ecological drift; Jurburg *et al.*, 2017).

Ecological drift was the dominant process that prevailed in summer when transient phytoplankton blooms occurred (Chapter 2). The different taxa that peaked during this period had various adaptations. For example, the small dinoflagellate *Prorocentrum minimum* primarily relies on photosynthesis for growth using inorganic nutrients. However, it compensates for low concentrations of inorganic nitrogen by mixotrophic utilization of organic nitrogen (Fan *et al.*, 2003) and probably other compounds released at the end of *P. globosa* bloom. The parasitic Syndiniales Group II showed infections in summer and autumn (Chapter 4). The most notable infection was observed with the *P. minimum* increase in June 2018. Pico- and nanophytoplankton can increase nutrient diffusion even in low concentrations due to their high surface/volume ratio (Raven, 1984), and thus were also relatively abundant in summer

(Chapter 2). The pennate diatoms *Leptocylindrus danicus* and *Pseudo-nitzschia pungens,* that bloomed in summer, are considered to be adapted to high light (Widdicombe *et al.*, 2010; Polimene *et al.*, 2014), and to low silicate conditions (Leynaert *et al.*, 2002; Marchetti *et al.*, 2004). Autumn was a transitional period characterised by diverse diatom communities and peaks of pico- and nanophytoplankton. This period was characterised by both deterministic and stochastic processes. As nutrients became more available for phytoplankton and light was still available, the impact of environmental filtering increased (Chapter 2).

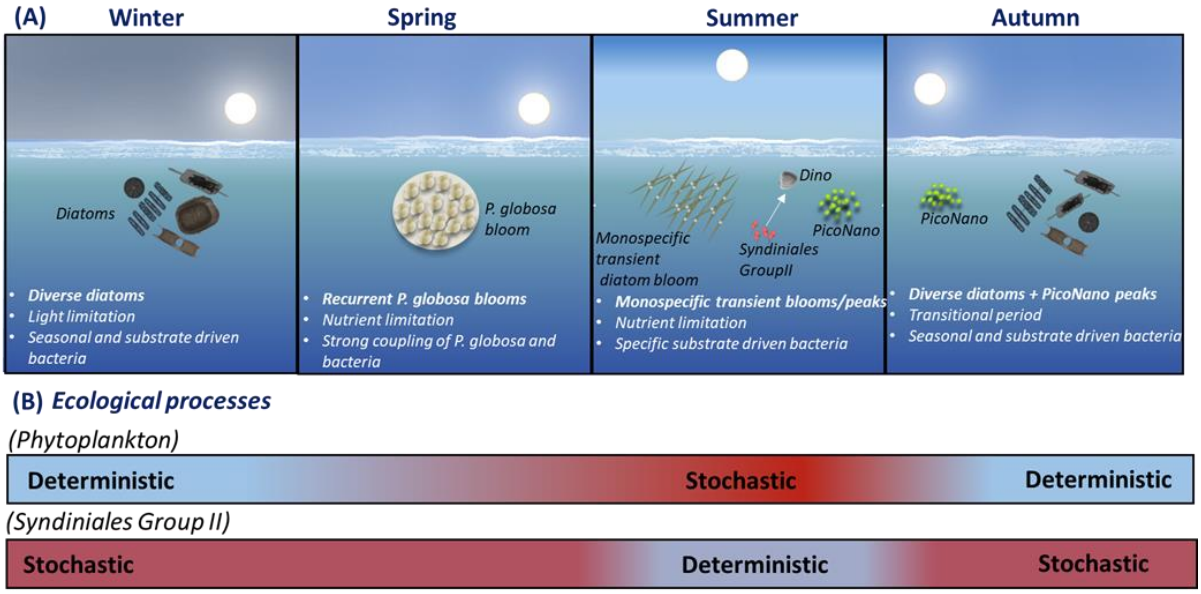

Figure 5.1. *(A) Schematic overview of the seasonal succession of planktonic microbes in the EEC. (B) The contributions of deterministic (blue colour), and stochastic processes (red colour) in phytoplankton and Syndiniales Group II Syndiniales are visualised in stripes. (PicoNano: pico- and nanophytoplankton, Dino: Dinoflagellates).*

5.2. Do similar ecological processes prevail across different microbial groups in the EEC?

It is generally accepted that both deterministic and stochastic processes play significant roles in the assembly of local communities (e.g., Chase *et al.*, 2009; and references therein). However, their relative importance may vary among different microbial groups and scales (i.e., spatial and temporal). This variation was observed in prokaryotes and picoeukaryotes across tropical and subtropical oceans (Logares *et al.*, 2020). Picoeukaryotes were found to be shaped primarily by dispersal limitation, while prokaryotes were influenced by the combined effects of dispersal limitation, selection (i.e., deterministic), and drift (i.e., stochastic). In another study conducted in limnic ecosystems in eastern Antarctica (ca. 411 km), it was observed that picoeukaryotes were influenced by drift, whereas prokaryotes were influenced by selection

(Logares *et al.*, 2018). Furthermore, the contribution of ecological processes varied between different phytoplankton groups (i.e., diatoms, *Synechococcus*, and haptophytes) at large spatial scales (Xu *et al.*, 2022).

The relative importance of ecological processes in shaping different microbial groups was investigated across seasons using the framework of Stegen (Chapters 2 and 4). The findings revealed varying patterns regarding dominance of deterministic and stochastic processes. In the case of phytoplankton, deterministic processes were found to dominate during winter and early spring, while stochastic processes took over in late spring and summer. Both deterministic and stochastic processes played significant roles in shaping phytoplankton communities in autumn (Chapter 2). In contrast, Syndiniales Group II displayed a different pattern, with stochastic processes being dominant throughout the year (Chapter 4). The seasonal variation in Syndiniales Group II was less evident compared to phytoplankton. This difference between the two groups can be attributed to several factors. Phytoplankton was more influenced by the abiotic environment (i.e., deterministic factors) compared to Syndiniales Group II. Distance-based RDA analysis evidenced that environmental variables contributed to 45 % of total variation of phytoplankton communities (Chapter 2; Fig. 2.1B). While previous studies have linked Syndiniales dynamics to environmental variables, this was not the case for our study (e.g., Yih and Coats, 2000; Alves-de-Souza *et al.*, 2012). Community size is another important factor. Phytoplankton communities consisted of a larger number of ASVs (i.e., 4,141 ASVs), compared to Syndiniales Group II (i.e., 663 ASVs). In smaller communities, such as Syndiniales Group II, stochastic processes can exert a strong influence on community structure, by increasing the probability of species going extinct locally (Chase *et al.*, 2009; Chase and Myers, 2011).

It is noteworthy that stochastic processes may be overestimated in phytoplankton and Syndiniales Group II datasets because of the rare taxa (e.g., representing < 0.1 % of reads), as they are more susceptible to such processes (e.g., Ramond *et al.*, 2023). In a technical aspect, the framework that was applied in this thesis (Stegen *et al.,* 2013) has been widely used (more than 1000 citations). Yet, there is a new methodology, using 'phylogenetic-bin based' null models (i.e., iCAMP; Ning *et al.*, 2020) instead of an entire community-based approach. According to the authors, this new method seems to offer better accuracy, sensitivity, and specificity. It might be worth considering testing this method to further validate our findings.

Regarding heterotrophic bacteria, is widely established that they are influenced by deterministic processes in marine coastal ecosystems (e.g., Teeling *et al.*, 2016; Chafee *et al.*, 2018). This observation is coherent with the significant interaction they have with phytoplankton. In fact, Chapter 3 showed that bacterial dynamics is seasonal and/or substrate driven, and it highlighted well-defined putative interactions with phytoplankton during non-blooming and blooming periods through network analysis. Considered together, deterministic and stochastic processes varied for different microbial groups and across seasons (Fig. 5.1 B).

5.3. Deterministic and stochastic processes in a changing world

As mentioned previously, the significance of deterministic and stochastic processes in shaping communities may vary across different groups. Therefore, it is reasonable to expect that these groups will exhibit distinct responses within a changing environment (e.g., increasing temperature, eutrophication). However, the question of how exactly these communities will respond remains unanswered, including whether deterministic or stochastic processes will predominate. Certain studies have indicated that eutrophication and climate warming may promote deterministic processes in fungal and bacterial communities respectively (Zhang *et al.*, 2021; Xu *et al.*, 2022). Furthermore, Beaugrand and Kirby, (2016) applied the 'METAL' model (MacroEcological Theory on the Arrangement of Life), which builds upon Hutchinson's ecological niche concept (1957), and using CPR (Continuous Plankton Recorder) copepod data focusing on two species. They also integrated a stochastic component into their model. These authors suggested that species' responses to climate warming were deterministic and hence predictable. However, Chapters 2 and 4 showed that stochastic processes outweigh deterministic ones across seasons, and thus responses to climate warming may not be predictable. This contrast may stem from the following factors: i) different methodologies in sampling acquisition (metabarcoding vs CPR data), iii) different types of organisms were studied (e.g., phytoplankton vs copepods), iv) different scales (e.g., small-scale vs regional), v) different ecology (e.g., community vs population ecology). Beaugrand and Kirby (2016) also stated that stochasticity was more important on local than on regional scale. This is in line with the small scale (ca. 15 km) that was considered in this thesis. We are still far from answering whether deterministic or stochastic processes will prevail in the future and how communities will respond to climate change. It is essential that microbial ecologists and modelers further collaborate to disentangle these processes at the population, community and metacommunity levels. For this, an appropriate methodology should be tested, including different planktonic groups and at various spatio-temporal scales (e.g., seasonal, local, regional and global).

5.4. Outlook for monitoring networks in French coastal ecosystems

Time series of molecular data have been started to developed in French coastal ecosystems since 2000. For example, molecular data have been acquired in SOMLIT and/or DYPHYRAD stations since 2008 at the LOG laboratory in Wimereux (Monchy *et al.*, 2012; Christaki *et al.*, 2014; Genitsaris *et al.*, 2016; Rachik *et al.*, 2018; this thesis). Similarly, the SOMLIT Astan station in Roscoff (Caracciolo *et al.*, 2022), the SOMLIT SOLA station in Banyuls-sur-mer (e.g., Lambert *et al.*, 2019), and recently the SOMLIT stations in the Bay of Brest (Lemonnier, 2019) have been also monitored for molecular data. However, these molecular surveys, among others, are not yet integrated into national labelled monitoring networks (like SOMLIT; https://www.somlit.fr/en/ and PHYTOBS; https://www.phytobs.fr/en), and there is not yet a standardized method to perform them. Depending on the study's goals, molecular surveys may target different organisms by using different primers, or target different size groups. For example, in LOG, samples are filtered on 0.2 µm, while in the Bay of Brest a successive filtration is used onto 0.2 µm, 3 µm, 20 µm to study separately pico-, nano- , and microphytoplankton (e.g., Ramond *et al.*, 2021). Furthermore, different DNA extraction kits are used, different sequencing and/or bioinformatic analysis are applied. In contrast to the Utermöhl method which is practically unchanged since 1931, metabarcoding evolve continuously. Utermöhl method is the most commonly used for data collection to monitor phytoplankton abundance and biomass in many microbial time series, being relatively rapid and inexpensive to set up. It is considered to be a standard method, although considerable variability occurs in the way the organisms are counted in the Utermöhl chamber, even though suggestions for standardized protocols have been made. (e.g., Zingone *et al.*, 2015). On the other hand, regarding metabarcoding, the ongoing improvements in extraction kits, sequencing technologies, primers, and bioinformatic analysis make the establishment of standardized molecular monitoring even more challenging.

Efforts have been made at the national European and international levels. At national level efforts have been made through discussions and workshops between different laboratories (e.g., the IR ILICO workshop organised in Wimereux, in January 2019). Also, ROME (https://rome.ifremer.fr/) is a new molecular network of IFREMER expanding from Western to South France (4 stations; since 2020). Its goal is to evaluate contaminations to monitor potential health risks from for humans and animals. The EMO BON (European Marine Omics Biodiversity Observation Network) has been recently established across 19 countries and includes three French stations in Banyuls-sur-mer, Villefranche and Roscoff, to better

understand biodiversity in a changing ocean (Santi *et al.*, 2023). At the international level, the OSD (Ocean Sampling Day), collects samples (16S and 18S rRNA data) worldwide on a specific day each year using the same methods, and holds a potential for making comparisons across time series data (Kopf *et al.*, 2015; Stern *et al.*, 2018). Even when standardisations will be made it is important to integrate the different time series carefully. During this thesis, an attempt was made to integrate 16S data, collected from 2013 to 2015 in the EEC, using the same primers (i.e., 341F, 785R; Klindworth *et al.,* 2013) that amplified the V3-V4 region, and using the same sequencing technology (i.e., Ilumina MiSeq 2x300 bp) with the data presented in this thesis collected from 2016 to 2020. However, data from 2013 to 2015 were not integrated as presented spurious patterns (i.e., absence of seasonal patterns, overrepresentation of a family contributing 90 % in relative abundance; see Annexes Fig. A1). This, could be attributed to: i) DNA extraction bias, ii) different sequencing companies, iii) difference in the number of samples sequenced in an Illumina-lane. Seventy samples were sequenced in one lane at each sequencing run for data from 2016 to 2020, while fifty-five samples were sequenced in one lane for data from 2013 to 2015. This may influence the sequencing depth (e.g., in RNA sequencing ; Sheng *et al.*, 2017). Sequencing depth refers to the average number of times a nucleotide base is read during the sequencing process. The samples in the lane with more samples will likely receive fewer reads each on average compared to the samples in the lane with fewer samples.

It is important to stress that 'omics' methods cannot replace direct observations provided by microscopy and cytometry data, but they complement them. This was evidenced during this thesis. In chapter 2, only two dinoflagellates (*Gymnodinium* sp., and *Prorocentrum minimum*) were kept from the metabarcoding dataset, that were also identified in microscopy to avoid misrepresentations. *Gymnodinium* is known to dominate dinoflagellate abundance and biomass in the eastern English Channel (Grattepanche *et al*., 2011), while *P. minimum* showed a momentary increase (Chapters 2 and 4). In Chapter 3, in the network analysis performed, phytoplankton enumerated by microscopy were considered instead of metabarcoding data to avoid discrepancies and because metabarcoding does not provide biomass data. However, it would be noteworthy to further test network analysis on metabarcoding data and see if the networks present the same interactions as those observed in our network based on microscopy. In Chapter 4, dinospores were enumerated by microscopy using the FISH method, to better study Syndiniales Group II dynamics, and to identify putative infections. Furthermore, it was shown that there was no relation between dinospore abundance and relative read abundance of

Syndiniales Group II (Fig. S4.8), suggesting that Syndiniales Group II reads cannot be used as a predictor for dinospore abundance and vice-versa.

The few existing studies that combine molecular and metabarcoding observations (e.g., Christaki *et al.*, 2021; Santi *et al.*, 2021; Caracciolo *et al.*, 2022), have clearly shown the overrepresentation of dinoflagellates due to high gene copies (Wisecaver and Hackett, 2011). This was also the case in this thesis. Based on microscopy, diatoms were the dominating group (in abundance and biomass), except during the blooming period of *P. globosa* in April and May. However, metabarcoding showed that dinoflagellates (29.7%) dominated protist communities, following by diatoms (i.e., 24.9 % read relative abundance; Chapter 4). It is important to note that variations in the compositions may result by the primers selected or the clustering technique. A previous study in the EEC using primers that amplify a shorter region of V2-V3 18S rRNA gene (470 – 480 bp), than the one applied here (i.e, V4; 527 bp), and different clustering technique (OTUs vs ASVs), showed that dinoflagellates were even more overrepresented. Diatoms contributed in 8%, and dinoflagellates 15% of the total read relative abundance (Christaki *et al.*, 2017). While considerable differences were detected between microscopic and metabarcoding datasets for protists, datasets had more similar compositions in higher taxonomic levels (e.g., families) than in genus or species level (e.g., Santi *et al.*, 2021). Despite the discrepancies, *P. globosa*, pico- and nanophytoplankton, and cryptophytes had similar seasonal trends in number of reads, cell abundance and biomass (5.2). Caracciolo *et al.,* (2022), applied a temporal analysis (i.e., db-MEM) using microscopic and metabarcoding protist data, and they showed similar temporal patterns.

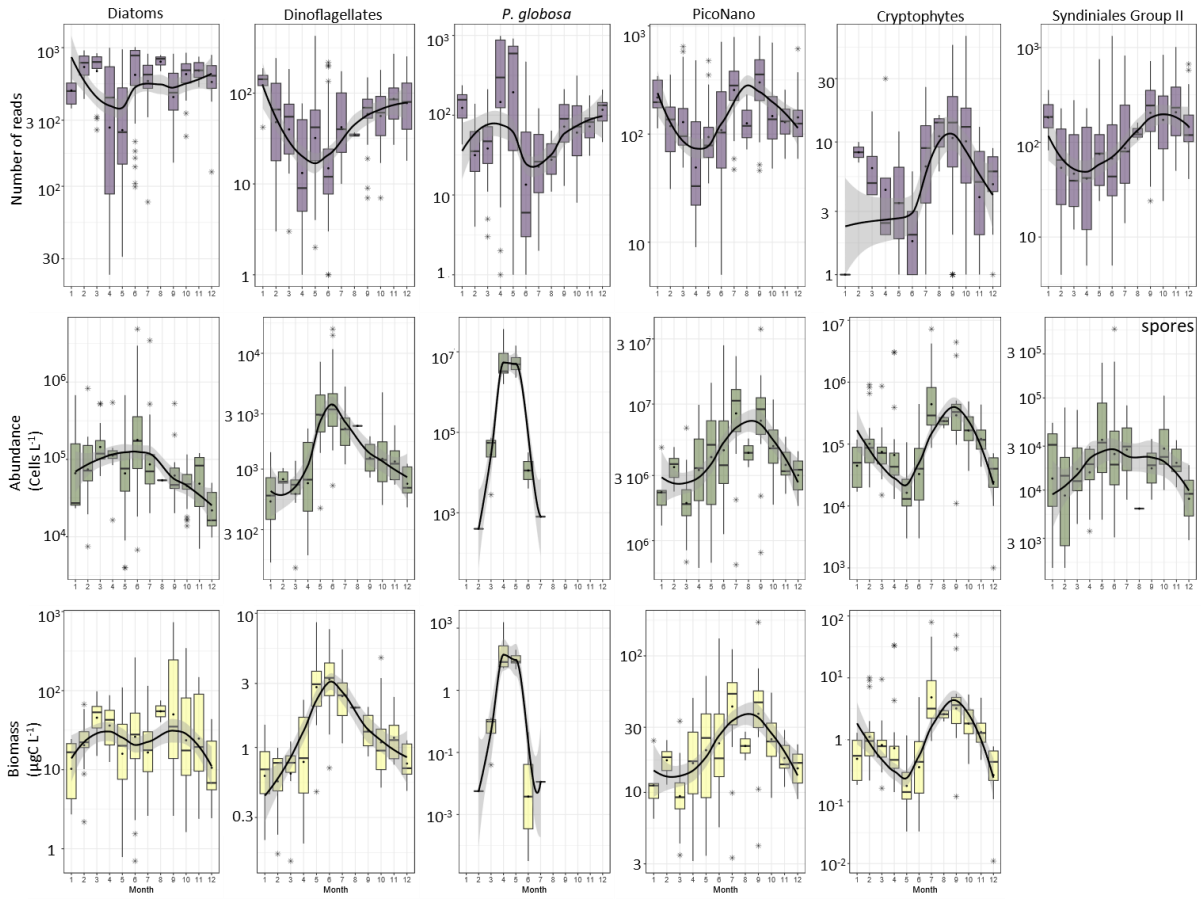

Figure 5.2. *Seasonal variation of protists: Diatoms, dinoflagellates, Phaeocystis globosa., pico-nanophytoplankton (PicoNano), cryptophytes, and Syndiniales Group II based on reads from metabarcoding data, and abundance and biomass from morphological data from SOMLIT and DYPHYRAD stations surface samples in the EEC, from March 2016 to October 2020. Y scale is log10 transformed. Solid black lines of boxplot represent the median, black dots the mean and the black stars the outliers. The solid line and ribbon represent LOESS smoothing and the 95% confidence interval.*

Regarding prokaryotes, direct observations are not possible. The FISH method provides quantification of certain families, and it has been showing a generally good accordance with metabarcoding data (Teeling *et al.*, 2016). In the marine realm, the unknown/ unassigned sequences contribute to 25 -58 % of microbial communities (Bernard *et al.*, 2018; Wyman *et al.*, 2018; Zamkovaya *et al.*, 2021). Considering this hidden diversity monitoring networks would benefit from including metagenomic and transcriptomic data. They also provide information on functional and metabolic diversity. Furthermore, metagenomic studies can limit the common overestimation of dinoflagellates and the underrepresentation of diatoms observed in metabarcoding studies (e.g., Genitsaris *et al.*, 2016).

In conclusion, this thesis has addressed a critical knowledge gap concerning the mechanisms underlying the seasonal succession of microbial communities and bloom-forming taxa in the EEC. By applying a phylogenetic null-model approach rooted in community ecology, this

study attempted to decipher the ecological processes governing seasonal organisation, and by applying network analysis and the FISH method explored interactions:

- Seasonal organisation of phytoplankton was regulated by deterministic and stochastic processes. Except winter and early spring, stochastic processes prevailed the rest of the year. Summer communities characterised by transient blooming taxa (diatoms, mixotrophic dinoflagellates) were mainly driven by stochastic processes. The prevalence of stochastic processes renders *a priori* seasonal dynamics less predictable.

- Heterotrophic bacteria showed seasonal patterns in winter, spring and autumn, and 'episodic' patterns in summer due to transient blooms. Also, diatom and *P. globosa* blooms harboured distinct bacterial communities.

- Syndiniales Group II (Clade 10+11, 14) were observed in consecutive years suggesting the existence of local populations. Clade 8 peaked in summer along with the mixotrophic dinoflagellates *Prorocentrum* and *Scrippsiella*, and showed infections (prevalence 38.5 %). Stochastic ecological processes prevailed in community assembly.

This thesis highlights the need for complementary approaches in observatory surveys, and advocates for higher sampling frequencies to gain more comprehensive understanding of the complex dynamics governing coastal marine ecosystems. Finally, to understand the complexity and the challenges that coastal ecosystems face we need collaborations between researchers of various backgrounds, standardized monitoring and analytical methods, and F.A.I.R. data (Findable, Accessible, Interoperable, Reusable).

Résumé détaillé en français

Chapitre 1 : Introduction

Généralités sur le plancton

Le plancton (Hensen, 1987) désigne les organismes dans la colonne d'eau qui ne peuvent pas se déplacer activement contre les courants. Le terme 'plancton' correspond à une définition fonctionnelle, et correspond à organismes diversifiés en termes de forme, de taille et de phylogénie (Woese *et al*., 1990; Worden *et al*., 2015; Barton *et al*., 2013). Le plancton couvre une large gamme de tailles, de quelques micromètres à plusieurs mètres, et représentant tous les domaines du domaine : les procaryotes, les protistes, les métazoaires et les virus. Malgré ces différences, ils partagent des caractéristiques écologiques telles que des taux de croissance élevés et des populations diversifiées. Cependant, ils diffèrent par leur physiologie, leurs capacités métaboliques et leur comportement trophique.

La compréhension de la distribution, de la composition et de l'écologie des communautés planctoniques est cruciale dans les questions et perspectives sur l'évolution et l'adaptation, du rôle fondamental dans les réseaux trophiques marins (plus de 60 % de la biomasse) et du cycle des nutriments (e.g., Bar-On and Milo, 2019). La faible biomasse du phytoplancton est responsable de près de la moitié de la production primaire nette globale (Falkowski *et al.*, 1998; Field *et al.*, 1998). Le renouvèlement rapide du plancton soutient les niveaux trophiques supérieurs ; les écosystèmes marins diffèrent de ceux terrestres en raison de ce renouvellement rapide. Le plancton joue un rôle majeur dans les cycles élémentaire de l'océan et de la Pompe à Carbone Biologique. Aussi, les organismes planctoniques servent de nourriture pour les niveaux trophiques supérieurs (zooplancton, necton), influençant le recrutement des espèces de poissons commercialement importantes (e.g., Platt *et al.*, 2003).

Un objectif fondamental en écologie microbienne marine est d'étudier la diversité et la dynamique des micro-organismes planctoniques et de déterminer les facteurs qui influencent leurs patrons de diversité. Cette connaissance est cruciale pour prédire comment cette dynamique peut être modifiée par les pressions anthropiques directes (comme les pollutions) et le changement global (comme l'élévation de la température, augmentation de la pCO_2 et acidification).

Théories, processus écologiques et diversité

Plusieurs théories de la biodiversité ont été formulées pour expliquer les assemblages de communautés et leur distribution spatio-temporelle. L'assemblage de la communauté est décrit comment les processus interagissent pour déterminer la composition des espèces et la biodiversité locale d'une communauté (par exemple, Chase et Myers, 2011). Ces théories, basées sur des principes différents, ne sont pas mutuellement exclusives. Elles impliquent des mécanismes environnementaux, des interactions et des mécanismes stochastiques.

Environnement

Il existe deux visions complémentaires concernant l'influence de l'environnement sur les assemblages de communautés. La théorie neutre de Hubbell, suppose que tous les individus ont les mêmes perspectives de reproduction et de mortalité (neutralité). La variabilité des abondances relatives entre les espèces est uniquement due à la stochasticité démographique. La théorie neutre de la biodiversité a été largement débattue, en particulier en raison de son postulat d'équivalence écologique. Cela signifie que les individus ont des taux de croissance, de mortalité, de spéciation et de dynamique spatiale similaires, et qu'il n'y a pas de différences significatives de *fitness* (compétitif vis-à-vis de la croissance). Par conséquent, la présence ou l'absence d'une espèce serait principalement déterminée par le hasard plutôt que par ses caractéristiques spécifiques ou ses avantages compétitifs. Bien que la théorie neutre suppose l'équivalence écologique de tous les individus, elle a réussi à prédire avec succès plusieurs schémas écologiques clés dans de nombreuses communautés, tels que les distributions d'abondance des espèces et les relations espèces-superficie, surpassant même la théorie des niches dans certains cas (Adler *et al*., 2007 ; Rosindell *et al*., 2012).

La deuxième théorie développée par Hutchinson (1957) considère la niche comme une caractéristique propre à chaque espèce. Elle est définie comme un espace multidimensionnel, chaque dimension représentant un paramètre environnemental. Chaque point dans cet espace correspond à un état environnemental permettant à une espèce de survivre indéfiniment (Hutchinson, 1957). Cependant, Hutchinson a observé que, dans le cas du phytoplancton, plusieurs espèces coexistaient malgré une même niche écologique (Hutchinson, 1961). Ceci contredisait le principe d'exclusion compétitive, créant le "paradoxe du plancton". Hutchinson a suggéré que l'équilibre environnemental n'est jamais atteint car des changements se

produisent avant l'équilibre à différentes échelles spatio-temporelles. Par conséquent, l'exclusion compétitive n'atteint jamais son maximum, permettant aux espèces de coexister. Plusieurs hypothèses ont été avancées pour résoudre ce paradoxe, notamment l'exclusion trophique, les processus stochastiques et l'impact de la reproduction asexuée sur la spéciation (Behrenfeld *et al*., 2021).

Interactions

Les interactions biologiques sont de plus en plus reconnues comme une force majeure modulant la structure et la fonction des communautés microbiennes, dans certains cas plus que les facteurs abiotiques (par exemple, Genitsaris et al., 2015 ; Lima-Mendez *et al*., 2015). Les interactions entre les microorganismes ont des effets importants sur le cycle des nutriments et l'efficacité du transfert vers les niveaux trophiques supérieurs (Worden *et al*., 2015).

Une des interactions le plus importantes dans les communautés microbiennes concerne celles entre le phytoplancton et les bactéries hétérotrophes, et elles peuvent varier de coopératives à compétitives. (Seymour *et al*., 2017). Les bactéries consomment la matière organique produite par le phytoplancton et agissant comme fournisseurs de nutriments pour la croissance des phytoplancton (Azam *et al*., 1983 ; Amin *et al*., 2012). Cependant, elles peuvent aussi entrer en compétition avec le phytoplancton pour les nutriments inorganiques (minéraux et sels nutritifs) et limiter ainsi leur croissance (Joint *et al*., 2002). Les interactions parasitaires sont également importantes et peu étudier, modifiant la dynamique des populations hôtes et influençant la composition des communautés, bien que leur compréhension reste encore limitée (Combes, 1996 ; Chambouvet *et al*., 2008). Par exemple, les Syndiniales, contrôlent les efflorescences de dinoflagellés et influencent les réseaux trophiques (Chambouvet *et al*., 2008). Ces interactions complexes façonnent les écosystèmes aquatiques.

Dispersion

En écologie des communautés la dispersion est définit comme le déplacement et à l'établissement réussi d'organismes dans l'espace. La dispersion peut être considérée comme un processus déterministe (c'est-à-dire les conditions biotiques et abiotiques sous lesquelles une espèce peut persister), stochastique (c'est-à-dire des changements aléatoires) ou les deux. Notre compréhension des processus de dispersion microbienne reste incomplète à l’heure actuelle. La dispersion microbienne est généralement considérée comme passive, et donc stochastique

(Zhou and Ning, 2017). Cependant au seins des systèmes marins, la dispersion physique dépend des propriétés morphologique des micro-organismes, telles que leur taille et leur forme.

Etudier les mécanismes qui déterminent la structure de communautés représente un défi en écologie. Vellend (2010) a proposé quatre processus : la spéciation, la sélection, 'le drift' et la dispersion. En attribuant des niveaux d'importance variables à ces processus, toutes les théories écologiques précédemment formulées peuvent être conceptualisées (Vellend, 2010). Pour étudier la diversité des organismes vivants et comprendre les mécanismes sous-jacents, il est nécessaire de quantifier la biodiversité, leurs propriétés et d'identifier leurs variations.

Méthodes pour étudier les microbes planctoniques

Dans cette thèse, des outils classiques tels que la microscopie et la cytométrie en flux ont été appliqués pour fournir des données sur l'abondance et la biomasse, ainsi que des techniques moléculaires (metabarcoding) pour fournir des données plus détaillées sur la diversité génétique.

La microscopie : En 1931, Utermöhl a inventé une méthode de sédimentation qui repose sur l'observation au microscope inversé pour identifier et dénombrer le microplancton. La méthode Utermöhl n'a guère évolué en près d'un siècle. Les échantillons naturels sont d'abord fixés pour conserver les caractéristiques des organismes observés, puis déposés dans un cylindre. Après 16 à 48 heures, les cellules déposées sont observées au microscope inversé pour identification et comptage. Cependant, cette méthode présente des limites, notamment sa lenteur et sa dépendance à l'expertise de l'observateur pour la discrimination des taxons, entraînant un biais dépendant de l'observateur

La cyrtométrie en flux : Contrairement à la microscopie, la cytométrie en flux est une méthode rapide, simple et précise pour quantifier l'abondance de petites cellules autotrophes et hétérotrophes en fonction de leurs propriétés optiques et spectrales (Trask *et al.*, 1982; Chisholm *et al.*, 1988; Amann *et al.*, 1990). La cytométrie en flux mesure et compte les cellules une par une, entrainé dans un liquide de gaine. Lorsqu'une cellule passe devant le faisceau laser, la lumière transmise (« forward scatter »), réfléchit à 90° (« side scatter ») va dépendre de sa taille et de sa forme. L'analyse permet d'identifier, quantifier et caractériser les propriétés des cellules (comme l'autofluorescence ou la fluorescence induite), mais ne fournit pas de discrimination taxonomique.

Metabarcoding : Les premières techniques de séquençage ont été décrites en 1977 : la méthode chimique de Maxam-Gilbert (Maxam et Gilbert, 1977) et la méthode enzymatique de Sanger (Sanger *et al*., 1977). La méthode de Sanger, toujours utilisée aujourd'hui, a rapidement été préférée à celle de Maxam-Gilbert, permettant le séquençage du premier génome humain. Cependant, la méthode de Sanger est limitée pour les génomes volumineux et est très coûteuse. De nouvelles méthodes de séquençage ont été développées au cours des dernières décennies, dont le metabarcoding environnemental qui a révolutionné l'étude de la diversité microbienne. Cette méthode utilise l'amplification PCR (Amplification en Chaine par Polymeration) pour cibler un fragment d'un gène marqueur d'ADN, permettant la description de la diversité moléculaire présente dans un échantillon environnemental. Bien que puissante, le metabarcoding a des biais potentiels, comme les biais de PCR et la sous- ou surestimation de certains taxons. En comparaison, le métagénomique et le métratranscriptomique permettent une caractérisation fonctionnelle des communautés microbiennes, mais sont plus coûteux et complexes à mettre en œuvre.

Fluorescence *in situ* par hybridation spécifique (*FISH*) : En raison des biais mentionnés liés au séquençage des gènes marqueurs, il est important de le compléter par des méthodes quantitatives précises. Une de ces techniques est l'hybridation in situ spécifique en présence d'une sonde fluorescente (FISH) de l'ARN ribosomal (Gall and Pardue, 1969). Cette méthode permet la détection, l'identification et le dénombrement (par microscopie, ou cytométrie) des microorganismes actifs dans l'environnement sans nécessiter de culture. Elle repose sur l'utilisation d'une sonde oligonucléotidique couplée à un fluorochrome qui se liera spécifiquement à une séquence cible. La méthode TSA-FISH (amplification du signal par tyramide) améliorée est essentielle pour les échantillons environnementaux pour lesquels la méthode conventionnelle ne fournit pas de signaux fluorescents suffisamment intenses. Cependant, cette méthode est limitée dans le temps, et la résolution taxonomique fine peut être difficile à obtenir en raison de la similarité génétique croissante entre les taxons.

Une approche multidimensionnelle avec différentes techniques complémentaires permet de comprendre de manière globale la composition des microorganismes planctoniques et d'assurer une surveillance à long terme.

La Manche

Les zones côtières sont des écosystèmes complexes à l'interface entre océans et milieux terestres. Elles jouent un rôle crucial dans les cycles biogéochimiques, contribuent significativement à la production primaire océanique et à l'accumulation de la matière organique, et abritent une grande partie de l'activité de pêche mondiale, ainsi que de la population humaine. La conservation de ces écosystèmes nécessite une compréhension approfondie de leur structure biologique et de leur fonctionnement, notamment en ce qui concerne le rôle central des microbes planctoniques. La Manche est une mer peu profonde située entre l'Angleterre et la France, divisée en Manche occidentale et orientale. La Manche orientale est caractérisée par un régime de marées méga-tidal avec des courants parallèles à la côte. Les apports fluviaux et la circulation résiduelle créent une zone côtière moins salée et plus turbide, séparée des eaux du large par un courant côtier riche en phytoplancton. Les conditions météorologiques variables tout au long de l'année affectent les propriétés de l'eau, avec des masses d'eau plus chaudes en été. La faible profondeur et les forts courants de marée empêchent la formation d'une thermocline saisonnière (e.g., Gentilhomme et Lizon, 1997).

Les microbes planctoniques en Manche Orientale

La Manche Orientale se caractérise par une dynamique de biodiversité répétitifs dans la succession du phytoplancton, notamment les efflorescences annuelles de printemps non toxiques de l'Haptophyte *Phaeocystis globosa*, qui peuvent représenter jusqu'à 90% de la biomasse du phytoplancton (par exemple, Schapira *et al*., 2008 ; Grattepanche *et al*., 2011a ; b, Breton et al., 2017). Au cours des deux dernières décennies, des recherches approfondies ont démontré les principaux facteurs définissant les efflorescences de *P. globosa* en Manche Oriental (Breton *et al*., 1999, 2006, Christaki *et al*., 2014 ; Genitsaris *et al*., 2015, 2015, 2016, Breton *et al*., 2021, 2022). Comme par exemple l'excès des nitrates et la limitation de silicates, la limitation du broutage par le zooplancton grâce à la formation de colonies. De plus, la ré-oligotrophication et la réduction des apports fluviaux observées le long de la côte au cours de la dernière décennie ont favorisé les efflorescences de *P. globosa* en modifiant le déséquilibre entre nitrates et phosphates (Breton *et al*., 2022).

Des observations microscopiques et le métabarcoding ont montré que l'efflorescence intense de *P. globosa* est encadrée par d'autres microorganismes planctoniques, dont les diatomées, les dinoflagellés, les bactéries et les parasites eucaryotes, et certains d'entre eux présentent des

efflorescences ou des augmentations relatives (Breton *et al*., 2000 ; Schapira *et al*., 2008 ; Lamy *et al*., 2009 ; Genitsaris *et al.,* 2015 ; 2016 ; Christaki *et al*., 2017). La structure et la succession saisonnière des communautés microbiennes ont été étudiées à l'aide d'approches par séquençage (par exemple, Christaki *et al*., 2014 ; Genitsaris *et al*., 2015, 2016). Genitsaris *et al*. (2015) ont montré que les interactions biotiques semblaient être le principal facteur gouvernant la structure et la succession temporelle des communautés. Aussi des observations microscopiques sur le phytoplancton à l'aide d'approches basées sur les traits fonctionnels ont montré que le phytoplancton est régulé par la compétition et la défense (Breton *et al*., 2021).

Cependant, nous manquons toujours de connaissances concernant les mécanismes régulant les successions d'autres microbes planctoniques et des efflorescences, à l'exception de *P. globosa*, car les études précédemment mentionnées étaient particulièrement axées sur les efflorescences de *P. globosa.* Dans cette thèse, le terme « blooming taxa » inclut les microorganismes planctoniques qui font des efflorescences ou présentent des augmentations relativement importantes.

Objectif de thèse

L'objectif de cette thèse était d'étudier les mécanismes d'organisation saisonnière des communautés microbiennes et des espèces responsables d'efflorescences issus de différents groupes phylogénétiques dans la Manche orientale. Plus précisément, cette thèse s'est penchée sur : i) les processus écologiques à travers une approche d'écologie des communautés, et ii) les interactions potentielles.

- Le Chapitre 2 vise à étudier les processus écologiques régulant les assemblages de phytoplancton dans les eaux côtières de la Manche Orientale.
- Le Chapitre 3 vise à décrire les dynamiques bactériennes et à identifier les interactions potentielles lors des efflorescences de *P. globosa* et des diatomées.
- Le Chapitre 4 vise à décrypter les dynamiques interannuelles, la diversité et à identifier les hôtes potentiels des Syndiniales Groupe II.

Chapitre 2 : Processus écologiques de phytoplancton en Manche Orientale

Historiquement, les assemblages de phytoplancton ont été étudiés d'une perspective déterministe basée sur leurs traits fonctionnels (par exemple, Tilman *et al*., 1982 ; Violle *et al*., 2007) et leur environnement (Longobardi *et al*., 2022). Néanmoins, les processus déterministes dans la structuration des communautés de phytoplancton (Litchman et Klausmeier, 2008) sont

insuffisants pour expliquer la structure globale de la communauté et les schémas de diversité (Behrenfeld *et al*., 2021). Les études sur le phytoplancton marin se sont partiellement concentrées sur les processus stochastiques (par exemple, Chust *et al*., 2013) ou les processus de dispersion (par exemple, Spatharis *et al*., 2019). Pourtant, il est nécessaire de comprendre comment les processus déterministes et stochastiques changent potentiellement dans un écosystème à différentes échelles de temps (Jia *et al*., 2018 ; Aguilar and Sommaruga, 2020). Deux études existantes sur le phytoplancton ont quantifié la contribution relative des processus déterministes et stochastiques axés sur une grande échelle spatiale (Xu *et al*., 2022) ou de courtes périodes de temps (moins d'un an ; Ramond *et al*., 2021). Cependant, la présente étude est la première à quantifier à la fois les processus d'assemblage déterministes et stochastiques du phytoplancton à une échelle saisonnière sur une période d'échantillonnage pluriannuelle.

Dans ce chapitre, nous avons émis l'hypothèse que les processus écologiques déterministes et stochastiques régulant le phytoplancton présentent des schémas saisonniers et répétitifs. Cette hypothèse a été explorée lors d'une étude de 5 ans (287 échantillons) menée à petite échelle spatiale (~15km). Les données de microscopie, cytométrie et de séquençage (metabarcoding) ont permis une évaluation approfondie de la diversité et l'exploration des processus écologiques régulant le phytoplancton, à l'aide d'une analyse de 'null modelling' (modèle nul). Le renouvellement temporel de la communauté (diversité bêta) a mis en évidence un schéma inter-annuel cohérent qui a déterminé la structure saisonnière du phytoplancton. En hiver et au début du printemps le déterminisme (sélection homogène) était le processus majeur dans l'assemblage de la communauté phytoplanctonique (moyenne global 38 %). Des processus stochastiques (ecological drift, dérive écologique) ont prévalu pendant le reste de l'année (moyenne globale 55 %) avec des valeurs maximales enregistrées à la fin du printemps et en été, qui présentaient souvent des pics phytoplanctoniques monospécifiques transitoires. Nous avons ainsi montré que globalement, la prévalence des processus stochastiques rend *a priori* moins prévisible la dynamique saisonnière des communautés phytoplanctoniques face aux changements environnementaux en cours et futurs.

Chapitre 3 : Dynamique des bactéries hétérotrophes et identification des interactions potentielles lors des efflorescences de *Phaeocystis globosa* récurrent de diatomées transitoires.

L'une des interactions les plus importantes au sein des communautés microbiennes concerne le phytoplancton et les bactéries hétérotrophes, et peut varier de la coopération à la compétition (Seymour *et al*., 2017). Les réponses rapides des bactéries sont directement liées aux

changements dans leur environnement physico-chimique et biologique, même si leur structure communautaire peut être relativement prévisible (par exemple, voir la revue de Fuhrman *et al*., 2015). Ainsi, les bactéries représentent le lien biologique intermédiaire entre les changements physico-chimiques dans l'environnement et les réponses de la communauté phytoplanctonique. Des études menées in situ ont examiné la dynamique des bactéries hétérotrophes et ont observé des schémas saisonniers récurrents et prévisibles aux niveaux taxonomique et fonctionnel, à la fois dans les écosystèmes oligotrophes et eutrophes. Ces schémas ont été influencés par une combinaison de facteurs environnementaux et biologiques, tels que la température, la stratification, la profondeur de la couche de mélange, la disponibilité des nutriments, les vents et particulièrement les efflorescences de phytoplancton (Buchan *et al*., 2014; Teeling *et al*., 2016; Bunse and Pinhassi, 2017). La majorité de nos connaissances concernant l'influence des efflorescences de phytoplancton sur la dynamique des bactéries est liée aux efflorescences dominées par les diatomées (par exemple, Teeling *et al*., 2012, 2016 ; Chafee *et al*., 2018 ; Arandia-Gorostidi *et al*., 2022). Cela est dû à l'importance écologique des diatomées à l'échelle mondiale (par exemple, Tréguer *et al*., 2018). Il reste à déterminer si la dynamique est similaire s'étendent à d'autres types de phytoplancton, en particulier ceux qui pourraient entrer en compétition avec les diatomées. *P. globosa* entre généralement en compétition avec les diatomées et domine souvent les efflorescences printanières dans les eaux côtières. Le deuxième chapitre a visé à contribuer à notre compréhension des interactions complexes entre le phytoplancton et les bactéries dans les écosystèmes côtiers. Pour cela, la dynamique du phytoplancton et des bactéries hétérotrophes en combinant le séquençage 16S rRNA, la microscopie et la cytométrie en flux dans un écosystème côtier mésotrophe sur une période de cinq ans (soit 282 échantillons). Cette étude s'est concentrée sur deux groupes de phytoplancton concurrents et phylogénétiquement éloignés (les Haptophytes, i.e., *P. globosa*, et les Bacillariophyta, i.e., les diatomées). L'analyse eLSA a été utilisée pour construire des réseaux pendant les périodes sans efflorescences et les périodes d'efflorescences. Dans l'ensemble, les résultats de cette étude ont mis en évidence l'importance des interactions saisonnières et spécifiques. L'hiver a était caractérisé par des communautés riches et diversifiées de diatomées, le printemps par des efflorescences de *P. globosa*, tandis que l'été était marqué par de courtes efflorescences monospécifiques de diatomées. L'hiver a montré des communautés bactériennes interconnectées, indiquant une dégradation synergique de divers substrats dérivés du phytoplancton. Au printemps, malgré des variations dans l'intensité des efflorescences de *P. globosa*, la composition des communautés bactériennes est restée constante d'une année sur

l'autre, suggérant l'établissement d'un environnement stable pour les communautés bactériennes pendant ces efflorescences. En été, des associations spécifiques entre les efflorescences transitoires monospécifiques de diatomées et les bactéries hétérotrophes ont été observées.

Chapitre 4 : Dynamique interannuelle, diversité et identification des hôtes potentiels du groupe II des Syndiniales.

Les endosymbiontes dans le milieu marin ont été largement mis en avant par les méthodes des metabarcoding, et récemment en Manche Orientale (Christaki *et al*., 2017). Cependant le metabarcoding ne permet d'avoir qu'une idée de l'abondance relative d'un taxon et non pas de son abondance absolue. Dans le cas des endosymbiotes, le metabarcoding ne permet pas de définir leurs hôtes et donc leur rôle. Pour cela il est important d'avoir des observations directes. Le quatrième chapitre vise à mieux comprendre la dynamique temporelle du groupe II des Syndiniales en combinant le séquençage des amplicons 18S rDNA et le dénombrement direct par microscopie (hybridation in situ en fluorescence - amplification du signal à la tyramide [FISH-TSA]) sur une période de 5 ans. L'étude a été menée dans un écosystème dominé par les diatomées, l'haptophyte *P. globosa* et présentant une abondance relativement faible de dinoflagellés. Une dynamique temporelle cohérente du groupe II des Syndiniales a été observé sur plusieurs années consécutives, mettant en évidence l'existence de populations locales. Selon les données de séquençage, le groupe II des Syndiniales a montré une abondance et une richesse croissantes en été et en automne. Les dinospores dénombrées par microscopie étaient présentes à de faibles abondances et étaient ponctuées par des pics transitoires. En été, l'abondance maximale de dinospores et leur prévalence ont coïncidé avec le pic d'abondance du dinoflagellé *Prorocentrum minimum*, tandis qu'en automne, le groupe II des Syndiniales avait probablement des hôtes plus diversifiés. Bien que plusieurs pics d'abondance de dinospores et de lectures (reads) coïncidassent, aucune relation cohérente n'a pu être mise en évidence entre eux. Les processus d'assemblage écologique à l'échelle saisonnière ont révélé que les processus stochastiques étaient les principaux moteurs (80 %) de l'assemblage de la communauté du groupe II, bien que des processus déterministes soient perceptibles (20 %) en juin et en juillet. Cette dernière observation pourrait refléter les interactions spécifiques entre les Syndiniales et les dinoflagellés en été.

Chapitre 5 : Discussion générale

Cette thèse a mis en évidence qu'appart les efflorescences printanières récurrentes de l'haptophyte *P. globosa*, des efflorescences transitoires des diatomées, de petits dinoflagellés mixotrophes (Chapitre 2) et des bactéries hétérotrophes (Chapitre 3) prédominaient et montraient des pics, en particulier en été. Les pico- et nanophytoplanctons (Chapitre 2) ont présenté des pics en été et en automne. Les Syndiniales du Groupe II (lectures -reads - et spores) ont montré des pics et des infections en été et en automne (Chapitre 4). Les processus écologiques qui façonnent l'organisation saisonnière du phytoplancton et du Groupe II des Syndiniales ont été étudiés. De plus, ce travail s'est concentré sur des relations spécifiques concernant : i) les hôtes potentiels et les parasites par le biais d'observations directes (en utilisant la méthode FISH et microscopie d'épifluorescence), et ii) le phytoplancton (les diatomées et *P. globosa*) et les bactéries hétérotrophes par le biais d'observations indirectes (l'inférence d'associations biologiques à l'aide de l'analyse de réseau). Dans ce chapitre a montré que les processus écologiques stochastiques et déterministes varient entres les saisons, ainsi qu'entre les diffèrent groupes microbiens. Par conséquent, il est raisonnable de s'attendre à ce que ces groupes présentent des réponses distinctes au sein d'un environnement changeant (par exemple, augmentation de la température, eutrophisation). Nous sommes encore loin de répondre à la question de savoir si les processus déterministes ou stochastiques vont dominer et comment les communautés réagiront aux changements locaux et globaux. Il est essentiel que les écologistes et les modélisateurs collaborent davantage pour mieux comprendre ces processus aux niveaux des populations, des communautés et des méta-communautés. Pour ce faire, une méthodologie appropriée devrait être testée, incluant différents groupes planctoniques et à différentes échelles spatio-temporelles (saisonnière, locale, régionale et mondiale). En fin, il a été montré dans la discussion que les reseaux d'observation en France ont besoin d'inclure des méthodes moléculaires comme le metabarcoding et la métagénomique mais il y a besoin de standardisation de ces méthodes afin que le différentes reseaux puissent comparer et combiner leurs résultats. Toutefois il est nécessaire de continuer appliquer des méthodes conventionnelles comme la microscopie et la cytométrie en flux pour compléter le mieux possible la vision du monde microbienne.

En conclusion, cette thèse a comblé une lacune critique de connaissance concernant les mécanismes sous-jacents à la succession saisonnière des communautés microbiennes et des taxons formant des efflorescences dans la Manche Orientale comme modèle d'étude à

appliquer sur d'autres écosystèmes marins côtiers. En appliquant une approche de modèle nul phylogénétique basé sur l'écologie des communautés, cette étude a essayé de décrypter les processus écologiques régissant l'organisation saisonnière, et en utilisant l'analyse de réseau et la méthode FISH, elle a exploré les interactions aboutissant aux conclusions suivantes :

- L'organisation saisonnière du phytoplancton était régulée par des processus déterministes et stochastiques. À l'exception de l'hiver et du début du printemps, les processus stochastiques ont prédominé le reste de l'année. Les communautés estivales caractérisées par des taxons transitoires (diatomées, dinoflagellés mixotrophes) étaient principalement régies par des processus stochastiques. La prévalence des processus stochastiques rend *a priori* les dynamiques saisonnières moins prévisibles.
- Les bactéries hétérotrophes ont montré une dynamique saisonnière, et « épisodique » dus à des efflorescences transitoires des diatomées. Il a été mis en évidence que les efflorescences de diatomées et de *P. globosa* sont associées à des communautés bactériennes distinctes qui étaient saisonnières et/ou liées aux types de substrats.
- Le Groupe II de Syndiniales a été observé pendant plusieurs années consécutives, suggérant l'existence de populations locales, et a présenté des patrons temporels cohérents. Ce Groupe II de Syndiniales a atteint son maximum en été avec le dinoflagellé mixotrophe *Prorocentrum minimum*, et a montré des infections (prévalence de 38,5 %). Les processus écologiques stochastiques ont prévalu dans l'assemblage de la communauté, mais les processus déterministes étaient remarquables en été, suggérant des interactions spécifiques entre les Syndiniales et les dinoflagellés.

Cette thèse souligne la nécessité d'approches complémentaires dans les recherches menées à partir des données d'observatoires, et plaide en faveur de fréquences d'échantillonnage plus élevées pour mieux comprendre les dynamiques complexes régissant les écosystèmes marins côtiers. Enfin, pour comprendre la complexité et les défis auxquels font face les écosystèmes côtiers, nous avons besoin de collaborations entre des chercheurs de divers horizons, de méthodes de surveillance et d'analyse normalisées, ainsi que de données F.A.I.R (Findable, Accessible, Interoperable, Reusable).

Annexes

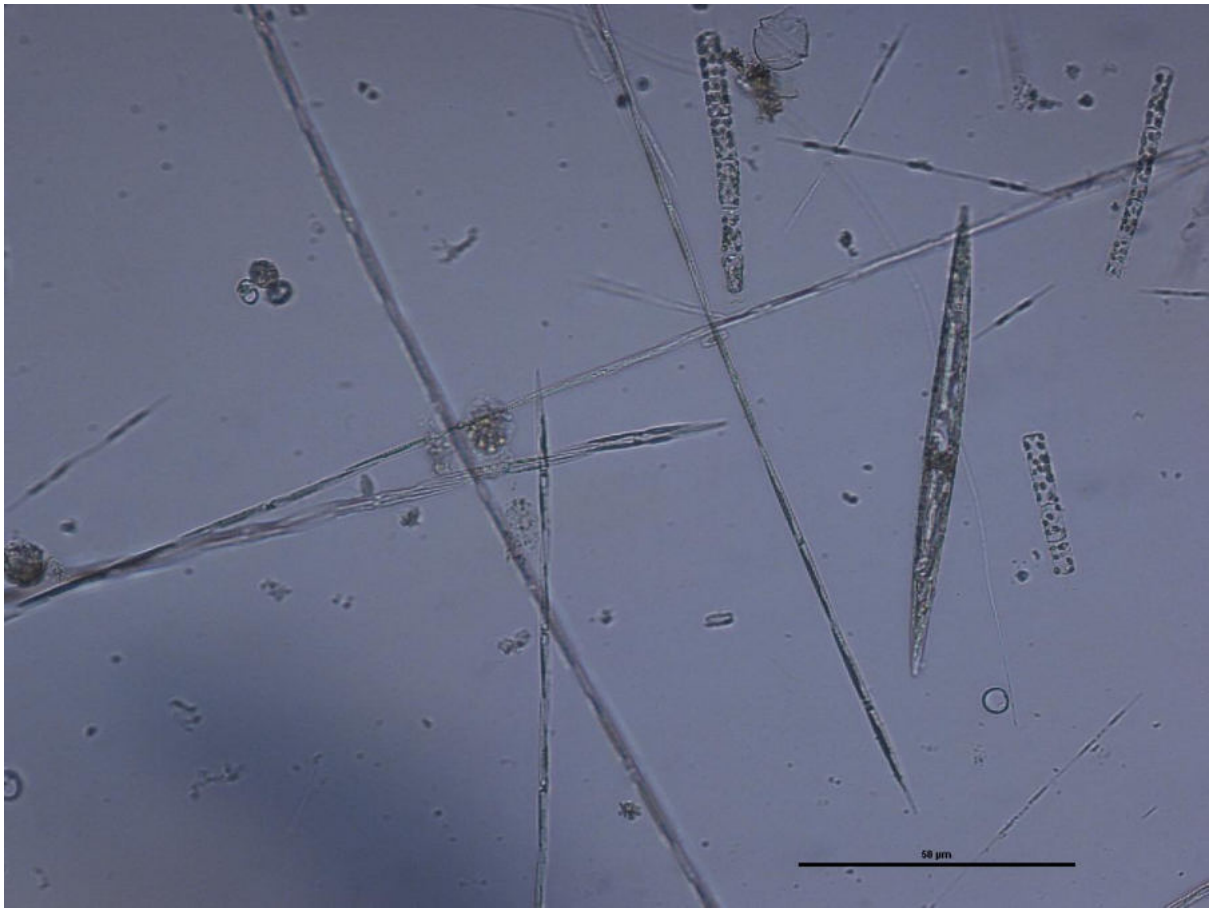

Merge 16S datasets

During this thesis, an attempt was made to integrate 16S data, collected from 2013 to 2015 in the EEC, using the same primers (i.e., 341F, 785R; Klindworth *et al.,* 2013) that amplified the V3-V4 region, and using the same sequencing technology (i.e., Ilumina MiSeq 2x300 bp) with the data presented in this thesis collected in the EEC from 2016 to 2020.

The different datasets derived from the sequencing runs (2013-2015, 2016-2020) were combined as described in the Big Data tutorial of dada2 (https://benjjneb.github.io/dada2/bigdata.html) using the *mergeSequenceTables* command. Chimeras' removal and taxonomy were assigned afterwards using the latest version of the Silva database. Then seasonal patterns of the ten dominant families were visualised. The data from 2013 to 2015 were not integrated as presented spurious patterns (i.e., absence of seasonal patterns, overrepresentation of Rubritaleaceae family contributing 90 % in relative abundance; Fig. A1).

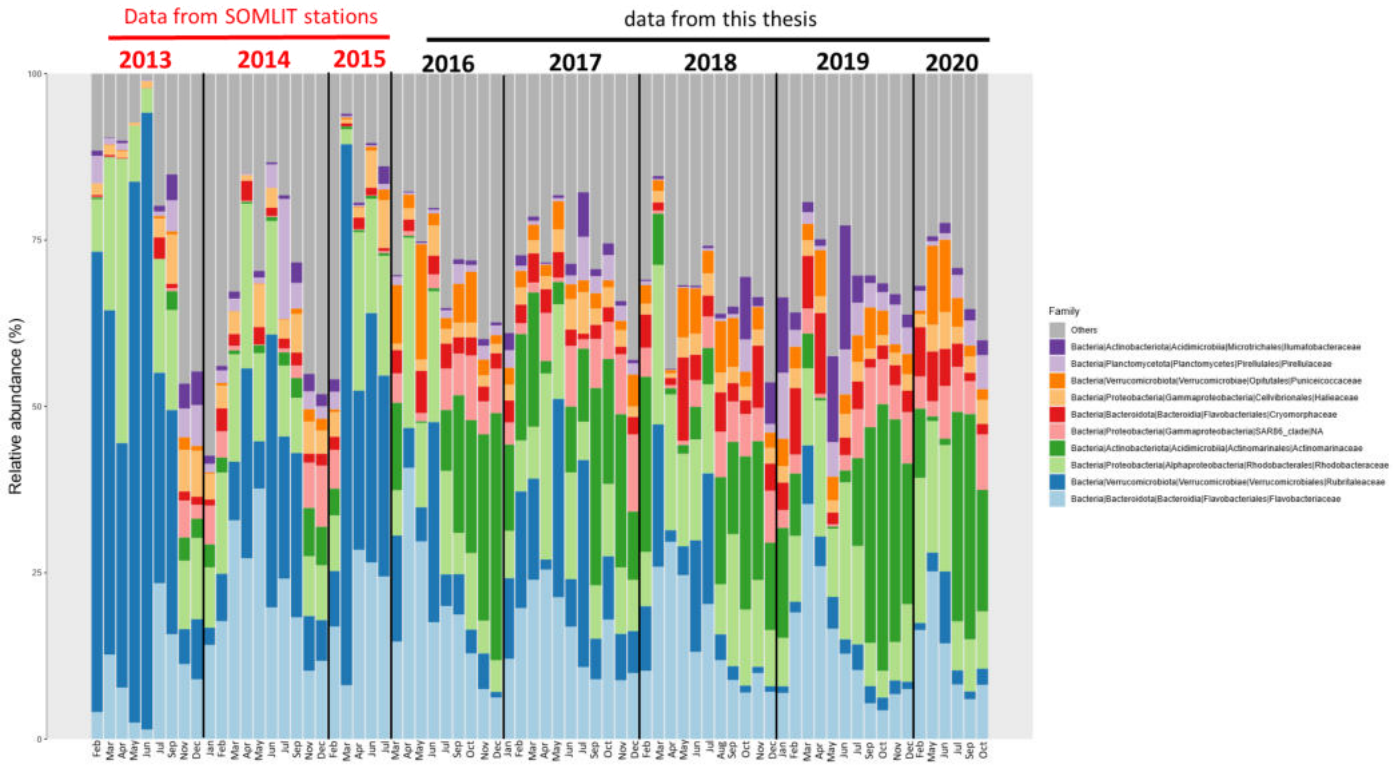

Figure A.1*: Seasonal variation of the ten most abundant families based on rRNA gene metabarcoding data in the EEC at the SOMLIT and DYPHYRAD stations from February 2013 to October 2020.*

The number of samples sequenced differ between the datasets, that may resulted in differences in sequencing depth. Fifty-five samples were sequenced in one lane from 2013 to 2015, while seventy samples sequenced at different sequencing runs from 2016 to 2018. From 2013 to 2015

each sample contained approximately 30,000 reads, before dada2 filtering, while from 2016 to 2020 each sample contained 80,000 before filtering in dada2. Furthermore, different extraction kits and sequencing companies were used.

Related papers, and book chapter as co-author

I was co-author on three papers, and three book chapters (CPER MARCO project 2015 -2021), presented in this section. All these studies used microscopy data to count plankton from the SNO-SOMLIT and/or REPHY/SRN, and applied niched-based analyses. I contributed by providing microscopy data for phytoplankton (i.e., diatoms and *Phaeocystis*), and/or microzooplankton data (i.e., dinoflagellates and ciliates).

The first paper by Breton et al., (2021) aimed to better understand the underline mechanisms of the seasonal species succession of diatoms and zooplankton communities from 2007 to 2013[1], in the coastal waters of the Eastern English Channel, by using a trait-based analysis. This study evidenced that the seasonal succession of diatoms and copepods is the result of several trade-offs among functional traits that are controlled by the seasonal abiotic and biotic pressure encountered by the plankton communities, and confirmed the key role of competition and predation in controlling annual plankton succession.

The second study by Breton et al., (2022) studied the effect of environmental change in phytoplankton communities by applying trait-based approach in the EEC from 1996 to 2019. This study showed that diatoms and *Phaeocystis* responded differently in anthropogenic pressure. The unbalanced nutrient reduction facilitated *Phaeocystis* blooms and may threaten diatom communities in the near future.

The third study by Houliez et al., (2023) investigated the drivers of the blooms of *Pseudo-nitzschia seriata* and *Pseudo-nitzschia delicatissima* complexes from 1992 to 2020, in the Eastern English Channel and Southern North Sea from. Phytoplankton data were analysed with a multivariate statistical approach based on the Hutchinson's niche concept (i.e., Outlying Mean Index to characterise realized ecological niche, and Within Outlying Mean Index to characterise the realized ecological sub-niches). This study showed that the complexes *P. delicatissima* and *P. seriata* were present year-round, but their bloom periods were different. This was attributed to the fact that the two complexes occupied different realized ecological niches, and to biotic interactions with other diatoms.

[1] *While the study investigated communities from 2007 to 2013, data from 1996 to 2019 (including the data in this thesis) were also included to calculate timing of bloom association.*

The book chapters concerned the CPER MARCO project (PI: François Schmitt), which will be published by 'Presses Universitaires du Septentrion'. Breton *et al*., have synthesized their results from the papers referred above (Breton et al., 2021 and 2022).

frontiers in Marine Science

ORIGINAL RESEARCH
published: 06 September 2021
doi: 10.3389/fmars.2021.656300

Seasonal Variations in the Biodiversity, Ecological Strategy, and Specialization of Diatoms and Copepods in a Coastal System With *Phaeocystis* Blooms: The Key Role of Trait Trade-Offs

Elsa Breton[1], Urania Christaki[1], Benoit Sautour[2], Oscar Demonio[3], Dimitra-Ioli Skouroliakou[1], Gregory Beaugrand[1], Laurent Seuront[1,4,5], Loïck Kléparski[1,6], Adrien Poquet[1,7], Antoine Nowaczyk[8], Muriel Crouvoisier[1], Sophie Ferreira[9], David Pecqueur[10], Christophe Salmeron[10], Jean-Michel Brylinski[1], Arnaud Lheureux[8] and Eric Goberville[3]*

[1] Univ. Littoral Côte d'Opale, CNRS, Univ. Lille, UMR 8187 LOG, Wimereux, France, [2] Univ. Bordeaux, CNRS, UMR 5805 EPOC, Rue Geoffroy Saint Hilaire – Bâtiment, Pessac, France, [3] Unité Biologie des Organismes et Ecosystémes Aquatiques (BOREA), Muséum National d'Histoire Naturelle, CNRS, IRD, Sorbonne Université, Université de Caen Normandie, Université des Antilles, Paris, France, [4] Department of Marine Resources and Energy, Tokyo University of Marine Science and Technology, Tokyo, Japan, [5] Department of Zoology and Entomology, Rhodes University, Grahamstown, South Africa, [6] Marine Biological Association, Citadel Hill, Plymouth, United Kingdom, [7] Univ. Côte d'Azur, CNRS, INSERM, IRCAN, Medical School of Nice, Nice, France, [8] Univ. Bordeaux, CNRS, UMR 5805 EPOC, Station Marine d'Arcachon, Arcachon, France, [9] Observatoire Océanologique de Banyuls s/mer, FR 3724 – Laboratoire Arago – SU/CNRS, Banyuls-sur-Mer, France, [10] Univ. Bordeaux, CNRS, OASU, UMS 2567 POREA, Allée Geoffroy Saint-Hilaire, Pessac, France

Although eutrophication induced by anthropogenic nutrient enrichment is a driver of shifts in community composition and eventually a threat to marine biodiversity, the causes and consequences on ecosystem functioning remain greatly unknown. In this study, by applying a trait-based approach and measuring niche breadth of diatoms and copepods, the drivers and underlying mechanisms of the seasonal species succession of these ecological communities in a coastal system dominated in spring by *Phaeocystis* blooms were explored. It is suggested that the seasonal succession of diatoms and copepods is the result of several trade-offs among functional traits that are controlled by the seasonal abiotic and biotic pressure encountered by the plankton communities. The results of this study highlight that a trade-off between competition and predator, i.e., weak competitors are better protected against predation, plays an important role in promoting plankton species richness and triggers the *Phaeocystis* bloom. As often observed in eutrophicated ecosystems, only the biotic homogenization of the copepod community and the shift in the diet of copepods toward *Phaeocystis* detrital materials have been detected during the *Phaeocystis* bloom. The diatom and copepod communities respond synchronously to fluctuating resources and biotic conditions by successively selecting species with specific traits. This study confirms the key role of competition and predation in controlling annual plankton succession.

Keywords: diatoms, copepods, *Phaeocystis*, biodiversity, functional traits, seasonality, trade-off

OPEN ACCESS

Edited by:
Maria Moustaka-Gouni, Aristotle University of Thessaloniki, Greece

Reviewed by:
Jun Sun, China University of Geosciences, China
Fabio Benedetti, ETH Zürich, Switzerland
Benjamin Alric, Centre National de la Recherche Scientifique (CNRS), France

****Correspondence:***
Elsa Breton
elsa.breton@univ-littoral.fr

Specialty section:
This article was submitted to Aquatic Microbiology, a section of the journal Frontiers in Marine Science

Received: *20 January 2021*
Accepted: *30 July 2021*
Published: *06 September 2021*

Citation:
Breton E, Christaki U, Sautour B, Demonio O, Skouroliakou D-I, Beaugrand G, Seuront L, Kléparski L, Poquet A, Nowaczyk A, Crouvoisier M, Ferreira S, Pecqueur D, Salmeron C, Brylinski J-M, Lheureux A and Goberville E (2021) Seasonal Variations in the Biodiversity, Ecological Strategy, and Specialization of Diatoms and Copepods in a Coastal System With Phaeocystis Blooms: The Key Role of Trait Trade-Offs. Front. Mar. Sci. 8:656300. doi: 10.3389/fmars.2021.656300

INTRODUCTION

Coastal eutrophication induced by anthropogenic nutrient enrichment is one of the major threats to biodiversity (Vitousek et al., 1997; Halpern et al., 2008; Howarth, 2008). However, assessing the impact of eutrophication on biodiversity is a difficult task, because the multiple drivers shaping biodiversity interact and operate at different interconnected temporal and spatial scales (e.g., White et al., 2010; Dray et al., 2012; Hill et al., 2016). Eutrophication may not only cause excessive blooms of opportunistic species, species loss (Smith and Schindler, 2009) but also, subtle changes in functional trait composition; and may even lead to a loss of functional diversity (FD) caused by a biotic homogenization by favoring generalist (species with broad environmental tolerances) over specialist (species well adapted to particular habitats) species: the latter showed narrower niche breadth and a lower tolerance to high nutrient levels (e.g., Clavel et al., 2011; Nelson et al., 2013; Villéger et al., 2014; Wengrat et al., 2018; Chihoub et al., 2020). Functional traits are biological characteristics that influence the performance and survival of organisms (Violle et al., 2007). Biotic changes may alter biodiversity by selecting species that possess functional traits that confer to them a selecting advantage. For instance, light limitation, which typically occurs under high primary production events, may select species with morphological features that allow them to enhance their buoyancy (Naselli-Flores et al., 2021 and references therein). Communities mainly composed of functionally redundant species may improve ecosystem resilience and stability (e.g., Biggs et al., 2020), but the loss of FD and/or specialist species may deteriorate ecosystem functioning (Olden et al., 2004; Pan et al., 2016; Alexander et al., 2017). Understanding how functional traits relate to associated ecological strategies (i.e., a combination of functional attributes reflecting how species cope with their environment) and ecological specialization across productivity gradients, which defines the degree of tolerance to changing environmental conditions, is, therefore, important to better measure ecosystem functioning and health.

Over the last decade, trait-based approaches have been increasingly used in plankton ecology to understand the drivers of biodiversity changes along environmental gradients and to propose ecological generalities and predictions across ecosystems. Because functional traits mediate the responses of the species to their abiotic and biotic environment (Violle et al., 2007), they help to: (i) better understand how organisms interact with their surrounding environment; and (ii) identify key processes that influence biodiversity such as trait trade-offs (e.g., Kneitel and Chase, 2004; Litchman et al., 2007). While functional identity informs on competitiveness and ecological strategies (e.g., predation avoidance, Shipley, 2010; Muscarella and Uriarte, 2016), FD, in combination with null modeling, informs on the degree of functional convergence of a community and detects mechanisms of community assembly (e.g., abiotic filtering and competitive interactions, Mason et al., 2013). As it may influence conclusions, trait choice is a critical issue (Zhu et al., 2017) when: studying resource traits (e.g., nutrient uptake and light absorption); under-dispersion of traits reflects environmental filtering and/or hierarchical competition (Mayfield and Levine, 2010); and over-dispersion of traits is related to a competition governed by niche differences (Macarthur and Levins, 1967; Cornwell and Ackerly, 2009). When focusing on defense traits against predation (e.g., setae and toxin production), under-dispersion is related to a high predation pressure by generalists, and over-dispersion to a high predation pressure by specialists (Cavender-Bares et al., 2009).

The Eastern English Channel (EEC) is a well-mixed meso-eutrophic sea undergoing multiple environmental disturbances such as temperature rise (McLean et al., 2019) and nutrient enrichment, mainly from the Seine and Somme rivers (Thieu et al., 2009) as a result of anthropogenic activities in the watersheds, especially intensive agriculture practices (e.g., Garnier et al., 2019). This nutrient enrichment is known to trigger the recurrent spring *Phaeocystis* blooms of EEC (Lancelot et al., 1987; Lancelot, 1995; Breton et al., 2000, Breton et al., 2017; Grattepanche et al., 2011a,b; Bonato et al., 2016; Ménesguen et al., 2018). By affecting the diatom and copepod communities, two interacting key compartments of the ecosystem trophodynamics (Smetacek, 1999; Tréguer and Pondaven, 2000; Beaugrand et al., 2003; Kiørboe, 2011; Mitra et al., 2014; Steinberg and Landry, 2017), this prymnesiophyte can disrupt the structure of the food web (Schoemann et al., 2005; Nejstgaard et al., 2007), especially during the late winter/spring and summer/autumn periods (Gasparini et al., 2000; Antajan, 2004).

By applying a functional trait-based approach to diatom and copepod communities collected over the period 2007–2013, and by measuring niche breadth of resources used and environmental conditions tolerated both at the species- and community level, the aims were to: (i) understand how diatoms and copepods in coastal waters of the EEC respond to seasonally changing environmental conditions; (ii) determine what drives plankton species richness and ecological specialization; and (iii) test whether taxonomic (species richness) and FD [functional richness (FRic), functional evenness (FEve), and functional divergence (Rao Quadratic entropy, RaoQ)] of plankton communities were affected by *Phaeocystis* blooms. Protozooplankton biomass (i.e., the sum of heterotrophic dinoflagellate, ciliate, and tintinnid biomass) and co-occurring phytoplankton groups were also considered in this study because of: (i) the diverse trophic regimes and feeding strategies of copepods depend on their food environment (Kleppel, 1993); (ii) diatoms may also be the prey of other predators other than copepods (e.g., Grattepanche et al., 2011b); and (iii) knowledge of the whole community composition may help to better depict trade-offs.

MATERIALS AND METHODS

Datasets

Hydrological and phytoplankton samples were collected at high tide at coastal station "C" (50°40′75 N; 1°31′17 E, 20–25 m maximum depth), which belongs to the French monitoring network SOMLIT[1]. Sampling was carried out on an average of every 3 weeks from February 2007 to December 2013. Subsurface (2 m depth) temperature (SST, °C) and salinity (S) were

[1] www.somlit.fr

measured with a conductivity temperature depth (CTD) Seabird profiler equipped with photosynthetically active radiation (PAR, E m^{-2} d^{-1}) sensor (QSP 2300; Biospherical Instruments Inc.). Dissolved inorganic phosphorous (DIP, μM), inorganic silica (DSi, μM), and inorganic nitrogen [the sum of nitrates, nitrites, and ammonium; (DIN, μM)], total suspended matter (TSM, mg L^{-1}), chlorophyll *a* (Chla, μg L^{-1}), particulate organic carbon (POC, μgC L^{-1}), phytoplankton, and protozooplankton were measured by means of a Niskin Water Sampler (8 L). Nutrient concentrations were quantified according to Aminot and Kérouel (2004) using autoanalyzer systems (Technicon, Alliance, and Seal Instruments), except for ammonium concentrations (NH4), which were assessed by fluorimetry according to Holmes et al. (1999) and Taylor et al. (2007). TSM was determined by filtrating a known volume of seawater through 47 mm precombusted and preweighed glass fiber filters (Whatman, GF/F, 47 mm), and drying it at 50°C for 24 h. POC was determined using a NA2100 Frisons CHN analyzer after filtration of 100–500 ml subsamples through precombusted glass fiber filters (Whatman, GF/F, 25 mm), then dried for at least 48 h at 50°C and exposed to HCl 1 N vapors for 5 h. Chla was estimated by fluorometry (Lorenzen, 1967) from subsample (100–250 ml) of seawater filtrated through glass fiber filters (Whatman, GF/F, 25 mm) and free of pigment (extraction in acetone 90% in the dark at 4°C for 12 h). The minimal volume values corresponded to the *Phaeocystis* bloom period that leads quickly to filter clogging. The maximal volume value corresponds to the maximal value fixed by the SOMLIT network. The average daily PAR experienced by phytoplankton in the water column, for 6 days before sampling, was obtained from a diffuse fraction (kd, m^{-1}) and global solar radiation (GSR, Wh m^{-2}) from the Copernicus Atmosphere Monitoring Service (CAMS) radiation service[2] using the formula of Riley (1957). GSR was converted into PAR by assuming PAR to be 50% of GSR and by considering 1 W m^{-2} = 0.36 E m^{-2} d^{-1} (Morel and Smith, 1974). Wind stress (Pa) and direction (i.e., eastward and northward components of horizontal winds), as proxies of regional turbulence (e.g., MacKenzie and Leggett, 1991), were obtained from the National Center for Atmospheric Research (NCAR, United States)[3] and the National Centers for Environmental Prediction (NCEP, United States). Subsurface and near-bottom environmental values were averaged for niche analysis (refer below "Ecological specialization").

Copepods were collected on 96 separate occasions (sampling frequency of 4 weeks) with vertical hauls from the bottom (ca. ∼ 20–25 m depth) to the surface using a 200-μm mesh size working party (WP) 2 plankton net. The volume filtered was measured with a Tsurumi – Seiki (TSK) *flowmeter* (Tokyo Seimitsu Co. Ltd) and mounted on the mouth of the net (0.25 m^2 mouth area). The volume of filtered seawater varied between 1 and 11 m^3, the lowest values being recorded during the *Phaeocystis* bloom (from mid-April to mid-May) as a result of rapid net clogging. All copepod samples were preserved with 4% formaldehyde buffered with borax. The composition and abundance of copepods were determined under stereomicroscopy (Nikon SMZ1500) with 10–100x magnification in Dollfus chambers according to the determination key provided by Rose (1933). Copepod carbon biomass was calculated from (i) the median of the minimum and maximum weights for the CV and CVI copepodite stages; and (ii) the regression equations relating wet weight and dry weight (mg) to carbon (mg C, Wiebe, 1988). The minimum and maximum weights were estimated from the range values of copepodite length reviewed by Conway (2006) for the North Atlantic sector and species-specific length-weight relationships (Durbin and Durbin, 1978; Cohen and Lough, 1981; Williams and Robins, 1982; Dam and Peterson, 1991; Zakaria et al., 2018). The list of the copepod species identified in this study, the final carbon conversion factor values and their corresponding frequencies (%) and average biomasses (μgC L^{-1}), are shown in **Supplementary Table 1**. Diatom, *Phaeocystis*, and dinoflagellate samples were fixed with Lugol-glutaraldehyde solution (1% v/v, a fixative that does not disrupt *Phaeocystis* colonies; Breton et al., 2006) and were kept at 4°C in the dark until microscopy analysis. Other protozooplankton samples, i.e., ciliates and tintinnids, were fixed with formaldehyde (Grattepanche et al., 2011a). Samples were examined using an inverted microscope (Nikon Eclipse TE2000-S) with 100–400x magnification after sedimentation in 5–25 ml and 25–100 ml Hydrobios chambers for phytoplankton and protozooplankton, respectively. Identifications were identified at the species level when possible, according to taxonomic literature (Halse and Syvertsen, 1996; Hoppenrath et al., 2009, for phytoplankton; Schiller, 1931–1937; Maar et al., 2002; Gómez and Souissi, 2007, for heterotrophic dinoflagellates; Kofoid and Campbell, 1929; Plankton Ciliate Project, 2002, for ciliates). For *Synechococcus* spp., picoeukaryotes, and cryptophytes, 5 ml samples were fixed with glutaraldehyde (1.33% v/v) and kept at −80°C until flow cytometry analysis (FACScan, BD Biosciences, Marie et al., 1999). Biovolumes were estimated using standard geometric forms according to Hillebrand et al. (1999). The number of *Phaeocystis* cells in the colonial stage of life was counted according to biovolume measurements of the colonies (Rousseau et al., 1990). Carbon biomass (μgC l^{-1}) of phytoplankton and heterotrophic dinoflagellates was calculated using the carbon conversion factors of Menden-Deuer and Lessard (2000). For *Phaeocystis* solitary cells, *Synechococcus* spp., and picoeukaryotes, the values of 89.5 pg C $cell^{-1}$ (van Rijssel et al., 1997), 154 fg $cell^{-1}$, and 1319 fg $cell^{-1}$ (Buitenhuis et al., 2012) were used, respectively. For flagellated and solitary colonial cells, only discriminated since 2007, the carbon conversion factors of 10.8 and 14.15 pg C/cell were applied, respectively (refer **Table 1** in Schoemann et al., 2005). The biomass of ciliates and tintinnids was calculated using a conversion factor of 0.19 pg μm^{-3} (Putt and Stoecker, 1989; refer **Supplementary Tables 1–4** and **Supplementary Data** for species list and biomass estimates).

Phytoplankton and Copepod Species Traits

Information on resource traits is scarce in the literature for most phytoplankton species (Litchman and Klausmeier, 2008; Breton et al., 2017). Consequently, an *a posteriori* approach

[2]http://www.soda-pro.com/web-services/radiation/cams-radiation-service

[3]https://psl.noaa.gov/data/gridded/data.ncep.html

TABLE 1 | List of the diatom and copepod traits used in this study and their functional meaning.

Traits	Type[a]	Range/Category	Ecological process/Functional meaning	References
Phytoplankton/diatoms				
Biovolume	Numerical (R and D)		The "master trait" for resource acquisition, reproduction, and predator avoidance	Litchman and Klausmeier, 2008
S/V cell ratio	Numerical (*R*)	0.02–4.62μm^{-1}	Competitive ability under nutrient limitation, silica requirement	Grover, 1989; Karp-Boss et al., 1996; Leynaert et al., 2004; Takabayashi et al., 2006; Musielak et al., 2009; Lovecchio et al., 2019
Coloniality	Ordinal (R and D)	0: No, 1: <5 cells, 2:[5–20], 3:[20, 100], 4:>100	Competitive ability under nutrient limitation	Grover, 1989; Karp-Boss et al., 1996; Takabayashi et al., 2006; Musielak et al., 2009; Bjærke et al., 2015; Lovecchio et al., 2019
		0: <500; 1:>501μm	vulnerability to predation	Djeghri et al., 2019
Apparent degree of signification	Ordinal (R and D)	1: Slightly, 2: Medium, 3: Heavily	Silica requirement, vulnerability to predation	Martin-Jézéquel et al., 2000; Martin-Jézéquel and Lopez, 2003; Pančić et al., 2019
Tychopelagic/Benthic occurrence	Binary	0: Pelagic; 1: Tychopelagic/Benthic	Use of resources and habitat	
Maximum Linear Dimension (MLD)	Numerical (R and D)	3–447 μm	Cell buoyancy, vulnerability to photo-inhibition	Grover, 1989; Key et al., 2010; Schwaderer et al., 2011; Naselli-Flores et al., 2021
			Capacity at capturing the fluctuating light and persisting in subsurface waters	Naselli-Flores et al., 2021
Defense	Ordinal (D)	0–4 (0: No defence, 4 many defence traits)[b]	Predator avoidance	Pančić and Kiørboe, 2018
Copepods				
Maximum size	Numerical (R and D)	1: ≤1 mm, 2: [1; 2], and 3: >2 mm	Feeding, growth, reproduction, survival	Litchman et al., 2013
Trophic regime	Fuzzy coded (R)	Carnivory, Herbivory, Detritivory, Omnivory[c]	Feeding, growth, reproduction, survival	Litchman et al., 2013
Feeding mode	Ordinal (R and D)	0: Passive, 0.5: Mixed, 1: Active	Feeding, survival	Kiørboe, 2011; Litchman et al., 2013

[a] *R and D: Resource and Defense trait, respectively.*
[b] *See **Supplementary Table 3** and **Supplementary Data**.*
[c] *See Chihoub et al. (2020) for more details.*

to defining resource use and requirement traits was used. For each species, biovolume (V, μm^3), maximum linear dimension (MLD, μm), and the surface to biovolume cell ratio (S/V ratio) were calculated from the median values of a series of microscopic measures over the entire 1996–2019 diatom datasets acquired at Station "C" (Breton unpublished data). The apparent degree of silicification (1: slight; 2: medium; 3: heavy) and Tychopelagic/benthic habit (0: pelagic; 1: tychopelagic/benthic) was based on information from phytoplankton taxonomic literature (e.g., Halse and Syvertsen, 1996; Hoppenrath et al., 2009). The potential degree of coloniality (0: None; 1: <5 cells; 2: 5–20 cells; 3: >20 cells) was assessed through the cultivation of each diatom species under F/20 medium and with a light: dark cycle of 12:12 h at an irradiance of 400 μmol photons m^{-2} s^{-1} (Daylight HQIT-WD 250 W F, OSRAM GmbH, Munich, Germany).

Biovolume is a key trait because it relates to the various ecophysiological attributes for resource acquisition, reproduction, and predator avoidance (Litchman and Klausmeier, 2008; **Table 1**). Species with high S/V cell ratio and long cellular chain length that favor cell suspension in the water column and increase nutrient flux have a great competitive ability under nutrient limitation (Grover, 1989; Karp-Boss et al., 1996; Takabayashi et al., 2006; Musielak et al., 2009; Lovecchio et al., 2019). Higher S/V cell ratio and weaker silicified species have also been related to lower silica requirement under laboratory conditions [(Leynaert et al., 2004) and to DSi limitation (Martin-Jézéquel et al., 2000; Martin-Jézéquel and Lopez, 2003)]. Cell elongation enhances both cell buoyancy (Grover, 1989; Naselli-Flores et al., 2021) and protection against photoinhibition, especially for larger cells (Key et al., 2010; Schwaderer et al., 2011). The binary trait "Tychopelagic/benthic habit" may be informative of resource use and requirement, as benthic diatoms are often highly photosynthetic efficient species and potentially facultative heterotrophs (Cahoon, 1999). This trait may be also an indicator of ecosystem health, as demonstrated by the positive relationship between the FD of benthic diatoms and the productivity of coastal waters in the Baltic Sea (Virta et al., 2019). Besides reflecting resource use and/or requirement, prey biovolume (Litchman and Klausmeier, 2008), the degree of coloniality (Bjærke et al., 2015), and the apparent degree of silicification (Pančić et al., 2019) mirror ecological processes/functions linked to predation. By including: (i) the capacity to produce mucous or toxins; (ii) the presence of

176

setae and/or spicules (that also favor buoyancy; Van den Hoek et al., 1995); (iii) the degree of silicification; and (iv) coloniality, the composite of defense traits reflect alteration of copepod grazing (Pančić and Kiørboe, 2018). The composite trait was obtained by summing the scores of each of these traits (refer **Supplementary Table 5** and **Supplementary Data**).

The carbon-to-chlorophyll ratio for phytoplankton (C/Chl*a* ratio, in μgC μgChla^{-1}) and timing of bloom initiation of diatoms (in months) were then calculated. Although not being traits *per se* (Litchman and Klausmeier, 2008), they are the outcome of processes linking the actual traits of species and the alleviation, or accentuation, of external limiting factors, such as grazing pressure or nutrients/light availability (Thackeray et al., 2008; Jakobsen and Markager, 2016). The C/Chl*a* ratio was calculated using microscopic counts and the cell carbon was computed from the equations of Menden-Deuer and Lessard (2000). Timing of bloom initiation of diatoms at Station "C" (refer **Supplementary Data**) was based on the cumulative biomass-based threshold method (Brody et al., 2013), using mean monthly diatom abundances over the period 1996–2019 and a limit value of 20%.

For copepods: (i) maximum size (mm); (ii) trophic preference (herbivory, carnivory, detritivory, and omnivory); and (iii) feeding mode (0: passive, 1: active, and 0.5: mixed feeding) were selected, as they directly/indirectly influence species fitness through growth, reproduction, and/or survival (Litchman et al., 2013; Kiørboe and Hirst, 2014). Most of them are responsive to changes in environmental conditions (McGinty et al., 2018). Data were obtained from the copepod trait database constructed by Benedetti et al. (2016) and completed by Brun et al. (2017), and references therein. For each copepod species, all available information on species size was compiled, and the maximum size value as representative of adult species was kept, note that sexual dimorphism was not considered. The degree of herbivory (carnivory, detritivory, or omnivory) was coded following Mondy and Usseglio-Polatera (2014). In this study, a coefficient of (i) 1/3 for omnivore; (ii) 2/3 for omnivore-herbivory (dominance of herbivory in copepod diet) or 2/3 for omnivore-carnivory (dominance of carnivory in copepod diet), with 1/4 for the two other diet categories; and (iii) 1 for species with carnivore/herbivore/detritivore diets, and 0 for the two other diet categories (refer Chihoub et al., 2020 for more details) was applied.

FD Metrics

In this study, four metrics (Step 1, refer **Supplementary Figure 1** for a description of the five main steps of the statistical method) to characterize the functional structure and diversity of diatom and copepod communities were used as follows: (i) community-weighted mean (CWM); (ii) FRic, (iii) FEve; and (iv) Rao Quadratic entropy (RaoQ) as a proxy of functional divergence. CWM, the mean trait value among each community weighted by the relative biomass of each species (Garnier et al., 2004), is a proxy of functional identity. FRic corresponds to the volume of functional niche space filled by a species within a community (Villéger et al., 2008). FEve corresponds to the regularity with which species biomass in a community is distributed along the minimum spanning tree that links all species in the multidimensional trait space (Mason et al., 2005). RaoQ is the sum of pairwise distances between species, weighted by the relative biomass within the multidimensional trait space. This index was selected over the functional divergence metric for its stronger ability to detect assembly rules (Botta-Dukát, 2005; Botta-Dukát and Czúcz, 2016). The FD indices of the diatom community were calculated from the biovolume, the apparent degree of silicification, coloniality, the S/V cell ratio, MLD, and defense traits (as shown in **Supplementary Table 5**). For each observation (i.e., sampling unit), functional metrics were computed on log-transformed species biomass, to reduce a potential influence of outliers, using the R package (R version 3.5.3, 2019) "FD" (Laliberté and Legendre, 2010). A preliminary principal coordinate analysis (PCoA; "vegan" package; and Oksanen et al., 2011) was performed to calculate the multidimensional trait space for each sampling day and FD was calculated from a dissimilarity matrix calculated using both the PCoA axis, as new functional traits, and the Gower distance (Gower, 1971). The Gower distance allows us to combine traits of different types, including ordinal (Podani, 1999; **Table 1**). A square root transformation ("sqrt"), or a Lingoes correction for negative values (Lingoes, 1971), was applied when the distance matrix "species × species" was not Euclidean. The quality of the functional space (i.e., the similarity between the functional space and initial functional trait values) based on the corrected distance matrix varied from 0.64 to 0.94. The inference of environmental filtering and biotic interactions (Step 2, **Supplementary Figure 1**) was estimated from the deviation [standardized effect size (SES); Gotelli and McCabe, 2002] between functional metrics calculated on a given (i.e., observed) diatom community and functional values obtained from a random community: for each sampling date, trait data were randomized 999 times ("permatfull" in the "vegan" package), while maintaining species richness and abundance constant. SES was calculated as follows:

$$SES = \frac{x_{obs} - \bar{x}_{ran}}{\sigma_{ran}} \quad (1)$$

where x_{obs} is the observed values of the functional metric at a given date; $\bar{x}_{ran}$ is the mean, and σ_{ran} is the SD of the FD of randomly assembled communities. Assuming a normal distribution of the random communities, the traits derived from the sampling dates falling into the 95th (or higher) percentile of the random distribution were considered "over-dispersed" (i.e., niche differentiation being the major process driving community assembly) and trait falling into the 5th (or lower) percentile were considered "under-dispersed" (i.e., environmental filtering as the major process).

Ecological Specialization

Ecological specialization (Step 3, **Supplementary Figure 1**) was estimated by means of the multidimensional outlying mean index (OMI, hereafter called "environmental tolerance," Dolédec et al., 2000) and unidimensional niche breadth analysis using the "ade4" (Chessel et al., 2004; Dray et al., 2007) and "hypervolume" packages (Blonder et al., 2014). The OMI was selected because it does not rely on any expected species response curves to environmental gradients and outperforms classical

177

methods such as canonical correspondence or redundancy analysis (Dolédec et al., 2000). The OMI analysis seeks combinations of environmental variables that maximize average species marginality, i.e., the squared Euclidean distance between the mean environmental conditions used by a species and the mean environmental conditions available to this species. Hypervolume estimates the niche breadth of one or several dimensions from the calculation of uni or multivariate kernel density. This method captures irregular shapes and does not require a specific density function, unlike OMI analysis that requires normal distribution: estimation of the hypervolume is, therefore, more accurate when high-dimensional or holey datasets are considered. An accurate estimate of kernel density requires high amounts of trait/environmental data, which rises as dimensionality increases, however (e.g., about >67 and >770 for three and five dimensions, respectively, Silverman, 1986). For a comprehensive assessment of environmental gradients, the calculation was, therefore, based on the ecological specialization of long-term diatom and copepods datasets, collected between 1996 and 2019 at the station "C," and from 2001 to 2017, respectively, in the downstream part of the Gironde estuary (Breton et al., 2000; Schapira et al., 2008; Breton et al., 2017; Richirt et al., 2019).

Environmental tolerance was based on species biomass, considering: (i) SST, S, Pa, nutrients, and PAR for diatoms; and (ii) SST, S, Pa, TSM, and POC for copepods. Unidimensional niche breadth related to resources (DIN, DIP, DSi, and light for diatoms; TSM and POC for copepods) was determined from kernel density using the environmental conditions encountered by species when present with a Silverman bandwidth estimator and a 0% quantile threshold (Blonder et al., 2014). An increase in these two indices of ecological specialization mirrors an decrease in the degree of specialization of the diatom or copepod community. Trophic homogenization within the copepod community was assessed from trophic preferences and feeding mode, as recommended by Mondy and Usseglio-Polatera (2014). For each copepod species and trophic trait, we first calculated the taxon specialization index (TSI) using the Gini-Simpson index (Gini, 1912; Simpson, 1949). Each TSI, where the trophic preference (the feeding mode) describes the degree of omnivory (the capacity to alternate between passive and active feeding), was then scaled by its respective minimum and maximum values to account for the different number of categories among traits (Mondy and Usseglio-Polatera, 2014). The community specialization index (CSI) was finally computed as the CWMs of each TSI: a value of 0 (1) corresponds to truly generalists (truly specialists).

All analyses were performed with R (R Development Core Team), version 3.5.3.

Exploratory Analyses

First, box plots (Step 4, **Supplementary Figure 1**) were computed combined with a locally weighted scatterplot smoothing (LOESS; Jacoby, 2000) curve in association with a 95% confidence interval (function "geom_smooth," package "ggplot2," Wickham, 2016) to depict the seasonal variations. Monthly differences were assessed by a Kruskal–Wallis test, followed by a *post hoc* Nemenyi test (Legendre and Legendre, 1998; package "PMCMRplus," Pohlert, 2014). To explore and summarize seasonal changes in the abiotic environment, a principal component analysis (PCA) was performed with the "ade4" package. To explore seasonal variations in both the mean values of key biological traits and in the degree of ecological specialization of the diatom and copepod communities, a PCoA (Step 4, **Supplementary Figure 1**) was computed on a community dissimilarity matrix (Gower distance) using monthly data of niche breadth and CWMs of different functional attributes. The coupling (Step 5, **Supplementary Figure 1**) between the environment and key biological attributes (species biomass, functional structure, ecological specialization, and FD of diatoms and copepods) was then estimated by computing two separated co-inertia analysis (COIA; Dolédec and Chessel, 1994; Dray et al., 2003) on monthly means using the "ade4" package. Prior to all multivariate analysis, and for each variable, skewness of the data was removed to reach normality and all variables were to have a mean of zero and a SD of one ("caret" package; Kuhn et al., 2016). The principle of COIA consists of finding co-inertia axis by maximizing the covariance between the row coordinates of two matrices (in this study, the environmental variables and either diatoms or copepods). It defines axis that simultaneously explain the highest possible variance in each of the two matrices and describes their closest common structure. First, a PCA was performed on each matrix, and then applied the COIA (Dray et al., 2003). Explanatory environmental variables were: Pa and direction, S, SST, DIN, DIP, DSi, and protozooplankton biomass. While PAR and copepods biomass were included as additional explanatory environmental variables for diatoms, diatom biomass was added, the defense trait against predation (expressed as CWM) for copepods, and the abundance of their main predators (i.e., Chaetognaths, fish larvae and jellyfish; Hirst and Kiørboe, 2002). The COIA was sequentially built for: (i) environment vs. diatoms; and (ii) environment vs. copepods, with a manual backward selection of the significant variables to obtain the highest coupling coefficients, the strength of the coupling being based on the multidimensional correlation coefficient (RV; Robert and Escoufier, 1976). The variables included in the final COIA were selected (i) only if they displayed a significant seasonal trend in box-plots (refer the final list above), and depending on both (ii) the RV value and (iii) the contribution of variables to the construction of the co-inertia axis. The latter was estimated by means of Pearson correlation calculated between the variables and the scores of samplings on the COIA axis. Although the loadings describe how each variable contributes to each co-inertia axis, such information can be retrieved by the correlation coefficient between the variables and the co-inertia axis. A Monte Carlo permutation procedure (1,000 permutations) was applied to compute the RV and statistical significance. For PCA, PCoA, and COIA analyses, an ascending hierarchical classification (AHC) was used with Ward's aggregation criterion on the two first component coordinates ("hclust" function of the "ade4" package) to reveal monthly clusters.

A variation partitioning (VP) analysis (Step 5, **Supplementary Figure 1**; "vegan" package; Borcard et al., 1992; Legendre and Legendre, 2012) was finally performed to estimate

178

the contribution of *Phaeocystis* blooms, water masses, hydrometeorological (Pa and/or direction as proxies), and local environmental conditions (S, nutrients, PAR, and predator and/or prey biomass) on changes in the functional structure (i.e., the CWMs), ecological specialization (i.e., environmental tolerance and niche breadths), and FD (SES-RaoQ) of the diatom and copepod communities. To explain variations in species richness of the diatom and copepod communities, the contribution of assembly rules was added using SES-RaoQ as a proxy. SES-RaoQ is known to be the most appropriate FD index (Botta-Dukát and Czúcz, 2016) to detect both environmental filtering (trait convergence) and competition based on niche difference (trait divergence). As for the COIA, variables that attest to the hydrometeorological and local environmental conditions (abiotic and prey biomass) were selected backward to obtain the lowest residual proportion. To explore the effect of *Phaeocystis* blooms on species richness, functional structure, ecological specialization, and FD of the diatom community, a Kruskal–Wallis test was performed using different classes of *Phaeocystis* biomass [1: <100; 2: (100, 500); 3: (500, 1000); 4: >1,000 μgC L^{-1}] coming from the 1996 to 2019 dataset (refer "Ecological specialization").

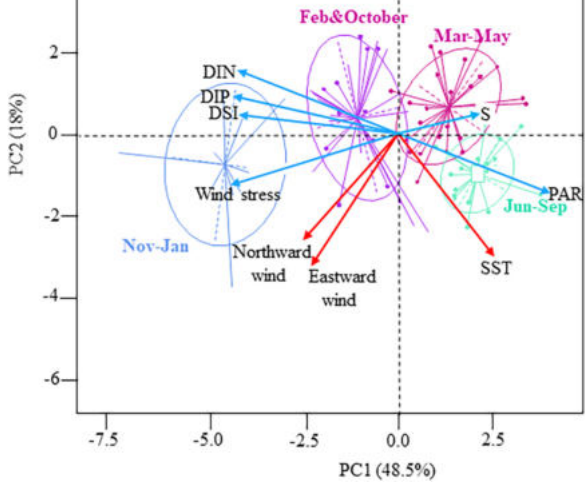

FIGURE 1 | Principal Component Analysis showing the seasonal variations of the abiotic environment in coastal waters of the eastern English Channel over the period 2007–2013. Projection of the variables and of the observations (from January to December) on the factorial map (Eigenvalues are given into brackets, 66.5% of the total inertia). Blue and red arrows: significant Pearson correlation with the first (PC1) and second (PC2) principal components. Blue, purple, pink and green ellipses: Hierarchical Agglomerative Clustering (HAC) of the observations on the factorial map using the Ward's linkage. Photosynthetic Active Radiation (PAR m^{-2} d^{-1}), Salinity (S, n.u), Sea Surface Temperature (SST, °C), Dissolved Inorganic Nitrogen (DIN, μM), Phosphorus (DIP, μM), Silica (DSi, μM), Northward and Eastward winds (m s^{-1}).

RESULTS

Abiotic Environment and Plankton Composition and Biomass

The first principal component (PC1, 48.5% of the total variance) showed a seasonal gradient from relatively high turbulent (Pa as a proxy), less saline, nutrient-rich (DIN, DIP, and DSi), and poor PAR winter conditions to calm and relatively lighted, but nutrient-limited (DSi < 2 μM, DIN < 1 μM, and DIP < 0.2 μM), and saline summer conditions (**Figure 1** and **Supplementary Figure 2**). The second principal component (PC2, 18% of the total variance) was mainly driven by wind direction (both north and eastward winds) and SST, suggesting that SST increased as north and eastward winds increased. The temperature-salinity diagrams mainly discriminated water masses according to temperature (**Supplementary Figure 3**). The vertical structure of water masses also showed seasonal variations; the spring-summer water masses (from March to August) being saltier and colder at the bottom depth; autumn-winter conditions (from September to February) were reversed.

Phytoplankton biomass was mainly composed of diatoms, except when *Phaeocystis* colonies prevailed (from March to mid-May, **Figure 2A**). Zooplankton biomass was mainly composed of copepods, except during the seasonal outburst of the meroplankton that was mainly composed of Echinodermata (in May, mainly *Pluteus* larvae, **Figure 2B**). While a slight decrease was observed during the peak of *Phaeocystis*, the biomass of diatoms followed the same seasonal dynamics as protozooplankton (sum of heterotrophic dinoflagellates and ciliates) and copepods (**Figures 3A–D**). Protozooplankton and copepod biomass progressively increased from winter months to May–June (**Figures 3C,D**), before decreasing. The C/Chl*a* ratio showed strong seasonal variations, with maxima in April–May and minima in winter (**Figure 3E**).

Functional Structure and Ecological Specialization of the Diatom and Copepod Communities

Seasonal variations in the functional structure and ecological specialization of the diatom community characterized with LOESS over the period 2007–2013 (**Supplementary Figures 4A,C,E,G,I,K,M,O** and **Supplementary Figures 5A,C,E,G,I,K**) were similar to those obtained over the period 1996–2019 (**Supplementary Figures 4B,D,F,H,J,L,N,P** and **5B,D,F,H,J,L**). However, Nemenyi tests revealed that monthly changes were more pronounced when using the 24-year time series. The PC1 of the PCoA (PCoA1; 51% of the total variance) (**Figure 4A**) suggested a seasonal shift in the functional structure and ecological specialization of diatom communities from the autumn fall winter to the spring period. This shift was characterized by a seesawing from communities exhibiting high silicification, low S/V ratio, presence of tychopelagic/benthic species, PAR specialization, and generalists relative to nutrient use, to more environmentally tolerant diatom communities (from May to July). During early spring and the *Phaeocystis* bloom period, communities exhibited an intermediate position

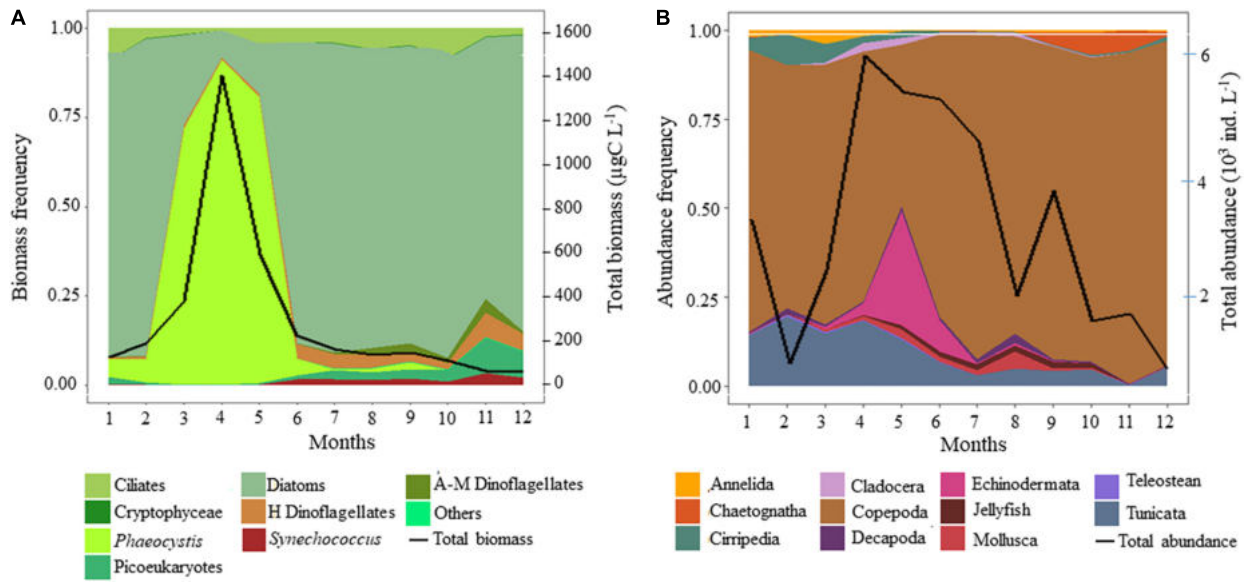

FIGURE 2 | Seasonal variations in panel **(A)** phytoplankton composition (carbon biomass frequency) and total phytoplankton biomass (black line, µgC L^{-1}), and **(B)** zooplankton composition (abundance frequency) and total zooplankton abundance (black line,10^3 ind. L^{-1}). A-M, Auto- Mixotrophic; H, Heterotrophic. Teleostean included fish larvae and eggs. Jellyfish included Cnidaria and Ctenaria.

(**Figure 4A**). The PC2 (PCoA2; 15% of the total variance) revealed that large-size diatom species with defense against predation prevailed from January to March and in October (**Figure 4A**). Although weakly associated with the first two principal components, we detected, for both time series, that CWM-MLD values peaked during the maximum of the *Phaeocystis* bloom (i.e., April; **Supplementary Figures 4E,F**).

For copepods, the PCoA (the PCoA1 and PCoA2 explaining 56% and 22% of the total inertia, respectively, **Figure 4B**) showed that the communities were mainly composed, from February to May, of large omnivorous active feeders (i.e., high CWM-feeding mode values), omnivores with a relatively high propensity to detritivory and environmentally tolerant species, and generalists for TSM and POC. A contrasting pattern between the CWM-omnivorous and the CSI-trophic regime was detected. From June to September, communities were mainly composed of small and passive feeders with a low propensity to detritivory and specialists for both TSM and POC. In October, carnivorous copepods, with specialized feeding modes and specialized environmental requirements, dominated the community.

Accordingly, the CSIs of copepods for trophic regime and feeding mode had high values. Concerning the functional structure of the copepod community (**Supplementary Figures 6A–M**), significant monthly changes were only seen for maximum size (**Supplementary Figure 6A**) and feeding mode (**Supplementary Figure 6B**).

Species Richness and FD of Diatom and Copepod Communities

The annual cycle of diatom species richness exhibited a bimodal pattern (**Figure 5A** and **Supplementary Figure 7A**), with a peak in February–March and September–October. No significant monthly change was detected (Nemenyi test, $p > 0.05$). The annual cycle of copepod species richness was unimodal, peaking in August–September (**Figure 5B**). No monthly variation was detected between the volume of filtered seawater and copepod species richness ($N = 96$, $r^2 = 10^{-5}$, $p > 0.05$).

Patterns of FD of the diatom community (**Figures 5C–H**, refer **Supplementary Table 5** and "diatom.defense.traits" in **Supplementary Data** for more details on the calculation), differed among functional indices, independently of the sampling period (**Supplementary Figures 7B–G**). FRic (SES-FRic, **Figures 5C,D** and **Supplementary Figures 7B,C**) and divergence (SES-RaoQ, **Figures 5E,F** and **Supplementary Figures 7D,E**) for resource use and predation avoidance were lower than expected by chance. FEve values (SES-FEve, **Figures 5G,H** and **Supplementary Figures 7F,G**) were also not different from those expected by chance. The SES-FRic and SES-RaoQ were significantly negatively correlated to species richness for both resource use and predation avoidance (SES-FRic: $r = -1$, $p < 0.001$ and $r = -0.98$, $p < 0.001$, respectively; SES-RaoQ: $r = -0.78$, $p < 0.001$, $r = -0.77$, $p < 0.001$, respectively). SES-FEve was not correlated with species richness ($r = 0.21$, $p > 0.05$ and $r = 0.01$, $p > 0.05$, respectively).

For copepods, the SES-FRic (**Figure 5I**) and SES-RaoQ (**Figure 5J**) were also significantly negatively correlated with species richness, but to a lesser extent ($r = -0.43$, $p < 0.001$, $r = -0.34$, $p < 0.001$, respectively). Omnivory and herbivory, because of their respective high significant correlation with detritivory ($r = 0.9$, $p < 0.001$) and carnivory ($r = -0.91$, $p < 0.001$), were discarded from the calculation. The SES-FRic (**Figure 5I**) values for copepods were not different from those expected by chance. SES-RaoQ (**Figure 5J**) and SES-FEve

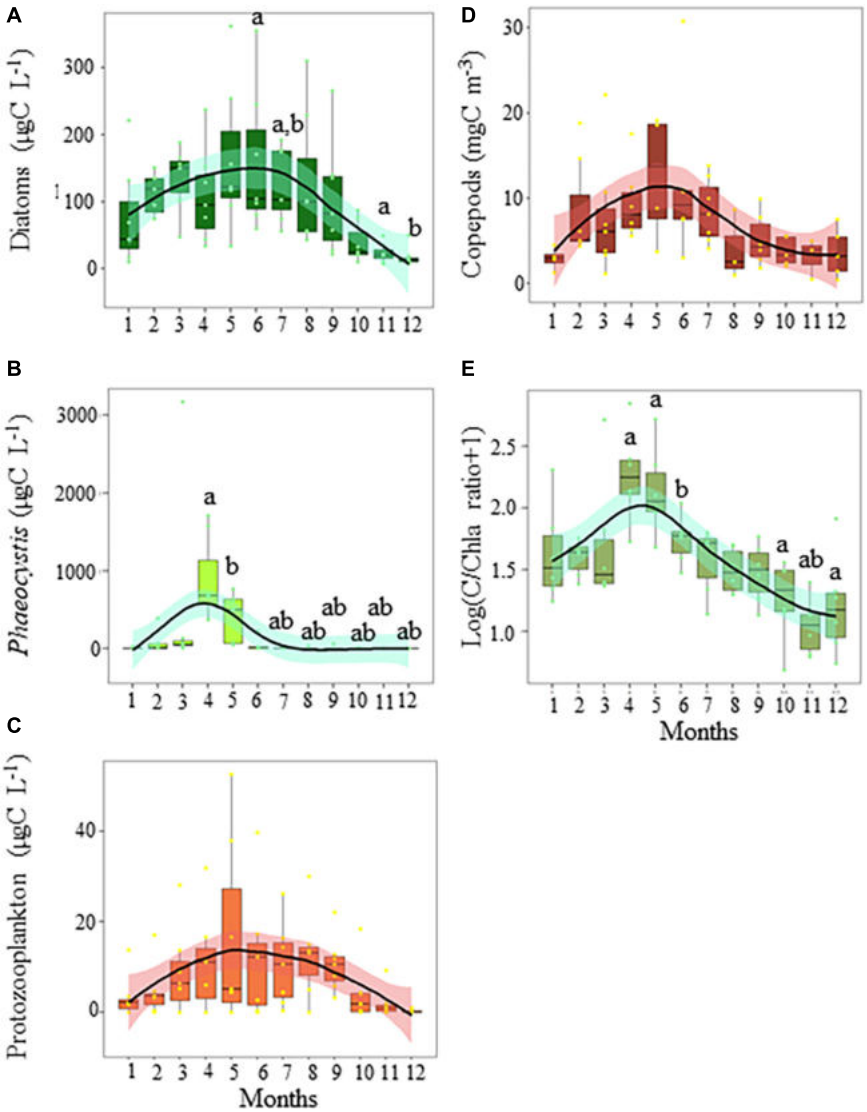

FIGURE 3 | Seasonal variations in the biomass (mgC L^{-1}) of panel **(A)** diatoms, **(B)** *Phaeocystis*, **(C)** protozooplankton (ciliates and dinoflagellates), **(D)** copepods (mgC m^{-3}), and **(E)** the C/Chla ratio in coastal waters of the eastern English Channel over the period 2007–2013. Black horizontal line inside box: median; box: first to third quartiles; whiskers: 1.5 times the interquartile range (IQR); dots: monthly data including outliers (>1.5 times IQR). The labels a and b show significant differences between months ($p = 0.05$, Nemenyi test). The solid line and ribbon represent LOESS smoothing and the 95% confidence interval, respectively.

(**Figure 5K**) values were mostly lower and higher, respectively, than expected by chance. FD indices did not show seasonal patterns (e.g., note the large 95% confidence intervals of the LOESS fits in **Figures 5I–K** and **Supplementary Figure 6A–M**).

Relationships Between the Functional Structure, Ecological Specialization, and FD, and the Abiotic and Biotic Environment

Co-inertia analysis showed a significant coupling (n = 63, RV = 0.49, $p = 10^{-3}$) between the structure of diatom communities and abiotic/biotic conditions (**Figures 6A,B**, **Supplementary Figures 8A,B**, and **Supplementary Table 6A**). A seasonal pattern was delineated by the COIA (**Supplementary Figures 8A,B**). Although all environmental parameters were significant in structuring the seasonality of diatom communities, some were more important than others (**Supplementary Table 6A**). The first COIA axis (explaining 86% of the total inertia, **Figure 6A**) showed that diatom communities, composed predominantly of slightly silicified species, with a relative high S/V cell ratio, and the ability to form colonies, were associated to calm weather conditions and more saline seawater with relatively higher PAR, but low nutrients. Diatom communities, with mainly specialist species for nutrients but generalists for PAR, were also sensitive to environmental variations (relatively

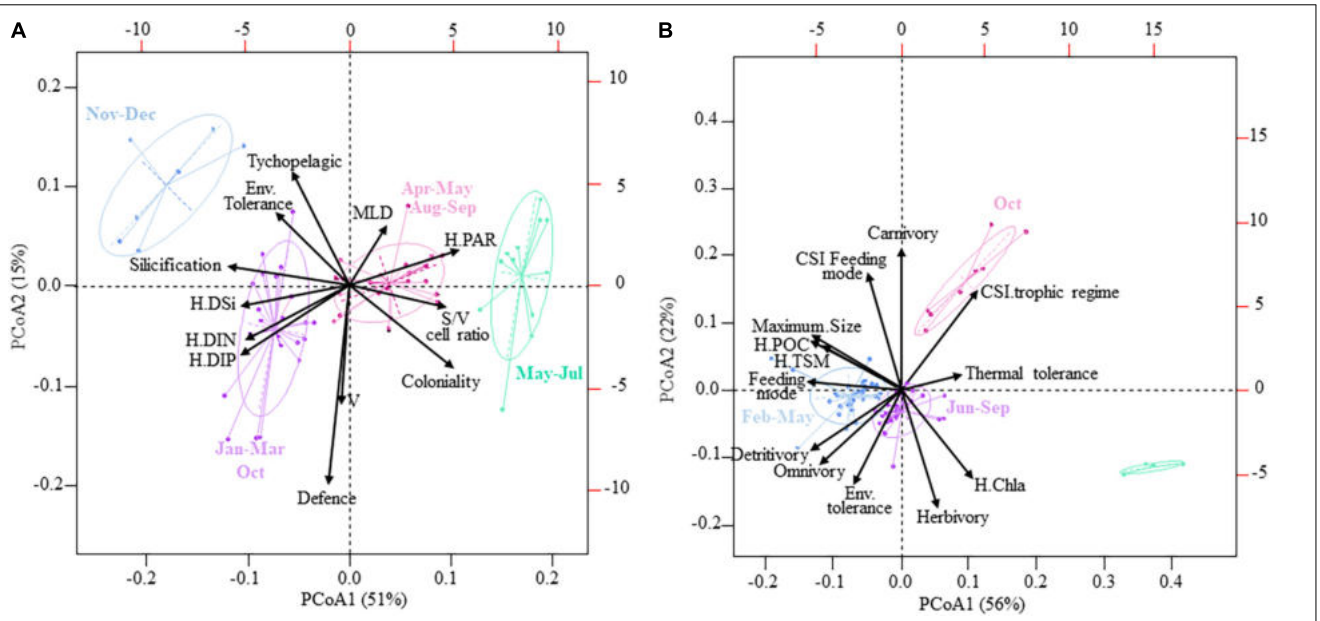

FIGURE 4 | Principal coordinates analysis (PCoA) of the functional structure and ecological specialization of the **(A)** diatom and **(B)** copepod community in coastal waters of the eastern English Channel over the period 2007–2013. The percentage of the total variance explained by each axis is shown in parentheses. Months are grouped together following the results of a Hierarchical Agglomerative Clustering (HAC) using the Ward's linkage and the two first coordinates of the PCoA. Each point represents a monthly averaged community sample. The ellipses show a 95% confidence level. H, niche breadth; PAR, Photosynthetic Active Radiation; DIN, DIP, DSi, Dissolved Inorganic Nitrogen and Phosphorous, and Silica; Chla, Chlorophyll *a*; S/V cell ratio, Surface to Volume cell ratio; MLD, Maximum Linear Dimension; Env. Tolerance, environmental tolerance; CSI, Community Specialization Index; TSM, Total Suspended Matter; POC, Particulate Organic Carbon. Thermal tolerance in panel **(A)** is not shown given its central position on the PCoA plane.

low "Tol" values); slightly silicified species bloomed later in the year. According to the second COIA axis (8% of the total inertia; **Figure 6A**), most diatoms with high defense levels against predation and DIN generalists were associated with colder seawater, rich in *Phaeocystis* biomass and characterized by a high C/Chla ratio, and large-bodied generalist omnivore copepod species. Under such conditions, diatom biomass was maximal. The third COIA axis (3% of the total inertia; **Figure 6B**) showed that species-rich diatom communities, characterized by the dominance of small MLD species, were associated with copepod communities dominated by specialist species. The SES-FRic and SES-RaoQ of the diatom community were the lowest for both resource use and predation avoidance (**Figure 6B**).

The coupling strength between functional structure (i.e., the CWMs), ecological specialization (i.e., environmental tolerance and niche breadth), and FD (SES-RaoQ and SES-FRic) of copepods, and environmental conditions (refer section "Materials and Methods") was low but significant (n = 63, RV = 0.36, p = 0.001, **Figure 6C**). The seasonality of the coupling was unclear (**Supplementary Figure 8C**). The first co-inertia axis (explaining 84% of the total inertia) revealed that large, active-feeding, and omnivore copepod species (i.e., low CSI-trophic regime values) were associated with relative calm weather conditions, more saline *Phaeocystis*-rich waters, characterized by higher proportions of diatoms with defense levels against predation (**Figure 6C** and **Supplementary Table 6B**), and relative high abundance of jellyfish and fish larvae, but low abundance of chaetognaths. Copepods were tolerant to environmental fluctuations, with a propensity to detritivory. The second co-inertia axis (12% of the total inertia) exhibited that species-rich copepod communities were mainly composed of passive-feeding and trophic specialist species (i.e., high CSI-trophic regime values) with a low propensity to detritivory. Copepod species were also sensitive to environmental variations, especially under warm conditions and a high protozooplankton and jellyfish biomass (**Figure 6C**); this coincides with the lowest SES-FRic and SES-RaoQ values occurring in the copepod communities.

Variation partitioning analysis (VP, **Figure 7A**) exhibited that seasonal variations of the functional structure and ecological specialization of the diatom and copepod communities were not related to seasonal changes in environmental conditions, as shown by the high residual values. It was detected that the local environment contributed the most to the explained variance (i.e., 49%) in the functional structure and ecological specialization of the diatom community (adjusted r^2 = 0.18, p = 0.001, i.e., 18% of the total variations of the diatom community), followed by hydrometeorological features (3%, p = 0.001) and the interaction between the local environment and hydrometeorological features is 16% (**Figure 7A**). The variations in the structure of the diatom community were also explained, but to a lesser extent, by the *Phaeocystis* bloom (1%, p = 0.001), predator biomass, and size (1%, p = 0.001), and their interactions (2%). The *Phaeocystis* bloom was the most contributing process to the functional structure and ecological specialization of the copepod community (15%, p = 0.001, **Figure 7B**). Hydrometeorological

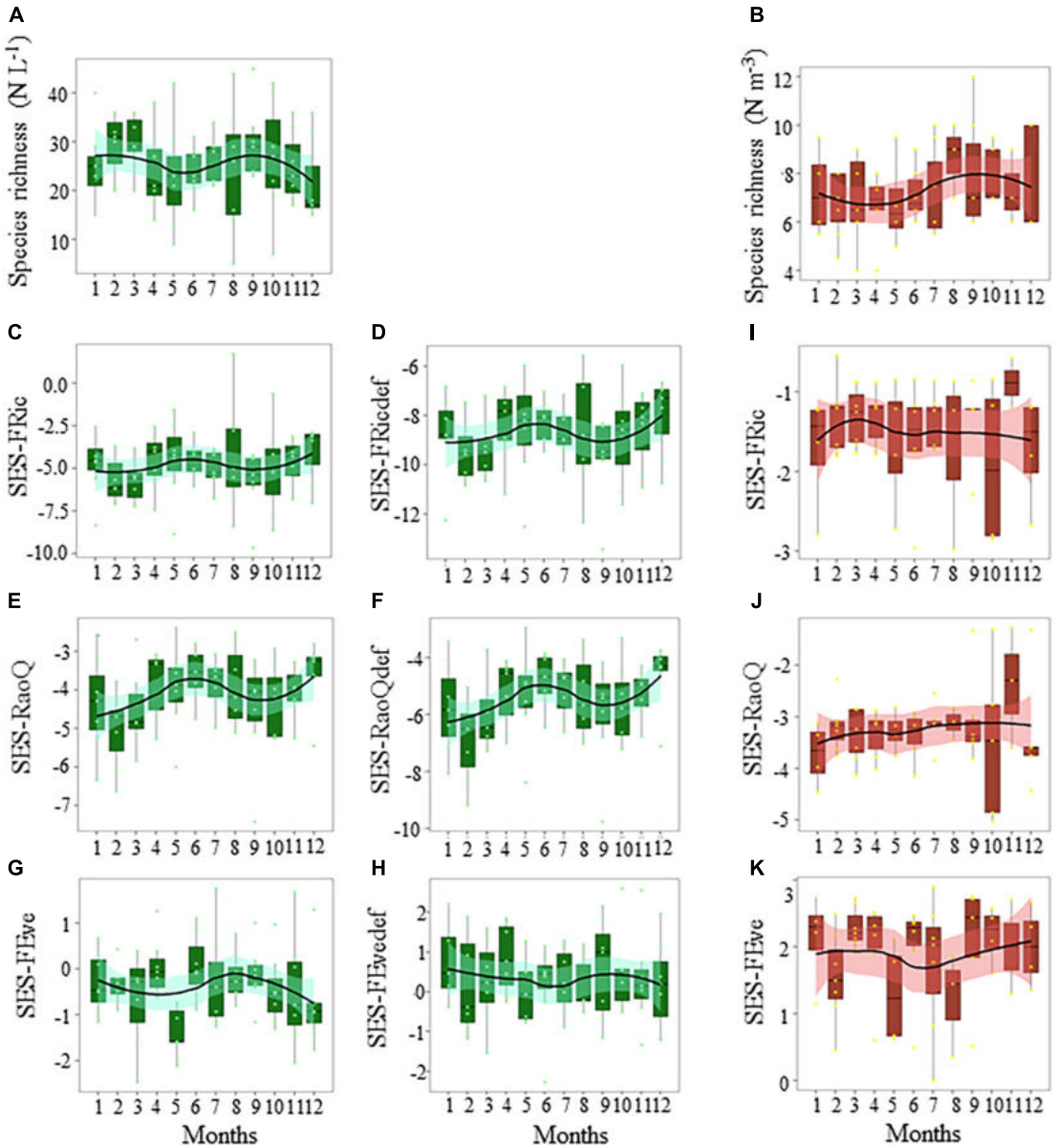

FIGURE 5 | Seasonal variations in the panels **(A,B)** species richness, **(C–E)** functional richness (SES-Fric), **(E,F,J)** functional divergence (SES-RaoQ), and **(G,H,K)** functional evenness (SES-Feve) of the diatom (**A–H**, in green) and copepod (**B,I–K**, in red) community in coastal waters of the eastern English Channel over the period 2007–2013. Def: defence traits against predation. Black horizontal line inside box: median; box: first to third quartiles; whiskers: 1.5 times the interquartile range (IQR); dots: monthly data including outliers (>1.5 times IQR). The solid line and ribbon represent LOESS smoothing and the 95% confidence interval. No difference between months ($p > 0.05$, Nemenyi test) was found between boxes for any of the variables.

features (5%, $p < 0.05$) and their interaction with the *Phaeocystis* bloom (4%), and the interaction between the local environment and predators (3%), played a minor role. In contrast to the functional structure and ecological specialization of diatom and copepod communities, the proportion of unexplained variance was low (3%) for diatom species richness. Diatom species richness was mainly explained by the convergence of a combination of traits: SES-RaoQ decreased as species richness decreased (92% of the total variations in diatom species richness, $p = 0.001$, **Figure 7C**). As for the functional structure and ecological specialization, most of the variations of copepod species richness remained unexplained (69%), and the most contributing drivers are both the convergence of a combination of traits (**Figure 7D**) and its indirect influence through interaction with the local environment (27%).

Phaeocystis biomass had no significant effect on the diatom species richness, biomass, FD (i.e., SES-FRic, SES-FEve, and SES-RaoQ), ecological specialization (i.e., niche breadths), or the functional structure (i.e., CWMs) of the diatom community (**Supplementary Figure 9**).

183

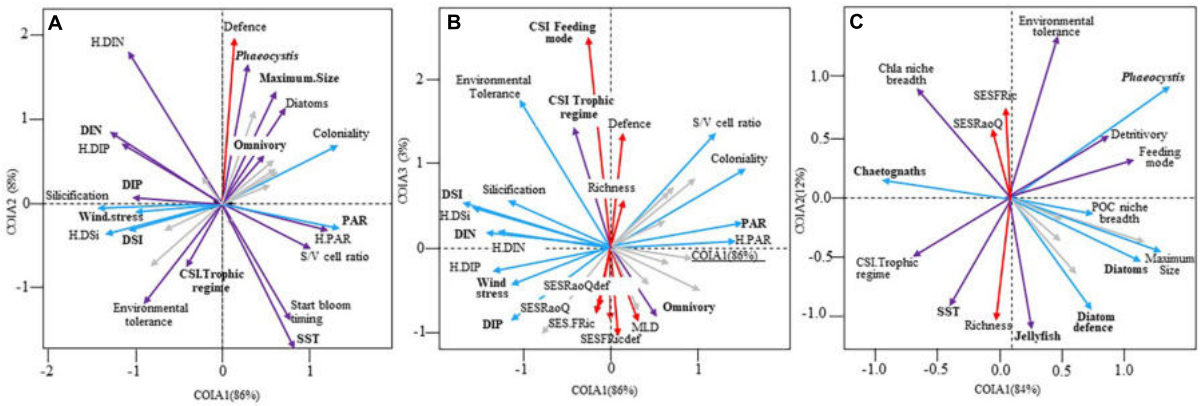

FIGURE 6 | Projection of the environmental variables, species richness, functional structure, ecological specialization and functional diversity of **(A,B)** diatoms (N = 63, RV = 0.49, $p = 10^{-3}$) and **(C)** copepods (N = 63, RV = 0.36, $p = 10^{-3}$) on the factorial maps (**A:** 1–2, **B:** 1–3 and **C:** 1–2) of the co-inertia analysis performed on the diatom and copepod community in coastal waters of the eastern English Channel over the period 2007–2013. Bold labels: "environmental" variables. Only the variables that contribute the most to the construction of the axes are labelled (see **Supplementary Table 6** for details). Gray arrows: no or low ($r < 0.5$) significant Pearson correlation between the variables and the first (blue arrows), second (red arrows) or both first and second or third (purple arrows) co-inertia axes. PAR, Photosynthetic Active Radiation; DIN, DIP, DSi, Dissolved Inorganic Nitrogen, Phosphorous, and Silica; SST, Sea Surface Temperature; S/V ratio, Surface to Volume cell ratio; MLD, Maximum Linear Dimension; CSI, Community Specialization Index; SES-FRic, the functional richness, SES-RaoQ, the functional divergence; def., defence against predation.

DISCUSSION

In this study, we investigated the challenging questions of linking the seasonal succession of planktonic organisms with resource and defense traits, and the identification of the conditions that shape species richness. The results showed that the diatom and copepod communities of the EEC respond synchronously to varying abiotic and biotic conditions. We highlighted that some environmental drivers acted on some trait combinations, through environmental filtering, leading to temporal succession in species composition. Such a pattern was possible through the expression of several well-established functional trait trade-offs that allowed us to optimize the fitness of a species in a particular environment. The results strongly suggested that the competition-defense trade-off (e.g., Hillebrand et al., 2000; Chase et al., 2002), a mechanism that favors weak competitors, better protected against predation, played a key role, not only in driving diatom and copepod species richness but also in triggering the *Phaeocystis* bloom (as shown below). We also revealed the key role of nutrient levels and competition for nutrients, and of prey-predator interactions in the seasonal succession of diatoms and copepods in the coastal waters of the EEC.

The seasonal succession of trait values within the diatom community along with the seasonal gradient of resource, turbulence, and grazing intensity, resulted from several trait trade-off effects: (i) a trade-off in the competitive ability for light vs. nutrients (i.e., S/V cell ratio, coloniality, and specialization for nutrients in opposition to silicification and specialization for light; as shown in **Figure 4A**; Huisman and Weissing, 1994; Leibold, 1997; Klausmeier and Litchman, 2001); (ii) a defense-competition trade-off (e.g., Hillebrand et al., 2000; Chase et al., 2002); and (iii) an opportunistic-gleaner strategy trade-off (Grover, 1990). We revealed a clear opposition in the dominance between *r*- and K-strategists: species with high maximum growth rate and photosynthetic efficiency adapted to low light but high nutrient and turbulent conditions on the one hand (e.g., diatoms: Armbrust, 2009, and *Phaeocystis* colony: Rousseau et al., 2007; Seuront et al., 2007; Nissen and Vogt, 2021), and species which have low maximum growth rate but high competitiveness for nutrients, such as *Synechococcus* and picoeukaryotes (Stawiarski, 2014), on the other hand. The defense-competition trade-off was deduced from the fact that the diatom communities with the highest proportion of level against predation species matched with periods of (i) high grazing intensity [i.e., late winter/spring (February–March) and late summer/autumn (September–October)] (Gasparini et al., 2000; Stelfox-Widdicombe et al., 2000; Antajan, 2004; Grattepanche et al., 2011b); and (ii) low competitiveness for nutrients (i.e., high silicification but low specialization for nutrients and low S/V cell ratio). The association between the defensive trait and cell biovolume was consistent with this functional trait trade-off (**Figure 4A**). To invest in defensive traits against predation, is generally metabolically costly, in such a way that prey with high defense levels has generally lower maximum growth rate, maximum resource uptake, and/or resource uptake affinity (Pančić and Kiørboe, 2018; Cadier et al., 2019; Ehrlich et al., 2020), all these types of defense costs being related to cell biovolume (Litchman and Klausmeier, 2008; Marañón, 2015).

We observed seasonal successions of copepod species of varying maximum size values, feeding strategies, trophic regimes, and vulnerability to predation along a seasonal gradient of turbulence, food level and composition, and predator abundance (**Figures 2A,B**, **3A–D**, **4B**, **6C**), in line with a competition-defense trade-off. Actively feeding copepods feed more efficiently on non-motile than on motile preys (i.e., competitive specialists), but they are more at predation risk

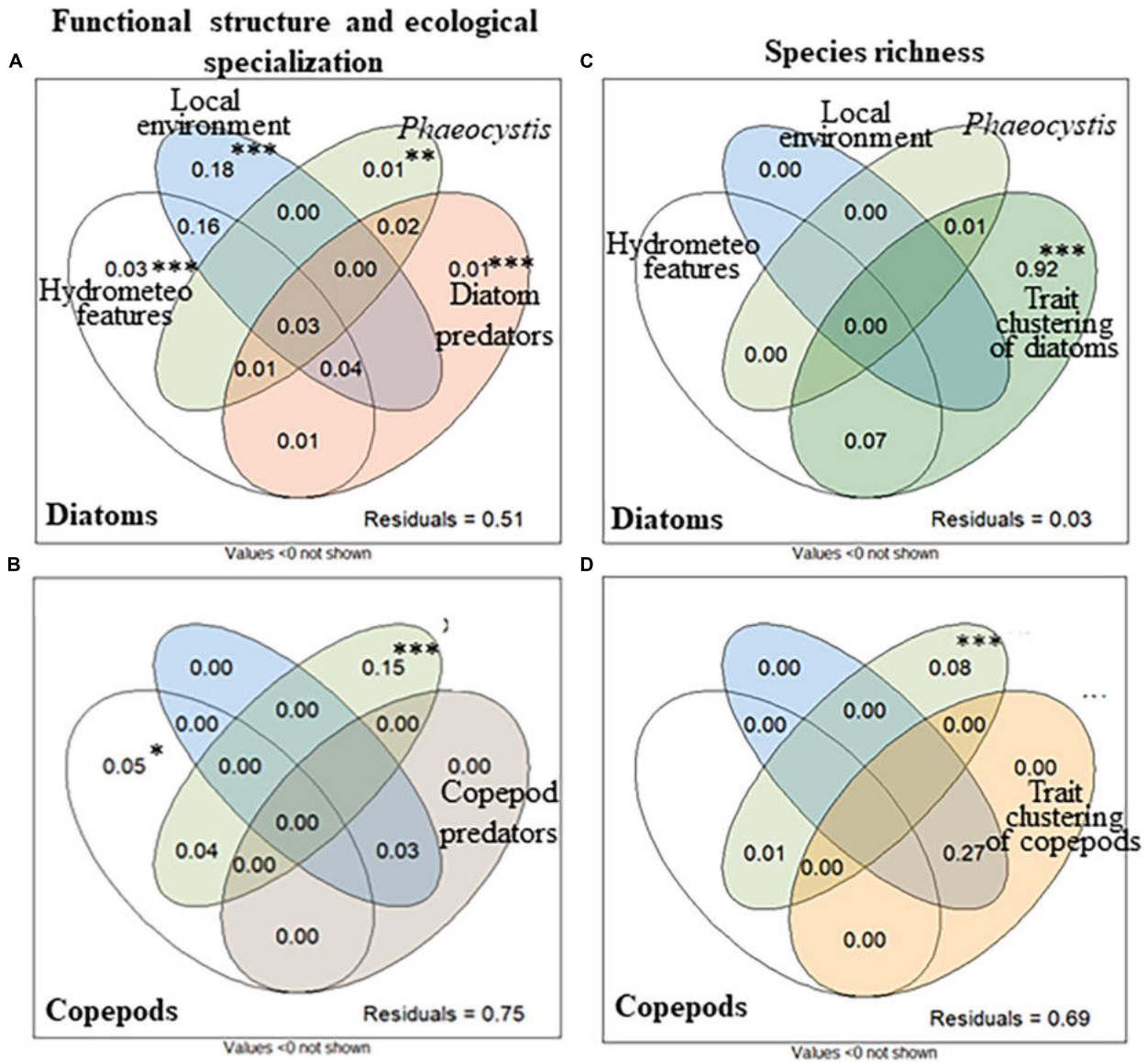

FIGURE 7 | Variation partitioning of the effect of water masses movement and hydrometeorological features (wind stress and direction, white circle), local environment (abiotic and prey biomass, blue circle), *Phaeocystis* biomass (light green circle), predator patterns (light brown: maximum.size of copepods, and biomass of copepods and protozooplankton for diatoms; dark brown: biomass of fish larvae, chaetognaths and jellyfish for copepods), biotic interaction (trait clustering as a proxy; dark green: diatoms, orange: copepods; using SES-RaoQ), the interactions, and the residual proportion on the **(A,B)** functional structure and the ecological specialization and **(C,D)** species richness of the **(A,C)** diatom and **(B,D)** copepod communities in coastal waters of the eastern English Channel over the period 2007–2013. Proportions of variations [adjusted r^2 calculated from redundancy analysis (rda)] in the response variables explained by the explanatory ones are shown. The statistical significance of proportions is calculated by permutation test for rda (***$p = 0.001$, **$p = 0.005$, and *$p < 0.05$). Variance values below are not shown. Note that the shared partitions cannot be tested for statistical significance.

than ambush feeders (i.e., defense specialists) (Almeda et al., 2018). This suggests that the shift toward the dominance of ambush copepod feeders (i.e., predators) during summer might result from strong predation pressure on active-feeding copepods by zooplanktivorous organisms, especially jellyfish (i.e., Cnidaria and Ctenaria). The increasing abundance of jellyfish during summer (**Figure 6C**) is known to exert strong top-down control on copepods (Hirst and Kiørboe, 2002). Ambush copepod feeders, mainly carnivores (**Figure 4B**), were also smaller, and with a lower metabolic cost (Kiørboe, 2011 and references therein) than actively feeding copepods. The presumed strong predation pressure of jellyfish on active-feeding copepods, in combination with the shift toward dominance of motile prey, might also explain the shift in maximum size and diet change that we observed for the copepod community from July (**Supplementary Figures 6A,C–F**). The dominance of active feeding-current feeders observed during the first quarter is consistent with the dominance of non-motile prey of high

food level (i.e., the spring bloom), their higher metabolic needs (Kiørboe, 2011 and references therein), and a lower abundance of zooplanktivore predators (**Figure 6C**). The prevalence of omnivory in winter and spring, which results from higher detritivory, is consistent with the high quantity of detrital material in winter, and both *Phaeocystis* aggregates and ghost colonies in spring (Becquevort et al., 1998; Mari et al., 2005). The significant decline in the grazing rate of copepods, often reported during a *Phaeocystis* bloom (Gasparini et al., 2000; Nejstgaard et al., 2007 and references therein), might result from a shift in the diet of copepods toward *Phaeocystis* detrital material.

We hypothesize that the increase in diatom species richness in early spring and autumn resulted from high grazing pressure by generalist copepods, which grazed the dominant highly competitive diatoms that displayed weak defensive traits. Annual maxima of diatom species richness (**Figure 5A** and **Supplementary Figure 7A**) matched with periods of annual maxima of defense level (**Figure 6B** and **Supplementary Figures 4O,P**) and high grazing pressure occurred at this time of the year (Gasparini et al., 2000; Antajan, 2004). Seasonal variations in diatom species richness were inversely related to functional divergence linked to resource and defense (SES-RaoQ and SES-RaoQdef) (**Figures 5A,E,F** and **Supplementary Figures 7A,D,E**). This indicates that species richness increased as the diatom community converged toward species of similar traits for resource and defense. Trait convergence, which results from abiotic stress (Cornwell and Ackerly, 2009) and/or competitive dominance and ensuing species exclusion (Mayfield and Levine, 2010), is unlikely given the increase in diatom biomass and species richness in early spring and autumn. Cavender-Bares et al. (2009) demonstrated that generalist consumers are expected to cluster prey communities toward species with high defense levels. Although we observed a pattern in line with Cavender-Bares et al. (2009) during the spring period, the autumnal peak in diatom species richness that we observed in the data was associated with specialist ambush and carnivore feeders: such a discrepancy may result from the high predation pressure exerted by jellyfish on generalist and actively feeding copepods (**Figure 6C**), which are more vulnerable to predation in comparison to passive ambush feeders (Kiørboe, 2011 and references therein). Copepod species richness also peaked in autumn, when the copepod community converged toward species of the similar maximum size, trophic preference, and feeding mode (**Figure 6C**) and when we observed dominance of copepod species less vulnerable to predation (i.e., passive ambush feeders; Kiørboe, 2011 and references therein, Almeda et al., 2018; refer also "feeding mode" in **Figure 6C** and **Supplementary Table 6**). However, the seasonal succession of copepod species was by far less evident than for diatoms. The lack of identification of the different copepodite stages, with sizes varying by one order of magnitude between the different copepodite stages (i.e., CI–CVI, Durbin and Durbin, 1978; Cohen and Lough, 1981), probably explained the result. Moreover, copepods live much longer than diatom cells (several months/up to 1 year for copepods, but a few days for diatoms) and their traits enable them to survive in unfavorable conditions. Large unexplained variance (>50%), as we quantified in the VP analysis, is common in ecological studies (Brasil et al., 2020 and references therein) and is often the result of (i) unmeasured environmental drivers, such as trace metals (Chappell et al., 2019); and (ii) potential antagonistic responses among species within a community (Brasil et al., 2020). Brasil et al. (2020) have also recently provided evidence that the assessment of biodiversity and FD is influenced by the presence/lack of rare species: rarity can contribute to large residuals when varpart models are computed. The uncertainty in plankton counts [estimated to be 10% for diatoms based on the table of Lund et al. (1958), and 3–40% for zooplankton (Mack et al., 2012; Kwong and Pakhomov, 2021) with an average of 30% (Frontier, 1969)] could have contributed to the large unexplained discrepancies found in the VP analyses (Brasil et al., 2020). Uncertainty in the species carbon conversion factors that we used for the calculation may have also influenced the estimations and the initial assumptions on how to capture the biological responses, such as linearity of the relationships between the response and explanatory matrices or statistical normality.

Despite potential shortcomings inherent to both the nature of the data and methodological assumptions, we characterized the important role of prey-predator interaction in shaping autumnal copepod community as a consequence of a strong predation pressure by jellyfish on the actively feeding copepods, which in turn induces relaxation of prey-prey competitive interactions. Because of the dominance of phytoplankton r- strategists in spring and autumn, generalist consumers might have grazed mainly on the dominant diatom species that displayed higher growth rates than diatom species with strongly defended cells. Several studies have suggested that species coexistence is possible only under both high grazing pressure and nutrient level conditions to allow the strongly grazed species to regrow after grazing (e.g., Proulx and Mazumder, 1998; Leibold, 1999; Worm et al., 2002). This could explain why diatom species richness declined in summer when nutrients are growth-limiting and the grazing pressure much lower than in spring and autumn (Gasparini et al., 2000; Stelfox-Widdicombe et al., 2000; Antajan, 2004; Grattepanche et al., 2011b). The defense-competition trade-offs could have reduced the frequency of well-defended, but poor-competitive, species and reduced diatom species richness in nutrient-limiting conditions that favor competitive exclusion. The relatively high S/V cell ratio and chain length values, but lowest silicification and defense level, observed in summer, reinforce this idea of the prevalence of competitive exclusion during this period. The concomitant shift toward niche differentiation through the tendency toward a decrease in functional divergence (e.g., Cornwell and Ackerly, 2009), according to the principle of limiting similarity (Macarthur and Levins, 1967), also suggested competitive exclusion. Such shift toward niche differentiation, paralleled by a decrease in species richness, started in April from the maximum of the *Phaeocystis* bloom. It suggests that the unbalancing of the defense-competition trade-off toward competitive exclusion began at the time *Phaeocystis* is a poor competitor for nitrate (Lancelot et al., 1998), has, in average, a lower maximum growth rate than diatoms (e.g., Breton et al., 2017 and reference therein), but strong protection against grazing by forming colonies that grow larger in the presence of predators (Jakobsen and Tang, 2002; Long et al., 2007; Nejstgaard et al., 2007, and references therein). *Phaeocystis* might have consequently benefited from the grazing

186

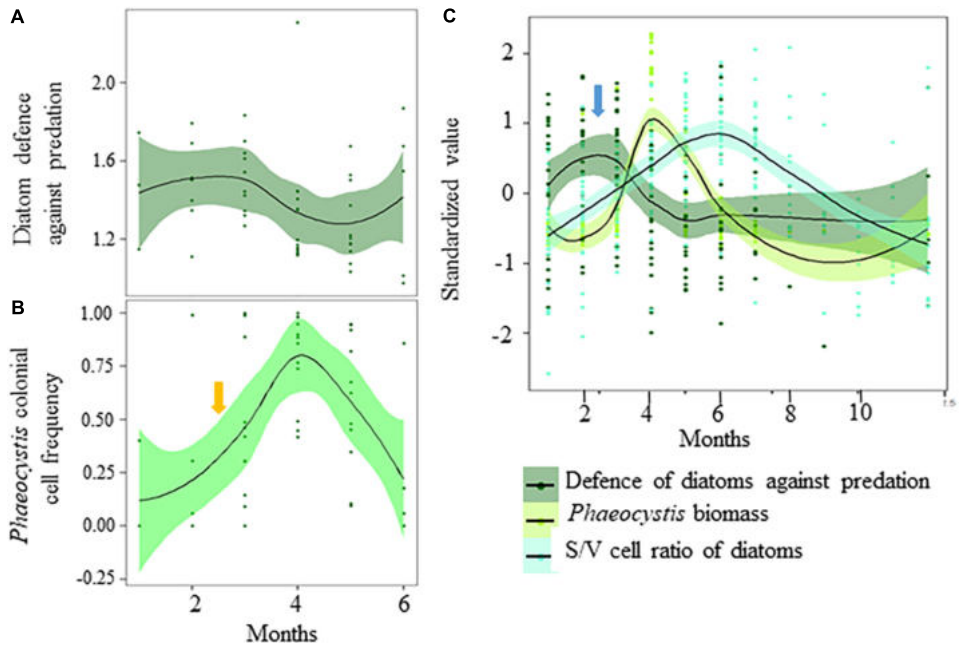

FIGURE 8 | Winter-spring variations in panel **(A)** the Community-Weight mean of Defence against predation of the diatom community (standardized value; black line and dark green shading), and **(B,C)** *Phaeocystis* colonial cell frequency and biomass (standardized value; black line and green shading) in coastal waters of the eastern English Channel over the **(A,B)** 2007–2019 and **(C)** 1996–2019. The solid line and ribbon represent LOESS smoothing and the 95% confidence interval, respectively. Standardized values were calculated per year. Note that **(A)** the seasonal maximum of the defense trait value, **(B)** the start of the transformation of *Phaeocystis* flagellate cells into colonial cells embedded into a mucopolysaccharide matrix (orange arrow) and **(C)** the start *Phaeocystis* bloom timing (blue arrow) are synchronised. Note that the S/V cell ratio of diatoms as proxy of competitiveness is low at this time **(C)**.

preference of generalists toward poor-defended, but highly competitive, species (**Figure 8**). The seasonal maximum of the defense trait value (**Figure 8A**), the start of the transformation of *Phaeocystis* flagellate cells into colonial cells embedded into a mucopolysaccharide matrix (**Figure 8B**, orange arrow), as well as the timing of bloom initiation of *Phaeocystis* (**Figure 8C**, blue arrow), were synchronized. The results highlight the potential key role in the defense-competition trade-off besides nutrient level in triggering the *Phaeocystis* bloom, and more generally, the cardinal role of generalist consumers in the initiation of the bloom. As observed for other ecological communities [Chihoub et al., 2020 (copepods); Wengrat et al., 2018 (diatoms); Villéger et al., 2014; Menezes et al., 2015; Alexander et al., 2017 (fish); Rogalski et al., 2017 (daphniids); Donohue et al., 2009; Zhang et al., 2019 (benthic invertebrates)], eutrophication favors biotic homogenization, which in turn may favor blooms of inedible species such as *Phaeocystis*. We did not detect any negative effect of the *Phaeocystis* bloom on the plankton community (**Supplementary Figure 9**), but a shift of the copepod community toward biotic homogenization was detected.

CONCLUSION

The application of a trait-based approach, combined with the assessment of ecological specialization, has made possible a better understanding of seasonal succession and biodiversity patterns in plankton along gradients of resources, turbulence, and grazing pressure. We have shown that species succession is driven by different trade-offs among functional traits, under the functional constraints dictated by the environmental pressure encountered by plankton communities across the seasons. We suggest that the competition-defense trade-off plays an important role in promoting plankton species richness and in triggering the *Phaeocystis* bloom in coastal waters of the EEC. By successively favoring species with ecological strategies that match environmental conditions, the diatom and copepod communities in coastal waters of the EEC respond synchronously to varying resources and biotic conditions.

DATA AVAILABILITY STATEMENT

The raw data supporting the conclusions of this article are available by the authors in **Supplementary Data**.

AUTHOR CONTRIBUTIONS

EB, BS, and EG conceptualized the study. EB and EG performed the investigation on methodology. EB, BS, D-IS, DP, CS, MC, SF, J-MB, and AL provided the abiotic and biological data. EB, AP, OD, and EG performed the data analysis. EB, UC, EG, BS, LK, GB, and LS contributed to the manuscript writing. All authors contributed to the article and approved the submitted version.

FUNDING

This work was a contribution of the project EVOLECO-NUPHY supported by the French National program LEFE (Les Enveloppes Fluides et l'Environnement).

ACKNOWLEDGMENTS

We acknowledge the three reviewers for their constructive comments, which allowed us to greatly improve the manuscript. We thank the crews who helped during long-term monitoring downstream of the Gironde estuary (2001–2017) and in coastal waters of the eastern English Channel (1996–2019), and the SOMLIT teams for sampling and physicochemical measurements and analysis, especially N. Degros, E. Lecuyer, and H. Derriennic. We also thank the students T. Rault and G. Parmentier for copepod identification and counts and S. Bosc and P. Faye for their contribution to diatom cell measurements. This work is dedicated to J.-M. Dewarumez, who managed SOMLIT at Wimereux, and P. Lebleu, who performed sampling in the Gironde estuary.

SUPPLEMENTARY MATERIAL

The Supplementary Material for this article can be found online at: https://www.frontiersin.org/articles/10.3389/fmars.2021.656300/full#supplementary-material

REFERENCES

Alexander, T. J., Vonlanthen, P., and Seehausen, O. (2017). Does eutrophication-driven evolution change aquatic ecosystems? *Philos. Trans. R. Soc. B Biol. Sci.* 19:372. doi: 10.1098/rstb.2016.0041

Almeda, R., van Someren Gréve, H., Kiørboe, T. (2018). Prey perception mechanism determines maximum clearance rates of planktonic copepods. *Limnol. Oceanogr.* 63, 2695–2707. doi: 10.1002/lno.10969

Aminot, A., and Kérouel, R. (2004). *Hydrologie des Écosystèmes Marins: Paramètres et Analyses*. Brest: Ifreme.

Antajan, E. (2004). *Responses of Calanoid Copepods to Changes in Phytoplankton Dominance in the Diatoms - Phaeocystis Globosa Dominated Belgium Coastal Waters*. Ph.D. thesis. Brussel: Vrije Universiteit Brussel, 142.

Armbrust, E. V. (2009). The life of diatoms in the world's oceans. *Nature* 459, 185–192. doi: 10.1038/nature08057

Beaugrand, G., Brander, K. M., Lindley, J. A., Souissi, S., Reid, P. C. (2003). Plankton effect on cod recruitment in the North Sea. *Nature* 426, 661–664. doi: 10.1038/nature02164

Becquevort, S., Rousseau, V., and Lancelot, C. (1998). Major and comparable roles for free-living and attached bacteria in the degradation of *Phaeocystis*-derived organic matter in coastal waters of the North Sea. *Aquat. Microb. Ecol.* 14, 39–48. doi: 10.3354/ame014039

Benedetti, F., Gasparini, S., and Ayata, S. D. (2016). Identifying copepod functional groups from species functional traits. *J. Plankton Res.* 38, 159–166. doi: 10.1093/plankt/fbv096

Bjærke, O., Jonsson, P. R., Alam, A., and Selander, E. (2015), Is chain length in phytoplankton regulated to evade predation? *J. Plankton Res.* 37, 1110–1119. doi: 10.1093/plankt/fbv076

Biggs, C. R., Yeager, L. A., Bolser, D. G., Bonsell, C., Dichiera, A. M., Hou, Z., et al. (2020). Does functional redundancy affect ecological stability and resilience? A review and meta-analysis. *Ecosphere* 11: e03184. doi: 10.1002/ecs2.3184

Blonder, B., Lamanna, C., Violle, C. and Enquist, B. J. (2014). The n-dimensional hypervolume. *Global Ecol. Biogeogr.* 23, 595–609. doi: 10.1111/geb.12146

Bonato, S., Breton, E., Didry, M., Lizon, F. (2016). Spatio-temporal patterns in phytoplankton assemblages in coastal-offshore gradients using flow cytometry: a case study in the eastern English Channel. *J. Mar. Syst.* 156, 76–85. doi: 10.1016/j.jmarsys.2015.11.009

Borcard, D. P, Legendre, P, Drapeau, P. (1992). Partialling out the spatial component of ecological variation. *Ecology* 73, 1045–1055. doi: 10.2307/1940179

Botta-Dukát, Z. (2005), Rao's quadratic entropy as a measure of functional diversity based on multiple traits. *J. Veg. Sci.* 16, 533–540. doi: 10.1111/j.1654-1103.2005.tb02393.x

Botta-Dukát, Z. and Czúcz, B. (2016). Testing the ability of functional diversity indices to detect trait convergence and divergence using individual-based simulation. *Methods Ecol. Evol.* 7, 114–126.

Brasil, L. S., Vieira, T. B., Andrade, A. F. A. (2020). The importance of common and the irrelevance of rare species for partition the variation of community matrix: implications for sampling and conservation. *Sci. Rep.* 10:19777.doi: 10.1038/s41598-020-76833-5

Breton E., Brunet C., Sautour B., and Brylinski, J. M. (2000). Annual variations of phytoplankton biomass in the eastern English Channel: comparison by pigment signatures and microscopic counts. *J. Plankton Res.* 22, 1423–1440. doi: 10.1093/plankt/22.8.1423

Breton, E., Rousseau, V., Parent, J. Y., Ozer, J., and Lancelot, C. (2006). Hydroclimatic modulation of diatom/*Phaeocystis* blooms in nutrient-enriched Belgian coastal waters (North Sea). *Limnol. Oceanogr.* 51, 1401–1409. doi: 10.4319/lo.2006.51.3.1401

Breton, E., Christaki, U., Bonato, S., Didry, M., and Artigas, L. F. (2017). Functional trait variation and nitrogen use efficiency in temperate coastal phytoplankton. *Mar. Ecol. Prog. Ser.* 563, 35–49. doi: 10.3354/meps11974

Brody, S. R., Lozier, M. S., and Dunne, J. P. (2013). A comparison of methods to determine phytoplankton bloom initiation. *J. Geophys. Res. Oceans*, 118, 2345–2357. doi: 10.1002/jgrc.20167

Brun, P., Payne, R., and Kiørboe, T. (2017). A trait database for marine copepods. *Earth Syst. Sci. Data* 9, 99–113. doi: 10.5194/essd-2016-30

Buitenhuis, E. T., Li, W. K. W., Vaulot D., Lomas M. W. (2012). Picophytoplankton biomass distribution in the global ocean. *Earth Syst. Sci. Data* 4, 37–46. doi: 10.5194/essd-4-37-2012

Cadier, M., Andersen, K. H., Visser, A. W. and Kiørboe, T. (2019). Competition–defense tradeoff increases the diversity of microbial plankton communities and dampens trophic cascades. *Oikos* 128, 1027–1040. doi: 10.1111/oik.06101

Cahoon, L. B. (1999). The role of benthic microalgae in neritic ecosystems. *Oceanogr. Mar. Biol. Annu. Rev.* 37, 47–86.

Cavender-Bares, J., Kozak, K. H., Fine, P. V. A., and Kembel, S. W. (2009). The merging of community ecology and phylogenetic biology. *Ecol. Lett.* 12, 693–715. doi: 10.1111/j.1461-0248.2009.01314.x

Chappell, P. D., Armbrust, E. V., Barbeau, K. A., Bundy, R. M., Moffett, J. W., Vedamati, J., and Jenkins, B. D. (2019). Patterns of diatom diversity correlate with dissolved trace metal concentrations and longitudinal position in the northeast Pacific coastal offshore transition zone. *Mar. Ecol. Prog. Ser.* 563, 35–49.

Chase, J. M., Abrams, P. A., Grover, J. P., Diehl, S., Chesson, P., Holt, R. D. et al. (2002). The interaction between predation and competition: a review and synthesis. *Ecol. Lett.* 5, 302–315. doi: 10.1046/j.1461-0248.2002.00315.x

Chessel, D., Dufour, A. B., and Thioulouse, J. (2004). The ade4 package-I-One-table methods. *R. News* 4, 5–10.

Chihoub, S., Christaki, U., Chelgham, S., Amara, R., Ramdane, Z., Zebboudj, A., Rachik, S., and Breton, E. (2020). Coastal eutrophication as a potential driver of functional homogenization of copepod species assemblages in the Mediterranean Sea. *Ecol. Ind.* 115:106388. doi: 10.1016/j.ecolind.2020.106388

Clavel, J., Julliard, R., and Devictor, V. (2011). Worldwide decline of specialist species: toward a global functional homogenization? *Front. Ecol. Environ.* 9, 222–228. doi: 10.1890/080216

Cohen, R. E. and Lough, R. G. (1981). Length-weight relationships for several copepods dominant in the Georges BankGulf of Maine area. *J. Northw. Atl. Fish. Sci.* 2, 47–52. doi: 10.2960/J.v2.a4

Conway, D. V. P. (2006). Identification of the copepodite developmental stages of twenty-six North Atlantic copepods. *J. Mar. Biolog. Assoc. U.K.* 21, 1–28.

Cornwell, W. K. and Ackerly, D. D. (2009). Community assembly and shifts in plant trait distributions across an environmental gradient in coastal California. *Ecol. Monogr.* 79, 109–126. doi: 10.1890/07-1134.1

Dam, H. G. and Peterson, W. T. (1991). *In situ* feeding behaviour of the copepod *Temora longicornis*: effects of seasonal changes in chlorophyll size fractions and female size. *Mar. Ecol. Prog. Ser.* 71, 113–123. doi: 10.3354/meps071113

Djeghri, N., Atkinson, A., Fileman, E. S., Harmer, R. A., Widdicombe, C. E., McEvoy, A. J., Cornwell, L., Mayor, D. J. (2019). High Prey-predator size ratios and unselective feeding in copepods: a seasonal comparison of five species with contrasting feeding modes, *Prog. Oceanogr.*177:102039. doi: 10.1016/j.pocean.2018.11.005

Dolédec, S., and Chessel, D. (1994). Co-inertia analysis: an alternative method for studying species–environment relationships. *Freshw. Biol.* 31, 277–294. doi: 10.1016/0269-7491(87)90079-0

Dolédec, S., Chessel, D. and Gimaret-Carpentier, C. (2000). Niche separation in community analysis: a new method. *Ecology* 81, 2914–2927. doi: 10.1890/0012-96582000081

Donohue, I., Jackson, A. L., Pusch, M. T., and Irvine, K. (2009). Nutrient enrichment homogenizes lake benthic assemblages at local and regional scales. *Ecology* 90, 3470–3477. doi: 10.1890/09-0415.1

Dray, S., Chessel, D., and Thioulouse, J. (2003). Co-inertia analysis and the linking of ecological data tables. *Ecology* 84, 3078–3089. doi: 10.1890/03-0178

Dray, S., Dufour, A.B., and Chessel, D. (2007). The ade4 Package-II: two-table and K-table methods. *R. News* 7, 47–52.

Dray, S., Pélissier, R., Couteron, P., Fortin, M., Legendre, P., Peres-Neto, P. R., et al. (2012). Community ecology in the age of multivariate multiscale spatial analysis. *Ecol. Monogr.* 82, 257–275. doi: 10.1890/11-1183.1

Durbin, E. G. and Durbin, A. G. (1978). Length and weight relationships of *Acartia clausi* from Narragansett Bay, R.I. *Limnol. Oceanogr.* 23, 958–969 doi: 10.4319/lo.1978.23.5.0958

Ehrlich, E., Kath, N. J., and Gaedke, U. (2020). The shape of a defense-growth trade-off governs seasonal trait dynamics in natural phytoplankton. *ISME J.* 14, 1451–1462. doi: 10.1038/s41396-020-0619-1

Frontier, S. (1969). Sur une méthode d'analyse faunistique rapide du zooplancton. exp. mar. *Biol. Ecol.* 3, 18–26.

Garnier, E., Cortez, J., Billes, G., Navas, M. L., Roumet, C., Debussche, M., Laurent, G., Blanchard, A., Aubry, D., Bellmann, A., Neill, C., and Toussaint, J. P. (2004). Plant functional markers capture ecosystem properties during secondary succession. *Ecology* 85, 2630–2637. doi: 10.1890/03-0799

Garnier, J., Riou, P., Le Gendre, R., Ramarson, A., Billen, G, Cugier, P., Schapira, M., Théry, S., Thieu, V., Ménesguen, A. (2019). Managing the agri-food system of watersheds to combat coastal eutrophication: a land-to-sea modelling approach to the french coastal english channel. Geosciences 9:441. doi: 10.3390/geosciences9100441

Gasparini, S., Daro, M. H., Antajan, E., Tackx, M., Rousseau, V., Parent, J. Y., and Lancelot, C. (2000). Mesozooplankton grazing during the *Phaeocystis globosa* bloom in the Southern Bight of the North Sea. *J. Sea Res.* 43, 345–356. doi: 10.1016/S1385-1101(00)00016-2

Gini, C., (1912). «Variabilità e Mutabilità», Studi Economico-Giuridici dell'Univ. Di Cagliari 3, 1–158. doi: 10.2307/2340052

Gómez, F. and Souissi, S. (2007). The distribution and life cycle of the dinoflagellate Spatulodinium pseudonoctiluca (Dinophyceae, Noctilucales) in the northeastern English Channel. *C. R. Biologies*, 330, 231–236. doi: 10.1016/j.crvi.2007.02.002

Gotelli, N. J. and McCabe, D. J. (2002). Species co-occurrence: a meta-analysis of J. M. Diamond's assembly rules model. *Ecology* 83, 2091–2096. doi: 10.1890/0012-96582002083

Gower, J. C. (1971). A general coefficient of similarity and some of its properties. *Biometrics* 27:857. doi: 10.2307/2528823

Grattepanche, J. D., Breton, E., Brylinski, J. M., Lecuyer, E., and Christaki, U. (2011a). Succession of primary producers and micrograzers in a coastal ecosystem dominated by *Phaeocystis globosa* blooms. *J. Plankton Res.* 33, 37–50. doi: 10.1093/plankt/fbq097

Grattepanche, J. D., Vincent, D., Breton, E., and Christaki, U. (2011b). Microzooplankton herbivory during the diatom-*Phaeocystis* spring succession in the eastern English Channel. *J. Exp. Mar. Biol. Ecol.* 404, 87–97. doi: 10.1016/j.jembe.2011.04.004

Grover, J. P. (1989). Influence of cell shape and size on algal competitive ability. *J. Phycology* 25, 402–405. doi: 10.1111/j.1529-8817.1989.tb00138.x

Grover, J. (1990). Resource competition in a variable environment: phytoplankton growing according to Monod's model. *Am. Nat.* 136, 771–789. doi: 10.1086/285131

Halpern, B. S., Walbridge, S., Selkoe, K. A., Kappel, C. V., Micheli, F. (2008). A global map of human impact on marine ecosystems. *Science* 319, 948–952. doi: 10.1126/science.1149345

Halse, G. R., and Syvertsen, E. E. (1996). "Chapter 2 - marine diatoms". ed C.R. *Tomas. Identifying Marine Diatoms and Dinoflagellates* (Cambridge, MA: Academic Press), 5–385.

Hill, S. L., Harfoot, M., Purvis, A., Purves, D. W., Collen, B., Newbold, T., Burgess, N. D. and Mace, G. M. (2016). Reconciling biodiversity indicators to guide understanding and action. *Conserv. Lett.* 9, 405–412. doi: 10.1111/conl.12291

Hillebrand, H., Worm, B., and Lotze, H. K. (2000). Marine microbenthic community structure regulated by nitrogen loading and grazing pressure. *Mar. Ecol. Prog. Ser.* 204, 27–38. doi: 10.3354/meps204027

Hillebrand, H., Dürselen, C. D., Kirschtel, D., Pollingher, U., and Zohary, T. (1999). Biovolume calculation for pelagic and benthic microalgae, *J. Phycol.* 35, 403–424. doi: 10.1046/j.1529-8817.1999.3520403.x

Hirst, A. G., and Kiørboe, T. (2002). Mortality of marine planktonic copepods: global rates and patterns. *Mar. Ecol. Prog. Ser.* 230, 195–209. doi: 10.3354/meps230195

Holmes, R. M., Aminot, A., Kérouel, R., Hooker, B. A., and Peterson, B. J. (1999). A simple and precise method for measuring ammonium in marine and freshwater ecosystems. *Can. J. Fish Aquat. Sci.* 56, 1801–1808. doi: 10.1139/f99-128

Hoppenrath, M., Elbrächter, M., Drebes, G. (2009). *Marine Phytoplankton. Selected Microphytoplankton From the North Sea Around Helgoland and Sylt, E.* Stuttgart: Schweizerbartsche Verlagsbuchhandlung, 264.

Howarth, R. W. (2008). Coastal nitrogen pollution: a review of sources and trends globally and regionally. *Harmful Algae* 8, 14–20. doi: 10.1016/j.hal.2008.08.015

Huisman, J. and Weissing, F. J. (1994). Light-limited growth and competition for light in well-mixed aquatic environments: an elementary model. *Ecology* 75, 507–520. doi: 10.2307/1939554

Jacoby, W. G. (2000). LOESS: a nonparametric, graphical tool for depicting relationships between variables. *Electoral Stud.* 19, 577–613. doi: 10.1016/S0261-3794(99)00028-1

Jakobsen, H. H., and Tang, K. W. (2002). Effects of protozoan grazing on colony formation in *Phaeocystis globosa* (Prymnesiophyceae) and the potential costs and benefits. *Aquat. Microb. Ecol.*, 27, 261–273. doi : 10.3354/ame027261

Jakobsen, H. H., and Markager, S. (2016). Carbon-to-chlorophyll ratio for phytoplankton in temperate coastal waters: seasonal patterns and relationship to nutrients. *Limnol. Oceanogr.* 61, 1853–1868. doi: 10.1002/lno.10338

Karp-Boss, L., Boss, E., and Jumars, P. A. (1996). Nutrient fluxes to planktonic osmotrophs in the presence of fluid motion. *Oceanogr. Mar. Biol.* 34, 71–107.

Key, T., McCarthy, A., Campbell, D. A., Six, C., Roy S. (2010). Cell size trade-offs govern light exploitation strategies in marine phytoplankton. *Environ. Microbiol.* 12, 95–104. doi: 10.1111/j.1462-2920.2009.02046.x

Kiørboe, T. (2011). How zooplankton feed: mechanisms, traits and trade-offs. *Biol. Rev.* 86, 311–339. doi: 10.1111/j.1469-185X.2010.00148.x

Kiørboe, T. and Hirst, A. G. (2014). Shifts in mass scaling of respiration, feeding, and growth rates across life-form transitions in marine pelagic organisms. *Am. Nat.* 183, 118–130. doi :10.1086/675241

Klausmeier, C. A. and Litchman, E. (2001). Algal games: the vertical distribution of phytoplankton in poorly mixed water columns. *Limnol. Oceanogr.* 46, 1998–2007. doi: 10.4319/lo.2001.46.8.1998

Kleppel, G. (1993). On the diets of calanoid copepods. *Mar. Ecol. Prog. Ser.* 99, 183–195.

Kneitel, J. M. and Chase, J. M. (2004). Trade-offs in community ecology: linking spatial scales and species coexistence. *Ecol. Lett.* 7, 69–80. doi: 10.1046/j.1461-0248.2003.00551.x

Kofoid, C. A. and Campbell, A. S. (1929). A conspectus of the marine and freshwater Ciliata belonging to the suborder Tintinnoinea with descriptions of new species, principally from the Agassiz Expedition to the eastern tropical Pacific, 1904–05. *Univ. Calif. Publ. Zool.* 34:403.

Kuhn, M., Wing, J., Weston, S., Williams, A., Keefer, C., Engelhardt, A., et al. (2016). *caret: Classification and Regression Training. R package version 6.0-71*. Available online at: https://CRAN.R-project.org/package=caret

Kwong, L. E, and Pakhomov, A. E. (2021). Zooplankton size spectra and production assessed by two different nets in the subarctic Northeast Pacific, *J. Plankton Res.* 43, 527–545. doi: 10.1093/plankt/fbab039

Laliberté, E. and Legendre, P. (2010). A distance-based framework for measuring functional diversity from multiple traits. *Ecology* 91, 299–305. doi: 10.1890/08-2244.1

Lancelot, C. (1995). The mucilage phenomenon in the continental coastal waters of the North Sea. *Sci. Tot. Environ. Mar. Mucilages* 165, 83–102. doi: 10.1016/0048-9697(95)04545-

Lancelot, C., Billen, G., Sournia, A., Weisse, T., Colijn, F., Veldhuis, M. J. W., et al. (1987). *Phaeocystis* blooms and nutrient enrichment in the continental coastal zones of the North Sea. *Ambio* 16, 38–46. doi: 10.1016/0198-0254(87)90379-7

Lancelot, C., Keller, M. D., Rousseau, V., Smith, W. O. Jr., and Mathot S. (1998). "Autoecology of the marine haptophyte *Phaeocystis* sp," in *Physiological Ecology of Harmful Algal Blooms NATO ASI Series*, eds D. M. Anderson, A. D. Cembella, and G. M. Hallegraeff (Berlin: Springer Verlag), 209–224

Legendre, P. and Legendre, L. (1998). *Numerical Ecology*, 2nd edn. Amsterdam: Elsevier ScienceBV.

Legendre, P. and Legendre, L. (2012). *Numerical Ecology: Developments in Environmental Modelling*, Vol. 24. Amsterdam: Elsevier Science and Technology.

Leibold, M.A. (1997). Do nutrient-competition models predict nutrient availabilities in limnetic ecosystems? *Oecologia* 110, 132–142. doi: 10.1007/s004420050141

Leibold, M. A. (1999). Biodiversity and nutrient enrichment in pond plankton communities. *Evol. Ecol. Res.* 1, 73–95.

Leynaert, A, Bucciarelli, E., Claquin, P., Dugdale, R. C., Martin-Jézéquel, V., Pondaven, P., and Ragueneau, O. (2004). Effect of iron deficiency on diatom cell size and silicic acid uptake kinetics. *Limnol. Oceanogr.* 49, 1134–1143. doi: 10.4319/lo.2004.49.4.1134

Lingoes, J. C. (1971). Some boundary conditions for a monotone analysis of symmetric matrices. *Psychometrika* 36, 195–203. doi: 10.1007/BF02291398

Litchman, E, Klausmeier, C. A, Schofield, O. M, Falkowski, P.G (2007). The role of functional traits and trade-offs in structuring phytoplankton communities: scaling from cellular to ecosystem level. *Ecol. Lett.* 10, 1170–1181. doi: 10.1111/j.1461-0248.2007.01117.x

Litchman, E., and Klausmeier, C. A. (2008). Trait-based community ecology of phytoplankton. *Annu. Rev. Ecol. Evol. Syst.* 39, 615-639. doi: 10.1146/annurev.ecolsys.39.110707.173549

Litchman, E., Ohman, M. D., and Kiørboe, T. (2013). Trait-based approaches to zooplankton communities. *J. Plankton Res.* 35, 473–484.

Long, J. D., Smalley, G. W., Barsby, T., Anderson, J. T; and Hay, M. E. (2007). Chemical cues induce consumer-specific defenses in a bloom forming marine phytoplankton. *Proc. Natl. Acad. Sci. U.S.A.* 104, 10512–10517.

Lorenzen, C. J. (1967). Determination of chlorophyll and pheopigments: spectrophotometric equations. *Limnol. Oceanogr.* 12, 343–346. doi: 10.4319/lo.1967.12.2.0343

Lovecchio, S., Climent, E., Stocker, R., and Durham, W. M. (2019). Chain formation can enhance the vertical migration of phytoplankton through turbulence. *Sci. Adv.* 5:eaaw7879. doi: 10.1126/sciadv.aaw7879

Lund, J. W. G., Kipling, C., and Le Cren, E. D. (1958). The inverted microscope method of estimating algal numbers and the statistical basis of estimations by counting. *Hydrobiologia* 11, 143–170. doi: 10.1007/BF00007865

Maar, M., Nielsen, T. G., Richardson, K. (2002). Spatial and temporal variability of food web structure during the spring bloom in the Skagerrak. *Mar. Ecol. Prog. Ser.* 239, 11–29.

Mack, H. R., Conroy, J. D., Blocksom, K. A., Stein, R. A., and Ludsin, S. A. (2012). A comparative analysis of zooplankton field collection and sample enumeration methods. *Limnol. Oceanogr. Methods* 10:41. doi: 10.4319/lom.2012.10.41

Marañón, E. (2015). Cell size as a key determinant of phytoplankton metabolism and community structure. *Annu. Rev. Mar. Sci.* 7, 241–264. doi: 10.1146/annurev-marine-010814-015955

Mari, X., Rassoulzadegan, F., Brussaard, C., and Wassmann, P. (2005). Dynamics of transparent exopolymeric particles (TEP) production by *Phaeocystis globosa* under N- or P limitation: a controlling factor of the retention/export balance? *Harmful Algae* 4, 895–914. doi: 10.1016/j.hal.2004.12.014

Marie, D., Brussaard, C. P. D., Partensky, F., and Vaulot, D. (1999). "Flow cytometric analysis of phytoplankton, bacteria and viruses," in *Current Protocols in Cytometry*, Vol. 11, ed. J. P. Robinson (New York: John Wiley & Sons), 1–15.

Martin-Jézéquel, V., and Lopez, P. J. (2003). Silicon – a central metabolite for diatom growth and morphogenesis. *Prog. Mol. Subcell. Biol.* 33, 99–124. doi: 10.1007/978-3-642-55486-5_4

Martin-Jézéquel, V., Hildebrand, M., Brzezinski, M. A. (2000). Silicon metabolism in diatoms: implications for growth. *J. Phycology* 36, 821–840. doi: 10.1104/pp.107.107094

Mason, N.W., de Bello, F., Mouillot, D., Pavoine, S., and Dray, S. (2013). A guide for using functional diversity indices to reveal changes in assembly processes along ecological gradients. *J. Veg. Sci.* 24, 794–806. doi: 10.1111/jvs.12013

Mayfield, M. M., and Levine, J. M. (2010). Opposing effects of competitive exclusion on the phylogenetic structure of communities. *Ecol. Lett.* 13, 1085–1093. doi: 10.1111/j.1461-0248.2010.01509.x

Macarthur, R., and Levins, R. (1967). Limiting similarity, convergence, and divergence of coexisting Species. *Am. Nat.* 101, 377–385. doi: 10.1086/282505

McGinty, N., Barton A. D., Record, N. R., Finkel, Z. V., and Irwin, A. J. (2018). Traits structure copepod niches in the North Atlantic and Southern Ocean. *Mar. Ecol. Prog. Ser.* 601, 109–126. doi: 10.3354/meps12660

MacKenzie, B. R., and Leggett, W. C. (1991). Quantifying the contribution of small-scale turbulence to the encounter rates between larval fish and their zooplankton prey: effects of wind and tide. *Mar. Ecol. Prog. Ser.* 73, 149–160. doi: 10.3354/meps213229

Mason, N. W. H., Mouillot, D., Lee, W. G., and Wilson, J. B. (2005). Functional richness, functional evenness and functional divergence: the primary components of functional diversity. *Oikos* 111, 112–118. doi: 10.1111/j.0030-1299.2005.13886.x

McLean, M. J., Mouillot, D., Goascoz, N., Schlaich, I., and Auber, A. (2019). Functional reorganization of marine fish nurseries under climate warming. *Glob. Chang. Biol.* 25, 660–674. doi: 10.1111/gcb.14501

Menden-Deuer, S., and Lessard, E. J. (2000). Carbon to volume relationships for dinoflagellates, diatoms, and other protist plankton. *Limnol. Oceanogr.* 45, 569–579. doi: 10.4319/lo.2000.45.3.0569

Ménesguen, A., Desmit, X., Dulière, V., Lacroix, G., Thouvenin, B., Thieu, V., Dussauze, M. (2018). How to avoid eutrophication in coastal seas? A new approach to derive river-specific combined nitrate and phosphate maximum concentrations. *Sci. Tot. Environ.* 628, 400–414. doi: 10.1016/j.scitotenv.2018.02.025

Menezes, R. F., Borchsenius, F., Svenning, J. C., Davidson, T. A., Søndergaard, M., Lauridsen, T. L., Landkildehus, F., and Jeppesen, E. (2015). Homogenization of fish assemblages in different lake depth strata at local and regional scales. *Fresh. Biol.* 60, 745–757. doi: 10.1111/fwb.12526

Mitra, A., Castellani, C., Gentleman, W. C., Jónasdóttir, S. H., Flynn, K. J, Bode, A., et al. (2014). Bridging the gap between marine biogeochemical and fisheries sciences; configuring the zooplankton link. *Prog. Oceanogr.* 129, 176–199. doi: 10.1016/j.pocean.2014.04.025

Mondy, C. P., and Usseglio-Polatera, P. (2014). Using fuzzy-coded traits to elucidate the nonrandom role of anthropogenic stress in the functional homogenisation of invertebrate assemblages. *Fresh. Biol.* 59, 584–600. doi: 10.1111/fwb.12289

Morel, A., and Smith, R. C. (1974). Relation between total quanta and total energy for aquatic photosynthesis. *Limnol. Oceanogr.* 19, 591–600. doi: 10.4319/lo.1974.19.4.0591

Muscarella, R., and Uriarte, M. (2016). Do community-weighted mean functional traits reflect optimal strategies? *Proc. Biol. Sci.* 283:20152434. doi: 10.1098/rspb.2015.2434

Musielak, M. M., Karp-Boss, L., Jumars, P. A., and Fauci, L. J. (2009). Nutrient transport and acquisition by diatom chains in a moving fluid. *J. Fluid Mech.* 638, 401–421.

Naselli-Flores, L., Zohary, T., and Padisák, J. (2021). Life in suspension and its impact on phytoplankton morphology: an homage to Colin S. Reynolds. *Hydrobiologia* 848, 7–30. doi: 10.1007/s10750-020-04217-x

Nejstgaard, J. C., Tang, K., Steinke, M., Dutz, J., Koski, M., Antajan, E., and Long, J. (2007). Zooplankton grazing on *Phaeocystis*: a quantitative review and future challenges. *Biogeochemistry* 83, 147–172. doi: 10.1007/s10533-007-9098-y

Nelson, C. E., Danuta, M. B., and Bradley, J. C. (2013). Consistency and sensitivity of stream periphyton community structural and functional responses to nutrient enrichment. *Ecol. Appl.* 23, 159–173. doi: 10.1890/12-0295.1

Nissen, C., and Vogt, M. (2021). Factors controlling the competition between Phaeocystis and diatoms in the Southern Ocean and implications for carbon export fluxes. *Biogeosciences* 18, 251–283. doi: 10.5194/bg-18-251-2021

Oksanen, J., Blanchet, G. F, Kindt, R., Legendre, P. (2011). *Vegan: Community Ecology Package*. Available online at: http://cran.r-project.org/web/packages/vegan/index.html

Olden, J. D., Poff, N. L., Douglas, M. R., Douglas, M. E., and Fausch, K. D. (2004). Ecological and evolutionary consequences of biotic homogenization. *Trends Ecol. Evol.* 19, 18–24. doi: 10.1016/j.tree.2003.09.010

Pan, Q., Tian, D., Naeem, S., Auerswald, K., Elser, J.J., Bai, Y., et al. (2016). Effects of functional diversity loss on ecosystem functions are influenced by compensation. *Ecology* 97: 2293-2302. doi: 10.1002/ecy.1460

Pančić, M., and Kiørboe, T. (2018). Phytoplankton defense mechanisms: traits and trade-offs. *Biological Reviews* 93: 1269–1303. doi: 10.1111/brv.12395

Pančić, M, Torres, R. R., Almeda, R, Kiørboe, T. (2019). Silicified cell walls as a defensive trait in diatoms. *Proc. Biol. Sci.* 24:20190184. doi: 10.1098/rspb.2019.0184

Plankton Ciliate Project (2002). *Plankton Ciliate Project. University of Liverpool*. Available online at: http://www.liv.ac.uk/ciliate/intro.htm

Podani, J. (1999). Extending Gower's general coefficient of similarity to ordinal characters. *Taxon* 48, 331–340. doi: 10.2307/1224438

Pohlert, T. (2014). *The Pairwise Multiple Comparison of Mean Ranks Package (PMCMR). R package*. Available online at: http://CRAN.R-project.org/package=PMCMR

Proulx, M. and Mazumder, A. (1998), Reversal of grazing impact on plant species richness in nutrient-poor vs. nutrient-rich ecosystems. Ecology 79, 2581–2592.

Putt, M., and Stoecker, D. K. (1989). An experimentally determined carbon: volume ratio for marine "oligotrichous" ciliates from estuarine and coastal waters. *Limnol. Oceanogr.*, 34, 1097–1103. doi: 10.4319/lo.1989.34.6.1097

R version 3.5.3 (2019). "Great Truth", the R Foundation for Statistical Computing Platform: i386-w64-mingw32/i386 (32-bit). Vienna: R Foundation for Statistical Computing.

Richirt, J., Goberville, E., Ruiz-Gonzalez, V., and Sautour, B. (2019). Local changes in copepod composition and diversity in two coastal systems of Western Europe, Estuar. Coast. Mar. Sci. 227:106304. doi: 10.1016/j.ecss.2019.106304

Riley, G. A. (1957). Phytoplankton of the north central Sargasso Sea. *Limnol. Oceanogr.* 2, 252–270. doi: 10.1002/lno.1957.2.3.0252

Robert P., and Escoufier Y. (1976). A unifying tool for linear multivariate statistical methods: the RV-coefficient. J. Appl. Stat., 25, 257–265.

Rogalski, M. A., Skelly, D. K., and Leavitt, P. R. (2017). Daphniid zooplankton assemblage shifts in response to eutrophication and metal contamination during the Anthropocene. *P. Roy. Soc. B Biol. Sci.*, 284:20170865. doi: 10.1098/rspb.2017.0865

Rose, M. (1933). *Copépodes pélagiques. – Faune de France*, Vol. 26, ed. P. Lechevalier (Paris), 374. Available online at: https://faunedefrance.org/bibliotheque/docs/M.ROSE(FdeFr26)Copepodes-pelagiques.pdf

Rousseau, V., Mathot, S., and Lancelot, C. (1990). Calculating carbon biomass of *Phaeocystis* sp. from microscopic observations. *Mar. Biol.* 107, 305–314. doi : 10.1007/BF01319830

Rousseau, V., Chrétiennot-Dinet, M. J., Jacobsen, A., Verity, P., and Whipple, S. (2007). The life cycle of *Phaeocystis*: state of knowledge and presumptive role in ecology. Biogeochemistry 83, 29–47. doi: 10.1007/s10533-007-9085-3

Schapira, M., Vincent, D., Gentilhomme, V., and Seuront, L. (2008). Temporal patterns of phytoplankton assemblages, size spectra and diversity during the wane of a *Phaeocystis globosa* spring bloom in hydrologically contrasted coastal waters. *J. Mar. Biol. Assoc.* U. K. 88, 649–662. doi: 10.1017/S0025315408001306

Schiller, J. (1931–1937). "Dinoflagellatae (Peridinineae) in monographischer Behandlung," in *Kryptogamen-Flora von Deutschland, Österreichs und der Schweiz. Akad, (Vol. 10 (3): Teil 1 (1–3) (1931–1933): Teil 2 (1–4) (1935–1937))* ed L. Rabenhorst (Leipzig: Verlag).

Schoemann, V., Becquevort, S., Stefels, J., Rousseau, V., and Lancelot, C. (2005). *Phaeocystis* blooms in the global ocean and their controlling mechanisms: a review. *J. Sea Res.* 53, 43–66. doi: 10.1016/j.seares.2004.01.008

Schwaderer, A. S., Yoshiyama, K., De Tezanos Pinto, P., Swenson, N. G., Klausmeier, C. A., and Litchman, E. (2011). Eco-evolutionary differences in light utilization traits and distributions of freshwater phytoplankton. *Limnol. Oceanogr.* 56, 589–598. doi: 10.4319/lo.2011.56.2.0589

Seuront, L., Lacheze, C., Doubell, M. J., Seymour, J. R., Van DongenVogels, V., Newton, K., Alderkamp, A. C., and Mitchell, J. G. (2007). The influence of *Phaeocystis globosa* on microscale spatial patterns of chlorphyll a and bulk-phase seawater viscosity. Biogeochemistry 83, 173–188.

Shipley, B. (2010). *From Plant Traits to Vegetation Structure: Chance and Selection in the Assembly of Ecological Communities*. Cambridge: Cambridge University Press.

Silverman, B. W. (1986). *Density Estimation for Statistics and Data Analysis*. London: Chapman and Hall.

Simpson, E. H. (1949). Measurement of diversity. *Nature* 163:688.

Smetacek, V. (1999). Diatoms and the ocean carbon cycle. *Protist* 150, 25–32. doi: 10.1016/S1434-4610(99)70006-4

Smith, V. H., and Schindler, D. W. (2009). Eutrophication science: where do we go from here? *Trends Ecol. Evol.* 24, 201–207. doi: 10.1016/j.tree.2008.11.009

Stawiarski, B. (2014). *The Physiological Response of Picophytoplankton to Light, Temperature and Nutrients Including Climate Change Model Simulations*. Ph.D. thesis. Norwich: Universityof East Anglia

Steinberg, D. K., and Landry, M. R. (2017). Zooplankton and the ocean carbon cycle. *Annu. Rev. Mar. Sci.* 9, 413–444. doi: 10.1146/annurev-marine-010814-015924

Stelfox-Widdicombe, C. E., Edwards, E. S., Burkill, P. H., and Sleigh, M. A. (2000). Microzooplankton grazing activity in the temperate and sub-tropical NE Atlantic: summer 1996. *Mar. Ecol. Prog. Ser.* 208, 10–12.

Takabayashi, M., Lew, K., Johnson, A., Marchi, A., Dugdale, R., and Wilkerson, F. P. (2006). The effect of nutrient availability and temperature on chain length of the diatom *Skeletonema costatum*. *J. Plankton Res.* 28, 831–840.

Taylor, B. W., Keep, C. F., Hall, R. O. Jr., Koch, B. J., Tronstad, L. M., Flecker, A., et al. (2007). Improving the fluorometric ammonium method: matrix effects, background fluorescence, and standard additions. *J. N. Am. Benthol. Soc.* 26, 167–177. doi: 10.1899/0887-3593200726

Thackeray, S. J., Jones, I. D. and Maberly, S. C. (2008). Long-term change in the phenology of spring phytoplankton: species-specific responses to nutrient enrichment and climatic change. *J. Ecol.* 96, 523–535. doi: 10.1111/j.1365-2745.2008.01355.x

Thieu, V., Billen, G., and Garnier, J. (2009). Nutrient transfer in three contrasting NW European watersheds: the seine, somme, and scheldt rivers. A comparative application of the Seneque/Riverstrahler model. *Water Res.* 43, 1740–1748.

Tréguer, P., and Pondaven, P. (2000). Global change: silica control of carbon dioxide. *Nature* 406, 358–359. doi: 10.1038/35019236

Van den Hoek, C., Mann, D. G. and Jahns, H. M. (1995). *Algae: An Introduction to Phycology*. Cambridge, MA: Cambridge University Press.

van Rijssel, M., Hamm, C., and Gieskes, W. (1997). *Phaeocystis globosa*(Prymnesiophyceae) colonies: hollow structures built with small amounts of polysaccharides. *Eur. J. Phycol.* 32, 185–192. doi: 10.1080/09670269710001737119

Villéger S., Mason N. W. H., and Mouillot, D. (2008). New multidimensional functional diversity indices for a multifaceted framework in functional ecology. *Ecology* 89, 2290–2301. 10.1890/07-1206.1.

Villéger, S., Grenouillet, G., and Brosse, S. (2014).Functional homogenization exceeds taxonomic homogenization among European fish assemblages. *Global Ecol. Biogeogr.* 23, 1450–1460. doi: 10.1111/geb.12226

Violle, C., Navas, M. L., Vile, D., Kazakou, E., Fortunel, C., Hummel, I.,et al. (2007). Let the concept of trait be functional! *Oikos* 116, 882–892. doi: 10.1111/j.0030-1299.2007.15559.x

Virta, L., Gammal, J., Järnström, M., Bernard, G., Soininen, J., Norkko, J., et al. (2019). The diversity of benthic diatoms affects ecosystem productivity in heterogeneous coastal environments. *Ecology* 100:e02765. doi: 10.1002/ecy.2765

Vitousek, P. M., Mooney, H. A., and Lubchenco, J. (1997). Human domination of Earth's ecosystems. *Science* 277, 494–499. doi: 10.1126/science.277.5325.494

Wengrat, S., Padial, A. A., Jeppesen, E., Davidson, T. A., Fontana, L., Costa-Boddeker, S., and Bicudo, D. C. (2018). Paleolimnological records reveal biotic homogenization driven by eutrophication in tropical reservoirs. *J. Paleolimnol.* 60, 299–309.

White, E. P., Ernest, S. K. M., Adler, P. B., Hurlbert, A. H., and Lyons, S. K. (2010). Integrating spatial and temporal approaches to understanding species richness. *Phil. Trans. R. Soc. B* 365, 3633–3643. doi: 10.1098/rstb.2010.0280

Wickham, H. (2016). *ggplot2: Elegant Graphics for Data Analysis*. New York, NY: Springer-Verlag New York.

Wiebe, P. H. (1988). Functional regression equations for zooplankton displacement volume, wet weight, dry weight, and carbon: a correction. *Fish. Bull.* 86, 833–835.

Williams, R., and Robins, D. B. (1982). Effects of preservation on wet weight, dry weight, nitrogen and carbon contents of *Calanus helgolandicus* (Crustacea: copepoda). *Mar. Biol.* 71, 271–281.

Worm, B., Lotze, H., Hillebrand, H. (2002). Consumer versus resource control of species diversity and ecosystem functioning. *Nature* 417, 848–851. doi: 10.1038/nature00830

Zakaria, H. Y., Hassan, A. M., El-Naggar, H. A., and Abo-Senna, F. M. (2018). Biomass determination based on the individual volume of the dominant copepod species in the Western Egyptian Mediterranean Coast. *Egyptian J. Aquatic Res.* 44, 89–99. doi: 10.1016/j.ejar.2018.05.002

Zhang, Y., Cheng, L., Li, K., Zhang, L., Cai, Y., Wang, X., et al. (2019). Nutrient enrichment homogenizes taxonomic and functional diversity of benthic macroinvertebrate assemblages in shallow lakes. *Limnol. Oceanogr.* 64, 1047–1058. doi: 10.1002/lno.11096

Zhu, L., Fu, B., Zhu, H. (2017). Trait choice profoundly affected the ecological conclusions drawn from functional diversity measures. *Sci. Rep.* 7:3643. doi: 10.1038/s41598-017-03812-8

Conflict of Interest: The authors declare that the research was conducted in the absence of any commercial or financial relationships that could be construed as a potential conflict of interest.

Publisher's Note: All claims expressed in this article are solely those of the authors and do not necessarily represent those of their affiliated organizations, or those of the publisher, the editors and the reviewers. Any product that may be evaluated in this article, or claim that may be made by its manufacturer, is not guaranteed or endorsed by the publisher.

frontiers | Frontiers in Marine Science

TYPE Original Research
PUBLISHED 06 October 2022
DOI 10.3389/fmars.2022.914475

OPEN ACCESS

EDITED BY
Alberto Basset,
University of Salento, Italy

REVIEWED BY
Kyle Edwards,
University of Hawaii at Manoa, United States
Márcio Silva de Souza,
Federal University of Rio Grande, Brazil

*CORRESPONDENCE
Elsa Breton
elsa.breton@univ-littoral.fr

SPECIALTY SECTION
This article was submitted to Marine Ecosystem Ecology, a section of the journal Frontiers in Marine Science

RECEIVED 06 April 2022
ACCEPTED 15 September 2022
PUBLISHED 06 October 2022

CITATION
Breton E, Goberville E, Sautour B, Ouadi A, Skouroliakou D-I, Seuront L, Beaugrand G, Kléparski L, Crouvoisier M, Pecqueur D, Salmeron C, Cauvin A, Poquet A, Garcia N, Gohin F and Christaki U (2022) Multiple phytoplankton community responses to environmental change in a temperate coastal system: A trait-based approach. *Front. Mar. Sci.* 9:914475. doi: 10.3389/fmars.2022.914475

Multiple phytoplankton community responses to environmental change in a temperate coastal system: A trait-based approach

Elsa Breton[1]*, Eric Goberville[2], Benoit Sautour[3], Anis Ouadi[3], Dimitra-Ioli Skouroliakou[1], Laurent Seuront[1,4,5], Gregory Beaugrand[1], Loïck Kléparski[1,6], Muriel Crouvoisier[1], David Pecqueur[7], Christophe Salmeron[7], Arnaud Cauvin[1], Adrien Poquet[1,8], Nicole Garcia[9], Francis Gohin[10] and Urania Christaki[1]

[1]Univ. Littoral Côte d'Opale, CNRS, Univ. Lille, UMR 8187 LOG, Wimereux, France, [2]Unité Biologie des Organismes et Ecosystèmes Aquatiques (BOREA), Muséum National d'Histoire Naturelle, CNRS, IRD, Sorbonne Université, Université de Caen Normandie, Université des Antilles, Paris, France, [3]Univ. Bordeaux, CNRS, UMR 5805 EPOC, Rue Geoffroy Saint Hilaire – Bâtiment B18N, Pessac, France, [4]Department of Marine Resources and Energy, Tokyo University of Marine Science and Technology, Tokyo, Japan, [5]Department of Zoology and Entomology, Rhodes University, Grahamstown, South Africa, [6]Continuous Plankton Recorder (CPR) Survey, Marine Biological Association, Plymouth, United Kingdom, [7]Observatoire Océanologique de Banyuls s/mer, FR 3724 - Laboratoire Arago - SU/CNRS, avenue Pierre Fabre Bât B, Banyuls sur Mer, France, [8]Univ. Côte d'Azur, CNRS, INSERM, IRCAN, Medical School of Nice, Nice, France, [9]Aix Marseille Univ., Université de Toulon, CNRS, IRD, MIO, Marseille, France, [10]Laboratoire d'écologie pélagique, IFREMER, DYNECO PELAGOS, CS 10070-29280 Plouzané, Brittany, France

The effect of environmental change in structuring the phytoplankton communities of the coastal waters of the Eastern English Channel was investigated by applying a trait-based approach on two decades (1996-2019) of monitoring on diatoms and *Phaeocystis*. We show that phytoplankton species richness in an unbalanced nutrient supply context was influenced by wind-driven processes, ecological specialization for dissolved inorganic phosphorous, temporal niche differentiation, and a competition-defense and/or a growth-defense trade-off, a coexistence mechanism where weak competitors (i.e., slower growing) are better protected against predation. Under the influence of both environmental perturbations (e.g., wind-driven processes, freshwater influence, unbalanced nutrient levels) and biotic interactions (e.g., competition, predation, facilitation), phytoplankton species exhibited specific survival strategies such as investment on growth, adaptation and tolerance of species to environmental stresses, silicification and resource specialization. These strategies have led to more speciose communities, higher productivity, functional redundancy and stability in the last decade. Our results revealed that the unbalanced nutrient reduction facilitated *Phaeocystis* blooms and that anthropogenic climate warming and nitrate reduction may threaten the diatom communities of the eastern English Channel in a near future. Our

results provide strong support for biogeographical historical and niche-based processes in structuring the phytoplankton community in this temperate region. The variety of species responses that we characterized in this region may help to better understand future changes in pelagic ecosystems, and can serve as a basis to consider functional approaches for future ecosystem management.

KEYWORDS

biodiversity, community assembly, diatoms, environmental change, functional traits, *Phaeocystis*, phytoplankton community, temporal niche partitioning

Introduction

Species functional traits reflect what species do, how they interact with and how they influence their environment (Violle et al., 2007). Trait-based approaches may therefore prove beneficial to significantly improve our knowledge of the interaction between community assembly and structure, species diversity and ecosystem functioning (McGill et al., 2006; Mayfield and Levine, 2010; Cadotte et al., 2011; Cardinale et al., 2012; Borja, 2014; 2015; De Laender et al., 2016).

Community ecologists typically infer the ecological processes of community assembly by considering that any local community is a subset of a regional species pool shaped by biogeographical and historical effects (Weiher et al., 1998; Grime, 2006): species thriving local community have successfully passed a hierarchy of ecological filters, including dispersal limitation, abiotic and biotic constraints (Zobel, 1997; Weiher et al., 1998; Grime, 2006). While the functional identity of a community often reflects optimal ecological strategies (*e.g.*, predation avoidance, Ackerly, 2003; Muscarella and Uriarte, 2016), functional diversity - in combination with null modelling - informs on the degree of niche overlap (functional convergence/similarity of a community as a proxy) and therefore on the mechanisms of community assembly (Mason et al., 2013). While over-dispersion of functional traits related to resources use is related to competition driven by niche differences (Mc Arthur and Levins, 1967; Cornwell and Ackerly, 2009), an under-dispersion reflects asymmetric competition for one limiting resource and/or abiotic filtering (Cornwell and Ackerly, 2009; Mayfield and Levine, 2010). However, facilitation, another biotic process known to occur in all environmental conditions (McIntire and Fajardo, 2014), may lead to a similar functional diversity outcome (Münkemüller et al., 2020 and references therein). Accordingly, over-dispersion is expected in the case of asymmetric facilitation (*i.e.*, one species favors another) whereas under-dispersion is expected in the case of symmetric facilitation (*i.e.*, species favor each other) (Gallien et al., 2018).

According to the modern coexistence theory (Chesson, 2000), coexistence under limiting resource conditions is maintained only if species either exhibit sufficient niche differentiation with respect to resource use, or are functionally similar (*i.e.*, fitness equalities). As the result of competition among species (Winder, 2009) or an increase in spatio-temporal environmental variability (*e.g.*, Adler et al., 2006; Stein et al., 2014), niche differentiation can be achieved by a multitude of processes, including resource niche partitioning (*e.g.*, Cardinale, 2011) and temporal niche differentiation (Shimadzu et al., 2013), the latter implying specialization of species to specific temporal niches (*e.g.*, Carscadden et al., 2020; Gao et al., 2020). Although trait trade-offs (*e.g.*, the defense-growth trade-off, Ehrlich et al., 2020) promote coexistence (*e.g.*, Kneitel and Chase, 2004; Litchman et al., 2007) by reducing the effect of differences among competitive ability of species, niche differentiation is required for stabilization of coexistence (Chesson, 2008).

The 'niche complementarity effect' hypothesizes that more diverse communities are more likely to favor species which use different resources, while the 'selection effect' promotes highly productive species (Tilman et al., 1997; Loreau, 2000). Both mechanisms facilitate ecosystem functioning (Worm et al., 2006; Ptacnik et al., 2008; Cardinale et al., 2012). Ecosystem functions may also be driven by mechanisms such as the particular traits of the dominant species within a community (the so-called 'mass ratio hypothesis'; Grime, 2006) or be induced by changes in population densities or species composition (Spaak et al., 2017). Given specialists (*i.e.*, species with narrow niche breadth resulting from their preference to particular environments/habitat; see Levins, 1962 and Carscadden et al., 2020) are considered to be more efficient at capturing and consuming resources than generalists (*i.e.*, species with broad environmental tolerance), a loss of specialists is expected to greatly affect material and energy transfer in ecosystems (Olden et al., 2004; Alexander et al., 2016), with putative consequences on ecosystem functioning. More diverse communities may also stabilize ecosystem processes and functions by steadying the

overall biomass of communities (the so-called 'portfolio effect'; Figge, 2004; Duffy, 2009) as a result of asynchrony in species fluctuations (*i.e*, compensation dynamics), evenness, overyielding, and how temporal variability in biomass scales with its mean (Cottingham et al., 2001). Increase in temporal stability may also be the result of a decrease in temporal variability of the dominant species (Steiner et al., 2005).

The Eastern English Channel (EEC) is a well-mixed mesoeutrophic sea under the influence of multiple environmental stressors such as temperature rise (McLean et al., 2019) and the effects of nutrient abatement measures implemented to reverse cultural eutrophication in the northwest European shelf seas (OSPAR, 1988; European Union, 1991a; European Union, 1991b). Over the last decades, these management measures led to a trend reversal in anthropogenic nutrients (Talarmin et al., 2016; Lheureux et al., 2021), with an increase in phosphate limitation in different marine coastal ecosystems (Loebl et al., 2009; Burson et al., 2016; Talarmin et al., 2016). Despite that reduction in nutrients loads to coastal waters, *Phaeocystis* (Phylum Haptophyta, Class Coccolithophyceae) - which forms the bulk of phytoplankton biomass with diatoms and is considered as a symptom of eutrophication (Tett et al., 2007; Burson et al., 2016; Breton et al., 2021) - still forms impressive spring blooms in the EEC (2006; 2017; 2021; Breton et al., 2000) and similar unexpected consequences have been observed elsewhere for diatoms abundance and chlorophyll *a* (McQuatters-Gollop et al., 2007; Duarte et al., 2009; Alvarez-Fernandez et al., 2012; Wiltshire et al., 2015; Xu et al., 2020). While an improvement in light conditions has been suggested as a potential triggering mechanism for phytoplankton increase (*e.g.*, McQuatters-Gollop et al., 2007; Xu et al., 2020), and as important for the maintenance of high *Phaeocystis* biomass given the higher light requirements of this microalga in comparison to diatoms (Jahnke, 1989; Peperzak et al., 1998; Breton et al., 2017); there is still a critical lack of full understanding of the underlying processes behind these unexpected observations. Phytoplankton increase could have been also induced by changes in seawater temperature, nutrient concentrations, and/or nutrient ratios observed in the study area.

Here, we applied a trait-based approach, null modelling and probabilistic hypervolumes to time-series (1996-2019) of diatoms and *Phaeocystis* collected in the EEC in order to (*i*) understand long-term changes in the assembly, structure and dynamic of species assemblages in relation to changing environmental conditions, especially unbalanced nutrient conditions, (*ii*) investigate the impact of environmental changes on different aggregate ecosystem functions and properties, and (*iii*) explore the role played by biodiversity on ecosystem functioning.

Material and methods

Monitoring datasets

Nutrient data (dissolved inorganic phosphorous [DIP], dissolved inorganic silica [DSi], and dissolved inorganic nitrogen as the sum of nitrates, nitrites and ammonium [DIN]), chlorophyll *a* (Chla, µg L^{-1}), Particulate Organic Nitrogen (PON, µg L^{-1}) and phytoplankton were collected at high tide by means of a Niskin Water Sampler (8 L) from subsurface (2m depth) samples originating from the coastal station "C" in the Eastern English Channel (50°40'75 N; 1° 31'17E, 20-25 m maximum depth) that belongs to the French coastal monitoring network SOMLIT (https://www.somlit.fr/). Nutrient concentrations were analyzed according to Aminot and Kérouel (2004) using autoanalyzer systems (Technicon, Alliance, and Seal Instruments), except for ammonium (NH4). Ammonium concentrations were assessed by spectrometry up to 2008 according to Koroleff (1970) and Solorzano (1969) and by fluorimetry from 2009 according to Holmes et al. (1999) and Taylor et al. (2007). Chlorophyll *a* was estimated by fluorometry (Lorenzen, 1967) from a 100-250 ml sample of seawater filtrated through glass fiber filters (Whatman, GF/F, 25 mm) and free of pigment (extraction in acetone 90% in the dark at 4°C for 12h). PON was assessed on a NA2100 Frisons CHN analyzer according to Aminot and Kérouel (2004).

Subsurface temperature (SST, °C) and salinity (S), and the mean diffuse attenuation coefficient for downwelling irradiance (Kd, m^{-1}) were assessed from instantaneous vertical CTD profiles with a Conductivity Temperature Depth (CTD) Seabird profiler equipped with a Photosynthetically Active Radiation (PAR, E m^{-2} d^{-1}) sensor (QSP 2300; Biospherical Instruments). Seawater density (D, kg m^{-3}) was calculated from the CTD data using SST, S and pressure (db), and the 1980 UNESCO International Equation of State (IES80, Millero et al., 1980; Millero and Poisson, 1981). The vertical stratification index (VSI) was calculated over the water column using separately temperature and density data according to the general formula:

$$VSI = \Sigma(x_z - x_{z-1}) \quad (1)$$

where X is the observed temperature or density value at a given depth z (m).

The average daily PAR experienced by phytoplankton in the water column, for a 6-day period before sampling, was obtained from Kd and global solar radiation (GSR, Wh m^{-2}) from the Copernicus Atmosphere Monitoring Service (CAMS) radiation service (http://www.soda-pro.com/web-services/radiation/cams-radiation-service) using the formula of Riley (1957). GSR was

converted into PAR by assuming PAR to be 50% of GSR and by considering 1 W m^{-2} = 0.36 E m^{-2} d^{-1} (Morel and Smith, 1974).

Local and regional meteorological data are described in Table S1 and details on large-scale hydro-climatological indices (the Northern Hemisphere Temperature (NHT), the East Atlantic (EA), the North Atlantic Oscillation (NAO), and the Arctic Oscillation (AO) are given in Lheureux et al. (2021). Information on the East Atlantic Western Russian (EAWR) pattern, one of most prominent teleconnection patterns that affects Eurasia throughout year, can be found at https://www.cpc.ncep.noaa.gov/data/teledoc/eawruss.shtml/.

Biological samples of diatoms and *Phaeocystis* were fixed with Lugol-glutaraldehyde solution (1% v/v; a fixative that does not disrupt *Phaeocystis* colonies; Breton et al., 2006) and examined using an inverted microscope (Nikon Eclipse TE2000-S) with 100-400x magnification after sedimentation in 5–25 mL Hydrobios chambers. Biovolume measurements were made over the entire period using standard geometric forms according to Hillebrand et al. (1999). Abundance and biovolume of *Phaeocystis* colonial cells were counted according to Rousseau et al. (1990). Carbon biomass of diatoms and *Phaeocystis* (µg C l^{-1}) were calculated using the carbon conversion factors of Menden-Deuer and Lessard (2000) and the value of 89.5 pg C $cell^{-1}$ (van Rijssel et al., 1997), respectively. The list of diatom species is provided in Supplementary Table S2, with information about occurrence frequency (%), and species average abundance (N L^{-1}) and biomass (µg C L^{-1}). Note that a subset of the phytoplankton count datasets used in this study has been previously published (Breton et al., 2021).

Given that at least some 80% of the total biomass are required to be representative of the functional identity of the communities (Pakeman and Quested, 2007; see '*Functional diversity metrics*' sub-section), available flow cytometry data of cryptophytes, picoeukaryotes and *Synechococcus* over the period 2009-2019 were used to ensure the dominant contribution of diatoms and *Phaeocystis* to total phytoplankton biomass. For flow cytometry, 5mL samples were fixed with glutaraldehyde (1.33% v/v) and kept at -80°C until analysis (FACSCan, BD Biosciences; Marie et al., 1999; abundance data are available at https://www.somlit.fr/). Dinoflagellates (auto- and mixotrophic) were counted by microscopy to complete the phytoplankton datasets. Identifications were made at the species level when possible, according to Schiller (1931–1937); Gómez and Souissi (2007); Hoppenrath et al. (2009) and Maar et al. (2002). Carbon biomass of auto- and mixo- dinoflagellates and cryptophytes were obtained from biovolume measurements according to Hillebrand et al. (1999) and the carbon conversion factors of Menden-Deuer and Lessard (2000). Carbon biomass of *Synechococcus* spp. and picoeukaryotes were determined using the carbon conversion factors of 154 fgC $cell^{-1}$ and 1319 fgC $cell^{-1}$ (Buitenhuis et al., 2012), respectively.

Phytoplankton species traits

For each of the 74 diatom species and *Phaeocystis*, biovolume (V, μm^3), Maximum Linear Dimension (MLD, µm), and the surface to biovolume cell ratio (S/V ratio) were calculated from the median values of microscopic measurements realized over the entire period (Breton unpublished data). The apparent degree of silicification (*i.e.*, 1: slight; 2: medium; 3: heavy) was based on Hasle and Syvertsen (1996) and Hoppenrath et al. (2009). The potential degree of coloniality for diatoms (*i.e.*, 0: None; 1:<5 cells; 2: 5-20 cells; 3: >20 cells; 4>50 cells) was assessed through the cultivation of each diatom species under F/20 medium and with a light:dark cycle of 12:12h at an irradiance of 400 µmol photons m^{-2} s^{-1} (Daylight HQIT-WD 250 W F, OSRAM Gmbh, Műnchen, Germany).

Biovolume is a key trait that relates to various ecophysiological attributes for resource acquisition, reproduction and predator avoidance (Litchman and Klausmeier, 2008; Karp-Boss and Boss, 2016). Species with high S/V cell ratio and long cellular chain length - that favor cell suspension in the water column and increase nutrient flux - have a great competitive ability under nutrient limitation (Grover, 1989; Karp-Boss et al., 1996; Tabakabayashi et al., 2006; Musielak et al., 2009; Lovecchio et al., 2019). Higher S/V cell ratio and weaker silicified species have also been related to lower silica requirement under laboratory (Leynaert et al., 2004) and DSi limitation conditions (Martin-Jézéquel et al., 2000; Martin-Jézéquel and Lopez, 2003). Cell elongation enhances both cell buoyancy (Grover, 1989; Naselli-Flores et al., 2021) and protection against photo-inhibition, especially for larger cells because of a lower cross-section for photoinactivation of PSII, and lower maximum metabolic rates than for smaller cells (Key et al., 2010; Schwaderer et al., 2011). Prey biovolume (Litchman and Klausmeier, 2008), the degree of coloniality (Bjærke et al., 2015), and the apparent degree of silicification (Pančić et al., 2019), reflect resource use and/or requirement and mirror ecological processes/functions linked to predation. A composite defense trait was then built based on the methodology described in Breton et al. (2021), i.e., by summing the scores of each of following traits: (i) the capacity to produce mucous or toxins (Yes: 1; No: 0), (ii) the presence of setae and/or spicules – which favor buoyancy; Van den Hoek et al., 1995 – (Yes: 1; No: 0), (iii) the degree of silicification (1: slight; 2: medium; 3: heavy), and (iv) coloniality (0: None; 1:<5 cells; 2: 5-20 cells; 3: >20 cells; 4>50 cells). More detail can be found in the supplementary material of Breton et al. (2021). All the trait values used in this study are given in supplementary data. Note that a subset of this dataset has been previously published (Breton et al., 2021).

The chlorophyll *a*-to-carbon ratio for phytoplankton (Chl *a*/C ratio, in µgChl *a* µgC $^{-1}$) was calculated using microscopic counts. The cell carbon was computed from the equations of

Menden-Deuer and Lessard (2000). Although the Chl *a*/C ratio is not a trait *sensu strictissimo* (Litchman and Klausmeier, 2008), it stems from processes linking the traits of species and the alleviation (or accentuation) of external limiting factors such as light/nutrients availability, in particular nitrogen (Thackeray et al., 2008; Jakobsen and Markager, 2016). This ratio is known to be a relevant proxy of phytoplankton growth rate (Cloern et al., 1995; Le Bouteiller et al., 2003).

Functional diversity metrics

In addition to species richness and Pielou's indices (Pielou, 1966, Step 1, Figure 1), we characterized the functional structure and functional diversity of phytoplankton communities by means of the (*i*) Community-Weighted Mean (CWM; the mean trait value among each community weighted by the relative biomass of each species; Garnier et al., 2004), (*ii*) functional richness (FRic), (*iii*) functional evenness (FEve), and (*iv*) Rao Quadratic entropy (RaoQ). CWM is a proxy of functional identity, *i.e.*, the optimal trait strategy (Ackerly, 2003; Muscarella and Uriarte, 2016). Functional richness corresponds to the volume of functional niche space filled by a species within a community (Villéger et al., 2008). Functional evenness is the regularity with which species biomass in a community is distributed along the minimum spanning tree that links all species in the multidimensional trait space (Mason et al., 2005). RaoQ is the sum of pairwise distances between species, weighted by the relative biomass within the multidimensional trait space (Botta-Dukát, 2005). This index is a relevant proxy of functional divergence and was selected over other similar metrics for its ability to detect assembly rules significantly better (Botta-Dukát and Czúcz, 2016).

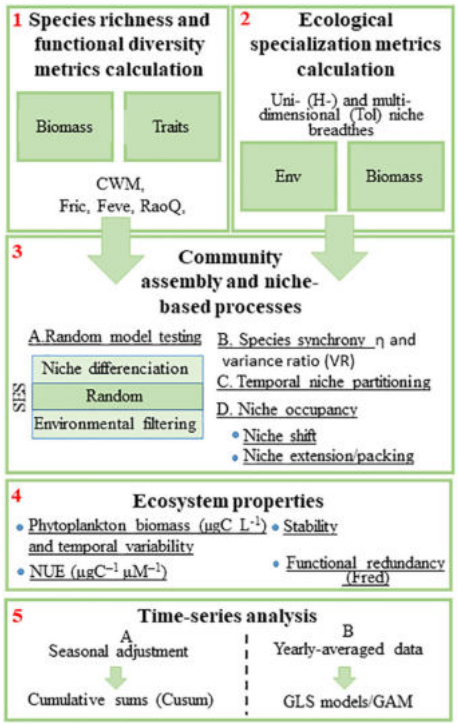

FIGURE 1
The 5 main steps in our statistical methodology to explore the link between the environment, phytoplankton biodiversity, and ecosystem functioning, and the underlying mechanisms and processes. Step 1: characterization of the plankton community trait distributions and biodiversity; Step 2: characterization of the ecological specialization of the phytoplankton community; Step 3: exploration of the mechanisms/niche-based processes of phytoplankton coexistence (SES, Standardized Effect Size); Step 4: Calculation of different ecosystem properties (phytoplankton biomass [µgC L^{-1}], Nitrogen Use Efficiency [NUE, µg C^{-1} μM^{-1}], Stability, and functional redundancy); Step 5: Time-series analysis. H, unidimensional niche; Tol, environmental tolerance; Env, environmental variables; CWM, community-weighted mean; RaoQ, functional divergence; FEve, functional evenness; Fric, functional richness; FRed, functional redundancy; GLS, Generalized Least Squares; GAM, Generalized Additive Models.

The precision of functional diversity indices, especially FRic and FEve, is sensitive to the incompleteness in species and/or traits data (Pakeman, 2014). Here, we considered 74 diatom species and *Phaeocystis*, which represented the majority of the phytoplankton species richness in coastal waters of the EEC (2021; Breton et al., 2017). Auto-/mixo dinoflagellates included 10 species (see Breton et al., 2021, Table S3). For smaller phytoplankton, which cannot be accurately identified by microscopy, several molecular surveys in the area (*e.g.*, 2016; Genitsaris et al., 2015) have previously found that pico eukaryotes were dominated by prasinophyceans (*Micromonas* spp., *Bathycoccus* spp.), *Teleaulax* spp. and *Plagioselmis* spp. for cryptophytes, and *Emiliania huxleyi* for coccolithophorids.

The functional indices for the diatoms and *Phaeocystis* communities were calculated from the biovolume, the apparent degree of silicification, coloniality, the S/V cell ratio, and MLD. For each observation (*i.e.*, sampling unit), the functional metrics were computed on log-transformed species biomass to reduce a potential influence of the most abundant species using the R package 'FD' (Functional Diversity; Laliberté and Legendre, 2010). For FRic, FEve, and RaoQ, a preliminary principal coordinate analysis (PCoA; 'vegan' package; Oksanen et al., 2011) was performed to calculate the multidimensional trait space for each sampling day. Functional diversity was computed from a dissimilarity matrix calculated using both the PCoA axes - as new functional traits - and the Gower distance (Gower, 1971). The Gower distance allows traits of different types, including ordinal (Podani, 1999; Table I), to be included. A square-root transformation ('sqrt') - or a Lingoes correction for negative values (Lingoes, 1971) - was applied when the distance matrix "species × species" was not Euclidean.

Ecological specialization metrics

Ecological specialization (Step 2, Figure 1) was estimated by means of the multi-dimensional Outlying Mean Index (OMI,

hereafter called 'environmental tolerance'; Dolédec et al., 2000) and uni-dimensional niche breadth analysis using the 'ade4' (Chessel et al., 2004; Dray et al., 2007) and 'hypervolume' R packages (Blonder et al., 2014). Environmental tolerance was based on species biomass, considering SST, salinity, wind stress, nutrients, and PAR. Unidimensional niche breadth (DIN, DIP, DSi, PAR, SST, and salinity) was determined from kernel density using (*i*) the environmental conditions encountered by each species, (*ii*) a Silverman bandwidth estimator and (*iii*) a 0% quantile threshold (Blonder et al., 2014). Niche breadth and environmental tolerance reflect the range of an abiotic factor determining the distribution and species biomass of a species, respectively. Advantages and disadvantages of each method are detailed in Breton et al. (2021). Considering one ecological dimension, we then calculated the Community-Weighted Mean (CWM; see '*Functional diversity metrics*') of the niche breadth to estimate the degree of ecological specialization at the community scale. A decrease in any CWM of the niche breadth for one dimension mirrors an increase in the degree of ecological specialization of the phytoplankton community.

Niche based-processes of community assembly

The inference of environmental filtering and biotic interactions (Step 3, Figure 1) were estimated from the deviation (Standardized Effect Size [SES]; Gotelli and McCabe, 2002) between functional diversity metrics (FRic, FEve, and RaoQ) calculated on a given (*i.e.*, observed) phytoplankton community and functional values obtained from a random community: for each sampling date, trait data were randomized arbitrarily (times=1000; 'permatfull' in the 'vegan' R package), while maintaining species richness and abundance constant. SES was calculated as follows:

$$SES = \frac{x_{obs} - \bar{x}_{ran}}{\sigma_{ran}} \quad (2)$$

where x_{obs} is the observed values of functional metric at a given date; $\bar{x}_{ran}$ is the mean; and σ_{ran} is the standard deviation of the functional diversity of randomly assembled communities. Assuming a normal distribution of the random communities, the traits derived from the sampling dates falling into the 95th (or higher) percentile of the random distribution were considered 'over-dispersed' (*i.e.*, niche differentiation being the major process driving community assembly); trait falling into the 5th (or lower) percentile were considered 'under-dispersed' (*i.e.*, environmental filtering as the major process).

The degree of temporal synchrony (η) between diatom and *Phaeocystis* species and the variance ratio (VR) were calculated for each year on monthly-averaged species biomass according to Gross et al. (2014) and Schluter (1984), respectively, using the 'codyn' R package (Hallett et al., 2020):

$$\eta = \frac{1}{n}\sum_{i} corr \qquad (Yi, \quad \sum_{j\neq 1} Yj) \quad (3)$$

and

$$VR = \frac{\sum_{i=1}^{n} Var\ (Y_i) + 2(\sum_{i=1}^{n-1}\sum_{j=i+1}^{n} Cov(Y_i, Y_j))}{\sum_{i}^{n} Var(Y_i)} \quad (4)$$

where n is the number of species, and Y_i and Y_j, the biomass of the species *i* and that of all other species than species *i*, respectively.

The approach of Gross et al. (2014) for synchrony calculation was preferred to the equation of Loreau and de Mazincourt (2008) because it equally weights species. This index varies between -1 (perfect asynchrony) and 1 (perfect synchrony). The variance ratio, VR = 1 indicates that species do not covary, whereas VR > 1 or<1 indicates predominately positive (*i.e.*, synchronous dynamics) and negative *(i.e.*, compensatory dynamics) covariance among species, respectively (Schluter, 1984). To test if the observed VR value was significantly different from 1, a thousand null communities were created by randomly selecting different starting points for each species' time series, allowing species biomass to vary independently while maintaining. within-species autocorrelation (Hallett et al., 2020). VR is considered to be significantly different from 1 when the observed VR value falls outside of the 2.5th and the 97.5th percentiles of the null distribution.

Potential temporal niche partitioning and its causes (niche shift *vs* niche packing/expansion processes) were assessed between successive pairs of phytoplankton communities by considering the DIP dimension (*i.e.*, the hypothesized main limiting resource for growth, see Loebl et al., 2009; Burson et al., 2016; Talarmin et al., 2016) and using the function *kernel.beta* (Carvalho and Cardoso, 2020; Mammola and Cardoso, 2020) from the 'BAT' R package (Cardoso et al., 2014) and by choosing the Jaccard similarity index. Niche shift corresponds to change in niche position of a given species from one community to another (*i.e.*, occupation of a different niche space between two successive communities); niche packing/expansion corresponds to the differences in niche breadth between two successive communities.

Ecosystem properties

Here, we focused on five ecological properties that are important for ecosystem functioning and for which data for their calculation were available: (*i*) phytoplankton biomass and (*ii*) its variability, (*iii*) the temporal stability of community-level biomass (reviewed in Cottingham et al., 2001; Loreau et al., 2002), (*iv*) the Nitrogen Use Efficiency (NUE; Ptacnik et al., 2008), and (*v*) functional redundancy (FRed). Temporal stability of community-level biomass - the inverse coefficient of variation

of biomass - was calculated on monthly log-transformed time-series of diatom and *Phaeocystis* carbon biomass using the 'codyn' R package (Hallett et al., 2020). Given that communities mainly composed of functionally redundant species may improve ecosystem resilience and stability (*e.g.*, Biggs et al., 2020), FRed - the difference between Simpson's diversity and RaoQ (de Bello et al., 2007) computed using the R package 'SYNCSA' (Debastiani and Pillar, 2012) - reflects ecosystem sustainability and the buffer capacity of communities to counteract environmental disturbances. NUE (biomass per unit of nitrogen available µg C^{-1} μM^{-1}) was calculated as:

$$NUE = biomass/(DIN + PON) \quad (5)$$

where DIN and PON are in µM. We did not consider the possibility of organic nitrogen uptake by phytoplankton due to lack of available measuring equipment. Phytoplankton of the English Channel and the southern North Sea has been found to primarily use dissolved inorganic nitrogen (L'Helguen et al., 1993; Moneta et al., 2014).

Data analyses

For each variable, we successively (i) calculated monthly average, (ii) applied the Kalman smoothing filter (Kalman, 1960) for data completion if needed, and (iii) decomposed the completed time-series for seasonal adjustment (*i.e.*, without the seasonal component) using the Loess method (Cleveland and Cleveland, 1990). Data completion and seasonal adjustment were performed using the R packages 'stlplus' (Hafen, 2016) and 'imputeTS' (Moritz and Bartz-Beielstein, 2017; Moritz, 2018), respectively. Before, *Phaeocystis* and diatom biomasses were log (x+1)-transformed. Note that an arbitrary time window of 5 years was chosen for time-series decomposition. To build an index of the wind conditions at a regional scale, we performed a PCA ('ade4' R package) on monthly wind values and their variations (CV), considering four regional weather stations monitored by Meteo-France (Dunkirk, Calais, Boulogne/mer, and Abbeville). A second PCA was calculated to summarize the abiotic conditions encountered by phytoplankton over the study period. Given that environmental heterogeneity may favor niche differentiation by increasing niche availability (*e.g.*, Stein et al., 2014), and because nutrient ratios may play an important role in the outcomes of competitive interactions, the CV of SST, salinity, seawater density, PAR, each nutrient between each pair of consecutive months, and the DIP/DIN, DSi/DIP and DSi/DIN molar ratios were considered in the PCA in addition to mean values. To explore the link between niche breadths along the different niche dimensions that we investigated (DSi, DIN, DIP, SST, salinity, and PAR) and to define the ecological specialization index of the phytoplankton community, we performed a third PCA on the CWMs of niche breadth of the different niche dimensions and environmental tolerance. Prior the three PCAs, skewness of the data was removed to reach normality and all variables were z-transformed to have a mean of zero and a standard deviation of one ('caret' package; Kuhn et al., 2016).

To explore the driver-response relationships of the phytoplankton community patterns/ecosystem properties to the environment, we successively calculated (step 5, Figure 1) cumulative sums (Cusum, Ibañez et al., 1993; Kirby et al., 2009; Regier et al., 2019) and performed Generalized Least Squares for linear regression modelling (GLS, Aitken, 1936) or Generalized Additive Models (GAM, Hastie and Tibshirani, 1990) for non-linear modelling. The Cusum method is particularly well-adapted to the study of environmental time-series because of its robustness for handling incomplete, non-normal, noisy data (Regier et al., 2019), and its potential to reduce the risk of misinterpretation which may result from the use of standard relationship analysis between variables (Regier et al., 2019). However, while previous studies correlated Cusum-transformed variables to explore the relationships between biotic patterns and the environment (*e.g.*, Ibañez et al., 1993; Breton et al., 2006; Glibert, 2010), such an approach violates the assumption of variable independence and is strongly discouraged (Cloern et al., 2012; Regier et al., 2019; but see Lancelot et al., 2012); instead, relationships are assessed by visually evaluating parallelism between Cusum-transformed variables using Cusum charts (Regier et al., 2019 and references therein). By contrast, GLS models and GAM allow accounting for the autocorrelation in time series data, and, therefore, a more quantitative assessment of the driver-response relationships and valid hypothesis testing. Cusum for each time series were obtained by subtracting the mean from all values of the given monthly time-series, and progressively adding the residuals. The Cusum function, called v in the formula, is calculated iteratively as follows (Ibañez et al., 1993; Kirby et al., 2009; Regier et al., 2019):

$$v_t = v_{t-1} + (x_t - \bar{x}) \quad (6)$$

where x_t is the monthly averaged variable at time t (ranging from 1 to n), and $\bar{x}$ is the variable averaged over the whole period of investigation. As a result, the distribution of the Cusum-transformed variables has a mean of 0 and a standard deviation of 1. The sign and the slope of the Cusum plots reveals trend and sub-cycle patterns, thresholds and changes in mean values along a time series of two or more variables (Regier et al., 2019). Positive v_t values indicate a deviation of x_t above the mean, while negative values indicate a deviation below the mean; increasing and decreasing slopes reveal values (on average) above and below and the mean of the time series, respectively. A transition from negative (positive) to positive (negative) slopes shows a shift in the time series from lower (higher) to higher (lower) than the mean (Regier et al., 2019). For regression modelling, we first computed Pearson correlations (package

'corrplot'; Wei and Simko, 2021) between the different variables using annual and standardized data. Each model was then built (i) by sequentially selecting (*i.e.*, forward selection) the significantly correlated variables, (ii) by accounting for a serial correlation AR(1) model for the errors and potential interaction between predictors when applicable, and (iii) using the Maximum-Likelihood method. The variance inflation factor (VIF) per variable was also calculated using the package 'car' (Fox and Weisberg, 2019) to ensure that multi-collinearity between predictors of the model was negligible (VIF<3). Based on the Akaike information criterion (AIC), we retained the most parsimonious model. All models were checked for accuracy by ensuring that the structure of the Autocorrelation and Partial-autocorrelation functions (ACF/PACF) of the model residuals meet the properties of an AR(1) model. GLS and GAM were performed using the R packages 'nlme' (Pinheiro et al., 2022) and 'mgcv' (Wood, 2017), respectively; and the function corAR1 (form=~year) for the correlation structure of the residuals.In our study, only the clear driver-response relationships (*i.e.*, parallelism or anti-parallelism for Cusums and significant ($p<0.05$) GLS or GAM models) are shown (Tables 3–5 and S3; and Figures 5A–F, 6A–E, 7, 9A–F, and 10A–C).

Results

The range, mean (± SD) and median values of the environmental conditions recorded at the monitoring coastal station "C" over the period 1996-2019 are given in Table 1. The values of nutrients and Kd were in the common range of coastal stations of the English Channel (*e.g.*, Lefebvre et al., 2011; Napoléon et al., 2012; Houliez et al., 2013; Saulquin et al., 2013; Bonato et al., 2016). Based on the Redfield and Brzezinski ratios (Redfield et al., 1963; Brzezinski, 1985), the nutrient molar ratio values recorded at station "C" showed that DIN was regularly in excess over DIP over the last two decades (Table 2). The trend towards DIP-limitation occurred from 2005 to 2015 and resulted from an increase in DIN : DIP and DSI : DIP peak events well above the Redfield (1963) and Brzezinski (1985) ratios (*i.e.*, >>16, Figures 2A, B). The DIN : DIP and DSI : DIP ratios decreased abruptly from 2015 to reach values similar to those recorded in the early 2000s, indicating an excess in DIP at both periods (DIN : DIP and DSI: DIP ratio value<<16). The analysis of the phytoplankton composition available for the last decade indicated that phytoplankton was mainly composed of diatoms and *Phaeocystis* biomass (86 ± 16%, Figures 3A, B), but for several dates from mid-2015 to end-2019 when picoeukaryotes and cryptophytes contributed altogether to more than 50% of the total phytoplankton biomass (20% of the observations). On a seasonal scale (Figure 3C), diatoms and *Phaeocystis* biomass contributed in average to 91% to phytoplankton biomass; the lowest and highest contributions occurring in November-December (78 and 80%, respectively) and in April during the maximum of the *Phaeocystis* bloom, respectively. The list of the ten most dominant diatom species in term of carbon biomass identified over the period 1996-2019 is given in Table 2 (see Table S2 for all the diatom species).

The cumulative sums calculated on the first three independent PCs (PC1-3, Figures 4A–C) of the PCA performed on the seasonally-adjusted mean abiotic environmental conditions and their variability (see Figures S1A–C for details) were synchronous with changes in twelve of the phytoplankton community patterns that we measured (Figures 5A–F, 6A–E, and 7). The Cusum of the inverse PC1 axis (INV-PC1, 20.3% of the total variability, Figures 4A and S1A-C) was synchronous with the Cusums of (*i*) the degree of silicification of the phytoplankton community (Figure 5A), (*ii*) the Chl *a*/C ratio (Figure 5B), (*iii*) the degree of generalism for nutrients and environmental tolerance (Figure 5C; Figure S2A, B), (*iv*) the temporal niche overlap for DIP which ranged from 66 to 92% (79 ± 4% niche overlap in average; Figure 5D), and (*v*) the temporal variability in phytoplankton biomass (0-104%, 64 ± 41%; Figure 5E). All Cusum values increased between 1996 and 2002 to reach a maximum in early 2002, followed by a second peak at end-2009, and a decrease until end-2019. The Cusum of the INV-PC1 (Figure 4A) was synchronous with the Cusums of the local wind speed (Figure S3A) and precipitation (3-206 mm, 73 ± 35 mm, Figure S3B). No synchrony between Cusums of precipitation and the INV-PC1 was found from 2012. Nutrients (positively), salinity (negatively), density (negatively), and the variability in both salinity, DIN, and DSi (positively) mainly contributed to the INV-PC1 (Figures S1A, C), and an increase in the Cusum of the INV-PC1 corresponded to an increase of both freshwater influence and wind-driven abiotic forcing (temporal environmental fluctuations). Note that the temporal niche differentiation, which started in early 2009, was mainly caused by a progressive niche shift of the communities (Figure S4). GLS modelling confirmed these driver-response relationships except for the temporal niche overlap for DIP (Table 3). Nevertheless, temporal niche overlap for DIP was indirectly related to the INV-PC1 through its relationships with DIN and PAR variability, themselves related to the INV-PC1 (Table S4). Note that refining driver-response relationships showed that the CWM of the degree of silicification and the variability in phytoplankton biomass were significantly related to DSI, whereas the Chla/C ratio and the degree of generalism were significantly related to the regional wind conditions (positively) and density (negatively) and the temporal niche overlap for DIP (positively), respectively (Table 3). The Cusum of the second principal component (PC2, 11.3% of the total variability, Figure 4B) was synchronous with the Cusums of (*i*) the contribution of *Phaeocystis* to total phytoplankton biomass (max 99%, Figure 6A), (*ii*) the duration of *Phaeocystis* seasonal occurrence (Figure 6B), (*iii*) the phytoplankton biomass (0.2-3221, 233 ± 420 μgCL^{-1}, Figure 6C), (*iv*) the total diatom abundance (0.16-64.4 10^5 $cellsL^{-1}$, 3.6 10^5 ± 6.3 10^5, Figure 6D), (*v*) the functional redundancy (Figure 6E), and the inverse of the

TABLE 1 Range, mean (± SD) and median values of the mean diffuse attenuation coefficient for downwelling irradiance (kd(PAR, m^{-1}), Photosynthetic Active Radiation at mid-depth (PAR_{10m}, E m^{-2} d^{-1}), sea surface temperature (SST, °C), density (D, kg m^{-3}), salinity (S), nutrients (dissolved inorganic nitrogen as the sum of nitrates, nitrites and ammonium [DIN, µM], dissolved inorganic phosphorous [DIP, µM], Dissolved inorganic silica [DSi, µM], and their molar ratios [DIN/DIP, DSi/DIP, and DSI/DIN, µM:µM], Chlorophyll a (Chla, µg L^{-1}), and diatom and *Phaeocystis* biomass (µgC L^{-1}) in coastal waters of the eastern English Channel over the period 1996-2019.

Variable	Unit	Range	Mean±SD	Median
kd	m^{-1}	0.01-0.83	0.33 ± 0.13	0.31
PAR_{10m}	E m^{-2} d^{-1}	0.57-23.15	6.6 ± 4.8	5.5
SST	°C	5-19.7	12.5 ± 4.3	12.3
D	kg m^{-3}	1023.4-1027	1025.6 ± 0.8	1025.6
S	nu	30.9-35.3	34.1 ± 0.5	34.2
DIN	µM	0.04-27.51	7 ± 7	4.31
DIP	µM	0.01-1.55	0.35 ± 0.29	0.28
DSi	µM	0.01-30.69	3.9 ± 4.1	2.44
DIN/DIP	µM:µM	0.3-443	24 ± 36	17
DSi/DIP	µM:µM	0.9-348	17 ± 30	11
DSi/DIN	µM:µM	0.003-40	1.7 ± 3.2	0.65
Chla	µg L^{-1}	0.34-24	4.87 ± 3.90	3.94
Diatoms	µgC L^{-1}	0.2-2338	110 ± 178	66
Phaeocystis	µgC L^{-1}	0-3174	122 ± 384	0

Pielou's evenness (Figure 6F). The Cusums of the contribution of *Phaeocystis* to total phytoplankton biomass and the *Phaeocystis* biomass were also synchronous (Figure S5). After a constant decrease from 1996 to mid-2004, all Cusum values increased until end-2014 - except for PC2, which showed a sharp decrease in 2013 - and slightly decreased until end-2019. Given that DIP level (negatively) and the DSI/DIP and DIN/DIP ratios (positively) contributed significantly to PC2 (Figure S1A and C), we revealed a noticeable DIP limitation. GLS modelling confirmed that the contribution of *Phaeocystis* to total phytoplankton biomass, the diatom and the total phytoplankton abundance, and the Pielou's evenness were significantly related to the PC2 (Table 4). Note that refining the driver-response relationships showed that the contribution of *Phaeocystis* to total phytoplankton biomass was

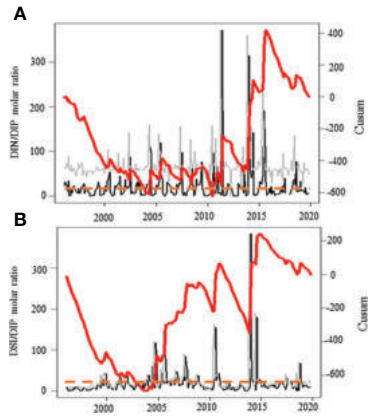

FIGURE 2
Temporal variations of the nutrient molar ratios (**A**: DIN/DIP, **B**: DSi/DIP, [µM:µM], with DIN and DIP as dissolved inorganic nitrogen [i.e., the sum of nitrates, nitrites and ammonium]) and phosphorus in coastal waters of the eastern English Channel over the period 1996-2019. Black line: monthly raw time-series. Grey line: seasonally adjusted, and red thick line: Cusum. Right axes are for seasonally adjusted and Cusum. Orange dashed line: the Redfield and Brzezinski nutrient molar ratios (Redfield 1963; Brzezinski 1985).

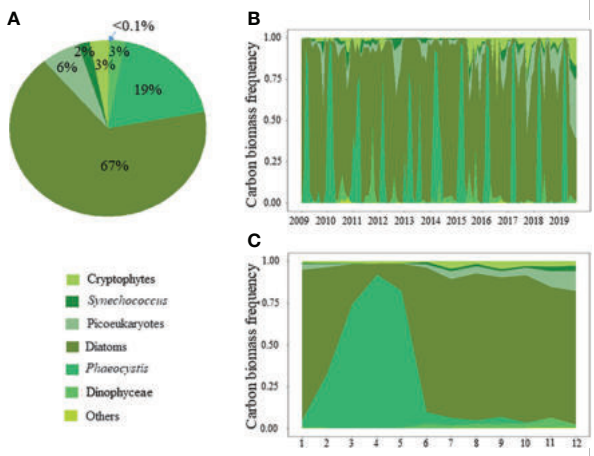

FIGURE 3
(A) Whole phytoplankton composition (carbon biomass frequency), and its **(B)** temporal and **(C)** average seasonal variations, respectively, in coastal waters of the eastern English Channel over the period 2009-2019.

TABLE 2 Rank biomass and abundance and occurrence frequency (%) of the ten most dominant diatom species in term of carbon biomass identified in coastal waters of the eastern English Channel over the period 1996-2019 (see Table S2 for all the diatom species).

Diatom species	Occurrence frequency %	Rank abundance	Average abundance NL^{-1}	Average biomass $\mu gC\ L^{-1}$
Rhizosolenia imbricata var. shrubsolei	69	1	21206	14.5
Guinardia striata	53	4.5	12080	13.86
Ditylum brightwelli	42	15	4449	6.74
Guinardia delicatula	70	1.5	22547	9.1
Guinardia flaccida	50	18	2164	8.83
Odontella sinensis	12	33	4680	2.93
Lauderia annulata/L. borealis	30	9	4545	1.88
Thalassiosira gravida	36	10	10292	5.46
Cerataulina pelagica	21	26	74232	4.04
Leptocylindrus danicus	41	2.5	157	0.89

Note that species rank was calculated on monthly time-series whereas occurrence frequency was calculated on sampling dates.

significantly related to the DIN/DIP ratio and the inverse of the variability in PAR and variance ratio. In the same way, diatom and phytoplankton abundance were related to the DSI/DIP ratio. and the diatom abundance and the contribution of *Phaeocystis* to total phytoplankton biomass, respectively. By contrast, the duration of *Phaeocystis* seasonal occurrence was inversely related to the regional wind conditions and the variance ratio. Moreover, the functional redundancy and phytoplankton biomass were related to DIP (negatively) and *Phaeocystis* biomass (positively), respectively. *Phaeocystis* biomass, was inversely related to the variability in PAR and the variance ratio (Table S3). The Cusum of the third component (PC3, 8.3% of the total variability, Figures 4C, Figures S1B, C) was similar to the Cusum of the diatom biomass (Figure 7). While not being related over the first years of monitoring, both Cusums increased from end-2002 until a maximum in mid-2005 and then decreased sharply from early 2015 to the end-2019. SST (negatively) and the variability in DIN and DSi (positively) were the variables that mainly contributed to PC3 (Figure S1B, C), indicating that diatom biomass was promoted under cold conditions and, to a lesser extent, favored by DIN and DSi pulses (*i.e.*, increase in their temporal variability). Note that no correspondence was found between the Cusum of PC3 and any meteorological parameter. GLS modelling showed that diatom biomass was only significantly related to the CWM of the S/V ratio (negatively, Table 4), itself being inversely related to DIN (Table S3). Note that, the variables used to compute the PC3 - yearly-averaged data - were different from the variables used to calculate the PC3 based on seasonally-adjusted data (Figure S1 and Table S4).

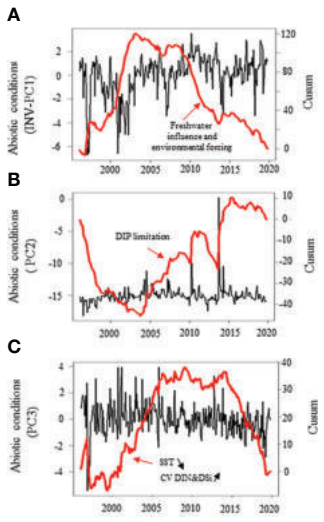

FIGURE 4
Temporal variations of the abiotic conditions (mean and variability) in coastal waters of the eastern English Channel over the period 1996-2019. **(A)** Principal component 1 [INV-PC1]; **(B)** Principal component 2 (PC2); and **(C)** Principal component 3 (PC3, see Figure S1 for PCA details). Black line: monthly seasonally adjusted ones. Red thick line: Cusum. Right axes are for Cusum. Note that PCs values in **(A)** have been inverted for ease of reading with next results (Figure 5).

In contrast to the Cusums of phytoplankton biomass (Figure 6C) and its variability (Figure 5E), the Cusum of the temporal stability of community-level biomass (Figure 8), which results from both biomass and its variability, is unlike any other. However, GLS modelling indicated that the temporal stability of community-level biomass was significantly related to diatom biomass.

Phytoplankton species richness and functional diversity (FRic and RaoQ) are displayed on Figures 9B–D. The FRic and RaoQ values for the diatom community and *Phaeocystis* were always significantly lower than values expected for random community analysis (*i.e.*, 5th< SES< 95th percentile of the random distribution, *i.e.* [-1.96<SES<1.96], in grey in Figures 9B, C and S7A, B), indicating a strong environmental filtering on phytoplankton communities from 1996 to 2019. The

TABLE 3 Significant (p-value<0.05) coefficient estimates (± SE) from Generalized Least Squares (GLS) models to explore the driver-responses relationships of the Community-weight mean of the degree of silicification (CWM), the degree of generalism, the chlorophyll *a*-to-carbon ratio (Chla/C ratio), the temporal DIP niche sharing and the variability of phytoplankton biomass in coastal waters of the eastern English Channel from 1996 to 2019.

	AIC	Estimates (±SE)	t-value	p-value
CWM of the degree of silicification				
DSI	-55.9	0.08 (0.01)	5.46	$<10^{-3}$
INV-PC1	-46.3	0.06 (0.02)	3.26	0.004
Chla/C ratio				
Regional Wind speed conditions		0.43 (0.11)	3.99	0.0007
INV-PC1		0.37 (0.09)	3.91	0.0009
Regional Wind speed conditions mPC1		0.43 (0.10)	4.21	0.0004
Generalism				
Density	24.6	-0.36 (0.09)	-3.75	0.001
Temporal DIP niche sharing		27.35 (4.51)	6.06	$<10^{-3}$
INV-PC1	43.5	031(0.14)	2.17	0.04
Temporal DIP miche sharing				
varPAR		0.009 (0.003)	3.07	0.006
DIN		0.01 (0.003)	3.36	0.003
Variability in phytoplankton biomass				
DSI	60.2	0.68 (0.15)	4.40	0.0002
INV-PC1	68.2	0.52 (0.17)	3.00	0.007

DSi: dissolved inorganic silicon; and the INV-PC1: the inverse coordinates of the first principal component of a PCA performed on the abiotic environment. GLS models were built with annual means and after accounting for a serial correlation AR(1) model for the errors and the potential interactions between the different predictors when applicable. The most parsimonious model was retained based on the Akaike Information Criterion (AIC) value. Note that the estimates of the intercept in each model are omitted r for ease of reading.

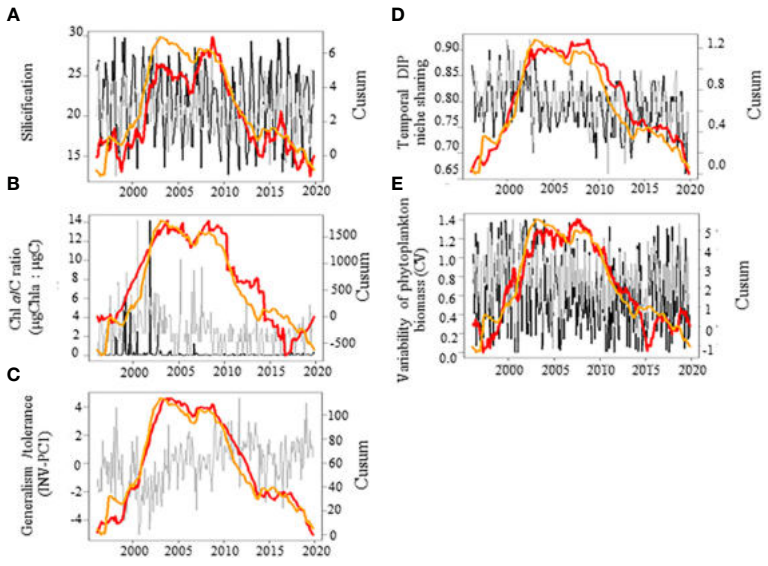

FIGURE 5
Temporal variations of the phytoplankton community patterns (red lines) in relation with the abiotic conditions (orange line, PC1, see Figure S1 for PCA details) in coastal waters of the eastern English Channel over the period 1996-2019. **(A)** The apparent degree of silicification, **(B)** the Chlorophyll a to phytoplankton carbon biomass (Chl a/C, µg Chla:µg C), **(C)** the degree of generalism for nutrients and environmental tolerance (INV-PC1, see Figure S2 for the PCA details); **(D)** temporal niche sharing for DIP; and **(E)** variability of phytoplankton biomass (CV). Black and grey line: monthly raw and seasonally adjusted time-series, respectively. Note that PCs in **(C)** represent yet seasonally adjusted time-series. Orange and red lines: Cusum. Right axes are for seasonally adjusted and Cusum. Note that PCs values in **(C)** have been inverted for ease of reading.

TABLE 4 Significant (p-value<0.05) coefficient estimates (± SE) from Generalized Least Squares (GLS) models to explore the driver-responses relationships of the contribution of *Phaeocystis* to total phytoplankton biomass (%), the duration of the seasonal *Phaeocystis* occurrence, the diatom abundance and biomass, the total phytoplankton abundance and biomass, the functional redundancy, and the Pielou's evenness of the phytoplankton community in coastal waters of the eastern English Channel from 1996 to 2019. were positively and negatively related to DIP, respectively.

	AIC	Estimates (±SE)	t-value	p-value
***Phaeocystis* biomass (%)**				
DIN/DIP ratio	-120.4	0.01 (0.003)	3.59	0.002
varPAR		-0.01 (0.004)	-3.48	0.002
Variance ratio		-0.02 (0.01)	-2.94	0.008
PC2	-104	0.01 (0.01)	2.61	0.02
Duration of *Phaeocystis* occurrence				
Regional Wind speed conditions		-0.49 (0.15)	-3.19	0.004
Variance ratio		-0.95 (0.31)	-3.06	0.006
Diatom abundance				
DSI/DIP ratio	59.7	0.41 (0.14)	2.83	0.01
PC2	60.5	0.46 (0.18)	2.54	0.02
Diatom biomass				
CWMS/V ratio			-4.03	<10
Phytoplankton abundance				
Diatom abundance	-48.1	0.13 (0.02)	7.59	<10
Phaeocystis biomass (%)		3.38 (0.66)	5.11	<10
PC2	-14.2	0.12 (0.04)	3.07	0.006
Phytoplauktom biomass				
Phaeocystis biomass		0.66 (0.13)	5.12	<10
Functional redundancy				
DIP		-0.06 (0.02)	-2.81	0.01
Pielou's index				
PC2		-0.43 (0.14)	-3.17	0.005
% of *Phaeocystis* biomass		-13.44 (5.61)	-2.40	0.03
INV-PC1		0.34 (0.15)	2.20	0.04

The GLS models were built with annual means and after accounting for a serial correlation AR(1) model for the errors and the potential interactions between the different predictors when applicable. The most parsimonious model was retained based on the Akaike Information Criterion (AIC) value. Note that the estimates of the intercept in each model are omitted r for ease of reading. DIP, DIN, and DSI: dissolved inorganic phosphorus, nitrogen, and silicon; the INV-PC1 and PC2: the two first principal components of a PCA performed on the abiotic environment; varPAR: variability in the Photosynthetic Active Radiation for phytoplankton; CWM.S/V ratio: the Community Weighted-Mean of the Surface to Biovolume cell ratio.

inspection of the Cusum of SES-RaoQ (Figure 9B) showed a tendency towards traits divergence from 1996 to early 2004, however, followed by a period of traits convergence. By contrast to the observed phytoplankton community patterns, the response of functional biodiversity (SES-RaoQ and SES-FRic), the degree of generalism for DIP (Figure 9E) and the variance ratio (Figure 9F) increased along with DIP (Figures 9A–C). Although the variance ratio showed a trend towards compensation over the last decade (VR<1), null model testing indicated that VR values were never significantly different from one, and consequently; that species did not significantly covary. We detected the inverse pattern described above for species richness and defense against predation (Figures 9D, G). This suggests that the contribution of specialists for acquiring/using DIP and well-defended species within the community, and for which the phytoplankton community tend towards compensation dynamics, increased as DIP decreased. We revealed that temporal changes in the Cusum of defense was synchronous with that of phytoplankton biomass and inversely related to that of the Pielou's evenness (see Figure S8). GLS modelling confirmed that the variance ratio and the niche breadth for DIP, and the CWM of defense against predation were positively and negatively related to DIP, respectively (Table 5). By contrast, the functional divergence (SES-RaoQ) was related to the total phytoplankton abundance. Moreover, species richness was inversely related to the functional divergence and the niche breadth for DIP. Note that although no clear driver-response relationships was found for synchrony based on the Cusum calculation, GLS modelling showed that synchrony was related to the regional wind speed conditions and the variance ratio (positively).

The Cusums of the ecological specialization for the acquisition and/or use of DIN (*i.e.*, the inverse niche breadth for DIN, Figure 10B) and the Nitrogen Use Efficiency (NUE,

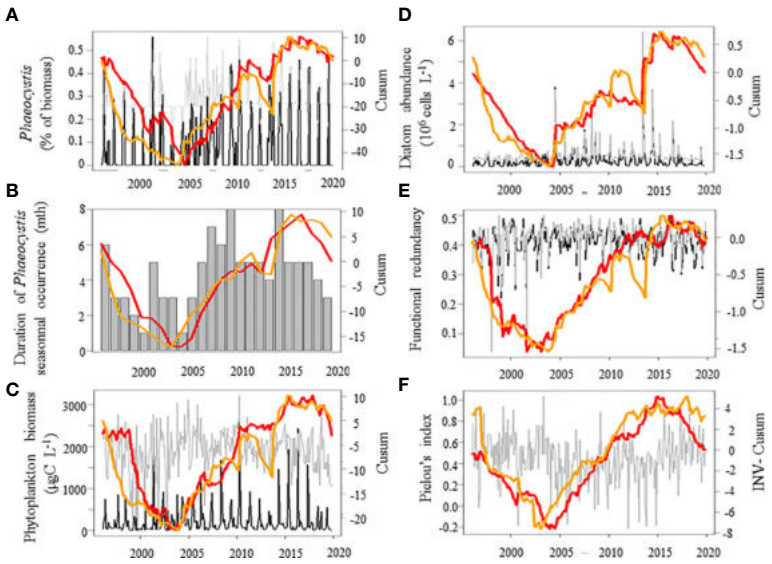

FIGURE 6
Temporal variations of phytoplankton patterns (red lines) in relation with the abiotic conditions (Principal component 2 [PC2], see Figure S1 for PCA details, orange line) over the period 1996-2019 in coastal waters of the eastern English Channel. **(A)** the % of *Phaeocystis* biomass, **(B)** the duration of *Phaeocystis* seasonal occurrence (months), **(C)** phytoplankton biomass (µgC L^{-1}), **(D)** diatom abundance (10^6 cells L^{-1}), **(E)** functional redundancy, and **(F)** Pielou's index (abundance-based) of the phytoplankton community. Black and grey lines: monthly raw and seasonally-adjusted time-series, respectively. Thick line: Cusum. Stick: seasonal value. Right axes are for seasonally adjusted and Cusum. Note that the Cusum of Pielou's evenness is inverted (INV-Cusum) for ease of reading.

Figure 10C) followed that of Kd, *i.e.*, a proxy of clarity in the seawater column (Figure 10A). The lower the Kd value (*i.e.*, higher light availability), the lower the number of DIN-specialists species, and the NUE. The Cusum of Kd paralleled the Cusum obtained for regional wind speed (Figure S3C; S6A, B). GLS modelling confirmed the relationships between NUE and the degree of ecological specialization for DIN but not for Kd (Table 5). The degree of ecological specialization for DIN was inversely related to DSI.

Finally, although no correspondence was found between the Cusums of the degree of coloniality of the phytoplankton community and any other variable, GLS analyses revealed that coloniality was inversely related to DIN and variability in density (Table S3).

Discussion

By studying resource requirement, acquisition and/or use traits over the last two decades, we demonstrated that environmental filtering (SES-RaoQ<-1.96) played a major role in structuring the phytoplankton communities of the coastal waters of the EEC. Such a general functional trait under-dispersion is in line with the finding that communities composed of functionally similar species are more frequent than previously reported (*e.g.*, Segura et al., 2013; Bottin et al., 2016; Burson et al., 2019; Keck and Kahlert, 2019). From our Cusum analyses, the opposition between SES-RaoQ and the CWM of defense, as shown at the seasonal scale with the same datasets (Breton et al., 2021), suggests strongly that a competition-defense trade off played a key role in the regulation of phytoplankton species richness over the two last decades. The competition-defense trade-off provide a refuge for weak competitors that are better protected against predator attacks (*e.g.*, Chase et al., 2002; Huot et al., 2014; Züst and Agrawal, 2017; Cadier et al., 2019; Ehrlich et al., 2020). The investment into defense mechanisms leads to relax competitive exclusion, through the predation pressure exerted on the competitively dominant species (Ehrlich et al., 2020), as we detected with the shift of SES-RaoQ towards higher functional clustering (Mayfield and Levine, 2010). Investing into defense has a metabolic cost at the expense of growth, however, such as a lower maximum growth rate or a lower competitive ability (Ehrlich et al., 2020). The suspicion of a competition-defense trade off was reinforced by the parallelism between the Cusums of defense and phytoplankton biomass, and the anti-parallelism between them and Pielou's evenness (see Figure S8). Accordingly, competition-defense theory predicts that predation increase prey richness in more productive environments (Chase et al., 2002), when prey communities have low evenness (Worm et al., 2002; Hillebrand et al., 2007). Although the theory predicts that defense leads to increased

TABLE 5 Significant (p-value<0.05) coefficient estimates (± SE) from Generalized Least Squares (GLS) models to explore the driver-responses relationships of the temporal stability of community-level biomass and the Nitrogen Use Efficiency (NUE), the functional divergence (SES-RaoQ), species richness, the niche breadth for DIP (HDIP), the variance ratio, the synchrony, and the community weighted-mean of defense against predation (CWM-Defense) of the phytoplankton community in coastal waters of the eastern English Channel from 1996 to 2019.

	AIC	Estimates (±SE)	t-value	p-value
Stability				
Diatom biomass		0.002 (0.0005)	3.83	<10-3
NUE				
HDIN		-137 (0.54)	-2.53	0.02
with HDIN:				
DSI		0.36 (0.078)	4.65	<10-3
SES-RaoQ				
Phytoplankton abundance		-1.42 (0.32)	-4.38	0.0002
Species richness (log scale)				
SES-RaoQ		-0.28 (0.05)	-5.81	<10-3
HDIP		-1.83 (0.56)	-3.25	0.004
HDIP				
generalism	-100	0.03 (0.007)	4.42	<10-3
Temporal DIP niche sharing	-101	1.03 (0.28)	3.72	0.001
DIP		0.14 (0.04)	325	0.004
varD		-0.01 (0.005)	-2.18	0.04
Variance ratio				
DIP		1.35 (0.44)	3.05	0.006
Synchrony				
Regional Wind speed conditions		0.57 (0.14)	3.92	0.0008
Variance ratio		1.11 (0.39)	2.82	0.01
CWM.Defeuse				
DIP		-0.67 (0.18)	-3.66	0.001

DIP and DSI: dissolved inorganic phosphorus and silicon; varD: variability in density (CV); HDIN: niche breadth for DIN. GLS models were built with annual means and after accounting for a serial correlation AR(1) model for the errors and the potential interactions between the different predictors when applicable.The most parsimonious model was retained based on the Akaike Information Criterion (AIC) value. Note that the estimates of the intercept in each model are omitted r for ease of reading.

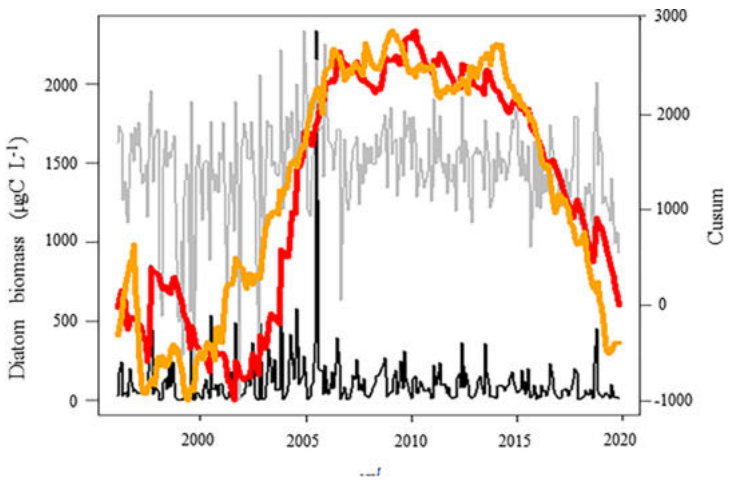

FIGURE 7
Temporal variations of the diatom biomass (µgC L^{-1}, red line) in coastal waters of the eastern English Channel over the period 1996-2019 in relation with the abiotic conditions (PC3, orange line, see Figure S1 for PCA details). Black and grey lines: monthly raw and seasonally adjusted time-series, respectively. Red and orange lines: Cusum. Right axes are for seasonally adjusted and Cusum.

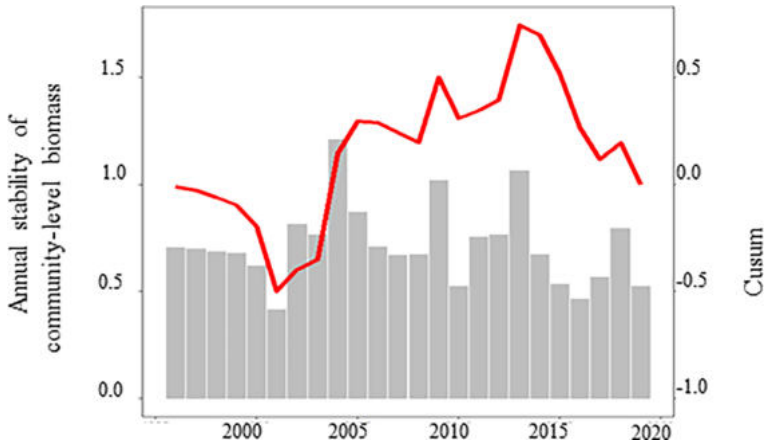

FIGURE 8
Temporal variations of the annual stability of community-level biomass (grey sticks) and its Cusum (red line).

coexistence only under eutrophic conditions (*i.e.*, high nutrient levels; Våge et al., 2014), we observed an inverse pattern both with Cusums and GLS modelling (*i.e.*, predation increased as DIP decreased). This discrepancy might be explained by the fact that nutrients levels are still high in our region of interest, despite significant re-oligotrophication.

Although we did not measure phytoplankton growth rate, the Chl *a*:C ratio is a potential relevant proxy for maximum growth rate (Cloern et al., 1995). Accordingly, this ratio decreases with increasing growth irradiance (Geider et al., 1986) and can be related to light-limited growth rate, rather than against irradiance directly (Langdon, 1988): the ratio increases linearly with growth rate when nutrients are limiting, and decreases curvilinearly with growth rate when light was limiting (Laws and Bannister, 1980). This suggests that phytoplankton growth rate in the EEC was maximal over the period 1996-2019 when nutrients were replete and light-limited, but slowed down as nutrients decreased. The trend towards an increase in the degree of coloniality of the phytoplankton community over time (*i.e.*, as DIN decreased) reinforce the suspicion of a trend towards a growth slowdown over time. Colony formation involve physiological costs related to growth (Yokota and Sterner, 2011) caused by nutrient shielding (Ploug et al., 1999; Lavrentovich et al., 2013), as shown for *Phaeocystis* (Ploug et al., 1999). Here, we indirectly revealed a patent link between the Chl *a*:C ratio, DIP level through the PCA computed on abiotic forcing, and the opposition between the Cusums of DIP level and defense, and the parallelism between the Cusums

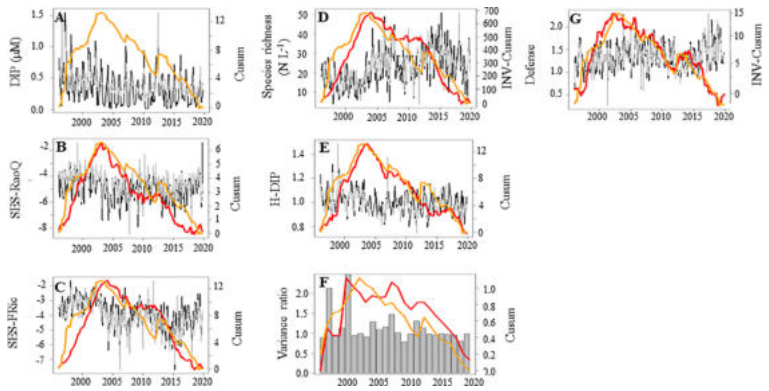

FIGURE 9
Temporal variations of the biodiversity (red lines) in relation with the concentration of dissolved inorganic phosphorous (DIP, µM, orange line) in coastal waters of the eastern English Channel over the period 1996-2019. **(A)** DIP (µM), **(B)** the functional divergence (SES-RaoQ), **(C)**: the functional richness (SES-FRic), **(D)**: the species richness (N L^{-1}), **(E)** the degree of specialization for DIP, **(F)** the variance ratio, and **(G)** the phytoplankton defense. Black and grey lines: monthly raw and seasonally adjusted time-series, respectively. Grey sticks: annual value. Orange line: the Cusum of DIP. Red line: the other Cusum. Right axes are for seasonally adjusted and Cusum. Note that the Cusums of species richness and defense are inverted (INV-Cusum) for ease of reading.

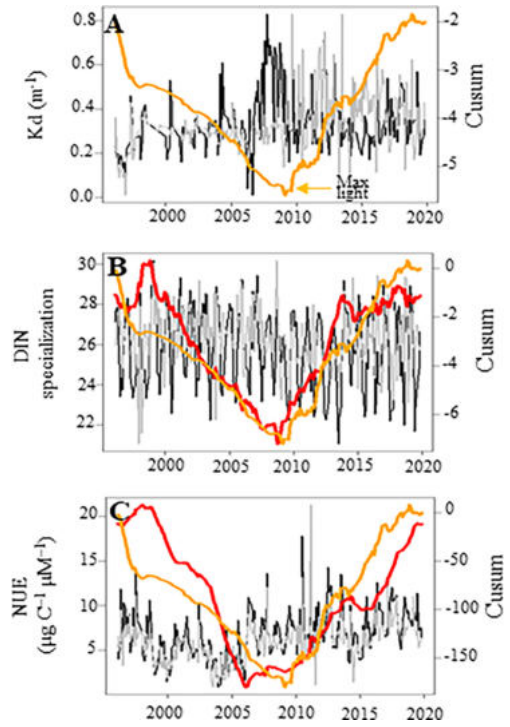

FIGURE 10
Temporal variations of **(A)** the vertical light attenuation coefficient (Kd, m^{-1}) as a proxy of the quantity of light available in the water column for phytoplankton, **(B)** the degree of specialization for DIN, and **(C)** Nitrogen Use Efficiency (µg C^{-1} μM^{-1}) in coastal waters of the eastern English Channel over the period 1996-2019. Black and grey lines: monthly raw and seasonally adjusted time-series, respectively, except for PC1 in **(A)**, which represents seasonal adjusted ones. Orange line: the Cusum of Kd. Red line: the other Cusum. Right axes are for seasonally adjusted and Cusum.

of Chl *a*:C ratio and DIP level suggest that a growth-defense trade off might have operated at the same time than a competition-defense trade off. During high Chl *a*:C ratio periods, the link between precipitation and environmental forcing suggested a potential influence of light-limiting conditions on ratio variations; even if no direct influence of light was found. We detected a shift towards random species distribution with increasing precipitation, wind stress, and nutrient concentrations, but a reduction in species richness, that suggests either a competition for light (*e.g.*, Sommer, 1988; Hautier et al., 2009) or stochastic effects under disturbed abiotic conditions (Weiher and Keddy, 1995). As stressed by Alvarez-Fernandez and Riegman (2014), the large variations in the Chl *a*: C ratio over the two last decades strengthened that using chlorophyll-*a* as a proxy of phytoplankton biomass must be done cautiously.

The correspondence between the apparent degree of silicification and wind-driven abiotic forcing/freshwater influence, as previously shown at the seasonal scale (Breton et al., 2021), is coherent with species requirements for cell wall rigidity (*i.e.*, heavily silicified) and to counteract cell wall expansion provoked by haline shock (Logares et al., 2009; Hoef-Emden, 2014; Suescún-Bolívar and Thomé, 2015). As we found in the present and at the seasonal scale (Breton et al., 2021) heavier silicified species are expected to occur in environments with higher DSi level (Martin-Jézéquel et al., 2000; Martin-Jézéquel and Lopez, 2003), but the progressive decrease in silicification observed over the period 1996-2019 may have increased species palatability, favoring species investment into defense against predators. Competition–defense/growth-defense trade-offs are known to promote species diversity by reducing the fitness of superior competitors (*i.e.*, slowing prey growth) and, therefore, fitness inequalities between competitors. Competition–defense/growth-defense trade-offs can therefore be considered as a fitness equalizing mechanism. In order to maintain long-term coexistence, stabilizing niche differences (*i.e.*, reduction in niche overlap) are, however, required besides the need of the superior competitor to survive to predation (Chesson, 2000; Chesson and Kuang, 2008). Although specialization is often associated to fine niche differences (McArthur, 1972; Mason et al., 2008; Pigot et al., 2016), our results showed that variations in functional similarity (*i.e.*, niche overlap) followed fluctuations of ecological specialization for DIP, as previously shown at the seasonal scale (Breton et al., 2021). The opposition between niche breadth for DIP and species richness that we revealed at the scale of the coastal waters of the EEC is consistent with the widespread pattern characterized by Granot and Belmaker (2019) for a large variety of taxa and ecosystems. The shift towards the dominance of generalists in response to abiotic forcing is clearly supported by the ability of such species to adapt to disturbed environments, eutrophicated systems, and unstable environmental conditions (Hautier et al., 2009; Hautier et al., 2015; Blüthgen et al., 2016; Pálffy and Vőrős, 2019). Ecological specialization of species may also reflect lower resource requirements (Carscadden et al., 2020).

While the traits used in this study may be too coarse to detect subtle niche partitioning, we showed a trend towards asynchronous variations (*i.e.*, a decrease in the variance ratio) between species' occurrences as DIP concentration decreased that suggest trade-off mechanisms related to competition for phosphate, such as competition versus defense against predation, or competition versus growth under high nutrient concentrations; mechanisms which can be invoked to explain niche differentiation. The correspondence between the temporal niche differentiation and abiotic forcing was explained by the key role of climatic stability on temporal niche differentiation. Environmental forcing - especially when severe and frequent - is known to synchronize population fluctuations (Loreau and de Mazancourt, 2008) and to favor stress-tolerant species over specialists (Levins, 1962; Purvis et al., 2000; Sultan and Spencer, 2002; Chase, 2007). Ecosystem stability requires some

form of temporal niche differentiation to allow species to respond specifically to environmental variations, leading to asynchronous fluctuations. This process was illustrated in the coastal waters of the EEC by both the trend towards synchronous response of species to wind-driven abiotic forcing and the opposition to the degree of ecological specialization and environmental tolerance. Taken together, our results highlighted that (*i*) biogeographical history, (*ii*) abiotic filtering through change in salinity and resources, and (*iii*) biotic interactions (competition, and predation) were the main mechanisms that shaped phytoplankton communities and influenced species diversity in the coastal waters of the EEC over the two last decades: heavily silicified phytoplankton species that resist to changes in salinity and wind-driven turbulence were favored, as well as species that are morphologically well-defended Nutrient levels, especially DIP, have clearly contributed to structure phytoplankton communities in the coastal waters of the EEC during the period 1996-2019.

We did not detect any deleterious effect of *Phaeocystis* on diatoms and phytoplankton diversity, as previously shown at the seasonal scale (Breton et al., 2021). The strong correspondence between the unbalanced DIP reduction (see the correlations between biotic variables and PC2; Figure S3C, and GLS modelling on Table 4) and the contribution of *Phaeocystis* to total phytoplankton biomass clearly demonstrates that this species is well-adapted to anthropogenic disturbance, such as the European unbalanced reduction of nutrient loads (Loebl et al., 2009; Burson et al., 2016). A high capacity for efficient phosphate (P) acquisition and conservation are key traits for the success of invasive plants under P-limited environments (Olde Venterink, 2011 and references therein; Funk, 2013). *Phaeocystis* is fundamentally characterized by its ability to grow on dissolved organic phosphorus compounds (DOP) through alkaline phosphatase activity (APA, van Boekel and Veldhuis, 1990) and to form mucilaginous colonies, which act as a P reservoir (Moestrup and Larsen, 1992; Schoemann et al., 2005; Rousseau et al., 2007) and provide protection against predation (Nejstgaard et al., 2007). Our results therefore support the need for DIN abatement and/or a rebalancing of the DIN : DIP ratio in order to mitigate *Phaeocystis* blooms in the future. Our results showed that variability in PAR was another significant negative predictor of *Phaeocystis* biomass. It's somewhat surprising given that *Phaeocystis* is considered to be able to photoadapt quickly to varying light conditions (Schoemann et al., 2005). By contrast, the fact that strong winds reduced significantly the seasonal duration of *Phaeocystis* occurrence is coherent with experimental works on the negative effect of turbulence on *Phaeocystis* (Schapira et al., 2006). The concurrent increase in *Phaeocystis* biomass, total diatom abundance, and functional clustering suggests that *Phaeocystis* (and also diatoms) might have also benefited from a density-dependent symmetric facilitation (*i.e.*, mutualism; Gallien et al., 2018) cascade induced by the increase in total phytoplankton abundance: a high abundance of benefactors gives more chance for DOP compounds to be present, which in turn positively contribute to stronger and more efficient facilitative interactions (Krichen et al., 2019; Zhang and Tielbörger, 2020). More generally, facilitation might arise from an increase in community complexity (McIntire and Fajardo, 2014; Münkemüller et al., 2020 and references therein).

We therefore recommend that future studies explore the role of density-dependent facilitation for *Phaeocystis* success and the diversity of available DOP compounds. Assessment of the multiple molecular expression in species assemblages of the EEC must be carry out to confirm that DIP niche partitioning did not occur in the coastal waters of this ecosystem.

It is well known that diatoms dominate in well-mixed nitrate-rich waters (*e.g.*, Breton et al., 2006). Our results suggest that diatoms were mainly influenced by seawater temperature, DIN concentration (indirectly through the relationship between the CWM-S/V ratio and DIN), and temporal variability in both DIN and DSi. The inverse Cusum pattern detected between diatom biomass and seawater temperature in the coastal waters of the EEC is consistent with *in situ* observations (Lürling et al., 2013 and references therein; Liu et al., 2020; Stockwell et al., 2020; Mancuso et al., 2021) and biogeochemical models (Bopp et al., 2005), raising concerns for the subsistence of diatom blooms under climate change conditions. Thermal stratification is often considered as the driving process of the decrease in diatom biomass (but see 2018; Kemp and Villareal, 2013), through the reduction of diatoms ability to stay in subsurface waters, where nutrient pulses typically occur (Falkowski and Oliver, 2008; Stockwell et al., 2020). In our study, no causal link between thermal stratification, nutrient concentrations and diatom biomass was found, however, with one hypothesis being that the combination of shallow waters and strong hydrodynamic conditions in the coastal waters of the EEC permanently mix the entire water column. The association between diatom biomass and temporal variability in DIN and DSi suggests a pivotal role of nutrient pulses in promoting diatom biomass. Climate warming may also directly affect the metabolism of species, or can act as a selection for the most thermally adapted species (Lewandowska et al., 2014). No link was detected with thermal niche breadth, however, and further analyses are needed to identify the underlying mechanisms behind temperature and diatom biomass in the coastal waters of the EEC.

We found no evidence that species richness and/or functional diversity are significant predictors of ecosystem functioning in the coastal waters of the EEC. Functional redundancy, crucial for ecosystem sustainability and for buffering the effects of environmental disturbances, was linked to phytoplankton productivity, the latter and NUE being driven by temporal changes in *Phaeocystis* biomass and the degree of specialization for DIN, respectively. In the same way, temporal

stability of community-level biomass was related to diatom biomass but not species richness. Long-term changes in the assembly, structure and dynamics of phytoplankton communities of the coastal waters of the EEC therefore corroborate the 'mass-ratio hypothesis' (Grime, 2006) that states that the effect of each species on an ecosystem process is proportional to the relative abundance of its functional trait values; here we revealed an important role in nitrogen storage capacity and productivity. Our study also strengthens previous results obtained for the same study region, but with coarse functional groups (Breton et al., 2017), and in both the Baltic (Filstrup et al., 2014) and Wadden seas (for NUE; Hodapp et al., 2015). In contrast to Ptacnik et al. (2008) who found a positive relationship between phosphorous use efficiency, resource use efficiency, and phytoplankton genus richness in Scandinavian lakes, we revealed that the dominance of a few species explained most of NUE and productivity of the coastal waters of the EEC.

Conclusion

Taken together, our results showed that phytoplankton communities in the coastal waters of the eastern English Channel were shaped over the last two decades by favoring either species specialized food resources, or species with ability to invest in growth, defense, chlorophyll-a and silicification levels, with a clear influence of environmental perturbations - such as wind-driven instability, riverine nutrient loads, and unbalanced nutrient reduction - and biotic interactions (competition, predation, facilitation). Our study provides strong support for both niche-based and facilitative processes, while highlighting the challenging choices faced by managers to preserve the integrity and sustainability of ecosystems in future, mainly because of the multiple responses of the phytoplankton communities to environmental change and the trade-offs - or lack of synergy - between ecosystem functions/properties.

Data availability statement

The original contributions presented in the study are publicly available. This data can be found here: https://doi.org/10.6084/m9.figshare.21196069.v1.

Author contributions

EB, EG, BS, LS, GB, DP, NG, and UC conceived the ideas and designed methodology; EB, EG, D-IS, MC, DP, CS, AC, and FG collected the data. EB, AO, and AP analysed the data; EB, EG, BS, LS, GB, D-IS, LK, MC, and UC led the writing of the manuscript. All authors contributed critically to the drafts and gave final approval for publication.

Acknowledgments

We thank the successive captains and crews of the RV Sepia II (INSU-CNRS), especially Charly Dollet, Jean-Claude Martin, Grégoire Leignel, Noël Lefiliatre, and Christophe Routier who helped during long-term monitoring in coastal waters of the eastern English Channel (1996-2019). We also thank the local SOMLIT team for sampling and physico-chemical measurements and analysis, especially N. Degros, E. Lecuyer, and Dr. V. Gentilhomme, as well as Emilie Grossteffan from the IUEM institute who analysed nutrients when local equipment was out of order. The other members of the SOMLIT Quality team (*i.e.*, L. Oriol, P. Rimmelin, T. Cariou, S. Ferreira, E. Sultan, O. Jolly, P. Pineau, S. Mas, H. De Lary, J. Lamoureux, A. Gueux and O. Crispi) are acknowledged for their investment all along the last two decades for improving the precision and the accuracy of the environmental data. The authors also thank the students for their assistance in water sample collection and help in nutrient analysis within the context of the SOMLIT program (INSU-CNRS), and the students S. Bosc and P. Faye for their contribution to diatom species size measurements. Finally, we thank the PHYTOBS network, especially Nadine Neaud-Masson (IFREMER) for its essential role in taxonomy expertise. Microscopy and harvesting equipment got several funding over the last decades including a BQR ULCO in 2007. This work was a contribution of the project EVOLECO-NUPHY supported by the French National program LEFE (Les Enveloppes Fluides et l'Environnement). ULCO is acknowledged for the payment of the publication.

Conflict of interest

The authors declare that the research was conducted in the absence of any commercial or financial relationships that could be construed as a potential conflict of interest.

Publisher's note

Supplementary material

The Supplementary Material for this article can be found online at: https://www.frontiersin.org/articles/10.3389/fmars.2022.914475/full#supplementary-material

References

Ackerly, D. D. (2003). Community assembly, niche conservatism, and adaptive evolution in changing environments. *Int. J. Plant Sci.* 164, S165–S184. doi: 10.1086/368401

Adler, P. B., HilleRisLambers, J., Kyriakidis, P. C., Guan, Q., and Levine, J. M. (2006). Climate variability has a stabilizing effect on the coexistence of prairie grasses. *PNAS* 103, 12793–12798. doi: 10.1073/pnas.0600599103

Aitken, A. C. (1936). On least-squares and linear combinations of observations. *PNAS* 55, 42–48. doi: 10.1017/S0370164600014346

Alexander, T. J., Vonlanthen, P., and Seehausen, O. (2016). Does eutrophication-driven evolution change aquatic ecosystem? *Philos. Trans. R. Soc Lond. B Biol. Sci.* 372, 20160041. doi: 10.1098/rstb.2016.0041

Alvarez-Fernandez, S., Lindeboom, H., and Meesters, E. (2012). Temporal changes in plankton of the north Sea: community shifts and environmental drivers. *Mar. Ecol. Prog. Ser.* 462, 21–38. doi: 10.3354/meps09817

Alvarez-Fernandez, S., and Riegman, R. (2014). Chlorophyll in north Sea coastal and offshore waters does not reflect long-term trends of phytoplankton biomass. *J. Sea Res.* 91, 35–44. doi: 10.1016/j.seares.2014.04.005

Aminot, A., and Kérouel, R. (2004). Hydrologie des écosystèmes marins: paramètres et analyses. *Eds. Ifremer, Brest*. 1, 335

Biggs, C. R., Yeager, L. A., Bolser, D. G., Bonsell, C., Dichiera, A. M., Hou, Z., et al. (2020). Does functional redundancy affect ecological stability and resilience? a review and meta-analysis. *Ecosphere* 117, e03184. doi: 10.1002/ecs2.3184

Bjærke, O., Jonsson, P. R., Alam, A., and Selander, E. (2015). Is chain length in phytoplankton regulated to evade predation? *J. Plankton Res.* 37, 1110–1119. doi: 10.1093/plankt/fbv076

Blonder, B., Lamanna, C., Violle, C., and Enquis, B. J. (2014). The n-dimensional hypervolume. *Glob. Ecol. Biogeogr.* 23, 595–609. doi: 10.1111/geb.12146

Blüthgen, N., Simons, N. K., Jung, K., Prati, D., Renner, S. C., Boch, S., et al. (2016). Land use imperils plant and animal community stability through changes in asynchrony rather than diversity. *Nat. Commun.* 12, 10697. doi: 10.1038/ncomms10697

Bonato, S., Breton, E., Didry, M., Lizon, F., Cornille, V., Lécuyer, E., et al. (2016). Spatio-temporal patterns in phytoplankton assemblages in coastal-offshore gradients using flow cytometry: a case study in the eastern English channel. *J. Mar. Syst.* 156, 76–85. doi: 10.1016/j.jmarsys.2015.11.009

Bopp, L., Aumont, O., Cadule, P., Alvain, S., and Gehlen, M. (2005). Response of diatoms distribution to global warming and potential implications: A global model study. *Geophys. Res. Lett.* 32, L19606. doi: 10.1029/2005GL023653

Borja, A. (2014). Grand challenges in marine ecosystems ecology. *Front. Mar. Sci.* 1. doi: 10.3389/fmars.2014.00001

Botta-Dukát, Z. (2005). Rao's quadratic entropy as a measure of functional diversity based on multiple traits. *J. Veg. Sci.* 16, 533–540. doi: 10.1111/j.1654-1103.2005.tb02393.x

Botta-Dukát, Z., and Czúcz, B. (2016). Testing the ability of functional diversity indices to detect trait convergence and divergence using individual-based simulation. *Methods Ecol. Evol.* 7, 114–126. doi: 10.1111/2041-210X.12450

Bottin, M., Soininen, J., Alard, D., and Rosebery, J. (2016). Diatom cooccurrence shows less segregation than predicted from niche modeling. *PloS One* 114, e0154581. doi: 10.1371/journal.pone.0154581

Breton, E., Brunet, C., Sautour, B., and Brylinski., J. M. (2000). Annual variations of phytoplankton biomass in the eastern English channel: comparison by pigment signatures and microscopic counts. *J. Plankton Res.* 22, 1423–1440. doi: 10.1093/plankt/22.8.1423

Breton, E., Christaki, U., Bonato, S., Didry, M., and Artigas, L. F. (2017). Functional trait variation and nitrogen use efficiency in temperate coastal phytoplankton. *Mar. Ecol. Prog. Ser.* 563, 35–49. doi: 10.3354/meps11974

Breton, E., Christaki, U., Sautour, B., Demonio, O., Skouroliakou, D.-I., Beaugrand, G., et al. (2021). Seasonal variations in the biodiversity, ecological strategy, and specialization of diatoms and copepods in a coastal system with phaeocystis blooms: The key role of trait trade-offs. *Front. Mar. Sci.* 8. doi: 10.3389/fmars.2021.656300

Breton, E., Rousseau, V., Parent, J. Y., Ozer, J., and Lancelot, C. (2006). Hydroclimatic modulation of diatom/*Phaeocystis* blooms in nutrient-enriched Belgian coastal waters north Sea. *Limnol. Oceanogr.* 51, 1401–1409. doi: 10.4319/lo.2006.51.3.1401

Brzezinski, M. A. (1985). The Si:C:N ratio of marine diatoms: interspecific variability and the effect of some environmental variables. *J. Phycol.* 21, 347–357. doi: 10.1111/j.0022-3646.1985.00347.x

Buitenhuis, E. T., Li, W. K. W., Vaulot, D., Lomas, M. W., Landry, M. R., Partensky, F., et al. (2012). Picophytoplankton biomass distribution in the global ocean. *Earth Syst. Sci. Data* 4, 37–46. doi: 10.5194/essd-4-37-2012

Burson, A., Stomp, M., Akil, L., Brussaard, C. P. D., and Huisman, J. (2016). Unbalanced reduction of nutrient loads has created an offshore gradient from phosphorus to nitrogen limitation in the north Sea. *Limnol. Oceanogr.* 61, 869–888. doi: 10.1002/lno.10257

Burson, A., Stomp, M., Mekkes, L., and Huisman, J. (2019). Stable coexistence of equivalent nutrient competitors through niche differentiation in the light spectrum. *Ecology* 10012, e02873. doi: 10.1002/ecy.2873

Cadier, M., Andersen, K. H., Visser, A. W., and Kiørboe, T. (2019). Competition–defense tradeoff increases the diversity of microbial plankton communities and dampens trophic cascades. *Oikos* 128, 1027–1040. doi: 10.1111/oik.06101

Cadotte, M. W., Carscadden, K., and Mirotchnick, N. (2011). Beyond species: functional diversity and the maintenance of ecological processes and services. *J. Appl. Ecol.* 48, 1079–1087. doi: 10.1111/j.1365-2664.2011.02048.x

Cardinale, B. J. (2011). Biodiversity improves water quality through niche partitioning. *Nature* 472, 86–89. doi: 10.1038/nature09904

Cardinale, B. J., Duffy, J. E., Gonzalez, A., Hooper, D. U., Perrings, C., Venail, P., et al. (2012). Biodiversity loss and its impact on humanity. *Nature* 486, 59–67. doi: 10.1038/nature11148

Cardoso, P., Rigal, F., and Carvalho, J. C. (2014) *BAT: Biodiversity AssessmentTools. r package version 1.0.1.* Available at: http://cran.r-project.org/package=BAT.

Carscadden, K. A., Emery, N. C., Arnillas, C. A., Cadotte, M. W., Afkhami, M. E., Gravel, D., et al. (2020). Niche breadth: Causes and consequences for ecology, evolution, and conservation. *Q. Rev. Biol.* 953, 179–214. doi: 10.1086/710388

Carvalho, J. C., and Cardoso, P. (2018). Decomposing the causes for niche differentiation between species using hypervolumes. *Front. Ecol. Evolution* 8. doi: 10.3389/fevo.2020.00243

Chase, J. M. (2007). Drought mediates the importance of stochastic community assembly. *PNAS* 104, 17430–17434. doi: 10.1073/pnas.07043501042007

Chase, J. M., Abrams, P. A., Grover, J. P., Diehl, S., Chesson, P., Holt, R. D., et al. (2002). The interaction between predation and competition: a review and synthesis. *Ecol. Lett.* 5, 302–315. doi: 10.1038/nature07248

Chessel, D., Dufour, A. B., and Thioulouse, J. (2004). The ade4 package-I-One-table methods. *R News* 4, 5–10. Available at: https://cran.r-project.org/doc/Rnews/

Chesson, P. (2000). Mechanisms of maintenance of species diversity. *Annu. Rev. Ecol. Evol. Syst.* 311, 343–366. doi: 10.1146/annurev.ecolsys.31.1.343

Chesson, P. (2008). "Quantifying and testing species coexistence mechanisms," in *Unity in diversity: Reflections on ecology after the legacy of ramon margalef*. Eds. F. Valladares, A. Camacho, A. Elosegui, C. Gracia, M. Estrada, J. C. Senar and J. M. Gili (Bilbao, Spain: Fundacion BBVA), 119–164.

Chesson, P., and Kuang, J. J. (2008). The interaction between predation and competition. *Nature* 4567219, 235–238. doi: 10.1038/nature07248

Cleveland, R.B., and Cleveland, W.S. (1990). STL: A Seasonal-Trend Decomposition Procedure Based on Loess. *J. Official Statistics* 6, 3–33.

Cloern, J. E., Grenz, C., and Vidergar-Lucas, L. (1995). An empirical model of the phytoplankton chlorophyll : carbon ratio-the conversion factor between productivity and growth rate. *Limnol. Oceanogr.* 40, 1313–1321. doi: 10.4319/lo.1995.40.7.1313

Cloern, J. E., Jassby, A. D., Carstensen, J., Bennett, W. A., Kimmerer, W., Nally, R. M., et al. (2012). Perils of correlating CUSUM-transformed variables to infer ecological relationships. *Limnol. Oceanogr.* 57, 665–668. doi: 10.4319/lo.2012.57.2.0665

Cornwell, W. K., and Ackerly, D. D. (2009). Community assembly and shifts in plant trait distributions across an environmental gradient in coastal California. *Ecol. Monogr.* 79, 109–126. doi: 10.1890/07-1134.1

Cottingham, K. L., Brown, B. L., and Lennon, J. T. (2001). Biodiversity may regulate the temporal variability of ecological systems. *Ecol. Lett.* 4, 72–85. doi: 10.1046/j.1461-0248.2001.00189.x

Debastiani, V., and Pillar, V. (2012). SYNCSA - r tool for analysis of metacommunities based on functional traits and phylogeny of the community components. *Bioinform.* 28, 2067–2068. doi: 10.1093/bioinformatics/bts325

de Bello, F., Lepš, J., Lavorel, S., and Moretti, M. (2007). Importance of species abundance for assessment of trait composition: an example based on pollinator communities. *Community Ecol.* 8, 163–170. doi: 10.1556/ComEc.8.2007.2.3

De Laender, F., Rohr, J. R., Ashauer, R., Baird, D. J., Berger, U., Eisenhauer, N., et al. (2016). Reintroducing environmental change drivers in biodiversity-ecosystem functioning research. *Trends Ecol. Evol.* 31, 905–915. doi: 10.1016/j.tree.2016.09.007

Dolédec, S., Chessel, D., and Gimaret-Carpentier, C. (2000). Niche separation in community analysis: a new method. *Ecology* 81, 2914–2927. doi: 10.1890/0012-96582000081

Dray, S., Dufour, A. B., and Chessel, D. (2007). The ade4 package-II: two-table and K-table methods. *R News* 7, 47–52. Available at: https://sdray.github.io/publication/dray-2007-a/.

Duarte, C. M., Conley, D. J., Carstensen, J., and Sánchez-Camacho, M. (2009). Return to neverland: shifting baselines affect eutrophication restoration targets. *Estuaries Coasts* 32, 29–36. doi: 10.1007/s12237-008-9111-2

Duffy, J. E. (2009). Why biodiversity is important to the functioning of real-world ecosystems. *Front. Ecol. Environ.* 7, 437–444. doi: 10.1890/070195

Ehrlich, E., Kath, N. J., and Gaedke, U. (2020). The shape of a defense-growth trade-off governs seasonal trait dynamics in natural phytoplankton. *ISME* 14, 1451–1462. doi: 10.1038/s41396-020-0619-1

European Union (1991a). Directive 91/676/EEC concerning the protection of waters against pollution caused by nitrates from agricultural sources. 1–8. Available at: https://eur-lex.europa.eu/legal-content/EN/ALL/?uri=celex%3A31991L0676

European Union (1991b). Council directive 91/271/EEC concerning urban wastewater treatment. 40–52. Available at: https://eur-lex.europa.eu/legal-content/EN/TXT/?uri=celex%3A31991L0271.

Falkowski, P., and Oliver, M. (2008). Diatoms in a future ocean — stirring it up: reply from falkowski and Oliver. *Nat. Rev. Microbiol.* 6, 407. doi: 10.1038/nrmicro1751-c2

Figge, F. (2004). Bio-folio: applying portfolio theory to biodiversity. *Biodivers. Conserv.* 13, 827–849. doi: 10.1023/B:BIOC.0000011729.93889.34

Filstrup, C. T., Hillebrand, H., Heathcote, A. J., Harpole, W. S., and Downing, J. A. (2014). Cyanobacteria dominance influences resource use efficiency and community turnover in phytoplankton and zooplankton communities. *Ecol. Lett.* 17, 464–474. doi: 10.1111/ele.12246

Fox, J., and Weisberg, S. (2019). *An r companion to applied regression. 3rd ed.* (Thousand Oaks CA: Sage). Available at: https://socialsciences.mcmaster.ca/jfox/Books/Companion/.

Funk, J. L. (2013). The physiology of invasive plants in low-resource environments. *Conserv. Physiol.* 11, cot026. doi: 10.1093/conphys/cot026

Gallien, L., Zurell, D., and Zimmermann, N. E. (2018). Frequency and intensity of facilitation reveal opposing patterns along a stress gradient. *Ecol. Evol.* 8, 2171–2181. doi: 10.1002/ece3.3855

Gao, V. D., Morley-Fletcher, S., Maccari, S., Vitaterna, M. H., and Turek, F. W. (2020). Resource competition shapes biological rhythms and promotes temporal niche differentiation in a community simulation. *Ecol. Evol.* 10, 11322–11334. doi: 10.1002/ece3.6770

Garnier, E., Cortez, J., Billes, G., Navas, M. L., Roumet, C., Debussche, M., et al. (2004). Plant functional markers capture ecosystem properties during secondary succession. *Ecology* 85, 2630–2637. doi: 10.1890/03-0799

Geider, R. J., Osborne, B. A., and Raven, I. A. (1986). Growth, photosynthesis and maintenance metabolic cost in the diatom phaeodactylum tricornutum at very low light levels. *J. Phycol.* 22, 39–48. doi: 10.1111/j.1529-8817.1986.tb02513.x

Genitsaris, S., Monchy, S., Breton, E., Lecuyer, E., and Christaki, U. (2016). Small-scale variability of protistan planktonic communities relative to environmental pressures and biotic interactions at two adjacent coastal stations. *Mar. Ecol. Prog. Ser.* 548, 61–75. doi: 10.3354/meps11647

Genitsaris, S., Monchy, S., Viscogliosi, E., Sime-Ngando, T., Ferreira, S., and Christaki., U. (2015). Seasonal variations of marine protist community structure based on taxon-specific traits using the eastern English channel as a model coastal system. *FEMS Microbiol. Ecol.* 91, fiv034. doi: 10.1093/femsec/fiv034

Glibert, P. M. (2010). Long-term changes in nutrient loading and stoichiometry and their relationships with changes in the foodweb and dominant pelagic fish species in the San Francisco estuary, California. *Rev. Fish. Sci.* 18, 211–232. doi: 10.1080/10641262.2010.492059

Gómez, F., and Souissi, S. (2007). The distribution and life cycle of the dinoflagellate spatulodinium pseudonoctiluca dinophyceae, noctilucales in the northeastern English channel. *C.R. Biol.* 330, 231–236. doi: 10.1016/j.crvi.2007.02.002

Gotelli, N. J., and McCabe, D. J. (2002). Species Co-occurrence: A meta-analysis of j. m. diamond's assembly rules model. *Ecology* 83, 2091–2096. doi: 10.1890/0012-96582002083

Gower, J. C. (1971). A general coefficient of similarity and some of its properties. *Biometrics* 27, 857. doi: 10.2307/2528823

Granot, I., and Belmaker, J. (2019). Niche breadth and species richness: Correlation strength, scale and mechanisms. *Glob. Ecol. Biogeogr.* 29, 159–170. doi: 10.1111/geb.13011

Grime, J. P. (2006). Trait convergence and trait divergence in herbaceous plant communities: mechanisms and consequences. *J. Veg. Sci.* 17, 255–260. doi: 10.1111/j.1654-1103.2006.tb02444.x

Gross, K., Cardinale, B. J., Fox, J. W., Gonzalez, A., Loreau, M., Wayne Polley, H., et al. (2014). Species richness and the temporal stability of biomass production: a new analysis of recent biodiversity experiments. *Am. Nat.* 183, 1–12. doi: 10.1086/673915

Grover, J. P. (1989). Influence of cell shape and size on algal competitive ability. *J. Phycol.* 25, 402–405. doi: 10.1111/j.1529-8817.1989.tb00138.x

Hafen, R. (2016) *Stlplus : Enhanced seasonal decomposition of time series by loess. r package version 0.5.1.* Available at: https://github.com/hafen/stlplus.

Hallett, L., Avolio, M., Carroll, I., Jones, S., MacDonald, A., Flynn, D., et al. (2020). doi: 10.5063/F1N877Z6

Hasle, G. R., and Syvertsen, E. E. (1996). "Chapter 2 - marine diatoms," in *Identifying marine diatoms and dinoflagellates*. Ed. C. R. Tomas (Academic Press), 5–385, ISBN: . doi: 10.1016/B978-012693015-3/50005-X

Hastie, T., and Tibshirani, R. (1990). *Generalized additive models* Vol. 1990 (New York, United States:Chapman & Hall/CRC), 352 p, ISBN: .

Hautier, Y., Niklaus, P. A., and Hector, A. (2009). Competition for light causes plant biodiversity loss after eutrophication. *Science* 324, 636–638. doi: 10.1126/science.1169640

Hautier, Y., Tilman, D., Forest, I., Seabloom, E. W., Borer, E. T., and Reich, P. B. (2015). Anthropogenic environmental changes affect ecosystem stability *via* biodiversity. *Science* 348, 336–340. doi: 10.1126/science.aaa1788

Hillebrand, H., Dürselen, C. D., Kirschtel, D., Pollingher, U., and Zohary, T. (1999). Biovolume calculation for pelagic and benthic microalgae. *J. Phycol.* 35, 403–424. doi: 10.1046/j.1529-8817.1999.3520403.x

Hillebrand, H., Gruner, D. S., Borer, E. T., Bracken, M. E., Cleland, E. E., Elser, J. J., et al. (2007). Consumer versus resource control of producer diversity depends on ecosystem type and producer community structure. *Proc. Natl. Acad. Sci. U.S.A.* 104, 10904–10909. doi: 10.1073/pnas.0701918104

Hodapp, D., Meier, S., Muijsers, F., Badewien, T. H., and Hillebrand, H. (2015). Structural equation modeling approach to the diversity-productivity relationship of wadden Sea phytoplankton. *Mar. Ecol. Prog. Ser.* 523, 31–40. doi: 10.3354/meps11153

Hoef-Emden, K. (2014). Osmotolerance in the cryptophyceae: jacks-of-all-trades in the chroomonas clade. *Protist* 165, 123–143. doi: 10.1016/j.protis.2014.01.001

Holmes, R. M., Aminot, A., Kérouel, R., Hooker, B. A., and Peterson, B. J. (1999). A simple and precise method for measuring ammonium in marine and freshwater ecosystems. *Can. Can. J. Fish. Aquat. Sci.* 56, 1801–1808. doi: 10.1139/f99-128

Hoppenrath, M., Elbrächter, M., and Drebes, G. (2009). *Marine phytoplankton. selected microphytoplankton from the north Sea around helgoland and sylt* (Stuttgart: E. Schweizerbartsche Verlagsbuchhandlung), 264, ISBN: .

Houliez, E., Lizon, F., Artigas, L. F., Lefebvre, S. F., and Schmitt, G. (2013). Spatio-temporal variability of phytoplankton photosynthetic activity in a macrotidal ecosystem the strait of Dover, eastern English channel. *Estuar. Coast. Shelf Sci.* 129, 37–48. doi: 10.1016/j.ecss.2013.06.009

Huot, B., Yao, J., Montgomery, B. L., and He, S. Y. (2014). Growth-defense tradeoffs in plants: a balancing act to optimize fitness. *Mol. Plant* 7, 1267–1287. doi: 10.1093/mp/ssu049

Ibañez, F., Fromentin, J. M., and Castel, J. (1993). Application de la méthode des sommes cumulées à l'analyse des séries chronologiques en océanographie. comptes rendus de l'Académie des sciences de Paris. *Sci. la Vie.* 316, 745–748.

Jahnke, J. (1989). The light and temperature dependence of growth rate and elemental composition of phaeocystis globosa scherffel and p. pouchetii (Har.) lagerh. in batchcultures. *Neth. J. Sea Res.* 23, 15–21. doi: 10.1016/0077-7579(89)90038-0

Jakobsen, H. H., and Markager, S. (2016). Carbon-to-chlorophyll ratio for phytoplankton in temperate coastal waters: Seasonal patterns and relationship to nutrients. *Limnol. Oceanogr.* 61, 1853–1868. doi: 10.1002/lno.10338

Kalman, R. E. (1960). A new approach to linear filtering and prediction problems ». *J. Basic Eng.* 82.1, 35–45. doi: 10.1115/1.3662552

Karp-Boss, L., and Boss, E. (2016). "The elongated, the squat and the spherical: Selective pressures for phytoplankton shape," in *Aquatic microbial ecology and biogeochemistry: A dual perspective*. Eds. P. M. Glibert and T. M. Kana (Cham: Springer International Publishing), 25–34. doi: 10.1007/978-3-319-30259-1_3

Karp-Boss, L., Boss, E., and Jumars, P. A. (1996). Nutrient fluxes to planktonic osmotrophs in the presence of fluid motion. *Oceanogr. Mar. Biol.* 34, 71–107.

Keck, F., and Kahlert, M. (2019). Community phylogenetic structure reveals the imprint of dispersal-related dynamics and environmental filtering by nutrient availability in freshwater diatoms. *Sci. Rep.* 12, 11590. doi: 10.1038/s41598-019-48125-0

Kemp, A. E. S., and Villareal, T. A. (2013). High diatom production and export in stratified waters – a potential negative feedback to global warming. *Prog. Oceanogr.* 119, 4–23. doi: 10.1016/j.pocean.2013.06.004

Kemp, A. E. S., and Villareal, T. A. (2018). The case of the diatoms and the muddled mandalas: Time to recognize diatom adaptations to stratified waters. *Prog. Oceanogr.* 167, 138–149. doi: 10.1016/j.pocean.2018.08.002

Key, T., McCarthy, A., Campbell, D. A., Six, C., Roy, S., and Finkel, Z.V. (2010). Cell size trade-offs govern light exploitation strategies in marine phytoplankton. *Environ. Microbiol.* 12, 95–104. doi: 10.1111/j.1462-2920.2009.02046.x

Kirby, R. R., Beaugrand, G., and Lindley, J. A. (2009). Synergistic effects of climate and fishing in a marine ecosystem. *Ecosystems* 12, 548–561. doi: 10.1007/s10021-009-9241-9

Kneitel, J. M., and Chase, J. M. (2004). Trade-offs in community ecology: linking spatial scales and species coexistence. *Ecol. Lett.* 7, 69–80. doi: 10.1046/j.1461-0248.2003.00551.x

Koroleff, F. (1970). Revised version of "Direct determination of ammonia in natural waters as indophenol blue, Int. Con. Explor. Sea, C. M. 1969/C:9. *ICES Information on Techniques and Methods for Sea Water Analysis Interlab*, 3 19–22.

Krichen, E., Rapaport, A., Le Floc'H, E., and Fouilland., E. (2019). Demonstration of facilitation between microalgae to face environmental stress. *Sci. Rep.* 9, 1–12. doi: 10.1038/s41598-019-52450-9ff.ffhal-02315867

Kuhn, M., Wing, J., Weston, S., Williams, A., Keefer, C., Engelhardt, A., et al. (2016) *Caret: Classification and regression training. r package version 6.0-71*. Available at: https://CRAN.R-project.org/package=caret.

Laliberté, E., and Legendre, P. (2010). A distance-based framework for measuring functional diversity from multiple traits. *Ecology* 91, 299–305. doi: 10.1890/08-2244.1

Lancelot, C., Grosjean, P., Rousseau, V., Breton, E., and Glibert, P. (2012). Rejoinder to "Perils of correlating CUSUM transformed variables to infer ecological relationships (Breton et al. 2006; Glibert 2010). *Limnol. Oceanogr.* 57, 669–670. doi: 10.4319/lo.2012.57.2.0669

Langdon, C. (1988). On the causes of interspecific differences in the growth-irradiance relationship for phytoplankton. II. a general review. *J. Plankton Res.* 10, 1291–1312. doi: 10.1093/plankt/10.6.1291

Lavrentovich, M. O., Koschwanez, J. H., and Nelson, D. R. (2013). Nutrient shielding in clusters of cells. *Phys. Rev. E Stat. Nonlin. Soft Matter Phys.* 87, 62703. doi: 10.1103/PhysRevE.87.062703

Laws, E. A., and Bannister, T. T. (1980). Nutrient- and light-limited growth of thalassiosira fluviatilis in continuous culture, with implications for phytoplankton growth in the ocean. *Limnol. Oceanogr.* 25, 457–473. doi: 10.4319/lo.1980.25.3.0457

Le Bouteiller, A., Leynaert, A., Landry, M. R., Le Borgne, R., Neveux, J., Rodier, M., et al. (2003). Primary production, new production, and growth rate in the equatorial pacific: Changes from mesotrophic to oligotrophic regime. *J. Geophys. Res.* 108, 8141. doi: 10.1029/2001JC000914

Lefebvre, A., Guiselin, N., Barbet, F., and Artigas, L. F. (2011). Long-term hydrological and phytoplankton monitoring 1992-2007 of three potentially eutrophic systems in the eastern English channel and the southern bight of the north Sea. *ICES Int. J. Mar. Sci.* 68, 2029–2043. doi: 10.1093/icesjms/fsr149

Levins, R. (1962). Theory of fitness in a heterogeneous environment. i. the fitness set and adaptive function. *Am. Nat.* 96, 361–373. doi: 10.1086/282245

Lewandowska, A. M., Boyce, D. G., Hofmann, M., Matthiessen, B., Sommer, U., and Worm, B. (2014). Effects of sea surface warming on marine plankton. *Ecol. Lett.* 17, 614–623. doi: 10.1111/ele.12265

Leynaert, A., Bucciarelli, E., Claquin, P., Dugdale, R. C., Martin-Jézéquel, V., Pondaven, P., et al. (2004). Effect of iron deficiency on diatom cell size and silicic acid uptake kinetics. *Limnol. Oceanogr.* 49, 1134–1143. doi: 10.4319/lo.2004.49.4.1134

L'Helguen, S., Madec, C., and Le Corre, P. (1993). Nutrition azotée du phytoplancton dans les eaux brassées de la manche occidentale. *Oceanol. Acta* 16, 653–660.

Lheureux, A., Savoye, N., Del Amo, Y., Goberville, E., Bozec, Y., Breton, E., et al. (2021). Bi-decadal variability in physico-biogeochemical characteristics of temperate coastal ecosystems: from large-scale to local drivers. *Mar. Ecol. Prog. Ser.* 660, 19–35. doi: 10.3354/meps13577

Lingoes, J. C. (1971). Some boundary conditions for a monotone analysis of symmetric matrices. *Psychometrika* 36, 195–203. doi: 10.1007/BF02291398

Litchman, E., and Klausmeier, C. A. (2008). Trait-based community ecology of phytoplankton. *Annu. Rev. Ecol. Evol. Syst.* 39, 615–639. doi: 10.1146/annurev.ecolsys.39.110707.173549

Litchman, E., Klausmeier, C. A., Schofield, O. M., and Falkowski, P. G. (2007). The role of functional traits and trade-offs in structuring phytoplankton communities: scaling from cellular to ecosystem level. *Ecol. Lett.* 10, 1170–1181. doi: 10.1111/j.1461-0248.2007.01117.x

Liu, H., Wu, C., Xu, W., Wang, X., Thangaraj, S., Zhang, G., et al. (2020). Surface phytoplankton assemblages and controlling factors in the strait of malacca and sunda shelf. *Front. Mar. Sci.* 7. doi: 10.3389/fmars.2020.00033

Loebl, M., Colijn, F., Justus, E. E., van Beusekom, J., Baretta-Bekker, G., Lancelot, C., et al. (2009). Recent patterns in potential phytoplankton limitation along the Northwest European continental coast. *J. Sea Res.* 61, 34–43. doi: 10.1016/j.seares.2008.10.002

Logares, R., Bråte, J., Bertilsson, S., Clasen, J. L., Shalchian-Tabrizi, K., and Rengefors, K. (2009). Infrequent marine–freshwater transitions in the microbial world. *Trends Microbiol.* 17, 414–422. doi: 10.1016/j.tim.2009.05.010

Loreau, M. (2000). Biodiversity and ecosystem functioning: recent theoretical advances. *Oikos* 91, 3–17. doi: 10.1034/j.1600-0706.2000.910101.x

Loreau, M., and de Mazancourt, C. (2008). Species Synchrony and Its Drivers: Neutral and Nonneutral Community Dynamics in Fluctuating Environments. *Am. Nat.* 172, 2.E48–2.E66. doi: 10.1086/589746

Loreau, M., Naeem, S., and Inchausti, P. (2002). *Biodiversity and ecosystem functioning: synthesis and perspectives* (Oxford: Oxford University Press).

Lorenzen, C. J. (1967). Determination of chlorophyll and pheopigments spectrophotometric equations. *Limnol. Oceanogr.* 12, 343–346. doi: 10.4319/lo.1967.12.2.0343

Lovecchio, S., Climent, E., Stocker, R., and Durham, W. M. (2019). Chain formation can enhance the vertical migration of phytoplankton through turbulence. *Adv. Sci.* 5, eaaw7879. doi: 10.1126/sciadv.aaw7879

Lürling, M., Eshetu, F., Faassen, E. J., Kosten, S., and Huszar, V. L. M. (2013). Comparison of cyanobacterial and green algal growth rates at different temperatures. *Freshw. Biol.* 58, 552–559. doi: 10.1111/j.1365-2427.2012.02866.x

Maar, M., Nielsen, T. G., Richardson, K., Christaki, U., Hansen,, O. S., Zervoudaki, S., et al. (2002). Spatial and temporal variability of food web structure during the spring bloom in the skagerrak. *Mar. Ecol. Prog. Ser.* 239, 11–29. doi: 10.3354/meps239011

Mammola, S., and Cardoso, P. (2020). Functional diversity metrics using kernel density n-dimensional hypervolumes. *Methods Ecol. Evol.* 11, 986–995. doi: 10.1111/2041-210X.13424

Mancuso, C. P., Lee, H., Abreu, C. I., Gore, J., and Khalil, A. S. (2021). Environmental fluctuations reshape an unexpected diversity-disturbance relationship in a microbial community. *J. Comput. Syst. Biol.* 10, e67175. doi: 10.7554/eLife.67175

Marie, D., Partensky, F., Vaulot, D., and Brussaard, C. (1999). Enumeration of Phytoplankton, Bacteria, and Viruses in Marine Samples. *Curr. Protoc. Cytom.*, 10, 11.11.1-11.11.15. doi: 10.1002/0471142956.cy1111s10

Martin-Jézéquel, V., Hildebrand, M., and Brzezinski, M. A. (2000). Silicon metabolism in diatoms: implications for growth. *J. Phycol.* 36, 821–840. doi: 10.1104/pp.107.107094

Martin-Jézéquel, V., and Lopez, P. J. (2003). Silicon – a central metabolite for diatom growth and morphogenesis. *Prog. Mol. subcell. Biol.* 33, 99–124. doi: 10.1007/978-3-642-55486-5_4

Mason, N. W., de Bello, F., Mouillot, D., Pavoine, S., and Dray, S. (2013). A guide for using functional diversity indices to reveal changes in assembly processes along ecological gradients. *J. Veg. Sci.* 24, 794–806. doi: 10.1111/jvs.12013

Mason, N. W. H., Irz, P., Lanoiselée, C., Mouillot, D., and Argillier, C. (2008). Evidence that niche specialization explains species–energy relationships in lake fish communities. *J. Anim. Ecol.* 77, 285–296. doi: 10.1111/j.1365-2656.2007.01350.x

Mason, N. W. H., Mouillot, D., Lee, W. G., and Wilson, J. B. (2005). Functional richness, functional evenness and functional divergence: the primary components of functional diversity. *Oikos* 111, 112–118. doi: 10.1111/j.0030-1299.2005.13886.x

Mayfield, M. M., and Levine, J. M. (2010). Opposing effects of competitive exclusion on the phylogenetic structure of communities. *Ecol. Lett.* 13, 1085–1093. doi: 10.1111/j.1461-0248.2010.01509.x

McArthur, R. H. (1972). *Geographical ecology* (New York: Harper and Row).

Mc Arthur, R., and Levins, R. (1967). Limiting similarity, convergence, and divergence of coexisting species. *Am. Nat.* 101, 377–385. doi: 10.1086/282505

McGill, B. J., Dornelas, M., Gotelli, N. J., and Magurran, A. E. (2015). Fifteen forms of biodiversity trend in the anthropocene. *Trends Ecol. Evol.* 30, 104–113. doi: 10.1016/j.tree.2014.11.006

McGill, B. J., Enquist, B. J., Weiher, E., and Westoby, M. (2006). Rebuilding community ecology from functional traits. *Trends Ecol. Evol.* 21, 178–185. doi: 10.1016/j.tree.2006.02.002

McIntire, E.J.B., and Fajardo, A. (2014). Facilitation as a ubiquitous driver of biodiversity. *New Phytol* 201, 403–416. doi: 10.1111/nph.12478

McLean, M. J., Mouillot, D., Goascoz, N., Schlaich, I., and Auber, A. (201). Functional reorganization of marine fish nurseries under climate warming. *Glob. Chang. Biol.* 25, 660–674. doi: 10.1111/gcb.14501

McQuatters-Gollop, A., Raitsos, D. E., Edwards, M., Pradhan, Y., Mee, L., Lavender, S. J., et al. (2007). A long-term chlorophyll data set reveals regime shift in

north Sea phytoplankton biomass unconnected to nutrient trends. *Limnol. Oceanogr.* 2, 635–648. doi: 10.4319/lo.2007.52.2.0635

Menden-Deuer, S., and Lessard, E. J. (2000). Carbon to volume relationships for dinoflagellates, diatoms, and other protist plankton. *Limnol. Oceanogr.* 45, 569–579. doi: 10.4319/lo.2000.45.3.0569

Millero, F. J., Chen, C.-T., Bradshaw, A., and Schleicher, K. (1980). A new high-pressure equation of state for seawater. *Deep Sea Res.* 27, 255–264. doi: 10.1016/0198-0149(80)90016-3

Millero, F. J., and Poisson, A. (1981). International one-atmosphere equations of state of seawater. *Deep-Sea Res.* 28, 625–629. doi: 10.1016/0198-0149(81)90122-9

Moestrup, Ø., and Larsen, J. (1992). "Potentially toxic phytoplankton: 1. haptophyceae prymnesiophyceae. ICES identification leaflets for plankton = fiches d'identification du plancton," in *ICES identification leaflets for plankton*, vol. 179 . Ed. J. A. Lindley (Copenhagen: ICES), 11, ISBN: .

Moneta, A., Veuger, B., van Rijswijk, P., Meysman, F., Soetaert, K., and Middelburg, J. J. (2014). Dissolved inorganic and organic nitrogen uptake in the coastal north Sea: a seasonal study. *Estuar. Coast. Shelf Sci.* 147, 78–86. doi: 10.1016/j.ecss.2014.05.022

Morel, A., and Smith, R. C. (1974). Relation between total quanta and total energy for aquatic photosynthesis. *Limnol. Oceanogr.* 19, 591–600. doi: 10.4319/lo.1974.19.4.0591

Moritz, S. (2018). *Time series missing value imputation package 'imputeTS'. Version2*. Available at: https://cran.r-project.org/web/packages/imputeTS/readme/README.html.

Moritz, S., and Bartz-Beielstein, T. (2017). ImputeTS: Time series missing value imputation in r. *R J.* 91, 207–218. doi: 10.32614/RJ-2017-009

Münkemüller, T., Gallien, L., Pollock, L. J., Barros, C., Carboni, M., Chalmandrier, L., et al. (2020). Dos and don'ts when inferring assembly rules from diversity patterns. *Global Ecol. Biogeogr.* 29, 1212–1229. doi: 10.1111/geb.13098

Muscarella, R., and Uriarte, M. (2016). Do community-weighted mean functional traits reflect optimal strategies? *Proc. R. Soc B: Biol. Sci.* 283, 20152434. doi: 10.1098/rspb.2015.2434

Musielak, M. M., Karp-Boss, L., Jumars, P. A., and Fauci, L. J. (2009). Nutrient transport and acquisition by diatom chains in a moving fluid. *J. Fluid Mech.* 638, 401–421. doi: 10.1017/S0022112009991108.401

Napoléon, C., Raimbault, V., Fiant, L., Riou, P., Lefebvre, S., Lampert, L., et al. (2012). Spatiotemporal dynamics of physicochemical and photosynthetic parameters in the central English channel. *J. Sea Res.* 69, 43–52. doi: 10.1016/j.seares.2012.01.005

Naselli-Flores, L., Zohary, T., and Padisák, J. (2021). Life in suspension and its impact on phytoplankton morphology: an homage to Colin s. reynolds. *Hydrobiologia* 848, 7–30. doi: 10.1007/s10750-020-04217-x

Nejstgaard, J. C., Tang, K., Steinke, M., Dutz, J., Koski, M., Antajan, E., et al. (2007). Zooplankton grazing on *Phaeocystis*: A quantitative review and future challenges. *Biogeochemistry* 83, 147–172. doi: 10.1007/s10533-007-9098-y

Oksanen, J., Blanchet, G. F., Kindt, R., Legendre, P., et al. (2011) *Vegan: community ecology package*. Available at: http://cran.r-project.org/web/packages/vegan/index.html.

Olden, J. D., Poff, N. L., Douglas, M. R., Douglas, M. E., and Fausch, K. D. (2004). Ecological and evolutionary consequences of biotic homogenization. *Trends Ecol. Evol.* 19, 18–24. doi: 10.1016/j.tree.2003.09.010

Olde Venterink, H. (2011). Does phosphorus limitation promote species rich plant communities? *Plant Soil* 345, 1–9. doi: 10.1007/s11104-011-0796-9

OSPAR (1988). *PARCOM recommendation 88/2 : On the reduction in nutrients to the Paris convention area* (Paris Commission). Available at: https://www.ospar.org/convention/agreements?q=PARCOM%20Recommendation%2088/2%20on%20the%20Reduction%20in%20Inputs%20of%20Nutrients%20to%20the%20Paris%20Convention%20Area.

Pakeman, R. J. (2014). Functional trait metrics are sensitive to the completeness of the species' trait data? *Methods Ecol. Evol.* 5, 9–15. doi: 10.1111/2041-210X.12136

Pakeman, R. J., and Quested, H. M. (2007). Sampling plant functional traits: what proportion of the species need to be measured? *Appl. Veg. Sci.* 10, 91–96. doi: 10.1658/1402-2001

Pálffy, K., and Vőrős, L. (2019). Phytoplankton functional composition shows higher seasonal variability in a large shallow lake after a eutrophic past. *Ecosphere* 10, e02684. doi: 10.1002/ecs2.2684

Pančić, M., Torres, R. R., Almeda, R., and Kiørboe, T. (2019). Silicified cell walls as a defensive trait in diatoms. *Proc. R. Soc B: Biol. Sci.* 24, 20190184. doi: 10.1098/rspb.2019.0184

Peperzak, L., Colijn, F., Gieskes, W. W. C., and Peeters, J. C. H. (1998). Development of the diatom-phaeocystis spring bloom in the Dutch coastal zone of the north Sea: the silicon depletion versus the daily irradiance threshold hypothesis. *J. Plankton Res.* 20, 517–537. doi: 10.1093/plankt/20.3.517

Pielou, E. (1966). The measurement of diversity in different types of biological collections. *J. Theor. Biol.* 13, 131–144. doi: 10.1016/0022-5193(66)90013-0

Pigot, A. L., Trisos, C. H., and Tobias, J. A. (2016). Functional traits reveal the expansion and packing of ecological niche space underlying an elevational diversity gradient in passerine birds. *Proc. R. Soc B: Biol. Sci.* 283, 20152013. doi: 10.1098/rspb.2015.2013

Pinheiro, J., Bates, D.R Core Team (2022) *Nlme: Linear and nonlinear mixed effects models. r package version 3*. Available at: https://CRAN.R-project.org/package=nlme.

Ploug, H. S., Jørgensen, W., and Barker, B. (1999). Diffusive boundary layers of the colony-forming plankton alga phaeocystis sp; implications for nutrient uptake and cellular growth. *Limnol. Oceanog.* 8. doi: 10.4319/lo.1999.44.8.1959

Podani, J. (1999). Extending gower's general coefficient of similarity to ordinal characters. *Taxon* 48, 331–340. doi: 10.2307/1224438

Ptacnik, R., Solimini, A. G., Andersen, T., Tamminen, T., Brettum, P., Lepistö, L., et al. (2008). Diversity predicts stability and resource use efficiency in natural phytoplankton communities. *PNAS* 105, 5134–5138. doi: 10.1073/pnas.0708328105

Purvis, A., Gittleman, J. L., Cowlishaw, G., and Mace, G. M. (2000). Predicting extinction risk in declining species. *Proc. R. Soc B: Biol. Sci.* 267, 1947–1952. doi: 10.1098/rspb.2000.1234

Redfield, A. C., Ketchum, B. A., and Richards, F. A. (1963). "The influence of organisms on the composition of sea-water: ideas and observations on progress in the study of the seas," in *The sea*, vol. Vol 2 . Ed. M. N. Hill (New York: Wiley), 26–77.

Regier, P., Briceño, H., and Boyer, J. N. (2019). Analyzing and comparing complex environmental time series using a cumulative sums approach. *MethodsX* 6, 779–787. doi: 10.1016/j.mex.2019.03.014

Riley, G. A. (1957). Phytoplankton of the north central Sargasso Sea. *Limnol. Oceanogr.* 2, 252–270. doi: 10.1002/lno.1957.2.3.0252

Rousseau, V., Chrétiennot-Dinet, M. J., Jacobsen, A., Verity, P., and Whipple, S. (2007). The life cycle of *Phaeocystis*: state of knowledge and presumptive role in ecology. *Biogeochemistry* 83, 29–47. doi: 10.1007/s10533-007-9085-3

Rousseau, V., Mathot, S., and Lancelot, C. (1990). Calculating carbon biomass of *Phaeocystis* sp. from microscopic observations. *Mar. Biol.* 107, 305–314. doi: 10.1007/BF01319830

Saulquin, B., Hamdi, A., Gohin, F., Populus, J., Mangin, A., and Fanton d'Andon, O. (2013). Estimation of the diffuse attenuation coefficient KdPAR using MERIS and application to seabed habitat mapping. *Remote Sens. Environ.* 128, 224–233. doi: 10.1016/j.rse.2012.10.002

Schapira, M., Seuront, L., and Gentilhomme, V. (2006). Effects of small-scale turbulence on phaeocystis globosa (Prymnesiophyceae) growth and life cycle. *J. Exp. Ma. Biol. Ecol.* 335, 27–38. doi: 10.1016/j.jembe.2006.02.018

Schiller, J. (1931–1937). "Dinoflagellatae peridinineae in monographischer behandlung," in *Kryptogamen-flora von deutschland, Österreichs und der schweiz*, vol. Vol. 10 . Ed. L. Rabenhorst (Leipzig: Akad. Verlag), 3.

Schluter, D. (1984). A variance test for detecting species associations, with some example applications. *Ecology* 65, 998–1005. doi: 10.2307/1938071

Schoemann, V., Becquevort, S., Stefels, J., Rousseau, V., and Lancelot, C. (2005). *Phaeocystis* blooms in the global ocean and their controlling mechanisms: a review. *J. Sea Res.* 53, 43–66. doi: 10.1016/j.seares.2004.01.008

Schwaderer, A. S., Yoshiyama, K., De Tezanos Pinto, P., Swenson, N. G., Klausmeier, C. A., and Litchman, E. (2011). Eco-evolutionary differences in light utilization traits and distributions of freshwater phytoplankton. *Limnol. Oceanogr.* 56, 589–598. doi: 10.4319/lo.2011.56.2.0589

Segura, A. M., Kruk, C., Calliari, D., García-Rodriguez, F., Conde, D., Widdicombe, C. E., et al. (2013). Competition drives clumpy species coexistence in estuarine phytoplankton. *Sci. Rep.* 3, 1037. doi: 10.1038/srep01037

Shimadzu, H., Dornelas, M., Henderson, P. A., and Magurran, A. E. (2013). Diversity is maintained by seasonal variation in species abundance. *BMC Biol.* 11, 98. doi: 10.1186/1741-7007-11-98

Solorzano, L. (1969). Determination of ammonia in natural waters by the phenolhypochlorite method. *Limnol. Oceanogr.* 14, 799–801. doi: 10.4319/lo.1969.14.5.0799

Sommer, U. (1988). Phytoplankton succession in microcosm experiments under simultaneous grazing pressure and resource limitation, limnol. *Oceanogr.* 33, 1037–1054. doi: 10.4319/lo.1988.33.5.1037

Spaak, J. W., Baert, J. M., Baird, D. J., Eisenhauer, N., Maltby, L., Pomati, F., et al. (2017). Shifts of community composition and population density substantially affect ecosystem function despite invariant richness. *Ecol. Lett.* 20, 1315–1324. doi: 10.1111/ele.12828

Steiner, C. F., Long, Z. T., Krumins, J. A., and Morin, P. J. (2005). Temporal stability of aquatic food webs: partitioning the effects of species diversity, species composition and enrichment. *Ecol. Lett.* 8, 819–828. doi: 10.1111/j.1461-0248.2005.00785.x

Stein, A., Gerstner, K., and Kreft, H. (2014). Environmental heterogeneity as a universal driver of species richness across taxa, biomes and spatial scales. *Ecol. Lett.* 17, 866–880. doi: 10.1111/ele.12277

Stockwell, J. D., Doubek, J. P., Adrian, R., Anneville, O., Carey, C. C., Carvalho, L., et al. (2020). Storm impacts on phytoplankton community dynamics in lakes. *Glob. Chang. Biol.* 26, 2756–2784. doi: 10.1111/gcb.15033

Suescún-Bolívar, L. P., and Thomé, P. E. (2015). Osmosensing and osmoregulation in unicellular eukaryotes. *World J. Microbiol. Biotechnol.* 313, 435–443. doi: 10.1007/s11274-015-1811-8

Sultan, S. E., and Spencer, H. G. (2002). Metapopulation structure favors plasticity over local adaptation. *Am. Nat.* 1602, 271–283. doi: 10.1086/341015

Tabakabayashi, M., Lew, K., Johnson, A., Marchi, A., Dugdale, R., and Wilkerson, F. P. (2006). The effect of nutrient availability and temperature on chain length of the diatom *Skeletonema costatum*. *J. Plankton Res.* 28, 831–840. doi: 10.1093/plankt/fbl018

Talarmin, A., Lomas, M. W., Bozec, Y., Savoye, N., Frigstad, H., Karl, D. M., et al. (2016). Seasonal and long-term changes in elemental concentrations and ratios of marine particulate organic matter. *Glob. Biogeochem. Cycles* 30, 1699–1711. doi: 10.1002/2016GB005409

Taylor, B. W., Keep, C. F., Hall, R. O.Jr., Koch, B. J., Tronstad, L. M., Flecker, A. S., et al. (2007). Improving the fluorometric ammonium method: matrix effects, background fluorescence, and standard additions. *J. North Am. Benthol. Soc.* 26, 167–177. doi: 10.1899/0887-3593200726

Tett, P., Gowen, R., Mills, D., Fernandes, T., Gilpin, L., Huxham, M., et al. (2007). Defining and detecting undesirable disturbance in the context of marine eutrophication. *Mar. pollut. Bull.* 55, 282–297. doi: 10.1016/j.marpolbul.2006.08.028

Thackeray, S. J., Jones, I. D., and Maberly, S. C. (2008). Long-term change in the phenology of spring phytoplankton: species-specific responses to nutrient enrichment and climatic change. *J. Ecol.* 96, 523–535. doi: 10.1111/j.1365-2745.2008.01355.x

Tilman, D., Knops, J., Wedin, D., Reich, P., Ritchie, M., and Siemann, E. (1997). The influence of functional diversity and composition on ecosystem processes. *Science* 277, 1300–1302. doi: 10.1126/science.277.5330.1300

Våge, S., Storesund, J. E., Giske, J., and Thingstad, T. F. (2014). Optimal defense strategies in an idealized microbial food web under trade-off between competition and defense. *PloS One* 9 (7), e101415. doi: 10.1371/journal.pone.0101415

van Boekel, W. H. M., and Veldhuis, M. J. W. (1990). Regulation of alkaline phosphatase synthesis in *Phaeocystis* sp. *Mar. Ecol. Prog. Ser.* 61, 282–289. doi: 10.3354/meps061281

Van den Hoek, C., Mann, D. G., and Jahns, H. M. (1995). *Algae: An introduction to phycology* (Cambridge: Cambridge University Press).

van Rijssel, M., Hamm, C., and Gieskes, W. (1997). *Phaeocystis globose* prymnesiophyceae colonies: hollow structures built with small amounts of polysaccharides. *Eur. J. Phycol.* 32, 185–192. doi: 10.1080/09670269710001737119

Villéger, S., Mason, N. W. H., and Mouillot, D. (2008). New multidimensional functional diversity indices for a multifaceted framework in functional ecology. *Ecology* 89, 2290–2301. doi: 10.1890/07-1206.1

Violle, C., Navas, M. L., Vile, D., Kazakou, E., Fortunel, C., Hummel, I., et al. (2007). Let the concept of trait be functional! *Oikos* 116, 882–892. doi: 10.1111/j.0030-1299.2007.15559.x

Weiher, E., Clarke, G. D. P., and Keddy, P. A. (1998). Community assembly rules, morphological dispersion, and the coexistence of plant species. *Oikos* 81, 309–322. doi: 10.2307/3547051

Weiher, E., and Keddy, P. A. (1995). Assembly rules, null models, and trait dispersion: new questions from old patterns. *Oikos* 74, 159–164. doi: 10.2307/3545686

Wei, T., and Simko, V. (2021) *R package 'corrplot': Visualization of a correlation matrix. (Version 0.92)*. Available at: https://github.com/taiyun/corrplot.

Wiltshire, K. H., Boersma, M., Carstens, K., Kraberg, A. C., Peters, S., and Scharfe, M. (2015). Control of phytoplankton in a shelf sea: Determination of the main drivers based on the helgoland roads time series. *J. Sea Res.* 105, 42–52. doi: 10.1016/j.seares.2015.06.022

Winder, M. (2009). Photosynthetic picoplankton dynamics in lake Tahoe: temporal and spatial niche partitioning among prokaryotic and eukaryotic cells. *J. Plankton Res.* 31, 1307–1320. doi: 10.1093/plankt/fbp074

Wood, S. (2017). Generalized Additive Models: An Introduction with R, 2nd edition. Chapman and Hall/CRC (Boca Raton, USA). 496 p. ISBN 9781498728331.

Worm, B., Barbier, E. B., Beaumont, N., Duffy, J. E., Folke, C., Halpern, B. S., et al. (2006). Impacts of biodiversity loss on ocean ecosystem services. *Science* 314, 787–790. doi: 10.1126/science.1132294

Worm, B., Lotze, H. K., Hillebrand, H., and Sommer, U. (2002). Consumer versus resource control of species diversity and ecosystem functioning. *Nature* 417, 848–851. doi: 10.1038/nature00830

Xu, X., Carsten, L., and Kai, W. W. (2020). Less nutrients but more phytoplankton: Long-term ecosystem dynamics of the southern north Sea. *Front. Mar. Sci.* 7. doi: 10.3389/fmars.2020.00662

Yokota, K., and Sterner, R. W. (2011). Trade-offs limiting the evolution of coloniality: ecological displacement rates used to measure small costs. *Proc. Biol. Sci.* 278, 458–463. doi: 10.1098/rspb.2010.1459

Zhang, R., and Tielbörger, K. (2020). Density-dependence tips the change of plant-plant interactions under environmental stress. *Nat. Commun.* 111, 2532. doi: 10.1038/s41467-020-16286-6

Zobel, M. (1997). The relative role of species pools in determining plant species richness: an alternative explanation of species coexistence? *Trends Ecol. Evol.* 127, 266–269. doi: 10.1016/S0169-5347(97)01096-3

Züst, T., and Agrawal, A. A. (2017). Trade-offs between plant growth and defense against insect herbivory: An emerging mechanistic synthesis. *Annu. Rev. Plant Biol.* 681, 513–534. doi: 10.1146/annurev-arplant-042916-040856

Harmful Algae 125 (2023) 102424

Contents lists available at ScienceDirect

Harmful Algae

journal homepage: www.elsevier.com/locate/hal

Original Article

On the conditions promoting *Pseudo-nitzschia* spp. blooms in the eastern English Channel and southern North Sea

Emilie Houliez *, François G. Schmitt, Elsa Breton, Dimitra-Ioli Skouroliakou, Urania Christaki

Univ. Littoral Côte d'Opale, CNRS, Univ. Lille, UMR 8187, LOG, Laboratoire d'Océanologie et de Géosciences, F-62930 Wimereux, France

ARTICLE INFO

Edited by Editor: Christopher Gobler

Keywords:
Harmful algal bloom
Domoic acid
Ecological niche
Pseudo-nitzschia
Biotic interactions
Phytoplankton

ABSTRACT

This study investigated the drivers of the blooms of *Pseudo-nitzschia seriata* and *Pseudo-nitzschia delicatissima* complexes in the eastern English Channel and southern North Sea. Phytoplankton data series acquired from 1992 to 2020 were analyzed with a multivariate statistical approach based on Hutchinson's niche concept. *P. seriata* and *P. delicatissima* complexes were found to be typically present year round, but they bloomed at different periods because they occupied different realized ecological niches. *P. delicatissima* complex occupied a more marginal niche and was less tolerant than *P. seriata* complex. *P. delicatissima* complex typically bloomed in April-May at the same time as *Phaeocystis globosa* while *P. seriata* complex blooms were more frequently observed in June during the decline of low intensity *P. globosa* blooms. *P. delicatissima* and *P. seriata* complexes were both favored by low-silicate environments and relatively low turbulence but they responded differently to water temperature, light, ammonium, phosphate and nitrite + nitrate conditions. Niche shifts and biotic interactions played important roles in the control of the blooms of *P. delicatissima* and *P. seriata* complexes. The two complexes occupied different sub-niches during their respective low abundance and bloom periods. The phytoplankton community structure and the number of other taxa presenting a niche overlapping the niches of *P. delicatissima* and *P. seriata* complexes also differed between these periods. *P. globosa* was the taxa contributing the most to the dissimilarity in community structure. *P. globosa* interacted positively with *P. delicatissima* complex and negatively with *P. seriata* complex.

1. Introduction

Blooms of the diatom *Pseudo-nitzschia* are recognized worldwide as a public health threat because several species in this genus are known to produce the neurotoxin domoic acid (DA) causing amnesic shellfish poisoning (ASP) (Bates et al., 2018; Grattan et al., 2016; Lelong et al., 2012; Petroff et al., 2021; Trainer et al., 2008). Since the report of the first ASP event in 1987 (Perl et al., 1990), *Pseudo-nitzschia* has become the focus of considerable international scientific attention. Temperature, salinity, nutrients, irradiance, photoperiod and upwelling events have been identified as factors influencing its growth and toxicity (Bates et al., 1998, 2018; Clark et al., 2019; Downes-Tettmar et al., 2013; Fehling et al., 2006; Klein et al., 2010; Lelong et al., 2012; Marchetti et al., 2004; McCabe et al., 2016; Thorel et al., 2017; Trainer et al., 2012, 2008). However, in spite of intense research, the current understanding of the conditions controlling *Pseudo-nitzschia* spp. blooms remains elusive since the aforementioned abiotic factors are generally insufficient to explain the occurrence, intensity and demise (often abrupt) of *Pseudo-nitzschia* spp. blooms (Azanza et al., 2018). A part of our lack of understanding is because environmental cues triggering *Pseudo-nitzschia* spp. blooms are complex and can be unique to the bay, coastal or open ocean region where they occur making any generalization of the findings almost impossible (Trainer et al., 2012). Another reason might be the methodology employed. Harmful algae (including *Pseudo-nitzschia* spp.) are usually studied in monospecific cultures in the laboratory and field studies often neglect to characterize surrounding phytoplankton community (Wells and Karlson, 2018). As such, competitive interactions are not taken into account.

Biotic interactions between *Pseudo-nitzschia* spp. and the other members of the phytoplankton community are of interest because competition for resources is well known to impact the dominance of certain phytoplankton species (Litchman, 2007; Sommer, 1989; Tilman, 1977). Besides, positive interactions such as facilitations (Bruno et al., 2003) have also recently been shown to play a role in some microalgae species successions (Krichen et al., 2019). Therefore, as it has already been demonstrated in terrestrial plants community successions

* Corresponding author.
E-mail address: emilie.houliez@outlook.fr (E. Houliez).

https://doi.org/10.1016/j.hal.2023.102424
Received 30 November 2022; Received in revised form 18 February 2023; Accepted 13 March 2023
Available online 15 March 2023

(Brooker et al., 2008), some pioneer microalgae species could modify their surrounding environment, making it more favorable for the subsequent colonization by other microalgae species. Some examples of *Pseudo-nitzschia* species attached on colonies of other phytoplankton species have also been observed in the field, such as *Pseudo-nitzschia pseudodelicatissima* on *Chaetoceros socialis, Pseudo-nitzschia americana* and *Pseudo-nitzschia linea* on *Chaetoceros* spp. and *Odontella* spp., *Pseudo-nitzschia delicatissima* on *Phaeocystis globosa* or *Pseudo-nitzschia* cf. *granii var. curvata* on *Phaeocystis pouchettii*, suggesting that some kind of relationships may exist between these species (Lelong et al., 2012 and references therein). However, to our knowledge, the potential role of biotic interactions influencing *Pseudo-nitzschia* spp. blooms has never been explored. Turbulence is another factor that has not been considered and would deserve more attention since it affects plankton dynamics (Estrada and Berdalet, 1997; Gibson, 2000; Mann and Lazier, 2013; Schmitt, 2020). There is evidence that turbulence affects most of the parameters influencing diatoms survival. It influences settling velocity and cell re-suspension (Estrada and Berdalet, 1997; Ruiz et al., 2004), nutrients acquisition and availability (Dell'Aquila et al., 2017; Estrada and Berdalet, 1997; Pahlow et al., 1997), genes expression (Amato et al., 2017), chain morphology (Amato et al., 2017; Clarson et al., 2009; Dell'Aquila et al., 2017) and encounter-based processes such as interactions with grazers and diatom-diatom encounter rate for reproduction and chain formation (Rothschild and Osborn, 1988).

Pseudo-nitzschia spp. are regularly present along all the French coasts (Belin et al., 2021) but in some regions, the blooms of *Pseudo-nitzschia* spp. have received few attention. This is the case of the eastern English Channel and southern North Sea. Phytoplankton research in this area has mainly focused on the understanding of the massive *P. globosa* blooms that occur every spring (Breton et al., 2000, 2022; Genitsaris et al., 2015; Grattepanche et al., 2011; Hernández-Fariñas et al., 2014; Peperzak, 2002). Consequently, the number of studies dealing with *Pseudo-nitzschia* spp. ecology in this region is very limited. Delegrange et al. (2018) described the diversity and toxicity of *Pseudo-nitzschia* spp. during one year (2012) at a single station in the southern Bight of the North Sea. Lefebvre and Dezécache (2020) studied the possibility to use *P. globosa* and diatoms (including *Pseudo-nitzschia* spp.) as indicators of eutrophication. Karasiewicz and Lefebvre (2022) found that *Pseudo-nitzschia* spp. could bloom several times during the same year or bloom over a large period of time; however, these blooms patterns could be driven by different species of *Pseudo-nitzschia*. Three *Pseudo-nitzschia* species (*P. delicatissima, P. fraudulenta* and *P. pungens*) belonging to two different complexes (*Pseudo-nitzschia delicatissima* complex and *Pseudo-nitzschia seriata* complex) have been detected in this region by Delegrange et al. (2018). In the present study, it was thus hypothesized that the two *Pseudo-nitzschia* complexes might occupy different ecological niches and present contrasted bloom periods controlled by different environmental factors. Understanding these potential differences in the ecology of the two *Pseudo-nitzschia* complexes is important because the species belonging to these complexes can present different levels of toxicity (e.g. Trainer et al., 2012). It was also thought that biotic interactions with the other members of the phytoplankton community and turbulence might influence *Pseudo-nitzschia* spp. blooms.

By using a methodology based on the concept of realized ecological niche (i.e. the set of favorable conditions under which a species survives, grows, reproduces and can be observed (Hutchinson, 1957)), the present study aimed: 1) to determine the bloom periods of *Pseudo-nitzschia delicatissima* complex and *Pseudo-nitzschia seriata* complex, 2) to investigate the main factors favoring these blooms and, 3) to define the role of the surrounding phytoplankton community by identifying potential biotic interactions between *Pseudo-nitzschia* spp. and the other phytoplankton species.

2. Materials and methods

2.1. Study area

The eastern English Channel and southern North Sea are temperate eutrophic shallow shelf seas with a macrotidal range (3–9 m). The water column is constantly well mixed. Tides are characterized by a residual water circulation parallel to the coast with coastal waters drifting from the English Channel to the North Sea. This so-called "coastal flow" separates the coastal waters from offshore waters by a transient tidally controlled frontal area (Brylinski et al., 1991). Coastal waters are influenced by freshwater runoffs from the Seine, Somme, Authie and Canche estuaries and from the Liane river. The eastern English Channel and southern North Sea present an unusual phytoplankton succession occurring every spring. Each year, the haptophyte *P. globosa* forms massive blooms between March and May and these blooms are preceded and followed by two diatom blooms with distinct species composition (Breton et al., 2000, 2022; Genitsaris et al., 2015; Grattepanche et al., 2011; Hernández-Fariñas et al., 2014).

2.2. Data sets and sampling strategy

Data come from three monitoring programs with similar methodology: 1) SNO-SOMLIT (National coastal observation service, www.somlit.fr), 2) IFREMER French Observation and Monitoring program for Phytoplankton and Hydrology in coastal waters (REPHY, 2021) and 3) Regional Observation and Monitoring Program for Phytoplankton and Hydrology in the eastern English Channel (SRN, 2017). The complete dataset comprised a total of 1213 samples collected over 28 years of phytoplankton observations (SNO-SOMLIT: 1996–2020 and REPHY/SRN: 1992–2019).

Samples were collected at 13 stations distributed along four coastal-offshore transects located in three main areas: the coasts of Boulogne-sur-Mer and Dunkerque and the Bay of Somme (Fig. 1). Water samples for laboratory analyses of nutrient concentrations and phytoplankton were collected at high tide in subsurface with a five-liter Niskin bottle. These sampling were done fortnightly during the SNO-SOMLIT monitoring while during the REPHY/SRN monitoring, samples were collected fortnightly from March to June and monthly the rest of the year. Phytoplankton samples (1 L) were fixed with neutral or acid Lugol's Iodine solution (final concentration 2%).

2.3. Abiotic parameters

Seawater temperature and salinity profiles were measured in situ with a CTD probe (conductivity, temperature, depth). Silicate ($SiOH_4$), nitrate + nitrite ($NO_3^- + NO_2^-$), ammonium (NH_4^+) and phosphate (PO_4^{3-}) concentrations were analyzed following the Aminot and Kérouel (2004, 2007)'s methodology. Turbulence was characterized by a proxy of the mean dissipation rate (ε in m^2/s^3) using MacKenzie and Leggett (1993)'s equation:

$$\varepsilon = \left(5.82\,10^{-6}\right) W^3 / z$$

with z = sampling depth (in m) and W = wind speed (in m s^{-1}). Wind speed was measured at the meteorological stations of Boulogne-sur-Mer, Dunkerque and Cayeux-sur-Mer and was provided by Meteo France. Daily photosynthetically active radiation (PAR in einstein m^{-2} day^{-1}) from 1998 to 2020 was downloaded on GlobColour website (https://hermes.acri.fr). PAR was estimated from satellite products using Frouin et al. (2003)'s algorithm. Five-day averages of turbulence and PAR values were used in the realized ecological niche analyses (four previous days and day of phytoplankton sampling) (Hernández Fariñas et al., 2015; Houliez et al., 2021).

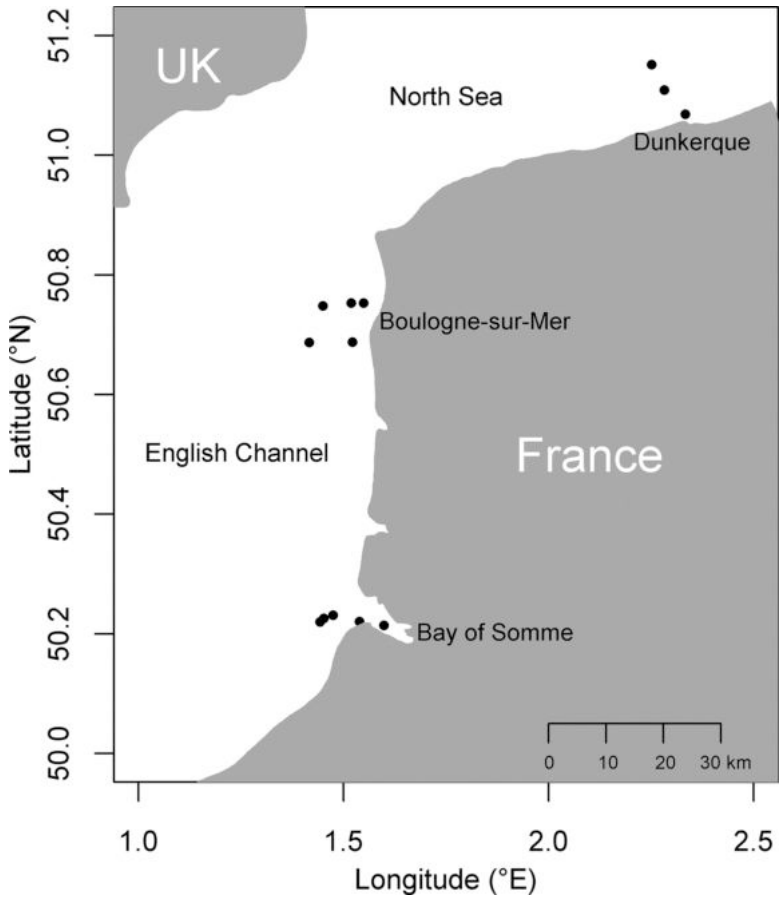

Fig. 1. Map of the eastern English Channel and southern North Sea showing the location of sampling stations (black points).

2.4. Taxonomic determination of phytoplankton species

10–100 mL of the fixed phytoplankton samples were settled for at least 24 h following the Utermöhl method (Utermöhl, 1958). Phytoplankton species were identified to the lowest possible taxonomic level and enumerated using an inverted optical microscope (x 200 to x 400 magnification). To reduce bias in the datasets due to difficulties in differentiating some species or genera using an optical microscope and to guarantee homogeneity over time and among sampling sites, some species and genera were grouped into taxonomic units. A taxonomic unit was thus composed either by a single species (easily identifiable) or a group of several species or genus difficult to distinguish. *Pseudo-nitzschia* spp. were separated into three groups: *Pseudo-nitzschia americana* and two complexes with different cell width and shape: *Pseudo-nitzschia delicatissima* complex (cell width <3 μm, linear shape, delicate forms with very fine structure) and *Pseudo-nitzschia seriata* complex (cell width >3 μm, lanceolate shape) (Hasle and Syvertsen, 1996). This classification based on the size and shape of the cells has already demonstrated its usefulness in the understanding of *Pseudo-nitzschia* spp. ecology (Ajani et al., 2020; Bowers et al., 2018; Delegrange et al., 2018; Downes-Tettmar et al., 2013; Stern et al., 2018; Thorel et al., 2017).

2.5. Statistical analyses

2.5.1. Realized ecological niches and sub-niches

The Outlying Mean Index (OMI, Dolédec et al., 2000) and Within Outlying Mean Indexes (WitOMI, Karasiewicz et al., 2017) were used to characterize respectively the realized ecological niche and realized ecological sub-niches of the two *Pseudo-nitzschia* complexes and of the other species composing surrounding phytoplankton community. OMI and WitOMI are both based on Hutchinson's (1957) realized ecological niche concept (for more details read the supplementary materials). The OMI analysis was carried out using the "niche" and "rtest" functions available in the R ade4 package (Dray and Dufour, 2007) while the WitOMI analysis was performed with the R subniche package (Karasiewicz et al., 2017).

The OMI analysis is a multivariate statistical analysis defining the realized ecological niche of each taxa composing a community along environmental gradients (Dolédec et al., 2000; Karasiewicz et al., 2020). It depends on the response of each taxa to their environment and describes their habitat. Three parameters characterize the realized niche of each taxa: tolerance, marginality, and residual tolerance. Tolerance (also known as niche breadth) corresponds to the niche extent. It describes the range of conditions tolerated and used by a given taxa. Taxa with high tolerance can persist under a wide range of environmental conditions. They are generalists. Inversely, a low tolerance corresponds to specialists i.e. taxa encountered under specific environmental conditions. Marginality (also known as niche position) is the distance between the average conditions (or resources) used by a given taxa and the average conditions (or resources) available in the study area. Taxa with high marginality occupy a marginal realized ecological niche and occur in atypical habitats within the study area. Inversely, taxa with low marginality occupy a non-marginal realized ecological niche and occur in habitats commonly found in the study area. Residual tolerance represents the part of variance that is not explained by marginality. It helps to determine whether the dataset of environmental conditions used to perform the OMI analysis is relevant to define the realized ecological niche of each taxa. The OMI analysis provides graphical outputs which are described in the supplementary materials.

The WitOMI analysis uses the environmental space delimited by the OMI axes as a reference. It decomposes the realized niche of each taxa into realized ecological sub-niches (Karasiewicz et al., 2017). This

analysis provides an estimation of niche shifts or conservatism in the realized ecological niche of each taxa, under specific sub-environmental conditions (called subsets) corresponding to a given time period or a sub-location within the study area. For each subset studied, two additional marginalities are provided: $WitOMI_G$ and $WitOMI_{GK}$. $WitOMI_G$ is the distance between the average conditions (or resources) used by the taxa within the studied subset and the average conditions (or resources) available within the whole sampling period or study area. $WitOMI_{GK}$ is the distance between the average conditions (or resources) used by the taxa within the studied subset and the average conditions (or resources) used by the community. Each of these marginalities is accompanied by an index of tolerance ($Tol_{WitOMIG}$ and $Tol_{WitOMIGK}$) and residual tolerances. For each subset considered, the WitOMI analysis provides a graphical representation of: 1) the environmental conditions (or resources) available (sub-environmental space), 2) the potential sub-niche of the taxa, 3) the realized ecological subniche of the taxa and 4) the biological constraints. The potential sub-niche of the taxa is the intersection between the sub-environmental space within the subset considered and the realized ecological niche defined by the OMI analysis. It corresponds to the niche which could be occupied by the taxa in the absence of biotic interactions. The realized ecological sub-niche is the niche currently occupied by the taxa. The biological constraints correspond to the difference in size between the potential sub-niche and realized ecological sub-niche, and represent the part of the niche that the taxa can't occupy due to biotic interactions (Houliez et al., 2021). In the present study, the environmental variables included in the OMI and WitOMI analyses were water temperature, salinity, nutrient concentrations, turbulence and PAR. These factors are known to influence harmful algal blooms and *Pseudo-nitzschia* spp. growth (e.g. Bates et al., 1998, 2018; Lelong et al., 2012; Wells and Karlson, 2018). The WitOMI analysis was used to decompose the realized ecological niche of *P. delicatissima* and *P. seriata* complexes by considering two subsets corresponding to two contrasted periods based on their abundance. For each *Pseudo-nitzschia* complex, the first subset corresponded to periods of low abundance $< 10^3$ cells L^{-1}. The second subset corresponded to bloom periods. Bloom periods were defined by using the French sanitary regulatory thresholds above which *Pseudo-nitzschia* species are considered as producing blooms potentially harmful, and samples are collected for domoic acid analysis in shellfish by the IFREMER REPHYTOX monitoring network (Belin et al., 2021). This threshold was $\geq 10^5$ cells L^{-1} for *P. seriata* complex and $\geq 3 \times 10^5$ cells L^{-1} for *P. delicatissima* complex. A Mann-Whitney U test (Hollander et al., 2013) was used to test the significance of differences in abiotic parameters between the blooms and periods of low abundance of *P. delicatissima* and *P. seriata* complexes.

2.5.2. Phytoplankton community structure and biotic interactions

For both *P. delicatissima* and *P. seriata* complexes, the taxa contributing the most to the dissimilarity in phytoplankton community structure between years with blooms and years without bloom were studied with a SIMPER (SIMilarity PERcentage) analysis performed on a data frame containing fourth root transformed phytoplankton species abundances using PRIMER 6 (PRIMER-E ltd, Plymouth, UK) (Clarke and Warwick, 2001). When taxa contribution was related to abundance changes, the significance of these changes was tested with a Mann-Whitney U test (Hollander et al., 2013).

To highlight potential biotic interactions between the *Pseudo-nitzschia* complexes (*P. delicatissima* and *P. seriata*) and the other members of the phytoplankton community, an interaction network was built using the Chiquet et al. (2021)'s multivariate Poisson-lognormal model (PLN model). This analysis was performed using the R PLNmodels package. PLN models offer the possibility to distinguish pairs of species that are truly interacting from indirect covariations due to similar response to environmental variables. From the matrix of partial correlation coefficients obtained with the PLN model, a simplified version of the network representing only the taxa interacting with *P. delicatissima* and *P. seriata* complexes was represented by using Cytoscape v.3.8.2.

2.5.3. Niche overlaps

The realized ecological niche, potential sub-niche and realized ecological sub-niche of *P. delicatissima* and *P. seriata* complexes were compared to the niches of the other taxa by using the R hypervolume (Blonder et al., 2014) and BAT (Biodiversity Assessment Tools) packages (Cardoso et al., 2021; Mammola, 2019). Niche hypervolumes were built by using the function "hypervolume_svm" on a data frame containing the coordinates of the realized ecological niche, potential sub-niche and realized ecological sub-niche along the first two axes of the OMI and WitOMI analyses. The total volume of each niche and sub-niche was calculated with the function "kernel.alpha" (Mammola and Cardoso, 2020). The function "kernel.similarity" was used to compare the different niches (Mammola and Cardoso, 2020). This function computes pairwise comparisons between kernel density niche hypervolumes of multiple species and characterizes the similarity between pairs of species niches with pairwise distance metrics (centroid and minimum distance) and similarity indices (intersection = niche overlap, Jaccard similarity index and Sørensen-Dice similarity index) (see Mammola, 2019 for details). In the present study, only the niche overlaps were reported. They were expressed as percentage of the volumes of the realized ecological niche, potential sub-niche and realized ecological sub-niches of *P. seriata* or *P. delicatissima* complex.

3. Results

3.1. Bloom periods

Pseudo-nitzschia delicatissima and *Pseudo-nitzschia seriata* complexes are typically present year round, but their bloom periods are different (Fig. 2 A&B). *P. delicatissima* complex blooms mainly at the same time as *P. globosa* blooms from April to May. From 2009, *P. delicatissima* complex blooms were observed every year (data not shown). *P. seriata* complex typically blooms from March to September but the blooms were more frequently observed in June during the decline periods of low intensity *P. globosa* blooms. *P. seriata* complex started to bloom either at the same time as *P. globosa* or with a small delay after the start of *P. globosa* blooms. However in all cases, the peak of the blooms of *P. seriata* complex was always reached during the decline of *P. globosa* blooms or shortly after. *P. globosa* bloomed every year but it was not the case for *P. seriata* complex (data not shown). During some years, low intensity *P. globosa* blooms were not accompanied by blooms of *P. seriata* complex.

3.2. Realized ecological niches of Pseudo-nitzschia spp

The OMI analysis revealed that *P. delicatissima* and *P. seriata* complexes occupied different realized ecological niches and presented different affinities for abiotic environmental conditions.

The first two axes of the OMI analysis explained 88.0% of total inertia (OMI1 = 70.3% and OMI2 = 17.6%, Fig. 3). OMI1 was mainly explained by $NO_3^- + NO_2^-$ and PAR while OMI2 was mainly explained by water temperature (T). The OMI plane reflected the seasonal variations of environmental conditions and delimited three main periods. The right side of the OMI plane corresponded to autumn-winter conditions characterized by high nutrient concentrations, well-mixed waters (high turbulence) and low PAR. The bottom left side corresponded to spring conditions with low nutrient concentrations, high PAR and high salinity. The top left side corresponded to summer conditions with also low nutrient concentrations, high PAR and high salinity but with higher temperature. The realized ecological niche center of gravity (marginality) of each taxa is positioned within this plane according to their affinities for environmental conditions. The position of the marginality of *P. delicatissima* and *P. seriata* complexes showed that *P. delicatissima* complex had affinity for spring conditions while *P. seriata* complex had

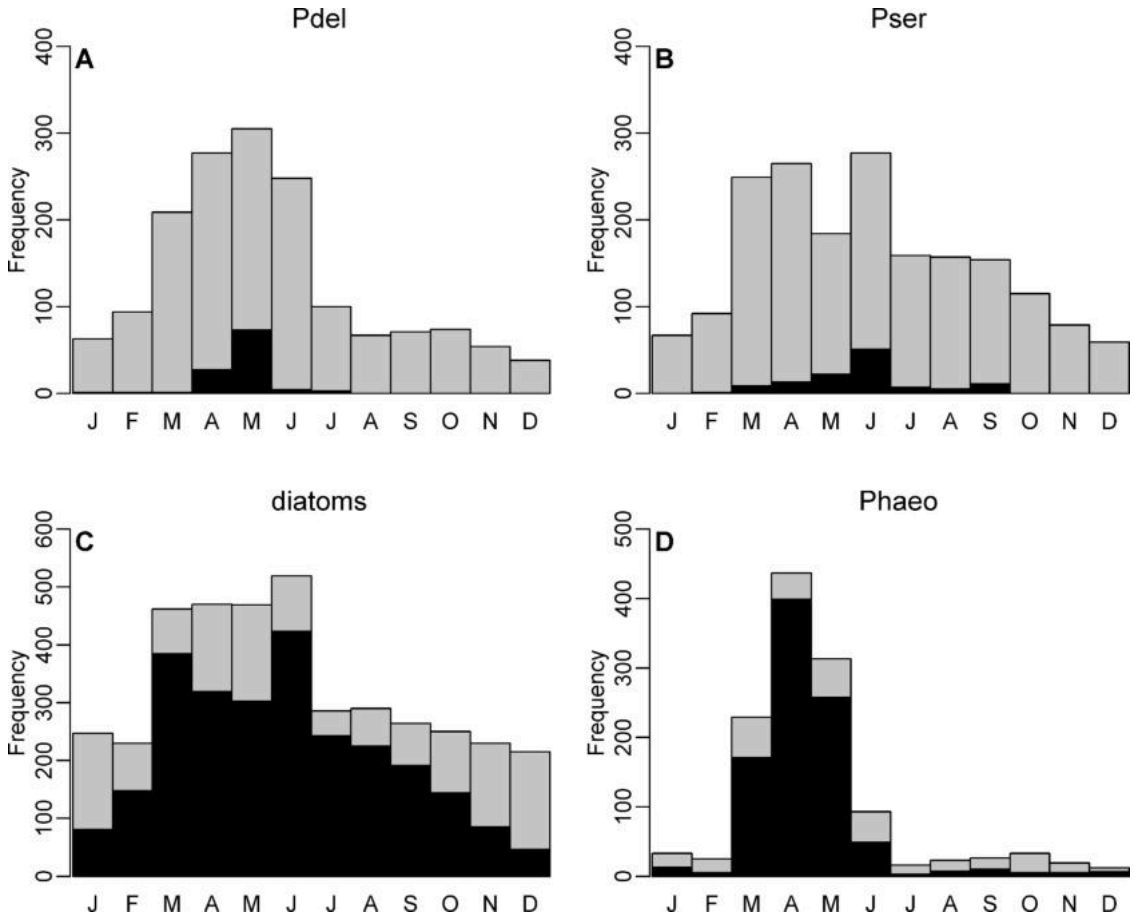

Fig. 2. Observation frequencies of A) *Pseudo-nitzschia delicatissima* complex (Pdel), B) *Pseudo-nitzschia seriata* (Pser) complex, C) all the other diatoms and D) *Phaeocystis globosa* (Phaeo) during the months of the year. Gray bars correspond to observation frequencies of the considered taxa whatever its abundance. Black bars correspond to observation frequencies of the bloom periods i.e. abundances $\geq 3 \times 10^5$ cells L^{-1} for *P. delicatissima* complex and $\geq 10^5$ cells L^{-1} for *P. seriata* complex, all the other diatoms and *P. globosa*. Note the different axes.

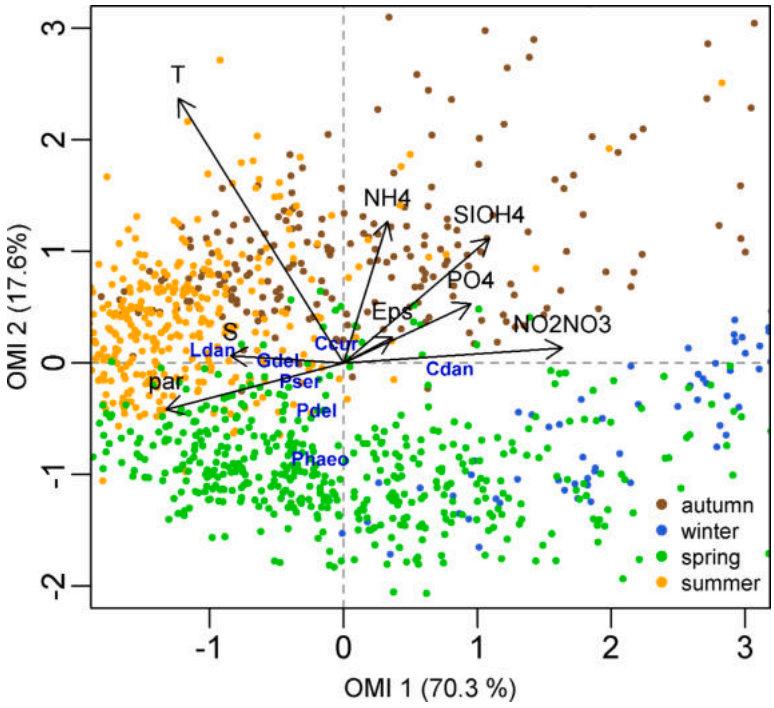

Fig. 3. Outlying Mean Index (OMI) analysis showing the projection of the environmental parameters (in black) and species niche marginality (in blue) along the two OMI axes (OMI1 and OMI2) delimiting the OMI plane. Dots are sampling units colored according to the seasons of the year. T = seawater temperature, par = photosynthetically active radiation, S = salinity, NH4 = ammonium concentration, SIOH4 = silicate concentration, PO4 = phosphate concentration, Eps = turbulent dissipation rate, Pdel = *Pseudo-nitzschia delicatissima* complex, Pser = *Pseudo-nitzschia seriata* complex, Phaeo = *Phaeocystis globosa*, Gdel = *Guinardia delicatula*, Ldan = *Leptocylindrus danicus*, Ccur = *Chaetoceros curvisetus* + *Chaetoceros debilis* and Cdan = *Chaetoceros danicus*.

affinity for spring-summer conditions. Along OMI2, the realized ecological niche of *P. seriata* complex was centered at a higher temperature than the realized ecological niche of *P. delicatissima* complex. High abundances of *P. delicatissima* complex were more frequently observed when temperature ranged from 11 to 14 °C while high abundances of *P. seriata* complex were more frequently observed when temperature ranged from 14 to 16 °C (supplementary materials Fig. S2). Along OMI1, the realized ecological niche of *P. seriata* complex was also centered at higher PAR than the realized ecological niche of *P. delicatissima* complex. High abundances of *P. delicatissima* complex were more frequently observed when PAR ranged from 25 to 45 einstein m^{-2} day^{-1} while high abundances of *P. seriata* complex were more frequently observed when PAR ranged from 40 to 55 einstein m^{-2} day^{-1}. *P. delicatissima* and *P. seriata* complexes also differed in their affinity for $NO_3^- + NO_2^-$ conditions. For both *P. delicatissima* and *P. seriata* complexes, high abundances were more frequently observed when $NO_3^- + NO_2^-$ concentrations were ≤ 1 µM. However, when $NO_3^- + NO_2^-$ concentrations ranged from 5 to 12 µM, high abundances of *P. delicatissima* complex were more frequently observed than high abundances of *P. seriata* complex.

P. delicatissima complex had a higher marginality and lower tolerance than *P. seriata* complex (Table 1). In comparison to the other taxa composing the phytoplankton community, *P. delicatissima* and *P. seriata* complexes were among the ten taxa with the lowest marginality. *P. delicatissima* complex was the 17th taxa with the lowest tolerance while *P. seriata* complex presented an intermediate tolerance (38th over the 74 diatoms with significant realized niches).

3.3. Realized ecological sub-niches of Pseudo-nitzschia spp

3.3.1. Environmental conditions

All abiotic environmental conditions differed between low abundance and bloom periods of *P. delicatissima* complex (Fig. 4). During the blooms of *P. delicatissima* complex, median water temperature, salinity, turbulence and nutrient concentrations (NH_4^-, $NO_2^- + NO_3^-$, $Si(OH)_4$ and PO_4^{3-}) were significantly lower and median PAR was significantly higher than during its low abundance periods. By contrast, only median turbulence, $NO_2^- + NO_3^-$ concentrations, $Si(OH)_4$ concentrations and PAR significantly differed between the blooms and low abundance periods of *P. seriata* complex. Median turbulence, $NO_2^- + NO_3^-$ concentrations and $Si(OH)_4$ concentrations were significantly lower while median PAR was significantly higher during the blooms of *P. seriata* complex than during its low abundance periods. During the years with blooms of *P. seriata* complex, $Si(OH)_4$ and $NO_2^- + NO_3^-$ winter stocks were lower than during the years without blooms of *P. seriata* complex (supplementary materials, Fig.S3).

3.3.2. WitOMI analysis

The WitOMI analysis showed that the sub-environmental space defined by the available environmental conditions was narrower during the blooms of *P. delicatissima* and *P. seriata* complexes than during their low abundance periods (Fig. 5). Consequently, the realized ecological sub-niches of *P. delicatissima* and *P. seriata* complexes shifted during their blooms. *P. delicatissima* and *P. seriata* complexes were both restricted by biological constraints during their respective low abundance periods and they could not take up the totality of their potential sub-niche. *P. delicatissima* and *P. seriata* complexes took up 63% and 90% of their potential sub-niche respectively (Table 1). By contrast, during their blooms, there was no biological constraint and they both took up the totality of their potential sub-niche. However, the realized ecological sub-niche occupied was more marginal than during their low abundance periods and their tolerance was lower.

3.4. Phytoplankton community structure and potential biotic interactions

To understand what were the biological constraints influencing the realized ecological sub-niches of *P. delicatissima* and *P. seriata* complexes, the surrounding phytoplankton community structure was compared between the years with blooms and years without bloom to determine the taxa influencing the most the bloom periods of *P. delicatissima* and *P. seriata* complexes. For both *P. delicatissima* and *P. seriata* complexes, the surrounding phytoplankton community structure was significantly different between their blooming years and the years without bloom (PERMANOVA, $p<0.001$). For *P. delicatissima* complex, the dissimilarity between the phytoplankton community present during the blooming years and that present during the years without bloom equaled 68% (SIMPER analysis, supplementary materials Table S1). Twenty-four taxa were identified as the most influential taxa explaining this dissimilarity. Among them, *P. globosa* was the major contributor. For *P. seriata* complex, the dissimilarity in phytoplankton community between the blooming years and years without bloom equaled 71%. Twenty-three taxa were identified as the most influential and *P. globosa* was also the major contributor to this dissimilarity.

However, contrasting interactions between *P. globosa* and each of the

Table 1
Realized ecological niche and sub-niches parameters of *Pseudo-nitzschia delicatissima* complex (Pdel), *Pseudo-nitzschia seriata* complex (Pser), *Phaeocystis globosa* (Phaeo), *Guinardia delicatula* (Gdel), *Leptocylindrus danicus* (Ldan), *Chaetoceros curvisetus* + *Chaetoceros debilis* (Ccur) and *Chaetoceros danicus* (Cdan).

	Niche parameters (OMI analysis)		Sub-niche parameters (WitOMI analysis)				
Taxa	Marginality	Tolerance	Periods	Marginality (WitOMIG)	Tolerance ($Tol_{WitOMIG}$)	Biological constraints	% PS occupied
Pdel	0.23	0.95	Pdel LA	0.35	4.19	37	63
			Pdel blooms	0.84	0.25	0	100
Pser	0.15	1.81	Pser LA	0.33	4.30	10	90
			Pser blooms	0.95	0.77	0	100
Phaeo	0.77	0.37	Pdel LA	0.58	0.84	51	49
			Pdel blooms	0.92	0.21	13	87
			Pser LA	0.76	0.40	26	74
			Pser blooms	1.21	0.11	44	56
Gdel	0.25	1.78	Pser LA	0.27	1.12	18	82
			Pser blooms	0.88	0.69	7	93
Ldan	1.08	0.99	Pser LA	0.85	0.84	21	79
			Pser blooms	1.72	0.87	5	95
Ccur	0.12	0.79	Pser LA	0.41	2.27	0	100
			Pser blooms	1.95	0.13	81	19
Cdan	0.68	3.24	Pser LA	1.77	3.83	10	90
			Pser blooms	1.16	0.67	27	73

OMI = Outlying Mean Index, WitOMI = Within Outlying Mean Indexes, Biological constraints = part of the potential sub-niche volume that could not be occupied due to biological constraints,% PS occupied = percentage of the potential sub-niche volume occupied by the realized ecological sub-niche, Pdel LA = low abundance periods of *Pseudo-nitzschia delicatissima* complex, Pdel blooms = blooms of *Pseudo-nitzschia delicatissima* complex, Pser LA = low abundance periods of *Pseudo-nitzschia seriata* complex, Pser blooms = blooms of *Pseudo-nitzschia seriata* complex.

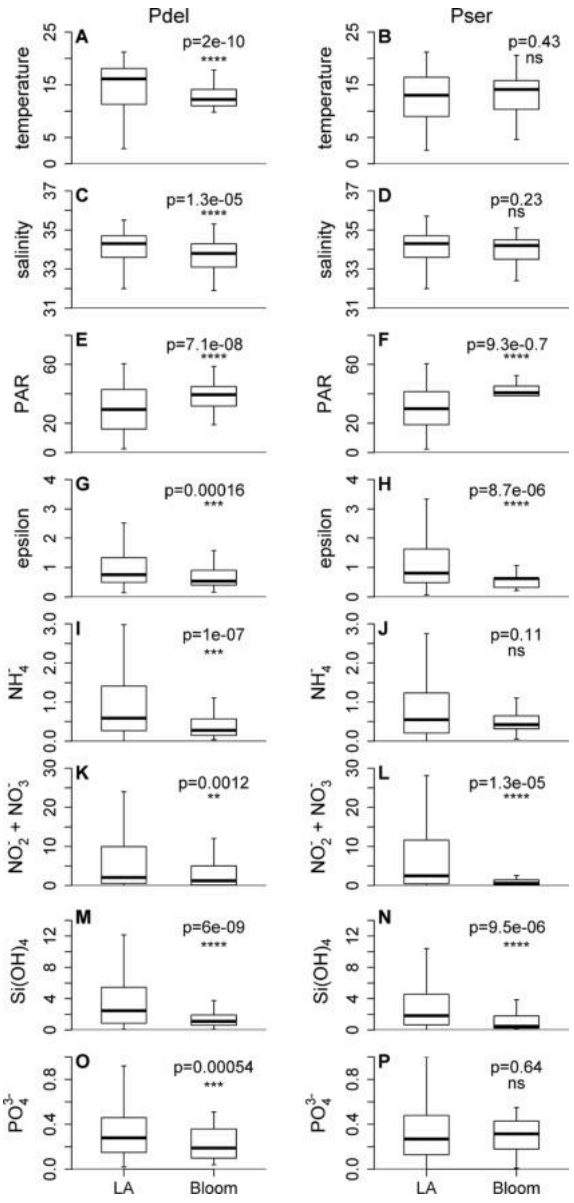

Fig. 4. Boxplots representing A & B) seawater temperature (in °C), C & D) salinity, D & E) photosynthetically active radiation (PAR in einstein m^{-2} day^{-1}), F & G) turbulent dissipation rate (epsilon in 10^{-3} W m^{-3}), I & J) ammonium concentration (NH_4^- in µM), K & L) nitrite + nitrate concentration (NO_2^- + NO_3^- in µM), M & N) silicate concentration ($Si(OH)_4$ in µM) and phosphate concentration (PO_4^{3-} in µM) during the low abundance (LA) and bloom periods of *Pseudo-nitzschia delicatissima* complex (Pdel, left panel) and *Pseudo-nitzschia seriata* complex (Pser, right panel). P values are Mann-Whitney U test results. ns = non significant.

Pseudo-nitzschia complexes (*P. delicatissima* and *P. seriata*) were observed. The interaction network highlighted a positive interaction between *P. delicatissima* complex and *P. globosa* while interaction between *P. seriata* complex and *P. globosa* was negative (Fig. 6). Positive interactions between *P. seriata* complex and 5 other diatoms: *Guinardia delicatula, Leptocylindrus danicus, Chaetoceros curvisetus* + *Chaetoceros debilis* and *Chaetoceros danicus* were also highlighted. *P. globosa* abundance was thus significantly higher during the blooms of *P. delicatissima* complex than during its low abundance periods (Fig. 7A) while the opposite trend was observed during the blooms and low abundance periods of *P. seriata* complex (Fig. 7B). *G. delicatula* (Fig. 7C), *C. curvisetus* + *C. debilis* (Fig. 7D) and *C. danicus* (Fig. 7E) abundances were significantly higher during the blooming years of *P. seriata* complex while for *L. danicus* (Fig. 7F), no significant difference was observed between the blooming years of *P. seriata* complex and years without bloom. *G. delicatula, C. curvisetus* + *C. debilis, C. danicus* and *L. danicus* were not present in high abundance at the same period. *G. delicatula* was present in high abundance ($\geq 10^5$ cells L^{-1}) from March to June during the blooms of *P. globosa* and *P. seriata* complex (Fig. 7G). *C. curvisetus* + *C. debilis* high abundances ($\geq 10^5$ cells L^{-1}) were typically observed from March to October but they were more frequently observed in March-April during the blooms of *P. globosa* and in June during the blooms of *P. seriata* complex (Fig. 7H). *C. danicus* high abundances ($\geq 10^4$ cells L^{-1}) were more frequently observed from February to March during the first diatom bloom and at the beginning of the *P. globosa* bloom period (Fig. 7I). *L. danicus* high abundances ($\geq 10^5$ cells L^{-1}) were more frequently observed during the blooms of *P. seriata* complex in June and July (Fig. 7J).

3.5. Realized ecological niches and sub-niches of the taxa interacting with *Pseudo-nitzschia spp.* and niche overlaps

Overlaps between the realized ecological sub-niches of the taxa composing the surrounding phytoplankton community and the realized ecological sub-niches of *P. delicatissima* and *P. seriata* complexes were calculated to better understand the biological constraints influencing the realized ecological sub-niches of *P. delicatissima* and *P. seriata* complexes.

The number of other taxa present and showing a niche overlapping the realized ecological sub-niche of *P. delicatissima* complex was lower during the blooms of *P. delicatissima* complex than during its low abundance periods. 113 other taxa were present during low abundance periods of *P. delicatissima* complex vs. 74 during its blooms. 86% of them had a realized ecological sub-niche overlapping the realized ecological sub-niche of *P. delicatissima* complex during its low abundance periods vs. 77% during its blooms. The same pattern was observed during low abundance periods and blooms of *P. seriata* complex. There were 108 other taxa during the low abundance periods of *P. seriata* complex vs. 64 during its blooms. 92% of them had a realized ecological sub-niche overlapping the realized ecological sub-niche of *P. seriata* complex during its low abundance periods vs. 77% during its blooms.

Among these taxa, *P. globosa, G. delicatula, L. danicus, C. curvisetus* + *C. debilis* and *C. danicus* were the taxa interacting the most with *P. delicatissima* complex and/or *P. seriata* complex. The realized ecological niche and sub-niches of *P. globosa, G. delicatula, L. danicus, C. curvisetus* + *C. debilis* and *C. danicus* differed from the realized ecological niche and sub-niches of *P. delicatissima* and *P. seriata* complexes (Figs. 8 and 5). *C. curvisetus* + *C. debilis* presented a lower marginality than *P. delicatissima* and *P. seriata* complexes while *P. globosa, G. delicatula, L. danicus* and *C. danicus* had a higher marginality (Table 1). Among these five taxa, *P. globosa* was the least tolerant while *C. danicus* was the more tolerant. *C. danicus* had affinity for winter-spring conditions, *C. curvisetus* + *C. debilis* for spring-summer-autumn conditions, *P. globosa* for spring conditions and *L. danicus* and *G. delicatula* for spring-summer conditions (Fig. 3).

The realized ecological niche of *P. globosa* was more similar to the realized ecological niche of *P. delicatissima* complex than the realized ecological niche of *P. seriata* complex. The realized ecological niche of *P. globosa* overlapped 56% of the realized ecological niche of *P. delicatissima* complex and 52% of the realized ecological niche of *P. seriata* complex (Table 2). The realized ecological niche of *P. globosa* differed from the realized ecological niches of *P. delicatissima* and *P. seriata* complexes mainly in the temperature, PAR and NO_2^- + NO_3^- conditions favoring its development (supplementary materials, Fig. S2). High *P. globosa* abundances were more frequently observed when PAR ranged from 30 to 45 einstein m^{-2} day^{-1} i.e. at values close to the PAR conditions favoring the development of *P. delicatissima* complex but at lower PAR than *P. seriata* complex. High *P. globosa* abundances were also more frequently observed at lower temperature (9–12 °C) and higher

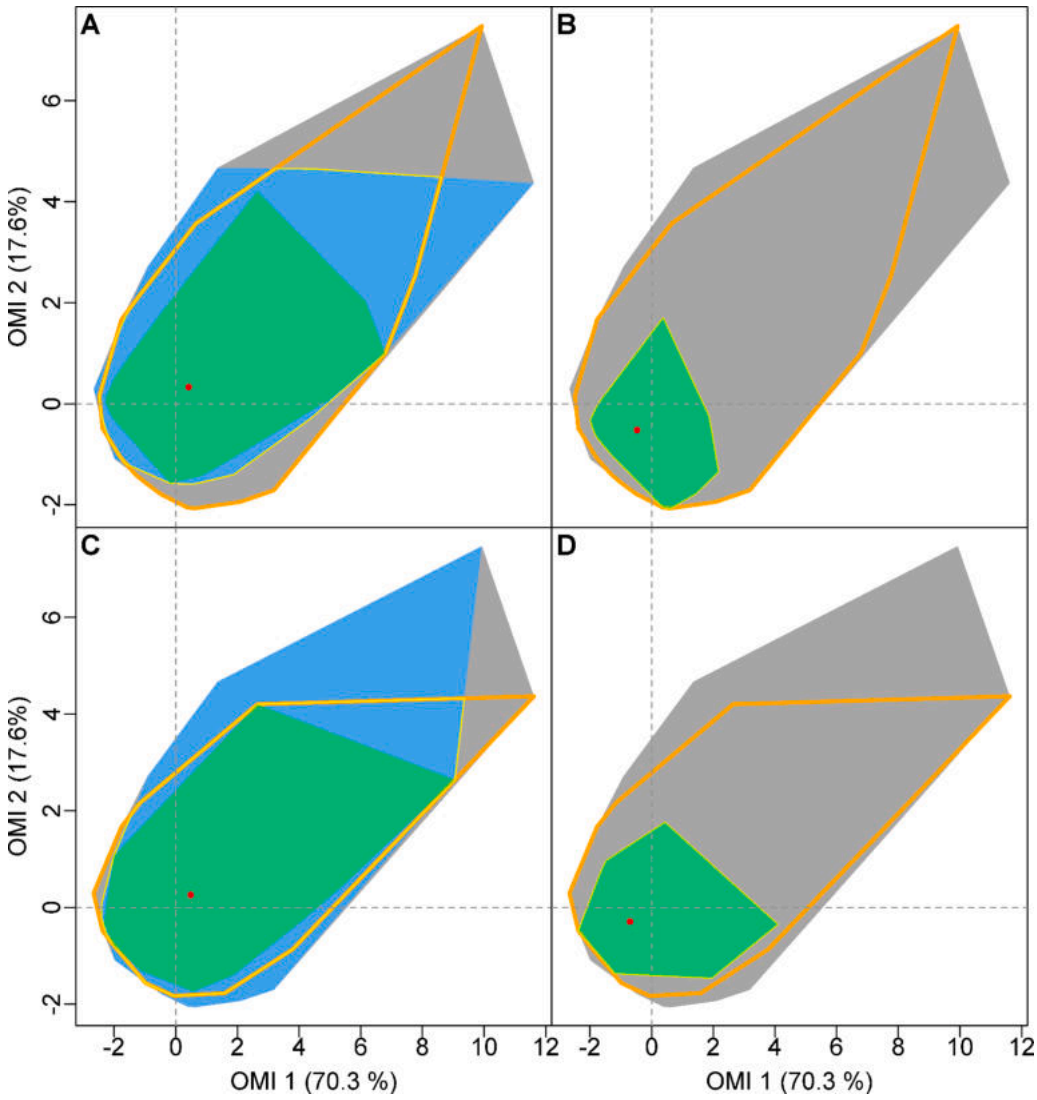

Fig. 5. Within Outlying Mean Index (WitOMI) analysis. sub-niches of A & B) *Pseudo-nitzschia delicatissima* complex and C & D) *Pseudo-nitzschia seriata* complex during their respective low abundance (left panel) and bloom (right panel) periods. gray polygon = environmental space, orange polygon = realized ecological niche (RN), blue polygon = sub-environmental space, yellow polygon = potential sub-niche (PS), green polygon = realized ecological sub-niche (RS). Red dot = $WitOMI_G$.

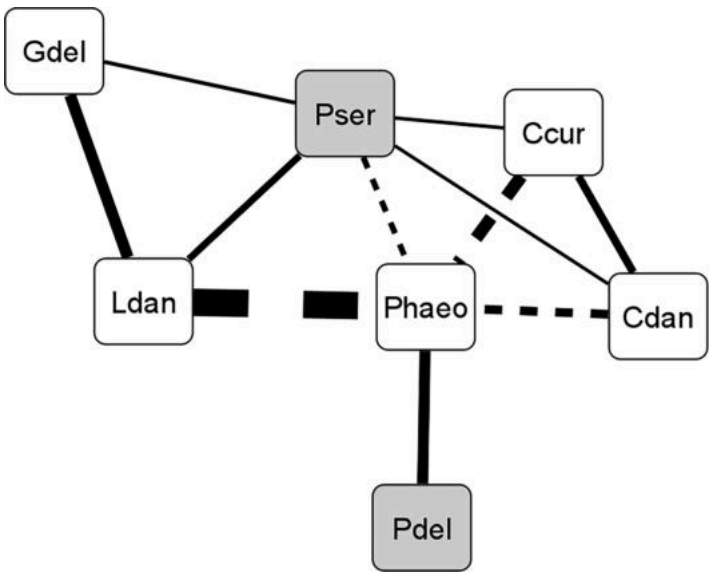

Fig. 6. Interaction network based on a Poisson lognormal model (PLN) showing the taxa interacting with *Pseudo-nitzschia delicatissima* complex (Pdel) and *Pseudo-nitzschia seriata* complex (Pser). Phaeo = *Phaeocystis globosa*, Gdel = *Guinardia delicatula*, Ldan = *Leptocylindrus danicus*, Ccur = *Chaetoceros curvisetus* + *Chaetoceros debilis* and Cdan = *Chaetoceros danicus*. Solid lines represent positive interactions while dashed lines represent negative interactions. Lines width is proportional to interaction strength.

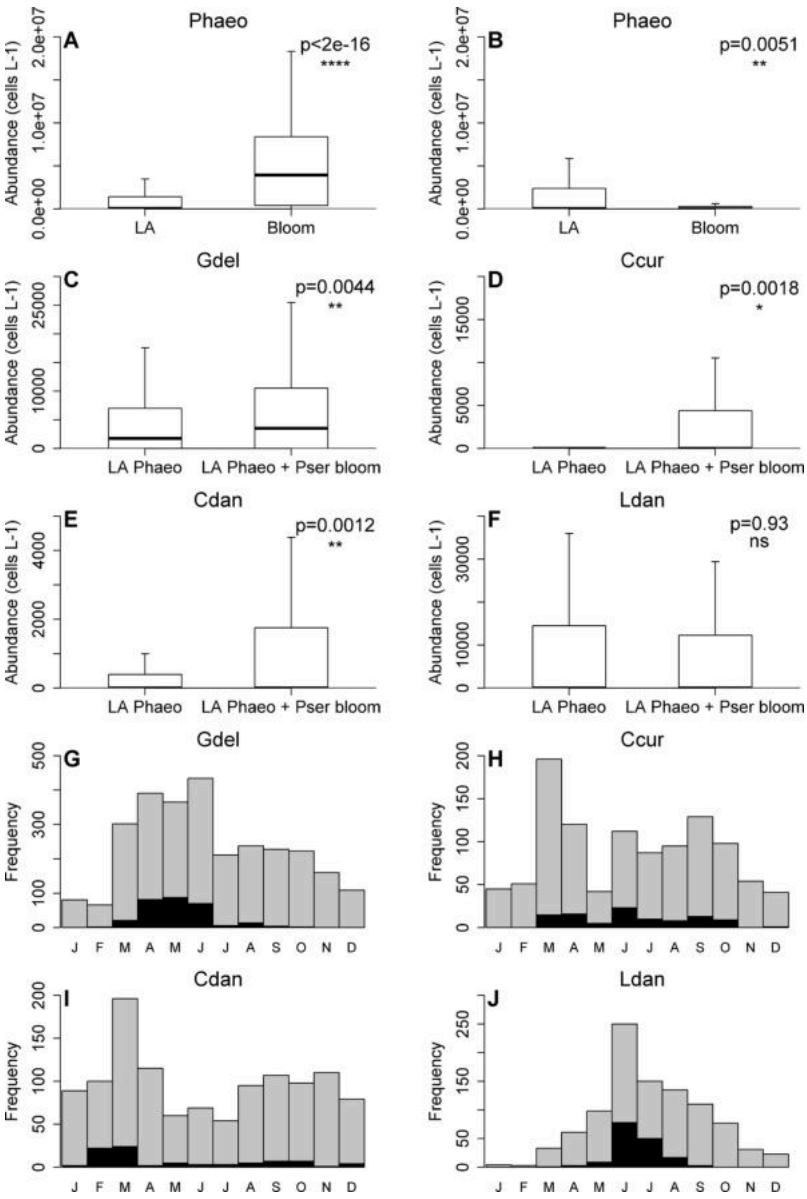

Fig. 7. Abundance of *Phaeocystis globosa* (Phaeo) during low abundance (LA) and bloom periods of A) *Pseudo-nitzschia delicatissima* complex and B) *Pseudo-nitzschia seriata* complex. Abundance of C) *Guinardia delicatula* (Gdel), D) *Chaetoceros curvisetus* + *Chaetoceros debilis* (Ccur), E) *Chaetoceros danicus* (Cdan) and F) *Leptocylindrus danicus* (Ldan) during years of low intensity *Phaeocystis globosa* blooms without bloom of *Pseudo-nitzschia seriata* complex (LA Phaeo) vs. years when the blooms of *Pseudo-nitzschia seriata* complex accompanied the low intensity *Phaeocystis globosa* blooms (LA Phaeo + Pser bloom). Observation frequencies of G) Gdel, H) Ccur, I) Cdan and J) Ldan during the months of the year. Gray bars correspond to observation frequencies of the considered taxa whatever its abundance. Black bars correspond to observation frequencies of high abundances. Note the different axes.

NO_3^- + NO_2^- concentrations than *P. delicatissima* and *P. seriata* complexes. Indeed, when NO_3^- + NO_2^- concentrations were > 10 μM high *P. globosa* abundances were more frequently observed than high abundances of *P. delicatissima* and *P. seriata* complexes.

During low abundance periods of *P. delicatissima* complex, *P. globosa* occupied 49% of its potential sub-niche (Table 1) and its realized ecological sub-niches were smaller than the realized ecological sub-niches of *P. delicatissima* complex (Fig. 8A) *P. globosa* potential and realized ecological sub-niches overlapped respectively 52% and 38% of the potential and realized ecological sub-niches of *P. delicatissima* complex (Table 2). During the blooms of *P. delicatissima* complex, the environmental conditions were different from its low abundance periods. The realized ecological sub-niches of *P. delicatissima* complex and *P. globosa* shifted (Figs. 5B and 8B). Consequently, the realized ecological sub-niches of *P. globosa* overlapped a higher proportion of the potential and realized ecological sub-niches of *P. delicatissima* complex (Table 2). Contrary to *P. delicatissima* complex that occupied the totality of its potential sub-niche, *P. globosa* only occupied 87% of its potential sub-niche.

During low abundance periods of *P. seriata* complex, *P. globosa* occupied 74% of its potential sub-niche and the sub-niches *P. globosa* were smaller than the sub-niches of *P. seriata* complex (Fig. 8C). The potential and realized ecological sub-niches of *P. globosa* overlapped respectively 57% and 43% of the potential and realized ecological sub-niches of *P. seriata* complex. During low abundance periods of *P. seriata* complex, *P. globosa* occupied a smaller proportion of its potential sub-niche due to stronger environmental and biological constraints (Table 1, Fig. 8D). Its potential sub-niche became identical to the potential sub-niche of *P. seriata* complex and the overlap between the realized ecological sub-niches of *P. globosa* and *P. seriata* complex increased (Table 2).

Among the diatoms interacting with *P. seriata* complex, the realized ecological niche of *G. delicatula* was the most similar to the realized ecological niche of *P. seriata* complex and completely overlapped it (Fig. 8E & F, Table 2). The realized ecological niche of *P. seriata* complex was however smaller than the realized ecological niche of *G. delicatula* (Figs. 8 & 5) since high abundances of *G. delicatula* occurred over a larger range of temperatures than high abundances of *P. seriata* complex (supplementary materials, Fig. S2). The other diatoms were ranked as follows: *C. danicus, C. curvisetus* + *C. debilis* and *L. danicus* with their realized ecological niches overlapping respectively 73%, 62% and 55% of the realized ecological niche of *P. seriata* complex (Table 2). High

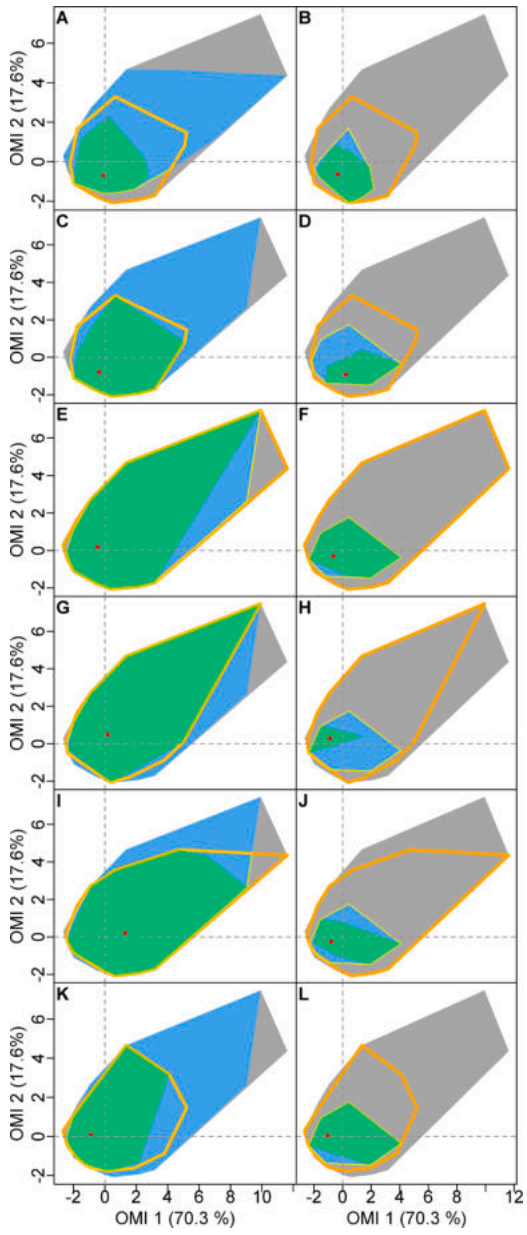

Fig. 8. Sub-niches of *Phaeocystis globosa* during the low abundance A) and B) bloom periods of *Pseudo-nitzschia delicatissima* complex. Sub-niches of C & D) *Phaeocystis globosa*, E & F) *Guinardia delicatula* (Gdel), G & H) *Chaetoceros curvisetus* + *Chaetoceros debilis* (Ccur), J & J) *Chaetoceros danicus* (Cdan) and K & L) *Leptocylindrus danicus* (Ldan) during the low abundance (left panel) and bloom (right panel) periods of *Pseudo-nitzschia seriata* complex. gray polygon = environmental space, orange polygon = realized ecological niche (RN), blue polygon = sub-environmental space, yellow polygon = potential sub-niche (PS), green polygon = realized ecological sub-niche (RS). Red dot = $WitOMI_G$.

abundances of *C. danicus* were frequently observed over a larger range of NO_3^- + NO_2^- concentrations than high abundances of *P. seriata* complex and at lower temperature and PAR (supplementary materials, Fig. S2). High abundances of *C. curvisetus* + *C. debilis* and *L. danicus* were frequently observed at higher temperatures than high abundances of *P. seriata* complex. However, high abundances of *C. curvisetus* + *C. debilis* were favored by lower PAR than *P. seriata* complex while *L. danicus* and *P. seriata* complex were favored by relatively similar PAR. High abundances of *C. curvisetus* + *C. debilis* were also observed over a larger range of NO_3^- + NO_2^- concentrations than *P. seriata* complex and *L. danicus*.

During low abundance periods of *P. seriata* complex, *C. curvisetus* + *C. debilis* occupied the totality of its potential sub-niche while *G. delicatula, C. danicus* and *L. danicus* occupied respectively 82%, 90% and 79% of their potential sub-niche (Fig. 8E, G, I, K & Table 1). The sub-niches of *G. delicatula, C. curvisetus* + *C. debilis* and *C. danicus* were larger than the sub-niches of *P. seriata* complex while the sub-niches of *L. danicus* were smaller. The potential sub-niches of *L. danicus, C. curvisetus* + *C. debilis* and *C. danicus* overlapped respectively 60%, 68%, and 96% of the potential sub-niche of *P. seriata* complex while the potential sub-niche of *G. delicatula* overlapped the totality of the potential sub-niche of *P. seriata* complex (Table 2). The realized ecological sub-niches of *L. danicus, C. curvisetus* + *C. debilis, C. danicus* and *G. delicatula* overlapped respectively 37%, 77%, 99% and 53% of the realized ecological sub-niche of *P. seriata* complex.

During the blooms of *P. seriata* complex, the environmental conditions constrained the realized ecological sub-niches of all the taxa interacting with *P. seriata* complex (Fig. 8F, H, J & L). Consequently, all of them had the same potential sub-niche as *P. seriata* complex. *G. delicatula* and *L. danicus* occupied almost the totality of their potential sub-niche while, due to stronger biological constraints, *C. curvisetus* + *C. debilis* and *C. danicus* occupied a smaller proportion of their potential sub-niche than during low abundance periods of *P. seriata* complex (Table 1). Overlaps between the realized ecological sub-niche of *P. seriata* complex and the realized ecological sub-niches of *C. curvisetus* + *C. debilis* and *C. danicus* were thus reduced. By contrast, overlaps between the realized ecological sub-niche of *P. seriata* complex and the realized ecological sub-niches of *G. delicatula* and *L. danicus* increased (Table 2). Overlaps between the realized ecological sub-niche of *P. globosa* and the realized ecological sub-niche of the other diatoms interacting with *P. seriata* complex were also modified. Overlap between the realized ecological sub-niche of *P. globosa* and the realized ecological sub-niche of *C. curvisetus* + *C. debilis* was reduced from 57% to 2%. By contrast, overlaps between the realized ecological sub-niche of *P. globosa* and the realized ecological sub-niches of *C. danicus* and *L. danicus* increased (*C. danicus*: from 56% to 71%, *L. danicus*: from 43% to 81%).

4. Discussion

The complexes *Pseudo-nitzschia delicatissima* and *Pseudo-nitzschia seriata* are typically present year round but they bloom at different periods and occupy different realized ecological niches.

P. delicatissima complex showed affinity for spring conditions and blooms more frequently from April to May at the same time as *P. globosa* blooms. *P. seriata* complex has affinity for spring-summer conditions. *P. seriata* complex is able to bloom within a larger seasonal window but its blooms are more frequently observed in June during the decline period of low intensity *P. globosa* blooms. A similar succession in the bloom seasonality of these two complexes has been observed by Fehling et al. (2006) in western Scottish coastal waters and Delegrange et al. (2018) in the southern North Sea. High abundances of *P. delicatissima* complex in spring have also been previously reported in the Skagerrak and Norwegian coastal waters (Hasle et al., 1996) and in the southern North Sea (Delegrange et al., 2018). This difference in seasonality can be explained by the two complexes occupying different realized ecological niches. *P. delicatissima* complex occupies a more marginal niche and is less tolerant than *P. seriata* complex. The realized ecological niches of *P. delicatissima* and *P. seriata* complexes differ mainly in the temperature, light and NO_2^- + NO_3^- conditions allowing their growth and survival. High abundances of *P. seriata* complex are observed at higher temperature and PAR than *P. delicatissima* complex but at lower NO_2^- + NO_3^- concentrations. The abiotic conditions favoring the blooms of *P. delicatissima* and *P. seriata* complexes also differ. The blooms of *P. delicatissima* complex are influenced by water temperature, salinity, turbulence, PAR and nutrients (NH_4^-, NO_2^- + NO_3^-, $Si(OH)_4$ and PO_4^{3-} concentrations). By contrast, the blooms of *P. seriata* complex are not influenced by water temperature, salinity and NH_4^- and PO_4^{3-} concentrations.

Table 2
Overlap percentages between the realized ecological niches, potential sub-niches and realized ecological sub-niches of *Pseudo-nitzschia delicatissima* complex, *Pseudo-nitzschia seriata* complex and their interacting taxa.

	Pdel RN	Pser RN		Pdel PS		Pser PS			Pdel RS		Pser RS	
				LA	Blooms	LA	Blooms		LA	Blooms	LA	Blooms
Phaeo RN	56	52	Phaeo PS	52	96	57	100	Phaeo RS	38	80	43	87
Gdel RN		100	Gdel PS			100	100	Gdel RS			53	87
Ldan RN		55	Ldan PS			60	100	Ldan RS			37	86
Ccur RN		62	Ccur PS			68	100	Ccur RS			77	17
Cdan RN		73	Cdan PS			96	100	Cdan RS			99	60

RN = realized ecological niche, PS = potential sub-niche, RS = realized ecological sub-niche, Pdel= *Pseudo-nitzschia delicatissima* complex, Pser = *Pseudo-nitzschia seriata* complex, Phaeo = *Phaeocystis globosa*, Gdel = *Guinardia delicatula*, Ldan = *Leptocylindrus danicus*, Ccur = *Chaetoceros curvisetus* + *Chaetoceros debilis,* Cdan = *Chaetoceros danicus*, LA = low abundance period.

In addition to environmental conditions, biotic interactions and niche shifts seem to play an important role in the control of the blooms of *P. delicatissima* and *P. seriata* complexes. During their respective low abundance periods, *P. delicatissima* and *P. seriata* complexes were limited by strong biological constraints and they could not occupy the totality of their potential sub-niche. For both complexes, surrounding community structure was different between their respective blooms and low abundance periods. The number of other taxa present and proportions of taxa presenting a niche overlapping the niches of *P. delicatissima* and *P. seriata* complexes were higher during their respective low abundance periods, suggesting that *P. delicatissima* and *P. seriata* complexes had potentially to compete with a higher number of other taxa during their respective low abundance periods than during their blooms. *P. globosa* is the taxa that contributed the most to the dissimilarity in community structure between these periods. *P. globosa* interacted positively with *P. delicatissima* complex, but negatively with *P. seriata* complex. *P. globosa* also occupied different sub-niches during the respective blooms and low abundance periods of *P. delicatissima* and *P. seriata* complexes.

The positive interaction between *P. delicatissima* complex and *P. globosa* is in line with observations frequently made in the eastern English Channel and southern North Sea. In these areas, during *P. globosa* blooms, it is very frequent to observe *P. globosa* colonies heavily colonized by *P. delicatissima* complex (e.g. Pannard et al., 2008; Sazhin et al., 2007). Sazhin et al. (2007) observed up to 130 cells of *P. delicatissima* complex per *P. globosa* colony. Cells of *P. delicatissima* complex associated with *P. globosa* colonies have also been commonly observed in the Gulf of Maine (northwestern Atlantic Ocean) (Fernandes et al., 2014). In the northern Adriatic Sea, Totti et al. (2005) observed higher proportions of *P. delicatissima* complex in large mucilage aggregates than in the water column. The reasons for the presence of *P. delicatissima* complex in mucilage aggregates and its association with *P. globosa* are currently unknown. However, it is thought that *P. delicatissima* complex would be able to use the organic substances contained in the mucus of *P. globosa* colonies and mucilage aggregates (Sazhin et al., 2007). *P. globosa* colonies would thus provide a favorable habitat for the growth of *P. delicatissima* complex (Sazhin et al., 2007). In accordance with this hypothesis, Loureiro et al. (2009) observed that in laboratory cultures, *P. delicatissima* is able to use organic nutrients to maintain its growth when inorganic nutrients are limiting. In the present study, the blooms of *P. globosa* and *P. delicatissima* complex occurred after a first diatom bloom that started to consume the nutrient stocks, and silicates were potentially limiting for diatoms during this period. Like any other diatom, *P. delicatissima* complex requires silicate to grow. However, since *Pseudo-nitzschia* spp. have lightly silicified frustules, they seem better adapted to low silicate conditions than many other diatoms (Marchetti et al., 2004). Indeed, several laboratory studies showed that *Pseudo-nitzschia* species were able to grow under low silicate concentrations (e.g. Fehling et al., 2004; Pan et al., 1996a, 1996b). Natural blooms of *Pseudo-nitzschia* spp. have also been repeatedly observed in association with depleted silicate concentrations and this genus has often been found to outcompete other phytoplankton species during the late stage of spring diatom blooms (Anderson et al., 2006, 2010; Bates et al., 1998; Davidson et al., 2012; Dortch et al., 1997; Fehling et al., 2004; Marchetti et al., 2004; Pan et al., 1996a, 1996b). It is thus frequent to find significant negative correlations between *Pseudo-nitzschia* spp. blooms and silicate concentrations, Si:N or Si:P ratios (e.g. Anderson et al., 2006, 2010). In the present study, high abundances of *P. delicatissima* complex were observed as associated with low Si:N ratios. Similar observations were made in the southern North Sea in 2012 (Delegrange et al., 2018) and in the Bay of Seine (central English Channel) in 2013 (Thorel et al., 2017). The capacity of *P. delicatissima* complex to grow at low silicate concentrations associated with its potential ability to use organic substances provided by *P. globosa* colonies mucus might be a competitive advantage over other diatoms and might explain the positive interaction between the blooms of *P. globosa* and *P. delicatissima* complex.

The negative interaction between *P. seriata* complex and *P. globosa* is more complex since other diatoms: *C. curvisetus* + *C. debilis, C. danicus, L. danicus* and *G. delicatula* also interacted with *P. globosa* and/or *P. seriata* complex. Interactions between *P. seriata* complex, *L. danicus* and *G. delicatula* seem to have been direct, while interactions between *C. curvisetus* + *C. debilis, C. danicus* and *P. seriata* seem to have been indirect because these species were not present with high abundance at the same period of the year and were not favored by the same environmental conditions. *P. seriata* complex was able to bloom after that a sequence of events created conditions favorable to its growth. Its bloom periods were accompanied by shifts in its realized ecological sub-niche but also in the realized ecological sub-niches of its interacting taxa. *P. seriata* complex always bloomed during years of low intensity *P. globosa* blooms. During the blooming years of *P. seriata* complex, the winter stocks of $NO_2^- + NO_3^-$ and $Si(OH)_4$ were lower while PAR and abundances of *C. danicus* and *C. curvisetus* + *C. debilis* were higher than during years without bloom of *P. seriata* complex. High abundances of *C. danicus* and *C. curvisetus* + *C. debilis* were observed during the diatom bloom preceding the blooms of *P. globosa*. During blooming years of *P. seriata* complex, *C. danicus, C. curvisetus* + *C. debilis* and the other diatoms consumed prematurely the winter stocks of $NO_2^- + NO_3^-$ and $Si(OH)_4$, so that the $NO_2^- + NO_3^-$ stock left over after the decline of this first diatom bloom was too low to support high intensity *P. globosa* blooms. In spite of this, since *P. globosa* is an haptophyte, it doesn't require $Si(OH)_4$ to grow, and it managed to dominate the phytoplankton community when diatoms became limited by $Si(OH)_4$. It was the dominant species until temperature and PAR increased and became less favorable to its growth. *P. globosa* and *P. seriata* complex did not occupy the same realized ecological niches. Since *P. seriata* complex tolerates higher temperature and PAR than *P. globosa*, it took advantage of this situation and started to bloom. In spite of their low intensity, *P. globosa* blooms continued to consume the $NO_2^- + NO_3^-$ stock. Consequently, $NO_2^- + NO_3^-$ concentrations left over during the decline of *P. globosa* blooms were lower than during years without blooms of *P. seriata* complex. Different forms of nitrogen as well as changes in the concentration of nitrogen and $Si(OH)_4$ can modify the competitive relationships between diatoms species (e.g. van Ruth et al., 2012). In this study, nitrogen and $Si(OH)_4$

appear to influence the ability of *P. seriata* complex to outcompete the other diatoms present. When *P. seriata* complex bloomed, the $Si(OH)_4$ concentrations were still relatively low, but since *P. seriata* complex is able to maintain viable cells under silicate limited conditions and is a good competitor under low Si:N ratios (Fehling et al., 2004), it still managed to grow. These blooms of *P. seriata* complex were accompanied by the presence of *G. delicatula* and *C. danicus* that interacted positively with *P. seriata* complex. The development of *P. globosa* blooms after *Chaetoceros* spp. blooms is common in the eastern English Channel and southern North Sea (Grattepanche et al., 2011; Rousseau et al., 2002). It was suggested that the winter nutrient stocks determines the composition of the first diatom bloom, and this composition in turn influences the intensity of the blooms of *P. globosa* through competitive relationships for nutrients (Karasiewicz et al., 2018). The association of low intensity *P. globosa* blooms with low $NO_2^- + NO_3^-$ concentrations is in accordance with observations made in the southern North Sea suggesting that *P. globosa* bloom intensity is controlled by nitrate left over after the decline of the first diatom bloom (Rousseau et al., 2002 and references therein). The presence of *P. seriata* complex during years of low intensity *P. globosa* blooms has been previously reported in a study examining the conditions favoring *P. globosa* blooms in the eastern English Channel (Karasiewicz et al., 2018) and in a study describing *Pseudo-nitzschia* spp. diversity and toxicity in 2012 in the southern North Sea (Delegrange et al., 2018). As in the present study, the bloom of *P. seriata* complex in 2012 in the southern North Sea was associated with low $NO_2^- + NO_3^-$ and $Si(OH)_4$ concentrations (Delegrange et al., 2018). Negative relationships between the occurrence of *P. seriata* complex and nitrate concentrations have also been previously reported in the western English Channel (Downes-Tettmar et al., 2013) and western Scottish waters (Fehling et al., 2006) suggesting that *P. seriata* complex responds mainly to nitrate concentrations in surface waters and is able to rapidly use nitrate when it becomes available. The capacity of *P. seriata* complex to outcompete other diatoms when $Si(OH)_4$ concentrations are low is also in line with competition experiments showing that in comparison with other diatoms, *Pseudo-nitzschia pungens* (that belongs to the *Pseudo-nitzschia seriata* complex) is able to dominate when Si:N ratios are relatively low (Sommer, 1994). The presence of *Leptocylindrus* species and/or *Guinardia* (*Rhizosolenia*) *delicatula* at the same time as *Pseudo--nitzschia* spp. seems to be recurrent. These taxa have been observed as associated with *Pseudo-nitzschia* spp. in the Bay of Seine (eastern English Channel) (Thorel et al., 2017), in the western Scottish waters (Fehling et al., 2006), on the Galician coasts (Casas et al., 1999), in the Adriatic Sea (Burić et al., 2008; Totti et al., 2005) and in the Mediterranean Sea (Quiroga, 2006). This suggests similarities in their environmental requirements. *G. delicatula* and *L. danicus* are often observed together (Tomas, 1997). As *Pseudo-nitzschia* spp., *G. delicatula* and *L. danicus* are lightly silicified chain forming diatoms (Conley et al., 1989; Davidson et al., 2012; Rousseau et al., 2002; Schlüter et al., 2012). The presence of *G. delicatula* is also frequently observed during periods of low $Si(OH)_4$ and nitrate concentrations since it generally appears after a succession of blooms (Del Amo et al., 1997; Rousseau et al., 2002 and references therein). In the present study, the OMI and WitOMI analyses showed that some similarities exist between the realized ecological niches and sub-niches of *P. seriata* complex, *G. delicatula* and *L. danicus*. They all have affinity for spring-summer conditions and tolerate higher temperature and PAR than *P. globosa*. However, in spite of these similarities, *P. seriata* complex, *G. delicatula* and *L. danicus* occupy different realized ecological niches and sub-niches. *G. delicatula* and *L. danicus* occupy a more marginal niche and are less tolerant than *P. seriata* complex.

5. Conclusion

This study showed that in the eastern English Channel and Southern North Sea, the complexes *P. delicatissima* and *P. seriata* are typically present year round but their bloom periods are different. This difference in seasonality can be explained by the two complexes occupying different realized ecological niches. The necessity to investigate surrounding phytoplankton community in addition to the environmental conditions was also highlighted. Indeed, niche shifts and biotic interactions played an important role in the control of the blooms of *P. delicatissima* and *P. seriata* complexes. *P. globosa* interacted with the two complexes but this interaction was positive with *P. delicatissima* complex and negative with *P. seriata* complex. Other diatoms also influenced the blooms of *P. seriata* complex. The positive interaction found between *P. delicatissima* complex and *P. globosa* is in accordance with previous observations reporting cells of the *P. delicatissima* complex associated with *P. globosa* colonies. However, the underlying processes explaining this association are currently unresolved. Laboratory experiments with co-cultures of *P. globosa* and *Pseudo-nitzschia* may help to better understand their relationships. The production of domoic acid associated with the presence of the two *Pseudo-nitzschia* complexes and its potential impacts for the food web have also not received adequate attention in this area.

CRediT authorship contribution statement

EH: conceptualization, data curation, formal analysis and wrote completely the first draft. All other authors read, commented and approved the final version of the manuscript. EB and DS: resources, identification and count of phytoplankton species from the SNO-SOMLIT monitoring program. UK and FS: funding acquisition and supervision of EH's post-doc.

Declaration of Competing Interest

The authors declare that they have no known competing financial interests or personal relationships that could have appeared to influence the work reported in this paper.

Data availability

Data will be made available on request.

Acknowledgements

We thank the reviewers for their constructive comments. We thank the Sepia II crew for operating the research vessel that was used to collect the water samples during the monitoring programs. We thank Eric Lecuyer for the SNO-SOMLIT sampling, operation of the CTD and analyses of ammonium concentrations. We thank Nicole Degros and Muriel Crouvoisier for measuring the SNO-SOMLIT nitrite, nitrate, silicate and phosphate concentrations. We thank Alain Lefebvre, Camille Blondel, Vincent Duquesne, Pascale Herbert, Remy Cordier, Catherine Belin, Antoine Huguet, Gaetane Durand, Dominique Soudan and David Devreker for collecting and analyzing the samples during the SRN monitoring program and for providing us the data set via SEANOE. We thank all the members of the REPHY monitoring program for collecting water samples, identifying and counting the phytoplankton species, operating the CTD, analyzing the nutrient concentrations and for providing us the data set via SEANOE. We thank Amélie Chédru for the work done during her master internship. This research was financially supported by: 1) the European Union (ERDF), the French State, the French region Hauts-de-France and IFREMER in the framework of the CPER project MARCO 2015-2021, 2) the French national program LEFE (Les Enveloppes Fluides et l'Environnement) in the framework of the project Turbu-diatox: "Effets de la turbulence sur la prolifération et la toxicité des diatomées" and 3) an inter-laboratories project funded by the GdR PHYCOTOX. [CG]

Supplementary materials

Supplementary material associated with this article can be found, in the online version, at doi:10.1016/j.hal.2023.102424.

References

Ajani, P.A., Larsson, M.E., Woodcock, S., Rubio, A., Farrell, H., Brett, S., Murray, S.A., 2020. Fifteen years of *Pseudo-nitzschia* in an Australian estuary, including the first potentially toxic *P. delicatissima* bloom in the southern hemisphere. Est. Coast. Shelf Sci. 236, 106651.

Amato, A., Dell'Aquila, G., Musacchia, F., Annunziata, R., Ugarte, A., Maillet, N., Carbone, A., Ribera d'Alcalà, M., Sanges, R., Iudicone, D., Ferrante, M.I., 2017. Marine diatoms change their gene expression profile when exposed to microscale turbulence under nutrient replete conditions. Sci. Rep. 7 (1), 3826.

Aminot, A., Kérouel, R., 2004. Hydrologie Des écosystèmes marins. Paramètres et analyses. Editions de l'Ifremer, Brest. pp. 335.

Aminot, A., Kérouel, R., 2007. Dosage automatique des nutriments dans les eaux marines. Editions de l'Ifremer 188.

Anderson, C.R., Brzezinski, M.A., Washburn, L., Kudela, R., 2006. Circulation and environmental conditions during a toxigenic *Pseudo-nitzschia australis* bloom in the Santa Barbara Channel, California. Mar. Ecol. Prog. Ser. 327, 119–133.

Anderson, C.R., Sapiano, M.R.P., Prasad, M.B.K., Long, W., Tango, P.J., Brown, C.W., Murtugudde, R., 2010. Predicting potentially toxigenic *Pseudo-nitzschia* blooms in the Chesapeake Bay. J. Mar. Syst. 83 (3), 127–140.

Azanza, R.V., Brosnahan, M.L., Anderson, D.M., Hense, I., Montresor, M., 2018. The role of life cycle characteristics in harmful algal bloom dynamics. In: Glibert, P., B, E., Burford, M., Pitcher, G., Zhou, M. (Eds.), Global Ecology and Oceanography of Harmful Algal Blooms. Springer, pp. 133–161.

Bates, S.S., Garrisson, D.L., Horner, R.A., 1998. Bloom dynamics and physiology of domoic-acid-producing *Pseudo-nitzschia* species. In: Anderson, D.M., Cembella, A.D., Hallegraeff, G.M. (Eds.), Physiological Ecology of Harmful Algal Blooms. Springer-Verlag, Heidelberg, pp. 267–292.

Bates, S.S., Hubbard, K.A., Lundholm, N., Montresor, M., Leaw, C.P., 2018. *Pseudo-nitzschia, Nitzschia*, and domoic acid: new research since 2011. Harmful Algae 79, 3–43.

Belin, C., Soudant, D., Amzil, Z., 2021. Three decades of data on phytoplankton and phycotoxins on the French coast: lessons from REPHY and REPHYTOX. Harmful Algae 102, 101733.

Blonder, B., Lamanna, C., Violle, C., Enquist, B.J., 2014. The n-dimensional hypervolume. Glob. Ecol. Biogeogr. 23 (5), 595–609.

Bowers, H.A., Ryan, J.P., Hayashi, K., Woods, A.L., Marin, R., Smith, G.J., Hubbard, K.A., Doucette, G.J., Mikulski, C.M., Gellene, A.G., Zhang, Y., Kudela, R.M., Caron, D.A., Birch, J.M., Scholin, C.A., 2018. Diversity and toxicity of *Pseudo-nitzschia* species in Monterey Bay: perspectives from targeted and adaptive sampling. Harmful Algae 78, 129–141.

Breton, E., Brunet, C., Sautour, B., Brylinski, J.M., 2000. Annual variations of phytoplankton biomass in the eastern English Channel: comparison by pigment signatures and microscopic counts. J. Plankton Res. 22 (8), 1423–1440.

Breton, E., Goberville, E., Sautour, B., Ouadi, A., Skouroliakou, D.-.I., Seuront, L., Beaugrand, G., Kléparski, L., Crouvoisier, M., Pecqueur, D., Salmeron, C., Cauvin, A., Poquet, A., Garcia, N., Gohin, F., Christaki, U., 2022. Multiple phytoplankton community responses to environmental change in a temperate coastal system: a trait-based approach. Front. Mar. Sci. 9, 914475.

Brooker, R.W., Maestre, F.T., Callaway, R.M., Lortie, C.L., Cavieres, L.A., Kunstler, G., Liancourt, P., Tielbörger, K., Travis, J.M.J., Anthelme, F., Armas, C., Coll, L., Corcket, E., Delzon, S., Forey, E., Kikvidze, Z., Olofsson, J., Pugnaire, F., Quiroz, C.L., Saccone, P., Schiffers, K., Seifan, M., Touzard, B., Michalet, R., 2008. Facilitation in plant communities: the past, the present, and the future. J. Ecol. 96 (1), 18–34.

Bruno, J.F., Stachowicz, J.J., Bertness, M.D., 2003. Inclusion of facilitation into ecological theory. Trends Ecol. Evol. 18 (3), 119–125.

Brylinski, J.M., Lagadeuc, Y., Gentilhomme, V., Dupont, J.P., Lafite, R., Dupeuple, P.A., Huault, M.F., Auger, Y., Puskaric, E., Wartel, M., Cabioch, L., 1991. Le "fleuve côtier": un phénomène hydrologique important en Manche orientale. Exemple du Pas-de-Calais. Oceanol. Acta 11, 197–203.

Burić, Z., Viličić, D., Mihalić, K.C., Carić, M., Kralj, K., Ljubešić, N., 2008. *Pseudo-nitzschia* blooms in the Zrmanja river estuary (eastern Adriactic Sea). Diatom Res 23 (1), 51–63.

Cardoso, P., Mammola, S., Rigal, F., Carvalho, J., 2021. BAT: biodiversity assessment tools. R package version 2.6.1. https://CRAN.R-project.org/package=BAT.

Casas, B., Varela, M., Bode, A., 1999. Seasonal succession of phytoplankton species on the coast of A Coruña (Galicia, northwest Spain). Bol. Inst. Esp. Oceanogr. 15 (1–4), 413–429.

Chiquet, J., Mariadassou, M., Robin, S., 2021. The Poisson-Lognormal model as a versatile framework for the joint analysis of species abundances. Front. Ecol. Evol. 9, 588292.

Clark, S., Hubbard, K.A., Anderson, D.M., McGillicuddy, J., Ralston, D.K., Townsend, D. W., 2019. *Pseudo-nitzschia* bloom dynamics in the Gulf of Maine: 2012-2016. Harmful Algae 88, 101656.

Clarke, K.R., Warwick, R.M., 2001. Changes in Marine communities: an Approach to Statistical Analysis and Interpretation, 2nd edition. PRIMER-E, Plymouth, p. 172.

Clarson, S.J., Steinitz-Kannan, M., Patwardhan, S.V., Kannan, R., Hartig, R., Schloesser, L., Hamilton, D.W., Fusaro, J.K.A., Beltz, R., 2009. Some observations of diatoms under turbulence. Silicon 1 (2), 79–90.

Conley, D.J., Kilham, S.S., Theriot, E., 1989. Differences in silica content between marine and freshwater diatoms. Limnol. Oceanogr. 34 (1), 205–212.

Davidson, K., Gowen, R., Tett, P., Bresnan, E., Harrison, P.J., McKinney, A., Milligan, S., Mills, D., Silke, J., Crooks, A., 2012. Harmful algal blooms: how strong is the evidence that nutrient ratios and forms influence their occurrence? Est. Coast. Shelf Sci. 115, 399–413.

Del Amo, Y., Queguiner, B., Treguer, P., Breton, H., Lampert, L., 1997. Impacts of high-nitrate freshwater inputs on macrotidal ecosystems. II. Specific role of the silicic acid pump in the year-round dominance of diatoms in the Bay of Brest (France). Mar. Ecol. Prog. Ser. 161, 225–237.

Delegrange, A., Lefebvre, A., Gohin, F., Courcot, L., Vincent, D., 2018. *Pseudo-nitzschia sp.* diversity and seasonality in the southern North Sea, domoic acid levels and associated phytoplankton communities. Est. Coast. Shelf Sci. 214, 194–206.

Dell'Aquila, G., Ferrante, M.I., Gherardi, M., Cosentino Lagomarsino, M., Ribera d'Alcalà, M., Iudicone, D., Amato, A., 2017. Nutrient consumption and chain tuning in diatoms exposed to storm-like turbulence. Sci. Rep. 7 (1), 1828.

Dolédec, S., Chessel, D., Gimaret-Carpentier, C., 2000. Niche separation in community analysis: a new method. Ecology 81 (10), 2914–2927.

Dortch, Q., Robichaux, R., Pool, S., Milsted, D., Mire, G., Rabalais, N., Soniat, T., Fryxell, G., Turner, R.E., Parsons, M., 1997. Abundance and vertical flux of *Pseudo-nitzschia* in the northern Gulf of Mexico. Mar. Ecol. Prog. Ser. 146, 249–264.

Downes-Tettmar, N., Rowland, S., Widdicombe, C., Woodward, M., Llewellyn, C., 2013. Seasonal variation in *Pseudo-nitzschia* spp. and domoic acid in the Western English Channel. Cont. Shelf Res. 53, 40–49.

Dray, S., Dufour, A.B., 2007. The ade4 package: implementing the duality diagram for ecologists. J. Stat. Softw. 22, 1–20.

Estrada, M., Berdalet, E., 1997. Phytoplankton in a turbulent world. Sci. Mar. 61, 125–140.

Fehling, J., Davidson, K., Bolch, C., Tett, P., 2006. Seasonality of *Pseudo-nitzschia* spp. (Bacillariophyceae) in western Scottish waters. Mar. Ecol. Prog. Ser. 323, 91–105.

Fehling, J., Davidson, K., Bolch, C.J., Bates, S.S., 2004. Growth and domoic acid production by *Pseudo-nitzschia seriata* (Bacillariophyceae) under phosphate and silicate limitation. J. Phycol. 40 (4), 674–683.

Fernandes, L.F., Hubbard, K.A., Richlen, M.L., Smith, J., Bates, S.S., Ehrman, J., Léger, C., Mafra, L.L., Kulis, D., Quilliam, M., 2014. Diversity and toxicity of the diatom *Pseudo-nitzschia* Peragallo in the Gulf of Maine, Northwestern Atlantic Ocean. Deep Sea Res. Part II Top. Stud. Oceanogr. 103, 139–162.

Frouin, R., Frantz, B.A., Werdell, P.J., 2003. The SeaWIFS PAR product. In: Hooker, SB, Firestone, ER (Eds.), Algorithm Updates For the Fourth SeaWIFS Data Reprocessing. CC NASA /TM, pp. 46–50.

Genitsaris, S., Monchy, S., Viscogliosi, E., Sime-Ngando, T., Ferreira, S., Christaki, U., 2015. Seasonal variations of marine protist community structure based on taxon-specific traits using the eastern English Channel as a model coastal system. FEMS Microbiol. Ecol. 91 (5).

Gibson, C.H., 2000. Laboratory and ocean studies of phytoplankton response to fossil turbulence. Dyn. Atmos. Oceans 31 (1), 295–306.

Grattan, L.M., Holobaugh, S., Morris, J.G., 2016. Harmful algal blooms and public health. Harmful Algae 57, 2–8.

Grattepanche, J.-.D., Breton, E., Brylinski, J.-.M., Lecuyer, E., Christaki, U., 2011. Succession of primary producers and micrograzers in a coastal ecosystem dominated by *Phaeocystis globosa* blooms. J. Plankton Res. 33 (1), 37–50.

Hasle, G.R., Lange, C.B., Syvertsen, E.E., 1996. A review of *Pseudo-nitzschia*, with special reference to the Skagerrak, North Atlantic, and adjacent waters. Helgolander Meeresun 50 (2), 131–175.

Hasle, G.R., Syvertsen, E.E., 1996. Chapter 2 - marine diatoms. In: Tomas, C.R. (Ed.), Identifying Marine Diatoms and Dinoflagellates. Academic Press, San Diego, pp. 5–385.

Hernández-Fariñas, T., Soudant, D., Barillé, L., Belin, C., Lefebvre, A., Bacher, C., 2014. Temporal changes in the phytoplankton community along the French coast of the eastern English Channel and the southern Bight of the North Sea. ICES J. Mar. Sci. 71 (4), 821–833.

Hernández Fariñas, T., Bacher, C., Soudant, D., Belin, C., Barillé, L., 2015. Assessing phytoplankton realized niches using a French national phytoplankton monitoring network. Est. Coast. Shelf Sci. 159, 15–27.

Hollander, M., Wolfe, D.A., Chicken, E., 2013. Nonparametric Statistical Methods, 3rd edition. John Wiley & Sons.

Houliez, E., Lefebvre, S., Dessier, A., Huret, M., Marquis, E., Bréret, M., Dupuy, C., 2021. Spatio-temporal drivers of microphytoplankton community in the Bay of Biscay: do species ecological niches matter? Prog. Oceanogr. 194, 102558.

Hutchinson, G.E., 1957. Concluding remarks. Cold Spring Harbor Symp. Quant. Biol. 22 (415–427).

Karasiewicz, S., Breton, E., Lefebvre, A., Hernandez Fariñas, T., Lefebvre, S., 2018. Realized niche analysis of phytoplankton communities involving HAB: *Phaeocystis* spp. as a case study. Harmful Algae 72, 1–13.

Karasiewicz, S., Chapelle, A., Bacher, C., Soudant, D., 2020. Harmful algae niche responses to environmental and community variation along the French coast. Harmful Algae 93, 101785.

Karasiewicz, S., Dolédec, S., Lefebvre, S., 2017. Within outlying mean indexes: refining the OMI analysis for the realized niche decomposition. Peer J 5, e3364.

Karasiewicz, S., Lefebvre, A., 2022. Environmental Impact on Harmful Species *Pseudo-nitzschia* spp. and *Phaeocystis globosa* Phenology and Niche. J. Mar. Sci. Eng. 10 (2), 174.

Klein, C., Claquin, P., Bouchart, V., Le Roy, B., Véron, B., 2010. Dynamics of *Pseudo-nitzschia* spp. and domoic acid production in a macrotidal ecosystem of the eastern English Channel (Normandy, France). Harmful Algae 9, 218–226.

Krichen, E., Rapaport, A., Le Floc'h, E., Fouilland, E., 2019. Demonstration of facilitation between microalgae to face environmental stress. Sci. Rep. 9 (1), 16076.
Lefebvre, A., Dezécache, C., 2020. Trajectories of changes in phytoplankton biomass, *Phaeocystis globosa* and Diatom (incl. *Pseudo-nitzschia* sp.) abundances related to nutrient pressures in the Eastern English Channel, Southern North Sea. J. Mar. Sci. Eng. 8 (6), 401.
Lelong, A., Hégaret, H., Soudant, P., Bates, S.S., 2012. *Pseudo-nitzschia* (Bacillariophyceae) species, domoic acid and amnesic shellfish poisoning: revisiting previous paradigms. Phycologia 51 (2), 168–216.
Litchman, E., 2007. CHAPTER 16 - Resource Competition and the Ecological Success of Phytoplankton. In: Falkowski, P., Knoll, A.H. (Eds.), Evolution of Primary Producers in the Sea. Academic Press, Burlington, pp. 351–375.
Loureiro, S., Jauzein, C., Garcés, E., Collos, Y., Camp, J., Vaqué, D., 2009. The significance of organic nutrients in the nutrition of *Pseudo-nitzschia delicatissima* (Bacillariophyceae). J. Plankton Res. 31 (4), 399–410.
MacKenzie, B.R., Leggett, W.C., 1993. Wind-based models for estimating the dissipation rates of turbulent energy in aquatic environments: empirical comparisons. Mar. Ecol. Prog. Ser. 94, 207.
Mammola, S., 2019. Assessing similarity of n-dimensional hypervolumes: which metric to use? J. Biogeogr. 46 (9), 2012–2023.
Mammola, S., Cardoso, P., 2020. Functional diversity metrics using kernel density n-dimensional hypervolumes. Methods Ecol. Evol. 11 (8), 986–995.
Mann, K.H., Lazier, J.R.N., 2013. Dynamics of Marine ecosystems: Biological-Physical Interactions in the Oceans, 3rd edition. Blackwell publishing.
Marchetti, A., Trainer, V.L., Harrison, P.J., 2004. Environmental conditions and phytoplankton dynamics associated with *Pseudo-nitzschia* abundance and domoic acid in the Juan de Fuca eddy. Mar. Ecol. Prog. Ser. 281, 1–12.
McCabe, R., Hickey, B.M., Kudela, R., Lefebvre, K.A., Adams, N.G., Bill, B.D., Gulland, F. M., Thomson, R.E., Cochlan, W.P., Trainer, V.L., 2016. An unprecedented coastwide toxic algal bloom linked to anomalous ocean conditions. Geophys. Res. Lett. 43, 10366–10376.
Pahlow, M., Riebesell, U., Wolf-Gladrow, D.A., 1997. Impact of cell shape and chain formation on nutrient acquisition by marine diatoms. Limnol. Oceanogr. 42 (8), 1660–1672.
Pan, Y., Dv, S.R., Mann, K.H., Brown, R.G., Pocklington, R., 1996a. Effects of silicate limitation on production of domoic acid, a neurotoxin, by the diatom *Pseudo-nitzschia multiseries*. I. Batch culture studies. Mar. Ecol. Prog. Ser. 131, 225–233.
Pan, Y., Dv, S.R., Mann, K.H., Li, W.K.W., Harrison, W.G., 1996b. Effects of silicate limitation on production of domoic acid, a neurotoxin, by the diatom *Pseudo-nitzschia multiseries*. II. Continuous culture studies. Mar. Ecol. Prog. Ser. 131, 235–243.
Pannard, A., Claquin, P., Klein, C., Le Roy, B., Véron, B., 2008. Short-term variability of the phytoplankton community in coastal ecosystem in response to physical and chemical conditions' changes. Est. Coast. Shelf Sci. 80 (2), 212–224.
Peperzak, L., 2002. The Wax and Wane of *Phaeocystis globosa* blooms. Doctoral dissertation. University of Groningen.
Perl, T.M., Bédard, L., Kosatsky, T., Hockin, J., Todd, E., Remis, R., 1990. An outbreak of toxic encephalopathy caused by eating mussels contaminated with domoic acid. N. Engl. J. Med. 322 (25), 1775–1780.
Petroff, R., Hendrix, A., Shum, S., Grant, K.S., Lefebvre, K.A., Burbacher, T.M., 2021. Public health risks associated with chronic, low-level domoic acid exposure: a review of the evidence. Pharmacol. Ther. 227, 107865.
Quiroga, I., 2006. *Pseudo-nitzschia* blooms in the Bay of Banyuls-sur-Mer, Northwestern Mediterranean Sea. Diatom Res 21 (1), 91–104.
REPHY, 2021. REPHY dataset. French Observation and Monitoring program for phytoplankton and Hydrology in coastal waters. Metropolitan data. SEANOE. 10.17882/47248.
Rothschild, B.J., Osborn, T.R., 1988. Small-scale turbulence and plankton contact rates. J. Plankton Res. 10 (3), 465–474.
Rousseau, V., Leynaert, A., Daoud, N., Lancelot, C., 2002. Diatom succession, silicification and silicic acid availability in Belgian coastal waters (Southern North Sea). Mar. Ecol. Prog. Ser. 236, 61–73.
Ruiz, J., Macias, D., Peters, F., 2004. Turbulence increases the average settling velocity of phytoplankton cells. Proc. Natl. Acad. Sci. USA 101 (51), 17720–17724.
Sazhin, A.F., Artigas, L.F., Nejstgaard, J.C., Frischer, M.E., 2007. The colonization of two *Phaeocystis* species (Prymnesiophyceae) by pennate diatoms and other protists: a significant contribution to colony biomass. Biogeochemistry 83, 137–145.
Schlüter, M.H., Kraberg, A., Wiltshire, K.H., 2012. Long-term changes in the seasonality of selected diatoms related to grazers and environmental conditions. J. Sea Res. 67 (1), 91–97.
Schmitt, F.G., 2020. Turbulence et écologie marine. Editions Ellipses.
Sommer, U., 1989. The role of competition for resources in phytoplankton succession. In: Sommer, U. (Ed.), Plankton Ecology: Succession in Plankton Communities. Springer Berlin Heidelberg, Berlin, Heidelberg, pp. 57–106.
Sommer, U., 1994. Are marine diatoms favoured by high Si: n ratios? Mar. Ecol. Prog. Ser. 115, 309–315.
SRN, 2017. SRN dataset. Regional Observation and Monitoring Program for Phytoplankton and Hydrology in the eastern English Channel. 1992-2016. SEANOE. https://doi.org/10.17882/50832.
Stern, R., Moore, S.K., Trainer, V.L., Bill, B.D., Fischer, A., Batten, S., 2018. Spatial and temporal patterns of *Pseudo-nitzschia* genetic diversity in the North Pacific Ocean from the Continuous Plankton Recorder survey. Mar. Ecol. Prog. Ser. 606, 7–28.
Thorel, M., Claquin, P., Schapira, M., Le Gendre, R., Riou, P., Goux, D., Le Roy, B., Raimbault, V., Deton-Cabanillas, A.-F., Bazin, P., Kientz-Bouchart, V., Fauchot, J., 2017. Nutrient ratios influence variability in *Pseudo-nitzschia* species diversity and particulate domoic acid production in the Bay of Seine (France). Harmful Algae 68, 192–205.
Tilman, D., 1977. Resource competition between plankton algae: an experimental and theoretical approach. Ecology 58 (2), 338–348.
Tomas, C.R., 1997. Identifying Marine Phytoplankton. Elsevier Academic Press, p. 875.
Totti, C., Cangini, M., Ferrari, C., Kraus, R., Pompei, M., Pugnetti, A., Romagnoli, T., Vanucci, S., Socal, G., 2005. Phytoplankton size-distribution and community structure in relation to mucilage occurrence in the northern Adriatic Sea. Sci. Total Environ. 353 (1–3), 204–217.
Trainer, V.L., Bates, S.S., Lundholm, N., Thessen, A.E., Cochlan, W.P., Adams, N.G., Trick, C.G., 2012. *Pseudo-nitzschia* physiological ecology, phylogeny, toxicity, monitoring and impacts on ecosystem health. Harmful Algae 14, 271–300.
Trainer, V.L., Hickley, B.M., Bates, S.S., 2008. Toxic diatoms, In: Walsh, P.J., Smith S.L., Fleming L.E., Solo-Gabriele H., Gerwick W.H. (Ed.), Oceans and Human Healths: Risks and Remedies from the Sea. Elsevier Science Publisher, New York, pp. 219–238.
Utermöhl, H., 1958. Zur Ver vollkommung der quantitativen phytoplankton-methodik. Mitt. Int. Ver. Theor. Amgew. Limnol. 9, 39.
van Ruth, P., Qin, J., Brandford, A., 2012. Size dependent competition in centric diatoms as a function of nitrogen and silicon availability. Open J. Mar. Sci. 2 (1), 33–42.
Wells, M.L., Karlson, B., 2018. Harmful algal blooms in a changing ocean. In: Glibert, P., B, E., Burford, M., Pitcher, G., Zhou, M. (Eds.), Global Ecology and Oceanography of Harmful Algal Blooms. Springer, pp. 77–90.

229

Inventaire taxonomique illustré des diatomées (Phylum : Ochrophyta, Classe: Bacillariophyceae) récoltées au point Côte (Manche orientale) des Services Nationaux d'Observation SOMLIT/PHYTOBS sur la période 1996-2019.

Breton Elsa1, Nadine Masson Neaud2, Lucie Courcot1, Dimitra-Ioli Skouroliakou1, et Urania Christaki1.

1Univ. Littoral Côte d'Opale, CNRS, Univ. Lille, UMR 8187 LOG, F-62930 Wimereux, France

2 Ifremer Centre Atlantique, Rue de l'Ile d'Yeu, BP 21105 - 44311 Nantes Cedex 03, France

Mots clés : biodiversité, diatomées, point Côte, SNO SOMLIT/PHYTOBS.

Résumé

Ce chapitre présente une liste validée des différentes espèces de diatomées (Phylum : Ochrophyta, Classe: Bacillariophyceae) recensées au point Côte (1 mile nautique des côtes au large du Portel, Manche orientale) des Services Nationaux d'Observation SOMLIT/PHYTOBS. Elle est issue d'échantillons phytoplanctoniques prélevés à la bouteille Niskin sur une base bi-mensuelle (1996-2019) pendant l'étale de pleine mer (marées en vive-eaux). Elle comprend 50 genres et 122 espèces, certaines rares (<1% d'occurrence) pour le site. Cette liste est illustrée par 122 photographies de spécimen vivants, la plupart prises au microscope optique inversé (X100-X400), après mise en culture. L'occurrence (%) de chaque espèce est donnée, ainsi que les dimensions et l'ultrastructure des *Pseudo-nitzschia* spp., recensées cette dernière décennie par microscopie électronique à balayage,

Introduction

Les diatomées sont des cellules eucaryotes unicellulaires et photosynthétiques, solitaires ou unies en colonie (chaîne, étoile, éventail…). Elles représentent à elles-seules 1/5ème de la production primaire planétaire[1] et l'un des groupes phytoplanctoniques le plus diversifié, au moins 100000 espèces[2]. Elles jouent un rôle majeur dans les cycles biogéochimiques[3,4], particulièrement celui de la silice et du carbone, et forment la base des réseaux trophiques des eaux côtières, particulièrement celles brassées par les vents et riches en nutriments, telle que celles de la Manche orientale.

La plupart des espèces sont identifiées par microscopie optique inversée (X100 à X400) en se basant sur des critères morphologiques (taille, forme, colonialité, présence de soies, couleur, etc..). Seules les espèces pseudo-cryptiques (*i.e.*, morphologiquement identiques bien que taxonomiquement différentes), telles que les *Pseudo-nitzschia*[5], nécessitent obligatoirement l'emploi d'un Microscope Electronique à Balayage pour les distinguer et les identifier.

La liste de diatomées donnée ici est issue d'échantillons phytoplanctoniques prélevés au point Côte (50°40.75 N 1°31.17 E, 1 mile nautique des côtes) dans le cadre des Services Nationaux d'Observation SOMLIT et PHYTOBS (voir encadré). Elle comprend un total de 50 genres et 122 espèces, dont les noms taxonomiques ont été vérifiés sur le site WoRM (http://www.marinespecies.org). Cette liste est accompagnée de 122 photographies de spécimen vivants, pris par microscopie optique inversée pour la plupart. L'occurrence (%) de chacune d'entre-elles est également donnée entre parenthèses. Enfin les dimensions et l'ultrastructure des différentes espèces de *Pseudo-nitzschia* récoltées au point Côte cette dernière décennie sont données dans le Tableau I.

Les Services Nationaux d'Observation SOMLIT et PHYTOBS

Le réseau SOMLIT (Service d'Observation en Milieu Littoral ; https://www.somlit.fr/) a été mis en place par le CNRS en 1997 pour augmenter nos connaissances sur les réponses des écosystèmes côtiers et littoraux français aux variations naturelles et anthropiques. Il est une composante de l'infrastructure de recherche ILICO, fédératrice de l'observation côtière nationale et sous la tutelle du Ministère de l'Enseignement Supérieur, de la Recherche et de l'Innovation. Le SOMLIT couvre une large gamme de conditions environnementales et trophiques représentatives des eaux côtières de la France métropolitaine grâce à un partenariat entre 11 institutions publiques dont l'Université du Littoral Côte d'Opale. Les protocoles pour le prélèvement, conditionnement, stockage et analyses sont communs à tout le personnel dédié. Toutes les données issues des mesures et analyses sont soumises à un contrôle qualité rigoureux selon la norme ISO 17025 (2017), et libre d'accès sur le site du réseau.

En chiffres, le SOMLIT c'est :

-12 écosystèmes répartis sur les 3 façades de la France métropolitaine et 20 points de suivis

-20 variables environnementales (16 en prélèvements discrets et 4 en profils verticaux)

-400 séries temporelles

-un quart de siècle de données pour les séries historiques (depuis 1996-1997)

Le réseau PHYTOBS (https://www.phytobs.fr/) a été créé en 2018 pour fédérer les différents taxonomistes français du phytoplancton et regrouper l'ensemble des données de comptages par microscopie optique inversée, issus d'échantillons prélevés par le SOMLIT et l'IFREMER (REPHY-SRN) en zone côtière et littoral de la France métropolitaine. Il est aussi une composante d'ILICO.

Matériel et méthodes

Les échantillons d'eau de mer ont été prélevés à la bouteille Niskin, puis fixés avec une solution de Lugol et de glutéraldehyde (1% v/v), et conservés au réfrigérateur en attendant les observations par microscopie optique inversée (Nikon Eclipse TE2000-S). Les identifications ont été effectuées aux grossissements X100-X400 après sédimentation dans une cuve Utermöhl d'un échantillon variant entre 5 et 25 ml, et guidées par divers ouvrages de références[6,7]. Les identifications des espèces du genre pseudo-cryptique *Pseudo-nitzschia* (Lundholm) ont été effectuées avec un microscope électronique de balayage (LEO 438VP), après pré-filtration de 20-100 ml sur des filtres en polycarbonate (Millipore, 0.8 µm), puis rinçage à l'eau distillée et traitement à l'acide (HCl 37%, à chaud) pour, respectivement, enlever le sel et nettoyer les frustules (*i.e.*, paroi silicifiée des diatomées). Après une phase de séchage, le sous-échantillon est placé sur une pastille et recouvert par une couche d'or et de palladium. Les identifications

[6]Halse, G. R., and Syvertsen, E. E., «Chapter 2 - marine diatoms», dans C.R. Tomas (éd.), *Identifying Marine Diatoms and Dinoflagellates,* Cambridge, 1996, p. 3-385.

[7]Hoppenrath, M., Elbrächter, M., and Drebes, G., *Marine Phytoplankton. Selected Microphytoplankton From the North Sea Around Helgoland and Sylt*, Stuttgart: Schweizerbartsche Verlagsbuchhandlung, 2009.

ont été guidées par divers travaux taxonomiques de référence[8,9,10,11,12,13,14], selon les critères morphologiques suivants: forme, longueur, largeur, présence d'un nodule central, le nombre de stries et fibules sur une longueur de frustule 10 µm, et le nombre de pores sur une longueur de 1 µm (Tableau I).

Liste des diatomées

Taxa pélagiques

Actinocyclus octonarius Ehrenberg (<1%)

Actinoptychus senarius Ehrenberg (6%)

Actinoptychus splendens (Shadbolt) Ralfs ex Pritchard (<1%)

Asterionella glacialis Castracane (41%)

Asterionella kariana Grunow (<1%)

Bacteriastrum hyalinum Lauder *var. princeps* (Castracane) Ikari (3%)

Bellerochea malleus (Brightwell) Van Heurck (<1%)

Trigonium alternans f. alternans Bailey (5%)

---

[8]Skov, Jette, Lundholm, Nina, Moestrup, Øjvind, Larsen, Jacob, «Potentially toxic phytoplankton. 4. The diatom genus *Pseudonitzschia* (Diatomophyceae/Bacillariophyceae)», dans JA Lindley (éd.), *ICES identification leaflets for plankton,* 1999, Copenhagen.

[9]Orsini, Luisa, Sarno, Diana, Procaccini, Gabriele, Poletti, Roberto, Dahlmann, Jens, Montresor, Marina. «Toxic *Pseudo-nitzschiamultistriata* (Bacillariophyceae) from the Gulf of Naples: morphology, toxin analysis and phylogenetic relationships with other *Pseudo-nitzschia* species», *European Journal of Phycology*, 37, 247-257, 2002.

[10] Lundholm, Nina, Moestrup, Øjvind, Hasle, Grethe Rytter, Hoef-Emden, Kerstin, «A study of the *P. pseudodelicatissima/cuspidata* complex (Bacillariophyceae). What is *Pseudo-nitzschia pseudodelicatissima*? » *Journal of Phycology*, 39, 797-813, 2003.

[11]Kaczmarska, Irena, Martin, Jennifer L., Ehrman, James M., Le Gresley, Murielle M., «*Pseudo-nitzschia* species population dynamics in the Quoddy Region, Bay of Fundy», *Harmful Algae*, 6, 861-874, 2007.

[12]Fehling J, Davidson K, Bolch CJ, Tett P, «Seasonality of *Pseudo-nitzschia* spp. (Bacillariophyceae) in western Scottish waters», *Marine Ecology Progress Series*, 323, 91–105, 2006.

[13] Churro, Catarina I., Carreira, Cátia C., Rodrigues, Francisco J., Craveiro, Sandra C., Calado, António J., Casteleyn, Griet, Lundholm, Nina, «Diversity and abundance of potentially toxic *Pseudo-nitzschia* Peragallo in Aveiro coastal lagoon, Portugal, and description of a new variety, *P. pungens var. aveirensis* var. nov. », *Diatom Research*, 24, 35-62, 2009.

[14]Klein, Cécile, Claquin, Pascal, Bouchart, Valérie, Le Roy, Bertrnd, Véron, Benoit, «Dynamics of *Pseudo-nitzschia* spp. and domoic acid production in a macrotidal ecosystem of the Eastern English Channel (Normandy, France) », *Harmful Algae*, 9, 218-226, 2010.

Plagiogramma brockmanni var. brockmanni Hustedt (15%)

Cerataulina bergonii Ostenfeld (21%)

Chaetoceros affinis Lauder (<1%)

Chaetoceros brevis Schütt (<1%)

Chaetoceros compressus Lauder (13%)

Chaetoceros costatus Pavillard (5%)

Chaetoceros curvisetus Cleve (28%)

Chaetoceros danicus Cleve (30%)

Chaetoceros debilis Cleve emend Xu, Li & Lundholm[15] (5%)

Chaetoceros decipiens Cleve (10%)

Chaetoceros densus (Cleve) Cleve (11%)

Chaetoceros diadema Ehrenberg (6%)

Chaetoceros didymus var. didymus Ehrenberg (6%)

Chaetoceros didymus var. protuberans (Lauder) Gran & Yendo (taxon incertain, phylogénie à vérifier) (<1%)

Chaetoceros ebeinii (Grunow) (taxon incertain, phylogénie à vérifier) (1%)

Chaetoceros lauderi Ralfs (taxon incertain, phylogénie à vérifier) (3%)

Chaetoceros lorenzianus Grunow (10%)

Chaetoceros mitra (Bailey) Cleve (non déterminé)

Chaetoceros muelleri Lemmermann (6%)

Chaetoceros perpusillus Cleve (taxon incertain, phylogénie à vérifier) (<1%)

Chaetoceros radians Schütt (taxon incertain, phylogénie à vérifier) (<1%)

Chaetoceros similis Cleve (<1%)

Chaetoceros simplex Ostenfeld (<1%)

Chaetoceros socialis Lauder (48%)

Chaetoceros tenuissimus Meunier (taxon incertain, phylogénie à vérifier) (6%)

Chaetoceros tortissimus Gran (taxon incertain, phylogénie à vérifier) (13%)

Chaetoceros wighamii Brightwell (10%)

---

[15] Xu, Xiaojing, Lundholm, Nina, Li, Yang, «A Study of *Chaetoceros debilis Sensu Lato* Species (Bacillariophyceae), with Ememdation of *C. debilis* and Description of *C. galeatus* Sp. Nov. », *Journal of Phycology*, 56, 784-797, 2020.

Corethron criophilum Castracane (taxon incertain, phylogénie à vérifier) (2%)

Coscinodiscus centralis Ehrenberg (taxon incertain, phylogénie à vérifier) (<1%)

Coscinodiscus concinnus Smith (2%)

Coscinodiscus granii Gough (<1%)

Coscinodiscus marginatus Ehrenberg (taxon incertain, phylogénie à vérifier) (<1%)

Coscinodiscus radiatus Ehrenberg (taxon incertain, phylogénie à vérifier) (10%)

Coscinodiscus wailesii Gran & Angst (taxon incertain, phylogénie à vérifier) (1%)

Cyclotella meneghiniana (Kützing) de Brébisson (1%)

Dactyliosolen fragilissimus (Bergon) Hasle (taxon incertain, phylogénie à vérifier) (28)

Dactyliosolen phuketensis (Sundström) Hasle (taxon incertain, phylogénie à vérifier, non distingué de *Guinardia striata*) (28%%)

Detonula pumila (Castracane) Gran (taxon incertain, phylogénie à vérifier) (<1%)

Ditylum brightwellii (West) Grunow (taxon incertain, phylogénie à vérifier) (42%)

Eucampia zodiacus Ehrenberg (taxon incertain, phylogénie à vérifier) (16%)

Guinardia delicatula (Cleve) Hasle (taxon incertain, phylogénie à vérifier) (70%)

Guinardia flaccida (Castracane) Peragallo (taxon incertain, phylogénie à vérifier) (50%)

Guinardia striata (Stolterfoth) Hasle Haslea (taxon incertain, phylogénie à vérifier) (53%)

Haslea wawrikae (Hustedt) Simonsen (<1%)

Helicotheca tamesis (Shrubsole) Ricard (taxon incertain, phylogénie à vérifier) (5%)

Lauderia annulata Cleve (taxon incertain, phylogénie à vérifier) (30%)

Leptocylindrus danicus Cleve (taxon incertain, phylogénie à vérifier) (41%)

Leptocylindrus minimus Gran (taxon incertain, phylogénie à vérifier) (14%)

Neocalyptrella robusta (Norman) Hernández-Becerril & Meave del Castillo (taxon incertain, phylogénie à vérifier) (2%)

Neomoelleria cornuta (Cleve) Blanco & Wetzel (<1%)

Neostreptotheca subindica Stosch (taxon incertain, phylogénie à vérifier) (2%)

Odontella aurita var. aurita Agardh (taxon incertain, phylogénie à vérifier) (<1%)

Odontella aurita var. minima (Grunow in Van Heurck) De Toni (taxon incertain, phylogénie à vérifier) (9%)

Odontella mobiliensis (Bailey) Grunow (taxon incertain, phylogénie à vérifier) (7%)

Odontella regia (Schultze) Simonsen (taxon incertain, phylogénie à vérifier) (6%)

Odontella rhombus (Ehrenberg) Kützing (taxon incertain, phylogénie à vérifier) (16%)

Odontella sinensis (Greville) Grunow (taxon incertain, phylogénie à vérifier) (12%)

Porosira glacialis (Grunow) Gran ((taxon incertain, phylogénie à vérifier) (1%)

Pseudo-nitzschia americana (Hasle) Fryxell (13%)

Pseudo-nitzschia delicatissima (Cleve) Heiden (57%)

Pseudo-nitzschia fraudulenta (Cleve) Hasle (37%)

Pseudo-nitzschia multistriata (Takano) Takano (1%)

Pseudo-nitzschia pungens (Grunow) Hasle) (26%)

Pseudo-nitzschia subpacifica (Hasle) Hasle (1%)

Rhizosolenia hebetata Bailey (<1%)

Rhizosolenia hebetata f. semispina (Hensen) Gran (<1%)

Rhizosolenia hyalina Ostenfeld (taxon incertain, phylogénie à vérifier) (<1%)

Rhizosolenia imbricata Brightwell (69%)

Rhizosolenia imbricata var. shrubsolei Brightwell (taxon incertain, phylogénie à vérifier) (69%)

Rhizosolenia setigera Brightwell (21%)

Rhizosolenia setigera f. pungens (Cleve-Euler) Brunel (17%)

Rhizosolenia styliformis Brightwell (5%)

Skeletonema dohrnii Sarno & Kooistra (34%)

Skeletonema marinoi Sarno & Zingone (34%)

Stauroneis membranacea (Cleve) Hustedt (taxon incertain, phylogénie à vérifier) (25%)

Stephanopyxis turris (Greville) Ralfs (1%)

Tenuicylindrus belgicus (Meunier) Nanjappa and Zingone (14%)

Thalassionema nitzschioides (Grunow) Mereschkowsky (48%)

Thalassiosira aestivalis Gran (taxon incertain, phylogénie à vérifier) (5%)

Thalassiosira angulata (Gregory) Hasle (taxon incertain, phylogénie à vérifier) (5%)

Thalassiosira constricta Gaarder (taxon incertain, phylogénie à vérifier) (5%)

Thalassiosira curviseriata Takano (taxon incertain, phylogénie à vérifier) (5%)

Thalassiosira delicatula Hustedt (taxon incertain, phylogénie à vérifier) (1%)

Thalassiosira eccentrica (Ehrenberg) Cleve (taxon incertain, phylogénie à vérifier) (2%)

Thalassiosira fallax Meunier (taxon incertain, phylogénie à vérifier) (3%)

Thalassiosira gravida Cleve (36%)

Thalassiosira levanderi Van Goor (taxon incertain, phylogénie à vérifier) (18%)

Thalassiosira minima Gaarder (taxon incertain, phylogénie à vérifier) (5%)

Thalassiosira nordenskioeldii Cleve (12%)

Thalassiosira oceanica (taxon incertain, phylogénie à vérifier) (<1%)

Thalassiosira punctigera (Castracane) Hasle (5%)

Thalassiosira rotula Cleve (36%)

Thalassiosira tenera Proschkina-Lavrenko (taxon incertain, phylogénie à vérifier) (<1%)

Taxa benthiques, tychopélagiques, et/ou épiphytiques

Asteromphalus Ehrenberg (<1%)

Bacillaria paxillifera (Müller) Marsson (taxon incertain, phylogénie à vérifier) (6%)

Ceratoneis closterium (Ehrenberg) (taxon incertain, phylogénie à vérifier) (54%)

Delphineis surirella (Ehrenberg) Andrews (taxon incertain, phylogénie à vérifier) (14%)

Diploneis (Ehrenberg) Cleve (18%)

Entomoneis Ehrenberg (<1%)

Flagilariopsis cylindrus Hustedt[16] (<1%)

Melosira moniliformis (Müller) Agardh (taxon incertain, phylogénie à vérifier) (<1%)

Melosira nummuloides Greville (taxon incertain, phylogénie à vérifier) (9%)

Navicula transitans Cleve (50%)

Nitzschia longissima (Brébisson) Ralfs (19%)

Nitzschia panduriformis f. panduriformis Gregory (5%)

Paralia sulcata (Ehrenberg) Cleve (64%)

Plagiogrammopsis vanheurckii (Grunow) Hasle (taxon incertain, phylogénie à vérifier) (5%)

Pleurosigma directum Grunow (33%)

Pleurosigma normanii Ralfs (5%)

Podosira stelligera (Bailey) Mann (1%)

Psammodictyon panduriforme (Gregory) Mann (taxon incertain, phylogénie à vérifier) (<1%)

Rhaphoneis amphiceros (Ehrenberg) Ehrenberg (60%)

Subsilicea fragilarioides von Stosch & Reimann (taxon incertain, phylogénie à vérifier) (5%)

Trachyneis Cleve (<1%)

[16] Schmidt, A., *Atlas der Diatomaceen-kunde*, Leipzig, O.R. Reisland, 1874.

Remerciements

Nous remercions les capitaines et marins successifs du bateau de recherché CNRS « *Sépia II* », Charly Dollet, Jean-Claude Martin, Grégoire Leignel, Noël Lefiliatre, et Christophe Routtier qui ont aidé aux prélèvements et rendu les conditions optimales pendant ces nombreuses années. Nous remercions également le personnel local du SOMLIT qui a effectué les prélèvements d'eau: Nicole Degros, Eric Lecuyer, Muriel Crouvoisier, et Arnaud Cauvin. Nous remercions également les réseaux SOMLIT et PHYTOBS, qui soutiennent le suivi long-terme des écosystèmes du littoral métropolitain incluant les communautés phytoplanctoniques.

Tableau 1. Dimensions et ultrastructure des différentes espèces de *Pseudo-nitzschia* récoltées au point Côte (Manche orientale) des réseaux SOMLIT/PHYTOBS sur la période 1996-2019. En italique: gamme des valeurs rencontrée dans la littérature spécialisée.

Espèce	**Longueur**	**Largeur**	**Biovolume**	**Striae**	**Fibulae**	**Rangée de pores**	**Pores**
	µm		μm^3	N/10 µm			N/1 µm
P. americana	20-28	2.2-2.7	102	30-32	20-22	2	10-12
	12-39	*1.8-3.7*		*24-38*	*16-23*		*7-10*
P. delicatissima	36-74	1-2.4	49	33-45	18-28	1-2	5-14
	14-78	*1-2.8*		*33-44*	*18-36*		*6-14*
P. fraudulenta	41-100	2-7.4	1261	16-28	14-24	2	6-7
	39-127	*3-10*		*18-26*	*12-26*		*4-7*
P. multistriata	52-59	1.1-2.8	231	28-42	23-24	2	12-13
	34-174	*2.3-4.1*		*36-46*	*22-32*		*9-13*
P. pungens	48-150	2.3-5.8	519	10-14	10-16	2-3	3-6
	37-174	*2-5.3*		*9-16*	*9-16*		*1-4*
P. subpacifica	50-73	1.6-4.7	514	28-32	16-22	2	7-10
	33-70	*4.1-7*		*26-32*	*15-20*		*7.5-10*

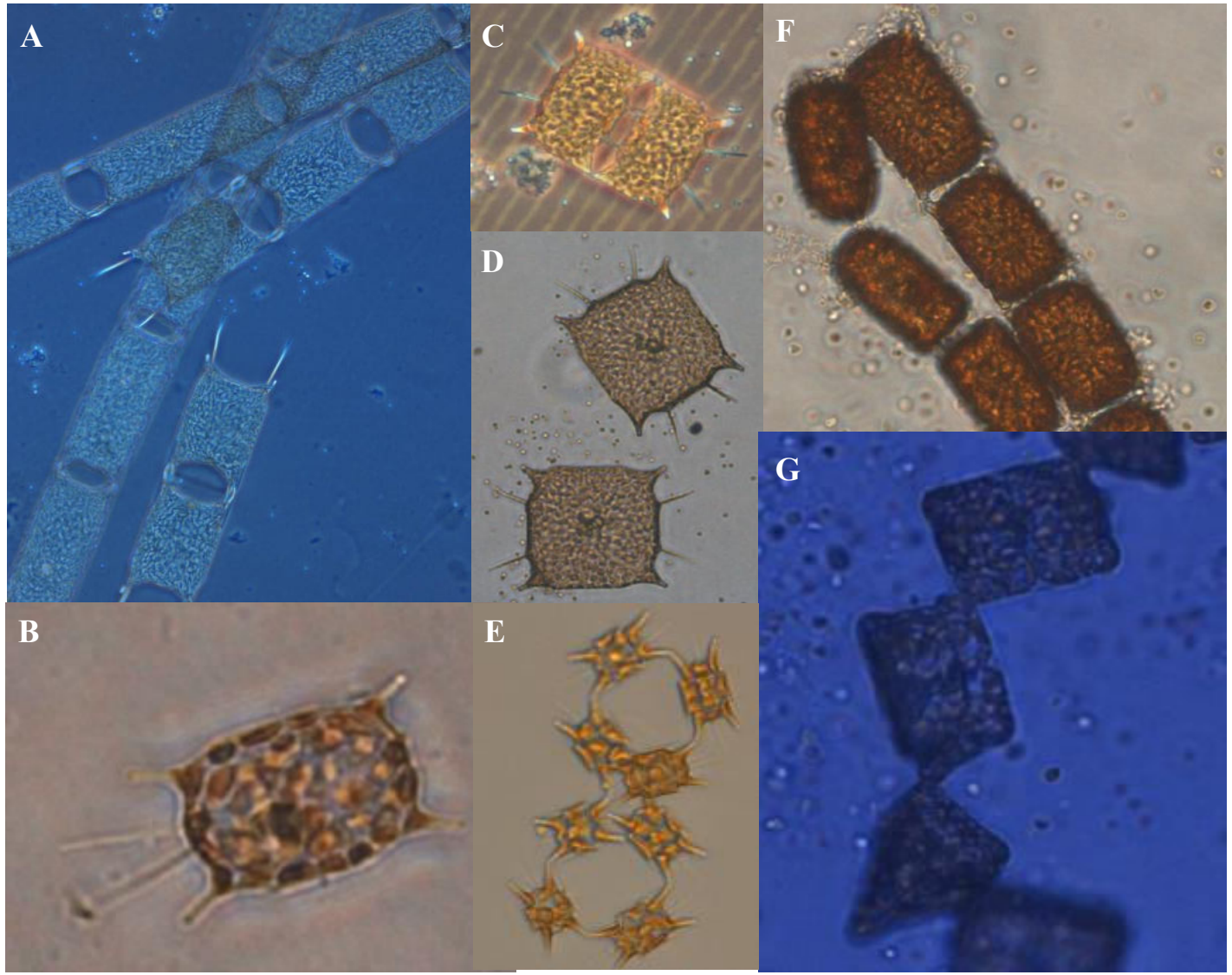

Figure 1. Diatomées pélagiques du genre *Odontella*, *Trieres*, et *Trigonium* au point Côte (Manche orientale) des réseaux SOMLIT/PHYTOBS sur la période 1996-2019. A*: Odontella sinensis*, B: *Trieres mobiliensis*, C: *Odontella granulata*, D: *Trieres regia*, E: *Odontella aurita var minima,* F: *Odontella rhombus*, G: *Trigonium alternans*. © E. Breton. A noter que la taille des espèces n'est pas respectée.

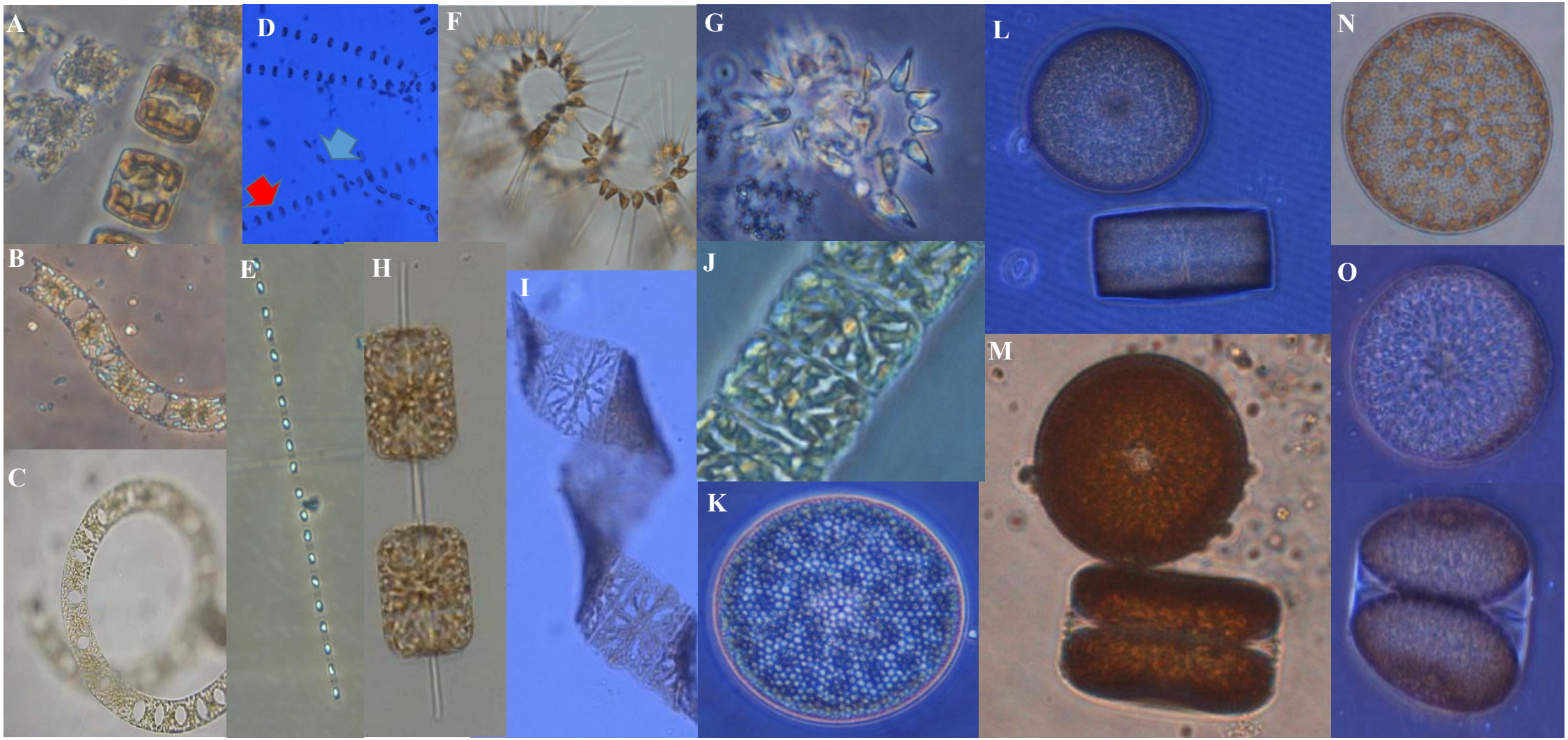

Figure 2. Diatomées pélagiques du genre *Cyclotella*, *Eucampia*, *Skeletonema*, *Helicotheca*, *Asterionella*, *Ditylum*, *Stauroneis*, et *Coscinodiscus* au point Côte (Manche orientale) des réseaux SOMLIT/PHYTOBS sur la période 1996-2019. A: *Cyclotella meneghiniana* , B: *Neomoelleria cornuta*, C: *Eucampia zodiacus*, D: *Skeletonema dohrnii* (flèche verte) et *Skeletonema marinoi* (flèche rouge), E: *Skeletonema costatum*, F: *Asterionella glacialis*, G: *Asterionella kariana*, H: *Ditylum brightwellii*, I: *Helicotheca tamesis,* J: *Stauroneis membranacea*, K: *Coscinodiscus centralis*, L: *Coscinodiscus wailesii*, M: *Coscinodiscus concinnus*, N: *Coscinodiscus radiatus*, et O: *Coscinodiscus granii*. © E. Breton. A noter que la taille des espèces n'est pas respectée.

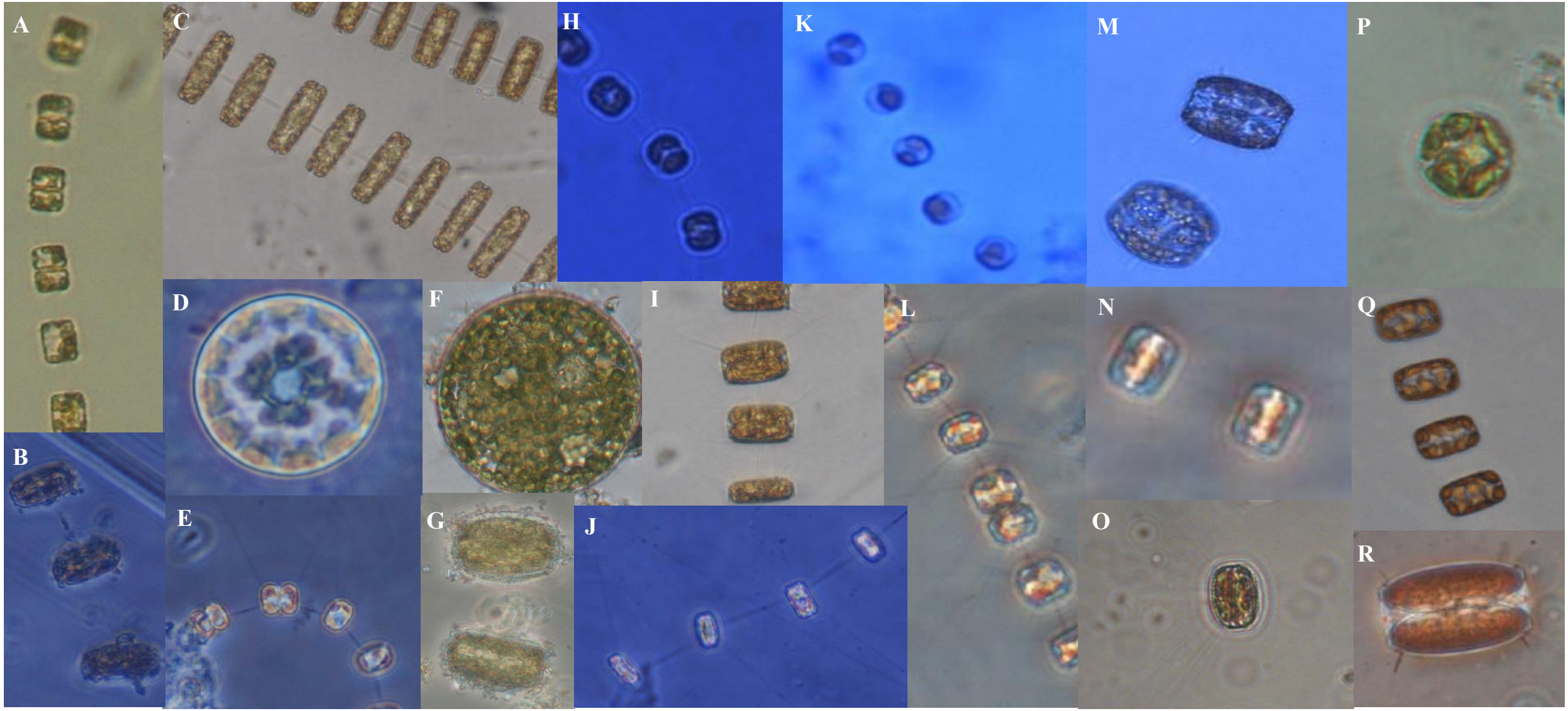

Figure 3. Diatomées pélagiques du genre *Thassasiosira* au point Côte (Manche orientale) des réseaux SOMLIT/PHYTOBS sur la période 1996-2019. A: *T. constricta,* B: *T. angulata*, C: *T. rotula*, D: *T. tenera*, E: *T. curviseriata*, F-G: *T. eccentrica*, H: *T. levanderi,* I: *T. decipiens*, J: *T. minima*, K: *T. pseudo-nana/mala,* L: *T. nordenskioldii,* M: *T. hendeyii*, N: *Thalassiosira* sp1. , O: *T. aestivalis, P: Thassiosira sp.2,* Q: *T. gravida,* et R: *T. punctigera*. © E. Breton. A noter que la taille des espèces n'est pas respectée.

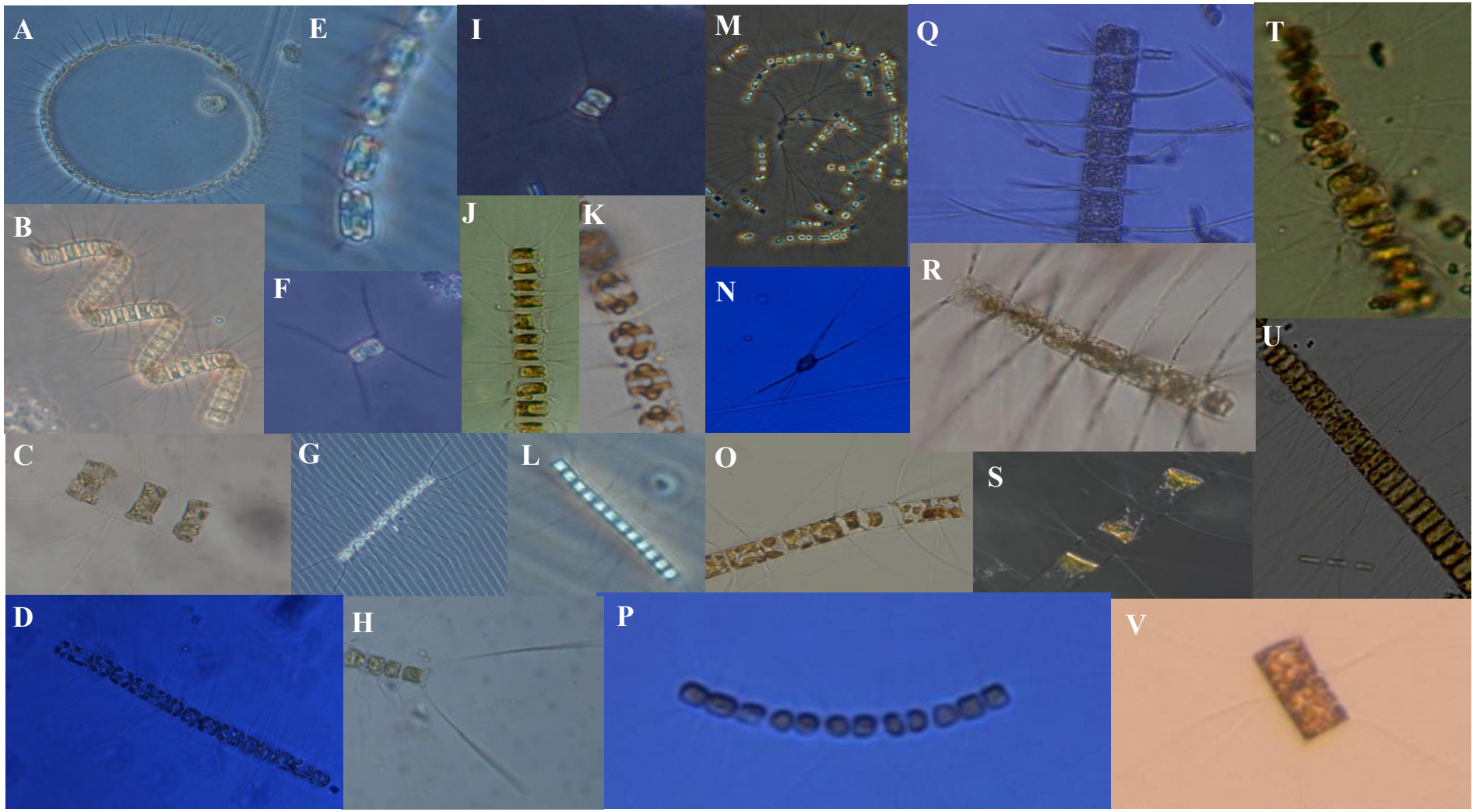

Figure 4. Diatomées du genre *Chaetoceros* au point Côte (Manche orientale) des réseaux SOMLIT/PHYTOBS sur la période 1996-2019. A: *C. curvisetus*, B: *C. debilis*, C: *C. decipiens*, D: *C. compressus*, E: *C. didymus var. protuberans*, F: *C. muelleri*, G: *C. affinis*, H: *C. castracanei*, I: *C. tenuissimus*, J: *C. dyadema*, K: *C. didymus var didymus*, L: *C crinitus*, M: *C. socialis*, N: *C. danicus*, O.: *C. lauderi*, P: *C. perpusillus,* Q: *C. ebeinii* (notez la présence de *Pseudo-nitzschia americana* sur les soies), R: *C. densus*, S: hypnospores de *C. mitra*, T: *C. tortissimus*, U: *C. costatus*, et V: *C. teres*. © E. Breton. A noter que la taille des espèces n'est pas respectée.

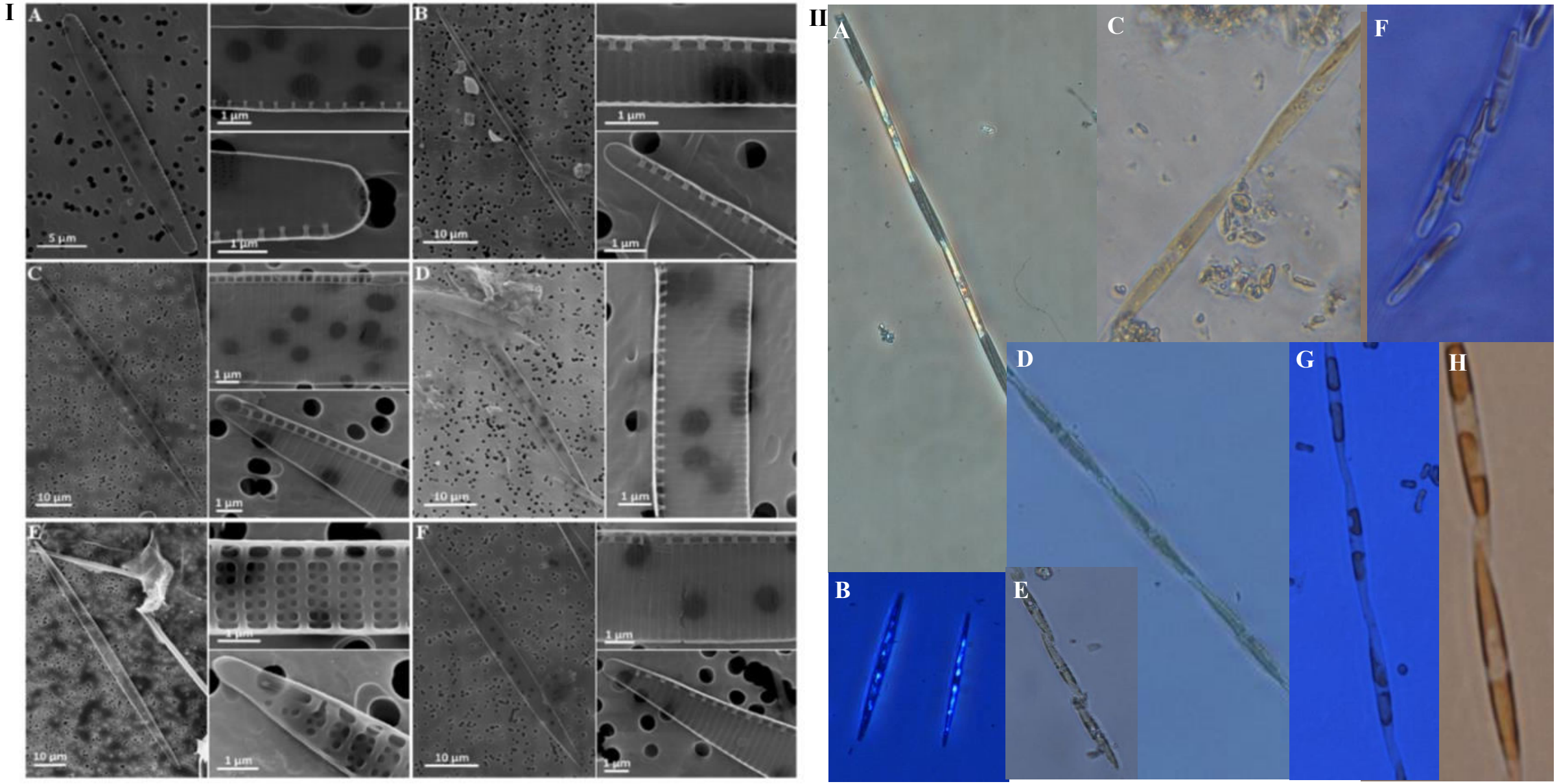

Figure 5. Diatomées pélagiques du genre *Pseudo-nitzschia* au point Côte des réseaux SOMLIT/PHYTOBS sur la période 1996-2019 (I: microscopie éléctronique de balayage [© L. Courcot]; II: microscopie optique inversée [© E. Breton]). IA&IIE: *P. americana*, IB&IIB: *P. delicatissima*, IC&IIF-G: *P. fraudulenta*, ID&IID-E: *P. multistriata*, IE&IIA: *P. pungens*, et IF&IID-E: *P. subpacifica*. A noter que la taille des espèces n'est pas respectée.

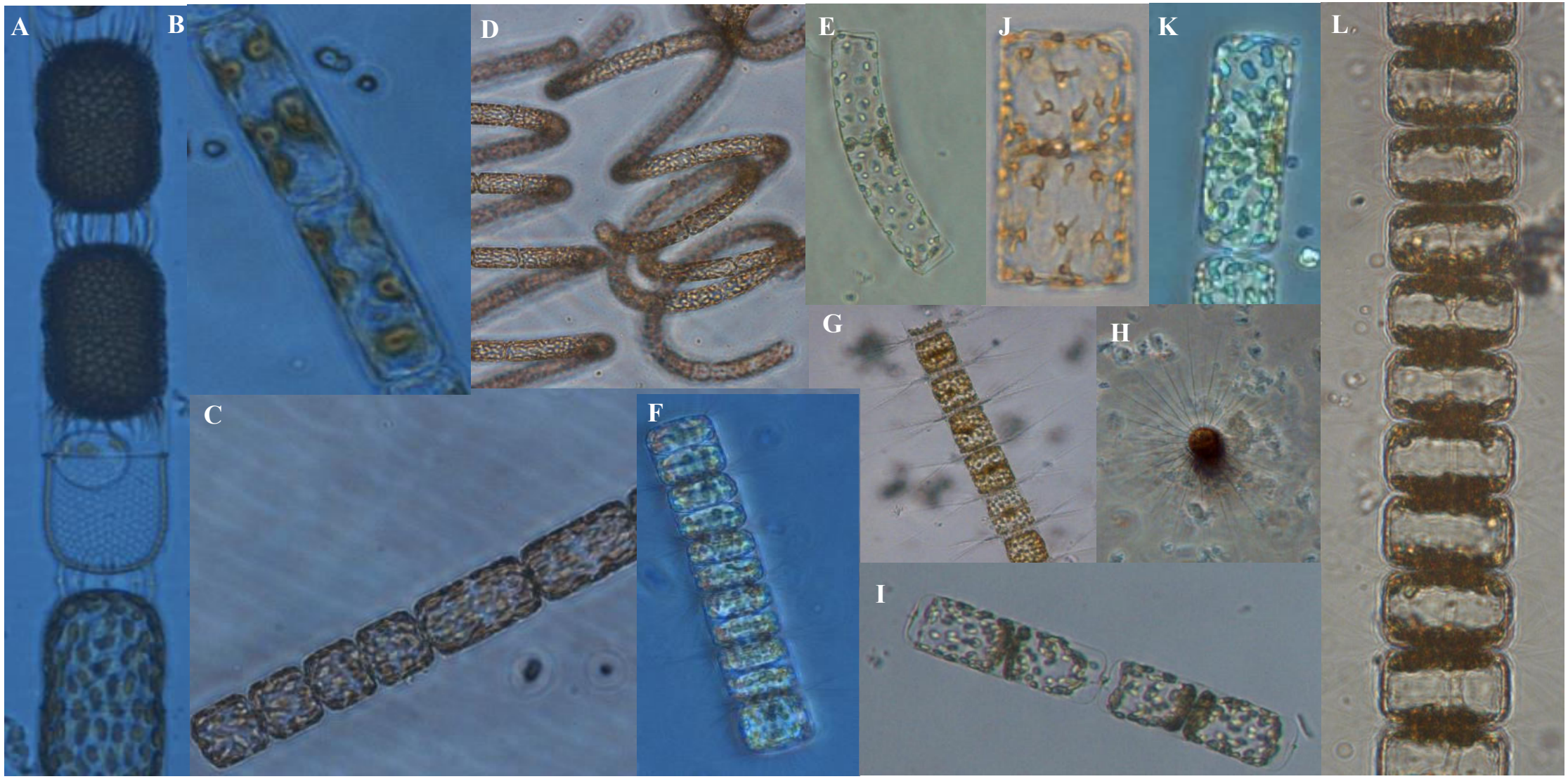

Figure 6. Diatomées pélagiques du genre *Stephanopyxis, Guinardia*, *Lauderia*, *Bacteriastrum, Dactyosolen, Cerataulina, Detonula,* et *Porosira* au point Côte des réseaux SOMLIT/PHYTOBS sur la période 1996-2019. A: *Stephanopyxis turris,* B: *Guinardia delicatula,* C: *Lauderia annulata,* D-E: *Guinardia striata,* F: *Porosira glacialis,* G-H: *Bacteriastrum hyalinum var. princeps,* I: *Dactyliosolen fragilissimus,* J: *Guinardia flaccida*, K: *Cerataulina bergonii,* et L: *Detonula pumilla.* © E. Breton. A noter que la taille des espèces n'est pas respectée.

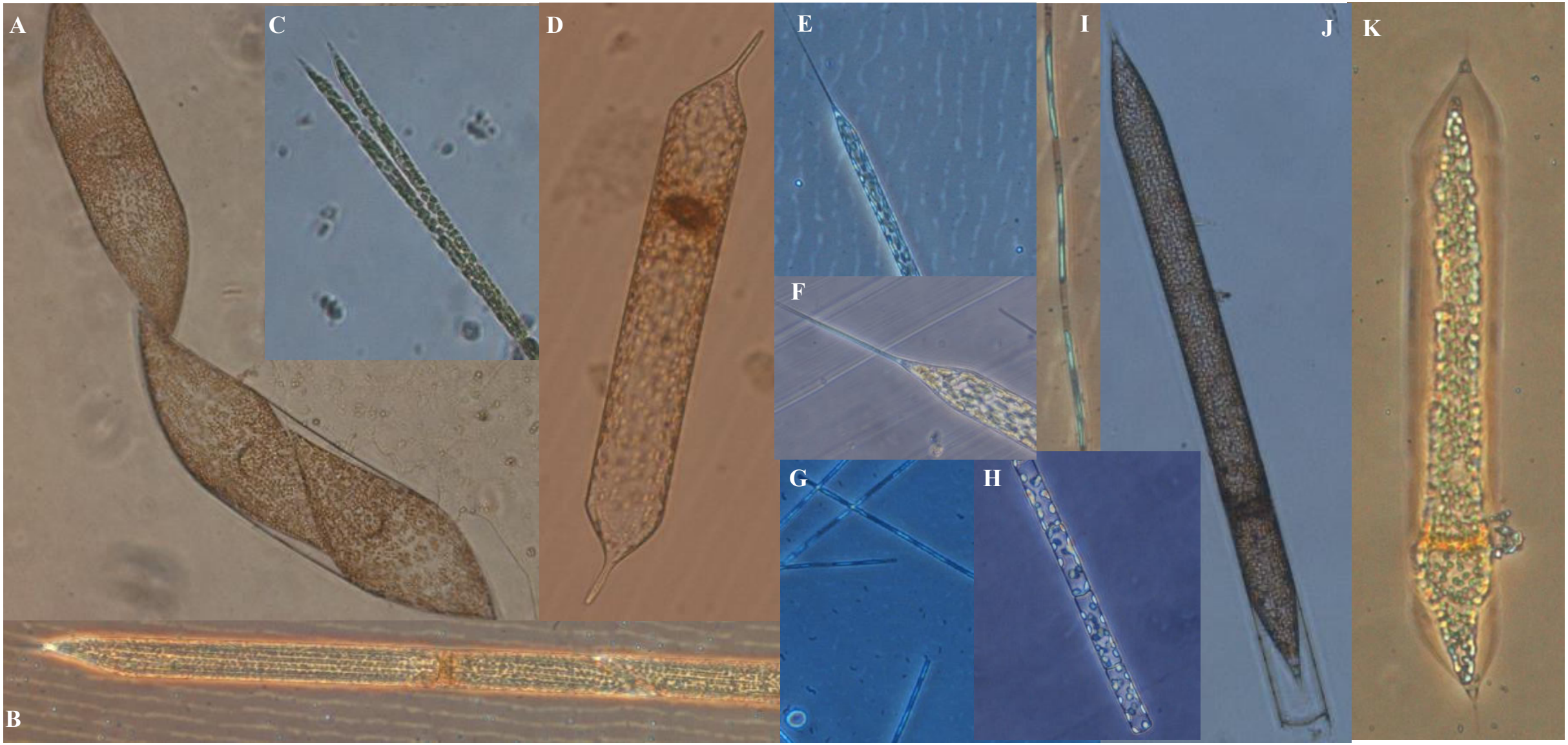

Figure 7. Diatomées pélagiques du genre *Neocalyptrella, Rhizosolenia, Neostreptotheca, Leptocylindrus, et Tenuicylindrus* au point Côte des réseaux SOMLIT/PHYTOBS sur la période 1996-2019. A: *Neocalyptrella robusta*, B: *R. shrubsolei*, C: R. *hebetata f. semispina,* D: *Neostreptotheca subindica*, E: *R. setigera,* F: *R. setigera var. pungens*, G: *L. minimus,* H: *L. danicus,* I: *T. Belgicus,* J: *Rhizosolenia styliformis,* et K: *Rhizosolenia hyalina.* © E. Breton. A noter que la taille des espèces n'est pas respectée.

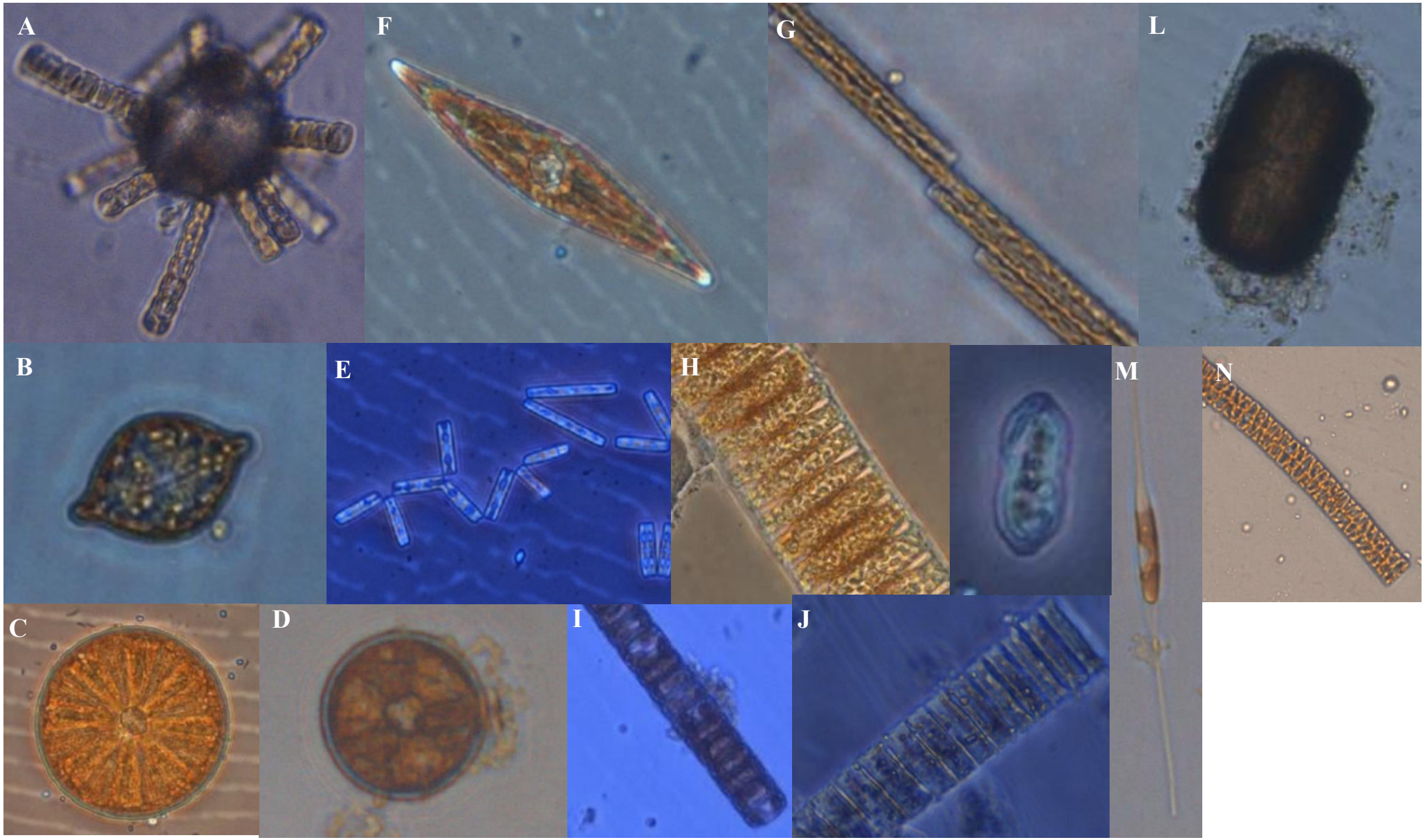

Figure 8. Diatomées benthiques et tychopélagiques au point Côte (Manche orientale) des réseaux SOMLIT/PHYTOBS sur la période 1996-2019. A: *Delphineis surirrella*; B: *Raphoneis amphiceros*; C: *Actinoptychus splendens*, D: *Actinoptychus serianus*, E: *Thalassionema nitzschoides*; F: *Pleurosigma directum*; G: *Bacillaria paradoxa*; H: *Lithodesmium undulatum*; I: *Paralia sulcata*; J: *Brockmaniella brockmanii*; K: *Nitzschia panduriformis f. panduriformis*, L: *Aulacodiscus argus*, M: *Ceratoneis closterium,* et N:. *Fragilariopsis* Photographies: E. Breton. A noter que la taille des espèces n'est pas respectée.

Dynamique et facteurs de contrôle des efflorescences de la micro-algue mucilagineuse du genre *Phaeocystis* : synthèse de 24 ans d'observation à la station « Wimereux Côte » des Services Nationaux d'Observation SOMLIT/PHYTOBS.

Breton Elsa1*, Eric Goberville2, Benoit Sautour3, Dimitra-Ioli Skouroliakou1, Muriel Crouvoisier1, Laurent Seuront1,4,5, Gregory Beaugrand1, David Pecqueur6, Christophe Salmeron6, Arnaud Cauvin1, Nicole Garcia7, et Urania Christaki1.

1-Univ. Littoral Côte d'Opale, CNRS, Univ. Lille, UMR 8187 LOG, F-62930 Wimereux, France

2- Unité Biologie des Organismes et Ecosystèmes Aquatiques (BOREA), Muséum National d'Histoire Naturelle, CNRS, IRD, Sorbonne Université, Université de Caen Normandie, Université des Antilles, Paris, France

3- Univ. Bordeaux, CNRS, UMR 5805 EPOC, Rue Geoffroy Saint Hilaire – Bâtiment B18N

33600 Pessac, France

4- Department of Marine Resources and Energy, Tokyo University of Marine Science and Technology, Tokyo, Japan

5- Department of Zoology and Entomology, Rhodes University, Grahamstown 6140, South Africa

6- Observatoire Océanologique de Banyuls/mer, FR 3724 - Laboratoire Arago - SU/CNRS, avenue Pierre Fabre Bât. B, F-66650 Banyuls sur Mer

7- Aix Marseille Univ., Université de Toulon, CNRS, IRD, MIO, Marseille, France

*elsa.breton@univ-littoral.fr

Mots clés : *Phaeocystis*, variations temporelles, facteurs de contrôle.

Résumé

La microalgue *Phaeocystis* (Phylum Haptophyta, Classe Prymnesiophyceae) - surnommée localement *« vert de mai »* - prolifère chaque printemps, depuis la fin des années 70, dans les eaux côtières de la Côte d'Opale. Formant des mousses impressionnantes - mais non toxiques - qui peuvent s'accumuler sur les plages lors de la dégradation de ses efflorescences, *Phaeocystis* a un impact notable sur l'écosystème et les activités économiques ; la surveillance de cette espèce est ainsi exigée par les directives européennes. Dans ce chapitre, nous synthétisons les connaissances sur la dynamique (1996-2019 ; 24 ans d'observation) et les facteurs de contrôle de *Phaeocystis* acquises par Breton et al. (2021, 2022) au point « Wimereux Côte » (au large du Portel, Manche orientale) suivi par les Services Nationaux d'Observation SOMLIT (Service d'Observation en Milieu Littoral) et PHYTOBS (Réseau d'observation du phytoplancton). Nos travaux démontrent (i) l'importance des interactions proie-prédateur pour la formation de colonies et des efflorescences chez *Phaeocystis,* et (ii) comment l'effet combiné d'une re-oligotrophisation et d'une diminution des apports fluviaux observées au cours de la dernière décennie à la côte ont favorisé les efflorescences de *Phaeocystis,* notamment en accentuant le déséquilibre entre les nitrates et les phosphates se traduisant par une tendance à la limitation en phosphates.

Introduction

La micro-algue cosmopolite *Phaeocystis* (Phylum Haptophyta, Classe Prymnesiophyceae) prolifère chaque printemps (mars-mai) dans les eaux côtières de la Côte d'Opale[1]. Elle suscite un grand intérêt scientifique car ses efflorescences agissent sur le climat en séquestrant de grandes quantités de CO_2 atmosphérique au fond des océans[2] et en influençant la formation des nuages par la production de diméthylsulfoxyde (DMSO)[3]. Le grand public connait surtout les formations impressionnantes de mousse qui peuvent s'accumuler le long du littoral lors de la phase de dégradation des efflorescences, comme observé sur la Côte d'Opale (Fig. 1A-B) depuis la fin des années 1970[4]. Ces formations et dépôts massifs de mousse peuvent perturber temporairement le fonctionnement des écosystèmes littoraux en provoquant une anoxie (i.e., réduction du taux d'oxygène) des milieux[5]. Malgré plusieurs décennies de recherche sur cette micro-algue, les facteurs qui la contrôle restent difficiles à identifier.

Les efflorescences de *Phaeocystis* dans les eaux côtières du nord-ouest de l'Europe sont considérées comme symptomatiques des apports excessifs du phosphore et de l'azote qui résultent des activités humaines dans les bassins versants[6,7]. Malgré la re-oligotrophisation (i.e., processus inverse de l'eutrophisation) des eaux côtières[8,9] initiée il y a plusieurs décennies pour

---

[1]Breton, Elsa, Goberville, Eric, Sautour, Benoit, Ouadi, Anis, Skouroliakou, Dimitra-Ioli, Seuront, Laurent, Beaugrand, Grégory, Kléparski, Loick, Crouvoisier, Muriel, Pecqueur, David, Salmeron, Christophe, Cauvin, Arnaud, Poquet, Adrien, Garcia, Nicole, Gohin, Francis, Christaki, Urania, «Multiple phytoplankton community responses to environmental change in a temperate coastal system: A trait-based approach», *Frontiers in Marine Science*, fmars.2022.914475, 2022.

[2]Arrigo, Kevin R., Robinson, Dale H., Worthen, Denise L, Dunbar, Robert B., DiTullio, Giacomo R., Van Woert, Michael, «Phytoplankton community structure and the drawdown of nutrients and CO2 in the Southern Ocean», *Science*, 283, 365–367, 1999.

[3]Schoemann, Véronique, Becquevort, Sylvie, Stefels, Jacqueline, Rousseau, Véronique, Lancelot, Christiane, «*Phaeocystis* blooms in the global ocean and their controlling mechanisms: a review», *Journal of Sea Research*, 53, 43−66, 2005.

[4]Schmitt, François G., Landry, Yannick, Revillion, Marc, Gentilhomme, Valérie, Borde, Christophe, Herbert, Vincent, « Efflorescences de *Phaeocystis* sur la Côte d'Opale : investigations historiques », dans F.G. Schmitt (éd.), *Du naturalisme à l'écologie*, Boulogne/mer, 2011.

[5]Spilmont, Nicolas, Denis, Lionel. Artigas, Luis F., Caloin, F., Courcot, Lucie, Créach, Anne, Desroy, Nicolas, Gevaert, François, Hacquebart, Pierre, Hubas, Christophe., Janquin, Marie-Andrée Lemoine, Yves, Luczak, Christophe, Migné, Aline, Rauch, Mathieu, Davoult, Dominique, «Impact of the *Phaeocystis globosa* spring bloom on the intertidal benthic compartment in the eastern English Channel: A synthesis», *Marine Pollution Bulletin*, 58, 55-63, 2009.

[6]Lancelot, Christiane, Billen, Gilles, Sournia, Alain, Weisse, Thomas, Colijn, Franciscus, Veldhuis, Marcel J. W., Davies Pamela A., Wassmann, Paul, «*Phaeocystis* blooms and nutrient enrichment in the continental coastal zones of the North Sea», *Ambio*, 16, 38–46, 1987.

[7]Tett, Paul, Gowen, Richard, Mills, Dave, Fernandes, Teresa, Gilpin, Linda, Huxham, Mark, Kennington, Kevin, Read, Paul, Service, Matthew, Wilkinson, Martin, Malcolm, Stephen, «Defining and detecting undesirable disturbance in the context of marine eutrophication», *Marine Pollution Bulletin*, 55, 282-97, 2007.

[8]Loebl, Martina, Colijn, Franciscus, van Beusekom, Justus E.E., Baretta-Bekker, Johanna G., Lancelot, Christiane, Philippart, Catharina J.M., Rousseau, Véronique, Wiltshire, Karen H., «Recent patterns in potential phytoplankton limitation along the Northwest European continental coast», *Journal of Sea Research*, 61, 34-43, 2009.

[9]Burson, Amanda, Stomp, Maayke, Akil, Larissa, Brussaard, Corina P. D., Huisman, Jef, «Unbalanced reduction of nutrient loads has created an offshore gradient from phosphorus to nitrogen limitation in the North Sea», *Limnology and Oceanography,* 61, 869–888, 2016.

combattre l'eutrophisation[10,11,12], *Phaeocystis* produit toujours une biomasse carbonée considérable dans les eaux côtières de la Côte d'Opale[1] et en Baie Sud de la Mer du Nord[9]. Il est possible que l'accentuation du déséquilibre entre les apports en nitrates et phosphates qui accompagne la re-oligotrophisation[8,9] soit à l'œuvre. En effet, les prymnésiophycées picoplanctoniques présentent des pics d'abondance dans les eaux ayant une valeur du rapport N/P bien supérieure (N/P>>16) à celle du rapport de Redfield[13] (i.e., la valeur moyenne du rapport entre concentrations en azote et en phosphore chez le phytoplancton, N/P=16), et la matière organique issue des efflorescences de *Phaeocystis* a un rapport N/P plus élevé que lorsqu'elle est issue de diatomées[2]. Mais il est également possible que le réchauffement des eaux de la Manche[14], et/ou une amélioration de l'éclairement de la colonne d'eau, soient à l'origine du maintien d'efflorescences importantes de *Phaeocystis*, comme suggéré[15,16] par le constat d'une augmentation de l'abondance des diatomées et des concentrations en chlorophylle *a* (indicateur de biomasse phytoplanctonique) en zone côtière de la Mer du Nord ; et ce, malgré une re-oligotrophisation.

Les facteurs environnementaux déclencheurs des efflorescences de *Phaeocystis* sont également flous. *Phaeocystis* a un cycle polymorphique complexe[17] qui alterne entre une phase solitaire et une phase coloniale. C'est la phase coloniale qui est à l'origine des efflorescences[17]. Bien qu'une limitation en silicates - nutriment utilisé uniquement par les diatomées, groupe phytoplanctonique majoritaire et potentiellement en compétition avec *Phaeocystis* en cas de limitation des ressources - déclenche la formation de colonies et l'efflorescence de *Phaeocystis* en laboratoire[18], ce n'est pas nécessairement le cas *in situ*[19]. En lien avec les besoins de *Phaeocystis*, considérés comme supérieurs à ceux des diatomées pour une croissance

[10]OSPAR, «PARCOM recommendation 88/2: On the reduction in nutrients to the Paris convention area (Paris Commission)», 1988.

[11]European Union, «Directive 91/676/EEC concerning the protection of waters against pollution caused by nitrates from agricultural sources», 1–8, 1991.

[12]European Union, Council directive 91/271/EEC concerning urban wastewater treatment», 40–52, 1991.

[13]Kirkham, Amy R., Lepère, Cécile, Jardillier, Ludwig E., Not, Fabrice, Bouman, Heather, Mead, Andrew, David J Scanlan, «A global perspective on marine photosynthetic picoeukaryote community structure», *ISME Journal*, 7, 922-36, 2013.

[14] McLean, Matthew J., Mouillot, David, Goascoz, Nicolas, Schlaich, Ivan, Auber, Arnaud, «Functional reorganization of marine fish nurseries under climate warming», *Global Change Biology*, 25,660–674, 2019.

[15]McQuatters-Gollop, Abigail, Raitsos, Dionysios E., Edwards, Martin, Pradhan, Yaswant, Mee, Laurence D., Lavender, Samantha J., Attrill, Martin, «A long-term chlorophyll data set reveals regime shift in North Sea phytoplankton biomass unconnected to nutrient trends». *Limnology and Oceanogaphy, 52*2, 635-648, 2007.

[16]Xu, Xu, Carsten, Lemmen, Wirtz, Kai W., «Less Nutrients but More Phytoplankton: Long-Term Ecosystem Dynamics of the Southern North Sea», *Frontiers in Marine Science*, 7, 662, 2020.

[17]Rousseau, Véronique, Chrétiennot-Dinet, Marie José, Jacobsen, Anita, Verity, Peter, Whipple, Stuart, «The life cycle of *Phaeocystis*: state of knowledge and presumptive role in ecology», *Biogeochemistry*, 83, 29−47, 2007.

[18]Egge, JK, Asknes DL, «Silicate as regulating nutrient in phytoplankton competition», *Marine Ecology Progress Series*, 83, 281−289, 1992.

[19]Peperzak, Louis, Colijn, Franciscus, Gieskes, W. W. C., Peeters, J. C. H., «Development of the diatom-*Phaeocystis* spring bloom in the Dutch coastal zone of the North Sea: the silicon depletion versus the daily irradiance threshold hypothesis», *Journal of Plankton Research*, 20*,* 517-537, 1998.

maximale[20,21], la nécessité d'une irradiance suffisante a été également suggérée[19]. Cette hypothèse n'a toutefois été formulée que sur la base de données recueillies au cours d'un seul cycle annuel[19]. Enfin, l'action de broutage par le zooplancton engendre une augmentation de la taille des colonies, *via* un signal chimique [22]. Néanmoins, et contrairement à ce qui est observé chez de nombreuses espèces phytoplanctoniques[23,24], ce broutage ne semble pas déclencher la formation de colonies[22], i.e., le passage d'un stade libre à colonial.

Dans ce chapitre, nous synthétisons les connaissances acquises ces dernières années[1,25] sur la dynamique et les facteurs de contrôle de cette micro-algue atypique. Notre analyse des données récoltées à la station Wimereux Côte (50°40'75 N; 1°31'17E, au large du Portel) des Services Nationaux d'Observation SOMLIT (Service d'Observation en Milieu Littoral, (https://www.somlit.fr) et PHYTOBS (Réseau d'observation du phytoplancton, https://www.phytobs.fr/) (i) révèle l'importance des interactions biotiques pour le succès de *Phaeocystis* et (ii) montre comment la re-oligotrophisation et la diminution des apports fluviaux à la côte observée au cours de la dernière décennie ont favorisé les efflorescences de *Phaeocystis*, en tendant à une limitation en phosphates et en accentuant le déséquilibre entre les nitrates et les phosphates.

Matériel et méthodes

Acquisition des données

Les prélèvements d'eau ont été effectués sur une base bimensuelle, avec une bouteille Niskin, en marées de vives-eaux à 2m de profondeur pendant l'étale de pleine mer à bord du bateau de recherche « *Sepia II* ». Pour connaitre la composition et estimer la biomasse du phytoplancton de taille > 5µm (i.e., diatomées et dinophycées) et de *Phaeocystis,* des échantillons d'eau ont été fixés avec une solution de Lugol-glutaraldéhyde (1% v/v) et examinés selon la méthode d'Utermöhl avec un microscope Nikon Eclipse TE2000-S équipé de grossissements ×100-400. A noter que la distinction entre les phases solitaire et coloniale a été effectuée à partir de 2007. La quantification des autres groupes phytoplanctoniques - i.e., les cryptophycées, les picoeucaryotes, et la cyanobactérie *Synechococcus* spp. - a été effectuée à partir de 2009 dans

[20]Jahnke, J., «The light and temperature dependence of growth rate and elemental composition of *Phaeocystis globosa* Scherffel and *P. pouchetii* (Har.) Lagerh. in batch cultures». *Netherlands Journal of Sea Research*, 23, 15−21, 1989.

[21]Breton, Elsa, Christaki, Urania, Bonato, Simon, Didry, Morgan, Artigas, Luis F., «Functional trait variation and nitrogen use efficiency in temperate coastal phytoplankton», *Marine Ecology Progress Series*, 563, 35–49, 2017.

[22]Jakobsen, Hans H., Tang, Kam W., «Effects of protozoan grazing on colony formation in *Phaeocystis globosa* (Prymnesiophyceae) and the potential costs and benefits», *Aquatic Microbial Ecology*, 27, 261−273, 2002.

[23]Kapsetaki, Stephania E., West, Stuart A., «The costs and benefits of multicellular group formation in algae», *Evolution*, 73, 1296-1308, 2019.

[24]Xiao, Man, Li, Ming, Reynolds, Colin S., «Colony formation in the cyanobacterium *Microcystis*», *Biological Reviews*, 93, 1399-1420, 2018.

[25]Breton, Elsa, Christaki, Urania, Sautour, Benoit., Demonio, Oscar, Skouroliakou, Dimitra-Ioli, Beaugrand, Gregory, Seuront, Laurent, Kléparski, Loick, Poquet, Adrien, Nowaczyk, Antoine, Crouvoisier, Muriel, Ferreira, Sohpie, Pecqueur, David, Salmeron, Christophe, Brylinski, Jean-Michel, Lheureux, Arnaud, Goberville, Eric, «Seasonal Variations in the Biodiversity, Ecological Strategy, and Specialization of Diatoms and Copepods in a Coastal System With *Phaeocystis* Blooms: The Key Role of Trait Trade-Offs», *Frontiers in Marine Science*, 8, 1178, 2021.

le cadre du SOMLIT par analyse cytométrique[26] des échantillons (FACSCan, BD Biosciences) au sein de la plate-forme labellisée BIOPIC (Biology Platform of Imaging and flow Cytometry ; https://www.obs-banyuls.fr/fr/rechercher/plateformes/biopic.html) : les échantillons ont été fixés avec une solution de glutaraldéhyde (1,33% v/v) et conservés à -80°C jusqu'à analyse. Toutes les données d'abondances acquises par microscopie et cytométrie en flux ont été converties en biomasse carbonée en utilisant des facteurs de conversion propres à chaque groupe phytoplanctonique[1,25].

Afin d'identifier les facteurs de contrôle de *Phaeocystis,* que ce soit à l'échelle saisonnière[25] et à long-terme[1], nous avons considéré l'ensemble des variables environnementales mesurées par le programme SOMLIT. Nous décrivons, ici, uniquement la méthodologie utilisée pour acquérir la mesure des variables qui se sont révélées déterminantes pour expliquer la dynamique de cette prymnésiophycée.

Les concentrations des sels nutritifs dans l'eau de mer (le phosphore dissous inorganique [DIP], la silice dissoute inorganique [DSi], et l'azote dissous inorganique [DIN], i.e., la somme des nitrates, nitrites, et ammonium) ont été déterminées selon la méthode colorimétrique[27] avec un autoanalyseur (Technicon, Alliance, puis Seal Instruments). A noter que pour l'ammonium, les concentrations ont été déterminées par spectrométrie[28,29] jusqu'en 2008, puis par fluorimétrie[30,31] à partir de 2009. La lumière disponible pour la photosynthèse a été estimée à partir (i) du coefficient d'atténuation de la lumière (Kd, m^{-1}) mesuré avec une sonde CTD Seabird équipée d'un capteur QSP 2300 (Biospherical Instruments) et (ii) des données de lumière incidente fournies par le Service d'observation atmosphérique du programme européen Copernicus (CAMS, http://www.soda-pro.com/web-services/radiation/cams-radiation-service). Les données de vents proviennent des stations météorologiques Météo-France de Dunkerque, Calais, Boulogne/mer, et Abbeville (https://donneespubliques.meteofrance.fr).

Analyse des données

La formation de colonies, ou le regroupement temporaire simple de cellules, peut se déclencher pour faire face à la prédation, à un stress, ou à l'épuisement/rareté des ressources (distribution hétérogène)[32]. Par conséquent, la limitation en phosphates et silicates (les nitrates sont en excès) et les variations du degré de protection des diatomées contre la prédation[1] (taille, degré de colonialité, présence de soies et/ou d'épines, production potentielle de mucus ou toxine) comme

[26]Marie, Dominique, Brussaard, Corina, Rigaut-Jalabert, Fabienne, Vaulot, Daniel, «Flow cytometric analysis of phytoplankton, bacteria and viruses», dans: John Wiley & Sons, (éd.) *Current Protocols in Cytometry*, Inc, 1999, 11.11.1-11.11.15.

[27]Aminot, Alain, Kérouel, Roger,«Hydrologie des écosystèmes marins: paramètres et analyses», Ifremer (éd), Brest, 2004, 335 p..

[28]Koroleff, F., «Direct determination of ammonia in natural waters as indophenol blue». *ICES C. M.* Reports, 1969, 94 pp.

[29]Solorzano, Lucia, «Determination of Ammonia in Natural Waters by the Phenolhypochlorite Method», *Limnology and Oceanography*, 14, 799-801, 1969.

[30]Holmes, Robert M., Aminot, Alain, Kérouel, Roger, Hooker, Bethanie. A., Peterson, Bruce J., «A simple and precise method for measuring ammonium in marine and freshwater ecosystems», *Canadian Journal of Fish Aquatic Science*, 56, 1801–1808, 1999.

[31]Taylor, Brad W., Keep, Christine F., Hall Jr., Robert O., Koch, Benjamin J., Tronstad, Lusha M., Flecker, Alexander S., Ulseth, Amber J., «Improving the fluorometric ammonium method: matrix effects, background fluorescence, and standard additions», *Journal of the North American Benthological Society*, 26, 167–177, 2007.

[32]Tong, Kai, Bozdag, G. Ozan, Ratcliff, William C., Selective drivers of simple multicellularity. *Current Opinion in Microbiology*, 67, 102141, 2022.

facteurs déclencheurs de la formation des colonies ont été étudiées sur la période 2007-2019. Les conditions d'éclairement et la température de l'eau au déclenchement de la phase coloniale ont aussi été étudiées. Pour cela, un seuil de 20% de cellules diploïdes (libres et coloniales) dans les échantillons a été considéré comme signal de changement de phase. Une analyse graphique a également été effectuée à l'échelle de la saison, après un lissage du nuage de points par régression locale selon la méthode LOESS[33] (Jacoby, 2000), i.e., par pondération locale où l'on considère qu'une observation est plus influencée par ses « k » plus proches voisins que par des voisins plus éloignés.

L'analyse exploratoire des facteurs de contrôle de la biomasse de *Phaeocystis* sur le long-terme (1996-2019) a été effectuée aux pas de temps mensuel et annuel. Les données mensualisées ont été désaisonnalisées puis transformées selon la méthode des sommes cumulées[34] (i.e., cumul des écarts à la moyenne ; Cusum). L'intérêt principal de cette méthode est sa robustesse pour traiter des données incomplètes, ayant une distribution non gaussienne, et/ou entachées de bruits parasites, ce qui est souvent le cas des séries chronologiques environnementales. Comme les séries Cusum sont auto-corrélées (i.e., la valeur d'une variable à un instant « t » dépend des valeurs précédentes ou suivantes), les relations significatives ne peuvent être estimées que visuellement en évaluant le degré de parallélisme entre les Cusums des variables étudiées. Afin d'avoir une mesure quantitative du degré de relation entre les variables (i.e., coefficient de régression r2 : variance expliquée sur une échelle de 0 à 1), les données annualisées ont été utilisées et modélisées à l'aide d'équations structurelles[35] (SEM) selon la méthode du maximum de vraisemblance, et en incluant un modèle des erreurs AR(1) (AR : autocorrélation). Un des grands intérêts des SEM est de pouvoir construire des modèles avec plusieurs variables expliquées, en plus de plusieurs variables explicatives. Le modèle final a été sélectionné selon le critère d'information d'Akaike. Avant cela - et afin de synthétiser l'information contenue dans les données abiotiques (température de l'eau, salinité, densité, sels nutritifs [DIP, DSi, DIN] et les rapports entre eux et la lumière disponible pour la photosynthèse) et de vent - des Analyses en Composantes Principales (ACP) ont été effectuées sur les valeurs moyennes et la variabilité mensuelle/annuelle (coefficient de variation en %) des variables abiotiques d'une part, et des vitesses de vent d'autre part. Cette méthode multivariée a permis de calculer de nouvelles variables indépendantes nommées Composantes Principales (CPs), concentrant l'information contenue dans le grand nombre de variables de départ.

Résultats et discussion

Dynamique saisonnière et long-terme (1996-2019) de Phaeocystis

Phaeocystis peut peupler les eaux côtières de la Côte d'Opale entre janvier et octobre, mais contribue majoritairement à la biomasse phytoplanctonique carbonée entre mars et mai (Fig. 2A). Sur la série de comptages phytoplanctoniques de 24 ans (1996-2019) au point Wimereux Côte, le maximum d'abondance a été atteint en avril 2011 : 4,5 10^7 cellules/litre sont observées, soit quatre fois moins que le maximum rapporté dans la littérature scientifique, comme dans la Baie Allemande[3]. L'ampleur des efflorescences de *Phaeocystis* (Fig. 2B) et la durée d'occurrence annuelle (Fig. 2C) sont très variables d'une année à l'autre.

[33]Jacoby, W. G., «LOESS: a nonparametric, graphical tool for depicting relationships between variables», *Electoral Studies*, 19, 577–613, 2000.

[34]Regier, Peter, Briceño, Henry, Boyer, Joseph N., «Analyzing and comparing complex environmental time series using a cumulative sums approach», *MethodsX*, 6, 779–787, 2019.

[35]Hoyle, R.H., «Structural Equation Modeling: Concepts, Issues, and Applications», dans Hoyle, R.H (ed.), Sage, Thousand Oaks, 1995.

Le cycle de *Phaeocystis* est complexe[17] (Fig. 3A-G) : il alterne entre une phase libre composée de cellules haploïdes flagellées d'une taille comprise entre 3 et 4µm (Fig. 3A) et une phase coloniale composée de colonies pourvues d'une enveloppe mucopolysaccharidique[36] (Fig. 3B-F). Les cellules dans les colonies sont diploïdes, sans flagelles, et d'une taille d'environ 8µm (Fig. 3E, G). Un cycle polymorphique est un atout écologique indéniable car il permet d'augmenter les chances de survie dans différentes conditions environnementales. Au point Wimereux Côte, les efflorescences de la phase coloniale peuvent être quasi mono-spécifiques : 99,96% de l'abondance totale du phytoplancton recensé par microscopie inversée (avril 2016), et 99,88% de biomasse carbonée (avril 2010). Les colonies grossissent (Fig. 3C), s'allongent, et bourgeonnent jusqu'à fin avril, (Fig. 3D). La taille des colonies peut varier entre 20µm (colonie de deux cellules environ) et 4mm (avril 2016) et montrent une taille médiane de 400µm (période 2007-2019). Lorsque mises en culture, les colonies dépassent fréquemment 5mm et peuvent atteindre des tailles supérieures au centimètre en présence de dinoflagellés hétérotrophes et en l'absence d'agitation (obs. pers.). Pendant la phase de déclin des efflorescences, les colonies vieillissantes sont progressivement colonisées par des bactéries (Fig. 3E, flèches en orange) et la diatomée *Pseudo-nitzschia delicatissima* (Fig. 3E, flèches en vert). Au cours de la période 1996-2019, seule cette espèce a été recensée sur les colonies de *Phaeocystis*, ce qui suggère un lien actif entre ces deux micro-algues, entre *Pseudo-nitzschia* et les bactéries attachées à *Phaeocystis*, voire le complexe *Pseudo-nitzschia*/*Phaeocystis*/bactéries. Des recherches complémentaires sont nécessaires pour éclaircir la(les) raison(s) de ce lien. La rupture de l'enveloppe coloniale (Fig. 3F) libère des milliers de cellules diploïdes (Fig. 3G), qui se transforment rapidement en cellules haploïdes flagellées (Fig. 3A). L'occurrence de ces cellules est généralement éphémère, i.e., environ une semaine. La disparition des échantillons de ces cellules haploïdes marque la fin des efflorescences annuelles de *Phaeocystis*. Il existe un troisième morphotype moins fréquent et jamais recensé dans nos échantillons[17] : une cellule coloniale diploïde flagellée.

Facteurs de contrôle des efflorescences de Phaeocystis

Nos résultats suggèrent que l'intensification de l'activité de broutage par le zooplancton à cette période de l'année[37,38] joue un rôle important dans le déclenchement de la formation des colonies et des efflorescences de *Phaeocystis* (Fig. 4A-B) ; et non la compétition pour acquérir des ressources limitées. Sur les treize ans de suivi (2007-2019), nos observations montrent que la formation des colonies s'est déclenchée quel que soit le niveau de ressources (phosphates, silicates, éclairement), limitée ou non limitées (Figure 1). Le rapport surface/volume (Fig. 4A, en marron), un indicateur de compétitivité pour acquérir les sels nutritifs lorsque ceux-ci sont limités[39,40], présente des valeurs bien inférieures au moment du changement de phase de *Phaeocystis* en comparaison des valeurs observées en été, lorsque les sels nutritifs sont épuisés[25]. La biomasse des diatomées ne diminue pas de manière significative pendant les

[36]Hamm, Christian E., Simson, Doris A., Merkel, Rudolf, Smetacek, Victor, «Colonies of *Phaeocystis globosa* are protected by a thin but tough skin», *Marine Ecology Progress Series*, 187, l0l-111, 1999.

[37]Antajan, Elvire, *Responses of Calanoid Copepods to Changes in Phytoplankton Dominance in the Diatoms - Phaeocystis Globosa Dominated Belgium Coastal Waters*, Vrije Universiteit Brussel, 2004.

[38]Gasparini, Stéphane, Daro, Marie-Hermande, Antajan, Elvire, Tackx, Michèle, Rousseau, Véronique, Parent, Jean- Yves, Lancelot, Christiane, «Mesozooplankton grazing during the *Phaeocystis globosa* bloom in the Southern Bight of the North Sea», *Journal of Sea Research*, 43, 345–356, 2000.

[39]Grover, James P., «Influence of cell shape and size on algal competitive ability», *Journal of Phycology*, 25, 402-405, 1989.

[40]Litchman, Elena, and Klausmeier, Christopher A., «Trait-based community ecology of phytoplankton», *Annual Review in Ecology Evolution and Systematics*, 39, 615−639, 2008.

efflorescences de *Phaeocystis*[25] et aucun effet négatif de *Phaeocystis* sur les diatomées n'a été détecté sur le long-terme[1]. Le déséquilibre nutritif (N/P>>16) s'installe avant le début des efflorescences et le déclenchement de changement de phase (Fig. 4C). Il est donc difficile de le considérer comme un facteur déclencheur des efflorescences.

Le déclenchement des efflorescences (20% de la biomasse totale produite par *Phaeocystis* ; Fig. 4A, en vert clair) et le seuil de 20% de cellules coloniales (Fig. 4B, en vert clair) coïncident avec le maximum saisonnier du degré de protection des diatomées contre la prédation (Fig. 4A-B). La Figure 4A révèle la présence d'un compromis physiologique résultant de l'histoire évolutive des espèces : les espèces les plus compétitives vis-à-vis de la ressource en sels nutritifs sont celles qui sont le moins bien protégées contre la prédation. Fabriquer une protection est métaboliquement coûteux et diminue d'autant les capacités de croissance et d'acquisition des ressources, comme l'affinité pour les ressources limitées[23,41,42]. Ces résultats suggèrent que les relations proie-prédateur jouent un rôle important dans la formation des colonies de *Phaeocystis* et le déclenchement des efflorescences, confortant l'idée que la compétition n'est pas le processus dominant de la structuration des communautés phytoplanctoniques à cette période de l'année. L'investissement dans des mécanismes de défense permet de relaxer la compétition[23,38,39] : les prédateurs contrôlent la dynamique des espèces dominantes, espèces les plus compétitives mais les moins équipées face à la prédation.

L'analyse des variations à long-terme de la contribution de *Phaeocytis* à la biomasse totale phytoplanctonique[5] montre que la tendance vers une limitation en phosphates (Fig. 5A, courbe ascendante en orange) favorise les efflorescences (Fig. 5A, courbe ascendante en rouge), et celle des diatomées, avec pour conséquence directe de prolonger également l'occurrence annuelle de *Phaeocytis*. Nos résultats montrent également une influence positive et significative de la diminution de la variabilité des conditions lumineuses sur la production de biomasse de *Phaeocystis* (coefficient d'estimation du modèle, C=-0,44) produite sur le long-terme (Fig. 5B). La durée d'occurrence annuelle de *Phaeocystis* dans les eaux côtières de la Côte d'Opale dépend principalement (r^2=0,62 ; Fig. 5B) de la quantité de biomasse produite pendant les efflorescences (C=0,62), de la tendance à une limitation en nitrates (N/P<<16 ; C=-0,41), et de la stabilité de la colonne d'eau (C=-0,41). La tendance à la limitation en phosphates observée au cours de la dernière décennie résulte d'une re-oligotrophisation déséquilibrée (i.e., augmentation des rapports N/P et Si/P) et de la diminution des apports fluviaux (C=0,85 ; Fig. 5B). Cette diminution en phosphates a engendré davantage de réponses différentes entre les espèces, et a donc augmenté l'asynchronisme annuel (C=-0,46). Ces résultats sont cohérents avec (i) une dominance des prymnésiophycées picoeucaryotes - classe à laquelle appartient *Phaeocystis* - dans des eaux ayant un rapport N/P plus élevé que celui de Redfield[13], (ii) des valeurs du rapport N/P plus élevées dans la matière organique issue des efflorescences de *Phaeocystis* que dans celle issue des diatomées[2], (iii) la capacité des colonies à être de véritables réservoirs à phosphore[3,43], et donc à énergie (ATP, NADP, etc…), donnant à *Phaeocystis* la capacité à synthétiser l'alcaline phosphatase pour utiliser le phosphore organique dissous[44]

[41]Cadier, Mathilde, Andersen, Ken H., Visser, Andre W., Kiørboe, Thomas, «Competition–defense tradeoff increases the diversity of microbial plankton communities and dampens trophic cascades», *Oikos*, 128, 1027-1040, 2019.

[42]Ehrlich, Elias, Kath, Nadja J., Gaedke, Ursula, «The shape of a defense-growth trade-off governs seasonal trait dynamics in natural phytoplankton», *ISME Journal*, 14, 1451–1462, 2020.

[43]Moestrup, Øjvind, Larsen, Jacob, «Potentially toxic phytoplankton: 1. Haptophyceae Prymnesiophyceae», dans Lindley, J.A. (éd.), *ICES Identification Leaflets for Plankton*, Copenhagen, 11 pp., 1992.

[44]van Boekel, W. H. M., Veldhuis, M. J. W., «Regulation of alkaline phosphatase synthesis in *Phaeocystis* sp. », *Marine Ecology Progress Series*, 61, 281–289, 1990.

résultant d'exsudas métaboliques ou issu du broutage. Nos résultats sont cohérents avec la stratégie de vie qualifiée de « survivaliste »[45], retrouvée chez les espèces très bien équipées pour l'acquisition des ressources limitées mais à la croissance plus lente que celles ayant une stratégie de « bloomer » ou « généraliste ». Le parallélisme entre la dynamique à long-terme de l'abondance des diatomées (Fig. 5A) et la contribution de *Phaeocystis* à la biomasse totale du phytoplancton suggère que l'activité métabolique des diatomées pourrait être une source importante de phosphore. L'augmentation de similarité fonctionnelle chez les communautés phytoplanctoniques au cours de la dernière décennie, synchrone à une augmentation de la richesse spécifique[1], conforte l'hypothèse d'un mutualisme entre les espèces.

Conclusion

Nos résultats suggèrent que les interactions proie-prédateur et mutualistes jouent un rôle important sur le déclenchement et l'ampleur des efflorescences de *Phaeocystis* dans les eaux côtières de la Côte d'Opale. Notre étude montre également comment la re-oligotrophisation observée au cours de la période de suivi au point Wimereux Côte a eu un effet inverse de celui initialement escompté : l'accentuation du déséquilibre entre les nitrates et les phosphates et la tendance à la limitation en phosphates pour une croissance optimale ont favorisé les efflorescences de *Phaeocystis* à partir de 2006. Nos analyses ne mettent pas en évidence d'effet négatif de *Phaeocystis* sur les diatomées et les copépodes. A l'ère de l'Anthropocène[46], ces efflorescences sont plus que jamais nécessaires pour tamponner, tout du moins en partie, les excès de CO_2 atmosphérique[47],[48].

Remerciements

Nous remercions les capitaines et marins successifs du bateau de recherche CNRS «*Sépia II*» : Charly Dollet, Jean-Claude Martin, Grégoire Leignel, Noël Lefiliatre, et Christophe Routtier qui ont aidé aux prélèvements et rendu les conditions optimales pendant ces nombreuses années. Nous remercions également le personnel local du SOMLIT qui a effectué les prélèvements et les analyses des paramètres physico-chimiques : Nicole Degros, Eric Lecuyer, et Dr. Valérie Gentilhomme, ainsi qu'Emilie Grossteffan de l'IUEM (Plouzané) qui a analysé les sels nutritifs lorsque l'appareil du LOG était en panne. Nous remercions également les réseaux SOMLIT et PHYTOBS qui soutiennent la poursuite du suivi long-terme des écosystèmes du littoral métropolitain incluant les communautés phytoplanctoniques.

[45]Arrigo, Kevin, «Marine microorganisms and global nutrient cycles», *Nature,* 437, 349–355, 2005.
[46]Crutzen, Paul J., «Geology of mankind: The Anthropocene», *Nature*. 2002, 415:23.
[47]https://www.climate.gov/news-features/understanding-climate/climate-change-atmospheric-carbon-dioxide
[48]Lüthi, Dieter, Le Floch, Martine, Bereiter, Bernhard, Blunier, Thomas, Barnola, Jean-Marc, Siegenthaler, Urs, Raynaud, Dominique, Jouzel, Jean, Fischer, Hubertus, Kawamura, Kenji, Stocker, Thomas F., «High-resolution carbon dioxide concentration record 650,000-800,000 years before present», *Nature*, 453, 379–82, 2008.

Tableau 1. Valeurs des ressources (lumière, phosphates, et silicates) et de la température de l'eau au déclenchement de la phase coloniale chez *Phaeocystis* (20% de cellules coloniales). Un milieu est considéré limité en lumière lorsque PAR<9 E m^{-2} j^{-1}, limité en phosphates lorsque la concentration en phosphates est <0.2 µM et les rapports N/P et Si/P>16 (µM:µM), et limité en silicates lorsque la concentration en silicates est <2 µM, et les rapports Si/P et Si/N, respectivement <10 et 1 (µM:µM). E: Einstein; CV: Coefficient de Variation (%).

Variable	Unité	Min-Max	Moyenne±CV(%)	Médiane	Fréquence de la limitation (%)
Température	°C	5,3-9,1	7±18	6,8	-
Lumière PAR	E m^{-2} j^{-1}	5-24	17±39	20	22
Silicates	µM	0,6-6,6	2,89±65	2,3	44
Phosphates	µM	0,14-0,6	0,38±48	0,34	22
Rapport N/P	µM:µM	9-115	40±85	31	-
Rapport Si/P	µM:µM	0,94-19	9±60	7	-
Rapport Si/N	µM:µM	0,32	0,7±75	0,44	-

Figure 1. Evènement mucilagineux sur la plage de Wimereux survenu en mai 2007. **A**: dépôt de mousse sur l'estran après une tempête; **B**: mousse fraiche, fabriquée au moment de l'échouage d'une vague sur la plage. Photographies: E. Breton.

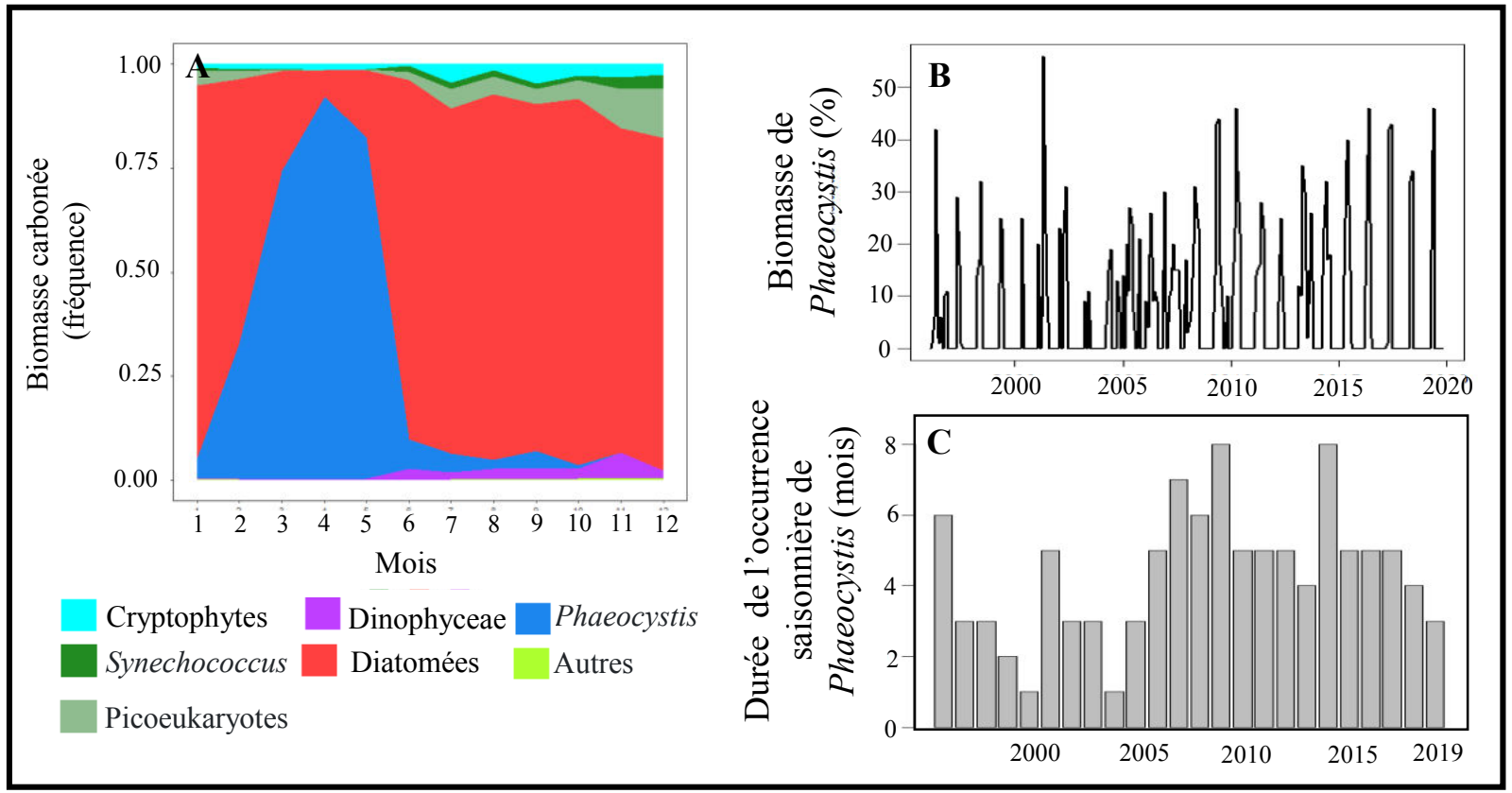

Figure 2. Dynamique saisonnière (2009-2019) et inter-annuelle (1996-2019) de *Phaeocystis*. **A**: composition et structure saisonnière des communautés phytoplanctoniques; Variations inter-annuelles **B**: de la biomasse de *Phaeocytis* (%) et **C**: de sa durée d'occurrence annuelle. D'après Breton et al. 2021, 2022.

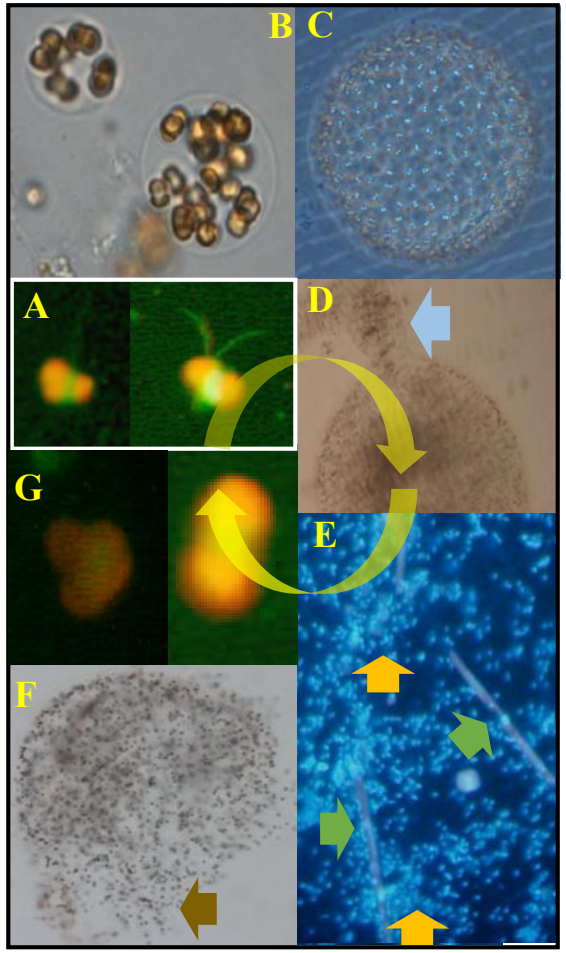

Figure 3. Cycle de vie de *Phaeocystis*.(**A-G**, d'après Rousseau et al. 1994, 2007). **A-B**: passage de la phase solitaire (**A**: cellules haploïdes flagellées) à la phase coloniale (**B**: petites colonies avec cellules diploïdes scellées dans une matrice mucopolysaccharidique); **B-D**: phase de grossissement (**B-C**) et de bourgeonnement (**D**, flèche bleue) des colonies; **E**: phase de vieillissement et colonisation des colonies. Notez les cellules diploïdes de *Phaeocystis* (flèches orange) scellées dans une matrice mucopolysaccharidique avec des bactéries (points blancs) et des cellules de la diatomée *Pseudo-nitzschia delicatissima* (flèches vertes) attachées à l'enveloppe coloniale; **F-G**: passage de la phase coloniale à la phase libre (**F**: rupture de l'enveloppe coloniale libérant des centaines de cellules diploïdes, flèche marron; **G**: cellules diploïdes libres ayant quitté la colonie). **A,E**, et **G**: microscopie à épifluorescence, X1000; **B**: microscopie inversée, X400, et **C**, **D** et **F**: microscopie inversée, X100. Photographies: E. Breton.

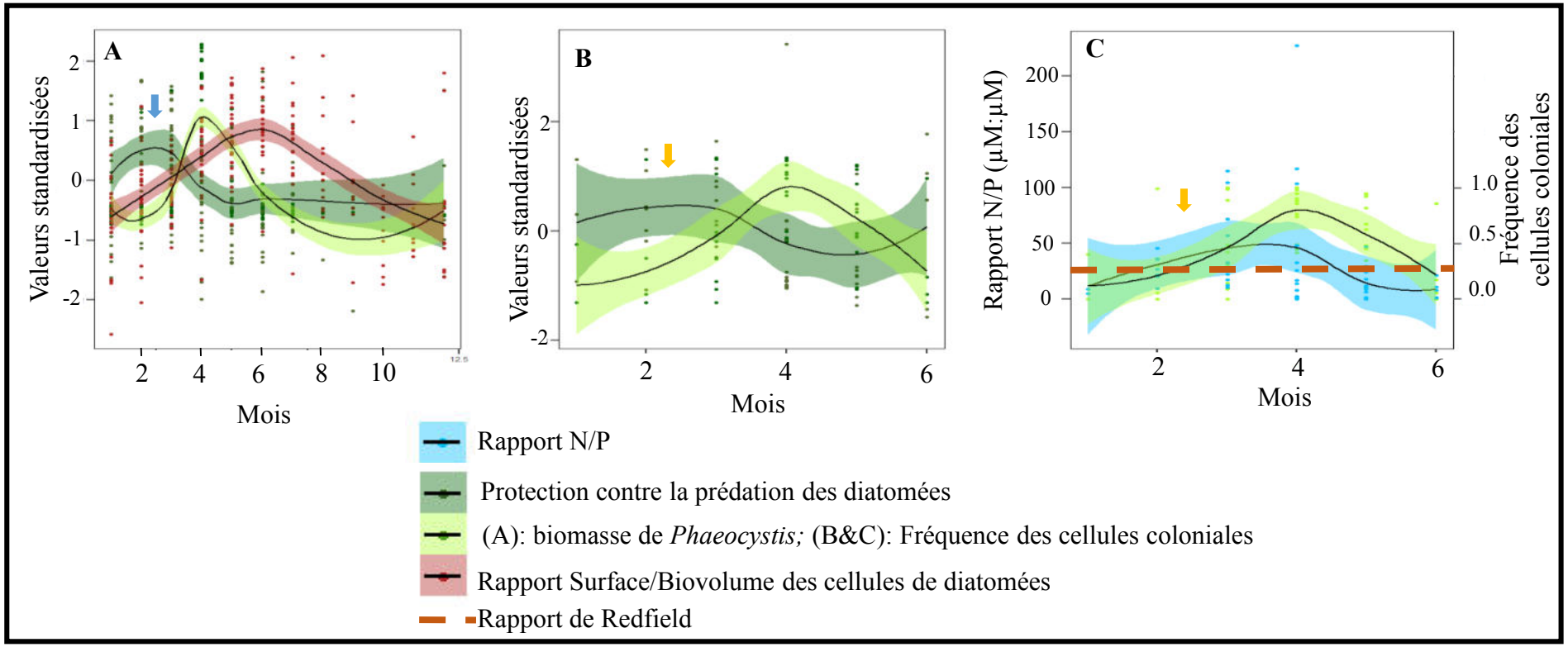

Figure 4. Facteurs de contrôle saisonnier du déclenchement des efflorescences de *Phaeocytis* dans les eaux côtières de la Manche orientale (**A**: période 1996-2019, **B**: 2007-2019). **A**: dynamique saisonnière de la biomasse de *Phaeocystis* (vert clair), du rapport Surface/Biovolume des diatomées (indicateur de compétitivité pour les nutriments; marron), et du degré de protection des diatomées contre la prédation (vert olive). **B**: dynamique saisonnière de la fréquence des cellules coloniales de *Phaeocystis* (vert clair) et du degré de protection des diatomées contre la prédation (vert olive). **C**: dynamique saisonnière de la fréquence des cellules coloniales de *Phaeocystis* (vert clair) et du rapport N/P (µM:µM; bleu). Les lignes représentent respectivement un lissage LOESS, et les rubans informant de l'intervalle de confiance à 95%. Les valeurs standardisées dans **A** (1996-2019) et **B** (2007-2019) ont été calculées par année. Noter la synchronisation entre la période de démarrage des efflorescences de *Phaeocystis* (**A**, flèche bleue), celle du déclenchement de la formation des colonies (20% de cellules coloniales, flèche orange) et le maximum saisonnier du degré de protection des diatomées contre la prédation (**A**, flèche bleue). Noter également les dynamiques temporelles opposées entre le rapport Surface/Biovolume des diatomées et le degré de protection des diatomées contre la prédation (i.e., compromis défense-compétitivité). **A&B** adaptés de Breton et al. 2021. Rapport N/P: le rapport entre concentrations en azote et en phosphore inorganiques dissous. Rapport de Redfield: N/P=16 (valeur moyenne chez le phytoplancton).

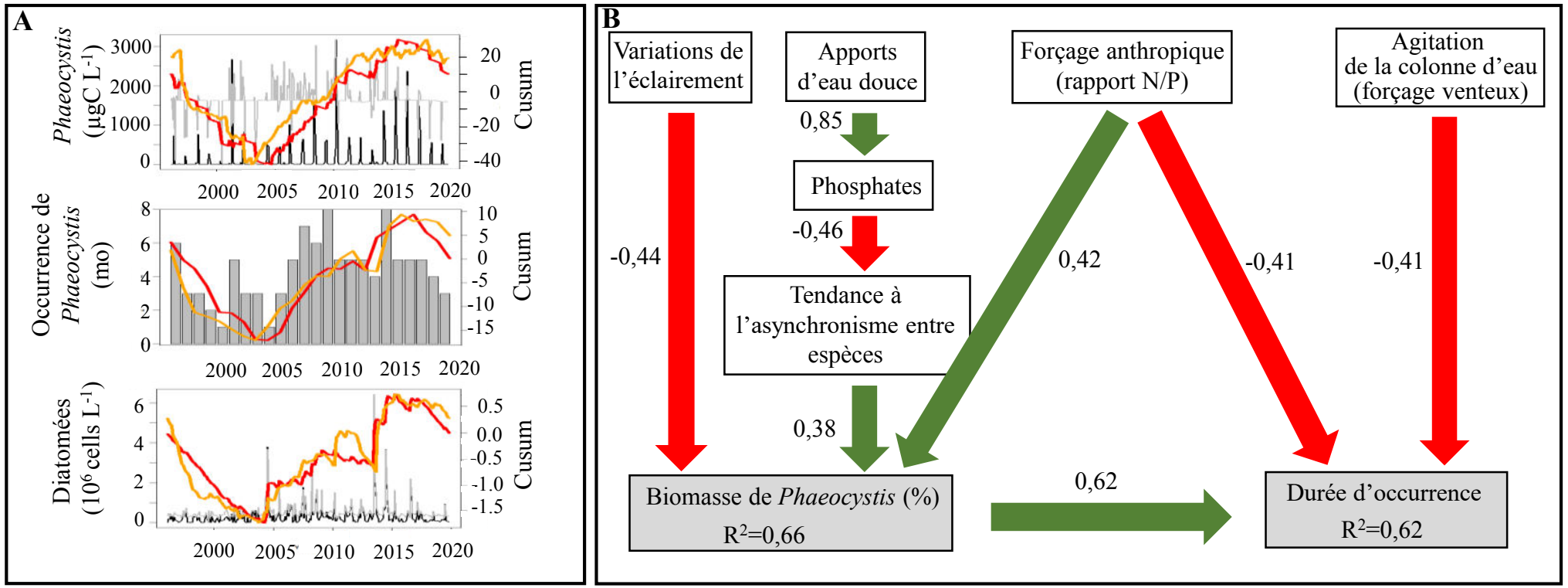

Figure 5. Facteurs de contrôle des variations à long-terme des efflorescences de *Phaeocystis* dans les eaux côtières de la Côte d'Opale. **A**: Relations à long-terme entre la limitation en phosphates (courbe orange) et la biomasse et la durée de l'occurrence annuelle de *Phaeocystis*, ainsi que l'abondance totale des diatomées. La courbe orange est issue d'une Analyse en Composantes Principales (ACP) effectuée sur les valeurs moyennes et la variabilité mensuelle de différentes variables abiotiques (température de l'eau, salinité, densité, sels nutritifs [phosphates, silicates, et azote inorganique dissous] et les rapports entre eux, et la lumière disponible pour la photosynthèse). Les apports d'eau douce dans (**B**) ont également été quantifiés à partir de cette ACP. Les variations temporelles de chacune des variables présentées dans (**A**) sont représentées sous la forme des sommes cumulées après avoir enlevé la composante saisonnière des séries. **B**: les relations ont été déterminées sur données annuelles par Modélisation d'Equations Structurelles (SEM) en tenant compte de l'autocorrélation des séries temporelles (1996-2019) avec un modèle des erreurs AR(1). Le modèle final a été sélectionné selon le critère d'information d'Akaike. Flèche rouge: effet négatif; flèche verte: effet positif. (**A**) adapté de Breton et al. (2022). Rapport N/P: le rapport entre concentrations en azote et en phosphore inorganiques dissous. AR: Auto Régression.

De l’intérêt des approches basées sur les traits de vie pour la compréhension des processus régulateurs de la biodiversité et leur rôle sur le fonctionnement des écosystèmes : exemples avec le plancton des eaux côtières de la Côte d’Opale.

Elsa Breton1, Urania Christaki1, Benoit Sautour2, Dimitra-Ioli Skouroliakou1, Muriel Crouvoisier1, Arnaud Cauvin1, et Eric Goberville3.

1-Univ. Littoral Côte d’Opale, CNRS, Univ. Lille, UMR 8187 LOG, F-62930 Wimereux, France

2-Univ. Bordeaux, CNRS, UMR 5805 EPOC, Rue Geoffroy Saint Hilaire – Bâtiment B18N

33600 Pessac, France

3-Unité Biologie des Organismes et Ecosystèmes Aquatiques (BOREA), Muséum National d’Histoire Naturelle, CNRS, IRD, Sorbonne Université, Université de Caen Normandie, Université des Antilles, Paris, France

Résumé

L'effondrement actuel de la biodiversité, son homogénéisation à l'échelle planétaire en lien avec les variations climatiques et l'intensification des activités humaines (*e.g.*, destruction des habitats, surexploitation des ressources, pollution/eutrophisation des milieux, introduction d'espèces exotiques envahissantes, …), ainsi que le besoin d'anticiper les impacts de ces changements globaux sur l'évolution des services écosystémiques, ont motivé l'urgence d'une compréhension mécanistique des liens entre biodiversité et processus écosystémiques : « *comment les assemblages d'espèces réagissent aux changements environnementaux, et pourquoi ?* ». Les traits de vie fonctionnels, reflètent la performance des espèces, ce qu'elles font, et comment elles interagissent avec leur environnement et les autres organismes. En s'appuyant sur une représentation simplifiée par rôle et non pas par espèce, l'étude de ces traits permet d'identifier les mécanismes sous-jacents responsables des liens entre environnement, biodiversité, et fonctionnement des écosystèmes, et donc de tendre vers une comparaison généralisable d'écosystèmes de compositions taxonomiques différentes. Bien qu'ayant atteint un certain degré de maturité en écologie terrestre, de nombreux verrous scientifiques doivent encore être levés en écologie marine, surtout pour la biodiversité « invisible », comme le plancton, compartiment essentiel du réseau trophique marin. Dans le cadre de ce chapitre, et après un rappel des fondements et des grands principes des approches fonctionnelles basées sur l'utilisation de traits de vie, nous montrons leur intérêt pour mieux comprendre comment les espèces planctoniques s'assemblent, répondent aux changements environnementaux et influent sur les processus écosystémiques. Nous nous appuyons sur l'étude de différentes séries planctoniques collectées dans les eaux côtières de la Côte d'Opale.

Pourquoi une approche basée sur les traits de vie ?

La responsabilité sans précédent des activités humaines (*e.g.*, destruction des habitats, surexploitation des ressources, pollution/eutrophisation des milieux, réchauffement climatique, introduction d'espèces invasives) dans l'érosion de la biodiversité (taxonomique et génétique) et l'homogénéisation écologique à l'échelle planétaire[1] (*i.e.*, remplacement progressif d'espèces spécialistes par des espèces généralistes) a motivé la nécessité (i) d'évaluer le rôle de la biodiversité sur le fonctionnement des écosystèmes[2,3], et (ii) d'une compréhension mécanistique de la réponse des espèces aux perturbations[4] – « Comment et pourquoi ? » – et de leurs effets sur les processus écosystémiques[5]. L'objectif final étant de pouvoir anticiper la réponse des écosystèmes aux changements globaux et l'évolution des services écosystémiques associés[4,5] (Fig. 1).

Comprendre la fonctionnalité d'un écosystème nécessite des informations sur ce que les espèces font, et comment elles interagissent avec leur environnement (les conditions abiotiques) et les autres organismes (les conditions biotiques)[4,6]. Les traits fonctionnels sont les caractéristiques morphologiques, physiologiques, ou phénologiques d'une espèce donnée (e.g., mode de reproduction, régime alimentaire, compétitivité, protection contre la prédation, ...) qui reflètent sa performance physiologique, reproductrice, et comportementale[7]. Ainsi, les approches basées sur l'étude de ces traits de vie offrent la possibilité d'identifier les mécanismes sous-jacents responsables du lien entre environnement, biodiversité, et fonctionnement des écosystèmes (Fig. 1)[4,5,6,7], et tiennent compte des interactions biotiques –encore largement négligées bien que déterminantes[8]- ainsi que des propriétés biologiques des espèces, et leurs différences[7]. Les premières études basées sur l'utilisation de traits remontent aux années 1930[9], en 1978 pour le phytoplancton[10]. Qualitatives, elles ne permettaient néanmoins pas de s'appuyer sur des relations établies pour anticiper la réponse des espèces aux possibles changements de leur environnement. A partir de la fin des années 1990[11], le regain d'intérêt pour ces approches

---

[1]IPBES, "Global assessment report on biodiversity and ecosystem services of the Intergovernmental Science-Policy Platform on Biodiversity and Ecosystem Services" dans E. S. Brondizio, J. Settele, S. Díaz, H. T. Ngo (ed), Bonn, 2019.

[2]Naeem Shahid, Duffy J Emmett, Zavaleta Erika, "The functions of biological diversity in an age of extinction", *Science*, 336:1401-6, 2012.

[3]Cardinale, B., Duffy, J., Gonzalez, A., Hooper, David U., Perrings, Charles, Venail, Patrick, Narwani, Anita, Mace, Georgina, M., Tilman, David, Wardle, David A., Kinzig, Ann P., Daily, Gretchen C., Loreau, Michel, Grace, James B., Larigauderie, Anne, Srivastava, Diane S., Naeem, Shahid, "Biodiversity loss and its impact on humanity", *Nature,* 486: 59–67, 2012.

[4]McGill, B. J., Enquist, B. J., Weiher, E., Westoby, M., "Rebuilding community ecology from functional traits", *Trends in Ecology & Evolution*, 21: 178–185, 2006.

[5]Cadotte, M. W., Carscadden K., Mirotchnick, N., "Beyond species: functional diversity and the maintenance of ecological processes and services", *Journal of Applied Ecology*, 48: 1079−1087, 2011.

[6]Cernansky, R., "The biodiversity revolution", *Nature*, 546: 22–24, 2017.

[7]Violle, C., Navas, M. L., Vile, D., Kazakou, E., Fortunel, C., HummelI, Garnier, E., "Let the concept of trait be functional!", *Oikos*, 116: 882−892, 2007.

[8]Van der Putten, W., Macel, Mirka, Visser, Marcel E., "Predicting species distribution and abundance responses to climate change: why it is essential to include biotic interactions across trophic levels.", *Philosophical Transactions of the Royal Society B,* 365: 2025– 2034, 2010.

[9] Raunkiær, C, "Life forms of plants and statistical plant geography", Oxford, Oxford University Press, 1934.

[10]Margalef, R., "Life forms of phytoplankton as survival alternatives in an unstable environment", Oceanologia Acta 1: 493–509, 1978.

[11]Tilman, D., Knops, J., Wedin, D., Reich, P., Ritchie, M., Siemann, E., "The influence of functional diversity and composition on ecosystem processes", *Science*, 277: 1300-1302, 1997.

résulte à la fois de l'urgence de mieux appréhender les impacts des changements globaux, mais également des avancées technologiques et statistiques permettant d'analyser un grand nombre de données de différentes natures (numérique, ordinal, binaire, nominal), et de développer des indices quantitatifs prédictifs[4,12,13]. Les approches fonctionnelles actuelles offrent l'opportunité d'établir des règles générales en écologie et d'établir des prédictions, quel que soit l'écosystème et sa composition taxonomique[4]. A terme, les approches basées sur les traits ont pour objectif de devenir des outils d'aide à la décision pour la gestion et la conservation des écosystèmes[14].

En écologie marine, ces approches ont majoritairement été appliquées aux communautés macro-benthiques et piscicoles[15]. La biodiversité « invisible », en particulier celle du plancton, compartiment essentiel du réseau trophique marin, n'est étudiée que de manière très récente[16,17]. Les priorités actuelles sont de (i) construire/compiler des bases de données de traits planctoniques[18,19,20,21,22,23], (ii) mieux comprendre les contraintes/compromis physiologiques ou évolutifs[24] à travers l'étude des syndromes (i.e., ensemble de traits corrélés entre eux), et (iii) tester les différentes théories écologiques connues pour mieux appréhender la complexité du vivant[22,23].

---

[12]Webb, C. T., Hoeting, J. A., Ames, G. M., Pyne, M.I., LeRoy, Poff N., "A structured and dynamic framework to advance traits-based theory and prediction in ecology", Ecology Letters, 13:267-83, 2010.
[13]Mouillot, D., Graham, N. A. J., Villeger, S., Mason, N. W. H., Bellwood,D. R., "A functional approach reveals community responses to disturbances", *Trends in Ecology & Evolution*, 28: 167–177, 2013.
[14]Laughlin, D. C., "Applying trait-based models to achieve functional targets for theory-driven ecological restoration", *Ecology Letters*, 17:771–784, 2014.
[15]Beauchard, O., Veríssimo, H., Queirós, A.M., Herman, P.M.J., "The use of multiple biological traits in marine community ecology and its potential in ecological indicator development", *Ecological Indicators*, 768: 1-96, 2017.
[16]Edwards, Kyle F., Litchman, Elena, Klausmeier, Christopher A., "Functional traits explain phytoplankton community structure and seasonal dynamics in a marine ecosystem", Ecology Letters, 16: 56–63, 2013.
[17]Pomerleau, Corinne, Sastri, Akash R., Beisner, Beatrix E., "Evaluation of functional trait diversity for marine zooplankton communities in the Northeast subarctic Pacific Ocean", *Journal of Plankton Research*, 37: 712–726, 2015.
[18]Litchman E, Klausmeier CA, "Trait-based community ecology of phytoplankton", *Annual Review in Ecology, Evolution and Systematics*, 39:615−639, 2008.
[19]Litchman, E., Ohman, Mark D., Kiørboe, T., "Trait-based approaches to zooplankton communities", *Journal of Plankton Research,* 35: 473–484, 2013.
[20]Benedetti F, Gasparini S, Ayata SD, "Identifying copepod functional groups from species functional traits.", Journal of Plankton Research, 38: 159-166, 2016.
[21]Benedetti, F., Wydler, J., Vogt, M., "Copepod functional traits and groups show divergent biogeographies in the global ocean". *Journal of Biogeography*, 00: 1– 15, 2022.
[22]Breton, Elsa, Christaki, Urania, Sautour, Benoit., Demonio, Oscar, Skouroliakou, Dimitra-Ioli, Beaugrand, Gregory, Seuront, Laurent, Kléparski, Loick, Poquet, Adrien, Nowaczyk, Antoine, Crouvoisier, Muriel, Ferreira, Sohpie, Pecqueur, David, Salmeron, Christophe, Brylinski, Jean-Michel, Lheureux, Arnaud, Goberville, Eric, «Seasonal Variations in the Biodiversity, Ecological Strategy, and Specialization of Diatoms and Copepods in a Coastal System With Phaeocystis Blooms: The Key Role of Trait Trade-Offs», *Frontiers in Marine Science*, 8, 1178, 2021.
[23]Breton, Elsa, Goberville, Eric, Sautour, Benoit, Ouadi, Anis, Skouroliakou, Dimitra-Ioli, Seuront, Laurent, Beaugrand, Grégory, Kléparski, Loick, Crouvoisier, Muriel, Pecqueur, David, Salmeron, Christophe, Cauvin, Arnaud, Poquet, Adrien, Garcia, Nicole, Gohin, Francis, Christaki, Urania, «Multiple phytoplankton community responses to environmental change in a temperate coastal system: A trait-based approach», Frontiers in Marine Science, fmars.2022.914475, 2022.
[24] Edwards K.F., Klausmeier C.A., Litcham E., "Evidence for a three-way trade-off between nitrogen and phosphorus competitive abilities and cell size in phytoplankton", *Ecology*, 92:2085–2095, 2011.

L'existence récente des approches quantitatives basées sur l'utilisation des traits de vie, et l'évolution rapide des méthodologies de traitement de l'information au cours de la dernière décennie sont souvent à l'origine de confusions et d'erreurs. Nous rappelons dans ce chapitre les principes à adopter et les erreurs classiques à éviter lorsqu'une approche fonctionnelle est adoptée. Dans ce chapitre, nous montrons leurs intérêts pour comprendre comment les espèces s'assemblent, répondent aux changements environnementaux et influent sur les processus écosystémiques. Afin d'étayer notre propos, nous nous appuyons sur des résultats obtenus au cours de ces trois dernières années[22,23,25,26], notamment par l'analyse des séries phytoplanctoniques et zooplanctoniques du point « Wimereux C » (au large du Portel, Manche orientale) des Services Nationaux d'Observation SOMLIT et PHYTOBS.

Quels traits planctoniques ?

L'évaluation de la pertinence/performance de traits chez le plancton marin pour comprendre la réponse des communautés planctoniques aux changements environnementaux, et leurs effets sur le fonctionnement des écosystèmes, est un volet de recherche actuel très actif[18,19,20,21,22,23]. Il s'agit d'identifier des traits fonctionnels, c'est-à-dire des traits qui influencent la performance (croissance, survie, reproduction, …) de l'organisme (**traits « réponse »**), un processus écosystémique (**traits « effet »**), ou les deux[7]. **Un trait fonctionnel est donc uniquement un trait qui covarie avec l'environnement et/ou un processus écosystémique. En d'autres termes, un trait neutre n'est donc pas fonctionnel, contrairement à ce qu'on peut lire dans certains travaux.** Les traits fonctionnels peuvent être identifiés par expertise. Par exemple, la taille des organismes est un « trait maître » car elle influence toutes les fonctions vitales : la reproduction, l'alimentation, la croissance, et la survie[18,19]. Ils peuvent également être caractérisé en recherchant, à l'échelle des communautés, des relations significatives entre traits et environnement et/ou processus écosystémiques[22,23]. Un gradient environnemental doit alors être clairement défini.

Contrairement à ce qu'il est parfois mentionné, **les traits ne peuvent être construits à partir de variables externes à l'organisme**[7] (e.g., environnement abiotique) : si l'information n'est pas inscrite dans le génome, il ne s'agit pas d'un trait[6]. Les préférences écologiques/physiologiques (e.g., largeur de niche ; tolérance au changement de salinité), la distribution verticale dans la colonne d'eau (i.e., épi-, méso-, bathypélagique), l'habitat (i.e., pélagique/benthique/tychopélagique pour les organismes planctoniques), la phénologie des espèces (e.g., démarrage saisonnier des efflorescences phytoplanctoniques) ne sont pas des traits *sensus stricto*. Ces informations restent néanmoins précieuses pour aider à comprendre la complexité du vivant et l'évolution d'un trait le long d'un gradient environnemental[22,23].

A titre d'exemple, la performance des traits « degré apparent de silicification »[22] et « degré de protection contre la prédation »[22] pour les organismes phytoplanctoniques, utilisés comme « trait réponse » et « trait effet », respectivement, est montrée sur la figure 2. L'hypothèse de départ est que le degré apparent de silicification des communautés phytoplanctoniques en zone côtière varie le long d'un gradient de silicates, salinité, et/ou de forçage venteux, car (i) une

[25]Breton, E., Christaki, U., Bonato, S., Didry, M., Artigas, L.F., "Functional trait variation and nitrogen use efficiency in temperate coastal phytoplankton", *Marine Ecological Progress Series*, 563: 35–49, 2017.

[26]Chihoub, S., Christaki, U., Chelgham, S., Amara, R., Ramdane, Z., Zebboudj, A., Rachik, S., Breton, E., "Coastal eutrophication as a potential driver of functional homogenization of copepod species assemblages in the Mediterranean Sea", *Ecological Indicators*, 115:106388, 2020.

espèce qui a un besoin en silice relativement faible est généralement moins silicifiée[27], (ii) les espèces fortement silicifiées sont généralement présentes dans un milieu riche en silicates[28], et (iii) les espèces ayant une paroi cellulaire rigide (i.e., fortement silicifiée) ont une chance de survie aux chocs halins plus importante[29,30,31]. En zone côtière, les chocs halins peuvent survenir lors de coups de vent qui favorisent les interactions fleuve-mer. Pour le « degré de protection contre la prédation », l'hypothèse est que la production primaire dépend, en partie, du degré de protection des espèces contre la prédation (régulation « top-down »). La figure 2A-E,G montre que ces deux postulats sont vérifiés. Le « degré apparent de silicification » des communautés phytoplanctoniques (« trait réponse », Fig. 2A,D) varie en fonction du vent (Fig.2 B,E), des concentrations en silicates de l'eau de mer (Fig. 2C), et de l'influence des apports fluviaux à la côte (Fig. 2A). La production primaire (en suivant la biomasse carbonée [µg C/L^{-1}] comme indicateur) varie en fonction du degré de protection du phytoplancton contre la prédation (« trait effet ») (Fig. 2G). Cette relation trait-environnement est confortée par les covariations entre le degré de généralisme/tolérance de la communauté phytoplanctonique et le degré apparent de silicification (Fig. 2F). En effet, les coups de vent augmentent la variabilité des conditions environnementales : seules les espèces tolérantes à des changements brusques en salinité, en sels nutritifs, et en lumière peuvent s'adapter.

Etant donné la grande richesse du plancton, il est fortement recommandé d'utiliser des traits faciles et rapides à quantifier. La liste non exhaustive (Figure 3) de traits communément utilisés pour caractériser le spectre fonctionnel des copépodes[19] - groupe zooplanctonique dominant- résume les différents aspects de l'écologie des copépodes qui sont considérés : alimentation, stratégies trophiques, taille, compétitivité, croissance, reproduction, et survie à la prédation ou au manque de nourriture. La présence de sacs ovigères informe sur la capacité de reproduction chez les copépodes : lorsque présents, les espèces ont un taux de fécondité relativement faible et une éclosion plus tardive[20,21]. La présence de myéline sur les antennes renseigne sur la capacité de l'organisme/espèce à survivre à la prédation (en augmentant la capacité à s'échapper) et au manque temporaire de nourriture (réserve lipidique)[20,21]. Enfin, la stratégie alimentaire atteste de la vulnérabilité à la prédation : les espèces suspensivores et celles qui se nourrissent en se déplaçant (« en mode croisière ») sont les plus vulnérables du fait des ondes engendrées par la filtration et/ou le déplacement[20,21].

Beaucoup de traits planctoniques restent à découvrir et/ou à mesurer. Par exemple, dans le cas du phytoplancton, les traits comme substituts des besoins en lumière et/ou de l'acquisition de l'énergie lumineuse manquent cruellement. La composition pigmentaire permet de discriminer uniquement les grands groupes phytoplanctoniques, mais la mesure de traits physiologiques à l'échelle de l'espèce (ex : capacité à croître sous une lumière faible, tolérance aux fortes lumières) demande un travail en laboratoire conséquent vu le grand nombre d'espèces existantes. La pertinence de la densité cellulaire en chloroplastes comme indicateur de la capacité photosynthétique et/ou le risque de photo-inhibition aux fortes lumières est en cours

[27] Leynaert, A., Bucciarelli, E., Claquin, P., Dugdale, R.C., Martin-Jézéquel, V., Pondaven, P., Ragueneau, O., "Effect of iron deficiency on diatom cell size and silicic acid uptake kinetics", *Limnology & Oceanography*, 49 :1134–1143, 2004.

[28]Martin-Jézéquel, V., Lopez, P.J., « Silicon – a central metabolite for diatom growth and morphogenesis". *Progress in molecular and subcellular biology*, 33:99–124, 2003.

[29]Logares, R., Bråte, J., Bertilsson, S., Clasen, J.L., Shalchian-Tabrizi, K., Rengefors, K., "Infrequent marine–freshwater transitions in the microbial world", *Trends in Microbiology,* 17:414–422, 2009.

[30]Hoef-Emden, K., "Osmotolerance in the Cryptophyceae: jacks-of-all-trades in the Chroomonas clade", *Protist*, 165:123–143. 2014.

[31]Suescún-Bolívar, L.P., Thomé, P.E., "Osmosensing and osmoregulation in unicellular eukaryotes", *World Journal of Microbiol. Biotechnology*, 313:435-43, 2015.

de test (com. pers.). Les résultats sur la recherche d'une relation générale entre le taux de croissance maximal potentiel du plancton et leur teneur structurale en phosphore (rapports C:P et N:P)[32,33,34] sont prometteurs, et devraient être poursuivis et élargis à d'autres espèces. Ces travaux s'appuient sur l'hypothèse du taux de croissance[32] qui mentionne que les espèces ayant une croissance maximale potentielle rapide auraient également une forte demande en ARN ribosomal riche en phosphore, mais une faible biomasse spécifique du fait de leur incapacité à faire des réserves : une espèce ayant des rapports stœchiométriques C:P et N:P élevés devraient avoir une croissance potentielle maximale faible, mais une grande capacité à faire des réserves et de la biomasse. L'examen de la performance de la structure de la lame masticatrice des mandibules chez les copépodes comme substitut du régime alimentaire[35] mérite également d'être poursuivie[20,21].

L'urgence est néanmoins de compléter les bases de données des traits les plus communément utilisés (cf. Figure 3) par des mesures pour les groupes zooplanctoniques souvent négligés, tels que les copépodes harpacticoïdes et cyclopoides[26], et pour la plupart des organismes gélatineux. Le plus grand défi actuel reste la quantification des traits à l'échelle individuelle, étape nécessaire pour une compréhension complète de la structuration des communautés en réponse aux changements environnementaux et de leur influence sur les processus écosystémiques. En ce sens, les nouvelles technologies d'acquisition d'image à haute fréquence[36,37,38] sont prometteuses[39], tout comme les approches de séquençage à haut débit et multi-omiques[40].

Traits fonctionnels et règles d'assemblage des communautés

Pour mieux appréhender la complexité des mécanismes de coexistence[18,19], les écologues s'appuient sur diverses théories écologiques qui ont, pour beaucoup, fait leurs preuves lors d'expérimentations en laboratoire. Mais leur évaluation dans le monde « réel » reste rare[22,23]. Deux théories/concepts majeur(e)s sont adopté(e)s pour expliquer la coexistence : la théorie

[32]Elser, James J., Dobberfuhl, Dean R., MacKay, Neil A., Schampel, John H., "Organism Size, Life History, and N:P Stoichiometry: Toward a unified view of cellular and ecosystem processes", *BioScience*, 46, 674–684, 1996,

[33]Elser, JJ, Acharya, K, Kyle, M, Cotner, J, Makino, W, Markow, T, Watts, T, Hobbie, S, Fagan, W, Schade, J., Hood, J, Sterner, R. W, "Growth rate–stoichiometry couplings in diverse biota", *Ecology Letters, 6: 936– 943, 2003.*

[34]Rees, T.A.V., Raven, J.A., "The maximum growth rate hypothesis is correct for eukaryotic photosynthetic organisms, but not cyanobacteria", *The New Phytologist*, 230: 601-611, 2021.

[35]Lapernat, Pascale-Emmanuelle, Razouls, Claude, "Functional analysis of the mandible in deep pelagic copepods from the Mediterranea (Malte)", *Vie et Milieu*, 52:17-30, 2002.

[36]Gorsky, G., Ohman, M. D. Picheral, M., Gasparini, S., Stemmann, L., Romagnan, J-B, Cawood, A, Pesant, S., Garcia-Comas, C., Prejger. F., "Digital zooplankton image analysis using the ZooScan integrated system", *Journal of Plankton Research*, 32: 285–303. 2010.

[37]Dubelaar, G.B.J., Gerritzen, P.L., "CytoBuoy: A Step Forward Towards Using Flow Cytometry in Operational Oceanography", *Scientia Marina,* 64(2), 2000.

[38]Sieracki CK, Sieracki ME, Yentsch CS, "An imagingin-flow system for automated analysis of marine microplankton", *Marine Ecology Progress Series*, 168: 285−296, 1998.

[39]Vilgrain, L., Maps, F., Picheral, M., Babin, M., Aubry, C., Irisson, J.-O., Ayata, S.-D., "Trait-based approach using in situ copepod images reveals contrasting ecological patterns across an Arctic ice melt zone", *Limnology and Oceanography,* 66: 1155-1167, 2021.

[40] McDaniel, E.A., van Steenbrugge, J.J.M., Noguera, D.R. et al, "TbasCO: trait-based comparative 'omics identifies ecosystem-level and niche-differentiating adaptations of an engineered microbiome", ISME Communication, 2, 111, 2022.

« habitat templets »[41] (Figure 4A-B) et le concept de « compromis physiologiques »[23,42] (Figure 5A-B). Traduire ces théories/concepts en indicateurs quantitatifs calculés à partir de valeurs de traits fonctionnels offre la possibilité d'identifier les mécanismes sous-jacents de l'assemblage des communautés. Néanmoins, le manque de connaissances sur les variations de traits entre individus d'une même espèce contraint, dans la plupart des cas, à travailler à l'échelle de l'espèce, empêchant de discriminer de manière robuste les règles d'assemblages des communautés. Beaucoup d'espoir est placé dans les nouvelles technologies telles que le Zooscan©[36], le CytoBuoy©[37], ou le Flowcam©[38], ainsi que dans les technologies multi-omiques[40].

La théorie « habitat templets » (Figure 4A), qui s'appuie sur le concept de différenciation des niches écologiques, stipule qu'une communauté écologique, à un temps et un endroit donné, est composée d'espèces issues d'un pool régional façonné par des processus évolutifs et qui ont passé des filtres écologiques successifs en lien avec les contraintes géographiques (capacité à se disperser), abiotiques/physiologiques (tolérance aux conditions climatiques, ressources, habitat, …) et biotiques (survie à la compétition, prédation, …)[40]. L'hypothèse est que plus les conditions de vie sont extrêmes (contraintes fortes) plus le tri des espèces est élevé et, par conséquent, plus le tri de traits (ou les valeurs de traits) est fort : une communauté fortement filtrée conduit à une sous-dispersion des valeurs de traits. L'acquisition d'une meilleure connaissance des règles d'assemblage des communautés, comme la découverte de la compétition asymétrique[43] (ou compétition hiérarchique) et de l'ubiquité des relations de facilitation[44], a néanmoins permis d'élargir la compréhension des mécanismes de coexistence. La compétition asymétrique considère que les espèces utilisent les mêmes ressources, mais certaines sont plus compétitives que d'autres. Une communauté dont les traits sont sous-dispersés traduit ainsi plusieurs mécanismes de coexistence : le filtrage abiotique, la compétition asymétrique, ou encore le mutualisme. Par conséquent, les mécanismes de coexistence ne peuvent être identifiés uniquement de cette manière et la connaissance de l'écosystème (ex. conditions environnementales), de la productivité, et de la richesse des communautés est indispensable pour discriminer les différentes règles d'assemblage[22,23]. De multiples indices, regroupés sous le terme de « diversité fonctionnelle », ont été élaborés pour caractériser et identifier les mécanismes d'assemblages au travers de la quantification de richesse, équitabilité, dispersion, et divergence fonctionnelle. En pratique, seuls les traits variant le long de gradients environnementaux- les traits réponses- peuvent être considérés pour tester si, et comment, les communautés écologiques diffèrent de communautés aléatoires, i.e., constituées en l'absence de mécanisme particulier[45]. La divergence fonctionnelle, exprimée sous la forme de l'entropie quadratique de Rao (RaoQ), est considérée comme l'indice le plus robuste et le plus consistent[46] (cf. encadré).

---

[41]Southwood, T.R.E., "Tactics, strategies, and templets", *Oikos*, 52:3-18, 1988.

[42]Litchman, E., Klausmeier, C.A., Schofield, O.M., Falkowski, P.G., "The role of functional traits and trade-offs in structuring phytoplankton communities: scaling from cellular to ecosystem level", *Ecology Letters*, 10:1170−1181, 2007.

[43]Mayfield, M.M., Levine, J.M., "Opposing effects of competitive exclusion on the phylogenetic structure of communities". *Ecology. Letters*, 13:1085−1093, 2010.

[44]McIntire, E.J.B. and Fajardo, "A. Facilitation as a ubiquitous driver of biodiversity", *New Phytologist*, 201: 403-416., 2014,

[45]Weiher, Evan, Keddy, Paul A., "Ecological assembly rules: perspectives, advances, retreats", 1999.

[46]Botta-Dukát, Z., Czúcz, B., "Testing the ability of functional diversity indices to detect trait convergence and divergence using individual-based simulation, *Methods in Ecology and Evolution*, 7:114-126, 2016.

SES-RaoQ, bioindicateur robuste des mécanismes de coexistence

Le calcul du bioindicateur SES-RaoQ (« standard effect size of Rao's quadratic entropy » ; entropie quadratique de Rao) nécessite (i) un tableau de traits fonctionnels, (ii) un tableau de biomasses spécifiques de chaque communauté, et (iii) un modèle nul générant aléatoirement des communautés écologiques pour lesquelles la richesse taxonomique est fixée par l'utilisateur, mais pas les valeurs de traits. Les valeurs de RaoQ observée et théorique moyenne (i.e. classiquement d'après 1000 communautés générées au hasard) sont ainsi obtenues, et l'indice SES-RaoQ est calculé à partir de la valeur moyenne et l'écart type des RaoQ observée et théorique[22,23]. Si la valeur de SES-RaoQ est :

- **Supérieure à 1,96** : les traits de la communauté écologique observée sont significativement **dispersés**, suggérant que la communauté écologique s'est constituée soit (i) à partir d'une **compétition basée sur l'utilisation de niches différentes,** soit (i) grâce à des interactions de **facilitation asymétrique** ; une espèce favorise une autre, mais l'inverse n'est pas vrai ;
- **Comprise entre -1,96 et 1,96** : la communauté est le résultat soit (i) de mécanismes purement **aléatoires** (e.g., la dispersion), soit (ii) d'un **mélange de mécanismes antagonistes** ; un mécanisme favorise la sur-dispersion de traits, un autre mécanisme favorise leur sous-dispersion ;
- **Inférieure à -1,96** : les traits composant la communauté sont **sous-dispersés**, suggérant que la communauté écologique s'est constituée à la suite soit (i) d'un **filtrage abiotique** (stress environnemental, manque de ressources, …), soit (ii) **d'interactions mutualistes**, soit (iii) **d'interactions de compétition hiérarchique**.

Les traits fonctionnels de la communauté phytoplanctonique en zone côtière de la Côte d'Opale ont été systématiquement sous-dispersés au cours des deux dernières décennies (Fig. 4Ba) et donc régulés par (i) l'effet d'un stress abiotique, (ii) compétition hiérarchique, ou (iii) mutualisme. La richesse phytoplanctonique et la productivité (en utilisant la biomasse comme estimateur ; Fig. 2G) ayant augmenté graduellement en parallèle, il est peu probable qu'un stress abiotique ou une compétition hiérarchique soient les mécanismes dominants, ces deux processus favorisant l'exclusion. Nos résultats suggèrent donc que cette sous-dispersion de traits soit consécutives d'un relâchement de la compétition (grâce, en partie, à l'utilisation des ressources à des périodes différentes de l'année[23]), d'une diminution de la croissance phytoplanctonique, et d'un renforcement de protection des espèces contre la prédation en réponse à la baisse des phosphates (Fig. 4Bb). Une telle conclusion est renforcée par le fait qu'une espèce bien équipée contre la prédation (Fig. 2G) présente généralement une croissance lente et une faible compétitivité (compromis compétitivité/prédation et croissance/prédation ; Figure 5A).

Le concept des compromis physiologiques[41] stipule que le développement d'une stratégie chez un organisme ne peut se faire qu'au détriment d'une autre, empêchant alors l'existence d'une « super-espèce » qui éliminerait toutes les autres, car totipotente. Dans le monde réel cela n'existe pas, chaque espèce étant contrainte par le stock d'énergie qu'elle possède : chaque stratégie écologique développée pour s'adapter aux conditions physiologiques, se nourrir, croître en taille, se reproduire, ou survivre à la prédation, a un coût métabolique et va donc se faire au dépend d'autres espèces. Les compromis physiologiques/écologiques bien connus chez le plancton sont listés Figure 5A, mais beaucoup restent à encore à découvrir. Certains sont communs à tous les organismes planctoniques, d'autres sont propres au phytoplancton ou au zooplancton. Cette connaissance sur les compromis physiologiques est indispensable pour décrypter les variations de traits observées et éclaircir les mécanismes d'assemblage des communautés. L'analyse saisonnière de 4 ans de données cytométriques obtenues au large de la Slack (Côte d'Opale ; Figure 5B) ont permis de distinguer les compromis (1) glaneur (*Synechocccus* et pico-eucaryotes ayant une stratégie K) *vs* opportunistes (*Phaeocystis* et diatomées, considérées comme ayant une stratégie r), (2) efficacité de croissance sous lumière faible (aμ) et les besoins en azote (faible rapport cellulaire C/N), et (3) entre compétitivité (rapport S/V) et résistance à la prédation (colonies de *Phaeocystis*). Dans cette étude, les traits ont été définis à l'échelle de chaque groupe phytoplanctonique identifié expérimentalement, et à partir d'une recherche exhaustive de valeurs de traits dans la littérature[25].

Métriques fonctionnelles de bio-indication pour évaluer l'état écologique des zones côtières

Le meilleur indicateur de l'état de santé d'un milieu est celui qui prend en compte les caractéristiques biologiques des communautés qui s'y trouvent. De nombreux indices fonctionnels ont été développés au cours de la dernière décennie dans le but, par exemple, d'alerter sur la dégradation d'un écosystème à la suite de diverses perturbations[13], et/ou d'identifier les habitats/écosystèmes à restaurer ou conserver en priorité[47,48]. Un travail conséquente doit encore être effectué avant de tendre vers des outils opérationnels, notamment en qualifiant leur transférabilité à une grande variété d'écosystèmes/écorégions[48,49]. Quelques exemples de métriques fonctionnelles de bio-indication sont données dans le Tableau I. Un suivi de l'indice CSI-trophique[26,52] - degré de spécialisation trophique d'une communauté – calculé sur des communautés de copépodes méditerranéennes, de l'estuaire de la Gironde, et de la Côte d'Opale a permis de détecter une homogénéisation trophique de ces communautés (baisse du degré de spécialisation des communautés) en réponse à l'eutrophisation (augmentation de la biomasse phytoplanctonique, avec la chlorophylle *a* comme estimateur) de ces eaux côtières et estuariennes. Bien que l'hypothèse soit que ces bioindicateurs -excepté la

[47]Pavoine,Sandrine, Bonsall, Michael B., Dupaix, Amaël, Jacob, Ute, Ricotta, Carlo, « From phylogenetic to functional originality: Guide through indices and new developments", *Ecological Indicators*, 82: 196-205, 2017.

[48]Vandewalle, M., de Bello, F., Bolger, M.P.B.T., Dolédec, S., Dubs, F., Feld, C.K., Harrington, R., Harrison, P.A., Lavorel, S., Silva, P.M., Moretti, M., Niemelä, J., Santos, P., Sattler, T., Sousa, J.P., Sykes, M.T., Vanbergen, A.J., Woodcock, B.A., "Functional traits as indicators of biodiversity response to land use changes across ecosystems and organisms", *Biodiversity and Conservation*, 19: 2921–2947, 2010.

[49]Brandl, S. J., Emslie, M. J., Ceccarelli, D. M. and Richards, Z. T., "Habitat degradation increases functional originality in highly diverse coral reef fish assemblages", *Ecosphere*, 7: e01557, 2016.

vulnérabilité et la redondance fonctionnelles- diminuent à la suite d'une perturbation[13], il est à noter que celle-ci n'est pas toujours vérifiée[50]

Conclusion

Ce chapitre a été écrit dans un but pédagogique afin de démocratiser les approches basées sur l'utilisation des traits de vie, en prenant le plancton comme modèle biologique. Malgré le manque actuel de connaissances sur les traits et la formulation probable de nouveaux concepts, de nouvelles méthodes, et de nouveaux bioindicateurs (notamment à l'échelle individuelle), les approches appliquées à l'échelle spécifiques permettent déjà d'améliorer notre compréhension de la structure et du fonctionnement des écosystèmes, et de comment ceux-ci répondent aux effets des changements environnementaux.

Remerciements

Nous remercions les capitaines et marins successifs du bateau de recherche CNRS « *Sépia II* » : Charly Dollet, Jean-Claude Martin, Grégoire Leignel, Noël Lefiliatre, et Christophe Routtier qui ont aidé aux prélèvements et rendu les conditions optimales pendant ces nombreuses années dans le cadre des programmes SOMLIT et PHYTOBS. Nous remercions également le personnel local du SOMLIT : Nicole Degros, Eric Lecuyer, et Dr. Valérie Gentilhomme, ainsi qu'Emilie Grossteffan de l'IUEM (Plouzané) qui a analysé les sels nutritifs lorsque l'appareil du LOG était en panne. Nous remercions également les réseaux SOMLIT et PHYTOBS qui soutiennent la poursuite du suivi long-terme des écosystèmes du littoral métropolitain incluant les communautés phytoplanctoniques et zooplanctoniques.

[50]Alric, Benjamin, Geffard, Olivier, Chaumot, Arnaud, "Metal bioavailable contamination engages richness decline, species turnover but unchanged functional diversity of stream macroinvertebrates at the scale of a French region", *Environmental Pollution*, 308, 119565, 2022.

[52]Mondy, C.P., Usseglio-Polatera, P., "Using fuzzy-coded traits to elucidate the nonrandom role of anthropogenic stress in the functional homogenisation of invertebrate assemblages », *Freshwater Biology*, 59, 584–600, 2014.

[53]de Bello, F., Lepš, J., Lavorel, S., and Moretti, M. Importance of species abundance for assessment of trait composition: an example based on pollinator communities. Community Ecol. 8: 163– 170, 2007.

[54]Mouillot, D., S. Villéger, V. Parravicini, M. Kulbicki, J. E. Arias-González, M. Bender, P. Chabanet, S. R. Floeter, A. Friedlander, L. Vigliola, and D. R. Bellwood, "Functional over-redundancy and high functional vulnerability in global fish faunas on tropical reefs", *Proceedings of the National Academy of Sciences*, 111:13757–13762, 2014.

Table I. Signification de quelques bio-indicateurs construits avec une métrique fonctionnelle et utilisés pour évaluer l'état de santé d'un écosystème.

Bio-indicateur fonctionnel	Signification
SES-RaoQ	Somme des distances entre paires d'espèces dans l'espace fonctionnel, pondérée par leur biomasse relative[46]
Originalité fonctionnelle	Distance moyenne entre chaque espèce et son plus proche voisin dans l'espace fonctionne[l3]
Spécialisation fonctionnelle	Distance moyenne des espèces par rapport au centre de l'espace fonctionnel[13]
Richesse fonctionnelle	Volume de l'enveloppe convexe de l'espace fonctionnel[50]
Indice de Spécialisation des Communautés	Degré de spécialisation trophique d'une communauté[52]
Redondance fonctionnelle	Différence entre l'indice de Simpson et l'indice de RaoQ[53]
Vulnérabilité fonctionnelle	Proportion d'une entité fonctionnelle d'un assemblage ou d'un groupe fonctionnel n'ayant qu'une seule espèce[54]

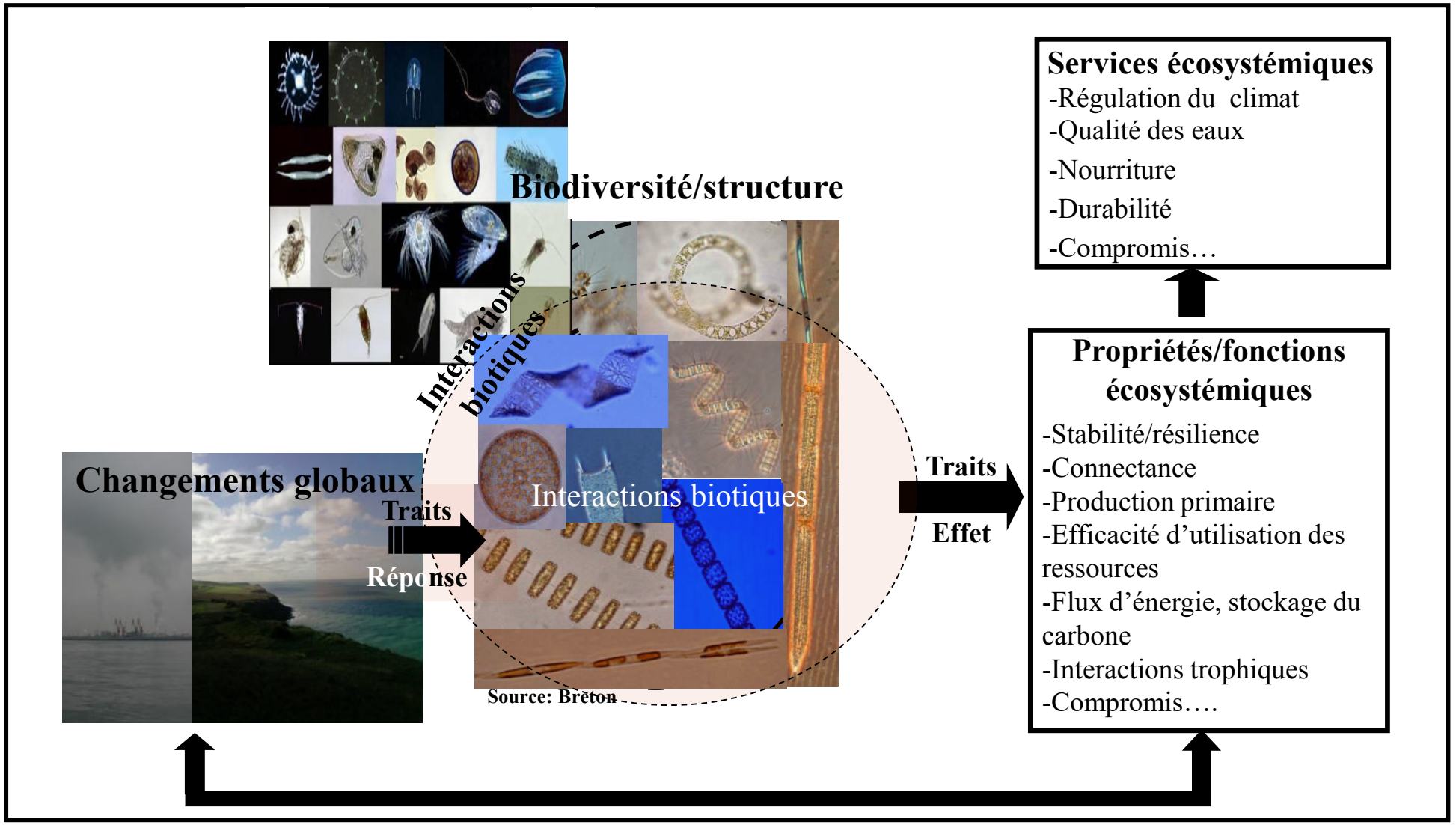

Figure 1. Relation entre les changements globaux, la biodiversité, et le fonctionnement des écosystèmes marins et les services écosystémiques associés. Les communautés écologiques répondent aux perturbations environnementales et climatiques via les traits réponses, et contrôlent les processus écosystémiques via les traits effets. Un trait réponse peut être aussi un trait effet: dans ce cas on peut directement prédire le fonctionnement des écosystèmes à partir de conditions environnementales données.

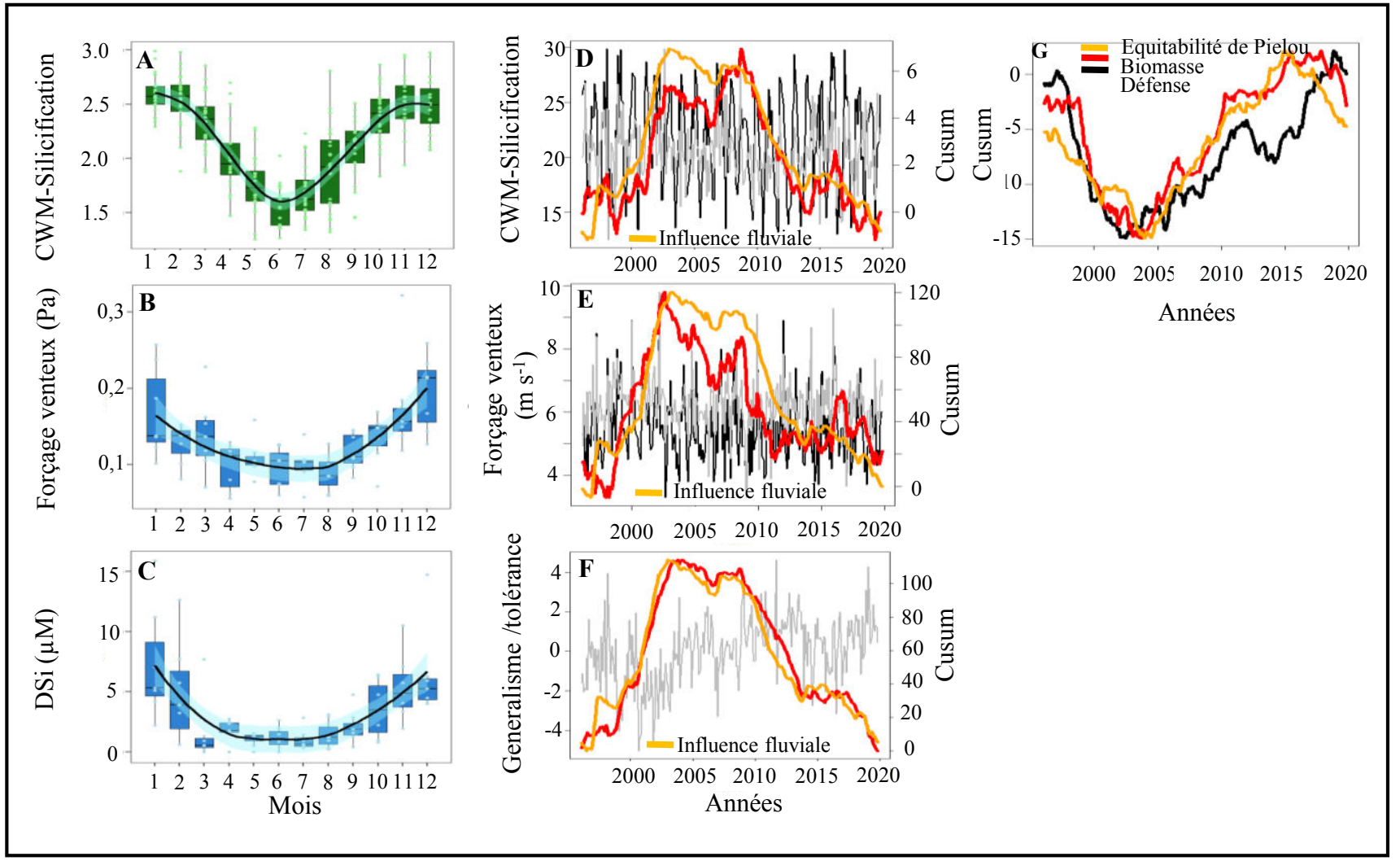

Figure 2. « Trait réponse » *vs* « trait effet ». (A-F) Pertinence du trait « degré apparent de silicification » chez le phytoplancton comme « trait réponse » à l'échelle de la saison (A-C) et sur le long terme (D-F) au point « Wimereux C » (au large du Portel, Manche orientale) des Service Nationaux d'Observation SOMLIT/PHYTOBS, et G: pertinence du trait défense comme « trait effet » sur la production primaire sur le long terme. A: Variations saisonnières de l'identité fonctionnelle (CWM-Silicification) des communautés de diatomées en fonction de (B) le forçage venteux (Pa) et (C) la concentration en silicates de l'eau de mer (DSi, µM); (D): Degré apparent de silicification (CWM-silicification, ligne rouge) en fonction des apports fluviaux à la côte (ligne orange) et (E) le forçage venteux (ligne rouge) survenus ces deux dernières décennies en zone côtière de la Côte d'Opale. F: Les espèces fortement silicifiées sont généralistes et tolérantes aux variations environnementales; CWM: Community Weighed Mean. La méthodologie est décrite dans Breton et al. 2021, 2022.

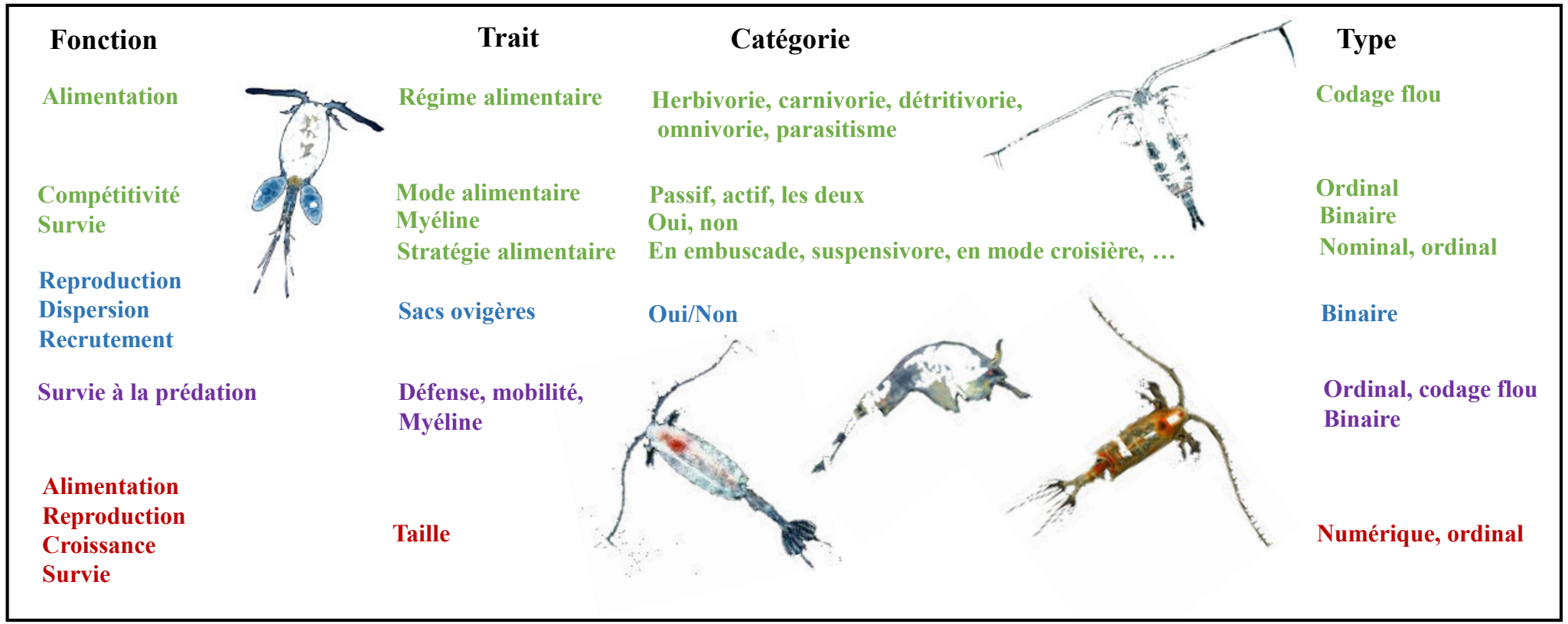

Figure 3. Liste non exhaustive de traits permettant de capturer le spectre fonctionnel des copépodes. D'après Litchman et al. 2013, Benedetti et al. 2016, 2022, et Breton et al. 2021. Les espèces portant leurs oeufs (présence de sacs ovigères) possèdent un taux de fécondité relativement faible et un temps d'éclosion plus long que ceux n'en possédant pas (Kiørboe & Sabatini, 1994). La présence de myéline sur la première antenne nous informe sur la capacité de l'organisme/espèce à survivre à la prédation (capacité à s'échapper) et au manque temporaire de nourriture (réserve lipidique). La stratégie alimentaire nous informe sur la vulnérabilité vis-à-vis de la prédation, les espèces suspensivores et en mode croisière étant les plus vulnérables.

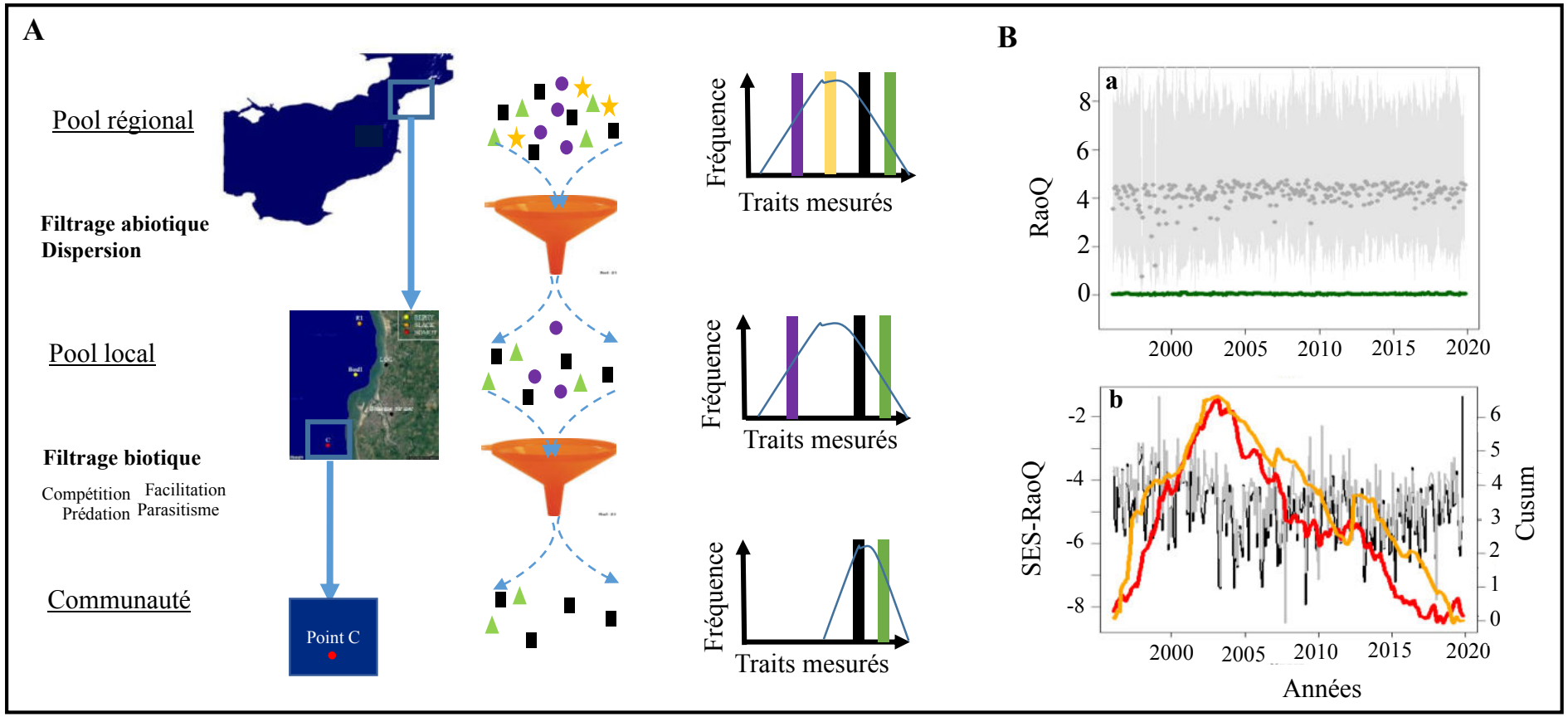

Figure 4. Règles d'assemblage des communautés (A) théorie « Habitat templets », Southwood, 1988). Toute communauté écologique à un temps et un endroit donnés est composée d'espèces issues d'un pool régional façonné par des processus évolutifs, et qui ont réussi à passer trois filtres successifs: la distance (capable de se disperser), les contraintes abiotiques/physiologiques (capables de tolérer les conditions climatiques, ressources, habitat ..) et biotiques (capables de survivre à la compétition, la prédation, …). Ba,b: d'après Breton et al. 2022.

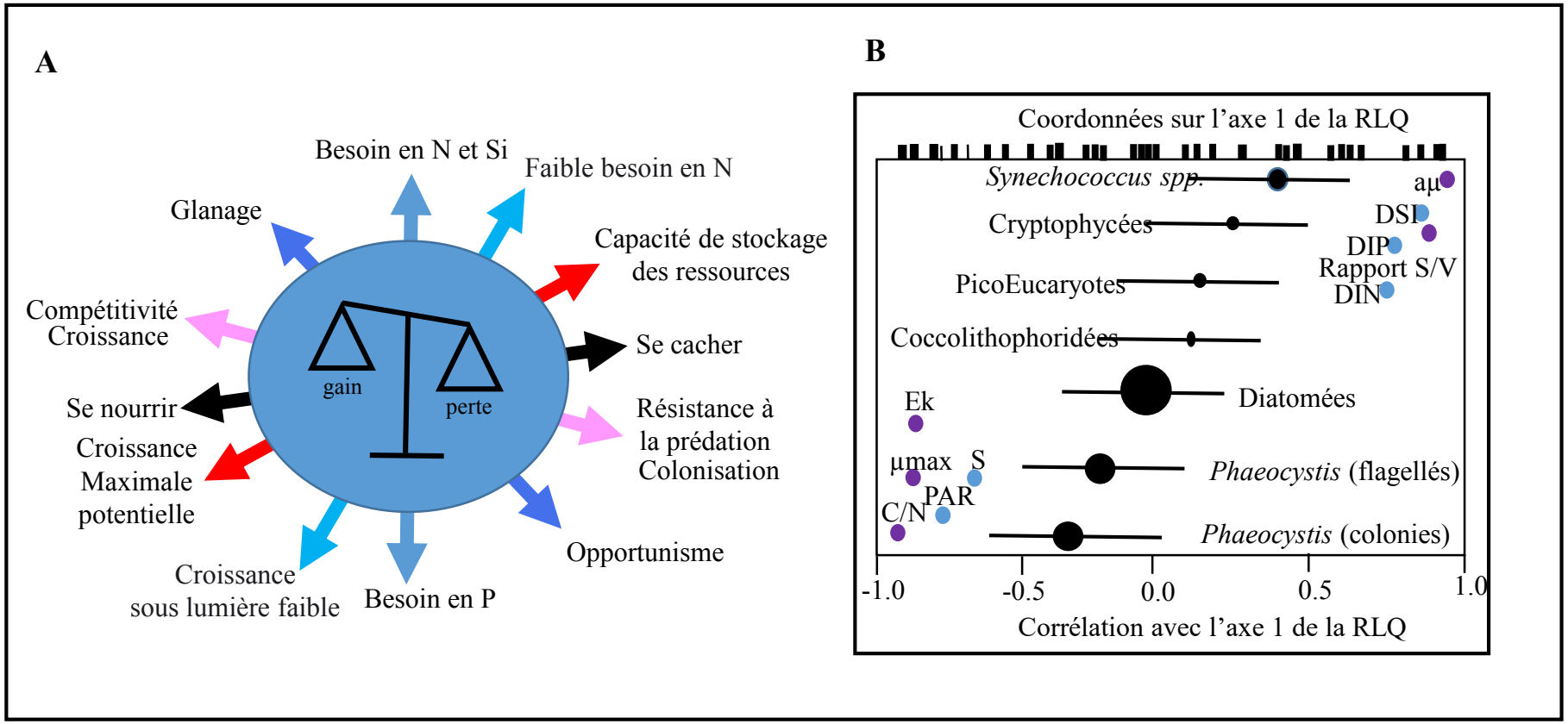

Figure 5. Règles d'assemblage des communautés écologiques: compromis physiologiques et évolutifs chez le plancton. A: compromis physiologiques connus chez le plancton. Flèche noire: uniquement chez le zooplancton; flèche rouge et rose: chez le phytoplancton et zooplancton; autres flèches: uniquement chez le phytoplancton. B: étude de cas chez le phytoplancton dans les eaux côtières de la Manche orientale (d'après Breton et al. 2017): (1) compromis glaneur (*Synechocccus* et picoeucaryotes ayant une stratégie K) *vs* opportunistes (*Phaeocystis* et diatomées, considérées ayant une stratégie r); (2) compromis entre l'efficacité de croissance sous lumière faible (aμ) et les besoins en azote (faible rapport cellulaire C/N); (3) compromis entre la compétitivité (rapport S/V) et la résistance à la predation (colonies de *Phaeocystis*).

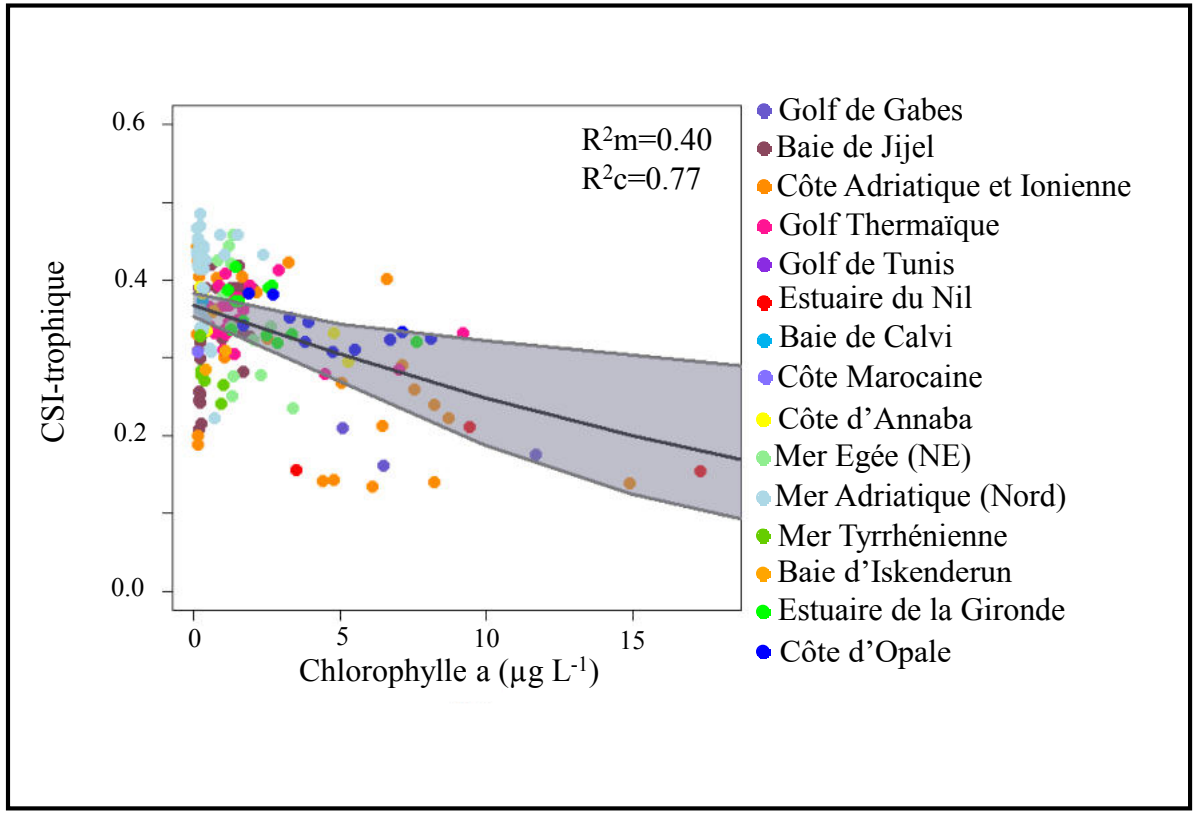

Figure 6: Exemple de bio-indicateur (CSI-trophique) utilisant une métrique fonctionnelle et révélant une homogénéisation trophique des communautés de copépodes (i.e., baisse du degré de spécialisation des communautés) en réponse à l'eutrophisation (i.e., augmentation de la biomasse phytoplanctonique avec la chlorophyll a comme proxy) des eaux côtières (Méditerranée occidentale et orientale, estuaire de la Gironde, et Côte d'Opale; N=176, R^2m=0,40; R^2c=0,77). R^2m et R^2c: coefficient de détermination du modèle et conditionnelle). D'après Chihoub et al. 2020.

References

Adler, P.B., HilleRisLambers, J., and Levine, J.M. (2007) A niche for neutrality. Ecology Letters 10: 95–104.

Aguilar, P. and Sommaruga, R. (2020) The balance between deterministic and stochastic processes in structuring lake bacterioplankton community over time. Molecular Ecology 29: 3117–3130.

Alderkamp, A.-C., Sintes, E., and Herndl, G. (2006) Abundance and activity of major groups of prokaryotic plankton in the coastal North Sea during spring and summer. Aquatic Microbial Ecology - AQUAT MICROB ECOL 45: 237–246.

Alvain, S., Moulin, C., Dandonneau, Y., and Bréon, F.M. (2005) Remote sensing of phytoplankton groups in case 1 waters from global SeaWiFS imagery. Deep Sea Research Part I: Oceanographic Research Papers 52: 1989–2004.

Alves-de-Souza, C., Pecqueur, D., Floc'h, E.L., Mas, S., Roques, C., Mostajir, B., et al. (2015) Significance of Plankton Community Structure and Nutrient Availability for the Control of Dinoflagellate Blooms by Parasites: A Modeling Approach. PLOS ONE 10: e0127623.

Alves-de-Souza, C., Varela, D., Iriarte, J., González, H., and Guillou, L. (2012) Infection dynamics of Amoebophryidae parasitoids on harmful dinoflagellates in a southern Chilean fjord dominated by diatoms. Aquat Microb Ecol 66: 183–197.

Amann, R I, Binder, B.J., Olson, R.J., Chisholm, S.W., Devereux, R., and Stahl, D.A. (1990) Combination of 16S rRNA-targeted oligonucleotide probes with flow cytometry for analyzing mixed microbial populations. Applied and Environmental Microbiology 56: 1919–1925.

Amann, R. I., Krumholz, L., and Stahl, D.A. (1990) Fluorescent-oligonucleotide probing of whole cells for determinative, phylogenetic, and environmental studies in microbiology. J Bacteriol 172: 762–770.

Amin, S.A., Hmelo, L.R., van Tol, H.M., Durham, B.P., Carlson, L.T., Heal, K.R., et al. (2015) Interaction and signalling between a cosmopolitan phytoplankton and associated bacteria. Nature 522: 98–101.

Amin, S.A., Parker, M.S., and Armbrust, E.V. (2012) Interactions between Diatoms and Bacteria. Microbiology and Molecular Biology Reviews 76: 667–684.

Aminot, A. and Kérouel, R. (2004) Dissolved organic carbon, nitrogen and phosphorus in the N-E Atlantic and the N-W Mediterranean with particular reference to non-refractory fractions and degradation. Deep Sea Research Part I: Oceanographic Research Papers 51: 1975–1999.

Andersen, K.S., Kirkegaard, R.H., Karst, Soeren M., and Albertsen, M. (2018) ampvis2: an R package to analyse and visualise 16S rRNA amplicon data. bioRxiv.

Andersen, K.S., Kirkegaard, R.H., Karst, Søren M., and Albertsen, M. (2018) ampvis2: an R package to analyse and visualise 16S rRNA amplicon data. 299537.

Anderson, D.M., Glibert, P.M., and Burkholder, J.M. (2002) Harmful algal blooms and eutrophication: Nutrient sources, composition, and consequences. *Estuaries* **25**: 704–726.

Anderson, S.R. and Harvey, E.L. (2020) Temporal Variability and Ecological Interactions of Parasitic Marine Syndiniales in Coastal Protist Communities. mSphere 5: e00209-20.

Arandia-Gorostidi, N., Krabberød, A.K., Logares, R., Deutschmann, I.M., Scharek, R., Morán, X.A.G., et al. (2022) Novel Interactions Between Phytoplankton and Bacteria Shape Microbial Seasonal Dynamics in Coastal Ocean Waters. Front Mar Sci 9: 901201.

Armbrust, E.V. (2009) The life of diatoms in the world's oceans. Nature 459: 185–192.

Azam, F., Fenchel, T., Field, J.G., Gray, J.S., Meyer-Reil, L.A., and Thingstad, F. (1983) The Ecological Role of Water-Column Microbes in the Sea. Marine Ecology Progress Series 10: 257–263.

Azam, F. and Malfatti, F. (2007) Microbial structuring of marine ecosystems. Nat Rev Microbiol 5: 782–791.

Bachy, C., Dolan, J.R., López-García, P., Deschamps, P., and Moreira, D. (2013) Accuracy of protist diversity assessments: morphology compared with cloning and direct pyrosequencing of 18S rRNA genes and ITS regions using the conspicuous tintinnid ciliates as a case study. ISME J 7: 244–255.

Bar-On, Y.M. and Milo, R. (2019) The Biomass Composition of the Oceans: A Blueprint of Our Blue Planet. Cell 179: 1451–1454.

Barton, A.D., Finkel, Z.V., Ward, B.A., Johns, D.G., and Follows, M.J. (2013) On the roles of cell size and trophic strategy in North Atlantic diatom and dinoflagellate communities. Limnology and Oceanography 58: 254–266.

Baas-Becking, L. G. M. (1934). Geobiologie; of inleiding tot de milieukunde. WP Van Stockum & Zoon NV.

Batten, S.D., Clark, R., Flinkman, J., Hays, G., John, E., John, A.W.G., et al. (2003) CPR sampling: the technical background, materials and methods, consistency and comparability. Progress in Oceanography 58: 193–215.

Bauer, J.E., Cai, W.-J., Raymond, P.A., Bianchi, T.S., Hopkinson, C.S., and Regnier, P.A.G. (2013) The changing carbon cycle of the coastal ocean. Nature 504: 61–70.

Beaugrand, G., Edwards, M., and Legendre, L. (2010) Marine biodiversity, ecosystem functioning, and carbon cycles. Proceedings of the National Academy of Sciences 107: 10120–10124.

Beaugrand, G., Edwards, M., Raybaud, V., Goberville, E., and Kirby, R.R. (2015) Future vulnerability of marine biodiversity compared with contemporary and past changes. Nature Clim Change 5: 695–701.

Beaugrand, G. and Kirby, R.R. (2010) Climate, plankton and cod. Global Change Biology 16: 1268–1280.

Beaugrand, G. and Kirby, R.R. (2016) Quasi-deterministic responses of marine species to climate change. Climate Research 69: 117–128.

Behrenfeld, M.J. and Boss, E.S. (2014) Resurrecting the Ecological Underpinnings of Ocean Plankton Blooms. Annu Rev Mar Sci 6: 167–194.

Behrenfeld, M.J., O'Malley, R., Boss, E., Karp-Boss, L., and Mundt, C. (2021) Phytoplankton biodiversity and the inverted paradox. ISME COMMUN 1: 52.

Belin, C., Soudant, D., and Zouher, A. (2021) Three decades of data on phytoplankton and phycotoxins on the French coast: Lessons from REPHY and REPHYTOX. Harmful Algae 102: 101733.

Benedetti, F., Vogt, M., Elizondo, U.H., Righetti, D., Zimmermann, N.E., and Gruber, N. (2021) Major restructuring of marine plankton assemblages under global warming. Nat Commun 12: 5226.

Bernard, G., Pathmanathan, J.S., Lannes, R., Lopez, P., and Bapteste, E. (2018) Microbial Dark Matter Investigations: How Microbial Studies Transform Biological Knowledge and Empirically Sketch a Logic of Scientific Discovery. Genome Biology and Evolution 10: 707–715.

Biard, T., Bigeard, E., Audic, S., Poulain, J., Gutierrez-Rodriguez, A., Pesant, S., et al. (2017) Biogeography and diversity of Collodaria (Radiolaria) in the global ocean. ISME J 11: 1331–1344.

Biegala, I.C., Not, F., Vaulot, D., and Simon, N. (2003) Quantitative Assessment of Picoeukaryotes in the Natural Environment by Using Taxon-Specific Oligonucleotide Probes in Association with Tyramide Signal Amplification-Fluorescence In Situ Hybridization and Flow Cytometry. Applied and Environmental Microbiology 69: 5519–5529.

Blanchet, F.G., Cazelles, K., and Gravel, D. (2020) Co-occurrence is not evidence of ecological interactions. Ecology Letters 23: 1050–1063.

van Boekel, W.H.M., Hansen, F.C., Riegman, R., and Bak, R.P.M. (1992) Lysis-induced decline of a *Phaeocystis* spring bloom and coupling with the microbial foodweb. Marine Ecology Progress Series 81: 269–276.

Bopp, L., Resplandy, L., Orr, J.C., Doney, S.C., Dunne, J.P., Gehlen, M., et al. (2013) Multiple stressors of ocean ecosystems in the 21st century: projections with CMIP5 models. Biogeosciences 10: 6225–6245.

Bottin, M., Soininen, J., Alard, D., and Rosebery, J. (2016) Diatom cooccurrence shows Less Segregation than Predicted from Niche Modeling. PLOS ONE 11: e0154581.

Bower, S.M., Carnegie, R.B., Goh, B., Jones, S.R.M., Lowe, G.J., and Mak, M.W.S. (2004) Preferential PCR Amplification of Parasitic Protistan Small Subunit rDNA from Metazoan Tissues. Journal of Eukaryotic Microbiology 51: 325–332.

Boyce, D.G., Lewis, M.R., and Worm, B. (2010) Global phytoplankton decline over the past century. Nature 466: 591–596.

Breton, E. (2000) Annual variations of phytoplankton biomass in the Eastern English Channel: comparison by pigment signatures and microscopic counts. Journal of Plankton Research 22: 1423–1440.

Breton, E., Christaki, U., Bonato, S., Didry, M., and Artigas, L. (2017) Functional trait variation and nitrogen use efficiency in temperate coastal phytoplankton. Mar Ecol Prog Ser 563: 35–49.

Breton, E., Christaki, U., Sautour, B., Demonio, O., Skouroliakou, D.-I., Beaugrand, G., et al. (2021) Seasonal Variations in the Biodiversity, Ecological Strategy, and Specialization of Diatoms and Copepods in a Coastal System With *Phaeocystis* Blooms: The Key Role of Trait Trade-Offs. Frontiers in Marine Science 8:.

Breton, E., Goberville, E., Sautour, B., Ouadi, A., Skouroliakou, D.-I., Seuront, L., et al. (2022) Multiple phytoplankton community responses to environmental change in a temperate coastal system: A trait-based approach. Frontiers in Marine Science 9:.

Breton, E., Rousseau, Vé., Parent, J.-Y., Ozer, J., and Lancelot, C. (2006) Hydroclimatic modulation of diatom/*Phaeocystis* blooms in nutrient-enriched Belgian coastal waters (North Sea). Limnology and Oceanography 51: 1401–1409.

Breton, E., Sautour, B., and Brylinski, J.-M. (1999) No feeding on *Phaeocystis* sp. as solitary cells (post-bloom period) by the copepod Temora longicornis in the coastal waters of the English Channel. Hydrobiologia 11.

Brown, E.A., Chain, F.J.J., Crease, T.J., MacIsaac, H.J., and Cristescu, M.E. (2015) Divergence thresholds and divergent biodiversity estimates: can metabarcoding reliably describe zooplankton communities? Ecology and Evolution 5: 2234–2251.

Brown, J.H., Gillooly, J.F., Allen, A.P., Savage, V.M., and West, G.B. (2004) Toward a Metabolic Theory of Ecology. Ecology 85: 1771–1789.

Bruggeman, J. (2011) A phylogenetic approach to the estimation of phytoplankton traits: phytoplankton traits from phylogeny. Journal of Phycology 47: 52–65.

Brussaard, C.P.D., Bratbak, G., Baudoux, A.-C., and Ruardij, P. (2007) *Phaeocystis* and its interaction with viruses. In *Phaeocystis*, major link in the biogeochemical cycling of climate-relevant elements. van Leeuwe, M.A., Stefels, J., Belviso, S., Lancelot, C., Verity, P.G., and Gieskes, W.W.C. (eds). Dordrecht: Springer Netherlands, pp. 201–215.

Brylinski, J.-M., Lagadeuc, Y., Gentilhomme, V., Dupont, J.-P., Lafite, R., Dupeuble, P.-A., et al. (1991) Le “fleuve cotier”: Un phenomene hydrologique important en Manche orientale. Exemple du Pas-de-Calais. Oceanologica Acta sp: 8.

Buchan, A., LeCleir, G.R., Gulvik, C.A., and González, J.M. (2014) Master recyclers: features and functions of bacteria associated with phytoplankton blooms. Nat Rev Microbiol 12: 686–698.

Bunse, C. and Pinhassi, J. (2017) Marine Bacterioplankton Seasonal Succession Dynamics. Trends in Microbiology 25: 494–505.

Burrows, M.T., Schoeman, D.S., Richardson, A.J., Molinos, J.G., Hoffmann, A., Buckley, L.B., et al. (2014) Geographical limits to species-range shifts are suggested by climate velocity. Nature 507: 492–495.

Burson, A., Stomp, M., Akil, L., Brussaard, C.P.D., and Huisman, J. (2016) Unbalanced reduction of nutrient loads has created an offshore gradient from phosphorus to nitrogen limitation in the North Sea. Limnology and Oceanography 61: 869–888.

Burson, A., Stomp, M., Mekkes, L., and Huisman, J. (2019) Stable coexistence of equivalent nutrient competitors through niche differentiation in the light spectrum. Ecology 100: e02873.

Cachon, J. (1964) Contribution à l'étude des péridiniens parasites. Cytologie, cycles évolutifs. Ann Sci Nat Zool 6: 1–158.

Cadée, G.C. and Hegeman, J. (2002) Phytoplankton in the Marsdiep at the end of the 20th century; 30 years monitoring biomass, primary production, and *Phaeocystis* blooms. *Journal of Sea Research* **48**: 97–110.

Cadotte, M.W. and Tucker, C.M. (2017) Should Environmental Filtering be Abandoned? Trends in Ecology & Evolution 32: 429–437.

Calbet, A. and Landry, M.R. (2004) Phytoplankton growth, microzooplankton grazing, and carbon cycling in marine systems. Limnology and Oceanography 49: 51–57.

Callahan, B.J., McMurdie, P.J., and Holmes, S.P. (2017) Exact sequence variants should replace operational taxonomic units in marker-gene data analysis. ISME J 11: 2639–2643.

Callahan, B.J., McMurdie, P.J., Rosen, M.J., Han, A.W., Johnson, A.J.A., and Holmes, S.P. (2016a) DADA2: High-resolution sample inference from Illumina amplicon data. Nature Methods 13: 581–583.

Callahan, B.J., McMurdie, P.J., Rosen, M.J., Han, A.W., Johnson, A.J.A., and Holmes, S.P. (2016b) DADA2: High-resolution sample inference from Illumina amplicon data. Nat Methods 13: 581–583.

Caporaso, J.G., Kuczynski, J., Stombaugh, J., Bittinger, K., Bushman, F.D., Costello, E.K., et al. (2010) QIIME allows analysis of high-throughput community sequencing data. Nature Methods 7: 335–336.

Caracciolo, M., Rigaut-Jalabert, F., Romac, S., Mahé, F., Forsans, S., Gac, J.-P., et al. (2022) Seasonal dynamics of marine protist communities in tidally mixed coastal waters. Molecular Ecology 31: 3761–3783.

Casotti, R., Brunet, C., Aronne, B., and d1Alcala, M.R. (2000) Mesoscale features of phytoplankton and planktonic bacteria in a coastal area as induced by external water masses. Marine Ecology Progress Series 195: 15–27.

Chafee, M., Fernàndez-Guerra, A., Buttigieg, P.L., Gerdts, G., Eren, A.M., Teeling, H., and Amann, R.I. (2018) Recurrent patterns of microdiversity in a temperate coastal marine environment. ISME J 12: 237–252.

Chai, F., Johnson, K.S., Claustre, H., Xing, X., Wang, Y., Boss, E., et al. (2020) Monitoring ocean biogeochemistry with autonomous platforms. Nat Rev Earth Environ 1: 315–326.

Chambouvet, A., Morin, P., Marie, D., and Guillou, L. (2008) Control of Toxic Marine Dinoflagellate Blooms by Serial Parasitic Killers. Science 322: 1254–1257.

Chan, A.T. (1980) Comparative physiological study of marine diatoms and dinoflagellates in relation to irradiance and cell size: Relationship between photosynthesis, growth, and carbon/chlorophyll ratio. Journal of Phycology 16: 428–432.

Chase, J.M. (2010) Stochastic Community Assembly Causes Higher Biodiversity in More Productive Environments. Science 328: 1388–1391.

Chase, J.M. (2005) Towards a Really Unified Theory for Metacommunities. Functional Ecology 19: 182–186.

Chase, J.M., Biro, E.G., Ryberg, W.A., and Smith, K.G. (2009) Predators temper the relative importance of stochastic processes in the assembly of prey metacommunities. Ecology Letters 12: 1210–1218.

Chase, J.M., Kraft, N.J.B., Smith, K.G., Vellend, M., and Inouye, B.D. (2011) Using null models to disentangle variation in community dissimilarity from variation in α-diversity. Ecosphere 2: art24.

Chase, J.M. and Myers, J.A. (2011) Disentangling the importance of ecological niches from stochastic processes across scales. Philosophical Transactions of the Royal Society B: Biological Sciences 366: 2351–2363.

Chesson, P. (2000a) General Theory of Competitive Coexistence in Spatially-Varying Environments. Theoretical Population Biology 58: 211–237.

Chesson, P. (2000b) Mechanisms of Maintenance of Species Diversity. Annu Rev Ecol Syst 31: 343–366.

Chisholm, S.W., Olson, R.J., and Yentsch, C.M. (1988) Flow cytometry in oceanography: Status and prospects. Eos, Transactions American Geophysical Union 69: 562–572.

Chivers, W.J., Edwards, M., and Hays, G.C. (2020) Phenological shuffling of major marine phytoplankton groups over the last six decades. Diversity and Distributions 26: 536–548.

Chivers, W.J., Walne, A.W., and Hays, G.C. (2017) Mismatch between marine plankton range movements and the velocity of climate change. Nat Commun 8: 14434.

Christaki, U., Courties, C., Massana, R., Catala, P., Lebaron, P., Gasol, J.M., and Zubkov, M.V. (2011) Optimized routine flow cytometric enumeration of heterotrophic flagellates using SYBR Green I: FC analysis of HF. Limnol Oceanogr Methods 9: 329–339.

Christaki, U., Genitsaris, S., Monchy, S., Li, L.L., Rachik, S., Breton, E., and Sime-Ngando, T. (2017) Parasitic Eukaryotes in a Meso-Eutrophic Coastal System with Marked *Phaeocystis globosa* Blooms. Front Mar Sci 4: 416.

Christaki, Urania, Kormas, K.A., Genitsaris, S., Georges, C., Sime-Ngando, T., Viscogliosi, E., and Monchy, S. (2014) Winter–Summer Succession of Unicellular Eukaryotes in a Meso-eutrophic Coastal System. Microb Ecol 67: 13–23.

Christaki, U., Lefèvre, D., Georges, C., Colombet, J., Catala, P., Courties, C., et al. (2014) Microbial food web dynamics during spring phytoplankton blooms in the naturally iron-fertilized Kerguelen area (Southern Ocean). Biogeosciences 11: 6739–6753.

Christaki, U., Skouroliakou, I.-D., Delegrange, A., Irion, S., Courcot, L., Jardillier, L., and Sassenhagen, I. (2021) Microzooplankton diversity and potential role in carbon cycling of contrasting Southern Ocean productivity regimes. Journal of Marine Systems 16.

Chun, S.-J., Cui, Y., Baek, S.H., Ahn, C.-Y., and Oh, H.-M. (2021) Seasonal succession of microbes in different size-fractions and their modular structures determined by both macro- and micro-environmental filtering in dynamic coastal waters. Science of The Total Environment 784: 147046.

Chust, G., Irigoien, X., Chave, J., and Harris, R.P. (2013) Latitudinal phytoplankton distribution and the neutral theory of biodiversity. Global Ecology and Biogeography 22: 531–543.

Cloern, J.E., Foster, S.Q., and Kleckner, A.E. (2014) Phytoplankton primary production in the world's estuarine-coastal ecosystems. Biogeosciences 11: 2477–2501.

Coats, D., Ej, A., Cl, G., and S, H. (1996) Parasitism of photosynthetic dinoflagellates in a shallow subestuary of Chesapeake Bay, USA. Aquatic Microbial Ecology 11: 1–9.

Coats, D.W. and Bockstahler, K.R. (1994) Occurrence of the Parasitic Dinoflagellate Amoebophrya ceratii in Chesapeake Bay Populations of Gymnodinium sanguineum. Journal of Eukaryotic Microbiology 41: 586–593.

Coats, D.W. and Park, M.G. (2002) Parasitism of Photosynthetic Dinoflagellates by Three Strains of Amoebophrya (dinophyta): Parasite Survival, Infectivity, Generation Time, and Host Specificity1. Journal of Phycology 38: 520–528.

Cole, J.J. (1982) Interactions Between Bacteria and Algae in Aquatic Ecosystems. Annual Review of Ecology and Systematics 13: 291–314.

Collins, F.S., Patrinos, A., Jordan, E., Chakravarti, A., Gesteland, R., Walters, L., and THE MEMBERS OF THE DOE AND NIH PLANNING GROUPS (1998) New Goals for the U.S. Human Genome Project: 1998-2003. Science 282: 682–689.

Colwell, R.K. and Rangel, T.F. (2009) Hutchinson's duality: The once and future niche. Proceedings of the National Academy of Sciences 106: 19651–19658.

Combes, C. (1996) Parasites, biodiversity and ecosystem stability. Biodivers Conserv 5: 953–962.

Connor, E.F. and Simberloff, D. (1979) The Assembly of Species Communities: Chance or Competition? Ecology 60: 1132.

Cooper, G.M. (2000) The Complexity of Eukaryotic Genomes. In The Cell: A Molecular Approach. 2nd edition. Sinauer Associates.

Cooper, M.B. and Smith, A.G. (2015) Exploring mutualistic interactions between microalgae and bacteria in the omics age. Current Opinion in Plant Biology 26: 147–153.

Costanza, R., d'Arge, R., de Groot, R., Farber, S., Grasso, M., Hannon, B., et al. (1997) The value of the world's ecosystem services and natural capital. Nature 387: 253–260.

Courties, C., Vaquer, A., Troussellier, M., Lautier, J., Chrétiennot-Dinet, M.J., Neveux, J., et al. (1994) Smallest eukaryotic organism. Nature 370: 255–255.

Dai, Y., Yang, S., Zhao, D., Hu, C., Xu, W., Anderson, D.M., et al. (2023) Coastal phytoplankton blooms expand and intensify in the 21st century. Nature 1–5.

Dauvin, J.-C. (2012) Are the eastern and western basins of the English Channel two separate ecosystems? Marine Pollution Bulletin 64: 463–471.

Davis, S.J., Caldeira, K., and Matthews, H.D. (2010) Future CO2 Emissions and Climate Change from Existing Energy Infrastructure. Science 329: 1330–1333.

De Luca, D., Piredda, R., Sarno, D., and Kooistra, W.H.C.F. (2021) Resolving cryptic species complexes in marine protists: phylogenetic haplotype networks meet global DNA metabarcoding datasets. ISME J 15: 1931–1942.

Delmas, E., Besson, M., Brice, M.-H., Burkle, L.A., Dalla Riva, G.V., Fortin, M.-J., et al. (2019) Analysing ecological networks of species interactions. Biological Reviews 94: 16–36.

Delmont, T.O., Hammar, K.M., Ducklow, H.W., Yager, P.L., and Post, A.F. (2014) *Phaeocystis antarctica* blooms strongly influence bacterial community structures in the Amundsen Sea polynya. Frontiers in Microbiology 5:.

Delmont, T.O., Quince, C., Shaiber, A., Esen, Ö.C., Lee, S.T., Rappé, M.S., et al. (2018) Nitrogen-fixing populations of Planctomycetes and Proteobacteria are abundant in surface ocean metagenomes. Nat Microbiol 3: 804–813.

Demuez, M., González-Fernández, C., and Ballesteros, M. (2015) Algicidal microorganisms and secreted algicides: New tools to induce microalgal cell disruption. Biotechnol Adv 33: 1615–1625.

Dini-Andreote, F., Stegen, J.C., van Elsas, J.D., and Salles, J.F. (2015) Disentangling mechanisms that mediate the balance between stochastic and deterministic processes in microbial succession. Proc Natl Acad Sci USA 112: E1326–E1332.

Doherty, S.J., Barbato, R.A., Grandy, A.S., Thomas, W.K., Monteux, S., Dorrepaal, E., et al. (2020) The Transition From Stochastic to Deterministic Bacterial Community Assembly During Permafrost Thaw Succession. Frontiers in Microbiology 11:.

Dray, S., Dufour, A.B., and Chessel, D. (2007) The ade4 Package — II: Two-table and K-table Methods. 7: 6.

Ducklow, H., Steinberg, D., and Buesseler, K. (2001) Upper Ocean Carbon Export and the Biological Pump. oceanog 14: 50–58.

Ducklow, H.W. and Carlson, C.A. (1992) Oceanic Bacterial Production. In Advances in Microbial Ecology. Advances in Microbial Ecology. Marshall, K.C. (ed). Boston, MA: Springer US, pp. 113–181.

Dunker, S., Boho, D., Wäldchen, J., and Mäder, P. (2018) Combining high-throughput imaging flow cytometry and deep learning for efficient species and life-cycle stage identification of phytoplankton. BMC Ecology 18: 51.

Durham, B.P., Sharma, S., Luo, H., Smith, C.B., Amin, S.A., Bender, S.J., et al. (2015) Cryptic carbon and sulfur cycling between surface ocean plankton. Proceedings of the National Academy of Sciences 112: 453–457.

Durkin, C.A., Cetinić, I., Estapa, M., Ljubešić, Z., Mucko, M., Neeley, A., and Omand, M. (2022) Tracing the path of carbon export in the ocean though DNA sequencing of individual sinking particles. ISME J 1–11.

Edwards, M., Bresnan, E., Cook, K., Heath, M., Helanaouet, P., Lynam, C., et al. (2013) Impacts of climate change on plankton. MCCIP Science Review 2013 15 pages.

Egge, J. and Aksnes, D. (1992) Silicate as regulating nutrient in phytoplankton competition. Mar Ecol Prog Ser 83: 281–289.

Eilers, H., Pernthaler, J., Glöckner, F.O., and Amann, R. (2000) Culturability and In Situ Abundance of Pelagic Bacteria from the North Sea. Applied and Environmental Microbiology 66: 3044–3051.

Ellison, A.M. (1987) Effect of Seed Dimorphism on the Density-Dependent Dynamics of Experimental Populations of Atriplex Triangularis (chenopodiaceae). American Journal of Botany 74: 1280–1288.

Emerson, B.C. and Gillespie, R.G. (2008) Phylogenetic analysis of community assembly and structure over space and time. Trends in Ecology & Evolution 23: 619–630.

Eren, A.M., Maignien, L., Sul, W.J., Murphy, L.G., Grim, S.L., Morrison, H.G., and Sogin, M.L. (2013) Oligotyping: differentiating between closely related microbial taxa using 16S rRNA gene data. Methods in Ecology and Evolution 4: 1111–1119.

Falkowski, P.G., Barber, R.T., and Smetacek, V. (1998) Biogeochemical Controls and Feedbacks on Ocean Primary Production. Science 281: 200–206.

Fan, C., Glibert, P., and Burkholder, J. (2003) Characterization of the affinity for nitrogen, uptake kinetics, and environmental relationships for Prorocentrum minimum in natural blooms and laboratory cultures. Harmful Algae 2: 283–299.

Faust, K. and Raes, J. (2012) Microbial interactions: from networks to models. Nat Rev Microbiol 10: 538–550.

Fenchel, T. (1988) Marine Plankton Food Chains. Annual Review of Ecology and Systematics 19: 19–38.

Fenchel, T. and Finlay, B.J. (2004) The Ubiquity of Small Species: Patterns of Local and Global Diversity. BioScience 54: 777–784.

Field, C.B., Behrenfeld, M.J., Randerson, J.T., and Falkowski, P. (1998) Primary production of the biosphere: integrating terrestrial and oceanic components. Science 281: 237–240.

Finkel, Z.V. (2001) Light absorption and size scaling of light-limited metabolism in marine diatoms. Limnol Oceanogr 46: 86–94.

Fodelianakis, S., Washburne, A.D., Bourquin, M., Pramateftaki, P., Kohler, T.J., Styllas, M., et al. (2021) Microdiversity characterizes prevalent phylogenetic clades in the glacier-fed stream microbiome. ISME J 16: 666–675.

Friedland, K.D., Mouw, C.B., Asch, R.G., Ferreira, A.S.A., Henson, S., Hyde, K.J.W., et al. (2018) Phenology and time series trends of the dominant seasonal phytoplankton bloom across global scales. *Global Ecology and Biogeography* **27**: 551–569.

Fuhrman, J.A., Cram, J.A., and Needham, D.M. (2015) Marine microbial community dynamics and their ecological interpretation. Nat Rev Microbiol 13: 133–146.

Gall, J.G. and Pardue, M.L. (1969) Molecular hybridization of radioactive dna to the dna of cytological preparations. Proceedings of the National Academy of Sciences 64: 600–604.

Gause, G.F. (1934) The struggle for existence, Baltimore: The Williams & Wilkins company.

Genitsaris, S., Monchy, S., Breton, E., Lecuyer, E., and Christaki, U. (2016) Small-scale variability of protistan planktonic communities relative to environmental pressures and biotic interactions at two adjacent coastal stations. Mar Ecol Prog Ser 548: 61–75.

Genitsaris, S., Monchy, S., Viscogliosi, E., Sime-Ngando, T., Ferreira, S., and Christaki, U. (2015) Seasonal variations of marine protist community structure based on taxon-specific traits using the eastern English Channel as a model coastal system. FEMS Microbiology Ecology 91:.

Gentilhomme, V. and Lizon, F. (1997) Seasonal cycle of nitrogen and phytoplankton biomass in a well-mixed coastal system (Eastern English Channel). Hydrobiologia 361: 191–199.

Georges, A.A., El-Swais, H., Craig, S.E., Li, W.K., and Walsh, D.A. (2014) Metaproteomic analysis of a winter to spring succession in coastal northwest Atlantic Ocean microbial plankton. ISME J 8: 1301–1313.

Georges, C., Monchy, S., Genitsaris, S., and Christaki, U. (2014) Protist community composition during early phytoplankton blooms in the naturally iron-fertilized Kerguelen area (Southern Ocean). Biogeosciences 11: 5847–5863.

Ghai, R., Mizuno, C.M., Picazo, A., Camacho, A., and Rodriguez-Valera, F. (2013) Metagenomics uncovers a new group of low GC and ultra-small marine Actinobacteria. Sci Rep 3: 2471.

Gibson, K., Song, H., and Chen, N. (2022) Metabarcoding analysis of microbiome dynamics during *a Phaeocystis globosa* bloom in the Beibu Gulf, China. Harmful Algae 114: 102217.

Gilbert, J.A. and Dupont, C.L. (2011) Microbial Metagenomics: Beyond the Genome. Annual Review of Marine Science 3: 347–371.

Giljan, G., Arnosti, C., Kirstein, I.V., Amann, R., and Fuchs, B.M. (2022) Strong seasonal differences of bacterial polysaccharide utilization in the North Sea over an annual cycle. Environmental Microbiology 24: 2333–2347.

Giovannoni, S.J., Cameron Thrash, J., and Temperton, B. (2014) Implications of streamlining theory for microbial ecology. ISME J 8: 1553–1565.

Gleason, F.H., Kagami, M., Lefevre, E., and Sime-Ngando, T. (2008) The ecology of chytrids in aquatic ecosystems: roles in food web dynamics. Fungal Biology Reviews 22: 17–25.

Glibert, P.M., Maranger, R., Sobota, D.J., and Bouwman, L. (2014) The Haber Bosch–harmful algal bloom (HB–HAB) link. Environ Res Lett 9: 105001.

Gómez, F. and Souissi, S. (2007a) The distribution and life cycle of the dinoflagellate Spatulodinium pseudonoctiluca (Dinophyceae, Noctilucales) in the northeastern English Channel. Comptes Rendus Biologies 330: 231–236.

Gómez, F. and Souissi, S. (2008) The impact of the 2003 summer heat wave and the 2005 late cold wave on the phytoplankton in the north-eastern English Channel. Comptes Rendus Biologies 331: 678–685.

Gómez, F. and Souissi, S. (2007b) Unusual diatoms linked to climatic events in the northeastern English Channel - ScienceDirect.

Gong, W. and Marchetti, A. (2019) Estimation of 18S Gene Copy Number in Marine Eukaryotic Plankton Using a Next-Generation Sequencing Approach. Front Mar Sci 6: 219.

González-Gil, S., Keafer, B.A., Jovine, R.V.M., Aguilera, A., Lu, S., and Anderson, D.M. (1998) Detection and quantification of alkaline phosphatase in single cells of phosphorus-starved marine phytoplankton. Marine Ecology Progress Series 164: 21–35.

Goodwin, S., McPherson, J.D., and McCombie, W.R. (2016) Coming of age: ten years of next-generation sequencing technologies. Nat Rev Genet 17: 333–351.

Grattepanche, J.-D., Breton, E., Brylinski, J.-M., Lecuyer, E., and Christaki, U. (2011) Succession of primary producers and micrograzers in a coastal ecosystem dominated by *Phaeocystis globosa* blooms. Journal of Plankton Research 33: 37–50.

Grattepanche, J.-D., Vincent, D., Breton, E., and Christaki, U. (2011) Microzooplankton herbivory during the diatom–*Phaeocystis* spring succession in the eastern English Channel. Journal of Experimental Marine Biology and Ecology 404: 87–97.

Grizzetti, B., Bouraoui, F., and Aloe, A. (2012) Changes of nitrogen and phosphorus loads to European seas. Global Change Biology 18: 769–782.

Grossart, H.-P., Levold, F., Allgaier, M., Simon, M., and Brinkhoff, T. (2005) Marine diatom species harbour distinct bacterial communities. Environmental Microbiology 7: 860–873.

Grzymski, J.J. and Dussaq, A.M. (2012) The significance of nitrogen cost minimization in proteomes of marine microorganisms. ISME J 6: 71–80.

Guan, C., Guo, X., Li, Y., Zhang, H., Lei, X., Cai, G., et al. (2015) Photoinhibition of *Phaeocystis globosa* resulting from oxidative stress induced by a marine algicidal bacterium Bacillus sp. LP-10. Sci Rep 5: 17002.

Guegueniat, P., du Bois, P.B., Salomon, J.C., Masson, M., and Cabioch, L. (1995) FLUXMANCHE radiotracers measurements: A contribution to the dynamics of the English Channel and North Sea. Journal of Marine Systems 6: 483–494.

Guillou, L., Bachar, D., Audic, S., Bass, D., Berney, C., Bittner, L., Boutte, C., Burgaud, G., de Vargas, C., Decelle, J., Del Campo, J., et al. (2013) The Protist Ribosomal Reference database (PR2): a catalog of unicellular eukaryote small sub-unit rRNA sequences with curated taxonomy. Nucleic Acids Res 41: D597-604.

Guillou, L., Bachar, D., Audic, S., Bass, D., Berney, C., Bittner, L., Boutte, C., Burgaud, G., de Vargas, C., Decelle, J., del Campo, J., et al. (2013) The Protist Ribosomal Reference database (PR2): a catalog of unicellular eukaryote Small Sub-Unit rRNA sequences with curated taxonomy. Nucleic Acids Res 41: D597–D604.

Guillou, L., Viprey, M., Chambouvet, A., Welsh, R.M., Kirkham, A.R., Massana, R., et al. (2008) Widespread occurrence and genetic diversity of marine parasitoids belonging to Syndiniales (Alveolata). Environmental Microbiology 10: 3349–3365.

Gutierrez-Zamora, M.-L. and Manefield, M. (2010) An appraisal of methods for linking environmental processes to specific microbial taxa. Rev Environ Sci Biotechnol 9: 153–185.

Halsey, K.H., Carter, A.E., and Giovannoni, S.J. (2012) Synergistic metabolism of a broad range of C1 compounds in the marine methylotrophic bacterium HTCC2181. Environmental Microbiology 14: 630–640.

Hansen, A.N. and Visser, A.W. (2019) The seasonal succession of optimal diatom traits. Limnology and Oceanography 64: 1442–1457.

Hanson, C.A., Fuhrman, J.A., Horner-Devine, M.C., and Martiny, J.B.H. (2012) Beyond biogeographic patterns: processes shaping the microbial landscape. Nat Rev Microbiol 10: 497–506.

Heino, J., Melo, A.S., Siqueira, T., Soininen, J., Valanko, S., and Bini, L.M. (2015) Metacommunity organisation, spatial extent and dispersal in aquatic systems: patterns, processes and prospects. Freshwater Biology 60: 845–869.

Hellweger, F.L. (2018) Heterotrophic substrate specificity in the aquatic environment: The role of microscale patchiness investigated using modelling. Environmental Microbiology 20: 3825–3835.

Hillebrand, H., Dürselen, C.-D., Kirschtel, D., Pollingher, U., and Zohary, T. (1999a) Biovolume Calculation for Pelagic and Benthic Microalgae. Journal of Phycology 35: 403–424.

Hillebrand, H., Dürselen, C.-D., Kirschtel, D., Pollingher, U., and Zohary, T. (1999b) Biovolume Calculation for Pelagic and Benthic Microalgae. Journal of Phycology 35: 403–424.

Hoef-Emden, K. (2014) Osmotolerance in the Cryptophyceae: Jacks-of-all-trades in the Chroomonas Clade. Protist 165: 123–143.

Houliez, E., Schmitt, F.G., Breton, E., Skouroliakou, D.-I., and Christaki, U. (2023) On the conditions promoting Pseudo-nitzschia spp. blooms in the eastern English Channel and southern North Sea. Harmful Algae 125: 102424.

Hu, X., Li, X., He, M., Long, A., and Xu, J. (2022) Regulation of Bacterial Metabolic Activities and Community Composition by Temperature in a Fringing Coral Reef. Journal of Geophysical Research: Oceans 127: e2022JC018823.

Hubas, C., Lamy, D., Artigas, L.F., and Davoult, D. (2007) Seasonal variability of intertidal bacterial metabolism and growth efficiency in an exposed sandy beach during low tide. Mar Biol 151: 41–52.

Hubbell, S.P. (2001) The Unified Neutral Theory of Biodiversity and Biogeography (MPB-32), Princeton University Press.

Hudson, P.J., Dobson, A.P., and Lafferty, K.D. (2006) Is a healthy ecosystem one that is rich in parasites? Trends in Ecology & Evolution 21: 381–385.

Husson, B., Hernández-Fariñas, T., Le Gendre, R., Schapira, M., and Chapelle, A. (2016) Two decades of Pseudo-nitzschia spp. blooms and king scallop (Pecten maximus) contamination by domoic acid along the French Atlantic and English Channel coasts: Seasonal dynamics, spatial heterogeneity and interannual variability. *Harmful Algae* **51**: 26–39.

Hutchinson, G.E. (1957) Population studies: animal ecology and demography - concluding remarks. Cold Spring Harb Symp Quant Biol 22: 415–427.

Hutchinson, G.E. (1961) The Paradox of the Plankton. The American Naturalist 95: 137–145.

IPCC AR6 Synthesis Report: Climate Change 2023 | Knowledge for policy.

Jia, X., Dini-Andreote, F., and Salles, J.F. (2018) Community Assembly Processes of the Microbial Rare Biosphere. Trends in Microbiology 26: 738–747.

Jo, J., Lee, H.-G., Kim, K.Y., Park, C., Jo, J., Lee, H.-G., et al. (2019) SoEM: a novel PCR-free biodiversity assessment method based on small-organelles enriched metagenomics. Algae 34: 57–70.

Joint, I., Henriksen, P., Flaten, G.A., Bourne, D., Thingstad, T.F., and Riemann, B. (2002) Competition for inorganic nutrients between phytoplankton and bacterioplankton in nutrient manipulated mesocosms. Aquatic Microbial Ecology - AQUAT MICROB ECOL 29: 145–159.

Jurburg, S.D., Nunes, I., Stegen, J.C., Le Roux, X., Priemé, A., Sørensen, S.J., and Salles, J.F. (2017) Autogenic succession and deterministic recovery following disturbance in soil bacterial communities. Sci Rep 7: 45691.

Kagami, M., de Bruin, A., Ibelings, B.W., and Van Donk, E. (2007) Parasitic chytrids: their effects on phytoplankton communities and food-web dynamics. Hydrobiologia 578: 113–129.

Kardol, P., Souza, L., and Classen, A.T. (2013) Resource availability mediates the importance of priority effects in plant community assembly and ecosystem function. Oikos 122: 84–94.

Karl, D.M., Bidigare, R.R., and Letelier, R.M. (2001) Long-term changes in plankton community structure and productivity in the North Pacific Subtropical Gyre: The domain shift hypothesis. Deep Sea Research Part II: Topical Studies in Oceanography 48: 1449–1470.

Käse, L., Metfies, K., Neuhaus, S., Boersma, M., Wiltshire, K.H., and Kraberg, A.C. (2021) Host-parasitoid associations in marine planktonic time series: Can metabarcoding help reveal them? PLOS ONE 16: e0244817.

Kassambara, A. and Mundt, F. (2020) factoextra: Extract and Visualize the Results of Multivariate Data Analyses.

Katoh, K. and Standley, D.M. (2013) MAFFT Multiple Sequence Alignment Software Version 7: Improvements in Performance and Usability. Molecular Biology and Evolution 30: 772–780.

Kembel, S.W., Cowan, P.D., Helmus, M.R., Cornwell, W.K., Morlon, H., Ackerly, D.D., et al. (2010) Picante: R tools for integrating phylogenies and ecology. Bioinformatics 26: 1463–1464.

Klais, R., Norros, V., Lehtinen, S., Tamminen, T., and Olli, K. (2017) Community assembly and drivers of phytoplankton functional structure. Functional Ecology 31: 760–767.

Klindworth, A., Pruesse, E., Schweer, T., Peplies, J., Quast, C., Horn, M., and Glöckner, F.O. (2013) Evaluation of general 16S ribosomal RNA gene PCR primers for classical and next-generation sequencing-based diversity studies. Nucleic Acids Research 41: e1–e1.

Koch, A.L. (2001) Oligotrophs versus copiotrophs. BioEssays 23: 657–661.

Kopf, A., Bicak, M., Kottmann, R., Schnetzer, J., Kostadinov, I., Lehmann, K., et al. (2015) The ocean sampling day consortium. GigaScience 4: 27.

Kraft, N.J.B., Adler, P.B., Godoy, O., James, E.C., Fuller, S., and Levine, J.M. (2015) Community assembly, coexistence and the environmental filtering metaphor. Functional Ecology 29: 592–599.

Kubota, K. (2013) CARD-FISH for Environmental Microorganisms: Technical Advancement and Future Applications. Microbes Environ 28: 3–12.

Kuhn, D.L., Plafkin, J.L., Cairns, J., and Lowe, R.L. (1981) Qualitative Characterization of Aquatic Environments Using Diatom Life-Form Strategies. Transactions of the American Microscopical Society 100: 165–182.

Kuwata, A., Hama, T., and Takahashi, M. (1993) Ecophysiological characterization of two life forms, resting spores and resting cells, of a marine planktonic diatom, Chaetoceros pseudocun/isetus, formed under nutrient depletion. Marine Ecology-progress Series - MAR ECOL-PROGR SER 102: 245–255.

Kwiatkowski, L., Torres, O., Bopp, L., Aumont, O., Chamberlain, M., Christian, J.R., et al. (2020) Twenty-first century ocean warming, acidification, deoxygenation, and upper-ocean nutrient and primary production decline from CMIP6 model projections. Biogeosciences 17: 3439–3470.

Lagadeuc, Y., Bouté, M., and Dodson, J.J. (1997) Effect of vertical mixing on the vertical distribution of copepods in coastal waters. J Plankton Res 19: 1183–1204.

Lamb, P.D., Hunter, E., Pinnegar, J.K., Creer, S., Davies, R.G., and Taylor, M.I. (2019) How quantitative is metabarcoding: A meta-analytical approach. Molecular Ecology 28: 420–430.

Lamy, D., Obernosterer, I., Laghdass, M., Artigas, F., Breton, E., Grattepanche, J., et al. (2009) Temporal changes of major bacterial groups and bacterial heterotrophic activity during a *Phaeocystis globosa* bloom in the eastern English Channel. Aquat Microb Ecol 58: 95–107.

Lancelot, C., Billen, G., Sournia, A., Weisse, T., Colijn, F., Veldhuis, M.J.W., et al. (1987) *Phaeocystis* Blooms and Nutrient Enrichment in the Continental Coastal Zones of the North Sea. Ambio 16: 38–46.

Lancelot, C. (1995) The mucilage phenomenon in the continental coastal waters of the North Sea. Science of The Total Environment 165: 83–102.

Lancelot, C., Keller, M., Rousseau, V., Smith, W.O.J., and Mathot, S. (1998) Autoecology of the Marine Haptophyte *Phaeocystis* sp. Springer, pp. 209–224.

Landa, M., Blain, S., Christaki, U., Monchy, S., and Obernosterer, I. (2016) Shifts in bacterial community composition associated with increased carbon cycling in a mosaic of phytoplankton blooms. ISME J 10: 39–50.

Lauro, F.M., McDougald, D., Thomas, T., Williams, T.J., Egan, S., Rice, S., et al. (2009) The genomic basis of trophic strategy in marine bacteria. Proceedings of the National Academy of Sciences 106: 15527–15533.

Lê, S., Josse, J., and Husson, F. (2008) FactoMineR: An R Package for Multivariate Analysis. Journal of Statistical Software 25: 1–18.

Leblanc, K., Lafond, A., Cornet, V., Legras, J., Marie, B., and Quéguiner, B. (2021) Deep particle stocks following the summer bloom around the Kerguelen islands: Insights into diatoms physiological state, community structure and mortality modes. Journal of Marine Systems 222: 103609.

Lefebvre, A., Guiselin, N., Barbet, F., and Artigas, F.L. (2011) Long-term hydrological and phytoplankton monitoring (1992–2007) of three potentially eutrophic systems in the eastern English Channel and the Southern Bight of the North Sea. ICES Journal of Marine Science 68: 2029–2043.

Legendre, P. and Anderson, M.J. (1999) Distance-based redundancy analysis: testing multispecies responses in multifactorial ecological experiments. Ecological Monographs 69: 24.

Lelong, A., Hégaret, H., Soudant, P., and Bates, S.S. (2012) Pseudo-nitzschia (Bacillariophyceae) species, domoic acid and amnesic shellfish poisoning: revisiting previous paradigms. Phycologia 51: 168–216.

Lemonnier, C. (2019) Effect of environmental variations on bacterial communities dynamics: evolution and adaptation of bacteria as part of a microbial observatory in the Bay of Brest and the Iroise Sea. 187.

Lemonnier, C., Perennou, M., Eveillard, D., Fernandez-Guerra, A., Leynaert, A., Marié, L., et al. (2020) Linking Spatial and Temporal Dynamic of Bacterioplankton Communities With Ecological Strategies Across a Coastal Frontal Area. Front Mar Sci 7: 376.

Leray, M. and Knowlton, N. (2016) Censusing marine eukaryotic diversity in the twenty-first century. Philosophical Transactions of the Royal Society B: Biological Sciences 371: 20150331.

Li, C., Song, S., Liu, Y., and Chen, T. (2014) Occurrence of Amoebophrya spp. infection in planktonic dinoflagellates in Changjiang (Yangtze River) Estuary, China. Harmful Algae 37: 117–124.

Lima-Mendez, G., Faust, K., Henry, N., Decelle, J., Colin, S., Carcillo, F., et al. (2015) Determinants of community structure in the global plankton interactome. Science 348: 1262073.

Liss, P.S., Malin, G., Turner, S.M., and Holligan, P.M. (1994) Dimethyl sulphide and *Phaeocystis*: A review. *Journal of Marine Systems* **5**: 41–53.

Litchman, E. and Klausmeier, C.A. (2008) Trait-Based Community Ecology of Phytoplankton. Annu Rev Ecol Evol Syst 39: 615–639.

Liu, C., Cui, Y., Li, X., and Yao, M. (2021) microeco : an R package for data mining in microbial community ecology. FEMS Microbiology Ecology 97: fiaa255.

Liu, C., Yao, M., Stegen, J.C., Rui, J., Li, J., and Li, X. (2017) Long-term nitrogen addition affects the phylogenetic turnover of soil microbial community responding to moisture pulse. Sci Rep 7: 17492.

Logares, R., Bråte, J., Bertilsson, S., Clasen, J.L., Shalchian-Tabrizi, K., and Rengefors, K. (2009) Infrequent marine-freshwater transitions in the microbial world. Trends Microbiol 17: 414–422.

Logares, R., Deutschmann, I.M., Junger, P.C., Giner, C.R., Krabberød, A.K., Schmidt, T.S.B., et al. (2020) Disentangling the mechanisms shaping the surface ocean microbiota. Microbiome 8: 55.

Logares, R., Tesson, S.V.M., Canbäck, B., Pontarp, M., Hedlund, K., and Rengefors, K. (2018) Contrasting prevalence of selection and drift in the community structuring of bacteria and microbial eukaryotes. Environmental Microbiology 20: 2231–2240.

Lomas, M.W., Bronk, D.A., and Van Den Engh, G. (2011) Use of Flow Cytometry to Measure Biogeochemical Rates and Processes in the Ocean. Annu Rev Mar Sci 3: 537–566.

Lombard, F., Boss, E., Waite, A.M., Vogt, M., Uitz, J., Stemmann, L., et al. (2019) Globally Consistent Quantitative Observations of Planktonic Ecosystems. Frontiers in Marine Science 6:.

Long, M., Marie, D., Szymczak, J., Toullec, J., Bigeard, E., Sourisseau, M., et al. (2021) Dinophyceae can use exudates as weapons against the parasite Amoebophrya sp. (Syndiniales). ISME COMMUN 1: 1–10.

Longhurst, A. (2007) Ecological Geography of the Sea - 2nd Edition.

Longobardi, L., Dubroca, L., Margiotta, F., Sarno, D., and Zingone, A. (2022) Photoperiod-driven rhythms reveal multi-decadal stability of phytoplankton communities in a highly fluctuating coastal environment. Sci Rep 12: 3908.

López-García, P., Rodríguez-Valera, F., Pedrós-Alió, C., and Moreira, D. (2001) Unexpected diversity of small eukaryotes in deep-sea Antarctic plankton. Nature 409: 603–607.

López-Pérez, M., Haro-Moreno, J.M., Iranzo, J., and Rodriguez-Valera, F. (2020) Genomes of the “Candidatus Actinomarinales” Order: Highly Streamlined Marine Epipelagic Actinobacteria. mSystems 5: e01041-20.

Lorenzen, C.J. (1966) A method for the continuous measurement of in vivo chlorophyll concentration. Deep Sea Research and Oceanographic Abstracts 13: 223–227.

Losos, J.B. (2008) Phylogenetic niche conservatism, phylogenetic signal and the relationship between phylogenetic relatedness and ecological similarity among species. Ecology Letters 11: 995–1003.

Louca, S., Parfrey, L.W., and Doebeli, M. (2016) Decoupling function and taxonomy in the global ocean microbiome. Science 353: 1272–1277.

Lowe, W.H. and McPeek, M.A. (2014) Is dispersal neutral? Trends in Ecology & Evolution 29: 444–450.

Luthi, D., Floch, M.L., Bereiter, B., Blunier, T., Barnola, J.-M., Siegenthaler, U., et al. (2008) High-resolution carbon dioxide concentration record 650,000-800,000 years before present. Nature 453: 379–383.

MacArthur, R.H. and Wilson, E.O. (1967) The Theory of Island Biogeography, REV-Revised. Princeton University Press.

Madsen, E.L. (2005) Identifying microorganisms responsible for ecologically significant biogeochemical processes. Nat Rev Microbiol 3: 439–446.

Mahé, F., Rognes, T., Quince, C., Vargas, C. de, and Dunthorn, M. (2015) Swarm v2: highly-scalable and high-resolution amplicon clustering. PeerJ 3: e1420.

Margalef, R. (1963) On Certain Unifying Principles in Ecology. The American Naturalist 97: 357–374.

Margalef, R. (1958) „Trophic" typology versus biotic typology, as exemplified in the regional limnology of Northern Spain. SIL Proceedings, 1922-2010 13: 339–349.

Marie, D., Brussaard, C.P.D., Thyrhaug, R., Bratbak, G., and Vaulot, D. (1999) Enumeration of Marine Viruses in Culture and Natural Samples by Flow Cytometry. Applied and Environmental Microbiology 65: 45–52.

Marie, D., Simon, N., Guillou, L., Partensky, F., and Vaulot, D. (2000) DNA/RNA Analysis of Phytoplankton by Flow Cytometry. Current Protocols in Cytometry 11: 11.12.1-11.12.14.

Mars Brisbin, M., Mitarai, S., Saito, M.A., and Alexander, H. (2022) Microbiomes of bloom-forming *Phaeocystis* algae are stable and consistently recruited, with both symbiotic and opportunistic modes. ISME J 1–10.

Mason, N.W.H., Mouillot, D., Lee, W.G., and Wilson, J.B. (2005) Functional richness, functional evenness and functional divergence: the primary components of functional diversity. Oikos 111: 112–118.

Massana, R., Gobet, A., Audic, S., Bass, D., Bittner, L., Boutte, C., et al. (2015) Marine protist diversity in European coastal waters and sediments as revealed by high-throughput sequencing. Environmental Microbiology 17: 4035–4049.

Massana, R. and Logares, R. (2013) Eukaryotic versus prokaryotic marine picoplankton ecology. Environmental Microbiology 15: 1254–1261.

Massana, R. and Pedrós-Alió, C. (2008) Unveiling new microbial eukaryotes in the surface ocean. Current Opinion in Microbiology 11: 213–218.

Maxam, A.M. and Gilbert, W. (1977) A new method for sequencing DNA. Proceedings of the National Academy of Sciences 74: 560–564.

Mayali, X. and Azam, F. (2004) Algicidal Bacteria in the Sea and their Impact on Algal Blooms1. Journal of Eukaryotic Microbiology 51: 139–144.

McLean, M.J., Mouillot, D., Goascoz, N., Schlaich, I., and Auber, A. (2019) Functional reorganization of marine fish nurseries under climate warming. Global Change Biology 25: 660–674.

McMurdie, P.J. and Holmes, S. (2013a) phyloseq: An R Package for Reproducible Interactive Analysis and Graphics of Microbiome Census Data. PLOS ONE 8: e61217.

McMurdie, P.J. and Holmes, S. (2013b) phyloseq: An R Package for Reproducible Interactive Analysis and Graphics of Microbiome Census Data. PLOS ONE 8: e61217.

Medinger, R., Nolte, V., Pandey, R.V., Jost, S., Ottenwälder, B., Schlötterer, C., and Boenigk, J. (2010) Diversity in a hidden world: potential and limitation of next-generation sequencing for surveys of molecular diversity of eukaryotic microorganisms. Molecular Ecology 19: 32–40.

Menden-Deuer, S. and Lessard, E.J. (2000) Carbon to volume relationships for dinoflagellates, diatoms, and other protist plankton. Limnology and Oceanography 45: 569–579.

Meyer, N., Bigalke, A., Kaulfuß, A., and Pohnert, G. (2017a) Strategies and ecological roles of algicidal bacteria. FEMS Microbiol Rev 41: 880–899.

Meyer, N., Bigalke, A., Kaulfuß, A., and Pohnert, G. (2017b) Strategies and ecological roles of algicidal bacteria. FEMS Microbiol Rev 41: 880–899.

Miloslavich, P., Bax, N.J., Simmons, S.E., Klein, E., Appeltans, W., Aburto-Oropeza, O., et al. (2018) Essential ocean variables for global sustained observations of biodiversity and ecosystem changes. Global Change Biology 24: 2416–2433.

Mineta, K. and Gojobori, T. (2016) Databases of the marine metagenomics. Gene 576: 724–728.

Mitchell, R. (1971) Role of Predators in the Reversal of Imbalances in Microbial Ecosystems. Nature 230: 257–258.

Monchy, S., Grattepanche, J.-D., Breton, E., Meloni, D., Sanciu, G., Chabé, M., et al. (2012) Microplanktonic Community Structure in a Coastal System Relative to a *Phaeocystis* Bloom Inferred from Morphological and Tag Pyrosequencing Methods. PLoS ONE 7: e39924.

Montagnes, D.J.S., Chambouvet, A., Guillou, L., and Fenton, A. (2008) Responsibility of microzooplankton and parasite pressure for the demise of toxic dinoflagellate blooms. Aquatic Microbial Ecology 53: 211–225.

Morel, A. and Smith, R.C. (1974) Relation between total quanta and total energy for aquatic photosynthesis. Limnology and Oceanography 19: 591–600.

Morris, B.E.L., Henneberger, R., Huber, H., and Moissl-Eichinger, C. (2013) Microbial syntrophy: interaction for the common good. FEMS Microbiology Reviews 37: 384–406.

Mou, X., Sun, S., Edwards, R.A., Hodson, R.E., and Moran, M.A. (2008) Bacterial carbon processing by generalist species in the coastal ocean. Nature 451: 708–711.

Mouillot, D., Graham, N.A.J., Villéger, S., Mason, N.W.H., and Bellwood, D.R. (2013) A functional approach reveals community responses to disturbances. Trends in Ecology & Evolution 28: 167–177.

Mühlenbruch, M., Grossart, H.-P., Eigemann, F., and Voss, M. (2018) Mini-review: Phytoplankton-derived polysaccharides in the marine environment and their interactions with heterotrophic bacteria. Environmental Microbiology 20: 2671–2685.

Napoléon, C., Fiant, L., Raimbault, V., Riou, P., and Claquin, P. (2014) Dynamics of phytoplankton diversity structure and primary productivity in the English Channel. Mar Ecol Prog Ser 505: 49–64.

Narwani, A., Alexandrou, M.A., Oakley, T.H., Carroll, I.T., and Cardinale, B.J. (2013) Experimental evidence that evolutionary relatedness does not affect the ecological mechanisms of coexistence in freshwater green algae. Ecol Lett 16: 1373–1381.

Nejstgaard, J.C., Tang, K.W., Steinke, M., Dutz, J., Koski, M., Antajan, E., and Long, J.D. (2007) Zooplankton grazing on *Phaeocystis*: a quantitative review and future challenges. Biogeochemistry 83: 147–172.

Nemergut, D.R., Schmidt, S.K., Fukami, T., O'Neill, S.P., Bilinski, T.M., Stanish, L.F., et al. (2013) Patterns and processes of microbial community assembly. Microbiol Mol Biol Rev 77: 342–356.

Newton, A., Icely, J., Cristina, S., Perillo, G.M.E., Turner, R.E., Ashan, D., et al. (2020) Anthropogenic, Direct Pressures on Coastal Wetlands. Frontiers in Ecology and Evolution 8:.

Nixon, S.W. and Buckley, B.A. (2002) "A strikingly rich zone"—Nutrient enrichment and secondary production in coastal marine ecosystems. Estuaries 25: 782–796.

Not, F., Latasa, M., Marie, D., Cariou, T., Vaulot, D., and Simon, N. (2004) A Single Species, Micromonas pusilla (Prasinophyceae), Dominates the Eukaryotic Picoplankton in the Western English Channel. Applied and Environmental Microbiology 70: 4064–4072.

Oksanen, J., Blanchet, F.G., Friendly, M., Kindt, R., Legendre, P., McGlinn, D., et al. (2020) vegan: Community Ecology Package.

Olson, R.J., Zettler, E.R., and Anderson, O.K. (1989) Discrimination of eukaryotic phytoplankton cell types from light scatter and autofluorescence properties measured by flow cytometry. Cytometry 10: 636–643.

Orellana, L.H., Francis, T.B., Ferraro, M., Hehemann, J.-H., Fuchs, B.M., and Amann, R.I. (2022) Verrucomicrobiota are specialist consumers of sulfated methyl pentoses during diatom blooms. ISME J 16: 630–641.

Orrock, J.L. and Watling, J.I. (2010) Local community size mediates ecological drift and competition in metacommunities. Proceedings of the Royal Society B: Biological Sciences 277: 2185–2191.

Park, M.G., Yih, W., and Coats, D.W. (2004) Parasites and phytoplankton, with special emphasis on dinoflagellate infections. J Eukaryot Microbiol 51: 145–155.

Peperzak, L., Colijn, F., Gieskes, W.W.C., and Peeters, J.C.H. (1998) Development of the diatom- *Phaeocystis* spring bloom in the Dutch coastal zone of the North Sea: the silicon depletion versus the daily irradiance threshold hypothesis. Journal of Plankton Research 20: 517–537.

Philippart, C.J.M., Cadée, G.C., van Raaphorst, W., and Riegman, R. (2000) Long-term phytoplankton-nutrient interactions in a shallow coastal sea: Algal community structure, nutrient budgets, and denitrification potential. Limnology and Oceanography 45: 131–144.

Pinhassi, J., Sala, M.M., Havskum, H., Peters, F., Guadayol, Ò., Malits, A., and Marrasé, C. (2004) Changes in Bacterioplankton Composition under Different Phytoplankton Regimens. Applied and Environmental Microbiology 70: 6753–6766.

Piredda, R., Claverie, J.-M., Decelle, J., de Vargas, C., Dunthorn, M., Edvardsen, B., et al. (2018) Diatom diversity through HTS-metabarcoding in coastal European seas. Sci Rep 8: 18059.

Piwosz, K., Mukherjee, I., Salcher, M.M., Grujčić, V., and Šimek, K. (2021) CARD-FISH in the Sequencing Era: Opening a New Universe of Protistan Ecology. Frontiers in Microbiology 12:.

Platt, T., Fuentes-Yaco, C., and Frank, K.T. (2003) Spring algal bloom and larval fish survival. Nature 423: 398–399.

Pohlert, T. (2015) PMCMR: calculate pairwise multiple comparisons of mean rank sums. R package version 1:.

Polimene, L., Brunet, C., Butenschön, M., Martinez-Vicente, V., Widdicombe, C., Torres, R., and Allen, J.I. (2014) Modelling a light-driven phytoplankton succession. Journal of Plankton Research 36: 214–229.

Poloczanska, E.S., Brown, C.J., Sydeman, W.J., Kiessling, W., Schoeman, D.S., Moore, P.J., et al. (2013) Global imprint of climate change on marine life. Nature Clim Change 3: 919–925.

Porter, K.G. and Feig, Y.S. (1980) The use of DAPI for identifying and counting aquatic microflora1. Limnology and Oceanography 25: 943–948.

Potvin, M. and Lovejoy, C. (2009) PCR-Based Diversity Estimates of Artificial and Environmental 18S rRNA Gene Libraries. Journal of Eukaryotic Microbiology 56: 174–181.

Powell, J.R., Karunaratne, S., Campbell, C.D., Yao, H., Robinson, L., and Singh, B.K. (2015) Deterministic processes vary during community assembly for ecologically dissimilar taxa. Nat Commun 6: 8444.

Price, M.N., Dehal, P.S., and Arkin, A.P. (2009) FastTree: Computing Large Minimum Evolution Trees with Profiles instead of a Distance Matrix. Molecular Biology and Evolution 26: 1641–1650.

Pulliam, H. r. (2000) On the relationship between niche and distribution. Ecology Letters 3: 349–361.

Quast, C., Pruesse, E., Yilmaz, P., Gerken, J., Schweer, T., Yarza, P., et al. (2013) The SILVA ribosomal RNA gene database project: improved data processing and web-based tools. Nucleic Acids Research 41: D590–D596.

R Core Team (2021) R: A language and environment for statistical computing. R Foundation for Statistical Computing, Vienna, Austria.

Rachik, S., Christaki, U., Li, L.L., Genitsaris, S., Breton, E., and Monchy, S. (2018) Diversity and potential activity patterns of planktonic eukaryotic microbes in a mesoeutrophic coastal area (eastern English Channel). PLoS ONE 13: e0196987.

Ramond, P., Siano, R., Schmitt, S., de Vargas, C., Marié, L., Memery, L., and Sourisseau, M. (2021) Phytoplankton taxonomic and functional diversity patterns across a coastal tidal front. Sci Rep 11: 2682.

Ramond, P., Siano, R., Sourisseau, M., and Logares, R. (2023) Assembly processes and functional diversity of marine protists and their rare biosphere. Environmental Microbiome 18: 59.

Rasconi, S., Jobard, M., and Sime-Ngando, T. (2011) Parasitic fungi of phytoplankton: ecological roles and implications for microbial food webs. Aquatic Microbial Ecology 62: 123–137.

Raven, J.A. (1984) A Cost-Benefit Analysis of Photon Absorption by Photosynthetic Unicells. New Phytologist 98: 593–625.

Redfield, A.C. (1958) The biological control of chemical factors in the environment. American Scientist 46: 230A–221.

Reynaud, J.Y., Teyssier, B., Auffret, J.P., Berné, S.S., Batist, M. de, Marsset, T., and Walker, P. (2003) The offshore sedimentary cover of the English Channel and its northern and western Approaches. J Quat Res 18: 261.

Reynolds, C.S. (1984) Phytoplankton periodicity: the interactions of form, function and environmental variability. Freshwater Biology 14: 111–142.

Richardson, A.J., Walne, A.W., John, A.W.G., Jonas, T.D., Lindley, J.A., Sims, D.W., et al. (2006) Using continuous plankton recorder data. Progress in Oceanography 68: 27–74.

Riemann, L., Steward, G.F., and Azam, F. (2000) Dynamics of Bacterial Community Composition and Activity during a Mesocosm Diatom Bloom. Applied and Environmental Microbiology 66: 578–587.

Rosindell, J., Hubbell, S.P., He, F., Harmon, L.J., and Etienne, R.S. (2012) The case for ecological neutral theory. Trends in Ecology & Evolution 27: 203–208.

Rousseau, V., Chrétiennot-Dinet, M.-J., Jacobsen, A., Verity, P., and Whipple, S. (2007) The life cycle of *Phaeocystis*: state of knowledge and presumptive role in ecology. Biogeochemistry 83: 29–47.

Ruan, Q., Dutta, D., Schwalbach, M.S., Steele, J.A., Fuhrman, J.A., and Sun, F. (2006) Local similarity analysis reveals unique associations among marine bacterioplankton species and environmental factors. Bioinformatics 22: 2532–2538.

Salomon, P.S., Granéli, E., Neves, M.H.C.B., and Rodriguez, E.G. (2009) Infection by Amoebophrya spp. parasitoids of dinoflagellates in a tropical marine coastal area. Aquatic Microbial Ecology 55: 143–153.

Salomon, P.S. and Stolte, W. (2010) Predicting the population dynamics in Amoebophrya parasitoids and their dinoflagellate hosts using a mathematical model. Marine Ecology Progress Series 419: 1–10.

Sanger, F., Nicklen, S., and Coulson, A.R. (1977) DNA sequencing with chain-terminating inhibitors. Proceedings of the National Academy of Sciences 74: 5463–5467.

Santi, I., Kasapidis, P., Karakassis, I., and Pitta, P. (2021) A Comparison of DNA Metabarcoding and Microscopy Methodologies for the Study of Aquatic Microbial Eukaryotes. Diversity 13: 180.

Sarthou, G., Timmermans, K.R., Blain, S., and Tréguer, P. (2005) Growth physiology and fate of diatoms in the ocean: a review. Journal of Sea Research 53: 25–42.

Sassenhagen, I., Irion, S., Jardillier, L., Moreira, D., and Christaki, U. (2020) Protist Interactions and Community Structure During Early Autumn in the Kerguelen Region (Southern Ocean). Protist 171: 125709.

Schapira, M., Vincent, D., Gentilhomme, V., and Seuront, L. (2008) Temporal patterns of phytoplankton assemblages, size spectra and diversity during the wane of a *Phaeocystis globosa* spring bloom in hydrologically contrasted coastal waters. J Mar Biol Ass 88: 649–662.

Schattenhofer, M., Fuchs, B.M., Amann, R., Zubkov, M.V., Tarran, G.A., and Pernthaler, J. (2009) Latitudinal distribution of prokaryotic picoplankton populations in the Atlantic Ocean. Environmental Microbiology 11: 2078–2093.

Schoemann, V., Becquevort, S., Stefels, J., Rousseau, V., and Lancelot, C. (2005) *Phaeocystis* blooms in the global ocean and their controlling mechanisms: a review. Journal of Sea Research 53: 43–66.

Schönhuber, W., Fuchs, B., Juretschko, S., and Amann, R. (1997) Improved sensitivity of whole-cell hybridization by the combination of horseradish peroxidase-labeled oligonucleotides and tyramide signal amplification. Applied and Environmental Microbiology 63: 3268–3273.

Segura, A.M., Kruk, C., Calliari, D., García-Rodriguez, F., Conde, D., Widdicombe, C.E., and Fort, H. (2013) Competition drives clumpy species coexistence in estuarine phytoplankton. Sci Rep 3: 1037.

Sehein, T.R., Gast, R.J., Pachiadaki, M., Guillou, L., and Edgcomb, V.P. (2022) Parasitic infections by Group II Syndiniales target selected dinoflagellate host populations within diverse protist assemblages in a model coastal pond. Environmental Microbiology 24: 1818–1834.

Sentchev, A., Yaremchuk, M., and Lyard, F. (2006) Residual circulation in the English Channel as a dynamically consistent synthesis of shore-based observations of sea level and currents. Continental Shelf Research 26: 1884–1904.

Seuront, L., Vincent, D., and Mitchell, J.G. (2006) Biologically induced modification of seawater viscosity in the Eastern English Channel during a *Phaeocystis globosa* spring bloom. Journal of Marine Systems 61: 118–133.

Seymour, J.R., Ahmed, T., and Stocker, R. (2009) Bacterial chemotaxis towards the extracellular products of the toxic phytoplankton Heterosigma akashiwo. Journal of Plankton Research 31: 1557–1561.

Seymour, J.R., Amin, S.A., Raina, J.-B., and Stocker, R. (2017) Zooming in on the phycosphere: the ecological interface for phytoplankton–bacteria relationships. Nat Microbiol 2: 17065.

Shade, A., Jones, S.E., Caporaso, J.G., Handelsman, J., Knight, R., Fierer, N., and Gilbert, J.A. (2014) Conditionally Rare Taxa Disproportionately Contribute to Temporal Changes in Microbial Diversity. mBio 5: e01371-14.

Shannon, P., Markiel, A., Ozier, O., Baliga, N.S., Wang, J.T., Ramage, D., et al. (2003) Cytoscape: A Software Environment for Integrated Models of Biomolecular Interaction Networks. Genome Res 13: 2498–2504.

Sheldon, R.W., Prakash, A., and Sutcliffe Jr., W.H. (1972) The Size Distribution of Particles in the Ocean1. Limnology and Oceanography 17: 327–340.

Shen, P., Qi, Y., Wang, Y., and Huang, L. (2011) *Phaeocystis globosa* Scherffel, a harmful microalga, and its production of dimethylsulfoniopropionate. Chin J Ocean Limnol 29: 869–873.

Sherr, E.B. and Sherr, B.F. (1994) Bacterivory and herbivory: Key roles of phagotrophic protists in pelagic food webs. Microb Ecol 28: 223–235.

Sherr, E.B. and Sherr, B.F. (2002) Significance of predation by protists in aquatic microbial food webs. Antonie Van Leeuwenhoek 81: 293–308.

Siano, R., Alves-de-Souza, C., Foulon, E., Bendif, E.M., Simon, N., Guillou, L., and Not, F. (2011) Distribution and host diversity of Amoebophryidae parasites across oligotrophic waters of the Mediterranean Sea. Biogeosciences 8: 267–278.

Siano, R., Lassudrie, M., Cuzin, P., Briant, N., Loizeau, V., Schmidt, S., et al. (2021) Sediment archives reveal irreversible shifts in plankton communities after World War II and agricultural pollution. *Current Biology* 31: 2682-2689.e7.

Siefert, R.L. and Plattner, G.-K. (2004) The role of coastal zones in global biogeochemical cycles. Eos, Transactions American Geophysical Union 85: 470–470.

Simon, N., Campbell, L., Örnolfsdottir, E., Groben, R., Guillou, L., Lange, M., and Medlin, L.K. (2000) Oligonucleotide Probes for the Identification of Three Algal Groups by Dot Blot and Fluorescent Whole-Cell Hybridization. Journal of Eukaryotic Microbiology 47: 76–84.

Sinclair, L., Osman, O.A., Bertilsson, S., and Eiler, A. (2015) Microbial Community Composition and Diversity via 16S rRNA Gene Amplicons: Evaluating the Illumina Platform. PLOS ONE 10: e0116955.

Skouroliakou, D.-I., Breton, E., Irion, S., Artigas, L.F., and Christaki, U. (2022) Stochastic and Deterministic Processes Regulate Phytoplankton Assemblages in a Temperate Coastal Ecosystem. Microbiology Spectrum 0: e02427-22.

Skovgaard, A. and Saiz, E. (2006) Seasonal occurrence and role of protistan parasites in coastal marine zooplankton. Marine Ecology Progress Series 327: 37–49.

Smayda, T.J. (2002) Turbulence, watermass stratification and harmful algal blooms: an alternative view and frontal zones as “pelagic seed banks.” Harmful Algae 1: 95–112.

Smith, S.D. (1988) Coefficients for sea surface wind stress, heat flux, and wind profiles as a function of wind speed and temperature. Journal of Geophysical Research: Oceans 93: 15467–15472.

Solomon, C.M., Lessard, E.J., Keil, R.G., and Foy, M.S. (2003) Characterization of extracellular polymers of *Phaeocystis globosa* and *P. antarctica*. Marine Ecology Progress Series 250: 81–89.

Spatharis, S., Lamprinou, V., Meziti, A., Kormas, K.A., Danielidis, D.D., Smeti, E., et al. (2019) Everything is not everywhere: can marine compartments shape phytoplankton assemblages? Proc Biol Sci 286: 20191890.

Spilmont, N., Denis, L., Artigas, L.F., Caloin, F., Courcot, L., Créach, A., et al. (2009) Impact of the *Phaeocystis globosa* spring bloom on the intertidal benthic compartment in the eastern English Channel: A synthesis. Marine Pollution Bulletin 58: 55–63.

Stackebrandt T, E. and Goebel B.M. (1994) Taxonomic Note: A Place for DNA-DNA Reassociation and 16S rRNA Sequence Analysis in the Present Species Definition in Bacteriology. International Journal of Systematic and Evolutionary Microbiology 44: 846–849.

Steele, D.J., Tarran, G.A., Widdicombe, C.E., Woodward, E.M.S., Kimmance, S.A., Franklin, D.J., and Airs, R.L. (2015) Abundance of a chlorophyll a precursor and the oxidation product hydroxychlorophyll a during seasonal phytoplankton community progression in the Western English Channel. Progress in Oceanography 137: 434–445.

Stegen, J.C., Lin, X., Fredrickson, J.K., Chen, X., Kennedy, D.W., Murray, C.J., et al. (2013) Quantifying community assembly processes and identifying features that impose them. ISME J 7: 2069–2079.

Stegen, J.C., Lin, X., Fredrickson, J.K., and Konopka, A.E. (2015) Estimating and mapping ecological processes influencing microbial community assembly. Frontiers in Microbiology 6: 370.

Stegen, J.C., Lin, X., Konopka, A.E., and Fredrickson, J. (2012) Stochastic and deterministic assembly processes in subsurface microbial communities. The ISME Journal 12.

Stern, R., Kraberg, A., Bresnan, E., Kooistra, W.H.C.F., Lovejoy, C., Montresor, M., et al. (2018) Molecular analyses of protists in long-term observation programmes—current status and future perspectives. Journal of Plankton Research 40: 519–536.

Stoecker, D.K., Hansen, P.J., Caron, D.A., and Mitra, A. (2017) Mixotrophy in the Marine Plankton. Annual Review of Marine Science 9: 311–335.

Storey, J.D. and Tibshirani, R. (2003) Statistical significance for genomewide studies. Proceedings of the National Academy of Sciences 100: 9440–9445.

Su, X., Pan, W., Song, B., Xu, J., and Ning, K. (2014) Parallel-META 2.0: Enhanced Metagenomic Data Analysis with Functional Annotation, High Performance Computing and Advanced Visualization. PLOS ONE 9: e89323.

Sunagawa, S., Acinas, S.G., Bork, P., Bowler, C., Tara Oceans Coordinators, Acinas, S.G., et al. (2020) Tara Oceans: towards global ocean ecosystems biology. Nat Rev Microbiol 18: 428–445.

Sverdrup, H.U. (1953) On Conditions for the Vernal Blooming of Phytoplankton. ICES Journal of Marine Science 18: 287–295.

Tada, Y., Taniguchi, A., Sato-Takabe, Y., and Hamasaki, K. (2012) Growth and succession patterns of major phylogenetic groups of marine bacteria during a mesocosm diatom bloom. J Oceanogr 68: 509–519.

Tappin, A.D. and Reid, P.C. (2000) The English Channel. Seas at the millennium - an environmental evaluation - Volume 1 65–82.

Teeling, H., Fuchs, B.M., Becher, D., Klockow, C., Gardebrecht, A., Bennke, C.M., et al. (2012) Substrate-Controlled Succession of Marine Bacterioplankton Populations Induced by a Phytoplankton Bloom. Science 336: 608–611.

Teeling, H., Fuchs, B.M., Bennke, C.M., Krüger, K., Chafee, M., Kappelmann, L., et al. (2016) Recurring patterns in bacterioplankton dynamics during coastal spring algae blooms. eLife 5: e11888.

Thompson, J.N. (1988) Variation in Interspecific Interactions. Annual Review of Ecology and Systematics 19: 65–87.

Tilman, D., Kilham, S.S., and Kilham, P. (1982) Phytoplankton Community Ecology: The Role of Limiting Nutrients. Annual Review of Ecology and Systematics 13: 349–372.

Trask, B.J., van den Engh, G.J., and Elgershuizen, J.H.B.W. (1982) Analysis of phytoplankton by flow cytometry. Cytometry 2: 258–264.

Tréguer, P., Bowler, C., Moriceau, B., Dutkiewicz, S., Gehlen, M., Aumont, O., et al. (2018) Influence of diatom diversity on the ocean biological carbon pump. Nature Geosci 11: 27–37.

Turner, R.E., Rabalais, N.N., Justic', D., and Dortch, Q. (2003) Global patterns of dissolved N, P and Si in large rivers. Biogeochemistry 64: 297–317.

Utermöhl, H. (1931) Neue Wege in der quantitativen Erfassung des Plankton. (Mit besonderer Berücksichtigung des Ultraplanktons.). SIL Proceedings, 1922-2010 5: 567–596.

Velegrakis, A.F., Michel, D., Collins, M.B., Lafite, R., Oikonomou, E.K., Dupont, J.P., et al. (1999) Sources, sinks and resuspension of suspended particulate matter in the eastern English Channel. Continental Shelf Research 19: 1933–1957.

Vellend, M. (2010) Conceptual Synthesis in Community Ecology. The Quarterly Review of Biology 85: 183–206.

Vellend, M., Srivastava, D.S., Anderson, K.M., Brown, C.D., Jankowski, J.E., Kleynhans, E.J., et al. (2014) Assessing the relative importance of neutral stochasticity in ecological communities. Oikos 123: 1420–1430.

Velo-Suárez, L., Brosnahan, M.L., Anderson, D.M., and McGillicuddy Jr, D.J. (2013) A quantitative assessment of the role of the parasite Amoebophrya in the termination of Alexandrium fundyense blooms within a small coastal embayment. PLoS One 8: e81150.

Verity, P.G., Robertson, C.Y., Tronzo, C.R., Andrews, M.G., Nelson, J.R., and Sieracki, M.E. (1992) Relationships between cell volume and the carbon and nitrogen content of marine photosynthetic nanoplankton. Limnology and Oceanography.

Violle, C., Navas, M.-L., Vile, D., Kazakou, E., Fortunel, C., Hummel, I., and Garnier, E. (2007) Let the concept of trait be functional! Oikos 116: 882–892.

Vrieling, E.G., Vriezekolk, G., Gieskes, W.W.C., Veenhuis, M., and Harder, W. (1996) Immuno-flow cytometric identification and enumeration of the ichthyotoxic dinoflagellate Gyrodinium aureolum Hulburt in artificially mixed algal populations. Journal of Plankton Research 18: 1503–1512.

Wang, J., Shen, J., Wu, Y., Tu, C., Soininen, J., Stegen, J.C., et al. (2013) Phylogenetic beta diversity in bacterial assemblages across ecosystems: deterministic versus stochastic processes. ISME J 7: 1310–1321.

Ward, C.S., Yung, C.-M., Davis, K.M., Blinebry, S.K., Williams, T.C., Johnson, Z.I., and Hunt, D.E. (2017) Annual community patterns are driven by seasonal switching between closely related marine bacteria. ISME J 11: 1412–1422.

Webb, C.O., Ackerly, D.D., McPeek, M.A., and Donoghue, M.J. (2002) Phylogenies and Community Ecology. Annu Rev Ecol Syst 33: 475–505.

Weiss, S., Van Treuren, W., Lozupone, C., Faust, K., Friedman, J., Deng, Y., et al. (2016) Correlation detection strategies in microbial data sets vary widely in sensitivity and precision. ISME J 10: 1669–1681.

Wickham, H. (2016) ggplot2, Cham: Springer International Publishing.

Widdicombe, C.E., Eloire, D., Harbour, D., Harris, R.P., and Somerfield, P.J. (2010) Long-term phytoplankton community dynamics in the Western English Channel. Journal of Plankton Research 32: 643–655.

Wisecaver, J.H. and Hackett, J.D. (2011) Dinoflagellate Genome Evolution. Annual Review of Microbiology 65: 369–387.

Woese, C.R., Kandler, O., and Wheelis, M.L. (1990) Towards a natural system of organisms: proposal for the domains Archaea, Bacteria, and Eucarya. PNAS 87: 4576–4579.

Worden, A.Z., Follows, M.J., Giovannoni, S.J., Wilken, S., Zimmerman, A.E., and Keeling, P.J. (2015) Rethinking the marine carbon cycle: Factoring in the multifarious lifestyles of microbes. Science 347: 1257594–1257594.

Wu, W., Lu, H.-P., Sastri, A., Yeh, Y.-C., Gong, G.-C., Chou, W.-C., and Hsieh, C.-H. (2018) Contrasting the relative importance of species sorting and dispersal limitation in shaping marine bacterial versus protist communities. ISME J 12: 485–494.

Wyman, S.K., Avila-Herrera, A., Nayfach, S., and Pollard, K.S. (2018) A most wanted list of conserved microbial protein families with no known domains. PLOS ONE 13: e0205749.

Xia, L.C., Steele, J.A., Cram, J.A., Cardon, Z.G., Simmons, S.L., Vallino, J.J., et al. (2011) Extended local similarity analysis (eLSA) of microbial community and other time series data with replicates. BMC Systems Biology 5: S15.

Xu, Z., Cheung, S., Endo, H., Xia, X., Wu, W., Chen, B., et al. (2022) Disentangling the Ecological Processes Shaping the Latitudinal Pattern of Phytoplankton Communities in the Pacific Ocean. mSystems 7: e01203-21.

Yih, W. and Coats, D.W. (2000) Infection of Gymnodinium sanguineum by the Dinoflagellate Amoebophryasp.: Effect of Nutrient Environment on Parasite Generation Time, Reproduction, and Infectivity. J Eukaryotic Microbiology 47: 504–510.

Zamkovaya, T., Foster, J.S., de Crécy-Lagard, V., and Conesa, A. (2021) A network approach to elucidate and prioritize microbial dark matter in microbial communities. ISME J 15: 228–244.

Zhang, B., Cai, G., Wang, H., Li, D., Yang, X., An, X., et al. (2014) Streptomyces alboflavus RPS and Its Novel and High Algicidal Activity against Harmful Algal Bloom Species *Phaeocystis globosa*. PLOS ONE 9: e92907.

Zhang, G., Liang, S., Shi, X., and Han, X. (2015) Dissolved organic nitrogen bioavailability indicated by amino acids during a diatom to dinoflagellate bloom succession in the Changjiang River estuary and its adjacent shelf. Marine Chemistry 176: 83–95.

Zhou, J. and Ning, D. (2017) Stochastic Community Assembly: Does It Matter in Microbial Ecology? Microbiol Mol Biol Rev 81:.

Zingone, A., Harrison, P.J., Kraberg, A., Lehtinen, S., McQuatters-Gollop, A., O'Brien, T., et al. (2015) Increasing the quality, comparability and accessibility of phytoplankton species composition time-series data. Estuarine, Coastal and Shelf Science 162: 151–160.

Résumé

Les efflorescences sont un phénomène naturel dans les écosystèmes marins côtiers, soutenant les chaînes alimentaires. Comprendre la dynamique des microbes marins est crucial pour améliorer notre capacité à prédire les conséquences environnementales des changements globaux. La Manche Orientale (MO) est un écosystème côtier, méso-eutrophe sous l'influence des marées, caractérisé par une efflorescence printanière de l'haptophyte *Phaeocystis globosa*. Outre *P. globosa*, d'autres microbes planctoniques, présentent des proliférations ou des augmentations de leur abondance. Si l'efflorescence de *Phaeocystis* est relativement bien étudiée, les mécanismes régulant les autres taxons proliférants dans la MO sont encore mal connus. L'objectif de cette thèse était d'étudier les mécanismes d'organisation saisonniers des communautés microbiennes et des taxons qui présentent des efflorescences de différents groupes microbiens. En particulier, cette thèse a examiné les processus écologiques par une approche d'écologie communautaire et par les interactions potentielles.

Le travail présenté dans ce manuscrit est basé sur l'analyse par microscopie, cytométrie, et métabarcoding de l'ADN (18S et 16S). Des échantillons en sub-surface ont été collectés sur cinq ans (2016-2020, 322 échantillons) dans cinq stations (15 km) aux le réseau national d'observation SOMLIT (S1, S2) et au transect local DYPHYRAD (R1, R2, R4). Deux fréquences d'échantillonnage différentes ont été utilisées pour mieux capturer les variations temporelles des communautés planctoniques (toutes les 2 semaines de 2016 à 2020 et à une fréquence plus élevée de 2018 à 2020). La microscopie et la cytométrie ont permis d'estimer l'abondance et la biomasse, et le metabarcoding a fourni une évaluation plus étendue de la diversité.

Dans la première partie de cette thèse, les processus écologiques régulant l'organisation saisonnière des communautés de phytoplancton ont été étudiés. Les processus déterministes ont dominé en hiver et au début du printemps, tandis que les processus stochastiques dominaient en été lorsque des proliférations transitoires se produisaient. Les processus déterministes et stochastiques ont joué tous deux un rôle significatif dans la formation des communautés de phytoplancton en automne. Dans la deuxième partie, la dynamique des bactéries hétérotrophes et leurs interactions potentielles ont été étudiées lors des proliférations récurrentes de *P. globosa* et de transitoires diatomées à l'aide de l'analyse de similarité locale étendue (eLSA). Les bactéries hétérotrophes ont présenté des patrons saisonniers et 'épisodiques' liés aux proliférations transitoires de diatomées. Il a été démontré que les efflorescences de diatomées et de *P. globosa* définissent des communautés bactériennes distinctes qui étaient saisonnières et/ou liées aux substrats phytoplanctoniques. Dans la troisième partie de cette thèse, les dynamiques interannuelles, la diversité, les processus écologiques et les hôtes potentiels des endosymbiotes du groupe II Syndiniales ont été étudiés. Cette étude a révélé l'existence de populations locales présentant des patrons temporels cohérents. Les Syndiniales du groupe II ont atteint leur maximum en été, en même temps que le dinoflagellé mixotrophe *Prorocentrum minimum*. Les processus écologiques stochastiques ont prédominé dans l'assemblage de la communauté, mais des processus déterministes ont été remarquables en été, suggérant des interactions spécifiques entre les Syndiniales et les dinoflagellés.

Dans l'ensemble, cette thèse a fourni une image complète des microbes planctoniques dans la MO. Elle a permis de souligner la nécessité d'approches complémentaires dans les recherches associées aux observatoires, et a plaidé en faveur de fréquences d'échantillonnage aussi élevées que possible. Dans un contexte plus large, la prévalence des processus stochastiques rend les dynamiques saisonnières moins prévisibles a priori face aux changements environnementaux futurs.

Mots clés : plancton, efflorescences, écologie des communautés, patrons temporels, métabarcoding, Manche Orientale.

Abstract

Blooms are an important, widespread natural phenomenon in coastal ecosystems supporting marine food webs. Understanding the dynamics of marine microbes is thus crucial for enhancing our ability to predict accurately the environmental consequences of local and global changes. The Eastern English Channel (EEC) is a tidally mixed meso-eutrophic coastal ecosystem, characterized by spring nontoxic bloom of the haptophyte *Phaeocystis globosa.* Besides *P. globosa,* other planktonic microbes, including diatoms, dinoflagellates, bacteria and eukaryotic parasites present blooms or increases in relative abundance. While the major drivers defining *P. globosa* are generally well studied, little is known about the mechanisms regulating other blooming taxa in the EEC. The objective of this thesis was to investigate the seasonal organisation mechanisms of plankton microbial communities of different groups. In particular, this thesis looked into ecological processes through a community ecology approach, and explored potential interactions.

The work presented in this manuscript is based on the analysis of microscopy, cytometry counts, and DNA metabarcoding (rRNA gene 18S V4 and16S V3-V4) data. Sub-surface samples were collected over five years (2016-2020, 322 samples) at five neighbouring stations (Wimereux, Eastern English Channel; ca. 15 km) belonging to the national observatory network SOMLIT (S1, S2; https://www.somlit.fr/en/) and to the local monitoring transect DYPHYRAD (R1, R2, R4). Two different sampling frequencies were conducted to better capture the temporal changes of plankton communities (bi-weekly during 2016–2020 and at a higher frequency during 2018–2020). Microscopy and cytometry allow estimating abundance and biomass, and metabarcoding provided a more extended evaluation of the diversity.

In the first part of this thesis, the ecological processes regulating seasonal organisation of phytoplankton communities were investigated. Deterministic processes dominated in winter and early spring, while stochastic processes dominated in summer, where transient bloom occurred. Both deterministic and stochastic processes played significant roles in shaping phytoplankton communities in autumn. In the second part of this thesis heterotrophic bacterial dynamics, and their potential interactions during *P. globosa* and transient diatom blooms were investigated by applying extended local similarity analysis (eLSA) to microscopic data for phytoplankton and 16S data for heterotrophic bacteria. Heterotrophic bacteria showed seasonal, and 'episodic' patterns related to transient diatom blooms. It was evidenced that diatom and *P. globosa* blooms harbour distinct bacterial communities that were seasonally and/or substrate driven. In the third part of this thesis the interannual dynamics, diversity, ecological processes and potential hosts of the endosymbionts Syndiniales group II were investigated. Syndiniales Group II evidenced the existence of local populations and featured consistent temporal patterns. Syndiniales Group II peaked in summer along with the mixotrophic dinoflagellate *Prorocentrum minimum* (prevalence up to 38.5 %). Stochastic ecological processes prevailed in community assembly, but deterministic ones were notable in summer suggesting specific Syndiniales-dinoflagellate interactions.

Overall, this thesis provided a complete picture of the microbial planktonic microbes in the EEC, highlighted the need for complementary approaches in observatory surveys, and advocated for as high as possible sampling frequencies. In a broader context, the prevalence of stochastic processes renders a priori less predictable the seasonal dynamics to future environmental change.

Keywords: plankton, blooms, community ecology, temporal patterns, metabarcoding, Eastern English Channel